Intracellular Mechanisms in Chronic Pain States

Ada Delaney

Thesis presented for the degree of Doctor of Philosophy

Centre for Neuroscience Research
College of Medicine and Veterinary Medicine
University of Edinburgh
2007

Declaration

I hereby declare that the composition of this thesis and the work presented in it are entirely my own with the exception of intrathecal administration of various pharmacological agents which were carried out in collaboration with Dr. E. M. Garry. Some of the studies presented have been published reprints and abstracts of all published work are included in the appendix.

Ada Delaney

Acknowledgements

This work was supported by the Wellcome Trust and a studentship awarded by the Medical Research Council. Many thanks to my supervisors, Professor Sue Fleetwood-Walker and Dr. Rory Mitchell for their encouragement, excellent advice and continued support and guidance throughout my PhD.

I would like to thank Professor S. Grant at the Wellcome Trust Sanger Institute, UK for providing the mutant mice, P. Robberecht, at the Free University of Brussels, Belgium for his gifts of the $VPAC_2$ receptor agonist, the $VPAC_1$ and $VPAC_2$ receptor antagonists, C. Garret, at Rhone-Poulenc Rorer, France for kindly providing the NK_1 receptor antagonist, X. Emonds-Alt at Sanofi Recherche, France for donating the NK_2 receptor antagonist and P. Birch at Glaxo Smith-Kline, UK for the gift of the NK_2 receptor agonist.

Thank you to all members of my thesis committee, Dr. Mike Cousins, Dr. Vladimir Buchman and Professor Vincent Molony for their continued encouragement and advice. I would like to extend my gratitude to Dr. Mayank Dutia, Dr. Richard Ribchester, Professor Peter Brophy and Professor Seth Grant for their continued support throughout my time at the Centre for Neuroscience Research. I would like to thank everyone that I have worked with throughout my PhD especially all those in the Division of Veterinary Biomedical Sciences, Centre for Neuroscience Research and Centre for Integrative Physiology for their expert and friendly assistance.

Specifically I would like to thank Dr. Rory Mitchell for designing all the pharmacological agents used and for his expert advice on all biochemical aspects of this thesis. I would like to thank Dr. Melaney Johnston and Bobbie Rosie at the MRC Membrane and Adapter Proteins Co-op for their advice and assistance with western immunobloting. Thank you to Heather Anderson and Mark Rockett for helping in the development of the immunofluoresence staining technique used here. I am grateful to Linda Wilson for all her guidance and assistance with the confocal microscope. Thank you to Mark Rockett

and Emer Garry for teaching me the surgical and behavioural techniques used and especially to Emer Garry for collaborating with all intrathecal studies.

Thank you to all the members of the lab for all your support and invaluable knowledge in particular, Emer, Heather, Bobbie, Mark, Francis, Clare and Anisha. I would also like to acknowledge and thank all lab members and collaborators who encouraged me to be part of the team effort in generating and publishing the research leading up to this thesis, such published papers showing the background research to this thesis are presented in the appendix.

A special thank you to my friends here and back home, especially Nora, Hara, Louise, Chris, Aoife and Arnaud and finally 'go raibh míle maith agat' to my family especially my parents for all your unending support.

Abstract

Neuropathic pain is a pervasive chronic condition that lacks adequate therapeutic treatment, making the identification of new candidate targets for drug development a priority. Underlying the development of this pathological pain state is a process of neuronal plasticity, termed central sensitisation that results in hyperexcitability of sensory neurons in the spinal cord. Stimulation of peripheral nociceptive inputs can cause downstream activation of kinases in the spinal dorsal horn that may contribute to the generation of this hyperexcitable state in the spinal cord. Here, using the chronic constriction injury (CCI) model of neuropathic pain, the role played by p42/44 and p38 mitogen-activated protein (MAP) kinases was addressed. Inhibition of both the p42/44 and p38 MAP kinase pathways attenuated the behavioural reflex sensitisation seen following nerve injury. The study explored the part played by spinal $VPAC_2$ and NK_2 receptors, (which respond to the afferent excitatory neuropeptides VIP and NKA respectively), in addition to glially mediated events in the activation of these kinases. Following nerve injury, both spinal activation of p42/44 and p38 MAP kinases and behavioural sensitisation (which was sensitive to p42/44 and p38 pathway inhibitors) was prevented by $VPAC_2$, NK_2 and NMDA receptor antagonists and glial or TNF-α inhibitors.

The NMDA receptor, which is thought to be crucially involved in central sensitisation in the spinal cord, binds to the multivalent adapter protein PSD-95; an interaction which is necessary for the development of neuropathic behavioural reflex sensitisation. Here we show that mutant mice expressing a single point mutation in the Src homology 3 (SH3) domain of PSD-95 ($PSD\text{-}95^{SH3W470L}$ mutants), have intact neuropathic behavioural reflexes but blunted inflammatory responses. These findings indicate that different domains of the same protein may contribute selectively to different pain states. Examining further the role played by PSD-95, we found that the expression of both PSD-95 and one of its signalling partner kinases, Pyk 2, was increased in the same superficial dorsal horn neurons following nerve injury. These studies suggest the importance of specific receptors and signalling pathways, non-neuronal cells and of protein:protein

complexes associated with the NMDA receptor in chronic pain states and point to their future potential in the design of novel therapeutic targets.

Contents

Chapter Contents

List of Figures

List of Tables

Abbreviations

°C	degrees celcius
(R)-CPP	3-((*R*)-2-Carboxypiperazin-4-yl)-propyl-1-phosphonic acid NMDA receptor antagonist
[Ac-His^{1}, D-Phe^{2}, Lys^{15}, Arg^{16}, Leu^{17}]-VIP(3-7)GRF(8-27)	$VPAC_1$ receptor antagonist
[des(1-4), Arg^{16}]-Ro 25-1553	$VPAC_2$ receptor antagonist
$AKAP_{79/150}$	A kinase-anchoring $protein_{79/150}$
AMPA	α-amino-3-hydroxy-5-methyl-4-isoxazole proprionic acid
ANOVA	analysis of variance
ARF	ADP-ribosylation factor
ATP	adenosine triphosphate
BDNF	brain derived neurotrophic factor
BSA	albumin bovine serum factor
Ca^{2+}	calcium
CADTK	calcium-dependent tyrosine kinase
CAK-β	cell adhesion kinase beta
CaMKII	calcium/calmodulin-dependent protein kinase II
cAMP	cyclic adenosine 3',5'-monophosphate
$CB_{1/2}$	cannabinoid receptor 1/2
CCI	chronic constriction injury
CCK	cholecystokinin
CFA	complete Freund's adjuvant
CGRP	calcitonin gene-related peptide
CNS	central nervous system
Con	contralateral
CREB	cAMP-response-element-binding protein
CRIPT	cysteine-rich interactor of PDZ3
CTb	cholera toxin B subunit

C-terminus	carboxy-terminal
DMF	dimethylformamide
DRG	dorsal root ganglion
EAA	excitatory amino acid
ERK1/2	extracellular signal regulated kinase 1/2 (p42/44)
FAK	focal adhesion kinase
FAK2	focal adhesion kinase 2
g; mg; kg	gram; milli; kilo- gram
G protein	guanyl regulatory protein
GABA	γ-amino-butyric acid
GAPDH	glyceraldehyde-3-phosphate dehydrogenase
GDNF	glial cell line derived neurotrophic factor
GFAP	glial fibrillary acidic protein
GK	guanylate kinase-like
GKAP	guanylate kinase-associated kinase
GPCR	g-protein coupled receptor
GR 64349	NK_2 receptor agonist
HIV	human immunodeficiency virus
IB_4	isolectin B_4
IHC	immunohistochemistry
IL-1	interleukin-1
IL-6	interleukin-6
IM	nucleus intermedio-medialis
Ipsi	ipsilateral
IT	intrathecal
JNK	Jun N-terminal kinase
K^+	potassium
KA	kainaite
kDa	kilo dalton
L; ml; μl	litre; mili; micro-litre
L3-6	lumbar 3-6 spinal nerves

LC	locus coeruleus
LI	lamina I
LII	lamina II
LII_i	lamina II inner zone
LIII	lamina III
LII_o	lamina II outer zone
LIV	lamina IV
LTP	long term potentiation
LV	lamina V
M; mM; nmol	molar; milimolar; nanomolar
MAGUK	membrane associated guanylate kinase
MAPK	mitogen-activated protein kinase (MAP-kinase)
Mg^{2+}	magnesium
mGluR1-7	metabotropic glutamate receptor subunits 1 to 7
MLK 2/3	mixed lineage kinases 2/3
m; mm; μm	metre; milli; micro-metres
mN/mm^2	force in milinewtons per unit area (square millimetre)
mRNA	messenger RNA
n	sample number
Na^+	sodium
$Na_v1.3$	sodium channel brain type III (TTX-sensitive)
SNS1	sodium channel type 1 ($Na_v1.8$; TTX-resistant)
SNS 2	sodium channel type 2 ($Na_v1.9$; TTX-resistant)
NF	neurofilament
NGF	nerve growth factor
NK	neurokinin
NKA / B	neurokinin A / B
$NK_{1/2/3}$	neurokinin 1/ 2/ 3 receptor
NMDA	*N*-methyl-D-aspartate
nNOS	neuronal nitric oxide synthase
NOS	nitric oxide synthase

NP γ	neuropeptide gamma
NPK	neuropeptide K
NPY	neuropeptide Y
NRM	nucleus raphe magnus
NSAID	non-steroidal anti-inflammatory drug
NT-3	neurotrophin-3
NT-4/5	neurotrophin-4/5
OX-42	microglia marker
$p \leq 0.05$	probability less than or equal to less than 0.05
$P130^{cas}$	focal contact protein
$P2X_3$	purinergic receptor
PAC1	VIP/PACAP receptor
PACAP	pituitary adenylate cyclase-activating polypeptide
PACAP-27/38	PACAP variant -27/-38
$PACAP_{6-38}$	PAC_1 receptor antagonist
PAG	periaqueductal gray
Pan	phosphorylation state-independent
PAP	pyk 2 C-terminus-associated protein
PBS	phosphate buffered saline
PD 098059	p42/44 MAP kinase pathway inhibitor
PDZ	PSD-Dlg-ZO-1 homology
PF	parafasicular neurones
Phos	phosphorylated (activated) state
PKA	protein kinase A
PKC	protein kinase C
PLC	phospholipase C
PNL	partial nerve ligation
PNS	peripheral nervous system
PP2	[4amino-5(4-chlorophenyl)-7(t-butyl)pyrazolo[3,4-d]pyrimidine]
PPT	Propentofylline
PPT I	perprotachykinin I

PPT II	perprotachykinin II
PSD	post synaptic density
PSD-95	post synaptic density protein 95
PSD-95^{SH3W470L}	mice carrying a targeted single point mutation of tryptophan 470 in the SH3 domain of PSD-95 substituting for leucine at this site
PSDC	post synaptic dorsal column
PVDF	polyvinyl difluoridine
PWL	paw withdrawal latency
PWT	paw withdrawal threshold
Pyk 2	proline-rich tyrosine kinase 2
Pyk 2-H	proline-rich tyrosine kinase 2 spliced isoform
R	receptor
RAFTK	related adhesion focal tyrosine kinase
RNA	ribonucleic acid
Ro 25-1553	$VPAC_2$ receptor agonist
ROI	region of interest
RP 67580	NK_1 receptor antagonist
RVM	rostral ventromedial medulla
SAP-102	synapse associated protein 102
SAP-90	synapse associated protein 90
SAP-97	synapse associated protein 97
SAPAP	synapse-associated protein-90-associated protein
SAPK	stress activated protein kinase
SB 203580	p38 MAP kinase inhibitor
SCT	spinocervical tract
SDS	sodium dodecyl sulphate
SDS-PAGE	sodium dodecyl sulphate polyacrylamide gel electrophoresis
SEM	standard error of the mean
SG	substantia gelatinosa
SH3	Src homology 3
SH3-/-	PSD-95^{SH3W470L} mutant mice

SMT	spinomesencephalic tract
SNI	spared nerve injury
SNL	spinal nerve ligation
SOM	somatostatin
SP	subsatance P
SPET	suspended paw elevation time
SR 48968	NK_2 receptor antagonist
SRT	spinoreticular tract
STT	spinothalamic tract
TNFα	tumor necrosis factor alpha
Topical	topical application
To-Pro	To-Pro-3 iodide
trk A	tropomyosin-related kinase A
trk B	tropomyosin-related kinase B
trk C	tropomyosin-related kinase C
TTX	tetrodotoxin
Tyr	tyrosine
U 0124	less active analogue of U 0126
U 0126	p42/44 MAP kinase pathway inhibitor
VIP	vasoactive intestinal polypeptide
$VPAC_{1/2}$	VIP/PACAP receptors
WB	western immunoblotting
WDR	wide dynamic range neurones
WP9QY	TNFα Antagonist
WT	wild type

1. Introduction

1.1 Pain

Pain is a complex sensation that is defined as "an unpleasant sensory and emotional experience associated with actual or potential tissue damage or expressed in terms of such damage" (Merskey and Bogduk, 1994). Pain sensation is a dynamic physiological process that involves the transduction of sensory information at the point of stimulation, transmission via peripheral nerve to the dorsal root ganglion then onto the spinal cord, which in turn relays this information to various centres in the brain, where it is combined with cognitive and emotional processing, resulting in the individual experience of pain. Nociception is the physiological process of transducing such sensory stimuli by specialised peripheral receptors and transmitting this information to the central nervous system, but is devoid of the emotional aspect of pain perception.

The ability to experience pain serves a protective role to warn of possible or actual tissue damage, thus allowing for the co-ordination of reflex and behavioural responses to limit the extent of such damage and enable the recovery and healing of the injury. Such acute (short-lasting) pain does not outlast the injury, to be precise the sensation of pain ceases once the inflammatory process abates or the initial noxious stimulus is removed. However, if pain sensation outlasts the injury or is out of proportion to the actual injury it is considered to be a pathological pain state. Such a chronic pain state is a maladaptive nociceptive process, where signal modulation and plasticity can occur at any stage of the process resulting in hyperexcitability of the nervous system. This hyperexcitability can lead to long term changes in nociception and the individual's perception of pain, thereby producing spontaneous and hypersensitive pain syndromes which can be so debilitating that the individual's quality of life is severely reduced. Chronic pain arising from damage to a peripheral nerve that is a neuropathic form of chronic pain will be the focus of this study, with some comparisons to chronic inflammatory pain being made. As the anatomy of sensory processing is essential to understanding how the system works and how the process may be at fault, resulting in hyperexcitability during chronic pain, each of these stages will be briefly discussed.

1.2 Peripheral transduction of sensory information

Primary afferent axons terminate in specialised nerve endings that are in close contact with well defined areas of skin from which they can be excited, this area is known as the receptive field. Sensory information about changes in the external environment of the animal is transmitted by a wide variety of cutaneous receptors and transduced into action potentials (electro-chemical activity) in primary afferent axons. Cutaneous receptors have been identified experimentally (by applying a series of test stimuli to the receptive field of the skin) to respond to specific stimuli in distinguishable classes of non-nociceptors and nociceptors (Lynn, 1994). Subgroups of receptors are activated by specific types of stimulus such as heat, cold, fine touch, pressure, vibration, and stretch and tissue pH. Primary afferent axons transmit the information evoked by stimulation of the skin to the first central synapse in the dorsal horn of the spinal cord in which afferents have highly structured termination patterns (Brown and Fuchs, 1975) thus forming an organised somatotopic map of peripheral structures (Swett and Woolf, 1985).

1.2.1 Primary afferent axons

The primary afferent axons associated with these sensory receptors run uninterrupted from their sensory endings in peripheral tissue to transmit sensory information to the spinal cord, where they have highly structured termination patterns in the dorsal horn of the spinal cord (Brown and Fuchs, 1975; Wall, 1960). These primary afferent axons can be subdivided into three types, classified according to their axonal diameter and conduction velocity.

Aβ-fibres have large diameters of greater than 10μm, are myelinated and are the most rapidly conducting fibres with conduction velocities of 30-100m/sec. These fibres are thought to be mostly non-nociceptive, innervating corpuscular endings or hair follicle receptors and respond to a variety of innocuous tactile sensations including fine touch, pressure, vibration, stretch, and hair movement under normal physiological conditions (Willis and Coggeshall, 1991; Lynn and Carpenter, 1982).

Aδ-fibres are also myelinated but have smaller axonal diameters of 2-6μm and therefore slower conduction velocities ranging from 12-30m/sec. Aδ-fibres supply hair follicle receptors or mechanical receptors and transmit both noxious and innocuous sensory information, responding to light and heavy pressure, heat and cooling and to noxious chemicals (Willis and Coggeshall, 1991). Aδ-fibre activation evokes a sensation termed 'first-pain' as it usually occurs rapidly after stimulation and is pricking or sharp in nature (Torebjork and Ochoa, 1980). There are two sub-types; Type I Aδ fibres are activated by high-intensity mechanical stimuli in the noxious range and are also weakly responsive to high-intensity heat and cold stimuli (Millan, 1999; Willis and Coggeshall, 1991). Type II Aδ fibres are less common and display a lower threshold to noxious heat stimuli and can therefore react more rapidly than type I (Willis and Coggeshall, 1991; Millan, 1999).

C-fibres have the smallest axonal diameters of 0.25-1.5μm, are unmyelinated and have slow conduction velocities of 1-2.5m/sec (Gasser, 1950). Many C-fibres are termed polymodal fibres as they respond to a range of noxious mechanical, thermal and chemical stimuli (Willis and Coggeshall, 1991). Stimulation of nociceptive C-fibres produces a sensation termed 'second pain' that usually has a relatively slow onset and is dull or burning in character (Ochoa and Torebjork, 1989; Yaksh, 1986).

1.2.2 Non-nociceptive Mechanoreceptors

Cutaneous mechanoreceptors, which are usually associated with myelinated primary afferent fibres, are highly sensitive receptors that respond to a variety of innocuous tactile sensations. This diverse group of receptors can be further subdivided:

Rapidly adapting cutaneous receptors respond to light touch, pressure and vibration of the receptive field of the skin but are not activated by hair movement. There are two classes of rapidly adapting mechanoreceptors, those associated with Meissner corpuscles and those associated with Pacinian corpuscles, both classes are associated with large Aβ fibres. Meissner corpuscles are thought to be responsible for fine or discriminative touch, while Pacinian corpuscles respond to mechanical distortion of the cutaneous receptive field caused by firm pressure (Willis and Coggeshall, 1991).

Slowly adapting cutaneous receptors are involved in stretch perception and shape discrimination, of which there are two types; slowly adapting type I and type II mechanoreceptors. Type I mechanoreceptors are low threshold receptors associated with Merkel cells and type II mechanoreceptors are associated with Ruffini corpuscles and respond to smaller displacements of skin receptive field as a result of stretching, both types are associated with Aβ fibres (Willis and Coggeshall, 1991).

Hair follicle receptors. Hairy skin has specific receptors that innervate hair follicles and respond to hair movement and bending (Brown and Iggo, 1967; Lynn and Carpenter, 1982). They can be classified according to the type of hair which they innervate (Brown and Iggo, 1967) and are associated with myelinated Aδ axons within rodent peripheral nerves (Lynn and Carpenter, 1982). *D–hair* receptors respond to the slow movement of the fine down hairs and are believed to have slowly conducting axons with large receptive fields, while *G–hair* receptors have large axons with relatively small receptive fields and liable to be activated as a result of fast movement of the guard hairs. The final class of receptor is the *T–hair* receptors which are the least numerous and are excited by movement of the large tylotrich hairs.

C–fibre mechanoreceptors. This class of mechanoreceptors is associated with unmyelinated afferent C–fibres, which are a distinct group of C–fibres that are sensitive to gentle mechanical stimulation and cooling of the skin (Bessou et al., 1971). They have a small receptive field (Bessou et al., 1971), are rapidly adapting (Bessou and Perl, 1969) and are found in the main on hairy skin. These receptors comprise approximately 15% of all C-fibres present in the saphenous nerve (Lynn and Carpenter, 1982) with a greater occurrence of approximately 30% in the sural nerve (Leem et al., 1993) in the rodent.

1.2.3 Non-nociceptive Thermoreceptors

Non-nociceptive cutaneous thermoreceptors respond to innocuous variations in temperature and can be further divided into warm or cold thermoreceptors:

Warm thermoreceptors are thought to be associated with unmyelinated axons (Iggo, 1959) and respond to slight warming of the skin. These receptors are activated by mild warmth in the non-noxious range, approximately 30-37°C.

Cold thermoreceptors are characterised by their sensitivity to miniscule reductions in skin temperature [as little as 0.1°C], the majority of which respond to stimuli in a restricted range of innocuous cold temperature [approximately 20-30°C] (Heinz et al., 1990; Iggo, 1969). These non-nociceptive cold cutaneous thermoreceptors are found in both the hairy and glabrous skin (Iggo, 1969) and are associated with Aδ-fibres [and to a lesser extent with cold-specific C-fibres] (Iggo, 1959; Iggo, 1969).

1.2.4 Nociceptors

Nociceptors respond to stimuli that can potentially or actually result in tissue damage, a concept that was first proposed a hundred years ago by Sherrington (Sherrington, 1906). Cutaneous nociceptors are functionally divided into two groups, the Aδ-fibre nociceptor or the C-fibre polymodal nociceptor.

Aδ-fibre mechanonociceptors are associated with Aδ-fibres, respond to noxious or high threshold mechanical stimulation of the skin such as pressure and pinch and are in both glabrous and hairy skin. These receptors while not normally responsive to thermal stimuli (Besson and Chaouch, 1987; Burgess and Perl, 1967) can become sensitized following a long-lasting thermal stimulation and subsequently result in a response to future thermal stimuli (Burgess and Perl, 1973; Fitzgerald and Lynn, 1977; Perl, 1984). Aδ-fibre nociceptors also show responses to noxious cold stimuli (Simone and Kajander, 1996; Simone and Kajander, 1997). In classifying Aδ-fibre nociceptors, the mechanonociceptors were found to be dominant (73%; Leem et al., 1993). Aδ nociceptive primary afferents originating from high threshold Aδ mechanonociceptors have been shown to terminate predominantly in lamina I, IV and V with some branching to lamina II and X of the spinal dorsal horn (see Figure 1.1 and Section 1.3.1 and 1.3.2 for description of Rexed's Laminae and also Figure 1.2; Cervero et al., 1976; Light and Perl, 1979; Rethelyi et al., 1983).

C-fibre polymodal nociceptors exist in both hairy and glabrous skin, have small receptive fields and respond to multiple high threshold stimuli. C-fibre polymodal nociceptors can be activated by high threshold heat stimulation (temperatures $\geq 42^{\circ}C$), by noxious mechanical stimulation, in addition to being excited by irritant chemicals (Bessou and Perl, 1969;Perl, 1984) and in some cases intense cold (Cervero and Iggo, 1980; Simone and Kajander, 1996; Willis and Coggeshall, 1991). Most C-fibre polymodal nociceptors have been shown to terminate in lamina I-II of the spinal dorsal horn (Figure 1.1 for Rexed Lamina and Figure 1.2; Cervero and Iggo, 1980; McMahon et al., 1984).

Other types of nociceptors have been identified including; cold nociceptors, that respond to close to $0^{\circ}C$, which are stimuli associated with Aδ nociceptors and possibly cold-sensitive C-fibres; chemical nociceptors, which respond specifically to changes in extracellular pH and acidosis; and 'silent' nociceptors, which may be completely inactive until sensitised, for example, by the onset of inflammation or the application of chemical irritants (Besson and Chaouch, 1987; Bessou and Perl, 1969; Clark et al., 2003; Schmidt et al., 1995; Simone and Kajander, 1996).

1.2.5 Sensory Neurones

The cell bodies of primary afferent fibres are located in the dorsal root ganglion (DRG) located close to either side of the spinal cord or in the cranial nerve ganglia at the base of the skull. Most afferent fibres pass through the dorsal root but some pass through the ventral root (Coggeshall et al., 1975), which generally carries efferent fibres whose cell bodies of origin are located in the spinal grey matter. There are different subpopulations of sensory neurones that can be identified by their size (diameter of the cell body) and ultrastructure and by immunocytochemical characteristics. The cell bodies of the primary afferent fibres can be characterised by their response to growth factors [such as nerve growth factor (NGF); glial cell-derived-neurotrophic factor (GDNF)] and by their expression of various substances. Markers that are expressed in a cell type restricted pattern include; neurofilament (NF) proteins, calcitonin gene related peptide (CGRP) and substance P (SP), nitric oxide synthase (NOS) as well as binding sites for isolectin B_4 (IB_4) (Bergman et al., 1999; Petruska et al., 2000). For example, *Type I* sensory neurones are large cells that do not express SP, account

for about 35% of cells and may be associated with Aβ-fibres (Bergman et al., 1999; Petruska et al., 2000). *Type II* sensory neurones are small cells identified by their binding of IB_4, account for approximately 50% of the cells and are mainly associated with C-fibres and Aδ-fibres (Bergman et al., 1999; Snider and McMahon, 1998). Another subpopulation is a small cell peptide–expressing group, which express SP and/or CGRP but are not IB_4 positive, and are associated with C-fibres, these cells are dependent on NGF and so express the NGF receptor TrkA (Braz et al., 2005).

1.3 Central transmission of sensory information

1.3.1 The Spinal Cord

The spinal cord is continuous rostrally with the medulla oblongata of the brain stem and is located in the spinal canal of the vertebral column. The dorsal horn of the spinal cord is the first stage involved in the processing of sensory information, providing the first central synapse where this information is transmitted from nociceptive primary afferent neurones, often onwards to the brain. The spinal cord in transverse section (see Figure 1.1) is composed of an 'H' or butterfly-shaped area of grey matter within white matter that is arranged around the central canal. The grey matter consists of neuronal cell bodies, fibres (axons and dendrites) and associated non-neuronal cells that can be subdivided into two main regions, namely the anterior or ventral horns and the posterior or dorsal horns. The work of Rexed (Rexed, 1952) in the spinal cord of the cat classified the grey matter into laminae according to their cytoarchitectonic characteristics. Rexed suggested an anatomical division of the spinal cord grey matter into nine laminae that comprised the dorsal and ventral horns and a tenth lamina surrounding the central canal (Rexed, 1952). Further investigations revealed that the laminar arrangement of the grey matter remained consistent between mammalian species (Molander et al., 1984). Rexed's laminae I to VI will be briefly discussed as these laminae comprise the primary area for receiving somatosensory input to the dorsal horn. In addition to this laminar organisation, the central terminals of primary afferent neurones in the dorsal horn are topographically organised (Doubell and McCulloch, 1999; Swett and Woolf, 1985).

1.3.2 Laminar organisation of the dorsal horn

Lamina I [The marginal zone]

Lamina I, also known as the 'marginal zone', is the thinnest and most superficial layer of the dorsal horn (Brown, 1981; Molander et al., 1984). It is classically characterized by large, horizontal neurones and a plexus of numerous horizontally arranged fine axons (Willis and Coggeshall, 1991). Both myelinated Aδ-fibres and unmyelinated C-fibres terminate in lamina I with Aδ-fibres being the predominant primary afferent input (Woolf and Doubell, 1994), while input from the large myelinated Aβ-fibres is not evident (Brown, 1981). Afferents from lamina I project to the brainstem, midbrain, thalamic nuclei and other parts of the spinal cord (Willis and Coggeshall, 1991). Lamina I is highly important in the transmission of noxious sensory information, as it appears to contain a substantial number of noci-specific neurones, which receive their projections from cutaneous high threshold Aδ-mechanoreceptors and C-fibre thermal nociceptors (Cervero et al., 1976; Cervero et al., 1979; Christensen and Perl, 1970; Light and Perl, 1979; Rethelyi et al., 1983), while studies have also revealed a large proportion of rat lamina I cells to be multireceptive (McMahon and Wall, 1983). Lamina I contains cells of origin of the spinothalamic (STT) and spinomesencephalic (SMT) tract (Giesler et al., 1976; Lima and Coimbra, 1989; Mehler et al., 1960). Lamina I neurones can be classified morphologically into three classes; firstly *fusiform cells* that have small spindle shaped somata and bipolar longitudinal dendritic arbors; secondly *pyramidal cells* with triangular soma and three main dendritic origins with primarily longitudinal arborisation; thirdly *multipolar cells* with larger multiangular somata and four or more radiating dendritic arbors directed longitudally and mediolaterally (Lima et al., 1991; Zhang et al., 1996). The dendrites of both fusiform and pyramidal cells remain in Lamina I whereas the dendrites of multipolar cells can enter Lamina II or III (Lima and Coimbra, 1986).

Lamina II [The substantia gelatinosa]

Lamina II is located ventral to lamina I and is also called the 'substantia gelatinosa' due to its gelatinous appearance as a result of the concentration of small neurones and the absence of myelinated fibres (Brown, 1981; Willis and Coggeshall, 1991). Lamina II consists of an outer zone (lamina II_o) that contains densely packed small cells and a less compact inner zone (lamina II_i; Light and Perl, 1979). Lamina II seems to be the main projection area for

unmyelinated C-fibres with a sparse input from the myelinated Aδ fibres (Willis and Coggeshall, 1991; Woolf and Doubell, 1994). While large myelinated Aβ-fibres can innervate this region, they appear largely excluded (Wilson and Kitchener, 1996). Lamina II neurones can be classified into two structural groups; namely *islet cells* that have dendrites which spread rostrocaudally within the lamina and axons that remain close to the cell body and *stalked cells* with dendrites that fan out ventrally and axons that pass dorsally into lamina I (Todd, 1988; Todd and Lewis, 1986). Very few (approximately 1%) lamina II neurones project to the brainstem, some neurones project into lamina I or are mainly intrinsic interneurones with extensive local integration (Giesler et al., 1976; Willis et al., 1979). Lamina II is primarily involved with the processing of sensory information from the skin and receives little input from non-cutaneous structures (such as muscle and viscera; Wilson and Kitchener, 1996). Together lamina I and lamina II are known as 'the superficial dorsal horn'.

Lamina III – IV [The nucleus proprius]

Lamina III lies ventral to lamina II and forms a broad band across the dorsal horn and is distinguished from lamina II by having slightly larger and more widely spaced cells (Rexed, 1952). There are two structural types of cells found in lamina III; firstly those that appear like lamina II islet cells and secondly other cells that resemble inverted stalked cells with dendrites which spread dorsally (Powell and Todd, 1992). Second order neurones send dendrites from lamina III to lamina I and IV, and this lamina contains cells of origin of the spinocervical (SCT), the postsynaptic dorsal column (PSDC) and STT tracts (Brown, 1981). Lamina IV is a slightly thicker layer ventral to lamina III and is distinguishable from lamina III by the heterogeneity of neuronal sizes in addition to the presence of some very large cells (Molander et al., 1984). Many of the large scattered cells of lamina IV project dendrites into lamina I-III; this distribution allows lamina IV cells to receive direct primary afferent input from fibres that enter the superficial layers. Again lamina IV contains cells of origin of the SCT, STT and the PSDC tracts. Lamina III-IV predominantly receives inputs from Aβ primary afferents of large hair follicles, slowly and rapidly adapting mechanoreceptors and non-nociceptive Aδ-fibres, while also receiving input from visceral afferents (Brown and Iggo, 1967; Gillette et al., 1994; Light and Perl, 1979) and is also known as the 'nucleus proprius'.

Lamina V - VI

Lamina V is a thick band across the narrowest part of the dorsal horn and can be identified by the presence of many large diameter cells and of myelinated fibres due to Aβ fibres terminating here (Molander et al., 1984; Willis and Coggeshall, 1991). Lamina VI exists only in the cervical and lumbosacral enlargements of the spinal cord and consists of a medial zone with small packed, compact cells and a lateral zone with slightly larger cells, with very few primary afferents terminating here (Brown, 1981; Willis and Coggeshall, 1991). This layer represents a transitional layer between the primary afferent-dominated dorsal horn and the ventral horn. Both Lamina V and VI contain cells of origin of the STT, SMT and SCT tract (Cao et al., 1993; Giesler et al., 1976; Mehler et al., 1960).

It is important to note that there are no precise cytoarchitectonic borderlines within the spinal cord and that the laminae are recognized primarily as zones of particular cell types that may have intermingled edges. Furthermore the borders between various laminae may differ slightly between different segmental sections (Molander et al, 1984). The remaining laminae, laminae VII-X which comprise the ventral horn are beyond the scope of this study.

1.3.3 Dorsal horn neurones

As outlined above the spinal dorsal horn is an important centre for the processing of sensory information from the periphery to the central nervous system and contains a number of cells of different sizes and appearance that can be categorised into three classes according to their response to peripheral sensory stimuli (see Figure 1.2).

Class I [Non-nociceptive neurones]

Class I neurones do not respond to noxious stimulation but only to innocuous mechanical stimulation of the receptive field via low threshold mechanosensitive A-fibres (Dubner and Bennett, 1983; Iggo and Ramsey, 1974).

Class II [multireceptive neurones]

Class II or wide-dynamic range (WDR) neurones respond to both innocuous and noxious cutaneous mechanical stimuli and or noxious thermal stimulation (Mendell, 1966; Price et

al., 1976; Price et al., 1978). Indeed these cells can respond to stimulation of all types of primary afferents, from the large myelinated Aβ-fibres to unmyelinated C-fibres and are most commonly found in laminae IV-VI of the dorsal horn, in particular lamina V (Besson and Chaouch, 1987), however they have also been documented in the superficial layers of the dorsal horn (McMahon and Wall, 1983; Menetrey and Besson, 1981; Woolf and Fitzgerald, 1983).

Class III [Noci-specific neurones]

Class III neurones appear to receive input only from myelinated (Aδ -fibres) and non-myelinated (C-fibres) nociceptive afferents, thereby responding only to high-threshold noxious stimuli (Cervero et al., 1976). These neurones have relatively small cutaneous receptive fields and display little spontaneous activity (Perl, 1984). While they are exclusively activated by noxious cutaneous stimulation, some of these noci-specific neurones can also be driven by non-cutaneous inputs from the muscle or viscera (Cervero, 1983; Craig and Kniffki, 1985). Noci-specific neurones tend to occur in lamina I and include neurones that project to the thalamic and brain stem regions (Cervero et al., 1976; Cervero et al., 1979; Christensen and Perl, 1970; Light and Perl, 1979). There is also a fourth class of dorsal horn neurones, consisting of proprioceptive neurones that for example respond to joint movement and pressure on deep tissues that will not be considered here.

In addition to the functional classification of dorsal horn neurones, they can also be grouped according to their axon projections. Such groups are projecting neurones, local circuit neurones and interneurones. Projecting neurones enter ascending spinal tracts and transmit sensory information to higher brain centres. The majority of dorsal horn neurones are interneurones, which can be excitatory or inhibitory. Dorsal horn neurones also receive inputs from descending neurones from the brain to exert modulatory influences on sensory information processing in the spinal cord. All of this is further discussed below.

Figure 1.1

Schematic diagram of Rexed's cytoarchitectonic scheme applied to the spinal cord of the rat.

The diagram represents a transverse section of the spinal grey matter. The laminae are indicated by roman numerals I-X and IM represents nucleus intermedio-medialis from Rexed (Rexed, 1952).

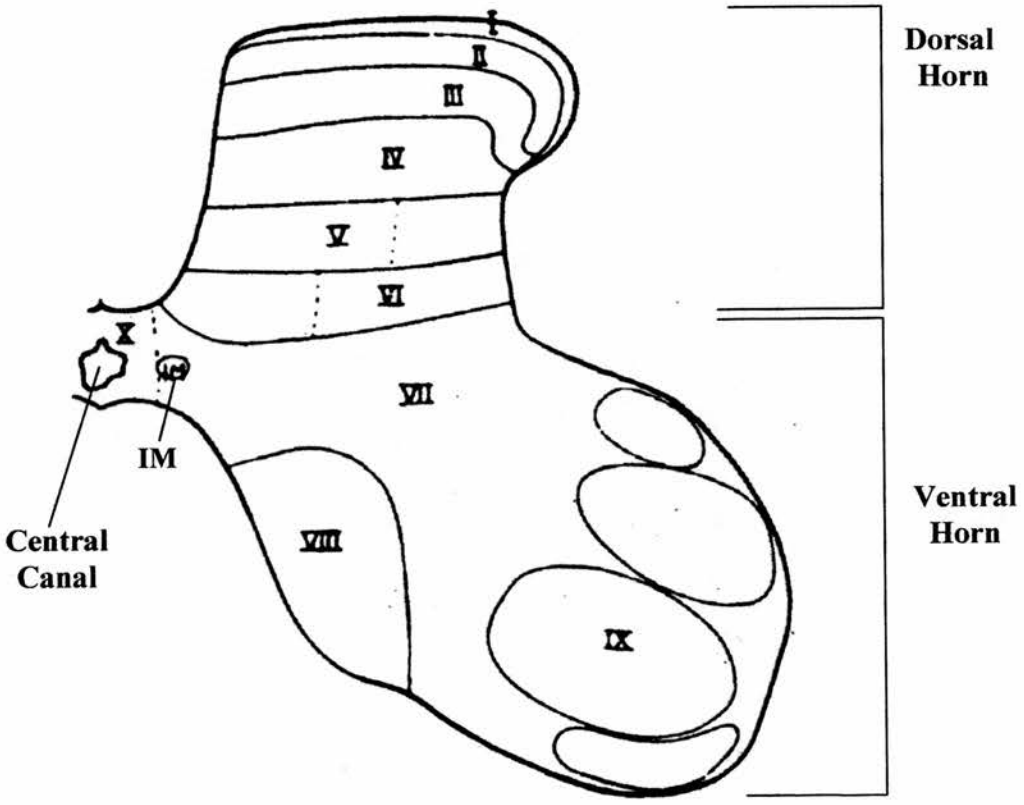
Dorsal
Horn
I
II
III
IV
V
VI
X
VII
IM
Central
Canal
VIII
IX
Ventral
Horn

Figure 1.2

Schematic diagram of the cutaneous afferent input to and neuronal organisation of the spinal dorsal horn.

A hypothetical cross section, showing the afferent fibres and neuronal elements found in the first four laminae of the spinal dorsal horn. The laminar divisions of Rexed (Rexed, 1952) are indicated to the right of the image. Afferent fibre types are listed to the left of the image, which are shown to project onto neuronal types typical of laminae I-IV. The neurones shown are a marginal cell, a substantia gelatinosa (SG) limiting cell, two SG central cells and two neurones of the nucleus proprius, the more superficial of which has dendrites penetrating lamina II (from Cervero and Iggo, 1980).

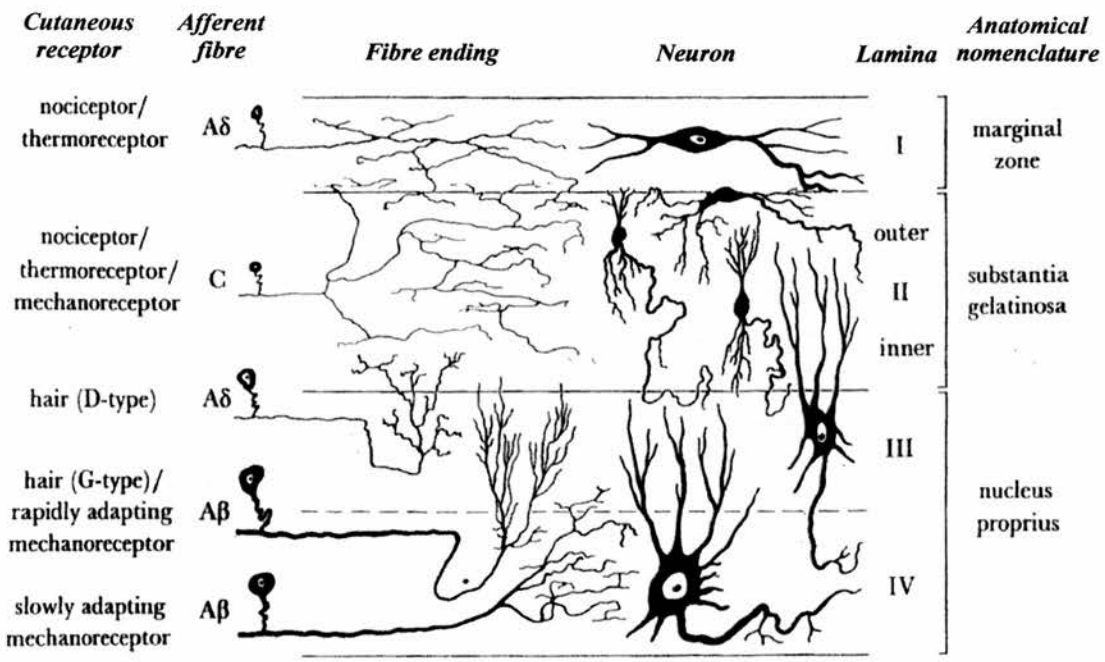
Cutaneous receptor
Afferent fibre
Fibre ending
Neuron
Lamina
Anatomical nomenclature
nociceptor/ thermoreceptor
Aδ
I
marginal zone
nociceptor/ thermoreceptor/ mechanoreceptor
C
outer
II
inner
substantia gelatinosa
hair (D-type)
Aδ
III
hair (G-type)/ rapidly adapting mechanoreceptor
Aβ
nucleus proprius
slowly adapting mechanoreceptor
Aβ
IV

1.3.4 Ascending somatosensory tracts

Many dorsal horn neurones are projection neurones which send their axons, via ascending tracts in the white matter to brainstem and midbrain regions. The main ascending tracts involved in the transmission of nociceptive information include;

Spinothalamic Tract [STT]

The STT carries information from the spinal dorsal horn to the thalamic nuclei, with its cells of origin located in laminae I, III and IV and V of the spinal dorsal horn (Giesler, Jr. et al., 1979; Todd et al., 2000; Todd, 2002). STT cells usually respond to noxious mechanical stimulation of the cutaneous receptive field but can also respond to innocuous mechanical and temperature stimuli (Giesler et al., 1976), thereby the STT is not solely involved in nociceptive transmission. Inhibition of the responses of STT cells from both noxious and innocuous stimuli (from myelinated fibres) can be seen when various regions of the brain are stimulated, such as the nucleus Raphe magnus (NRM; Willis et al., 1977).

Spinoreticular Tract [SRT]

The SRT projects from the dorsal horn in the ventrolateral region of the spinal cord to the brain stem reticular formation, particularly within the medulla. SRT cells of origin appear to be concentrated in laminae VII and VIII in the ventral horn (Chaouch et al., 1983) with few cells found in the superficial layers of the dorsal horn. Studies revealed that some SRT cells could be activated by noxious sensory stimuli (Menetrey et al., 1980).

Spinomesencephalic tract [SMT]

The SMT projects from cells of origin in laminae I, V and VI to the mesencephalic reticular formation including the periaqueductal grey area (PAG) and to other sites in the midbrain (Mehler et al., 1960). A significant proportion of SMT neurones which originate in lamina I appear to be nociceptive in nature (Menetrey et al., 1980; Menetrey et al., 1982).

Dorsal Column Pathways

This ascending group can be divided into the postsynaptic dorsal column system (PSDC) and the spinocervical tract (SCT). ***PSDC:*** The PSDC cells of origin are located primarily in

lamina III of the spinal cord and projects through the dorsal funiculus to the nucleus gracilis and nucleus cuneatus of the medulla (Giesler, Jr. et al., 1984). PSDC neurones are excited by innocuous hair movement, pressure, pinching and cooling in addition to nociceptive stimuli (Angaut-Petit, 1975). ***SCT:*** The SCT originates from cells in laminae III-VII and projects ipsilaterally to the lateral funiculus (Cao et al., 1993). Some fibres of this tract project into the PSDC or cross the mid-line into the contralateral ascending ventral funiculus (Cao et al., 1993). Most SCT neurones respond to innocuous hair movement, however many are multireceptive responding to nociceptive stimulation (Brown et al., 1983; Cervero et al., 1979; Fleetwood-Walker et al., 1988).

1.3.5 Descending control

Dorsal horn neurones also receive efferent inputs from descending fibres, the effects of which may be direct or indirect through involvement of interneurones at the spinal cord level. Melzack and Wall were first to describe the existence of a specific modulatory system within the CNS in their 'Gate Control Theory of Pain' (Melzack and Wall, 1965). They proposed that spinal nociceptive transmission could be influenced by impulses from the brain which had the potential to exert a form of descending control mediated by cutaneous stimulation of large afferent fibres. This inhibitory influence by stimulation of large A fibres, on C-fibre and noxious stimulation evoked excitation of dorsal horn neurones has been confirmed experimentally (Besson and Chaouch, 1987; Woolf and Wall, 1982). Descending inhibitory pathways from the brain may augment local inhibitory mechanisms to reduce nociceptive transmission (Besson and Chaouch, 1987; Polgar et al., 2002). While many modifications of the detail of this theory have been made, the hypothesis remains relevant when investigating transmission of nociceptive information.

Tonic descending modulation

Many areas of the brain are known to be involved in the descending control of nociceptive transmission, the exact origin of tonic descending inhibition is unclear. Lesion studies revealed the lateral reticular nuclei in the brainstem as a source of descending pathways (Foong and Duggan, 1986; Morton et al., 1983). Two regions in the brainstem, the medullary nucleus raphae magnus (NRM) and adjacent structures of the rostral ventromedial medulla

(RVM) are key regions involved in descending control of nociceptive transmission. The NRM provides a major serotonergic input to laminae I, II and V cells of the dorsal horn (Basbaum and Fields, 1984; Polgar et al., 2002). Electrical stimulation of this area has been shown to produce analgesia to noxious stimuli (Duggan and Griersmith, 1979; Guilbaud et al., 1977; Oliveras et al., 1974; Willis et al., 1977). Electrical stimulation in the RVM produces a biphasic modulatory effect with facilitation at low intensities and inhibition at higher intensities (Calejesan et al., 2000). Under mild noxious stimulation, RVM cells with inhibitory projections to the dorsal horn may inhibit spinal dorsal horn relay neurones (Gilbert and Franklin, 2001). However intense noxious stimulation may result in the release of GABA onto RVM cells, which in turn inhibits descending inhibitory fibres to allow transmission of nociceptive input via the dorsal horn (Gilbert and Franklin, 2001). The RVM may also be activated via opioid-mediated activation of the RVM from higher brain centres such as the amygdale (McGaraughty and Heinricher, 2002), the anterior cingulate cortex (Calejesan et al., 2000). The locus coeruleus (LC) is also involved in modulating nociceptive transmission through its actions on the parafascicular neurones (PF) of the thalamus (Zhang et al., 1997a). The LC can exert two effects on nociceptive transmission through the PF; firstly descending noradrenergic fibres from the LC to spinal cord play a predominantly inhibitory role on nociceptive information transmitted rostrally from the spinal cord and secondly ascending fibres play a facilitatory role on the responsiveness of PF to noxious input (Zhang et al., 1997a). Thus descending modulation of nociceptive transmission in the spinal cord requires the involvement of complex interactions between various brain regions.

Segmental controls

Segmental control is noted as the inhibitory effect produced by the large diameter Aβ-fibres on the responses of spinal neurones to nociceptive stimulation, which can selectively inhibit C-fibre and noxious stimulation evoked excitation of dorsal horn neurones (Besson and Chaouch, 1987; Woolf and Wall, 1982). Such an inhibitory influence can be exerted on both multireceptive and noci-specific dorsal horn neurones either directly by activation of spinal interneurones by primary afferent fibres or indirectly by activation of descending pathways from the brain. Inhibitory transmitters present in the spinal cord and brainstem include the amino acids γ-aminobutyric acid (GABA), glycine and the endogenous opioids (discussed

below). In addition to this, monoamines (such as serotonin and noradrenaline) can be directly released by descending control systems to exert inhibitory effects (Besson and Chaouch, 1987).

γ-aminobutyric acid (GABA)

GABA is an inhibitory neurotransmitter found in approximately one-third of laminae I-III dorsal horn interneurones (Barber et al., 1982; Hunt et al., 1981; Todd and McKenzie, 1989), in addition to neurones of the rostral ventral lateral medulla which projects to the spinal cord (Reichling and Basbaum, 1990). GABA-like immunoreactivity is shown in 28% of lamina I, 31% of lamina II and 46% of lamina III cells (Todd and Sullivan, 1990) and is generally considered to be present in interneurones (Todd and McKenzie, 1989). In addition a proportion of GABAergic cells contain the cotransmitter glycine (Todd and Sullivan, 1990). Ionophoretic application of GABA results in inhibition of dorsal horn neuron activity, including lamina II neurones (Curtis et al., 1977; Zieglgansberger and Sutor, 1983).

Glycine

Glycine is another important neurotransmitter that is expressed in laminae I-III of the spinal cord, where it is often colocalised with GABA (Todd and Sullivan, 1990). Ionophoretic application of glycine can inhibit dorsal horn neuronal activity (Zieglgansberger and Sutor, 1983). Glycine can have opposing functions as it can exert (or gate) an excitatory action as a co-agonist at the NMDA receptor in addition to having an inhibitory action by acting via the strychnine-sensitive glycine receptor (Budai et al., 1992). Intrathecal application of glycine has been shown to inhibit substance P (SP)-evoked biting and scratching behaviours, while use of a glycine antagonist (strychnine) facilitates nociceptive flexor reflex (Beyer et al., 1989; Sivilotti and Woolf, 1994).

Endogenous opioids

Endogenous opioid peptides such as enkephalin and dynorphin are present within the synaptic terminals of the spinal dorsal horn (Cruz and Basbaum, 1985; Glazer and Basbaum, 1981; Willis and Coggeshall, 1991). The importance of this system is illustrated by the powerful and long-lasting analgesic effects seen in animals after the intrathecal

administration of morphine (Yaksh, 1981). This principle is further supported by studies where ionophoretic application of opioids in lamina II produces a robust inhibition of dorsal horn neuron response to noxious peripheral stimulation (Duggan and North, 1983; Fleetwood-Walker et al., 1988). Opiate receptors; μ (mu), δ (delta) and κ (kappa) receptors have been identified on primary afferent terminals and located in the superficial dorsal horn (Atweh and Kuhar, 1977). In the rat spinal cord, μ receptors represent 70% of the opioid receptors while δ receptors make up 24% and κ receptors are the remaining 6% of opioid receptors (Besse et al., 1990). The inhibitory action of the endogenous opioid peptides may be pre-synaptic or may be an indirect action as a result of interneuron activation.

Endogenous cannabinoids

An alternative spinal modulatory system that can elicit selective antinociceptive effects is the endogenous cannabinoid system (Fox et al., 2001; Herzberg et al., 1997; Richardson et al., 1998). This system is of particular interest due to the evidence that natural and synthetic cannabinoid compounds can exert analgesic effects in chronic pain states (Robson, 2001). The thus far identified cannabinoid receptors are CB_1 and CB_2 (Pertwee, 1997; Pertwee, 1998). CB_1 receptors have been identified in the CNS, in particular in an area associated with nociceptive processing, namely the superficial laminae of the spinal cord (Farquhar-Smith et al., 2000; Herkenham et al., 1991). CB_2 receptors are believed to be largely restricted to the peripheral nervous system. The endogenous cannabinoids have demonstrated an antinociceptive role in both behavioural and electrophysiological studies of acute pain (Drew et al., 2000; Lichtman and Martin, 1997; Smith and Martin, 1992), with initial studies into the effect on neuropathic pain behaviours showing positive results (La Rana et al., 2006). It is possible that cannabinoids and opioids may interact in their action on the processing of nociceptive information, as CB_1 and μ- opioid receptors are colocalised in lamina II interneurones (Salio et al., 2001). The expression of CB_1 receptors has been shown to increase in a time dependent manner following chronic constriction injury (CCI) of the sciatic nerve primarily within the superficial dorsal horn of the spinal cord (Lim et al., 2003), although CB_1 receptor knockout mice have similar pain behaviour responses following partial nerve ligation (PNL) of the sciatic nerve to wild-type mice (Castane et al., 2006). Expression of CB_2 receptors is induced in the spinal cord following CCI nerve-injury but not

as a result of peripheral inflammation (CFA model of persistent inflammation), with expression thought to be localised to activated spinal microglia (Zhang et al., 2003b) and expression is also increased ipsilaterally in the spinal nerve ligation model (SNL; Beltramo et al., 2006). More recently an increase in the expression of CB_1 and CB_2 receptors has been shown ipsilaterally in skin, DRG and spinal cord in a new model of nerve-injury, namely the saphenous partial ligation model (Walczak et al., 2005).

1.4 Neurotransmitters/peptides and their receptors involved in nociception

Primary afferent nociceptors as outlined above are composed of a cell body (located in the DRG) and nerve fibres which project in a dual manner both centrally and peripherally (Willis and Coggeshall, 1991). Peripheral stimuli of sufficient intensity, such as an intense mechanical, thermal or chemical stimulus, trigger action potentials in the primary afferent fibres resulting in the release of a variety of neurotransmitters and neuropeptides from their nerve terminals. These neurotransmitters and neuropeptides act upon dorsal horn neurones, via binding to postsynaptic receptors, to mediate the transmission of nociceptive information. Excitatory amino acids (EAAs) and several peptides have been implicated in synaptic transmission through primary afferents and many have been shown to co-exist within primary afferents and sensory neurones (Ju et al., 1987; Smith et al., 1993). The dorsal horn is an important centre for the processing of nociceptive input and thus the co-existence of EAAs and peptides may allow for the co-release of various transmitters from primary afferents at the same time, which in turn may act on a number of different postsynaptic receptors to either differentially or similarly modulate the threshold of the postsynaptic membrane of the dorsal horn neuron.

1.4.1 Glutamate

The excitatory amino acid, L-glutamate, is a neurotransmitter that elicits fast excitatory responses in the CNS and appears to be the main neurotransmitter released from primary afferents (Watkins and Evans, 1981). Electrical nerve stimulation causes glutamate release from terminals of both myelinated and unmyelinated axons, consistent with the idea that glutamate plays a role in the transmission of both noxious and non-noxious information

(Davies et al., 1979; Duggan and Johnston, 1970). Ionophoretic application of glutamate results in excitation of dorsal horn neurones (Curtis et al., 1959). Intrathecal administration of glutamate can result in behavioural hyperalgesia and spontaneous nociceptive behaviour (Aanonsen and Wilcox, 1986; Aanonsen and Wilcox, 1987). Glutamate has been found, using immunocytochemistry, in all types of somatosensory fibres (De Biasi and Rustioni, 1988), in DRG (Salt and Hill, 1983) and in dorsal roots (Duggan and Johnston, 1970). Glutamate has been identified as a key EAA neurotransmitter for primary afferent fibres transmitting mechanical, chemical and thermal stimuli (Gerber and Randic, 1989; King and Lopez-Garcia, 1993). This evidence indicates the importance of glutamate's role in the transmission of nociceptive information. Glutamate can mediate its actions through several receptor subtypes, which can be divided into two groups, firstly ionotropic glutamate receptors and secondly metabotropic G-protein linked glutamate receptors (mGluRs).

1.4.2 Ionotropic glutamate receptors

The ionotropic group of receptors are ligand-gated ion channels that can be divided into two groups as a result of their pharmacological response characteristics to various agonists; the two groups are the N-methyl-D-aspartate (NMDA) and the non-NMDA ionotropic glutamate receptors (Young and Fagg, 1990). The non-NMDA group of ionotropic glutamate receptors comprises the α-amino-3-hydroxy-5-isoxazole-4-propionic acid (AMPA) and kainate (KA) receptor subtypes.

Kainate receptors

KA receptors are composed of glutamate receptor subunits 5-7 (GluR5-7) and KA1-2 subunits, but their role in somatosensory processing has been difficult to study due to a lack of selective agonists and antagonists (Lerma et al., 2001), as available pharmacological agents mostly cross react with AMPA receptors. KA receptors (with a GluR5 subunit) have been found on small diameter primary afferent neurones (Sato et al., 1993) and in the superficial layers of the dorsal spinal cord (Hwang et al., 2001; Yung, 1998). Electrophysiological studies have shown KA receptors on intrinsic dorsal horn neurones (Li et al., 1999), that were a different type to those expressed on DRG neurones as most were insensitive to the GluR5-preferring agonist ATPA (Kerchner et al., 2001a; Kerchner et al.,

2001b). Electrophysiological investigations also showed KA receptors are selectively activated by stimulation of high threshold (not low threshold) primary afferents, suggesting the localisation of KA receptors to synapses receiving input from high threshold (nociceptive) primary afferents (Li et al., 1999). A recent study suggests that KA receptor-expressing nociceptive DRG neurones were approximately six times more likely to co-express a non-peptidergic marker, the $P2X_3$ purinergic receptor than a peptidergic marker (substance P), and a possible role for presynaptic KA receptors in nociceptive processing during neuropathic pain states has been proposed (Lucifora et al., 2006).

AMPA receptors

AMPA receptors are composed of various combinations of its four subunits, termed GluR1-4 (Wisden and Seeburg, 1993). AMPA receptors are thought to mediate the fast synaptic transmission as a result of glutamate release and their activation leads to depolarization of dorsal horn neurons (Gerber and Randic, 1989; Jahr and Jessell, 1985; Jessell et al., 1986). Blocking AMPA receptors can attenuate the activation of dorsal horn neurones by noxious and innocuous stimuli (Dougherty et al., 1992), indeed AMPA receptors are involved in the fast transmission of both noxious and innocuous stimuli (Procter et al., 1998; Stanfa and Dickenson, 1999). AMPA receptor subunits, in particular subunits GluR1 and GluR2, have been localized to the superficial spinal dorsal horn (Coggeshall and Carlton, 1997; Furuyama et al., 1993; Henley, 1993; Popratiloff et al., 1996; Tolle et al., 1993). A high proportion of GABA-positive neurones in the dorsal horn were also found to be positive for the expression of the GluR1 AMPA receptor subunit (Albuquerque et al., 1999; Kerr et al., 1998).

NMDA receptors

Due to the focus of this study on second messenger events downstream of the NMDA receptor, this receptor will be considered more extensively. The NMDA receptor is an ionotropic glutamate receptor that is permeable to calcium and sodium ions. The NMDA receptor, which has two principal subunits termed NR1 and NR2, is thought to form a tetramer with the NR1 subunit comprising the core functional unit and the NR2 subunit subtypes (A-D) determining the specific channel characteristics (Monyer et al., 1992). NMDA receptor subunits have been shown to be distributed throughout the brain and spinal

cord, particularly in the superficial dorsal horn (Furuyama et al., 1993; Greenamyre et al., 1984; Monaghan and Cotman, 1985). NMDA receptors are blocked in a voltage-dependent manner by magnesium ions, thus during transmission of acute pain, NMDA receptors are largely inactive (Nishiyama, 2000). However, following prolonged noxious stimulation, NMDA receptors may be activated as a result of the dorsal horn neurones being sufficiently depolarised to remove the magnesium block. The dorsal horn neuron may become depolarised by alternative glutamate (such as AMPA) receptor activation or the receptor itself may be phosphorylated via second messenger cascades triggered by activation of the non-NMDA and peptidergic receptors. Therefore activation of the NMDA receptor occurs following a reduction in the receptor's affinity for the magnesium ion, bought about either by the progressive depolarization of the neuron or via a conformational change following phosphorylation of the receptor itself. This illustrates the idea that glutamate produces a fast excitatory potential when acting at the AMPA receptor and a long synaptic potential when acting at the NMDA receptor site.

The NMDA receptor has been demonstrated to play a crucial role in activity-dependent excitability changes such as long term potentiation (LTP), which may be necessary for spatial learning and memory formation in the hippocampus (Collingridge et al., 1983; Morris et al., 1986). NMDA receptor-dependent LTP may be considered to share some similarities with events that occur during central sensitisation of the spinal cord in hyperalgesic pain states (Dougherty et al., 1992; Ji et al., 2003; Zhou et al., 1996). It must be noted that there are significant mechanistic differences between the two processes of LTP and central sensitisation. Central sensitisation is the facilitation of neuronal activity in response to heterosynaptic input that can be triggered by relatively low frequency (natural) input from more than one source, whereas LTP requires high frequency neuronal stimulation (Ji et al., 2003). Indeed the similarities between LTP and central sensitisation have been shown to be more complex, with evidence of different forms of plasticity in the spinal cord emerging, for example while an LTP-like event could be triggered using high frequency stimulation in spinal cord slices, it was not seen in the intact spinal cord (with the presence of segmental and descending modulation in place; Chiang et al., 1998; Ji et al., 2003; Sandkuhler, 2000; Sandkuhler and Liu, 1998).

Application of NMDA can alter the excitability of spinal neurones (Chaplan et al., 1997; Haley et al., 1990; Leem et al., 1996) and intrathecal administration of NMDA has been shown to result in thermal hyperalgesia in the rat (Kolhekar et al., 1994). NMDA receptor antagonists result in the inhibition of dorsal horn neuron responses induced by prolonged chemical nociception, joint inflammation or by repetitive C-fibre stimulation ('wind-up') (Davies and Lodge, 1987; Haley et al., 1990; Neugebauer et al., 1993). Pre and post-injury administration of an NMDA antagonist may result in the prevention or attenuation of thermal and mechanical hyperalgesia for a period of time after injury (Mao et al., 1992c; Mao et al., 1992b; Smith et al., 1994). Studies in humans have demonstrated the potential of the NMDA antagonist, ketamine in the treatment of various chronic pain conditions, however with significant side effects (Hocking and Cousins, 2003). The effect of glutamate binding to the NMDA receptor may be modulated by a regulatory glycine binding site (Kleckner and Dingledine, 1988) as mentioned above (see section 1.3.5). Glycine may be important in regulating a number of NMDA receptor-mediated responses and has been termed a co-agonist of the NMDA receptor. Blocking the glycine recognition site on the NMDA receptor (Gly_{NMDA} site) has been shown to inhibit NMDA-induced thermal hyperalgesia, by increasing the threshold to noxious radiant heat (Kolhekar et al., 1994). Antagonists to the Gly_{NMDA} site can decrease the enhanced responses of spinal neurones that occur as a result of repetitive C-fibre stimulation (Dickenson and Aydar, 1991) and can block a neurokinin (NK_1) receptor facilitation of the NMDA receptor (Heppenstall and Fleetwood-Walker, 1997). The evidence outlined here indicates that the activation of NMDA receptors appears to be central to the generation of prolonged states of nociception and of pain-related behaviours as a result of nerve injury.

1.4.3 Metabotropic glutamate receptors

The mGluRs are members of the super family of seven transmembrane domain G protein-coupled receptors. They are divided into three groups; Group I mGluRs which are coupled to $G_{q/11}$ proteins, and consist of mGluR1 and mGluR5. Group II mGluRs comprise mGluR2 and mGluR3, group III mGluRs consist of mGluR4, 6, 7 and 8; both of the latter groups are negatively coupled to adenylate cyclase via $G_{i/o}$ proteins (Abe et al., 1992; Aramori and

Nakanishi, 1992; De Blasi et al., 2001; Pin and Duvoisin, 1995). Group II mGluRs and group III mGluRs will not be further discussed here. Group I mGluRs are concentrated in the superficial dorsal horn of the spinal cord (Berthele et al., 1999; Jia et al., 1999) and activation of these receptors leads to activation of intracellular kinases such as protein kinase C (PKC), release of intracellular calcium and possibly increasing intracellular cyclic adenosine monophosphate (cAMP; Abe et al., 1992; Aramori and Nakanishi, 1992) all of which could contribute to regulating cell excitability. The use of an antagonist to mGluR1 resulted in a marked reduction in the electrophysiological response of dorsal horn neurones to a noxious (mustard oil) but not to an innocuous (brushing) stimulus (Young et al., 1997), and the ionophoretic application of another selective mGluR1 antagonist also reversed the sensitisation observed in dorsal horn neurones following a noxious stimuli (Young et al., 1995). Dorsal horn neurones were shown to have a normal response to innocuous stimuli and a significant reduction in their response to noxious stimuli following the removal of mGluR1 via antisense ablation (Young et al., 1998). Intrathecal administration of a specific mGluR5 antagonist caused reversal of mechanical hyperalgesia in chronic inflammation and of thermal hyperalgesia in neuropathic pain states (Dogrul et al., 2000; Walker et al., 2001). These investigations illustrate the important role played by group I mGluRs in mediating nociceptive transmission at the spinal cord level.

1.4.4 Neuropeptides

There are clearly numerous ways in which glutamate exerts its function as a neurotransmitter in the spinal cord. However, neuropeptides are often co-released with glutamate from peripheral afferent terminals and can lead to various synergistic effects on postsynaptic dorsal horn neurones. A range of neuropeptides are synthesised in DRG neurones and play an important role in nociceptive transmission. Indeed a key event that occurs following peripheral nerve injury is the characteristic phenotypic changes that occur in many primary afferent neurones, demonstrated by an altered expression of neuropeptides in their cell bodies in DRG (Hokfelt et al., 1994; Villar et al., 1991), in their terminals and relevant receptors within the dorsal spinal cord (Dickinson and Fleetwood-Walker, 1999). These long-lasting changes in the production and expression of neuropeptides are thought to contribute to the

altered sensory transmission observed in chronic pain states. Some of the main changes observed following peripheral nerve injury will be discussed here.

Tachykinins

The tachykinins are a family of neuropeptides characterised by a common carboxy-terminal sequence and consist of the peptides substance P (SP), neurokinin A (NKA), neurokinin B (NKB), neuropeptides K (NPK) and neuropeptide γ (NP γ). The two preprotachykinin genes responsible for this family are preprotachykinin I (PPT I) and preprotachykinin II (PPT II). Firstly PPT I has three variants α-, β-, and γ- PPT I of which α-PPT I encodes for SP only and both β- and γ- PPT I encode for SP and NKA mRNA expression, while NPK is derived from β-PPT I and γ- PPT I results in NP γ production (Krause et al., 1987; Nawa et al., 1984). The PPT II gene results in the production of NKB (Bonner et al., 1987). In situ hybridisation studies revealed PPT I to be expressed in lamina I and II while PPT II was found to be expressed within lamina III (Warden and Young, III, 1988). Looking specifically at each PPT I variant, α-PPT I mRNA expression accounted for approximately 0.5% of the total level of PPT I mRNA expression, with β-PPT I accounting for 22% and γ-PPT I 78% of overall PPT I expression in the CNS (Carter and Krause, 1990). There are three receptors through which tachykinins exert their effects, they are the NK_1, NK_2 and NK_3 neurokinin receptors for which SP, NKA and NKB are the preferential endogenous ligands respectively (Maggi et al., 1993; Regoli et al., 1987).

SP has been found to be expressed in small diameter primary afferent neurones, in small diameter DRG cells and in the superficial dorsal horn (and the ventral horn; Hokfelt et al., 1975; Hokfelt et al., 1977; Hokfelt et al., 1980; Hokfelt et al., 1993; Gibson et al., 1981;Ju et al., 1987). In DRG neurones, most SP-positive cells have been found to contain other substances, such as calcitonin gene-related peptide (CGRP), somatostatin (SOM) and glutamate (Battaglia and Rustioni, 1988; Ju et al., 1987). When SP is released, it mediates its effects via the NK_1 receptor, which has been found to be expressed in the superficial layers of the spinal cord, with a lower concentration detected in laminae III – V (Brown et al., 1995; Helke et al., 1986; Naim et al., 1997; Nasstrom et al., 1992; Quirion et al., 1983; Yashpal et al., 1991). NKA has also been localised in the spinal cord and in small diameter primary

afferent neurones (Dalsgaard et al., 1985; Kanazawa et al., 1984; Ogawa et al., 1985). NKB has also been found in the spinal cord although it does not appear to be associated with cutaneous afferent fibre (Kanazawa et al., 1984). NKA is the preferential ligand for NK_2 receptors, which were found to be expressed in the dorsal horn of the spinal cord (Yashpal et al., 1990; Yashpal et al., 1991). The distribution of the NK_2 receptor was revealed to be distinct from that of the NK_1 and NK_3 receptors in the spinal cord, which appeared to be expressed in neuronal cell bodies and dendrites (Ding et al., 1996; Mantyh et al., 1996; Moussaoui et al., 1992; Zerari et al., 1995; Zerari et al., 1997), whereas a proportion of NK_2 receptor expression was found to be localised to astrocytes, perhaps designating astroglial cells as a major target for NKA (Zerari et al., 1998).

There is a large amount of evidence implicating the involvement of the tachykinins and their receptors in nociceptive processing in the dorsal horn of the spinal cord. Intrathecal injection of SP in naïve animals evokes scratching and biting behaviours that may be indicative of painful sensations and reduced tail-flick latency response to peripheral stimuli (Courteix et al., 1993; Hayes and Tyers, 1979; Hylden and Wilcox, 1981; Yashpal and Henry, 1984). Ionophoretic application of SP resulted in excitation of dorsal horn neurones (Henry, 1976; Zieglgansberger and Tulloch, 1979). However NK_1 receptor antagonists have not been shown to be greatly effective in reducing dorsal horn neuron responses to brief noxious stimuli (Fleetwood-Walker et al., 1990), and do not appear to be particularly efficacious as analgesic agents in clinical trials of chronic pain states (Hill, 2000). Interestingly noxious mechanical and thermal stimuli can specifically evoke SP release from primary afferents (Duggan et al., 1995; Duggan and Furmidge, 1994; Kuraishi et al., 1989). Ablation of SP-containing dorsal horn neurones resulted in the attenuation of behavioural responses only to highly noxious stimuli (Mantyh et al., 1997). The pre-emptive use of a NK_1 receptor antagonist has recently been shown to prevent the development of mechanical and cold allodynia following nerve injury (Cahill and Coderre, 2002). The mRNA of SP is significantly decreased in its expression following axotomy in small to medium diameter DRG neurons, with this reduction being most prominent ten to fourteen days after injury, and accompanied by a parallel reduction in dorsal spinal SP levels (Barbut et al., 1981; Jessell et al., 1979; Noguchi et al., 1993; Shehab and Atkinson, 1986). Such reduction in SP

production in DRG is also noted following CCI, with a decrease in SP levels in the ipsilateral spinal cord also observed (Cameron et al., 1991; Cameron et al., 1997; Kajander and Xu, 1995; Nahin et al., 1994). The reduction following CCI is not as great as that seen after axotomy, which may be due to the fact that CCI results in a partial denervation compared to axotomy. These findings of a reduction in SP may suggest a lesser role for SP in nociceptive processing in neuropathic pain states.

NKA, the preferential ligand for NK_2 receptors, is capable of producing spinal hyperexcitability (Henry and Salter, 1987; Hokfelt et al., 1994; Xu et al., 1991). Application of NKA can facilitate dorsal horn neuron responses to noxious thermal stimuli, suggesting an NKA involvement in the processing of inputs from thermal nociceptive afferents (Fleetwood-Walker et al., 1990). NKA has been shown to be released from primary sensory terminals in the dorsal horn as a result of peripheral noxious stimulation (Duggan et al., 1990). There is evidence that NKA but not SP is able to diffuse a considerable distance from its primary afferent site of release in the superficial dorsal horn following noxious stimulation in the periphery, which may be due to the greater metabolic stability of NKA (compared with that of SP; Duggan et al., 1988; Duggan et al., 1990; Hope et al., 1990; Regoli et al., 1994; Theodorsson-Norheim et al., 1987). This potential ability of NKA to diffuse may allow for this peptide to bind to the NK_2 receptors located on astroglial cells when released from primary afferents as a result of peripheral stimulation. Intrathecal administration of an NK_2 receptor agonist evoked a reduction in the reaction time in the tail-flick in naïve animals (Picard et al., 1993), while NK_2 receptor antagonists block both the increased dorsal horn neuron excitability (including the attenuation of thermal nociceptive responses) and behavioural sensitisation following nerve damage (Coudore-Civiale et al., 1998; Fleetwood-Walker et al., 1990; Yashpal et al., 1996). The expression of NKA following nerve injury has not been determined, although the preferential receptor for this ligand, the NK_2 receptor has been demonstrated to have an important role in nociceptive processing, thereby suggesting a role for NKA (Coudore-Civiale et al., 1998; Fleetwood-Walker et al., 1990; Fleetwood-Walker et al., 1993; Munro et al., 1993; Yashpal et al., 1996). These results indicate an important role for the tachykinins and their receptors in processing nociceptive inputs in the dorsal spinal cord.

Calcitonin gene related peptide [CGRP]

CGRP is found in approximately 30% of all primary afferent axons (Levine et al., 1993), mainly in unmyelinated C-fibres or small diameter myelinated Aδ-fibres that terminate in laminae I, II and V of the spinal cord (Carlton et al 1988). CGRP can be released into the superficial dorsal horn as a result of noxious thermal and mechanical stimulation of primary afferents (Morton and Hutchison, 1990). Subpopulations of CGRP-expressing DRG neurones also contain SP, SOM or galanin, indeed a high proportion (approximately 80%) of SP-expressing DRG neurones also contain CGRP (Battaglia and Rustioni, 1988; Ju et al., 1987; Smith et al., 1993; Villar et al., 1989). These two peptides are largely co-released and CGRP can potentiate the effects of SP (Mao et al., 1992a), possibly by inhibiting the degradation of SP (Le Greves et al., 1985; Mao et al., 1992a). Ionophoretic application of CGRP results in a slow-onset excitation of dorsal horn neurones that is long-lasting (Miletic and Tan, 1988). However the application of CGRP can also increase the effect of SP on dorsal horn neurones (Biella et al., 1991) and enhance the release of SP from spinal cord slices (Oku et al., 1987). Administration of a selective CGRP receptor antagonist can result in the reversal of mechanical hyperalgesia observed following cutaneous capsaicin injection (Sun et al., 2003). Following axotomy, the expression of CGRP mRNA was markedly reduced in primary sensory neurones, with maximal reduction observed seven to fourteen days after injury (Noguchi et al., 1989; Noguchi et al., 1990; Noguchi et al., 1993; Shehab and Atkinson, 1986). A reduction in the expression levels of CGRP was also found in the superficial dorsal horn (Carlton and Coggeshall, 1996). Similar reductions were also noted following CCI, which resulted in an approximately 50% decrease in CGRP mRNA levels in DRG within seven to fourteen days after nerve injury (Nahin et al., 1994). However spinal levels of CGRP expression were not found to decrease until approximately sixty days post CCI injury (Kajander and Xu, 1995).

Somatostatin [SOM]

Expression of SOM is seen in a population of small diameter primary afferents, different to those that are SP-positive (Hokfelt et al., 1976; Nagy and Hunt, 1982), and in lamina II cells of the dorsal horn (Finley et al., 1981; Hokfelt et al., 1976; Yin, 1995). SOM expression has been found to be localised to lumbar DRG neurones that are IB_4-positive neurones and

express the GDNF receptor (Kashiba et al., 2001). The application of GDNF to the spinal dorsal horn promotes an activity-induced release of SOM from the central terminals of sensory neurones (Lever and Malcangio, 2002). However the role of SOM in nociceptive processing is unclear as electrophysiological studies report both inhibitory and excitatory actions on dorsal horn neurones (Macdonald and Nowak, 1981; Murase et al., 1982; Randic and Miletic, 1978; Salt et al., 1982). Intrathecal administration of SOM has been reported to increase dorsal horn neuron responses to mechanical and thermal stimuli (Wiesenfeld-Hallin, 1985). In contrast, intrathecal and epidural administration of SOM in humans results in analgesia (Carlton et al., 2001). It has been proposed that SOM may modulate the effect of other neurotransmitters (Macdonald and Nowak, 1981) perhaps acting in a pro-nociceptive or analgesic manner depending on the circumstances, thus possibly explaining the discrepancies noted in the above electrophysiological studies. SOM while normally present in about 20% of small to medium diameter DRG (Ju et al., 1987; Smith et al., 1993), has been found to be markedly decreased following nerve damage and a corresponding reduction in SOM levels is seen in the superficial dorsal horn (Shehab and Atkinson, 1986; Villar et al., 1989; Zhang et al., 1993b).

Cholecystokinin [CCK]

CCK is expressed in small DRG neurones, peripheral nerves and the superficial dorsal horn of the spinal cord (Fuji et al., 1983), with expression seen in low levels in naïve animals (Ju et al., 1987; Noguchi et al., 1993). Although CCK has an excitatory role within the CNS, due to the low concentration found in the naïve state it may be predicted that its role will only become important following injury when its levels are markedly up-regulated (Hokfelt et al., 1994; Noguchi et al., 1989), with the expression of CCK mRNA increasing in primary afferent neurones following nerve injury (Villar et al., 1989). While the exact role of CCK in neuropathic pain states is not clear, it does appear to decrease the analgesic effect of both morphine and β-endorphin (Faris et al., 1983). The upregulation of CCK following nerve injury may have a role in explaining the decreased effectiveness of opioid treatment observed in many neuropathic patients.

Galanin

Galanin is a peptide with a low level of expression in small to medium diameter DRG neurones that co-exists with various neurotransmitters such as CGRP and SP (Baranowski et al., 1994; Ju et al., 1987; Ma and Bisby, 1997; Zhang et al., 1993a). Galanin can be found concentrated in laminae I-III and to a lesser extent in laminae IV-V of the spinal cord (Kar and Quirion, 1995). Galanin may act as a neuromodulator, as intrathecal administration of galanin antagonises the excitatory effects of CGRP and SP when used as a pre-treatment (Wiesenfeld-Hallin et al., 1991b; Xu et al., 1990). Galanin also inhibits the analgesic effect of morphine on noxious thermal and mechanical stimuli in naïve animals (Wiesenfeld-Hallin et al., 1991a). Again as with SOM, galanin's main effects may occur following injury when levels are up-regulated, with peripheral nerve injury resulting in an increase in galanin mRNA expression in DRG cells in addition to an increase in expression in the ipsilateral dorsal horn (Ma and Bisby, 1997; Nahin et al., 1994; Romualdi et al., 1990; Zhang et al., 1995c). Furthermore the pattern of co-expression of galanin with other neuropeptides can also alter following nerve injury, with reduced levels of galanin co-expressing with CGRP and increased levels of galanin co-expressing with NPY and VIP (Nahin et al., 1994). Galanin's inhibitory role has been found to be more pronounced following nerve injury (Wiesenfeld-Hallin and Xu, 1996).

Neuropeptide Y [NPY]

NPY is not expressed by DRG neurones under normal conditions (Lundberg et al., 1983). Nonetheless there are many NPY-positive fibres present in the superficial dorsal horn, which originate both locally and from supraspinal descending tracts (Wakisaka et al., 1991), where NPY may co-exist with galanin or GABA (Laing et al., 1994; Zhang et al., 1993a; Zhang et al., 1993c). Intrathecally administered NPY appears to be excitatory at low doses, whereas high doses produce an inhibitory effect (Scherer et al., 1994; Ullstrom et al., 1999). Following nerve injury, administration of NPY antiserum enabled a reduction in the injury-induced tactile hypersensitivity but not thermal hyperalgesia (Ossipov et al., 2002). NPY may also have a modulatory role that occurs following an insult, as following nerve injury a marked upregulation in the levels of NPY is seen not only in large or medium diameter primary afferent neurons, but also in axons of laminae III-V of the spinal dorsal horn (Kar

and Quirion, 1992; Nahin et al., 1994; Zhang et al., 1994). NPY may play an inhibitory role within the CNS as systemic administration of NPY resulted in marked antinociceptive effects (Hua et al., 1991).

Vasoactive intestinal polypeptide [VIP] and pituitary adenylate cyclase-activating polypeptide [PACAP]

VIP and PACAP are widely expressed within the CNS (Yaksh et al., 1988). In normal conditions a low level of VIP expression is observed in DRG neurones, in the spinal cord (with a higher concentration in the superficial layers) and in spinal glial cells (Brenneman et al., 1990; Gibson et al., 1981; Kar and Quirion, 1995; Knyihar-Csillik et al., 1991). Similarly low levels of PACAP are expressed in the DRG and spinal cord of naïve animals (Dun et al., 1996; Moller et al., 1993; Nahin et al., 1994; Zhang et al., 1995a). VIP and PACAP share a high degree of sequence homology. As a result they can combine with the same receptor binding sites (Harmar and Lutz, 1994), to activate a family of three receptors, namely $VPAC_1$, $VPAC_2$ and PAC_1 receptors (Hosoya et al., 1993; Ishihara et al., 1992; Lutz et al., 1993). VIP activates both $VPAC_1$ and $VPAC_2$ receptors and to a lesser degree the PAC_1 receptor (Hashimoto et al., 1997; Ishihara et al., 1992), with the PAC_1 receptor displaying a higher affinity for PACAP than VIP (Hashimoto et al., 1993; Shivers et al., 1991). All three receptors comprise seven trans-membrane domains with intracellular loops that couple to signalling cascades involving G_s and/or G_q proteins, which when activated stimulate either adenylate cyclase or PLC second messenger pathways respectively (Ishihara et al., 1992; Lutz et al., 1993; Spengler et al., 1993). Expression of mRNA for $VPAC_1$, $VPAC_2$ and PAC_1 receptors is seen in the spinal cord, in particular the superficial dorsal horn (Arimura and Shioda, 1995; Ishihara et al., 1992; Lutz et al., 1993), with expression also found in astrocytes (Grimaldi and Cavallaro, 1999; Jaworski, 2000; Joo et al., 2004).

Following injury, the levels of PACAP in DRG increase in the early stage returning to basal levels seven to fourteen days following injury (Hokfelt et al., 1994; Zhang et al., 1995b). Axotomy results in a major increase in PACAP mRNA in around 75% of DRG cells with a maximal increase observed by day three that begins to decline by day ten following injury (Zhang et al., 1995a). PACAP's role is not entirely clear as it may have inhibitory or

excitatory properties, as intrathecal administration of PACAP-38 (which activates both $VPAC_{1,2}$ and PAC_1 receptors) can reverse thermal hyperalgesia at low doses yet causes biting and scratching pain behaviours at higher doses (Narita et al., 1996). While administration of the other PACAP variant (PACAP-27) resulted in a long-lasting suppression of a C-fibre evoked reflex (Zhang et al., 1993c). Electrical stimulation of afferents at or above C/Aδ-fibre intensity has been demonstrated to produce an increase in VIP levels in the spinal cord, whereas low threshold fibre intensity stimulation did not have this effect (Yaksh et al., 1982). The expression of VIP is dramatically increased in DRG neurones following axotomy, and is often co-expressed with galanin (Nahin et al., 1994; Zhang et al., 1995b). The level of VIP in the spinal dorsal horn has been found to increase following nerve crush but returns to control levels when fibre regeneration occurs (Knyihar-Csillik et al., 1991; Knyihar-Csillik et al., 1993). VIP has an excitatory role and as such this peptide may take over the role of SP as the primary neuropeptide involved in the CNS in neuropathic pain states, that is, there may be a functional switch from SP to VIP in mediating some part of the C-fibre input. The rapid increase in PACAP expression suggests that it may be important in the early onset of neuropathic pain. VIP levels have been shown to gradually increase in the first weeks following injury but remain elevated for longer (Nahin et al., 1994; Zhang et al., 1995c) and so may have an important role in the maintenance of neuropathic pain states. Looking closer at the receptors for VIP, it has been shown that selective antagonists for $VPAC_1$, $VPAC_2$ and PAC_1 receptors had no effect on innocuous sensory transmission in nerve injured animals and the application of $VPAC_1$ and PAC_1 receptors agonists did not increase the neuronal response observed as a result of nerve injury (Dickinson et al., 1999). However, a $VPAC_2$ receptor agonist significantly amplified the response, and the expression of the receptor itself increased as a result of nerve injury (Dickinson et al., 1999). Indeed experiments blocking the $VPAC_2$ receptor resulted in suppression of the neuronal response to noxious input in naïve and nerve-injured animals (Dickinson et al., 1999). Moreover the expression of the receptors to VIP and PACAP found that following nerve injury only the expression of $VPAC_2$ receptor increases in the spinal cord, while the expression of the $VPAC_1$ receptor is decreased and PAC_1 receptor remains unaltered (Dickinson et al., 1999). These findings suggest that the $VPAC_2$ receptor is important in the processing of nociceptive information especially following nerve injury.

1.5 Neuropathic pain

Neuropathic pain is an intractable pervasive pain that does not serve to protect the individual and is often debilitating. The development of neuropathic pain may be a result of various factors such as damage to peripheral nerves, trauma to the spinal cord, as a consequence of specific infections such as the herpes zoster virus and the human immunodeficiency virus (HIV) or due to systemic nerve-injury disorders such as diabetes or rheumatoid arthritis (Hewitt et al., 1997; Mohamed and Carr, 1994; Scadding, 1984). Independent of its origin, neuropathic pain is characterised by a neuronal hyperexcitability in damaged areas of the nervous system. The associated symptoms of neuropathic pain include numbness, weakness, abnormal sensations and pain (Scadding, 1981). The pain experienced can be characterised into different types of pain sensation, namely stimulus-independent pain (spontaneous pain) or stimulus-evoked pain (hypersensitivity to a stimulus). Stimulus-evoked pain includes *hyperalgesia*, which is an exaggerated response to a noxious stimulus and *allodynia*, which is pain in response to normally innocuous stimuli. Neuropathic pain persists long after the initiating event resolves and is not effectively treated by classical analgesics. Understanding the mechanisms involved in neuropathic pain states requires the use of animal models of nerve injury that mimic as far as possible the clinical conditions in man.

1.5.1 Animal models of chronic pain

Progress in understanding some of the mechanisms that underlie the hyperalgesia and allodynia induced by nerve injury has involved the use of animal models of human pain conditions. Several models of chronic pain have been developed to replicate the pathophysiological changes present in man while ensuring the minimum of distress to the animal. A number of investigations into chronic pain states use animal models that rely on nerve injury involving the sciatic nerve for reasons of simplicity and reproducibility (Boucher and McMahon, 2001). Analysis of the pain experienced in animal models involves measuring the behavioural response to cutaneous stimuli, as the affective character of the pain can not be readily assessed. The behavioural responses measured generally involve spinal reflexes, specifically the nocifensive hindpaw flexor reflex; the magnitude of this reflex as a result of electrical or physiological stimuli has been shown to correlate to spinal

dorsal horn neuronal activity (Schouenborg and Sjolund, 1983). Alterations in the magnitude and latency of this nocifensive reflex can be measured using a number of behavioural tests that evaluate different sensory stimuli. Thermal hyperalgesia can be assessed using an apparatus developed by Hargreaves that measures the latency of hindpaw withdrawal from a calibrated heat source (Hargreaves et al., 1988; see section 3.4.4). Mechanical allodynia can be assessed using calibrated Semmes-Weinstein Von Frey filaments, which exert a fixed pressure before bending (see section 3.4.2). Cold allodynia can be measured by the animal's response to iced water (4°C; see section 3.4.3). In the animal models most frequently studied a mixture of intact and injured nerve fibres is created which allows for some correlation of changes that occur as a result of the nerve injury with pain-related behavioural responses. Behavioural tests as outlined above are performed to measure alterations in the behavioural response of the affected (ipsilateral) hindlimb.

The chronic constriction injury model [CCI]

This chronic constriction injury model developed by Bennett and Xie (Bennett and Xie, 1988) is a frequently used model that is produced by tying four loose chromic cat gut ligatures around the sciatic nerve at thigh level (see section 3.2.1). Animals guard the affected limb in a protective manner, which is thought to be an abnormal behaviour indicative of the presence of spontaneous pain. Neuropathic pain behaviours are observed within one week of nerve injury, with the affected hindlimb demonstrating hyperalgesic and allodynic behaviours. Indeed cold allodynia is a marked feature of this model. While these behavioural changes can be observed within three to four days of nerve injury they are most pronounced ten to fourteen days after nerve injury and can last for up to three months. Of note in this model is that the loose tying of the ligatures does not sever the nerve, the blood supply is maintained and many of the axons within the nerve remain viable. In this model some selective involvement of the sympathetic nervous system is seen, as surgical sympathectomy alleviates the increased response to thermal stimuli but has not been shown to affect responses to mechanical stimuli (Attal et al., 1990; Desmeules et al., 1995).

The partial nerve ligation model [PNL]

The partial nerve ligation model was developed by Seltzer and colleagues (Seltzer et al., 1990), uses a single tight ligation of one third to one half of the sciatic nerve. Following this injury, animals in addition to abnormal grooming (licking and biting) of the affected hindlimb also hold the affected hindlimb in a protective manner, which may indicate the presence of spontaneous pain. No signs of autotomy (where animals gnaw at the affected hindlimb) are observed in this model. As a result of PNL, animals show signs of hyperalgesia and mechanical allodynia within a few days of injury and can last for up to seven months and can lead to the development of bilateral ('mirror') sensitivity (Seltzer et al., 1990). However no signs of cold allodynia are observed in this model. An important contribution of the sympathetic nervous system in the development of PNL induced is noted, as chemical or surgical sympathectomy has been shown to reduce or prevent the development of such neuropathic pain sensitisation (Shir and Seltzer, 1991).

The spinal nerve ligation model [SNL]

Developed by Kim and Chung (Kim and Chung, 1992) the spinal nerve ligation involves the tight ligation of either the L5 or L5 and L6 spinal nerves from the common sciatic nerve just distal to the DRG. SNL injured animals show no signs of autotomy and develop abnormal grooming (licking and biting) behaviours which may indicate spontaneous pain presence (Na et al., 1993). Animals show signs of hyperalgesia and mechanical allodynia within the first few days of injury and can last for up to five months (Kim and Chung, 1992). In the SNL model no signs of cold allodynia are observed. In this model the sympathetic nervous system contributes significantly to the behavioural responses noted as surgical sympathectomy almost completely abolishes these behaviours (Choi et al., 1994; Kim et al., 1993). This model is especially useful for investigating the contribution of the sympathetic nervous system in the development of neuropathic pain.

The spared nerve injury model [SNI]

This model recently developed by Decosterd and Woolf (Decosterd and Woolf, 2000) is a variant of partial denervation involving a lesion (where the nerve is ligated and cut) of two of the three terminal branches of the sciatic nerve (tibial and common peroneal nerves) leaving

the remaining sural nerve intact. The SNI model results in a rapid (one day post injury) and a prolonged (up to six months) behavioural sensitisation in the skin area adjacent to the denervation, with behavioural signs of mechanical and cold allodynia observed. The extent to which the sympathetic nervous system contributes to the behavioural responses noted in this model has not yet been assessed through either chemical or surgical sympathectomy.

In addition to the models involving peripheral nerve injury outlined above, other models of neuropathic pain have been developed, including for example bone cancer, diabetic and viral neuropathy, which are beyond the scope of this study. The CCI model by Bennett and Xie (Bennett and Xie, 1988) was used in this investigation as it is displays many prominent signs of ongoing pain, has a small selective involvement of the sympathetic nervous system and has been widely studied (Kim et al., 1997b). In addition this model does not show bilateral sensitisation of behavioural responses, allowing comparison of the responses of the affected (ipsilateral) hindlimb to the contralateral hindlimb (in addition to control animals). It is of interest to look briefly at some of the potential causes of nerve injury in this model of neuropathic pain: The aetiology of nerve injury and subsequent development of behavioural sensitisation in the CCI model may be due to a number of factors. In this model the type of material used for the ligatures may be important. A study using either, chromic cat gut, plain gut or polyglactin (Vicryl) sutures, for ligatures in the CCI model resulted in a number of different outcomes (Kajander et al., 1996). The position of the affected hindpaw was altered dependent upon the type of ligature used, with a greater effect seen with chromic cat gut whereby animals held their affected paw in abnormal positions for longer (Kajander et al., 1996). The use of chromic cat gut decreased the expression levels of CGRP and SP in the spinal cord while the other ligatures did not affect their expression levels (Xu et al., 1996). Since all types of ligatures induced the behavioural changes associated with this model it is therefore thought that the physical constriction probably plays the most important part in the development of such abnormal behavioural responses (with a constituent of chromic gut having an additional influence). Indeed it has been suggested that provision of an acidic environment around the sciatic nerve for seven days can lead to the development of thermal hyperalgesia (Maves et al., 1995). Additional changes that may be important include alterations in local blood flow in the injured nerve, as decreased blood flow is found at the

site of nerve injury when thermal hyperalgesia is observed (Myers et al., 1993). The inflammatory response is also essential in the development of neuropathic pain states, illustrated by the finding that daily injections of dexamethasone (an anti-inflammatory glucocorticoid) decreased not only the inflammatory response induced by chromic gut ligatures but additionally decreased the guarding behaviour and thermal hyperalgesia observed in this model (Clatworthy et al., 1995).

While the focus of this study is the neuropathic pain state, where possible, models of inflammatory pain were utilised, to compare potential mechanistic differences between inflammatory and neuropathic chronic pain states. Unlike neuropathic pain, which is a formidable clinical problem, inflammatory pain responds to existing analgesics, for example NSAIDs (non-sterodial anti-inflammatory drugs) and opioids, for example loperamide (an mu opioid receptor agonist) has antinociceptive effects in inflammatory conditions (Kidd and Urban, 2001). An element of many chronic pain states is the release of inflammatory mediators which act on nociceptive transmission as outlined above, while most surgical models of peripheral nerve injury incorporate a component of local inflammation, specific models of chronic inflammation have been developed.

Formalin-induced model of inflammatory pain

The formalin model involves the subcutaneous injection of formalin into the hindpaw, which results in a response characterised as flinching, flicking and licking of the affected hind paw. The formalin test has been shown to elicit a biphasic nociceptive response (Dubuisson and Dennis, 1977). The biphasic response consists of an early intense response (first phase) produced by direct excitation of nociceptors at the site of injection (i.e. of peripheral origin). The more prolonged response (second phase), which typically follows a small quiescent interval is more complex involving both ongoing peripheral activity and central sensitisation in the spinal cord (Chaplan et al., 1997; Coderre et al., 1990; Coderre and Melzack, 1992; Dickenson and Sullivan, 1990; Haley et al., 1990; Villetti et al., 2003). This formalin-induced model of inflammatory pain has been useful in the pharmacological characterisation of pain since direct nociception and facilitated sensory processing can mainly be dissociated into these two phases of the test.

Models of persistent inflammatory pain

The use of irritant agents has been employed to develop models of persistent inflammation. Examples of the irritant agents that can be used include Complete Freund's Adjuvant (CFA), carrageenan, turpentine, acidic saline and capsaicin. This study uses CFA for subcutaneous injection into the hindpaw. The CFA model of persistent inflammation results in a striking increased sensitivity to innocuous mechanical stimuli (mechanical allodynia), in addition to thermal hyperalgesia. Animals display such signs of behavioural sensitisation from as early as a few hours after CFA injection, which can continue up to 2-3 days later, with recovery observed from 5 days onwards following CFA injection (Ji et al., 2002b; Molliver et al., 2005; Zhang et al., 2003a). However, unlike the formalin test, the CFA response cannot distinguish which stage of the response is due to direct peripheral activity and/or central sensitisation in the spinal cord.

1.6 Changes in the peripheral nervous system following nerve injury

1.6.1 Ectopic activity and remodelling of voltage-gated sodium channel expression

Many changes occur in the peripheral nervous system as a result of nerve injury. Increasing the excitability of the nociceptor terminal membrane (reducing the amount of depolarisation required to initiate an action potential) occurs when terminals are exposed to sensitising agents such as inflammatory mediators or neurotrophic factors released during tissue/nerve damage (Woolf and Salter, 2000). Voltage-gated sodium channels are mainly responsible for the rising phase of the action potential and are also important along with potassium channels in determining the excitability of the nerve (Woolf and Costigan, 1999). After nerve injury, sodium channels accumulate in the axon at the injury site and along its length, resulting in foci of hyperexcitability and ectopic action potential discharge in the axon and cell body of injured sensory neurones (Woolf and Mannion, 1999). Electrophysiological investigations revealed an abnormally high level of spontaneous activity following nerve injury in primary sensory neurones, which appeared to be mediated mainly by Aβ and Aδ fibres (Kajander et al., 1992; Kajander and Bennett, 1992; Laird and Bennett, 1993; Palecek et al., 1992). Spontaneous discharge from C-fibres contributes slightly later than that noted from A-fibres (approximately from day 10 versus day 1-3 respectively after nerve injury), which

corresponds to maximal behavioural sensitisation observed in the CCI model (Attal et al., 1990; Bennett and Xie, 1988; Xie and Xiao, 1990). In addition to firing spontaneously, ectopic pacemaker sites are often excited as a result of mechanical forces applied to them during movement that can result in spontaneous and movement-evoked pain (Devor and Seltzer, 1999). The exact site initiating this ectopic action potential discharge remains unclear; investigations in primary afferents have indicated that the spontaneous activity originates from the site of nerve injury (Xie and Xiao, 1990), while other reports show this ectopic discharge to originate from the DRG (Kajander et al., 1992; Zhang et al., 1997b). It is probable that both the nerve injury site and the DRG contribute to the ectopic firing of primary afferents (Tal and Eliav, 1996). This can probably result in not only transmission to the central nervous system (to trigger and maintain central sensitisation) but also to the peripheral terminals leading to further excitation of the peripheral axons (Kim et al., 1998; Xie et al., 1995).

Nerve injury can lead to an increased excitability of terminal membranes, which can be brought about by the remodelling of expression and location of voltage-gated sodium (Na^+) and potassium (K^+) ion channels in neuronal membranes. As Na^+ channels are essential for the propagation of action potentials and following nerve injury Na^+ channels accumulate at the injury site and along the axon, turning these sites into areas of hyperexcitability, they will be briefly discussed (Devor and Seltzer, 1999; Matzner and Devor, 1994; Omana-Zapata et al., 1997; Woolf and Mannion, 1999). Alterations in the expression of Na^+ channels are observed in DRG neurones as a result of various disease states, including chronic pain (Waxman et al., 1999b). Normally DRG neurones express a number of Na^+ channel transcripts (Waxman et al., 1999b) that can be distinguished by their sensitivity to tetrodotoxin (TTX) (Black and Waxman, 1996). For example some TTX-resistant Na^+ channels, such as SNS 1/Na_v1.8 (Akopian et al., 1996) and SNS 2/Na_v1.9 (Tate et al., 1998) have been shown to be specifically expressed in sensory neurones, thereby suggesting a possible involvement in pain states (Akopian et al., 1996). Specifically, SNS 1/Na_v1.8 channels are expressed in approximately 50% of small diameter unmyelinated cells and in 20% of larger diameter myelinated cells of the DRG, while SNS 2/Na_v1.9 channels are only expressed in unmyelinated cells of the DRG (Amaya et al., 2000). These two TTX-resistant

Na^+ channels produce slowly inactivating currents and the decrease in expression noted following nerve injury may lead to a hyperpolarizing shift in resting potential allowing for a possible increase in the TTX-sensitive channels available for activation (Akopian et al., 1996; Decosterd et al., 2002; Dib-Hajj et al., 1999; Waxman et al., 1999a; Waxman et al., 2000). A SNS 1/Na_v1.8-null mutation results in a partial analgesia to noxious mechanical and thermal stimuli and delayed development of inflammatory induced thermal hyperalgesia in mice (Akopian et al., 1999). Animals with a null mutation of SNS 1/Na_v1.8 also show neuropathic induced behaviours but do not show action potential spontaneous activity, suggesting the involvement of this channel in the development of spontaneous activity in sensitised nociceptors (Kerr et al., 2001; Laird et al., 2002; Roza et al., 2003). A TTX-sensitive Na^+ channel of interest, the brain type III Na^+ channel/Na_v1.3 is normally found in DRG neurones only during early development but its expression is upregulated in sensory neurones following nerve injury (Black et al., 1999), which can lead to an enhancement of TTX-sensitive currents (to produce a rapidly repriming current), that could sustain frequent ectopic discharges (Cummins and Waxman, 1997; Waxman et al., 1999b). This suggests that DRG neurones expressing brain type III Na^+/Na_v1.3 channels may be able to sustain a greater frequency of firing which in turn may lead to hyperexcitability of the cell.

1.6.2 Ephaptic interaction of peripheral nerve fibres

In normal conditions, a single sensory neuron represents an independent signal conduction pathway. However following nerve injury, Schwann cells around myelinated fibres can degenerate (Gautron et al., 1990), which can compromise the normal insulation of the fibre. Nerve injury can result in cross-excitation in the peripheral nervous system (PNS), where a stable electrical (ephaptic) interaction forms between neighbouring injured and uninjured sensory axons (Seltzer and Devor, 1979; Tal and Eliav, 1996). Ephaptic interaction can occur in neuromas, regenerating nerve and at patches of demyelination (Rasminsky, 1978). This ephaptic interaction can occur between neighbouring fibres of different origins, for example Aδ-fibres may now be stimulated by the large Aβ-fibres, suggesting that pathways normally only activated via noxious stimulation may now be activated by non-noxious stimuli or movement in the periphery (Fried et al., 1993; Seltzer and Devor, 1979). This cross-

excitation may underlie changes in excitability of uninjured afferents that perhaps cannot be explained by alterations in ion channels alone.

1.6.3 Morphological changes in the sciatic nerve in the CCI model

The sciatic nerve originates from the spinal segments L4-L6 and comprises fibres of sensory, motor and sympathetic origin. At mid thigh level the nerve is composed of approximately 27,000 axons of which 48% are unmyelinated sensory axons and 23% are myelinated sensory axons (with a further 6% motor and 23% unmyelinated sympathetic axons; Schmalbruch, 1986). Following CCI there are striking morphological changes in the fibre composition of the sciatic nerve. There are two main stages involved in these changes (Coggeshall et al., 1993). Firstly an early degenerative phase occurs, which may be a result of the inflammation and swelling at the nerve injury site where the chromic cat gut ligatures were applied, leading to a slow strangulation of the axons. This swelling becomes maximal by three days and can last for up to twenty-eight days after CCI injury, by which time a neuroma is often evident (Coggeshall et al., 1993). Changes also occur in the sciatic nerve distal to the site of injury; by three days post injury a steady and extensive reduction in axon numbers of all types occurs. The main change is a profound loss of the large myelinated axons, the Aβ-fibres, with the smaller myelinated and unmyelinated fibres being relatively less affected. The few remaining large diameter Aβ-fibres were found to be in an advanced state of degeneration (Basbaum et al., 1991). It could be suggested that this great loss of the large myelinated fibres distal to the injury may lead to some loss of the central inhibitory input (normally exerted via these afferents). The morphology of the sciatic nerve proximal to the site of injury appears normal, with no evidence of degenerating fibres being observed (Basbaum et al., 1991; Coggeshall et al., 1993; Gautron et al., 1990).

The second stage of change observed is a regenerative phase that occurs from around four weeks onwards following CCI injury by which point the sutures have been reabsorbed (around fourteen days) and the neuroma and swelling are diminishing (Coggeshall et al., 1993). During this phase there is a gradual recovery of axonal numbers and an eventual recovery of normal sensation in the affected hindlimb (seen by a recovery of neuropathic pain behaviours; Guilbaud et al., 1993). The time course of the phases of morphological

changes in the injured nerve have been studied alongside the development of behavioural changes, revealing hyperalgesia to be maximal around ten to fourteen days after injury, corresponding to the time point for the degenerative phase (Attal et al., 1990; Basbaum et al., 1991; Bennett and Xie, 1988; Coggeshall et al., 1993; Gautron et al., 1990). The onset of allodynia also appears maximal around two weeks after injury, with progressive recovery noted from three to four weeks following injury (Guilbaud et al., 1993). It has been shown that at week two (post injury) there is a massive Wallerian degeneration of the large myelinated fibres and recovery is observed from three weeks onwards, coinciding with recovery of behavioural changes (Ramer et al., 1997). Nevertheless the largest fibres had not recovered by fifteen weeks after the injury, which does not correspond with the recovery of the behavioural changes seen around eight to ten weeks post injury (Guilbaud et al., 1993). This indicates that while the morphological changes observed is an important link to the development and maintenance of neuropathic behavioural sensitisation, additional factors must also be involved given the discrepancy between the time courses of change outlined above.

1.6.4 Sympathetic nervous system

A number of investigations have suggested a link between the sympathetic nervous system and the development of nerve injury-induced behavioural sensitisation. As outlined above (section 1.5.1) surgical or chemical sympathectomies have resulted in a reduction in the development of abnormal pain behaviours associated with a number of different animal models of neuropathy (Kim et al., 1997b; Kim et al., 1993; Kim and Chung, 1991; Shir and Seltzer, 1991). These findings suggest that the sympathetic nervous system may be involved to some extent in the development of neuropathic pain states. However this involvement is variable and may be dependent upon the site of nerve injury and distance of injury from the spinal cord in addition to the type of injury (Kim et al., 1997b), all of which may explain why the treatment of neuropathic pain involving the manipulation of sympathetic inputs has variable results (Loh and Nathan, 1978; Luo and Wiesenfeld-Hallin, 1995). Additionally, following nerve injury, sympathetic axons have been shown to sprout into the DRG from the injured nerve (Chung and Chung, 2001) in a manner that parallels the development of behavioural sensitisation (McLachlan et al., 1993; Ramer and Bisby, 1997). In axotomised

animals, noradrenergic axons were found to sprout into the DRG, where they form 'baskets' around the cell bodies of sensory neurones which provides a coupling pathway for sympathetic-sensory fibres within the DRG (McLachlan et al., 1993). In the CCI model, a slightly more rapid sprouting of sympathetic axons in DRG was noted (Ramer and Bisby, 1997). A direct coupling of sympathetic and somatosensory systems has been implicated from findings showing the ectopic discharge of injured axons can be altered by electrical stimulation of the sympathetic nervous system (Devor et al., 1994; Habler et al., 1987; Korenman and Devor, 1981). However this coupling in DRG may change over the time course of the nerve injury (Michaelis et al., 1996). These findings reveal the role played by the sympathetic nervous system in the neuropathic pain states and how this role may change during the course of the nerve injury, which may aid in the recovery of normal sensitisation.

1.6.5 Neuropeptides

Some of the characteristic alterations in the expression of neuropeptides in their cell bodies in DRG, in their terminals and relevant receptors within the dorsal spinal cord observed following peripheral nerve injury have been discussed above (Section 1.4.4).

1.6.6 Neurotrophic factors

Neurotrophins are a family of molecules that promote survival, growth and maintenance of populations of neurones and are essential for normal neuronal development. The classic neurotrophin family includes nerve growth factor (NGF), brain derived neurotrophic factor (BDNF), neurotrophin-3 (NT-3) and neurotrophin-4/5 (NT-4/5) (Thoenen, 1991). Neurotrophins have been found to play a role in the development of normal functional properties of sensory neurones, such as the ability to respond to peripheral stimuli (Carroll et al., 1998). These neurotrophins signal via binding to their relevant tyrosine kinase receptors which are the trkA (NGF), trkB (BDNF and NT-4/5) and trkC (NT-3) and the p75 receptor which is capable of binding all neurotrophins with low affinity (Mendell et al., 2001). A second family of neurotrophic factors is the glial cell line-derived neurotrophic factor (GDNF) family, which are also important for the normal functioning of sensory neurones and include GDNF, neurturin, artemin and persephin. These neurotrophins all signal through a tyrosine kinase receptor, ret (Boucher and McMahon, 2001). Peripheral nerve injury has been

shown to result in altered expression of the neurotrophins and their receptors in DRG neurones (Cameron et al., 1997; Nahin et al., 1994; Sebert and Shooter, 1993). The expression of SP in DRG neurones has been shown to depend on the availability of NGF (Lindsay and Harmar, 1989; Otten et al., 1980; Verge et al., 1995). While the expression of VIP in cultured DRG neurones appears to be independent of NGF's presence or absence (Mulderry and Lindsay, 1990), the expression of VIP *in vivo* following axotomy may be dependent on the reduced availability of NGF as a result of axotomy (Shadiack et al., 2001). Intrathecal administration of NGF can prevent axotomy-induced reductions in the levels of SP and CGRP (Fitzgerald et al., 1985). In the SNL model, NGF appears to increase after injury and application of anti-NGF antibodies to the spinal nerve adjacent to the site of spinal nerve ligation can prevent development of thermal hyperalgesia for up to six days following injury (Fukuoka et al., 2001). GDNF also plays a role, as demonstrated by the observation that continuous administration of GDNF during either PNL or SNL prevents the development of subsequent abnormal pain behaviours (Bennett et al., 2000). While the precise role of these neurotrophic factors in neuropathic pain states is under investigation, it is clear from some of the conflicting evidence shown here that a particular balance of neurotrophic factors may be needed for normal functioning of sensory neurones.

1.7 Changes in the central nervous system following nerve injury

Stimulus-evoked pain, such as mechanical hyperalgesia, is one of the most common manifestations of neuropathic pain and is the consequence of an increased central response to primary afferent input. Following nerve injury the changes in the periphery, such as the appearance of ectopic discharges, results in an altered input to the CNS that induces changes in the sensory processing mechanisms within the spinal dorsal horn. This gives rise to the phenomenon of *central sensitisation* resulting from the increased afferent input generated by injury and noxious stimuli. This increased excitability of nociceptive neurones in the dorsal horn leads to an exaggerated and extended response to subsequent sensory inputs (Ji and Woolf, 2001). As a result, stimuli that would normally be innocuous now result in the sensation of pain. Central sensitisation manifests in three ways: enlargement of the area in the periphery where sensory neurones are activated by a noxious stimulus (i.e. the peripheral

receptive field); increasing the response to a suprathreshold input; and prior subthreshold inputs reaching threshold to initiate action potential discharge.

1.7.1 A-fibre sprouting in the dorsal horn

Central terminals of A-fibres exist in all the laminae of the dorsal spinal cord apart from lamina II of the superficial dorsal horn, which receives input exclusively from C-fibres. After nerve injury, sprouting of Aβ-fibre central terminals into lamina II can occur (Lekan et al., 1996; Woolf et al., 1992). This sprouting of Aβ-fibres that normally transmit innocuous stimuli into an area involved in nociceptive processing may lead to misinterpretation of information, whereby innocuous stimuli is interpreted as noxious. Sprouting of Aβ-fibres was observed to be maximal at two weeks following nerve injury and persisted for over six months (Woolf et al., 1992). However it must be noted that doubts are emerging about these findings, as sprouting was assessed by an anterograde labeling technique that utilizes cholera toxin B subunit (CTb) as a selective tracer for A-fibres (Tong et al., 1999). The selectivity of this tracer is in doubt, as recent studies have shown that CTb also labels unmyelinated C-fibre afferents in lamina II (Bao et al., 2002; Shehab et al., 2003). Another study using intra-axonal neurobiotin, as a label for sciatic A-fibres in both intact and axotomised nerves, revealed no fibres extending further dorsally than the ventral aspect of lamina II (Hughes et al., 2003). Nonetheless, despite the lack of concrete evidence for sprouting of A-fibres, it appears that Aβ-fibres have the ability to monosynaptically excite neurones in the superficial dorsal horn after nerve injury (Kohama et al., 2000). It has also been demonstrated that following sciatic nerve section (in a spinal cord slice preparation for electrophysiology) large myelinated A-fibres can establish synaptic contact with interneurones and newly transmit innocuous information to the substantia gelatinosa (Okamoto et al., 2001). This finding represents a functional reorganization of the spinal cord circuitry and may account in part for associated sensory abnormalities in neuropathic pain (Okamoto et al., 2001).

1.7.2 Inhibition and central sensitisation

Inhibitory mechanisms are active both locally within the dorsal horn and from descending pathways (Sotgui, 1993). Loss of this inhibitory input onto excitatory neurones may aid central sensitisation. However, evidence regarding the effects of CCI on the levels of

inhibitory transmitters is conflicting. A marked loss of GABA-positive cells in lamina I-III in the ipsilateral dorsal horn has been noted (Ibuki et al., 1997) and an increase in glycine and GABA levels within the spinal cord has also been observed following nerve injury (Satoh and Omote, 1996). Conversely, others have found that the proportion of cells in laminae I-III that are GABA and or glycine positive was unaltered as a result of nerve injury (Polgar et al., 2003). Another study revealed the return of GABA expression to pre-injury levels with recovery from CCI (Ibuki et al., 1997). It is possible that the inhibitory effects of GABA and glycine may be altered at different stages in the development of nerve injury induced sensitisation, which may explain why differences were found in the above studies. Altered activity in descending pathways may also play a role in central sensitisation, in particular the rostral ventromedial medulla (RVM) and the medullary nucleus raphe magnus (NRM) are key regions involved in descending modulatory projections to the spinal cord (Calejesan et al., 1998; Zhuo and Gebhart, 1990). Loss of specific RVM cells that project to the spinal cord to inhibit or facilitate transmission of noxious information both prevents and reverses development of experimental neuropathic pain behaviours (Porreca et al., 2001). Inactivation of RVM or spinal transection results in the suppression of mechanical allodynia following nerve injury (Bian et al., 1998; Kauppila et al., 1998; Sung et al., 1998).

1.7.3 NMDA receptor complex and central sensitisation

Central sensitisation is an immediate onset, activity-dependent increase in the excitability of nociceptive neurones in the spinal dorsal horn as a result of (and outlasting) an intense peripheral noxious stimulus, tissue injury or nerve damage (Baranauskas and Nistri, 1998; Ji et al., 2003; Woolf, 1996). Some of the factors leading to central sensitisation as discussed above include: presynaptic transmitter/peptide release (such as glutamate, SP, VIP) acting on various metabotropic and ionotropic receptors (such as NMDA, mGlu, AMPA, NK_1, $VPAC_2$ receptors) in the dorsal horn to result in increased intracellular calcium and trigger production of second messengers (Ji and Woolf, 2001; Woolf and Costigan, 1999; Woolf and Mannion, 1999). While clearly a number of receptors and subsequent signalling pathways are involved in central sensitisation, changes in NMDA receptor activation are consistently thought to be a crucial factor underlying central sensitisation (Chaplan et al., 1997; Dickenson and Sullivan, 1987; Woolf and Costigan, 1999). Indeed the NMDA receptor has

been shown to be involved in central sensitisation occurring as a result of inflammation of tissues or joints, from repetitive low frequency electrical stimulation of afferents ('wind-up'), from demyelination of afferents as well as peripheral nerve injury (Davies and Lodge, 1987; Gillespie et al., 2000; Haley et al., 1990; Mao et al., 1993; Neugebauer et al., 1993; Tal and Bennett, 1993; Wallace et al., 2003).

NMDA receptors as outlined above (section 1.4.2) are expressed in the superficial dorsal horn of the spinal cord, an area essential for processing of nociceptive information (Furuyama et al., 1993; Greenamyre et al., 1984). The NMDA receptor requires a combination of the NR1 subunit (the core functional unit) with at least one of the NR2 $_{(A-D)}$ subunits (Monyer et al., 1992; Mori and Mishina, 1995). The NMDA receptor is a bi-ligand gated receptor, activated by binding of glycine and glutamate (Laube et al., 1997; Moriyoshi et al., 1991). The NMDA receptor is usually blocked in a voltage-dependent manner by magnesium ions and is activated by the progressive depolarization of the neuron or by a reduction in the receptor's affinity for the magnesium ion when both binding sites of the receptor are ligand-bound. Studies have shown that many properties of the NMDA receptor, such as sensitivity to magnesium block, susceptibility to modulation by glycine, kinetic differences, phosphorylation, affinity for agonists and antagonists may be dependent upon the type of NR2 subunit found in the receptor's heteromeric complex (Cull-Candy et al., 2001; Yamakura and Shimoji, 1999). An example of such a subunit-dependent property of the NMDA receptor can be seen when assessing the channel conductance and sensitivity to magnesium block. NMDA receptors incorporating an NR2A or NR2B subunit generate high-conductance channel openings that have a high sensitivity to the magnesium block, whereas receptors containing an NR2C or NR2D subunit have low-conductance channel openings with a lower sensitivity to magnesium block (Ciabarra et al., 1995; Nishi et al., 2001; Sucher et al., 1995). NR1 receptor subunit protein levels have been found to be reduced in the superficial dorsal horn following CCI (Hama et al., 1995; Wilson et al., 2005), while the levels of NR2B increase in the superficial dorsal horn following nerve injury (Boyce et al., 1999a; Wilson et al., 2005), suggesting a possible role for this subunit in nociceptive processing.

NMDA receptor antagonists can attenuate behavioural sensitisation and can reduce neuronal responses to noxious stimuli and electrical stimulation of afferents (see section 1.4.2; (Davies and Lodge, 1987; Haley et al., 1990; Mao et al., 1992b; Mao et al., 1992c; Neugebauer et al., 1993; Smith et al., 1994; Dickenson and Aydar, 1991; Woolf and Thompson, 1991; Mao et al., 1993: Sotgiu and Biella, 2000). These findings illustrate the importance of NMDA receptor activation in the plastic changes underlying nociceptive processing and behavioural sensitisation as a result of nerve injury. NMDA receptors are embedded in the postsynaptic density (PSD), a structure that is visible by electron microscopy as a thickening of the postsynaptic membrane, containing the NMDA receptor complex (Sheng and Kim, 2002). The signalling pathways acting downstream from NMDA receptors that are crucial to the development of the neuropathic pain state are under investigation. One challenge in understanding these pathways is the composition of NMDA receptor complexes, which in overview represent multi-protein complex of receptors, adhesion and associated adaptor proteins in addition to signalling enzymes, all of which are currently believed to total around 185 proteins (Grant et al., 2005). Different varieties of complex may well occur in different situations. The proteins that can interact with the NMDA receptor have numerous functions, such as adapter, scaffolding, cytoskeletal or signalling functions (Husi et al., 2000). Of all the various proteins interacting with the NMDA receptor, one of the multivalent adapter proteins was noteworthy, because of its prominent presence in central synapses, namely postsynaptic density 95kDa protein (PSD-95). PSD-95 interacts with the cytoplasmic carboxy (C)–terminal tail of NR2 subunits of the NMDA receptor (Kornau et al., 1995; Niethammer et al., 1996).

Membrane associated guanylate kinases (MAGUK)

PSD-95 belongs to the membrane associated guanylate kinases (MAGUK) family of multivalent adapter proteins (Sheng, 1996). In mammals, the MAGUK family of proteins comprises of PSD-95 (also known as synapse-associated protein 90, SAP-90), synapse associated protein 97 (SAP-97), postsynaptic density 93 (PSD-93, also known as chapsyn 110) and synapse associated protein 102 (SAP-102) (Garner et al., 2000; Sheng and Kim, 1996). All four MAGUK proteins share approximately 70% sequence homology and contain multiple protein interaction domains, namely three N-terminal PDZ (PSD-Dlg-ZO-1

homology) domains, an SH3 (Src homology 3) domain and a GK (guanylate kinase-like) domain in their C-terminal region. It is the PDZ domains of the MAGUK proteins that have been found to bind to motifs within the C-terminal of NR2 subunits of the NMDA receptor (Garner et al., 2000; see Figure 1.3). This family of proteins can cluster ion channels on postsynaptic membranes at excitatory synapses and also interact with signalling molecules and the cytoskeleton (Sheng, 2001; Sheng and Kim, 2002). All the MAGUK proteins have been found in glutamatergic synapses but their expression in the spinal cord appear to have distinct patterns. Both PSD-95 and SAP-102 are mainly found in lamina I and outer lamina II of the superficial dorsal horn (Garry et al., 2003; Tao et al., 2000) and PSD-93 is expressed mostly in laminae I and II and outer lamina III (Tao et al., 2003b; Zhang et al., 2003). Localisation of these MAGUKs in the superficial dorsal horn of the spinal cord, the primary area for processing noxious information, encourages the idea of their potential role in nociceptive processing. On the other hand the expression of SAP-97 has not yet been localised to specific laminae of the spinal cord (Tao et al., 2001; Zhang et al., 2003a). The expression of either the mRNA or protein of all four MAGUKs was not reported in dorsal root ganglion (Tao et al., 2000; Tao et al., 2003b; Zhang et al., 2003a). The expression of PSD-95 and PSD-93 is of interest as their distribution overlaps with that of the NMDA receptor subunits, in particular NR2B, which is found in lamina I and II, whereas NR2A has a wider dorsal horn distribution (Boyce et al., 1999b; Dickenson and Aydar, 1991; Tao et al., 2000), suggesting that PSD-95 and PSD-93 could possibly associate with NMDA receptor complexes of different subunit composition.

Two of the MAGUK proteins, PSD-95 and PSD-93, have through genetic and antisense techniques been implicated in chronic pain states (Garry et al., 2003; Tao et al., 2003b; Tao et al., 2001; Tao et al., 2003a;Tao et al., 2000 Zhang et al., 2003a), the role SAP-102 or -97 may play has yet to be addressed and is beyond the scope of this study. PSD-93 plays a role in the mechanism of both chronic inflammatory and neuropathic pain. PSD-93 mutant mice and knockdown of spinal PSD-93 prevented the development of behavioural sensitisation observed following CFA injection and the SNL model of nerve injury (Tao et al., 2003b; Zhang et al., 2003a). Spinal knockdown of PSD-95 resulted in a reduction in both the development and maintenance of SNL nerve injury induced behavioural sensitisations (Tao

et al., 2001; Tao et al., 2003a). While investigations using PSD-95 mutant mice resulted in a complete absence of behavioural sensitisation to mechanical, thermal and cold stimuli following CCI nerve injury, normal responses to the formalin test were displayed (Garry et al., 2003). A closer inspection of the genetic mutations show that PSD-93 and PSD-95 mutant mice have different disruptions, that is different PDZ domains were targeted in each mutation. The PSD-93 mutant construct has a complete deletion of the second PDZ domain, whereas the PSD-95 construct, leaves the first two PDZ domains intact (McGee et al., 2001b; Migaud et al., 1998). This difference may explain why PSD-93 was implicated in both chronic inflammatory and neuropathic pain states whereas PSD-95 appeared to be involved in neuropathic pain states. Furthermore, the second PDZ domain (in addition to the first PDZ domain) can bind directly to the NMDA receptor, which might explain the differences noted between these two strains of mice. That is, the impaired cell surface expression of NR2A and NR2B subunits and impaired functioning of synaptic NMDA receptors in PSD-93 mutants may be a result of the site of mutation, which is not seen in the PSD-95 mutant mice. Migaud et al (Migaud et al., 1998) state that the expression and localisation of NR1, 2A and 2B is the same in wild type and PSD-95 mutant mice and NMDA receptor channel properties are unaffected by the mutation and the receptor is normally localised to synapses in the mutants. In the two mutants, the PSD-93 mutant has impaired expression of NMDA subunits whereas the PSD-95 mutant does not have such an impairment, while the surface localisation of PSD-95 itself was unaltered (as it is ~10fold less in 95 mutants), this might explain the differences seen in the prevention of behavioural sensitisation (Migaud et al., 1998; Tao et al., 2003b). In order to fully ascertain if these proteins have different roles in chronic pain states, equivalent mutant or knockdown animals would have to be assessed using identical models of chronic pain.

The interaction of PSD-95 with the NMDA receptor in the spinal dorsal horn has been revealed by our lab to be necessary for neuropathic reflex sensitisation (Garry et al., 2003). Given the larger number of proteins incorporated in the NMDA receptor complex and the fact that PSD-95 has multiple protein interaction domains, the list of potential binding partners of PSD-95 is vast, with more and more interactions being continually discovered. PSD-95, in addition to its involvement in anchoring and clustering the NMDA receptor at

synapses, can couple the NMDA receptor to signalling proteins to mediate downstream signalling. One of the potential binding partners is neuronal nitric oxide synthase (nNOS), which is a Ca^{2+}/calmodulin-regulated enzyme. The PDZ ligand motif of nNOS can bind to the second PDZ domain of PSD-95, and a ternary complex of NR2-PSD-95-nNOS has been identified in the spinal cord (Tao et al., 2000). However the role played by spinal nNOS in nociceptive signalling in chronic pain states is unclear. Treatment with nNOS inhibitor did not prevent the development of allodynia as a result of nerve injury, whereas a general NOS inhibitor did inhibit allodynia in nerve injured animals (Luo et al., 1999; Yoon et al., 1998). Another protein of interest in this complex is the Ca^{2+}/calmodulin-dependent kinase II (CaMKII), which can interact directly with NR2A and NR2B subunits of the NMDA receptor (Gardoni et al., 1999; Garry et al., 2003; Strack and Colbran, 1998). CaMKII does appear to play a role in nociceptive processing, CaMKII coimmunoprecipitation with NR2A and NR2B subunits is increased following nerve injury and use of CaMKII antagonists prevented development of behavioural sensitisation as a result of nerve injury (Garry et al., 2003). The disruption of CaMKII interaction with PSD-95 and the NMDA receptor is thought to be responsible for the lack of neuropathic pain in the PSD-95 mutant mice (Garry et al., 2003). CaMKII expression has also been found to increase in DRG cells as a result of the formalin model of inflammatory pain (Carlton, 2002) and to increase in the superficial dorsal horn and DRG cells following injection of capsaicin (Fang et al., 2002). These findings indicate that CaMKII may play a role downstream of the NMDA receptor-PSD-95 complex to bring about a sensitized state following nerve injury. In addition to its effect on the NMDA receptor, CaMKII can regulate other proteins, such as GluR1 subunits, leading to an enhancement of AMPA receptor currents and contributing to the translocation of GluR1 to synapses (Derkach et al., 1999; Hayashi et al., 2000).

SynGAP is another PDZ domain-interacting protein that has been demonstrated to be of importance in hippocampal plasticity (Kim et al., 2003; Komiyama et al., 2002). SynGAP is a Ras-GTPase activating protein, which is involved in regulation of the MAPK cascade, thus providing a potential functional link between the NMDA receptor and the MAPK pathway (O'Brien et al., 1998). However this protein has not been detected in the spinal cord by our lab and will not be discussed further (unpublished communication). Cysteine-rich interactor

of PDZ3 (CRIPT) has been identified to bind selectively to the third PDZ domain of PSD-95, CRIPT also binds directly to microtubulues thereby linking the mictotubule cytoskeleton to PSD-95, which may contribute to the synaptic clustering of PSD-95 (Passafaro et al., 1999). There are many other PDZ domain binding proteins that theoretically might interact with PSD-95, including for example, subunits of various ion channels and receptors other than the NMDA receptor, scaffolding, cytoskeletal and cell-adhesion proteins, which are beyond the scope of this study.

The two remaining interacting domains of PSD-95 are the GK and SH3 domains. The GK (guanylate kinase) domain does not have a conserved ATP binding site, therefore exhibits no enzymatic activity, but the domain can bind GMP in a relatively specific manner (Kistner et al., 1995). Kim and colleagues (Kim et al., 1997a) hypothesized that in the absence of enzymatic (catalytic) activity, the GK domain's primary function was as a protein binding site and using a yeast two hybrid screen, they cloned a novel binding partner, guanylate kinase-associated protein, GKAP (also called synapse-associated protein 90-associated protein, SAPAP). GKAP is believed to function as a scaffolding protein that anchors and links glutamate receptors and other PSD proteins to synaptic proteins (Romorini et al., 2004). Indeed, GKAP has been shown to bind to the SHANK family of proteins, which in turn, via binding to the mGluR-interacting protein Homer, results in a physical link between the NMDA receptor complex and metabotropic glutamate receptors (mGluR), thereby possibly connecting the NMDA receptor complex to downstream effectors in the mGluR signalling pathway (Takeuchi et al., 1997; Tu et al., 1999). Whether such a connection occurs in the spinal cord or if it is involved in the processing of nociceptive information remains to be determined.

The remaining domain of PSD-95 is the SH3 domain (see section 5.1), which has a binding specificity for proline-rich sequences containing a PXXP motif (Erpel et al., 1995; Lim and Richards, 1994; Mayer and Eck, 1995; Pawson and Scott, 1997). The majority of SH3 domains characterized to date recognize class I and/or class II peptides that share a core PXXP motif (Cohen et al., 1995; Mayer, 2001; Sparks et al., 1998). However, it must be noted that the SH3 domain of PSD-95 has an atypical structure (Borchert et al., 1994;

Guruprasad et al., 1995; Musacchio et al., 1992; Musacchio et al., 1994; Noble et al., 1993). A novel feature found in the SH3 domain of PSD-95 include the ability of the SH3 domain to interact with the GK domain at a site that does not involve the proline binding site of the SH3 domain, and it is thought that this intramolecular binding may be favoured over intermolecular binding (McGee and Bredt, 1999; Nix et al., 2000; Shin et al., 2000; Tavares et al., 2001). The SH3 and GK domains form an integrated structural unit, whereby four β strands (A-D) of the SH3 domain are followed by a large hinge region (separating β strands D and E) and the GK domain is inserted between β strands E and F (Shin et al., 2000; Tavares et al., 2001; see Figure 1.4). The recent development of mutant mice with a single point mutation of the SH3 domain of PSD-95, that targets the highly conserved tryptophan residue (tryptophan 470; see Figure 1.4) in SH3 domains, which is thought to be crucial for the interaction of SH3 domains with proline-rich ligands (Erpel et al., 1995) by Prof. Seth Grant and colleagues [Section 5.2] enables evaluation of the possible role of the SH3 domain of PSD-95 in the development and maintenance of neuropathic behavioural sensitisation. Binding partners of the SH3 domain include: Pyk 2, a non-receptor tyrosine kinase (Huang et al., 2001; Seabold et al., 2003), the KA2 subunit of kainate receptor (Garcia et al., 1998), Huntingtin protein (Sun et al., 2001), A-Kinase-anchoring Protein (AKAP) 79/150 (Colledge et al., 2000) and Mixed lineage kinases (MLK) 2 and 3 (Savinainen et al., 2001; see also Section 6.1). The focus of this study is the binding partner proline-rich tyrosine kinase 2, Pyk 2 (Huang et al., 2001; Seabold et al., 2003).

Figure 1.3

Schematic diagram of the NMDA receptor complex, in the postsynaptic density assembled by PSD-95

The PDZ domains of PSD-95, a member of the MAGUK (membrane-associated guanylate kinase) family of proteins, interact with the cytoplasmic carboxy (C-) terminal tail of the NMDA receptor NR2 subunits. The PDZ domains of PSD-95 can also interact with, for example, the PDZ domain of neuronal nitric oxide synthase (nNOS) and with Cysteine-rich interactor of PDZ3 (CRIPT). The Src homology region 3 (SH3) domain of PSD-95 can bind to the proline-rich tyrosine kinase 2, Pyk 2. The guanylate kinase (GK) domain can link the NMDA receptor complex to the metabotropic glutamate (mGlu) receptor via a scaffold assembled from guanylate kinase-associated protein (GKAP), Shank and Homer.

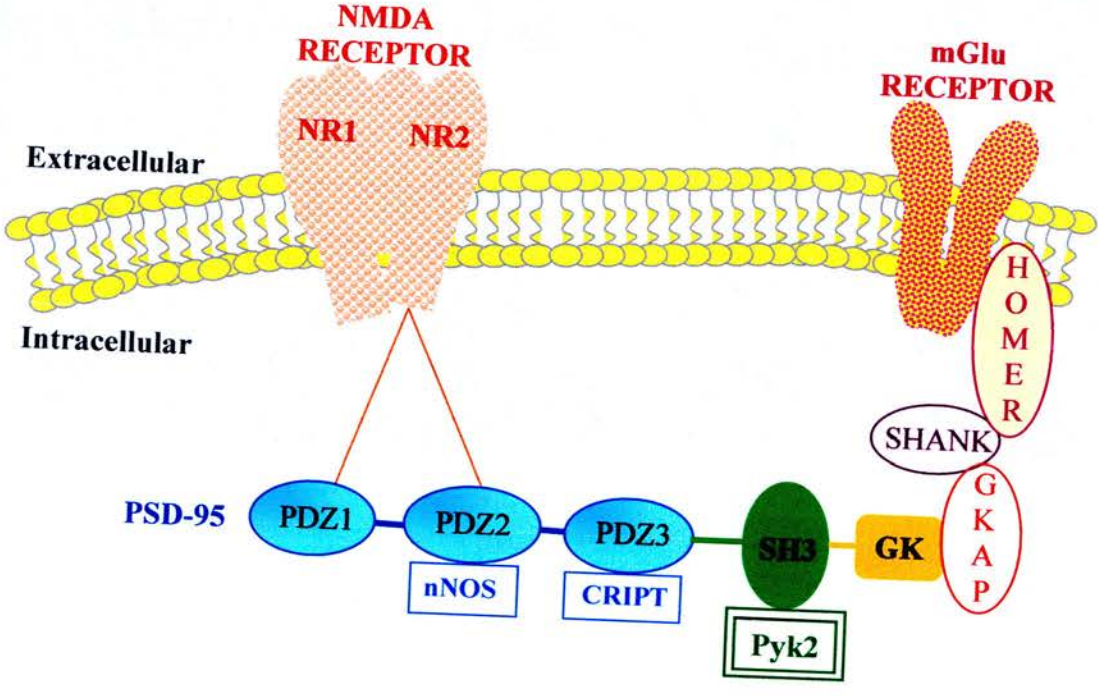
NMDA
RECEPTOR
NR1
NR2
mGlu
RECEPTOR
Extracellular
Intracellular
H
O
M
E
R
SHANK
G
K
A
P
PSD-95
PDZ1
PDZ2
PDZ3
SH3
GK
nNOS
CRIPT
Pyk2

Figure 1.4

Schematic diagram of the integrated structural unit formed by the SH3 and GK domains of PSD-95.

The integrated unit formed is comprised of four β strands (A-D) of the SH3 domain, followed by a large hinge region (separating β strands D and E) and the GK domain is inserted between β strands E and F (from McGee et al., 2001a). A point is marked to illustrate the single point targeted mutation of the SH3 domain of PSD-95 that resulted in the development of the PSD-95$^{SH3 50W470L}$ mutant mouse used in this study [Generated by Prof. Seth Grant's laboratory (Wellcome Trust Sanger Institute, Cambridgeshire, UK)].

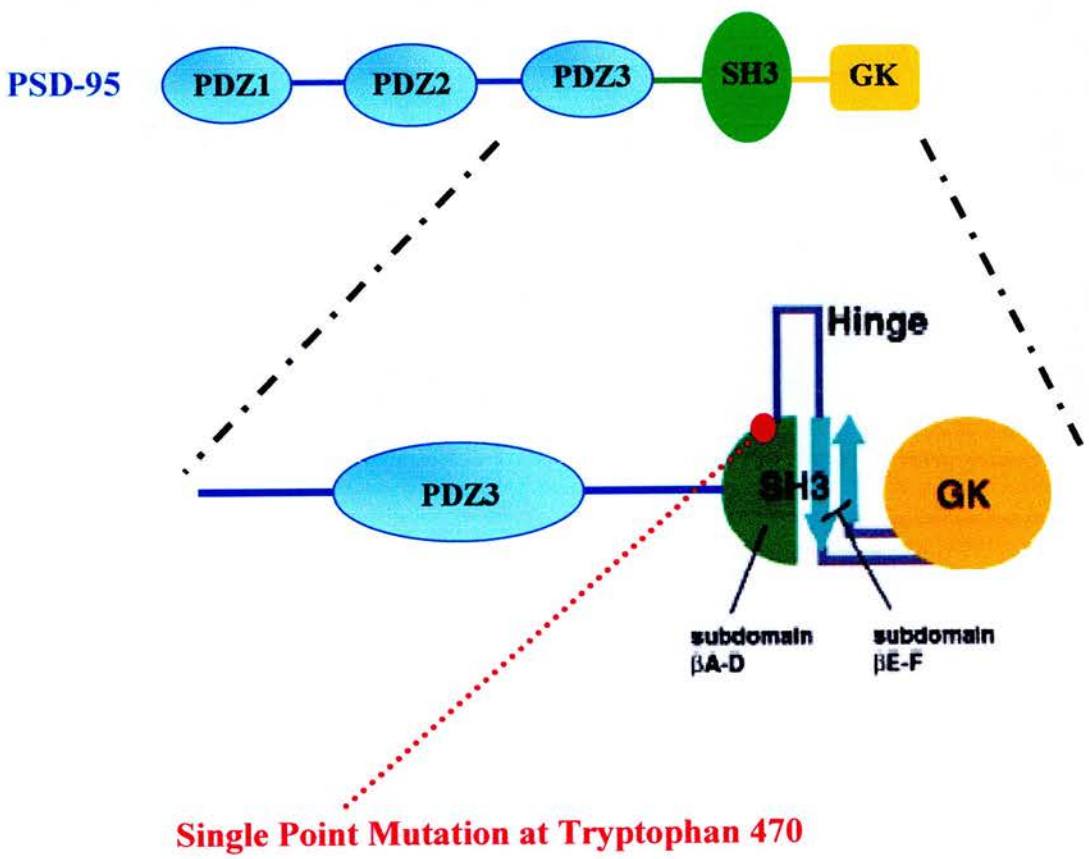
PSD-95
PDZ1
PDZ2
PDZ3
SH3
GK
Hinge
PDZ3
SH3
GK
subdomain
βA-D
subdomain
βE-F
Single Point Mutation at Tryptophan 470

Proline-rich tyrosine kinase 2 [Pyk 2]

Proline-rich tyrosine kinase 2 (Pyk 2) is a non-receptor protein tyrosine kinase which is intracellularly located and is classified based on its sequence similarity and distinct structural characteristics into the focal adhesion kinase family, a subfamily of the non-receptor protein tyrosine kinases (Hanks and Quinn, 1991). The focal adhesion family is composed of focal adhesion kinase (FAK) and Pyk 2 (Neet and Hunter, 1996). Pyk 2 is also known as cell adhesion kinase β (CAK-β), calcium-dependent tyrosine kinase (CADTK), related adhesion focal tyrosine kinase (RAFTK) and focal adhesion kinase 2 (FAK2) (Avraham et al., 1995; Herzog et al., 1996; Lev et al., 1995; Sasaki et al., 1995; Yu et al., 1996). Pyk 2 displays a high degree of sequence similarity with that of FAK (Lev et al., 1995; Sasaki et al., 1995). The structure of Pyk 2 comprises an N-terminus, a centrally located protein tyrosine kinase domain and two proline-rich regions at the C-terminus; these two proline rich motifs are sites for SH3 mediated protein-protein interactions (Avraham et al., 2000). While FAK is expressed in most tissues, Pyk 2 is predominantly expressed in the central nervous system and cells derived from hematopoietic lineages, whereas its alternatively spliced isoform (Pyk 2-H) is specifically expressed in T and B lymphocytes, monocytes, and natural killer cells (Avraham et al., 2000; Dikic et al., 1998; Lev et al., 1995).

Pyk 2 is phosphorylated in response to various external stimuli (such as depolarization, growth factor receptor activation) that increase the intracellular calcium concentration, as well as by protein kinase C (PKC) activation (Lev et al., 1995; Park et al., 2000). Pyk 2 is also activated for example by adhesion-mediated signalling in platelets and B cells (Astier et al., 1997; Tokiwa et al., 1996). It has also been shown that Pyk 2 (but not FAK) can be activated in response to stress signals (such as tumor necrosis factor-α, changes in osmolarity) and in such cases can trigger activation of the Jun N-terminal kinase (JNK) cascade (Tokiwa et al., 1996; Yu et al., 1996). Activation of Pyk 2 in response to an increase in intracellular free Ca^{2+} can be prevented by use of PKC inhibitors (Hiregowdara et al., 1997; Ohba et al., 1998; Raja et al., 1997; Siciliano et al., 1996; Soltoff et al., 1998), although the precise mechanism of PKC's involvement is not known. An increase in intracellular free Ca^{2+}, via receptor activation resulting in release of calcium from intracellular stores and an increase in calcium influx into the cell, can trigger activation of

calcium-dependent enzymes, such as protein kinase C (PKC) and calcium/calmodulin-dependent protein kinase II (CaMKII discussed above), calcium-dependent adenylate cyclase isoforms and tyrosine kinases (Bortolotto and Collingridge, 1998; Malmberg et al., 1997; Munro et al., 1994; Silva et al., 1992). These kinases may act to regulate membrane bound receptors and ion channels, such as the NMDA receptor. Indeed kinase activation by G protein-coupled metabotropic receptors is believed to lead to phosphorylation of the NMDA receptor resulting in a conformational change that diminishes the Mg^{2+} blockade (Bleakman et al., 1992; Bond and Lodge, 1995; Chen and Huang, 1992) and leads to increased NMDA receptor-mediated influx of Ca^{++} into the cell. Such calcium influx through the NMDA receptor may then activate the nitric oxide/cGMP/PKG pathways, and blockade of these pathways has been found to alleviate pain induced by formalin (Coderre and Yashpal, 1994) and peripheral nerve injury (Meller et al., 1992). Similarly, calcium-dependent camp generation would lead to the activation of protein kinase A (PKA), which has also been implicated in central sensitisation, as it is required for the second phase of formalin-induced inflammatory mechanical allodynia (Coderre and Yashpal, 1994).

Pyk 2 is a possible mediator of various extracellular signals that elevate intracellular Ca^{2+} concentration. Pyk 2 was recently shown to directly interact with PSD-95 in rat brain (independent of the presence of the NMDA receptor) and, through GST fusion protein constructs, it was shown that Pyk 2 bound specifically to the SH3 domain only and not to the GK domain (Huang et al., 2001; Seabold et al., 2003). Whether association of Pyk 2 with the SH3 domain binding of PSD-95 occurs in the spinal cord will be looked at in this study, as well as its possible activation in pain models. Whichever stimulus is involved, Pyk 2 is activated by autophosphorylation at Tyr402 (tyrosine402) and Tyr579/580 sites, this then enables Pyk 2 to bind to the SH2 domain of Src (another family of the non-receptor protein tyrosine kinases) (Dikic et al., 1996) leading to the activation of Src by relieving autoinhibition (Thomas and Brugge, 1997; Xu et al., 1997). Activation of Pyk 2, leading to the recruitment of Src, can also result in modulation of ion channel function and trigger a number of further signalling pathways, such as activation of the MAPK signalling cascade (Avraham et al., 1995; Lev et al., 1995). Pyk 2 can act with Src to link G protein-coupled receptors via Grb2 to the Ras/MAP kinase signalling pathway (Dikic et al., 1996; Girault et

al., 1999). Src itself has a number of important substrates which include the NMDA receptor (Wang and Salter, 1994; Zheng et al., 1998), $GABA_A$ receptors (Moss et al., 1995) and voltage-gated K^+ channels (Holmes et al., 1996; Huang et al., 1993). Pyk 2/Src-mediated regulation of NMDA receptors may play an important role in regulating synaptic plasticity (Huang et al., 2001). Pyk 2 has also been suggested to be important in pathological conditions such as ischaemia and convulsions (Liu et al., 2005; Tian et al., 2000). Pyk 2 activation may therefore play a significant part in the array of mechanisms for calcium-dependent signalling events (Lev et al., 1995), making Pyk 2 a candidate for the coupling of depolarisation and activation of various receptors (such as the NMDA receptor) to downstream signalling pathways, such as the MAP kinase pathway.

Mitogen-activated protein [MAP] kinase pathway

Long lasting changes in neuronal excitability occur through activation of transcription factors via signalling pathways, to result in the alteration of gene expression and protein synthesis in the DRG and spinal dorsal horn (Hokfelt et al., 1994; Ji and Woolf, 2001). Indeed the effect of nerve damage on gene expression has recently, through cDNA microarray techniques, demonstrated an alteration in the expression of numerous genes following injury, some of which are known to be involved in neurotransmission, signal transduction, myelination and transcriptional regulation (Rabert et al., 2004). A key signalling pathway involved in the activation of such transcription factors is the mitogen-activated protein (MAP) kinase cascade (Widmann et al., 1999). MAP kinases are serine/threonine protein kinases localized in the cytoplasm until activated by dual phosphorylation on both threonine and tyrosine residues when they can translocate towards the nucleus (Raingeaud et al., 1995; Seger and Krebs, 1995; Widmann et al., 1999). They are crucially involved in many important intracellular signalling pathways transmitting signals from the cell surface to the nucleus (Derkinderen et al., 1999). The better characterised members of the MAP kinase family are firstly the p42/44 MAP kinases, known also as extracellular signal regulated kinase (ERK) ERK1/2, secondly, the p38 MAP kinase and finally c-Jun N-terminal kinase (JNK) also known as stress-activated protein kinase (SAPK). JNK/SAPK originally identified by its response to cellular stressors, was found to be associated with the apoptotic pathway of cell death and has recently been investigated in persistent pain states. JNK MAP kinase activation

(in addition to ERK activation) has been reported in astrocytes of the spinal dorsal horn in the PNL model of neuropathic pain (Ma and Quirion, 2002). Peripheral axotomy has been shown to induce JNK/SAPK activation in DRG neurones (Kenney and Kocsis, 1998). JNK activation is also observed in injured DRG neurones following the SNL model of neuropathic pain (in addition to ERK and p38 activation) and use of a JNK inhibitor reversed the SNL-induced mechanical allodynia (Obata et al., 2004b). More recently it has been shown that SNL induced the activation of JNK in injured DRG neurones and in spinal cord astrocytes and SNL-induced mechanical allodynia was reversed by use of a JNK inhibitor (Zhuang et al., 2006).

While the p42/44 MAP kinases have been clearly implicated in neuronal plasticity states, such as long-term potentiation, learning and memory (Impey et al., 1999; Sweatt, 2001) they, along with p38 MAP kinase, are also involved in the plasticity underlying chronic pain states. Indeed p38 MAP kinase activation occurs in DRG neurones as a result of both peripheral inflammation and nerve injury (Ji et al., 2002b; Kim et al., 2002; Mizushima et al., 2005; Schafers et al., 2003), in addition to activation of p38 MAP kinase occurring in the spinal dorsal horn (Bessou et al., 1971; Brown and Iggo, 1967; Jin et al., 2003; Kim et al., 2002; Svensson et al., 2003). Indeed it has been shown that p38 MAP kinase inhibition results in the reduction of both inflammation and nerve injury induced behavioural sensitisation (Ji et al., 2002b; Jin et al., 2003; Schafers et al., 2003). The activation of p42/44 MAP kinase as a result of peripheral inflammation occurs in the spinal dorsal horn and use of p42/44 MAP kinase inhibitors prevents the development of inflammatory behavioural sensitisation (Galan et al., 2002; Ji et al., 1999; Ji et al., 2002a; Leem et al., 1993; Sammons et al., 2000). Recently, it has also been found that activation of p42/44 MAP kinase is localised to both dorsal spinal cord and DRG neurones as a result of peripheral nerve injury (Obata et al., 2004a; Obata et al., 2004b; Zhuang et al., 2005). Additionally p38 MAP kinase activation can be localised to microglia after peripheral inflammation and nerve injury (Jin et al., 2003; Kawasaki et al., 1997; Kim et al., 2002; Svensson et al., 2003; Tsuda et al., 2004) and p42/44 MAP kinase activation can be seen in astrocytes and microglia following nerve injury (Ma and Quirion, 2002; Zhuang et al., 2005). These findings clearly illustrate the important role the MAP kinase cascade plays in the neuropathic pain state; some of the receptors possibly

involved in their activation will be investigated in this study. In addition, it seems likely that not just neurons, but also glia may well play an important role in chronic sensitised pain states.

1.8 Spinal Glia

The central nervous system is comprised of neurones and glial cells. There are three types of glial cells in the CNS, termed astrocytes, microglia and oligodendrocytes. Traditionally glial cells were thought of as cells that provide support and protection for neuronal cells and became known as the 'supporting cells' of the nervous system. However, glial cells are now known to communicate bidirectionally with neurones, express multiple types of neurotransmitter receptors, play a role in transmitter uptake and release a number of bioactive substances, therefore they may play a more direct role in modulating neuronal transmission than previously believed (Millan, 1999). Indeed the activation of spinal cord glial cells, namely microglia and astrocytes, has recently been implicated in the pathogenesis of pain, ending the idea that pain hypersensitivity results solely from altered neuronal function (DeLeo and Yezierski, 2001; Meller et al., 1994; Watkins et al., 1997; Watkins et al., 2001b; Watkins et al., 2001a). Astrocytes and microglia can be activated by several substances, including excitatory amino acids (EAAs), prostaglandins and adenosine triphosphate (ATP); however these substances can also activate neurones (Bezzi et al., 1998; Hide et al., 2000; Takuma et al., 1996). Astrocyte activation is characterised by an increase in the production of filaments (involving proteins such as glial fibrillary acidic protein, GFAP) and also by an increased release of pro-inflammatory substances (Pekny, 2001). The activation of microglia results in numerous responses which include alterations in receptor expression, cell-surface markers and production of pro-inflammatory substances (Watkins and Maier, 2003). The first studies to implicate glial activation in neuropathic pain states showed that spinal glial cell activation was prevented by an NMDA receptor antagonist, which also prevented the behavioural sensitisation noted following peripheral nerve chronic constriction injury (Garrison et al., 1991; Garrison et al., 1994). These initial findings suggesting that glial activation aided the development of neuropathic behavioural sensitisation needed to be tested rigorously before glia could be considered as a possible therapeutic target. The use of two

pharmacological agents to disrupt glial function, namely fluorocitrate, which disrupts glial function and minocycline, which prevents the activation of microglia, blocked the development of both allodynia and hyperalgesia following various models of nerve injury (Ledeboer et al., 2005; Meller et al., 1994; Milligan et al., 2003; Raghavendra et al., 2003a; Watkins et al., 1997). The mechanisms of how glial activation can enhance neuronal transmission are not fully understood. It is believed that activated glia release substances that affect neurones either directly to increase excitation, or indirectly to induce the release of other transmitters to act on nociceptive neurones or cause upregulation of neuronal receptors. It is known that activated glia can release the pro-inflammatory cytokines, tumor necrosis factor-alpha (TNFα), interleukin-1 (IL-1) and interleukin-6 (IL-6), which have been shown to activate neurones as well as glia via binding to specific receptors on these cells (Sawada et al., 1989; Vitkovic et al., 2000). TNFα, IL-1 and IL-6 are grouped as pro-inflammatory cytokines not because of structural similarities but due to their co-ordinated responses to infection and injury (Watkins and Maier, 2003). Injection of pro-inflammatory cytokines around the spinal cord enhances dorsal horn neuronal responses to noxious stimuli (Onda et al., 2002; Reeve et al., 2000). Inhibiting these pro-inflammatory cytokines by intrathecal injection of antagonists resulted in the prevention or reversal of allodynia and hyperalgesia in models of both inflammation and nerve injury (Milligan et al., 2003; Sweitzer et al., 2001a; Watkins et al., 1997). Furthermore, thalidomide (a selective inhibitor of TNFα synthesis) and propentofylline (an inhibitor of glial function possibly via adenosine-independent or adenosine-dependent mechanisms; Sweitzer et al., 2001b) can also prevent behavioural sensitisation seen following peripheral nerve injury (George et al., 2000; Raghavendra et al., 2003b; Sommer et al., 1998; Sweitzer et al., 2001b). Release of pro-inflammatory cytokines results in the activation of intracellular pathways, one of which is the p38 MAP kinase cascade (see section 1.7.3; Clark et al., 2003; Watkins et al., 1999), where a reduction in nerve injury-induced p38 activation can be seen by blocking the pro-inflammatory cytokine, TNFα (Svensson et al., 2005). The anti-inflammatory cytokine, IL-10, which can suppress the production and actions of TNFα, IL-1 and IL-6, is under investigation for its potential use as an analgesic. Current research into glial cell involvement in chronic pain states is also trying to establish the role of astrocytes and microglia by using markers for activation of astrocytes (GFAP) and microglia (OX-42). This work, looking at the pattern of glial

activation following nerve injury, has led to the idea that early microglial activation may lead to astrocyte activation, which could then maintain the chronic pain state (Colburn et al., 1999; Hashizume et al., 2000; Raghavendra et al., 2003a; Winkelstein and DeLeo, 2002). The complex role played by glial cells in modulating nociceptive processing is still being investigated.

1.9 Aims

This study will examine some of the possible mechanisms involved in the development and maintenance of neuropathic pain. The sciatic chronic constriction injury (CCI) model (Bennett and Xie, 1988) will be used in this study and at times compared to the formalin-induced model of inflammation and the Complete Freund's Adjuvant model of persistent inflammation to look at possible mechanistic differences involved in neuropathic and inflammatory chronic pain states. It is clear from previous investigations that several receptor types are involved in the mechanisms of central sensitisation. Of all these receptors, the ionotropic glutamate NMDA receptor and the peptidergic NK_2 and $VPAC_2$ receptors, all of which have been crucially implicated in mediating nociceptive processing in neuropathic pain states, will be further investigated here. The involvement of these receptors in activating the MAP kinase signalling pathway and the involvement of the p42/44 and p38 MAP kinases in the development of neuropathic pain will be addressed. Given the importance of glial cells in neuropathic pain states, their potential participation in the activation of the p42/44 and p38 MAP kinases will also be examined. Following on from the work of Garry and colleagues (Garry et al., 2003) into the role of the NMDA receptor complex adapter protein, PSD-95 in neuropathic pain states, the potential association of this protein with a downstream signalling partner Pyk 2, in addition to the involvement of the SH3 domain of PSD-95 in the neuropathic pain state, will be examined. This study was designed to add to our current understanding of the intracellular mechanisms involved in neuropathic pain, thereby potentially aiding the development of novel therapeutic targets.

2. Materials

2.1 Animals

- Adult male Wistar rats (250-320g; Charles River, UK)
- Adult male and female MF1 mice either PSD-95^{SH3W470L} mutant or wild-type littermates (20-30g; Gift from Seth Grant, Wellcome Trust Sanger Institute, Cambridgeshire, UK).

2.2 Anaesthetics

- Halothane (Merial Animal Health Ltd., Essex, UK)
- Sodium pentobarbital (Sagatal; Rhone Merieux Ltd., Hertfordshire, UK)

2.3 Materials for animal models

- 4/0 Chromic cat gut sterilized surgical ligatures (SMI AG, Belgium)
- 5/0 Sterile surgical chromic cat gut ligatures (Medgut, South Africa)
- Hibitane (Zeneca Ltd., Cheshire, UK)
- 5.0 Coated vicryl absorbable suture with curved needle (Ethicon, Edinburgh, UK)
- 1ml microsyringe (Terumo, Belgium)
- 25-gauge needle (Terumo, Belgium)
- Micro fine 0.3ml Insulin syringe U100 with attached needle (BD Medical, Oxford, UK)
- Complete Freund's adjuvant (CFA; Sigma, UK)
- Formalin (36.5-38% formaldehyde; Sigma, UK)
- Saline, Sodium chloride solution 0.9% (Sigma, UK)
- All surgical instruments (Fine Science Tools, Germany)

2.4 Behavioural Somatosensory Reflex Testing Equipment

- Semmes-Weinstein von Frey filaments (Stoelting Co., Wood Dale, Illinois, USA)
- Hargreaves' thermal stimulator (Ugo Basile Model; Linton Instrumentation, UK)
- Clear Perspex box with raised aluminium floor for cold test (made on site)

2.5 Materials for intrathecal injections

- 25-gauge needle (Terumo, Belgium)
- 1ml microsyringe (Terumo, Belgium)
- Saline, Sodium chloride solution 0.9% (Sigma, UK)
- Dimethylformamide (DMF; Sigma, UK)

2.6 Drugs used for intrathecal administration and spinal cord incubation [Table 2.1]

- p38 MAP kinase inhibitor SB 203580 (Merck Biosciences, UK)
- p42/44 MAP kinase pathway inhibitor PD 098059, (Merck Biosciences, UK)
- p42/44 MAP kinase pathway inhibitor U 0126, (Merck Biosciences, UK)
- p42/44 MAP kinase pathway inhibitor less active analogue U 0124, (Merck Biosciences, UK)
- Glial inhibitor propentofylline (PPT; Sigma, UK)
- TNF-α receptor antagonist, WP9QY (Merck Biosciences, UK)
- $VPAC_2$ receptor antagonist, ([des(1-4), Arg^{16}]-Ro 25-1553; Gift from P. Robberecht, Free University of Brussels, Belgium)
- $VPAC_1$ receptor antagonist, ([Ac-His^1, D-Phe^2, Lys^{15}, Arg^{16}, Leu^{17}]-VIP(3-7)GRF(8-27) ; Gift from P. Robberecht, Free University of Brussels, Belgium)
- PAC_1 receptor antagonist, $PACAP_{6-38}$ (Bachem UK Ltd., UK)
- NK_1 receptor antagonist, RP 67580 (Gift from C Garret, Rhone-Poulenc Rorer, France)
- NK_2 receptor antagonist, SR 48968 (Gift from X. Emonds-Alt, Sanofi Recherche, France)
- NMDA receptor antagonist, (R)-CPP (3-((R)-2-carboxypiperazine-4-yl)-propyl-1-phosphonic acid; Tocris, Cookson Ltd., UK)
- NK_2 receptor agonist GR 64349 (Gift from P. Birch, Glaxo, Smith-Kline, UK)
- $VPAC_2$ receptor agonist, Ro 25-1553 (Gift from P. Robberecht, Free University of Brussels, Belgium)
- TNF-α synthesis inhibitor, Thalidomide (Sigma, UK)
- Saline, Sodium chloride solution (Sigma, UK)

2.7 Western Immunoblotting

- Hand-held mini-borosilicate glass homogenisers (Fisher Scientific, Ltd., UK)
- NuPage Novex pre-cast 4-12% Bis-Tris Gels, 1.0mm x12 well pH6.4 (Invitrogen Ltd., UK)
- NuPage XCell *Sure*Lock™ Minicell gel electrophoresis system (Invitrogen Ltd., UK)
- Immobilon-P^{sq}, polyvinylidene difluoride (PVDF) transfer membranes (Millipore, USA)
- See blue Plus 2 prestained protein standard (Invitrogen Ltd., UK)
- Polyoxyethylenesorbitan monolaurate (Tween-20, Sigma, UK)
- LumiGLO reagent (luminol chemiluminescent substrate) and peroxide (Cell Signaling, UK)
- High performance chemiluminesence film (Amersham, USA)
- Lammeli Lysis buffer (2% SDS, 50mM Tris-hydroxymethylaminoethane pH7.5, 5% β-mercaptoethanol)
- Coomassie brilliant blue R-250 protein stain (Pierce, Perbio Science Ltd., UK)
- Destaining reagent (10% (v/v) acetic acid, 30% (v/v) methanol)
- Protein transfer buffer (500mM Bicine, 500mM Bis-Tris, 20.5mM EDTA; pH7.2)
- NuPage MOPS (1M Tris Base, 1M MOPS, 20.5mM EDTA 69.3mM SDS; pH7.7) or MES (1M Tris Base, 1M MES, 20.5mM EDTA 69.3mM SDS; pH7.3) Running Buffers for electrophoresis (Invitrogen Ltd., UK)
- Blocking buffer, 5% (w/v) non-fat milk (Marvel) made up in PBS containing 0.1% Tween 20
- Albumin Bovine Serum Fraction V (BSA; Sigma, UK)
- Primary Antibody buffers, 5%, 3% (w/v) non-fat milk (Marvel) or 2% or 5% (w/v) bovine serum albumin (BSA; Sigma, UK) made up in PBS containing 0.1% Tween 20
- Secondary Antibody buffers, 5%, 3% (w/v) non-fat milk (Marvel) or 2% (w/v) BSA (Sigma, UK) made up in PBS containing 0.1% Tween 20

- Phosphate Buffered Solution (PBS; Di-Sodium hydrogen orthophosphate dihydrate (Fisher Scientific, UK); Sodium dihydrogen orthophosphate dihydrate (Fisher Scientific, UK); Sodium Chloride (Fisher Scientific, UK); made up in ultra high purity water, pH 7.4)
- PBS-Tween (PBS containing 0.1% (v/v) Tween 20)

2.8 Immunohistochemistry

- Agar (VWR International Ltd., UK)
- Freezing microtome: Leitz Kryomat 1700 (Leitz, Germany)
- Heparin (Sigma, UK)
- Paraformaldehyde (Sigma, UK)
- Perfusion pump (Watson-Marlow Ltd., UK)
- Sucrose (Sigma, UK)
- To-Pro-3 iodide, nuclear marker (Molecular Probes, UK)
- Normal goat serum (Vector Laboratories, USA)
- Fish skin gelatin (Sigma, UK)
- Triton X-100 (Sigma, UK)
- Vecta-Shield (Vector Laboratories, USA)
- Glass coverslips (22 x 50mm) (Merck-BDH, UK)
- Glass slides pre-coated with poly-L-lysine (VWR International, UK)
- Fluorescein Tyramide Reagent Kit (Perkin Elmer, USA)
- PBS as above

2.9 Primary Antibodies [see Table 2.2]

- Rabbit polyclonal anti-phospho-[Thr180/Tyr182]-p38 MAP kinase (Cell Signaling, UK)
- Rabbit polyclonal anti-p38 MAP kinase ('pan': phosphorylation state-independent; Cell Signaling, UK)
- Rabbit polyclonal anti-phospho-[Thr1202/Tyr204]-p42/44 MAP kinase (Cell Signaling, UK)

- Rabbit polyclonal anti-p42/44 MAP kinase ('pan': phosphorylation state-independent; 1: Cell Signaling, UK)
- Rabbit polyclonal anti-NR1 (Chemicon, UK)
- Rabbit polyclonal anti-NR2A (Upstate, UK)
- Rabbit polyclonal anti-NR2B (Chemicon, UK)
- Mouse monoclonal anti-PSD-95 (Transduction Labs, USA)
- Mouse monoclonal anti-PSD-95 (Upstate, UK)
- Rabbit polyclonal anti-SAP-97 (Abcam, UK)
- Rabbit polyclonal anti-SAP-102 (Chemicon, UK)
- Rabbit polyclonal anti-PSD-93/Chapsyn 110 (Chemicon, UK)
- Rabbit polyclonal anti-phospho-(Tyr^{402})-Pyk 2 (Cell Signaling, UK)
- Rabbit polyclonal anti-Pyk 2 (Upstate, UK)
- Mouse monoclonal anti-glyceraldehyde-3-phosphate dehydrogenase (GAPDH; Chemicon, UK)

2.10 Secondary antibodies [see Table 2.2]

- Goat-anti-rabbit Alexa Fluor 568 (Molecular Probes, UK)
- Peroxidase-linked goat-anti-rabbit (Cell Signaling, UK)
- Peroxidase-linked goat-anti-mouse (Chemicon, UK)
- Peroxidase-linked goat-anti-rabbit (Chemicon, UK)

2.11 Analysis programs

- Leica TCSNT Confocal system (Leica Microsystems, Germany)
- Scion Image (Scion Image Beta 4.02 Win, Scion Corporation, USA)
- LCS-lite software Version 2051347a (Leica Microsystems, Germany)
- Adobe Photoshop Version 7.0 (Adobe Systems Inc., USA)
- SigmaStat for windows v2.03 (SPSS Inc., UK)
- Scan analysis software (Scion Image GelPro, Scion Corporation, USA)

Table 2.1

Drugs used for intrathecal administration and/or spinal cord incubation

The table presented provides a brief summary of all the drugs used in investigating the involvement of spinal $VPAC_2$ and NK_2 receptors and glially mediated events in the activation of both p38 and p42/44 MAP kinases in an experimental model of mononeuropathy (Results presented in Chapter 4). This table provides the name and source of all drugs in addition to the specific dose used for either intrathecal (IT) administration or for incubation on the spinal cord (Incubation) and general information on the action of each compound.

Drugs used for intrathecal (IT) and/or spinal cord incubation				
Name	**Source**	**Dose**		**Action**
		IT	**Incubation**	
SB 203580	Merck Biosciences, UK	5nmol	-	p38 MAP kinase inhibitor
PD 098059	Merck Biosciences, UK	2.5nmol	-	p42/44 MAP kinase pathway inhibitor
U 0126	Merck Biosciences, UK	1.5nmol	-	p42/44 MAP kinase pathway inhibitor
U 0124	Merck Biosciences, UK	1.5nmol	-	Less active analogue of U 0126
Propentofylline (PPT)	Sigma, UK	0.5μmol	10 mM	Glial inhibitor
WP9QY	Merck Biosciences, UK	25μg	0.5mg/ml	Antagonises TNF-α binding to TNF receptor 1
[des(1-4), Arg^{16}]-Ro 25-1553	Gift - P. Robberecht, Free University of Brussels, Belgium	0.1 nmol	2μM	Selective $VPAC_2$ receptor antagonist
[Ac-His^1, D-Phe^2, Lys^{15}, Arg^{16}, Leu^{17}]-VIP(3-7)GRF(8-27)	Gift - P. Robberecht, Free University of Brussels, Belgium	0.1 nmol	-	Selective $VPAC_1$ receptor antagonist
$PACAP_{6-38}$	Bachem UK Ltd., UK	0.1 nmol	-	Selective PAC_1 receptor antagonist
RP 67580	Gift - C. Garret, Rhone-Poulenc Rorer, France	5 nmol	-	Selective NK_1 receptor antagonist
SR 48968	Gift - X. Emonds-Alt, Sanofi Recherche, France	5 nmol	100μM	Selective NK_2 receptor antagonist
(R)-CPP	Tocris, Cookson Ltd., UK	-	10 μM	Selective NMDA receptor antagonist
GR 64349	Gift – P. Birch, Glaxo, Smith-Kline, UK	1.5 nmol	50μM	Selective NK_2 receptor agonist
Ro 25-1553	Gift - P. Robberecht, Free University of Brussels, Belgium	0.5 nmol	30μM	Selective $VPAC_2$ receptor agonist
Thalidomide	Sigma, UK	-	200μM	TNF-α synthesis inhibitor

Table 2.2

Antibodies used for western immunoblot and immunohistochemical investigations

The table presented provides a brief summary of all the antibodies used throughout this thesis (Results presented in Chapter 4, 5 and 6). This table shows the name, source and product number of all primary and secondary antibodies used for Western immunoblot (WB) and immunohistocehmical (IHC) investigations in addition to the dilution factor used and details the above information for the nuclear marker used in immunohistocehmical experiments.

Antibody	Source	Product Number	Dilution Factor	
			IHC	WB
Primary Antibodies				
Rabbit polyclonal anti-phospho-[Thr180/Tyr182]-p38 MAP kinase IgG	Cell Signaling, UK	9211	-	1:250
Rabbit polyclonal anti-p38 MAP kinase ('pan': phosphorylation state-independent) IgG	Cell Signaling, UK	9212	-	1:500
Rabbit polyclonal anti-phospho-[Thr1202/Tyr204]-p42/44 MAP kinase IgG	Cell Signaling, UK	9101	-	1:250
Rabbit polyclonal anti-p42/44 MAP kinase ('pan': phosphorylation state-independent) IgG	Cell Signaling, UK	9102	-	1:500
Rabbit polyclonal anti-NR1 IgG	Chemicon, UK	AB1516	-	1:100
Rabbit polyclonal anti-NR2A IgG	Upstate, UK	07-632	-	1:100
Rabbit polyclonal anti-NR2B IgG	Chemicon, UK	AB1557P	-	1:100
Mouse monoclonal anti-PSD-95 IgG	Transduction Labs, USA	610496	-	1:100
Mouse monoclonal anti-PSD-95 IgG	Upstate, UK	05-494	1:50	-
Rabbit polyclonal anti-SAP-97 IgG	Abcam, UK	AB3437	-	1:100
Rabbit polyclonal anti-SAP-102 IgG	Chemicon, UK	AB5170	-	1:100
Rabbit polyclonal anti-PSD-93/Chapsyn 110 IgG	Chemicon, UK	AB5168	-	1:100
Rabbit polyclonal anti-phospho-(Tyr 402)-Pyk 2 IgG	Cell Signaling, UK	3291	-	1:100
Rabbit polyclonal anti-Pyk 2 IgG	Upstate, UK	06-559	1:50	1:100
Mouse monoclonal anti-GAPDH IgG	Chemicon, UK	MAB374	-	1:750
Secondary Antibodies and Nuclear Marker				
Goat-anti-rabbit Alexa Fluor 568	Molecular Probes, UK	A11011	1:1000	-
Peroxidase-linked goat-anti-rabbit	Cell Signaling, UK	7074	-	1:2000
Peroxidase-linked goat-anti-mouse	Chemicon, UK	AP130P	1:200	1:10,000
Peroxidase-linked goat-anti-rabbit	Chemicon, UK	AP132P	-	1:5000
To-Pro-3 iodide [nuclear marker]	Molecular Probes, UK	T3605	1:1000	-

3. Methods

All experiments were carried out in accordance with the U.K. Animals (Scientific Procedures) Act 1986. The use of animals in this thesis was necessary to explore the underlying mechanisms involved in the development of chronic pain states, which is crucial for the advancement of novel efficacious analgesics.

3.1 Animals

Studies were carried out using adult male Wistar rats (250-320g), which were housed in groups of three to five per cage. For studies using mice, adult male and female MF1 mice either PSD $95^{SH3W470L}$ mutant or wild-type littermates (20-30g) were housed in groups of two to six per cage. In all cases free access to water and food was provided and all cages were housed in a controlled environment of a 12-hour light/dark cycle and a temperature range of 22-24°C.

3.2. Surgical preparation of animal models

All surgical procedures were carried out under aseptic conditions.

3.2.1 The chronic constriction injury (CCI) model of experimental mononeuropathy

Adult male Wistar rats were anaesthetised with halothane and oxygen (oxygen flow rate of 2L/min), always ensuring that the pinch reflex of the front limb was abolished and assessing the respiratory rate before continuing with surgery. The right hind limb was shaved and the skin sterilised by wiping with Hibitane skin disinfectant (0.5% in 70% alcohol). A small (1cm) skin incision was made over the sciatic nerve at the mid-thigh level. The sciatic nerve was exposed by blunt dissection and approximately 1cm of the nerve was freed from surrounding tissues. Using an operating microscope (x40 objective lens), four chromic cat gut ligatures (4.0) were loosely tied, around the tibial and peroneal branches of the sciatic nerve leaving the smallest sural branch of the sciatic nerve intact, at approximately 1mm intervals.

For studies using mice, due to the greater susceptibility to inhalation anaesthetic adult mice were anaesthetised with sodium pentobarbital (Sagatal; 0.3ml 25% Sagatal in sterile saline (0.9%); intraperitoneal injection) and supplemented with halothane and oxygen (oxygen flow rate of 2L/min), no difference was noted in the post-surgical recovery time for either methods of anaesthesia, again the pinch reflex of the front limb was ensured to be abolished and the respiratory rate was assessed before continuing with surgery. The right hind limb was shaved and the skin sterilised by wiping with Hibitane skin disinfectant (0.5% in 70% alcohol). A small (0.5cm) skin incision was made over the sciatic nerve at the mid-thigh level. As with the rats, the sciatic nerve was exposed by blunt dissection and approximately 0.5cm of the nerve was freed from surrounding tissues and three chromic cat gut ligatures (5.0) were loosely tied around the tibial and peroneal branches of the sciatic nerve leaving the smallest sural branch of the sciatic nerve intact, at approximately 1mm intervals, viewed under an operating microscope (x40 objective lens).

In both cases the chromic cat gut ligatures were tightened to prevent slippage without blocking the circulation through the superficial epineurium. The overlying muscle and skin were closed with resorbable sutures (5.0 vicryl) using a continuous subcutaneous technique. The wound was re-sterilised with Hibitane to prevent any infection, and the animals were allowed to recover from surgery and anaesthesia before returning to their original cages. The animals were checked regularly and allowed five days (in the case of the rats) and three days (in the case of the mice) to recover before behavioural testing commenced.

3.2.2 Complete Freund's adjuvant model of experimental persistent inflammation

For studies using adult rats and mice, both were briefly anaesthetised with halothane and oxygen (oxygen flow rate of 2L/min). Complete Freund's adjuvant (CFA) was injected subcutaneously into the dorsum surface of the right hind paw, 80µl for the rats and 20µl for the mice. Control animals were injected with the same volume of saline (0.9%) in the same manner. The animals were checked regularly and allowed to recover before behavioural testing commenced 30 minutes after injection.

3.2.3 Formalin-induced model of inflammatory pain

For studies using adult rats and mice, both were briefly anaesthetised with halothane and oxygen (oxygen flow rate of 2L/min). Formalin was injected subcutaneously into the dorsum surface of the right hind paw, 70µl of a 5% solution in saline (0.9%) for the rats and 10µl of a 1.5% solution in saline (0.9%) for the mice. Control animals were injected with the same volume of saline (0.9%) in the same manner. Animals were allowed five minutes to recover from anaesthesia before responses to formalin were assessed.

3.3 Formalin-induced behavioural response

To assess the formalin-induced behavioural response, animals were placed in perspex cages on a glass table with mirrors in place to ensure the animals hind paws were clearly visible at all times. The response to formalin is characterised as flinching, flicking and licking of the affected hind paw. The formalin-induced response was measured as the number of flinches, flicking and licking per minute and counted every five minutes until recovery.

3.4 Behavioural Somatosensory Reflex Tests

The behavioural signs investigated represent three different components of neuropathic pain: mechanical allodynia, cold allodynia and thermal hyperalgesia. Behavioural testing was carried out prior to surgery to establish a baseline for comparison to post-surgical values, with values for the uninjured contralateral and injured ipsilateral paw measured from day five for the rats and day three for the mice following CCI surgery or from 30 minutes following CFA injection. Behavioural testing was carried out to assess the development and progression of these chronic pain states, animals that displayed injury-induced behavioural reflex sensitisation were used for further pharmacological or biochemical study, in order to explore the underlying mechanisms involved in the development of these chronic pain states, which is vital for the development of new effective analgesics.

3.4.1 General Observations

Inspections were made on a regular basis, to assess the animal's posture, gait and condition of the injured hind limb and normal behaviour (for example exploratory, feeding and grooming behaviours). If any animal displayed signs of autotomy, such as biting or gnawing of the injured paw or leg (rarely observed), this resulted in immediate euthanasia. All animals used in this study showed, normal behaviours, posture and gait.

3.4.2 Mechanical allodynia

To assess mechanical allodynia each animal was placed on a metal mesh floor allowing the experimenter to reach the plantar surface of the hind paw from beneath unobserved by the animal (Figure 3.1a). The paw withdrawal threshold (PWT) in response to normally innocuous mechanical stimuli was measured by presenting to the mid-plantar surface of the hindpaw calibrated Semmes-Weinstein Von Frey filaments, which exert a fixed bending force ranging from 318.19mN/mm^2 to 4830.62 mN/mm^2. Each filament was applied perpendicularly to the mid-plantar surface of the foot until it flexed. The filaments were applied in ascending order (starting from the weakest) with each application repeated 10 times at two second intervals. The response was characterized as a quick paw flick with or without shaking. Threshold was defined as the indentation pressure (mN/mm^2) required to elicit a response/paw withdrawal to at least 5 out of the 10 applications (i.e. to at least 50% of application). Each test was carried out three times alternatively on each paw with a minimum of five minutes between tests.

3.4.3 Cold allodynia

Cold allodynia was detected by the animal's response to iced water (4°C). Animals were placed in a perspex box on an aluminium floor (elevated by a wire-mesh stage) where the depth of the iced water was approximately 1cm above the aluminium floor to ensure that both the glabrous and hairy skin of the animal's hindpaw were submerged (Figure 3.1b). The animals were allowed 10 seconds to acclimatise then measurements of the Suspended Paw Elevation Time (SPET) were taken during a 20 second time period (Figure 3.1c), that is the number of seconds the animal raised its hind paw above the water during the test period. Each test was repeated three times with a minimum 10

minute interval between test periods to allow the animal's paws to return to body temperature before the next test.

3.4.4 Thermal Hyperalgesia

Animals were placed in perspex cages on a glass table and allowed to acclimatise to their environment. Thermal hyperalgesia was monitored using a Hargreaves' thermal apparatus, to determine the paw withdrawal latency (PWL) to a noxious heat stimulus (42°C). The Hargreaves' thermal apparatus consists of a moveable infra red heat source connected to a thermal detector and electronic timer (Figure 3.1d). The radiant heat source was placed under the mid-plantar surface of the animal's hind paw beneath the glass table and switched on, causing both the timer and heat source to activate, which are automatically cut off with the withdrawal of the animal's paw. This enables the PWL to be measured to the nearest 0.1 of a second and a standard cut-off limit of 20 seconds was employed to ensure there was no tissue damage when the animal did not respond. The withdrawal response was characterized as a brief paw flick. Testing was carried out five times alternatively on each paw with a minimum of five minutes between tests.

Figure 3.1

Apparatus used for assessment of behavioural somatosensory reflex tests

(A) Illustrates the calibrated Semmes-Weinstein Von Frey filaments, which exert a fixed bending force (mN/mm^2) and the elevated metal mesh floor used to assess the paw withdrawal threshold to mechanical stimuli. **(B)** Shows the perspex tank used for measurement of suspended paw elevation time in response to iced water (4°C; at a depth of approx. 1cm). **(C)** Showing an experimental animal (that has undergone a unilateral CCI of the sciatic nerve, Section 3.2.1) exhibiting an elevated paw in response to the iced water/cold stimulus. **(D)** Illustrates the Hargreaves' thermal apparatus used for the measurement of paw withdrawal latency to a noxious radiant heat source, showing the moveable infra red heat source connected to a thermal detector and electronic timer. [See Section 3.4 for information on behavioural somatosensory reflex tests illustrated]

A.

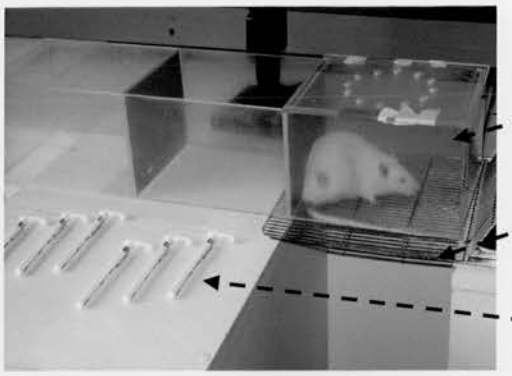
Perspex cage
Elevated mesh floor
Von Frey filaments

B.

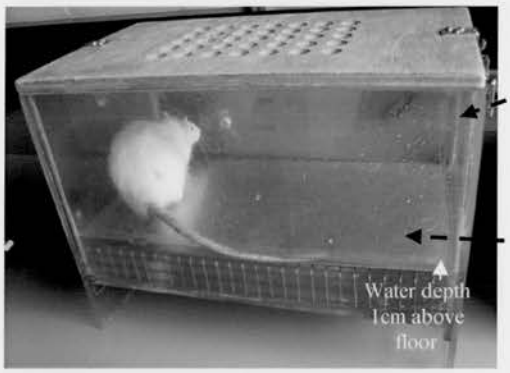
Perspex Tank
Aluminium floor with iced water (1cm depth; 4°C)
Water depth 1cm above floor

C.

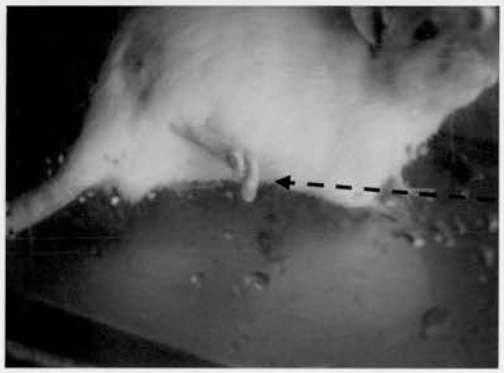
Paw elevated above iced water (4°C)

D.


Moveable infra red heat source (42°C)
Thermal detector and electronic timer

3.5 Intrathecal administration of drug

Naïve animals were used for intrathecal injections of agonists and combinations of agonist and antagonist/inhibitor. Animals that had undergone a unilateral chronic constriction injury of the sciatic nerve and were at the peak of neuropathic behavioural reflex sensitisation were used for intrathecal injections of antagonists/inhibitors. For all injections, baseline measurements for mechanical allodynia and thermal hyperalgesia were recorded prior to injection. All animals were briefly anaesthetised with halothane and oxygen (oxygen flow rate of 2L/min) and injected intrathecally at the L4/5 level of the spinal cord using a 25-gauge needle microsyringe with the pharmacological agent of interest at a volume of 50μl in sterile saline. Injections were performed blinded to the pharmacological agent used so as to eliminate bias. In each experimental group there was a minimum of six animals used, with no one animal used for more than three injections. If an animal was injected on more than one occasion, there was a minimum 48-hour interval between injections with pre-injection behavioural measurements taken to ensure there was no residual effect from the previous injection. To determine the effects of each drug on both mechanical allodynia and thermal hyperalgesia, quantitative sensory reflex testing (as outlined above Section 3.4.2 and 3.4.4) began 15 minutes following injection. This allowed for recovery from anaesthesia, testing continued every 5 minutes thereafter until recovery to pre-injection values.

Animals that had undergone chronic constriction injury and were at the peak of neuropathic behavioural reflex sensitisation were used for intrathecal administration of the following drugs:

- **The p38, p42/44 MAP kinase pathway inhibitors**

The p38 MAP kinase inhibitor SB 203580 was injected at a concentration of 5nmol in sterile saline (0.9%) with 0.3% dimethylformamide (DMF). The p42/44 MAP kinase pathway inhibitors PD 098059, U 0126 and its less active analogue U 0124 were injected at a concentration of 2.5nmol in sterile saline (0.9%) with 0.3% DMF, 1.5nmol in sterile saline (0.9%) with 0.1% DMF and 1.5nmol in sterile saline (0.9%) with 0.1% DMF respectively.

• **Glial inhibitor**

The glial inhibitor propentofylline (PPT) was injected at a concentration of 0.5μmol in sterile saline (0.9%).

• **TNF-α receptor antagonist**

The TNF-α receptor peptide antagonist WP9QY was injected at a concentration of 25μg in sterile saline (0.9%).

• **$VPAC_1$, $VPAC_2$ and PAC_1 receptor antagonists**

The selective $VPAC_1$ receptor antagonist, [Ac-His^1, D-Phe^2, Lys^{15}, Arg^{16}, Leu^{17}]-VIP(3-7)GRF(8-27), $VPAC_2$ receptor antagonist, [des(1-4), Arg^{16}]-Ro 25-1553 and PAC_1 receptor antagonist, $PACAP_{6-38}$ were all injected at a concentration of 0.1nmol in sterile saline (0.9%).

• **NK_1, and NK_2 receptor antagonists**

The selective NK_1 receptor antagonist, RP 67580, and NK_2 receptor antagonist, SR 48968 were both injected at a concentration of 5nmol in sterile saline (0.9%).

Naïve animals were used to assess the effect of intrathecal administration of the following drugs:

• **$VPAC_2$ receptor agonist**

The selective $VPAC_2$ receptor agonist, Ro 25-1553 was injected at a concentration of 0.5nmol in sterile saline (0.9%).

• **NK_2 receptor agonist**

The NK_2 receptor agonist GR 64349 was injected at a concentration of 1.5nmol in sterile saline (0.9%).

• **Combination of agonist and inhibitor**

The following drugs were combined and injected at the same concentration as outlined above. All combined drug injections were carried out in naïve animals. The $VPAC_2$ receptor agonist Ro 25-1553 was combined with the p38 MAP kinase inhibitor SB 203580. The NK_2 receptor agonist GR 64349 was combined with the p42/44 MAP kinase pathway inhibitor U 0126.

3.6 Western Immunoblotting

3.6.1 Tissue preparation

Animals were terminally anaesthetised under a halothane oxygen mix as outlined above (section 3.2.1) prior to and during dissection of all tissues, while under anaesthetic a laminectomy of the lumbar region was performed. The spinal cord from L3 -L6 was hemisected to separate ipsilateral and contralateral sides in experimental animals, with spinal cords from naïve animals taken intact (unhemisected). Spinal cord samples were rapidly removed and homogenized in Laemmli lysis buffer on ice in hand-held glass homogenisers to prepare whole lysates and denatured at 100°C for five minutes, allowed to cool and stored at -70°C.

3.6.2 Tissue preparation of spinal cord incubated with drug

Animals were terminally anaesthetised under a halothane oxygen mix as outlined above (section 3.2.1) prior to and during dissection of all tissues, while under anaesthetic a laminectomy of the lumbar region was performed. Animals were maintained on anaesthetic, while the spinal cord was incubated with sterile saline (500µl, 0.9%) or with the pharmacological agent of interest (500µl in sterile saline 0.9%) for 30minutes at room temperature. After which the spinal cord from L3 -L6 was hemisected to separate ipsilateral and contralateral sides in experimental animals or in naïve animals unhemisected spinal cords were prepared as outlined above (section 3.6.1).

Naïve spinal cords were incubated with the following: sterile saline (0.9%) as a control, $VPAC_2$ receptor agonist, Ro 25-1553 (30µM), the NK_2 receptor agonist, GR 64349 (50µM) or with a combination of the $VPAC_2$ receptor agonist Ro 25-1553 or the NK_2 receptor agonist GR 64349 and the glial inhibitor, propentofylline (PPT; 10mM). In nerve-injured animals (CCI model of experimental mononeuropathy see section 3.2.1; in animals that were at the peak of neuropathic behavioural reflex sensitisation), the spinal cords were incubated with the following: sterile saline (0.9%) as a control, the selective $VPAC_2$ receptor antagonist, [des(1-4), Arg^{16}]-Ro 25-1553 (2µM), the selective NMDA receptor antagonist, (R)-CPP (10µM), the selective NK_2 receptor antagonist, SR 48968

(100μM), or with the glial inhibitor, propentofylline (PPT; 10mM), the TNF-α receptor antagonist, WP9QY (0.5mg/ml) or with the TNF-α synthesis inhibitor, thalidomide (200μM).

3.6.3 Immunobloting procedure

Samples (as prepared above; Section 3.6.1) were separated by electrophoresis on pre-cast 4-12% Bis-Tris Gels using the NuPage XCell *Sure*Lock™ Minicell gel electrophoresis system, then transferred to polyvinylidene difluoride (PVDF) membranes. Prior to immunoblotting, membranes were temporarily stained with a prestained standard (Coomassie brilliant blue R-250 protein stain and destained with destaining reagent (10% (v/v) acetic acid, 30% (v/v) methanol) to ensure even protein loading and protein transfer. Membranes were blocked overnight at 4°C in 5% Marvel, containing 0.1% Tween 20 (unless otherwise stated). Blots were washed in phosphate buffered saline (PBS; pH7.4, containing 0.1% Tween 20), and incubated with antibodies diluted in primary antibody buffer containing 2% bovine serum albumin (BSA, in PBS containing 0.1% Tween 20) at room temperature for 90 minutes (unless otherwise stated). Antibodies were used at the following concentrations: rabbit polyclonal anti-phospho-[Thr180/Tyr182]-p38 MAP kinase (1:250, Cell Signalling) and rabbit polyclonal anti-p38 MAP kinase ('pan': phosphorylation state-independent; 1:500, Cell Signalling), rabbit polyclonal anti-phospho-[Thr1202/Tyr204]-p42/44 MAP kinase (1:250, Cell Signalling) and rabbit polyclonal anti-p42/44 MAP kinase ('pan': phosphorylation state-independent; 1:500, Cell Signalling), rabbit polyclonal anti-NR1 (Chemicon; 1:100; incubated overnight at 4°C), rabbit polyclonal anti-NR2A (Upstate; 1:100; incubated overnight at 4°C), rabbit polyclonal anti-NR2B (Chemicon; 1:100; incubated overnight at 4°C), mouse monoclonal anti-PSD-95 (Transduction Labs; 1:100), rabbit polyclonal anti-Sap 97 (Abcam; 1:100; incubated overnight at 4°C), rabbit polyclonal anti-Sap 102 (Chemicon; 1:100; incubated overnight at 4°C), rabbit polyclonal anti-PSD-93/Chapsyn 110 (Chemicon; 1:100; incubated overnight at 4°C in 5% marvel containing 0.1% Tween 20), rabbit polyclonal anti-phospho-(Tyr402)-Pyk2 (1:100; Cell Signalling; incubated overnight at 4°C in 5% BSA containing 0.1% Tween 20), rabbit polyclonal anti-Pyk2 (1:100; Upstate; incubated overnight at 4°C in 3% marvel containing 0.1% Tween 20)

and mouse monoclonal anti-glyceraldehyde -3-phosphate dehydrogenase (GAPDH, 1:750; Chemicon) a ubiquitous housekeeping protein used as a control for protein level normalisation. In all cases detection was by peroxidase-linked secondary antibodies, goat-anti-rabbit (1:2000; Cell Signalling), goat-anti-mouse (1:10,000; Chemicon) or goat-anti-rabbit (1:5000; Chemicon), incubated in 2% BSA containing 0.1% Tween 20 for 50 minutes at room temperature, [except for anti-phospho-(Tyr402)-Pyk2 (Cell Signalling) where the secondary antibody was incubated in 5% marvel containing 0.1% Tween 20 for 60 minutes at room temperature and anti-Pyk2 (Upstate) with the secondary antibody incubated in 3% marvel containing 0.1% Tween 20 for 90 minutes at room temperature] and enhanced chemiluminescence and exposed to high performance chemiluminescence film (X-ray film).

3.7 Immunohistochemistry

3.7.1 Tissue preparation

Experimental and naïve animals were terminally anaesthetized with halothane and oxygen (oxygen flow rate of 2L/min) and were transcardially perfused with 200mls of heparinised vascular flush (0.1M PBS containing 0.6mg/ml heparin) using a small rotary pump at 30mls/minute, followed by 250-300mls of fixative solution (0.1M PBS containing 4% paraformaldehyde). Post perfusion a laminectomy was performed of the lumbar region and L3-L6 of the spinal cord was dissected out under an operating microscope (x20 objective lens). Tissue samples were post-fixed with post-fixative solution (0.1M PBS containing 4% paraformaldehyde) overnight at 4°C, transferred through increasing concentrations of sucrose solutions (sucrose in 0.1M PBS) to a 30% solution overnight, then transferred to a 0.1M PBS solution and stored at 4°C.

3.7.2 Immunohistochemistry procedure

Spinal cords were embedded in 0.25% agar (in 0.1M PBS) and sectioned (at -15°C; 40μm thickness) on a freezing micortome (Leitz Kyromat 1700). Experimental spinal cords were marked in the contralateral ventral horn by a pinhole to identify ipsilateral and contralateral dorsal horns. Spinal cord sections were transferred to a 36 well plate

containing 0.1M PBS. The free-floating sections were washed in 0.1M PBS, quenched in a hydrogen peroxide solution (1.5% in 0.1M PBS) for 20 minutes at room temperature, followed by an antigen retrieval step of suspending the sections in a 3M Urea solution for 10 minutes at 75°C, and blocked for 90 minutes at room temperature with blocking buffer (0.5% blocking reagent in 0.1M PBS; part of Fluorescein Tyramide Reagent Kit, Perkin Elmer). Primary antibody was incubated overnight at room temperature with agitation, antibodies were used at the following concentrations: mouse monoclonal anti-PSD 95 (Upstate; 1:50 in 0.1M PBS) and rabbit polyclonal anti-Pyk2 (Upstate; 1:50 in 0.1M PBS). Sections were incubated with the appropriate secondary antibodies in 0.1M PBS for 90 minutes at room temperature at the following concentrations: fluorescent goat-anti-rabbit (Alexa Fluor 568; Molecular Probes; 1:1000) and peroxidase-linked goat-anti-mouse (1:200; Cell Signalling), Sections were washed in 0.1M PBS and incubated in fluorescein tyramide (amplification reagent) for 25 minutes at room temperature (1:50 in 1x amplification dilutent, part of Fluorescein Tyramide Reagent Kit, Perkin Elmer). Following washing with 0.1M PBS sections were incubated with To-pro (To-pro-3-iodide; Molecular Probes; 1:1000) for 1-2 minutes at room temperature. Two final washes in deionised water were conducted prior to mounting of sections onto pre-coated microscope slides (with poly-L-lysine) and cover-slipped with Vecta Shield (mounting medium), sealed with clear varnish and stored at 4°C in a light sensitive box before confocal microscopy. Control sections were processed as above omitting the primary antisera (see Figure 3.2 and 3.3).

3.8 Analysis

3.8.1 Analysis of behavioural studies

In each behavioural study, data was pooled for each test day, with group averages shown ± the standard error of the mean (SEM). For responses to mechanical stimulus (Von Frey filaments) differences between paw withdrawal thresholds (PWT) ipsilateral to contralateral were determined by a Wilcoxon test (significance set at $p \leq 0.05$) and differences between post-operative and pre-operative values were determined by a Friedman test on ranks followed by Dunn's post-hoc analysis (significance set at $p \leq 0.05$). Tests conducted on mechanical data were non-parametric in nature due to Von Frey forces being a graded series of forces in intervals. For responses to a noxious thermal stimulus, differences between paw withdrawal latency (PWL) ipsilateral to contralateral were determined by a Student's t-test (significance set at $p \leq 0.05$) and differences between post-operative and pre-operative values were determined by a one-way repeated measures ANOVA followed by a Dunnett's post-hoc analysis (significance set at $p \leq 0.05$). These tests conducted on thermal data are parametric as thermal data is continuous. For responses to cold stimulus, differences between suspended paw elevation time (SPET) scores ipsilateral to contralateral were determined by a Wilcoxon test (significance set at $p \leq 0.05$) and differences between post-operative and pre-operative values were determined by a Friedman test on ranks followed by Dunn's post-hoc analysis (significance set at $p \leq 0.05$). In all cases no significant difference was noted in the contralateral response.

For analysis of the formalin response in mice where the PSD $95^{SH3W470L}$ mutant response was compared to wild type littermates response, significant differences were determined by a student's t-test (significance set at $p \leq 0.05$) and for the formalin response in rats, differences between pre-injection to post-injection values were determined by a one way repeated measures ANOVA followed by Dunnett's post hoc analysis (significance set at $p \leq 0.05$).

3.8.2 Analysis of behavioural studies following intrathecal administration

In each intrathecal study, data was pooled for each test time, with group averages shown ± SEM. For responses to mechanical stimulus (Von Frey filaments), differences between paw withdrawal thresholds ipsilateral to contralateral were determined by a Wilcoxon test (significance set at $p \leq 0.05$) and differences between post-injection and pre-injection values were determined by a Friedman test on ranks followed by Dunn's post-hoc analysis (significance set at $p \leq 0.05$). For thermal behavioural tests differences between paw withdrawal latencys ipsilateral to contralateral were determined by a Student's t-test (significance set at $p \leq 0.05$) and differences between post-injection and pre-injection values were determined by a one-way repeated measures ANOVA followed by a Dunnett's post-hoc analysis (significance set at $p \leq 0.05$). In all cases there was no significant alteration seen in the contralateral response and full recovery to pre-drug response levels were observed.

3.8.3 Analysis of western immunobloting studies

Exposed chemiluminescence films were scanned and densitometry was performed using 'Scan Analysis' software, whereby grey levels of positive protein bands and background grey levels were quantitatively measured, with the absolute numerical values derived being arbitrary. All densities were measured relative to the ubiquitous housekeeping enzyme GAPDH and all samples that were compared were run on the same gels or run under similar conditions. In the case of the phosphorylated form of both p38- and p42/44-MAP kinases the grey levels were calculated as densitometric ratios against 'pan' (phosphorylation state-independent) p38- and p42/44-MAP kinase levels.

3.8.4 Analysis of immunohistochemical studies

Spinal cord sections were examined using the Leica TCSNT Confocal system to aquire single optical section images (slice width 0.8μm) at both low and higher (with x5 and x20 objective lens) magnification. Digital images captured were stored on TDK CD-R media for analysis using LCS-lite software and Scion Image analysis. Single optical section images were acquired at low magnification (x5 objective lens) of whole dorsal spinal cord sections and at high magnification (x20 objective lens) of each spinal dorsal horn.

Images captured at low magnification, are 2000 x 2000μm in size as such were able to include both dorsal horns in the one image. Images captured at high magnification are 500 x 500μm in size therefore only lamina I to III of the spinal dorsal horn was captured, with the lateral aspect of the dorsal horn on each image, that is where the superficial laminae of the dorsal horn curve in a ventral direction. In analyzing all images the experimenter was blinded as to whether images were from experimental or naïve animals as all images when captured were labeled with a coded name.

Capturing images using the Leica TCSNT Confocal system involves sequentially scanning the section with individual lasers to detect fluorescence in each channel ensuring that any possible spectral bleed through is minimized to produce an accurate merged image of fluorophore distribution. Control sections were prepared (processed as experimental sections as outlined above (Section 3.7.2) omitting the primary antisera). Omitting the primary antisera and labeling the section with each fluorophore acts as a control for assessing possible spectral bleed through. Sample control sections at low magnification (x5 objective lens; Figure 3.2) and at higher magnification (x20 objective lens; Figure 3.3) show a clear signal for the nuclear marker To-pro (blue) whereas the fluorescent signal for either PSD-95 (green) or Pyk 2 (red) is not observed.

For analysis of the expression of PSD-95 and Pyk 2 in the spinal dorsal horn at low magnification (x5 objective lens), Scion Image analysis was used to measure the mean fluorescent intensity of PSD-95 or Pyk 2 in lamina I and II or lamina III, or IV of the ipsilateral and contralateral sides in CCI injured and naïve spinal dorsal horns. Analysis was carried out within the region's of interest (ROI) that is from the mediolateral region to the start of the curved lateral region of the dorsal horn, thus focusing the area of attention on the region of afferent input from the hind limb (see Figure 3.2 for illustration of ROIs). Analysis was carried out on 8-10 randomly selected sections from each of 4 naïve animals and of 6 CCI injured animals. Within Lamina I and II, the area was subdivided into three, the mediolateral, intermediate and lateral regions for analysis (see Figure 3.2). The fluorescence intensity (arbitrary values) was measured, data was pooled for each experimental group, with the mean fluorescence intensity shown ± SEM (in

arbitrary units). Differences between fluorescent intensity ipsilateral to contralateral were determined by a Student's paired t-test (significance set at $p \leq 0.05$) and differences between experimental compared to naïve were determined by a Student's unpaired t-test (significance set at $p \leq 0.05$).

For analysis of the cellular expression of PSD-95 and Pyk 2 in the spinal dorsal horn, images were captured at higher magnification (x20 objective lens), cells were analyzed in the ROI from the mediolateral region to the start of the curved lateral region of the dorsal horn (to focus analysis in the area of afferent input from the hind limb). Analysis was carried out in the following manner using LCS-lite software; within each ROI, the number of PSD-95 immunopositive cells (green) and the number of Pyk 2-immunopositive cells (red) were counted from 6-8 randomly selected sections from each of 4 naïve and 6 CCI injured animals (see Figure 3.3 for illustration of ROIs). The number of PSD-95 or Pyk 2-immunopositive cells were counted in lamina I, II and III, (see Figure 3.3) where only cells that were associated with To-pro staining (nuclear marker) and whose intensity was at least twice background intensity were counted as immunopositive (data expressed as the total cell number of immunopositive cells per ROI ± SEM). Differences between the number of immunopositive cells in each laminae ipsilateral compared to contralateral were determined by a Student's paired t-test (significance set at $p \leq 0.05$) and experimental compared to naïve were assessed by a Student's unpaired t-test (significance set at $p \leq 0.05$).

Colocalisation analysis was carried out using a profile tool on the LCS-lite software, which enabled each cell in the region of interest to be profiled at the same time for the intensity of each fluorochrome, thereby measuring the intensity of fluorescence of PSD-95 (green), Pyk2 (red) and the nuclear marker To-pro (blue; see Figure 3.4). Profiling each cell involved a line of approx. 16μm in length being drawn through each cell and the intensity of each fluorochrome was measured along the line. The resulting intensities were graphed and colocalisation was determined to be positive, if the fluorochrome graph for PSD-95 and Pyk 2 overlapped in a cell that again was To-pro positive and signal was at least twice background intensity for both PSD-95 and Pyk 2. If the profile of the cell

showed the intensities not to overlap then the cell was counted as a non-colocalised cell that was either PSD-95 or Pyk 2 immunopositive. The number of colocalised and non-colocalised cells were counted within each ROI, namely lamina I, II and III as outlined above (see Figure 3.3) from 6-8 randomly selected sections from each of 4 naïve and 6 CCI injured animals. Data is expressed as the total number of colocalised cells per ROI ± SEM or the total number of non-colocalised cells (that are either PSD-95 or Pyk 2 immunopositive) per ROI ± SEM. Differences between the number of colocalised and non-colocalised cells in each laminae ipsilateral compared to contralateral were determined by a student's paired t-test (significance set at $p \leq 0.05$) and experimental compared to naïve were assessed by a student's unpaired t-test (significance set at $p \leq 0.05$).

Figure 3.2

Immunohistochemical analysis of fluorescence intensity in the spinal dorsal horn of naïve and CCI injured animals at low magnification

(A) An example of the spinal cord at low magnification (x5 objective lens) is illustrated (for demonstration purposes showing PSD-95 immunoreactivity (green)). The image shows the regions of interest (ROI of equal size) used in analysis; **Area A, B and C** are within laminae I and II, showing the (A) mediolateral, (B) intermediate and (C) lateral regions used for analysis of intensity of PSD-95 and Pyk 2 fluorescent staining. **Area D** shows the ROI used to assess intensity of PSD-95 and Pyk 2 fluorescent staining in lamina III. **Area E** illustrates the ROI used to assess intensity of PSD-95 and Pyk 2 fluorescent staining in lamina IV. The mean fluorescence intensity (arbitrary values) was measured using Scion Image analysis, from ipsilateral and contralateral sides in CCI injured and naïve dorsal horns from 8-10 randomly selected sections from naïve or CCI injured animals. (L= Lateral edge of the dorsal horn, M= medial edge of the dorsal horn; scale bar 45μm; Results of analysis presented in Chapter 6, see Figure 6.7 and 6.8). **(B)** Image illustrates a control spinal cord section at low magnification (x5 objective lens), whereby sections were processed as in Section 3.7.2 omitting the primary antisera but with the nuclear marker (To-pro; blue), with an example of the pinhole in the contralateral ventral horn. The signal for To-pro (blue) is clearly visible whereas the fluorescent signal for either PSD-95 (green) or Pyk 2 (red) cannot be seen. (L= Lateral edge of the dorsal horn, M= medial edge of the dorsal horn; scale bar 50μm).

A.

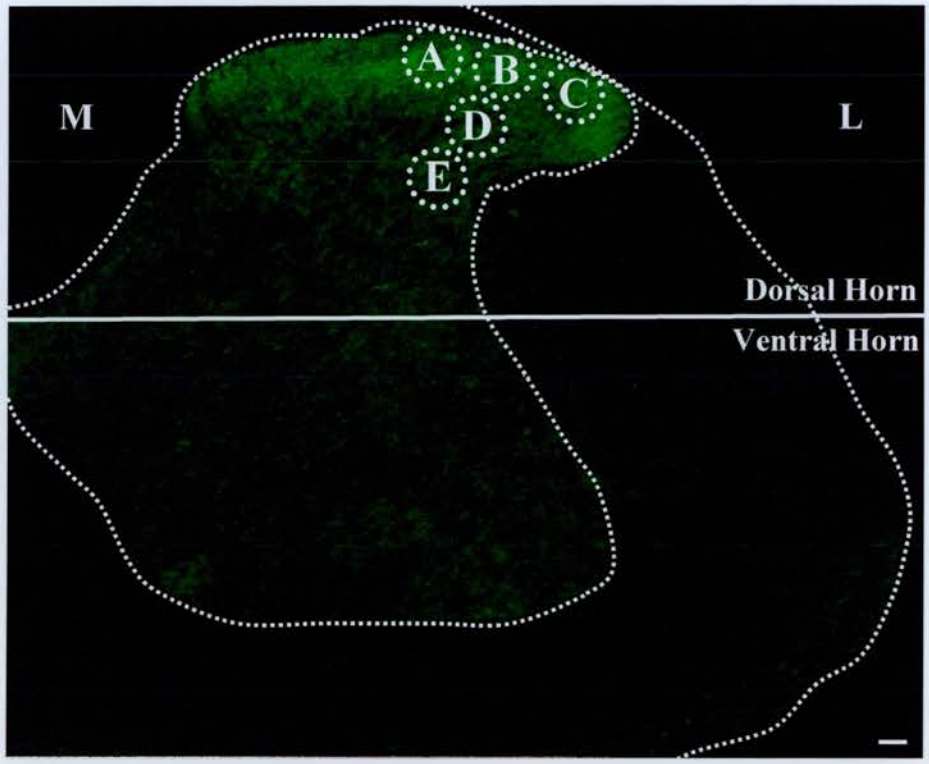
A
B
C
D
E
M
L
Dorsal Horn
Ventral Horn

B.

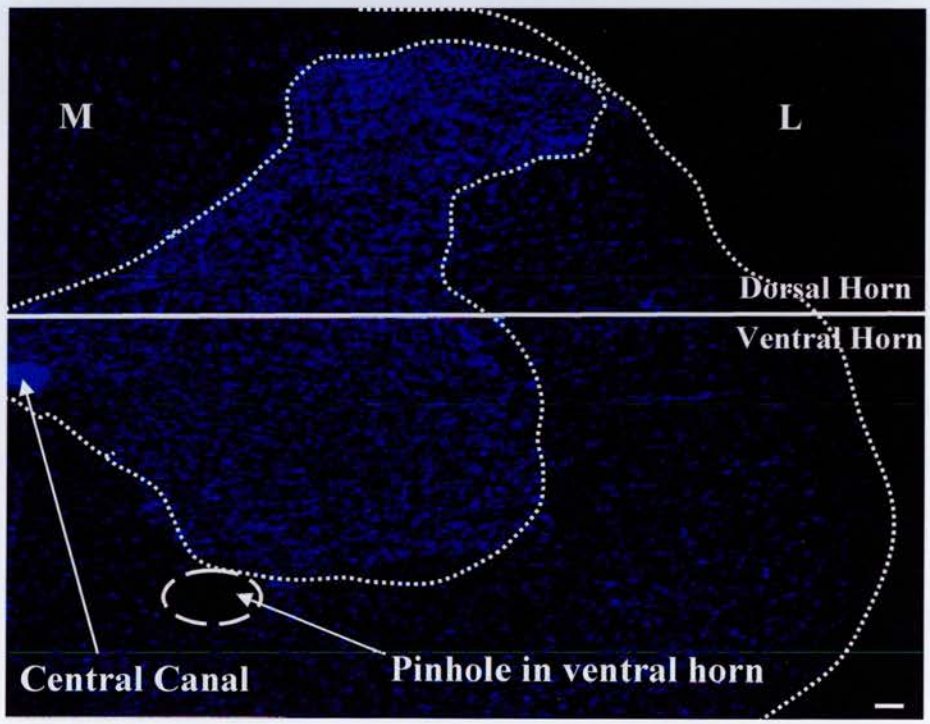
M
L
Dorsal Horn
Ventral Horn
Central Canal
Pinhole in ventral horn

Figure 3.3

Immunohistochemical analysis of the cellular expression of PSD-95 and Pyk 2 in the spinal dorsal horn of naïve and CCI injured animals

(A) An example image of the spinal dorsal horn with boundaries marked for Lamina I, II and III used in counting PSD-95 or Pyk 2 immunopositive cells is illustrated (for demonstration purposes showing PSD-95 immunoreactivity (green) and To-pro immunoreactivity (blue)). The total numbers of PSD-95 and Pan Pyk 2 immunopositive cells were counted in lamina I to III, where only cells that were associated with To-pro staining (nuclear marker) and whose intensity was at least twice background intensity were counted as immunopositive using LCS-Lite software, from 6-8 randomly selected sections per 4 naïve animals and 6 CCI injured animals. (L= Lateral edge of the dorsal horn; scale bar 20μm; Results of analysis presented in Chapter 6, see Figure 6.9 to 6.12). **(B)** Image illustrates a control spinal cord section, whereby sections were processed as in Section 3.7.2 omitting the primary antisera, captured at higher magnification (x20 objective lens). The spinal dorsal horn is visible with a strong signal for To-pro (blue), and with no clear fluorescent signal for either PSD-95 (green) or Pyk 2 (red) observed, when compared to signal observed in experimental sections (see Figure 6.9 and 6.11 for comparison; L= Lateral edge of the dorsal horn; scale bar 20μm).

A.

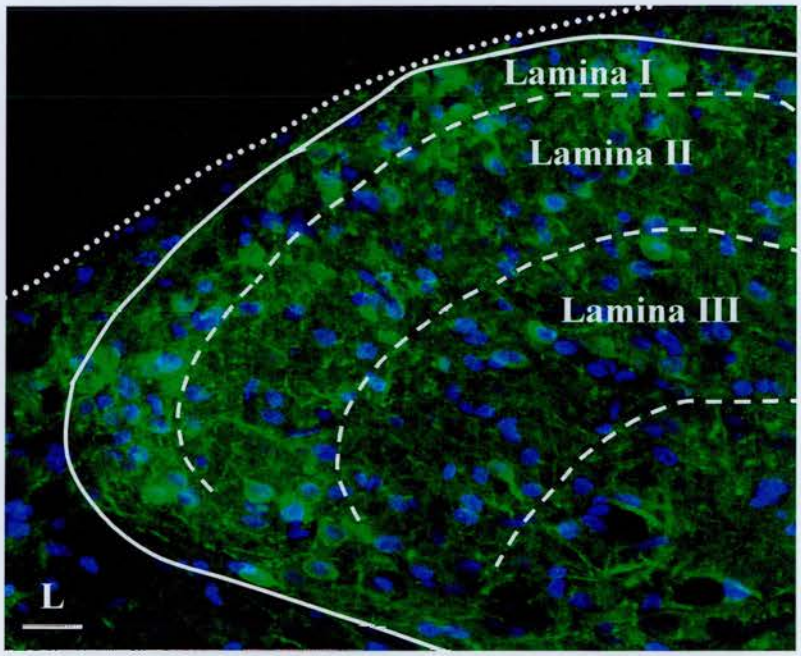
Lamina I
Lamina II
Lamina III
L

B.

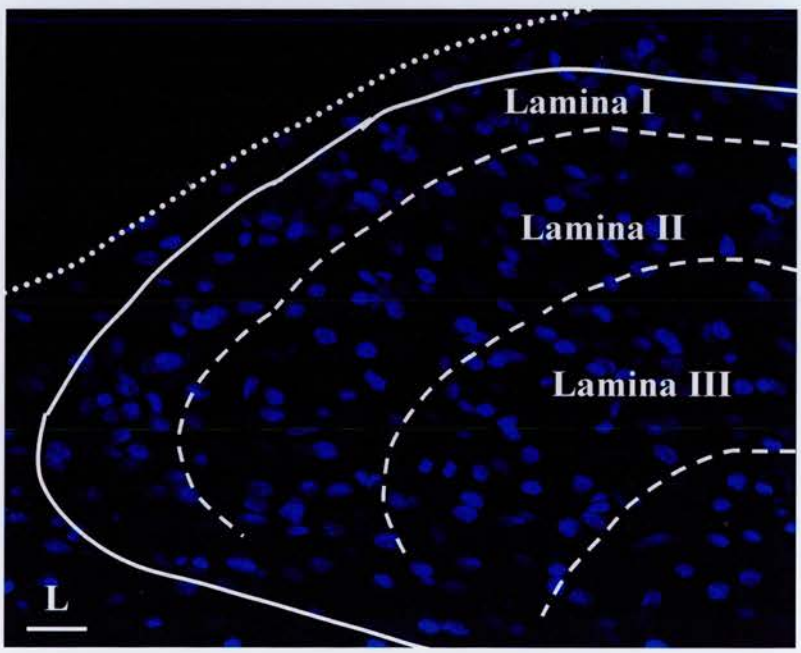
Lamina I
Lamina II
Lamina III
L

Figure 3.4

Immunohistochemical analysis of the colocalisation of PSD-95 and Pyk 2 in the spinal dorsal horn of naïve and CCI injured animals

The images illustrate sample cells from Lamina II (for demonstration purposes) of the spinal dorsal horn showing PSD-95 (green), Pyk 2 (red) and To-pro (nuclear marker; blue) immunoreactivity. Colocalisation was determined by profiling each cell using LCS-Lite software, whereby the intensity of each fluorochrome was measured in each cell and graphed, the corresponding fluorochrome intensity graphs of each cell is shown below each image. The graphs show the intensity of each fluorochrome channel, either green (PSD-95), red (Pyk 2) or blue (Nuclear marker) on the y-axis and the length of the profile line drawn on the x-axis (16μm). **(A)** An example of a PSD-95 immunopositive cell with the corresponding graphs of each fluorochrome below. The blue channel (nuclear marker) shows the cell is To-pro positive, the red channel (Pyk 2) shows that the fluorescent intensity is not twice background, whereas the green channel (PSD-95) shows fluorescent intensity to be at least twice that of background level, thereby demonstrating this cell to be PSD-95 immunopositive. **(B)** An example of a Pyk 2 immunopositive cell with the corresponding graphs of each fluorochrome below. The blue channel (nuclear marker) shows the cell is To-pro positive, the red channel (Pyk 2) shows fluorescent intensity is at least twice that of background level, while the green channel (PSD-95) illustrates the fluorescent intensity is not twice background, thereby demonstrating this cell to be Pyk 2 immunopositive. **(C)** An example of a colocalised cell with the corresponding graphs of each fluorochrome below. The blue channel (nuclear marker) shows the cell is To-pro positive, the red channel (Pyk 2) and the green channel (PSD-95) show fluorescent intensity at least twice that of background level, the graphs also illustrates that the red and green fluorescent signal overlap indicating that PSD-95 is colocalised with Pyk 2 in this cell (results of analysis are presented in Chapter 6, see Figure 6.13 to 6.16).

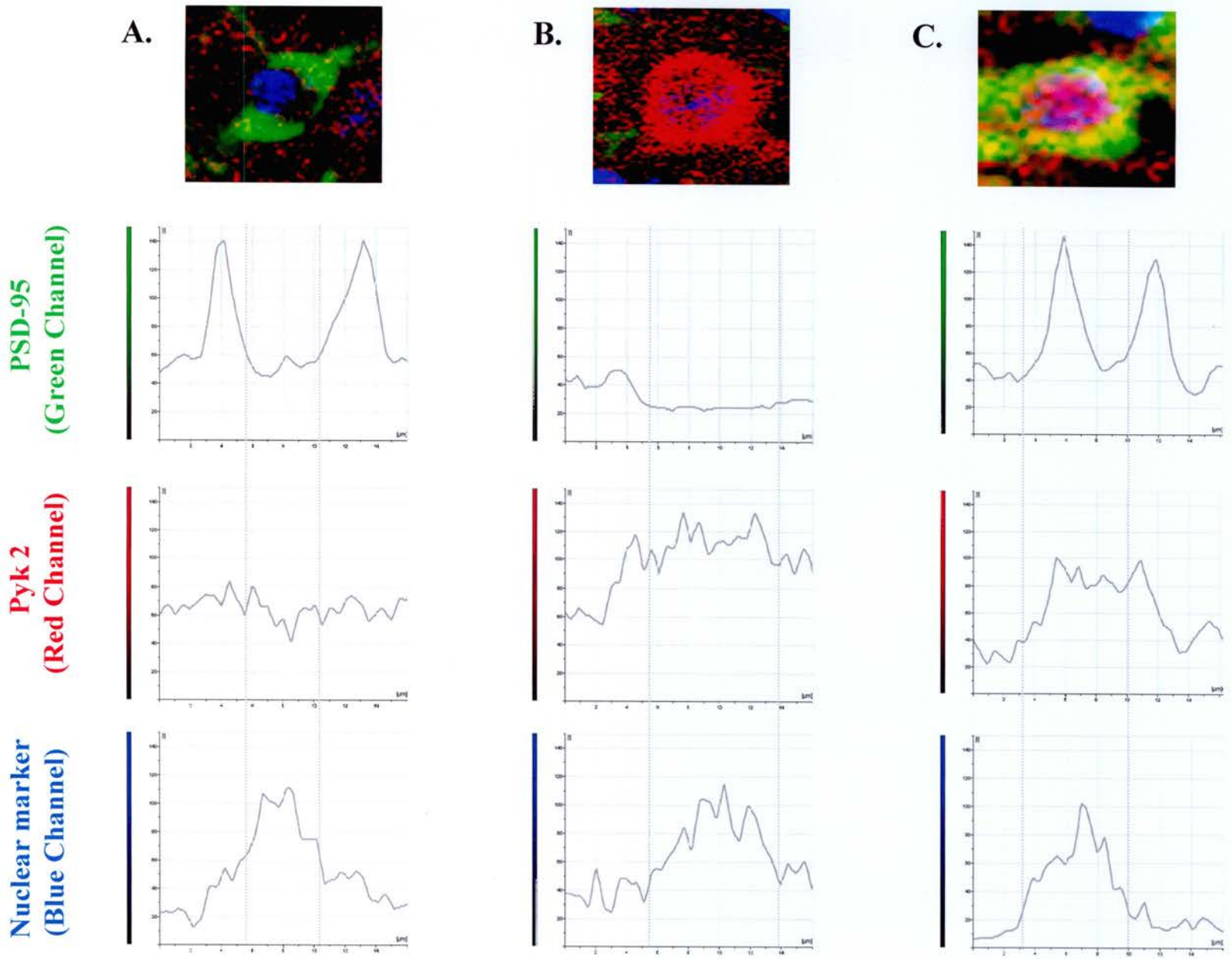
A.
B.
C.
PSD-95
(Green Channel)
Pyk 2
(Red Channel)
Nuclear marker
(Blue Channel)
PSD-95
immunopositive cell
Pyk 2
immunopositive cell
Colocalised
cell

4. Involvement of spinal $VPAC_2$ and NK_2 receptors and glially-mediated events in the activation of both p38 and p42/44 MAP kinases in an experimental model of mononeuropathy

4.1 Introduction

Mitogen-activated protein kinases (MAP kinases) are serine/threonine protein kinases that are instrumental in many important intracellular signalling pathways transmitting signals from the cell surface to the nucleus (reviewed in Section 1.7.3; Derkinderen et al., 1999). These kinases are localized in the cytoplasm until activated by dual phosphorylation on both threonine and tyrosine residues (Raingeaud et al., 1995; Seger and Krebs, 1995; Widmann et al., 1999). The focus of this study was to look at the involvement of two members of the MAP kinase family, firstly the p42/44 MAP kinases, known also as extracellular signal regulated kinase (ERK), with ERK1 being p44 MAP kinase and ERK2 being p42 MAP kinase and secondly the p38 MAP kinase. The p42/44 MAP kinases are known to be one of the intracellular signalling pathways implicated in neuronal plasticity, such as long-term potentiation, learning and memory (Impey et al., 1999; Sweatt, 2001). It is thought p38 MAP kinase exerts effects in the hippocampus that may oppose that of p42/44 MAP kinase, indeed the p38 MAP kinase pathway has been shown to be involved in the induction of metabotropic glutamate receptor-dependent long-term depression (Bolshakov et al., 2000). Chronic pain also involves neuronal plasticity that leads to the development of a hyperalgesic state in spinal cord sensory neurons. Although repetitive afferent activity plays a key part in this, multiple mediators are involved and the changes are heterosynaptic, so the process is not identical to LTP. Nevertheless, there is accumulating evidence that both the p42/44 and p38 classes of the MAP kinase family are believed to be involved in the mechanisms of sensitisation in chronic pain states.

Peripheral inflammation and nerve injury induce activation of p38 MAP kinase in primary sensory neurons of the dorsal root ganglion (Ji et al., 2002b). In addition to this, peripheral inflammation and nerve injury also activate p38 MAP kinase in the dorsal horn

of the spinal cord ipsilateral to injury (Jin et al., 2003; Kim et al., 2002; Svensson et al., 2003). Inhibition of p38 MAP kinase reduces inflammation and nerve injury-induced behavioural sensitisation (Ji et al., 2002b; Jin et al., 2003; Schafers et al., 2003). It has also been shown that p42/44 MAP kinases are activated in spinal dorsal horn neurons following selective C-fibre stimulation (Ji et al., 1999). A number of studies have revealed that peripheral inflammation results in phosphorylation of p42/44 MAP kinase in the spinal dorsal horn and inflammatory behavioural sensitisation is prevented by use of p42/44 MAP kinase inhibitors (Galan et al., 2002; Ji et al., 1999; Ji et al., 2002a; Sammons et al., 2000). It has also been demonstrated recently that p42/44 MAP kinase is activated following peripheral nerve injury in both dorsal spinal cord and primary sensory neurons (Obata et al., 2004; Zhuang et al., 2005) and noxious stimulation similarly induces phosphorylation of p42/44 MAP kinase in the trigeminal nucleus (Huang et al., 2000). Activation of both p38 and p42/44 MAP kinases in the spinal dorsal horn following nerve injury is believed to be localised not only to neurons but also to spinal glial cells (Jin et al., 2003; Ma and Quirion, 2002; Tsuda et al., 2004; Zhuang et al., 2005). Glial cells are non-neuronal cells, which are not overtly electrically excitable; the major types in the central nervous system are astrocytes, oligodendrocytes, and microglia, which are traditionally thought to play a supportive role to neurons. Following peripheral inflammation and nerve injury it has been shown that p38 MAP kinase activation can be localised to microglia (Jin et al., 2003 ;Kawasaki et al., 1997; Kim et al., 2002; Svensson et al., 2003; Tsuda et al., 2004) and activation of p42/44 MAP kinase has been shown in astrocytes (Ma and Quirion, 2002), with a more recent study reporting activation of p42/44 MAP kinase occurring in both microglia and astrocytes following nerve injury (Zhuang et al., 2005).

Pain hypersensitivity has previously been thought to result exclusively from altered neuronal activity, however the activation of spinal cord glial cells, including microglia and astrocytes, has increasingly been implicated in the pathogenesis of pain (DeLeo and Yezierski, 2001; Meller et al., 1994; Watkins et al., 1997; Watkins et al., 2001b; Watkins et al., 2001a). The idea that glial cells could be activated (and be functionally important) in pain states originated when peripheral nerve damage was shown to activate spinal cord

glia and that this activation was inhibited by an NMDA receptor antagonist that also inhibited the behavioural sensitisation observed (Garrison et al., 1991; Garrison et al., 1994). This was the first study to link glial activation to the functional outcome (behavioural sensitisation) of peripheral nerve injury. To discover whether glia are necessary for the development of behavioural sensitisation, several studies have investigated whether such sensitisation would occur if glial function was disrupted. Two inhibitors were utilised, firstly fluorocitrate, which disrupts glial function and secondly minocycline, which prevents the activation of microglia in particular; both agents were effective in attenuating allodynia and hyperalgesia in various nerve injury models (Ledeboer et al., 2005; Meller et al., 1994; Milligan et al., 2003; Raghavendra et al., 2003a; Watkins et al., 1997).

It is not completely understood how activation of spinal glia contributes to hyperalgesia and allodynia; which substances glia release to act on neurons and the subsequent actions of these substances are not clear and in need of further investigation. The actions of these substances could be manifold, such as acting directly on neurons to increase excitability, acting to induce the release of other transmitters that then influence nociceptive neurons or by acting to upregulate neuronal receptors. Activated glia, for example, can release the pro-inflammatory cytokines, tumor necrosis factor-alpha (TNF-α), interleukin-1 (IL-1) and interleukin-6 (IL-6), which can activate neurons as well as glia via binding to specific receptors on these cells (Vitkovic et al., 2000), suggesting a possible way in which glia can transmit signals to neurons. A selective inhibitor of TNF-α synthesis, thalidomide, has proven to be effective in delaying sensitisation development induced by peripheral nerve injury (George et al., 2000; Sommer et al., 1998a). Inhibition of these pro-inflammatory cytokines, by intrathecal injection of antagonists also prevented or reversed allodynia and hyperalgesia in models of inflammation and nerve injury (Milligan et al., 2003; Sweitzer et al., 2001a; Watkins et al., 1997), suggesting that these proteins induced by glial activation may be involved in the maintenance of behavioural sensitisation observed in such pain models. In addition to this, the inhibitor of glial-generation of pro-inflammatory cytokines, propentofylline, which has been shown to reduce microglial and astrocyte activation in the spinal cord, was also reported to have an analgesic effect on

sensitisation caused by nerve injury (Raghavendra et al., 2003b; Sweitzer et al., 2001b). Another approach to control the effects of pro-inflammatory cytokines is to block the intracellular pathways that are activated upon the binding of these cytokines to their receptors. Although many cascades are activated, one known pathway, which has been implicated in both pro-inflammatory cytokine signalling and production, is the p38 MAP kinase cascade (Clark et al., 2003; Watkins et al., 1999). Indeed it has recently been demonstrated that blockade of TNF-α can reduce nerve injury-induced p38 activation (Svensson et al., 2005).

A number of events can result in the downstream activation of the p38 and p42/44 MAP kinase pathways, for example an increase in intracellular calcium, pro-inflammatory cytokines (which can be released by activated glia), activation of calcium-permeable ionotropic glutamate receptors such as the NMDA receptor (Kawasaki et al., 1997; Xia et al., 1996), as well as a number of G protein-coupled receptors (GPCRs) (Marinissen and Gutkind, 2001; Yamauchi et al., 1997). As previously elaborated (Section 1.4.2 and 1.7.3) the NMDA receptor is crucially involved in sensitisation of spinal dorsal horn neurons (Coderre and Melzack, 1992; Davies and Lodge, 1987; Dickenson and Sullivan, 1987; Suzuki et al., 2001; Woolf and Thompson, 1991). Examples of GPCRs that may be involved include the peptidergic GPCRs for neurokinin peptides (NK receptors) and for vasoactive intestinal polypeptide (VPAC and PAC receptors). Both of these types of peptidergic receptor, which were reviewed in chapter one (Section 1.4.4) are importantly involved in nociception and behavioural sensitisation (Coderre and Melzack, 1992; Dickinson and Fleetwood-Walker, 1999; Laird et al., 1993). The neurokinin receptors (NK_1, NK_2, and NK_3) are activated by the tachykinins substance P (SP), neurokinin A (NKA) and neurokinin B (NKB) respectively. The focus of this investigation is the NK_2 receptor whose ligand NKA, is localised to unmyelinated C-fibres, is capable of producing spinal hyperexcitability and depletion of which occurs following nerve transection (Dalsgaard et al., 1985; Hokfelt et al., 1994; Ogawa et al., 1985; Xu et al., 1991). NK_2 receptor antagonists have been demonstrated to block both the increased dorsal horn neuron excitability and behavioural sensitisation following nerve damage (Coudore-Civiale et al., 1998; Fleetwood-Walker et al., 1990; Yashpal et al., 1996). NK_2

receptors are located in the spinal cord where a proportion are believed to be localised to astrocytes (Quirion and Davey, 1988; Zerari et al., 1998). There are three receptors that respond to the excitatory peptide VIP, namely the $VPAC_1$, the $VPAC_2$ and PAC_1 receptors, in the spinal cord. The expression of VIP in fine afferents and of the $VPAC_2$ receptor in the spinal dorsal horn increases following nerve injury (Dickinson et al., 1999; Nahin et al., 1994). The $VPAC_2$ receptor (in addition to the other VPAC and PAC receptors) has also been demonstrated to be localised to astrocytes (Brenneman et al., 1990). As a result of these investigations showing that the $VPAC_2$ receptor is upregulated in neuropathic pain states, this receptor will be focused on in this investigation. (Grimaldi and Cavallaro, 1999; Jaworski, 2000; Joo et al., 2004).

This study aims to investigate the activation of both the p38 and p42/44 MAP kinases in the spinal cord following the induction of an experimental model of mononeuropathy and to explore their functional role in behavioural sensitisation as a result of such nerve injury. The contribution of the NK_2, $VPAC_2$ and NMDA receptors and spinal glia to the effects of nerve injury-induced activation of both the p38 and p42/44 MAP kinases was also assessed.

4.2 Methods

Experiments were carried out using adult male Wistar rats (180-250g). As detailed in Chapter three; Animals (n=25) underwent a unilateral chronic constriction injury to the sciatic nerve, a model of experimental mononeuropathy (CCI; Section 3.2.1). All animals were assessed behaviourally prior to surgery (to obtain baseline values) and post surgery (from day 6) until recovery (day 19-25 post surgery) from CCI induced-injury (Section 3.4). All animals were tested for signs of mechanical allodynia using calibrated Von Frey filaments (Section 3.4.2) and for signs of thermal hyperalgesia using the Hargreaves' thermal apparatus (Section 3.4.4) and for cold allodynia by use of iced water (Section 3.4.3). For analysis of the effects of intrathecal administration of specific inhibitors, receptor antagonists and agonists on somatosensory behavioural reflexes; naïve animals were used for intrathecal injections of receptor agonists and combinations of agonist and

inhibitor and animals that had undergone chronic constriction injury and were at the peak of neuropathic behavioural reflex sensitisation were used for intrathecal injections of receptor antagonists and inhibitors.

Prior to intrathecal injection of drugs, measurements of mechanical allodynia (Section 3.4.2) and thermal hyperalgesia (Section 3.4.4) were recorded to obtain baseline values. All animals were briefly anaesthetised with halothane and oxygen and injected intrathecally at the L4/5 level of the spinal cord with the pharmacological agent of interest (Section 3.5). To determine the effects of each drug, quantitative sensory reflex testing began 15 minutes post injection for signs of mechanical allodynia (Section 3.4.2) and thermal hyperalgesia (Section 3.4.4), with testing continuing every 5 minutes thereafter until recovery to pre-injection values. The following drugs were used on animals displaying peak behavioural reflex sensitisation following CCI: MAPK pathway inhibitors, p38 MAP kinase inhibitor, SB 203580 (5nmol; n=6) and p42/44 MAP kinase pathway inhibitors PD 098059 (2.5nmol; n=6), U 0126 (1.5nmol; n=8) and its less active analogue U 0124 (1.5nmol; n=6; Section 3.5.1). The glial inhibitor propentofylline (PPT; 0.5μmol; n=5; Section 3.5.2). The TNF-α receptor antagonist WP9QY (25μg; n=5; Section 3.5.3). The selective $VPAC_2$ receptor antagonist ([des(1-4), Arg^{16}]-Ro 25-1553); 0.1 nmol; n=7), the $VPAC_1$ receptor antagonist ([Ac-His^1, D-Phe^2, Lys^{15}, Arg^{16}, Leu^{17}]-VIP(3-7)GRF(8-27); 0.1 nmol; n=6) and the PAC_1 receptor antagonist ($(PACAP_{6-38})$; 0.1 nmol; n=6; Section 3.5.3). The antagonist for NK_1 (RP 67580; 5 nmol; n=6; Section 3.5.3) and for NK_2 (SR 48968; 5 nmol; n=5; Section 3.5.3) receptors. The following drugs were used on naïve animals: The selective $VPAC_2$ receptor agonist, (Ro 25-1553; 0.5 nmol; n=6; Section 3.5.4). The NK_2 receptor agonist (GR 64349; 1.5 nmol; n=6; Section 3.5.5). The following combinations of drugs were also assessed: The $VPAC_2$ receptor agonist (Ro 25-1553; 0.5 nmol) was combined with the p38 MAP kinase inhibitor (SB 203580; 5nmol; n=6; Section 3.5.6) and the NK_2 receptor agonist (GR 64349; 1.5 nmol) was combined with the p42/44 MAP kinase pathway inhibitor (U 0126; 1.5nmol; n=6; Section 3.5.6). The effects of the intrathecal administration of the drugs were analysed as described above (Section 3.8.2).

Using phospho-specific (activation state-dependent) antibodies, the expression of total and activated p38 MAP kinase and of total and activated p42/44 MAP kinase proteins in the spinal cord was assessed in naïve (n=5) and in animals displaying peak behavioural reflex sensitisation following CCI nerve injury (n=5). Animals were terminally anaesthetised prior to and during dissection of all tissues and a laminectomy of the lumbar region of the rats was performed and spinal cord tissue was homogenised in Laemmli lysis buffer to prepare spinal cord extracts (Section 3.6.1). In the case of incubation of drugs on the spinal cord, animals were terminally anaesthetised prior to and during dissection of all tissues, following a laminectomy the spinal cord was incubated with saline or of the pharmacological agent of interest (Section 3.6.2) then spinal cord tissue was homogenised in Laemmli lysis buffer to prepare the spinal cord extracts (Section 3.6.1). The following drugs were incubated on naïve spinal cords: saline (0.9%; n=5), the agonists for $VPAC_2$ receptor (Ro 25-1553; 30 μM; n=5), the NK_2 receptor agonist (GR 64349; 50 μM; n=5) and a combination of the $VPAC_2$ receptor agonist (Ro 25-1553; 30 μM) or the NK_2 receptor agonist (GR 64349; 50 μM) with the glial inhibitor, propentofylline (PPT; 10 mM; n=5; Section 3.6.2). In nerve-injured (CCI see section 3.2.1) animals, spinal cords were incubated with the following: saline (0.9%; n=5), the $VPAC_2$ receptor antagonist ([des(1-4), arg^{16}]-Ro 25-1553; 2μM; n=5), the NK_2 receptor antagonist (SR 48968; 100μM; n=5), the NMDA receptor antagonist, ((R)-CPP; 10 μM; n=5), the glial inhibitor, propentofylline (PPT; 10mM; n=5) and with the TNF-α receptor antagonist (WP9QY; 0.5mg/ml; n=5) or with the TNF-α synthesis inhibitor, thalidomide (200μM; n=5; Section 3.6.2). Prepared spinal cord extracts were then separated by electrophoresis and transferred to PVDF membranes, blocked and probed for rabbit polyclonal anti-phospho-[Thr180/Tyr182]-p38 MAP kinase, rabbit polyclonal anti-p38 MAP kinase ('pan': phosphorylation state-independent), as well as rabbit polyclonal anti-phospho-[Thr202/Tyr204]-p42/44 MAP kinase and rabbit polyclonal anti-p42/44 MAP kinase ('pan': phosphorylation state-independent) and detected by peroxidase-linked secondary antibodies (goat-anti-rabbit) and enhanced chemiluminescence (Section 3.6.4). Densitometry was performed to measure quantitatively the grey levels of positive protein bands and background grey levels to give a ratio of phosphorylated p38 or p42/44 to total

(pan) p38 or p42/44 MAP kinase (with the absolute numerical values derived being arbitrary; Section 3.8.3).

4.3 Results

4.3.1 Analysis of the development of behavioural reflex sensitisation ipsilateral to sciatic nerve injury in the chronic constriction injury (CCI) model of experimental mononeuropathy.

The majority of nerve-injured animals showed the behavioural changes characteristic of the CCI model. All of the animals that underwent CCI surgery (Section 3.2.1) held the affected limb in a protective manner, keeping it held flexed with claws tightly clasped. The animals developed a limp gait and favoured the contralateral hind limb in locomotion. These abnormalities are thought to be indications of spontaneous pain[71]. Apart from these changes post-operative animals appeared healthy, had no signs of weight loss and were handled without any distress being evident. During this study none of the animals developed any signs of autotomy.

Thermal hyperalgesia ***[see Figure 4.1 A]***

All animals were behaviourally tested for signs of thermal hyperalgesia, using the Hargreaves' thermal apparatus (Section 3.4.4). In a series of experiments designed to characterise the behavioural reflex changes occurring, baseline (pre-surgical) paw withdrawal latency (PWL) was measured as ipsilateral, 13.0 ± 1.8 seconds and contralateral 12.8 ± 1.7 seconds (mean latency ± SEM ; n=25). At all time points from the sixth day until the twenty fourth day post-surgery, all animals showed significantly reduced PWL ipsilateral to the injury as compared to the contralateral side ($p<0.05$ by Student's t-test) and a significant reduction in PWL was also seen between post-surgical and pre-surgery values ($p<0.05$; One Way Repeated Measures ANOVA followed by Dunnett's post-hoc analysis), no significant difference remained in the PWL by the twenty fifth day post-surgery. All animals reached a peak of thermal hyperalgesia between the thirteenth and nineteenth days post-surgery when the ipsilateral PWL was 3.4 ± 0.1 seconds and contralateral was 11.9 ± 1.2 seconds (mean latency ± SEM). The

contralateral PWL showed no significant alterations in its response. In addition to developing such a reduced ipsilateral response to a noxious heat stimulus, the animals also altered their response from a rapid flick of the hind paw returning to a resting posture (observed in pre-operative animals) to that of a flick where the animals tended to hold the limb elevated for a longer period or shake and or lick the affected paw before returning to a resting posture (observed in post-operative animals).

Mechanical allodynia *[see Figure 4.1 B]*

All animals were tested for signs of mechanical allodynia using calibrated Von Frey filaments (Section 3.4.2). The baseline (pre-surgical) paw withdrawal threshold (PWT) required to elicit a paw withdrawal response was ipsilateral 4831 ± 0 mN/mm^2 and contralateral 4831 ± 0 mN/mm^2 (mean threshold ± SEM; n=25). The baseline values here with zero error bars is due to the sensitivity of the Von Frey apparatus, which have a wide range of forces, with each filament having a fixed bending force, here a force of 4381 mN/mm^2 was required to elicit a paw withdrawal and a lower graded force applied to the mid-plantar hindpaw could not elicit such a paw withdrawal. The Von Frey filaments range of forces is not discreet enough to detect At all time points from the sixth day until the nineteenth day post-surgery, all animals demonstrated an increased sensitivity to mechanical stimuli with a significantly reduced PWT ipsilateral to the injury as compared to the contralateral side ($p<0.05$ Wilcoxon test) and a significant reduction in PWT was also seen between post-surgical and pre-surgery values ($p<0.05$; Friedman test on ranks followed by Dunn's post-hoc analysis). Animals reached a peak of mechanical allodynia around the fourteenth day post-surgery when the ipsilateral PWT was 1429 ± 117 mN/mm^2 and the contralateral was 4831 ± 44 mN/mm^2 (mean threshold ± SEM). Contralateral PWT responses showed no significant alterations.

Cold allodynia *[see Figure 4.1 C]*

All animals were tested for signs of cold allodynia by detecting the animal's response to iced water (4°C; Section 3.4.3), measuring the Suspended Paw Elevation Time (SPET) during a 20 second time period. Prior to surgery naïve rats showed no behavioural response to iced water with both an ipsilateral and contralateral baseline value of 0 ± 0

seconds (mean SPET ± SEM; n=25). At all time points from the sixth day until the nineteenth day post-surgery, all animals demonstrated an increased sensitivity to a cold stimulus with a significantly increased SPET ipsilateral to the injury (for example to 7.0 ± 0.6 seconds [mean SPET ± SEM] on day eight post nerve injury) as compared to the contralateral side (of 0 ± 0 seconds [mean SPET ± SEM]; $p<0.05$; Wilcoxon test) and a significant increase in SPET was also seen between post-surgical and pre-surgery values ($p<0.05$; Friedman test on ranks followed by Dunn's post-hoc analysis). Animals reached a peak of cold allodynia around the thirteenth day post-surgery when the ipsilateral SPET was 14.0 ± 1.3 mN/mm^2 and contralateral remained unaffected at 0 ± 0 SPET (mean ± SEM responses). No significant increases were observed in the SPET response of the contralateral limb.

4.3.2 Intrathecal administration of either the p38 or p42/44 MAP kinase pathway inhibitors attenuated nerve-injury induced behavioural reflex sensitisation

The effects of the intrathecal administration of the p38 MAP kinase inhibitor, SB 203580 or the p42/44 MAP kinase pathway inhibitors, PD 098059 or U 0126 (and its less active analogue U 0124) on nerve injury-induced thermal hyperalgesia and mechanical allodynia were assessed. Intrathecal administration of all drugs was carried out in animals that displayed peak ipsilateral behavioural reflex sensitisation, with the effects of all drugs being assessed until recovery to pre-injection values. None of the drugs tested had any significant effects on responses from the contralateral hindpaw. Previous series of experiments in the lab had shown that intrathecal injection of the vehicle used for these experiments (0-0.3% dimethylformamide (DMF) in saline) had no effect on any behavioural reflex responses in CCI or naïve animals with all animals assessed here and previously being of the same age, sex, weight and strain it was felt unwarranted here to repeat such experiments again.

The p38 MAP kinase inhibitor SB 203580 ***[see Figure 4.2 A and B]***

The p38 MAP kinase inhibitor SB 203580 (5nmol) was injected in animals at the peak of ipsilateral behavioural reflex sensitisation following CCI. The baseline (pre-injection) paw withdrawal latency (PWL) was measured as ipsilateral, 9.4 ± 0.5 seconds and

contralateral 14.8 ± 1.3 seconds (mean latency ± SEM; n=6). Injection of SB 203580 caused a significant reversal of the thermal hyperalgesia that had been seen prior to injection, for up to 75 min post-injection († $p<0.05$; One Way Repeated Measures ANOVA followed by Dunnett's post-hoc analysis), with maximal reversal of ipsilateral thermal hyperalgesia to 18.1 ± 0.7 seconds and contralateral was 17.3 ± 1.2 seconds (mean latency ± SEM) at 35 minutes post injection. The baseline (pre-injection) paw withdrawal threshold (PWT) required to elicit a response was ipsilateral 1610 ± 273 mN/mm^2 and contralateral 4831 ± 0 mN/mm^2 (mean threshold ± SEM; n=6). Injection of SB 203580 caused a significant reversal of the mechanical allodynia seen prior to injection for 55 minutes post-injection († $p<0.05$; Friedman test on ranks followed by Dunn's pos- hoc analysis), with maximal reversal of ipsilateral mechanical allodynia to 3929 ± 368 mN/mm^2 and contralateral was 4831 ± 0 mN/mm^2 (mean threshold ± SEM) at 15 minutes post injection.

The p42/44 MAP kinase pathway inhibitor PD 098059 ***[see Figure 4.2 C and D]***

The p42/44 MAP kinase pathway inhibitor PD 098059 (2.5nmol) was injected in animals at the peak of ipsilateral behavioural reflex sensitisation following CCI. The baseline (pre-injection) paw withdrawal latency (PWL) was measured as ipsilateral, 9.6 ± 0.4 seconds and contralateral 15.5 ± 0.3 seconds (mean latency ± SEM; n=6). Injection of PD 098059 caused a significant reversal of the thermal hyperalgesia that had been seen prior to injection, for up to 55 min post-injection († $p<0.05$; One Way Repeated Measures ANOVA followed by Dunnett's post-hoc analysis), with maximal reversal of ipsilateral thermal hyperalgesia to 17.2 ± 1.1 seconds and contralateral was 15.4 ± 0.5 seconds (mean latency ± SEM) at 20 minutes post injection. The baseline (pre-injection) paw withdrawal threshold (PWT) required to elicit a response was ipsilateral 978 ± 126 mN/mm^2 and contralateral 4831 ± 0 mN/mm^2 (mean threshold ± SEM; n=6). Injection of PD 098059 caused a significant reversal of the mechanical allodynia seen prior to injection for 40 minutes post-injection († $p<0.05$; Friedman test on ranks followed by Dunn's post-hoc analysis), with maximal reversal of ipsilateral mechanical allodynia to 3929 ± 368 mN/mm^2 and contralateral 4831 ± 0 mN/mm^2 (mean threshold ± SEM) at 35 minutes post injection.

The p42/44 MAP kinase pathway inhibitor U 0126 ***[see Figure 4.3 A and B]***

The p42/44 MAP kinase pathway inhibitor U 0126 (1.5nmol) was injected in animals at the peak of ipsilateral behavioural reflex sensitisation following CCI. The baseline (pre-injection) paw withdrawal latency (PWL) was measured as ipsilateral, 8.8 ± 0.5 seconds and contralateral 13.2 ± 1.4 seconds (mean latency ± SEM; n=8). Injection of U 0126 caused a significant reversal of the thermal hyperalgesia that had been seen prior to injection, for up to 60 min post-injection († $p<0.05$; One Way Repeated Measures ANOVA followed by Dunnett's post-hoc analysis), with maximal reversal of ipsilateral thermal hyperalgesia to 19.1 ± 0.6 seconds and contralateral was 16.2 ± 3.1 seconds (mean latency ± SEM) at 25 minutes post injection. The baseline (pre-injection) paw withdrawal threshold (PWT) required to elicit a response was ipsilateral 1294 ± 182 mN/mm^2 and contralateral 4831 ± 0 mN/mm^2 (mean threshold ± SEM; n=8). Injection of U 0126 caused a significant reversal of the mechanical allodynia seen prior to injection for 35 minutes post-injection († $p<0.05$; Friedman test on ranks followed by Dunn's post-hoc analysis), with maximal reversal of ipsilateral mechanical allodynia to 3274 ± 658 mN/mm^2 and contralateral 4831 ± 0 mN/mm^2 (mean threshold ± SEM) at 15 minutes post injection.

U 0124, an less active analogue of U 0126 ***[see Figure 4.3 C and D]***

The less active analogue of U 0126, U 0124 (1.5nmol) was injected in animals at the peak of ipsilateral behavioural reflex sensitisation following CCI. The baseline (pre-injection) paw withdrawal latency (PWL) was measured as ipsilateral, 9.2 ± 0.7 seconds and contralateral 17.3 ± 0.1 seconds (mean latency ± SEM; n=6). Injection of U 0124 caused a significant reversal of the thermal hyperalgesia that had been seen prior to injection, at 20-25 minutes post-injection († $p<0.05$; One Way Repeated Measures ANOVA followed by Dunnett's post-hoc analysis), with maximal reversal of ipsilateral thermal hyperalgesia to 13.1 ± 3.0 seconds and contralateral 18.1 ± 1.1 seconds (mean latency ± SEM) at 20 minutes post injection. This reversal of thermal hyperalgesia seen was to a very much smaller extent than that seen with the active compound U 0126 and indeed had a greater error margin. The baseline (pre-injection) paw withdrawal threshold (PWT) required to

elicit a response was ipsilateral 1827 ± 286 mN/mm^2 and contralateral 4831 ± 0 mN/mm^2 (mean threshold ± SEM; n=6). Injection of U 0124 did not cause a significant reversal of the mechanical allodynia seen prior to injection.

4.3.3 The activation of p38 and p42/44 MAP kinases following nerve injury compared to naïve controls *[see Figure 4.4 and Table 4.1 A]*

The levels of phosphorylated (activated) p38 and p42/44 and corresponding pan (i.e. total) p38 and p42/44 expression in the spinal cord extracts of animals displaying peak behavioural reflex sensitisation following CCI were assessed by immunoblot, on the ipsilateral (Ipsi) and contralateral (Con) sides of nerve injured animals and in naïve animals. Following CCI there was an ipsilateral increase in the level of phospho-p38 and phospho-p42/44 compared to the contralateral side and naïve animals. No significant alterations occurred in the overall levels of p38 (pan-p38) or p42/44 (pan-p42/44) as a result of nerve injury. The densitometric ratio of phosphorylated to pan p38 immunoreactivity showed a significant increase, due to CCI to 63.5 ± 5.7 arbitrary density units ipsilateral compared to contralateral value of 48.4 ± 6.2 arbitrary density units and naïve value of 44.6 ± 4.6 arbitrary density units (mean ± SEM; values derived from quantitative densitometry; $p<0.05$; Wilcoxon test; n=5 in all cases). The densitometric ratio of phosphorylated to pan p42/44 immunoreactivity also showed a significant increase due to CCI, to 56.1 ± 4.8 arbitrary density units ipsilateral compared to contralateral value of 35.9 ± 3.6 arbitrary density units and naïve value of 39.6 ± 7.1 arbitrary density units (mean ± SEM; $p<0.05$ Wilcoxon test; n=5 in all cases). The levels of phosphorylated p38 expression and p42/44 expression on the contralateral side of CCI were not significantly different from those in naïve animals.

4.3.4 Intrathecal administration of either the glial inhibitor propentofylline (PPT) or the TNF-α receptor antagonist (WP9QY) attenuated nerve-injury induced behavioural reflex sensitisation

The effects of intrathecal administration of the glial inhibitor propentofylline, PPT and of the TNF-α receptor antagonist, WP9QY on nerve injury-induced thermal hyperalgesia and mechanical allodynia were assessed. Intrathecal injections were made in animals that

displayed peak ipsilateral behavioural reflex sensitisation, with the effect of all drugs assessed until recovery to pre-injection values. Neither of these drugs had any significant effects on responses mediated by the contralateral hindpaw.

The glial inhibitor propentofylline, PPT *[see Figure 4.5 A and B]*

When the glial inhibitor PPT (0.5μmol) was injected in CCI animals, the baseline (pre-injection) paw withdrawal latency (PWL) was measured as ipsilateral, 9.8 ± 0.5 seconds and contralateral 16.5 ± 0.5 seconds (mean latency ± SEM; n=5). Injection of PPT caused a significant reversal of the thermal hyperalgesia that had been seen prior to injection for up to 40 min post-injection († $p<0.05$; One Way Repeated Measures ANOVA followed by Dunnett's post-hoc analysis), with maximal reversal of ipsilateral thermal hyperalgesia to 15.9 ± 0.5 seconds and contralateral 14.4 ± 1.2 seconds (mean latency ± SEM) at 20 minutes post injection. The baseline (pre-injection) paw withdrawal threshold (PWT) required to elicit a response was ipsilateral 1610 ± 573 mN/mm^2 and contralateral 4831 ± 0 mN/mm^2 (mean threshold ± SEM; n=5). Injection of PPT caused a significant reversal of the mechanical allodynia seen prior to injection for 45 minutes post-injection († $p<0.05$; Friedman test on ranks followed by Dunn's post-hoc analysis), with maximal reversal of ipsilateral mechanical allodynia to 3256 ± 931 mN/mm^2 and contralateral 4831 ± 0 mN/mm^2 (mean threshold ± SEM; n=5) at 20 minutes post injection.

The TNF-α receptor antagonist, WP9QY *[see Figure 4.5 C and D]*

When the TNF-α receptor peptide antagonist, WP9QY (25μg), which efficiently antagonises the effect of TNF-α binding to the TNF receptor 1 (Takasaki et al., 1997), was injected in CCI animals, the baseline (pre-injection) paw withdrawal latency (PWL) was measured as ipsilateral, 9.9 ± 0.7 seconds and contralateral 15.7 ± 0.9 seconds (mean latency ± SEM; n=5). Injection of WP9QY caused a significant reversal of the thermal hyperalgesia that had been seen prior to injection for up to 35 min post-injection († $p<0.05$; One Way Repeated Measures ANOVA followed by Dunnett's post-hoc analysis), with maximal reversal of ipsilateral thermal hyperalgesia to 16.2 ± 1.2 seconds and contralateral 14.9 ± 1.3 seconds (mean latency ± SEM) at 35 minutes post injection. The baseline (pre-injection) paw withdrawal threshold (PWT) required to elicit a

response was ipsilateral 1610 ± 126 mN/mm^2 and contralateral 4831 ± 0 mN/mm^2 (mean threshold ± SEM; n=5). Injection of WP9QY caused a significant reversal of the mechanical allodynia seen prior to injection for 30 minutes post-injection († $p<0.05$; Friedman test on ranks followed by Dunn's post-hoc analysis), with maximal reversal of ipsilateral mechanical allodynia to 3929 ± 658 mN/mm^2 and contralateral 4831 ± 0 mN/mm^2 (mean threshold ± SEM) at 15-20 minutes post injection.

4.3.5 The activation of p38 and p42/44 MAP kinases following nerve injury is attenuated by incubation of the spinal cord with the glial inhibitor propentofylline (PPT) or the TNF-α receptor antagonist (WP9QY) and the TNF-α synthesis inhibitor thalidomide compared to saline controls ***[see Figure 4.6 and Table 4.2 A, C]***

CCI nerve injury results in an ipsilateral increase in the level of activated (phosphorylated) p38 and p42/44 as shown above (Section 4.3.3). Glial cells are known to express p38 and p42/44 MAP kinases, so the effect of glial blockade on MAP kinase activation was examined. Incubation of the spinal cord with of the glial inhibitor propentofylline, PPT (10mM), the TNF-α receptor antagonist, WP9QY (0.5mg/ml) and the TNF-α synthesis inhibitor, thalidomide (200μM), to the dorsal surface of the spinal cord for 30 minutes resulted in the suppression of increased activation of both p38 (phospho-p38) and p42/44 (phospho-p42/44) MAP kinases that occurs following nerve injury when compared to saline controls. In saline (0.9%) controls the densitometric ratio of phosphorylated to pan p38 MAP kinase immunoreactivity showed a significant ipsilateral increase to 63.5 ±5.7 arbitrary density units compared to a contralateral value of 48.4 ± 6.2 arbitrary density units (mean ± SEM; values derived from quantitative densitometry; $p<0.05$ Wilcoxon test; n=5). The densitometric ratio of phosphorylated to pan p42/44 MAP kinase immunoreactivity also shows a significant increase to 56.1 ± 4.8 arbitrary density units compared to contralateral value of 35.9 ± 3.6 arbitrary density units in saline controls (mean ± SEM; $p<0.05$ Wilcoxon test; n=5).

The incubation of the spinal cord with PPT suppressed this increased level of phosphorylated p38 to a phospho:pan densitometric ratio of 37.4 ± 5.9 arbitrary density units ipsilateral, similar to the contralateral level of 39.8 ± 4.4 arbitrary density units and

phosphorylated p42/44 to 30.9 ± 4.3 arbitrary density units ipsilateral, similar to the contralateral level of 38.3 ± 4.6 arbitrary density units (mean ± SEM; n=5). The incubation of the spinal cord with WP9QY suppressed the CCI-induced increased level of phosphorylated p38 to 40.3 ± 5.0 arbitrary density units ipsilateral, similar to the contralateral level of 36.3 ± 7.5 arbitrary density units and phosphorylated p42/44 to 41.3 ± 8.3 arbitrary density units ipsilateral, similar to the contralateral level of 34.8 ± 5.2 arbitrary density units (mean ± SEM; n=5). The incubation of the spinal cord with thalidomide suppressed a CCI-induced increased level of phosphorylated p38 to 41.5 ± 6.8 arbitrary density units ipsilateral, similar to the contralateral level of 39.6 ± 4.8 arbitrary density units (mean ± SEM; n=5). Thalidomide also suppressed the level of phosphorylated p42/44 to 35.0 ± 6.2 arbitrary density units ipsilateral, similar to the contralateral level of 45.9 ± 6.9 arbitrary density units (mean ± SEM). The incubation of the spinal cord with each of these drugs suppressed the nerve injury-induced increase in phosphorylated p38 and p42/44 MAP kinases resulting, such that there was now no statistically significant difference between ipsilateral and contralateral values for each drug or with the contralateral side of the saline treated control (as determined by Wilcoxon test). There was no significant change in the overall (pan) levels of p38 or p42/44 MAP kinase following the application of any of these drugs.

4.3.6 The effect of intrathecal administration of the selective antagonists for the $VPAC_1$, $VPAC_2$, PAC_1, NK_1 and NK_2 and the receptors on nerve injury-induced behavioural reflex sensitisation

The effects of the intrathecal administration of the selective antagonists for $VPAC_1$ ([Ac-His^1, D-Phe^2, Lys^{15}, Arg^{16}, Leu^{17}]-VIP(3-7)GRF(8-27)), $VPAC_2$ ([des(1-4), Arg^{16}]-Ro 25-1553), PAC_1 ($PACAP_{6-38}$), NK_1 (RP 67580) and NK_2 (SR 48968) receptors on nerve injury-induced thermal hyperalgesia and mechanical allodynia was assessed. Animals that displayed peak ipsilateral behavioural reflex sensitisation were used for the intrathecal administration of all drugs, with the effect of all drugs being assessed until recovery to pre-injection values. None of the drugs tested had any significant effects on the contralateral hindpaw. Marked effects were seen only with the $VPAC_2$ and NK_2 receptor antagonists.

$VPAC_2$ receptor antagonist ***[see Figure 4.7 A and B and Table 4.3]***

The selective antagonist for the $VPAC_2$ receptor [des(1-4), Arg^{16}]-Ro 25-1553 (0.1nmol) was injected in animals at the peak of ipsilateral behavioural reflex sensitisation following CCI. The baseline (pre-injection) paw withdrawal latency (PWL) was measured as ipsilateral, 12.2 ± 1.0 seconds and contralateral 19.8 ± 0.4 seconds (mean latency ± SEM; n=7). Injection of [Des(1-4), Arg^{16}]-Ro 25-1553 caused a significant reversal of the ipsilateral thermal hyperalgesia seen prior to injection for 70 min post-injection († $p<0.05$; One Way Repeated Measures ANOVA followed by Dunnett's post-hoc analysis), with maximal reversal of ipsilateral thermal hyperalgesia to 20.0 ± 1.1 seconds and contralateral 18.1 ± 1.8 seconds (mean latency ± SEM) at 15-40 minutes post injection. The baseline (pre-injection) paw withdrawal threshold (PWT) required to elicit a response was ipsilateral 1610 ± 126 mN/mm^2 and contralateral 4831 ± 0 mN/mm^2 (mean threshold ± SEM; n=7). Injection of [Des(1-4), Arg^{16}]-Ro 25-1553 caused a significant reversal of the mechanical allodynia seen prior to injection for 35 minutes post-injection († $p<0.05$; Friedman test on ranks followed by Dunn's post-hoc analysis), with maximal reversal of ipsilateral mechanical allodynia to 3256 ± 658 mN/mm^2 and contralateral 4831 ± 0 mN/mm^2 (mean threshold ± SEM) at 15-25 minutes post injection. The mean percent reversal of ipsilateral sensitisation from 15-30 min following intrathecal administration of [Des(1-4), Arg^{16}]-Ro 25-1553 was 93.6 ± 5.2% for thermal hyperalgesia (*$p < 0.05$, One Way Repeated Measures ANOVA followed by Dunnett's pot-hoc analysis test) and 41.2 ± 6.1% for mechanical allodynia (*$p < 0.05$, Friedman test on ranks followed by a Dunn's post-hoc test; means ± SEM).

NK_2 receptor antagonist ***[see Figure 4.7 C and D and Table 4.3]***

The selective antagonist for the NK_2 receptor SR 48968 (5nmol) was injected in animals at the peak of ipsilateral behavioural reflex sensitisation following CCI. The baseline (pre-injection) paw withdrawal latency (PWL) was measured as ipsilateral, 9.3 ± 0.2 seconds and contralateral 15.9 ± 0.5 seconds (mean latency ± SEM; n=6). The NK_2 receptor antagonist caused a significant reversal of the ipsilateral thermal hyperalgesia seen prior to injection for 35 mins post-injection († $p<0.05$; One Way Repeated Measures

ANOVA followed by Dunnett's post-hoc analysis), with maximal reversal of ipsilateral thermal hyperalgesia to 13.8 ± 1.8 seconds and contralateral 14.3 ± 0.9 seconds (mean latency ± SEM) at 15-25 minutes post injection. The baseline (pre-injection) paw withdrawal threshold (PWT) required to elicit a response was ipsilateral 1294 ± 141 mN/mm^2 and contralateral 4831 ± 0 mN/mm^2 (mean threshold ± SEM; n=6). Injection of SR 48968 caused a significant reversal of the ipsilateral mechanical allodynia seen prior to injection for 45 minutes post-injection († $p<0.05$; Friedman test on ranks followed by Dunn's post-hoc analysis), with maximal reversal of ipsilateral mechanical allodynia to 4079 ± 589 mN/mm^2 and contralateral 4831 ± 0 mN/mm^2 (mean threshold ± SEM) at 20 minutes post injection. The mean percent reversal of ipsilateral sensitisation from 15-30 min following intrathecal administration of SR 48968 was 89.6 ± 4.3% for thermal hyperalgesia (*$p < 0.05$, One Way Repeated Measures ANOVA followed by Dunnett's post-hoc analysis) and 73.2 ± 6.5% for mechanical allodynia (*$p < 0.05$, Friedman test on ranks followed by a Dunn's post-hoc test; means ± SEM).

$VPAC_1$ receptor antagonist ***[see Table 4.3]***

The selective antagonist for the $VPAC_1$ receptor ([Ac-His^1, D-Phe^2, Lys^{15}, Arg^{16}, Leu^{17}]-VIP(3-7)GRF(8-27); 0.1 nmol) was injected in animals at the peak of ipsilateral behavioural reflex sensitisation following CCI. The baseline (pre-injection) paw withdrawal latency (PWL) was measured as ipsilateral, 8.9 ± 0.5 seconds and contralateral 15.0 ± 0.5 seconds (mean latency ± SEM; n=6). Injection of [Ac-His^1, D-Phe^2, Lys^{15}, Arg^{16}, Leu^{17}]-VIP(3-7)GRF(8-27) did not result in a significant reversal of the ipsilateral thermal hyperalgesia seen prior to injection, with values remaining similar to baseline values. The baseline (pre-injection) paw withdrawal threshold (PWT) required to elicit a response was ipsilateral 978 ± 0 mN/mm^2 and contralateral 4831 ± 0 mN/mm^2 (mean threshold ± SEM; n=6). Injection of [Ac-His^1, D-Phe^2, Lys^{15}, Arg^{16}, Leu^{17}]-VIP(3-7)GRF(8-27) did not cause a significant reversal of the ipsilateral mechanical allodynia seen prior to injection, values remained similar to baseline values. The mean percent reversal of ipsilateral sensitisation from 15-30 min following intrathecal administration of [Ac-His^1, D-Phe^2, Lys^{15}, Arg^{16}, Leu^{17}]-VIP(3-7)GRF(8-27) was 8.3 ± 2.0% for thermal hyperalgesia and 12.4 ± 4.6% for mechanical allodynia (means ± SEM).

PAC_1 receptor antagonist ***[see Table 4.3]***

The selective antagonist for the PAC_1 receptor ($PACAP_{6-38}$; 0.1 nmol) was injected in animals at the peak of ipsilateral behavioural reflex sensitisation following CCI. The baseline (pre-injection) paw withdrawal latency (PWL) was measured as ipsilateral, 7.9 ± 0.7 seconds and contralateral 14.9 ± 0.6 seconds (mean latency ± SEM; n=6). Injection of $PACAP_{6-38}$ caused a significant reversal of the ipsilateral thermal hyperalgesia seen prior to injection for 30 min post-injection († $p<0.05$; One Way Repeated Measures ANOVA followed by Dunnett's post-hoc analysis), with maximal reversal of ipsilateral thermal hyperalgesia to 10.3 ± 1.1 seconds and contralateral 13.1 ± 1.8 (mean latency ± SEM) at 15 minutes post injection. The baseline (pre-injection) paw withdrawal threshold (PWT) required to elicit a response was ipsilateral 978 ± 126 mN/mm^2 and contralateral 4831 ± 0 mN/mm^2 (mean threshold ± SEM; n=6). Injection of $PACAP_{6-38}$ caused a significant reversal of the ipsilateral mechanical allodynia seen prior to injection for 25 minutes post-injection († $p<0.05$; Friedman test on ranks followed by Dunn's post-hoc analysis), with maximal reversal of ipsilateral mechanical allodynia to 2182 ± 573 mN/mm^2 and contralateral 4831 ± 0 mN/mm^2 (mean threshold ± SEM) at 15-25 minutes post injection. The mean percent reversal of ipsilateral sensitisation from 15-30 min following intrathecal administration of $PACAP_{6-38}$ was 27.6 ± 4.1% for thermal hyperalgesia (*$p < 0.05$, One Way Repeated Measures ANOVA followed by Dunnett's pot-hoc analysis) and 19.5 ± 3.3% for mechanical allodynia (*$p < 0.05$, Friedman test on ranks followed by a Dunn's post-hoc test; means ± SEM). The significant reversal of thermal hyperalgesia and mechanical allodynia observed here was notably less than that produced by the intrathecal injection of the selective antagonist for the $VPAC_2$ receptor.

NK_1 receptor antagonist ***[see Table 4.3]***

The selective antagonist for the NK_1 receptor (RP 67580; 5nmol) was injected in animals at the peak of ipsilateral behavioural reflex sensitisation following CCI. The baseline (pre-injection) paw withdrawal latency (PWL) was measured as ipsilateral, 9.2 ± 1.0 seconds and contralateral 16.0 ± 0.9 seconds (mean latency ± SEM; n=6). Injection of RP 67580 did not result in a significant reversal of the ipsilateral thermal hyperalgesia seen

prior to injection, with values remaining similar to baseline values. The baseline (pre-injection) paw withdrawal threshold (PWT) required to elicit a response was ipsilateral 1609 ± 126 mN/mm^2 and contralateral 4831 ± 0 mN/mm^2 (mean threshold ± SEM; n=6). Injection of RP 67580 caused a significant reversal of the ipsilateral mechanical allodynia seen prior to injection for 30 minutes post-injection († $p<0.05$; Friedman test on ranks followed by Dunn's post-hoc analysis), with maximal reversal of ipsilateral mechanical allodynia to 3829 ± 501 mN/mm^2 and contralateral 4831 ± 0 mN/mm^2 (mean threshold ± SEM) at 15-20 minutes post injection. The mean percent reversal of ipsilateral sensitisation from 15-30 min following intrathecal administration of RP 67580 was 11.6 ± 4.8% for thermal hyperalgesia (not significant) and 22.9 ± 6.1% for mechanical allodynia (*$p < 0.05$, Friedman test on ranks followed by a Dunn's post-hoc test; means ± SEM). The significant reversal of mechanical allodynia observed here was notably less than that produced by the intrathecal injection of the selective NK_2 receptor antagonist.

4.3.7 The activation of p38 and p42/44 MAP kinases following nerve injury is prevented by incubation of the spinal cord with selective antagonists for $VPAC_2$, NK_2 or NMDA receptors *[see Figure 4.8 and Table 4.2 B, C]*

CCI nerve injury results in an ipsilateral increase in the level of both phosphorylated p38 and p42/44 as shown above (Section 4.3.3). The incubation of the spinal cord with the selective antagonists for $VPAC_2$ ([des(1-4), Arg^{16}]-Ro 25-1553; 2μM), NK_2 (SR 48968; 100μM) or NMDA ((R)-CPP; 10μM) receptors to spinal cord resulted in suppression of increased activation of both p38 (phospho-p38) and p42/44 (phospho-p42/44) MAP kinases that occurred following nerve injury when compared to saline controls. As outlined above (Section 4.3.5) the incubation of the spinal cord with saline had no effect on the CCI-induced increase in phosphorylated p38 to 63.5 ±5.7 arbitrary density units compared to contralateral value of 48.4 ± 6.2 arbitrary density units (mean ± SEM; values derived from quantitative densitometry; $p<0.05$ Wilcoxon test; n=5), or on the increase in phosphorylated p42/44 to 56.1 ± 4.8 arbitrary density units compared to contralateral value of 35.9 ± 3.6 arbitrary density units in saline controls (mean ± SEM; $p<0.05$ Wilcoxon test; n=5). The incubation of the spinal cord with [des(1-4), Arg^{16}]-Ro 25-1553 suppressed this CCI-induced activation of p38 to 39.3 ± 7.3 arbitrary density units

ipsilateral, similar to the contralateral level of 35.8 ± 6.0 arbitrary density units and p42/44 to 39.7 ± 4.4 arbitrary density units ipsilateral, similar to the contralateral level of 41.4 ± 5.0 arbitrary density units (mean ± SEM; n=5). SR 48968 suppressed the CCI-induced activation of p38 to 47.3 ± 5.5 arbitrary density units ipsilateral, similar to the contralateral level of 45.6 ± 4.8 arbitrary density units (mean ± SEM; n=5). SR 48968 also suppressed the CCI-induced activation of p42/44 to 37.9 ± 3.9 arbitrary density units ipsilateral, similar to the contralateral level of 37.1 ± 5.2 arbitrary density units (mean ± SEM n=5). In addition, incubation of the spinal cord with (R)-CPP suppressed the CCI-induced activation of p38 to 42.3 ± 7.6 arbitrary density units ipsilateral, similar to the contralateral level of 44.1 ± 7.1 arbitrary density units and of p42/44 to 39.6 ± 4.9 arbitrary density units ipsilateral, similar to the contralateral level of 42.8 ± 4.3 arbitrary density units (mean ± SEM n=5). The incubation of the spinal cord with each of these drugs were sufficient to fully suppress the nerve injury induced increase in phosphorylated p38 and p42/44 MAP kinases resulting in no statistically significant difference between ipsilateral and contralateral values for each drug or compared with the contralateral side of the saline treated control (as determined by Wilcoxon test). There was no significant change in the overall (pan) levels of p38 or p42/44 MAP kinase following the application of any of these drugs.

4.3.8 Intrathecal administration of $VPAC_2$ or NK_2 receptor agonist results in behavioural reflex sensitisation, which is prevented by co-administration of either p38 or p42/44 MAP kinase pathway inhibitors in naïve animals

The effects of the intrathecal administration of agonists for the $VPAC_2$ or NK2 receptor (Ro 25-1553 and GR 64349 respectively) on naïve animal's responses to a noxious heat stimulus were measured as (bilateral) paw withdrawal latency (due to time constraints responses to mechanical stimuli were not measured for the agonist study). The effects of co-administration of the p38 MAP kinase inhibitor SB 203580 or the p42/44 MAP kinase pathway inhibitor U 0126 was also assessed. The effects of all drugs were measured until recovery to pre-injection values. Since Ro 25-1553 caused relatively greater activation of p38 than p42/44 and GR 64349 caused relatively greater activation of p42/44 than p38

(see Section 4.3.9 below) and both time and resources were limited, only the blocker for the more strongly implicated MAP kinase was tested on each agonist.

$VPAC_2$ receptor agonist *[see Figure 4.9 A]*

The agonist for the $VPAC_2$ receptor, Ro 25-1553 (0.5nmol) was injected in naïve animals. The baseline (pre-injection) bilateral paw withdrawal latency (PWL) was measured as 15.4 ± 0.2 seconds (mean latency ± SEM; n=6). Ro 25-1553 caused a significant sensitisation of the thermal response compared to that prior to injection for 55 mins post-injection († $p<0.05$; One Way Repeated Measures ANOVA followed by Dunnett's post-hoc analysis), with maximal reduction of latency to 10.5 ± 1.2 seconds (mean latency ± SEM) at 30 minutes post injection.

$VPAC_2$ receptor agonist co-administered with the p38 MAP kinase inhibitor *[see Figure 4.9 B]*

The agonist for the $VPAC_2$ receptor Ro 25-1553 (0.5nmol) and the p38 MAP kinase inhibitor SB 203580 (5nmol) were injected in naïve animals. The baseline (pre-injection) bilateral paw withdrawal latency (PWL) was measured as 14.8 ± 0.4 seconds (mean latency ± SEM; n=6), co-administration of the agonist Ro 25-1553 with SB 203580 prevented the development of the thermal sensitisation seen when Ro 25-1553 was administered alone, such that co-administration resulted in reversal of latency to 14.5 ± 1.3 seconds (mean latency ± SEM) at 20-30 minutes post-injection, which was not significantly different to pre-drug (baseline) values.

NK_2 receptor agonist *[see Figure 4.9 C]*

The agonist for the NK_2 receptor, GR 64349 (1.5nmol) was injected in naïve animals. The baseline (pre-injection) bilateral paw withdrawal latency (PWL) was measured as 14.6 ± 0.3 seconds (mean latency ± SEM; n=6). GR 64349 caused a significant sensitisation of the thermal response compared to prior to injection for 35 mins post-injection († $p<0.05$; One Way Repeated Measures ANOVA followed by Dunnett's post-hoc analysis), with maximal reduction of latency to 11.4 ± 0.7 seconds (mean latency ± SEM) at 20 minutes post injection.

NK_2 receptor agonist co-administered with p42/44 MAP kinase pathway inhibitor ***[see Figure 4.9 D]***

The agonist for the NK_2 receptor, GR 64349 (1.5nmol) and the p42/44 MAP kinase pathway inhibitor U 0126 (1.5nmol) were injected in naïve animals. The baseline (pre-injection) bilateral paw withdrawal latency (PWL) was measured as 14.4 ± 0.3 seconds (mean latency ± SEM; n=6), co-administration of the agonist GR 64349 with U 0126 blocked the development of the thermal sensitisation seen when GR 64349 was administered alone. That is co-administration resulted in reversal to 14.2 ± 1.4 seconds (mean latency ± SEM) at 20-30 minutes post-injection, which was not significantly different to pre-drug (baseline) values.

4.3.9 The incubation of the spinal cord with the $VPAC_2$ and the NK_2 receptor agonists in naïve animals resulted in increased activation of p38 and p42/44 MAP kinases that was prevented by co-incubation of the glial inhibitor propentofylline ***[see Figure 4.10 and Table 4.1 B]***

CCI nerve injury results in an ipsilateral increase in the level of both phosphorylated p38 and p42/44 as shown above (Section 4.3.3). The incubation of the spinal cord with the agonist for $VPAC_2$ (Ro 25-1553; 30μM) and NK_2 (GR 64349; 50μM) receptors resulted in increased activation of both p38 (phospho-p38) and p42/44 (phospho-p42/44) MAP kinases in naïve animals when compared to saline controls. The incubation of the spinal cord with saline (0.9%) did not significantly increase the levels of phosphorylated p38 (36.5 ± 4.2 arbitrary density units), or of phosphorylated p42/44 (39.0 ± 7.3 arbitrary density units; from those in naïve controls see Section 4.3.3; mean ± SEM; n=5). Incubation of the spinal cord with Ro 25-1553 significantly increased the phosphorylation ratios of both p38 to 60.7 ± 6.3 arbitrary density units and p42/44 to 67.1 ± 4.0 arbitrary density units (mean ± SEM; $p<0.05$ Wilcoxon test; n=5) compared to saline controls. The incubation of the spinal cord with GR 64349 significantly increased the phosphorylation ratios of p38 to 53.2 ± 4.8 arbitrary density units and of p42/44 to 94.4 ± 5.8 arbitrary density units (mean ± SEM; $p<0.05$ Wilcoxon test; n=5) compared to saline controls. The $VPAC_2$ receptor agonist caused a relatively greater activation of p38 MAP kinase than

did the NK_2 receptor agonist and the NK_2 receptor agonist caused a relatively greater activation of p42/44 than p38 MAP kinase.

The co-incubation of PPT (10mM) with Ro 25-1553 (30μM) blocked the Ro 25-1553-induced increase in the phosphorylation of p38 and p42/44, that is co-incubation did not significantly increase the levels of phosphorylated p38 (39.9 ± 5.3 arbitrary density units) or p42/44 (34.8 ± 4.6 arbitrary density units) compared to saline controls (mean ± SEM; n=5). The co-incubation of PPT (10mM) with GR 64349 (50μM) blocked the GR 64349-induced increase in the phosphorylation of both p38 and p42/44, such that co-incubation did not significantly increase the levels of phosphorylated p38 (43.3 ± 6.0 arbitrary density units) or p42/44 (40.0 ± 5.7 arbitrary density units) compared to saline controls (mean ± SEM; n=5). The co-incubation of PPT with Ro 25-1553 and GR 64 349 suppressed the increased phosphorylation of both p38 and p42/44 MAP kinases, to levels that were not significantly different from saline controls. There was no significant change in the overall (pan) levels of p38 or p42/44 MAP kinase following the incubation of the spinal cord with any of these drugs.

Figure 4.1

The time course of development of thermal hyperalgesia, mechanical and cold allodynia ipsilateral to nerve injury in a model of experimental mononeuropathy (CCI).

Data show mean ± SEM responses prior to surgery (baseline) and following the induction of CCI (post surgery; n=25). **(A)** Paw withdrawal latency (PWL) from a noxious thermal stimulus (Hargreaves' thermal stimulator) ipsilateral to CCI (O) showed significant differences between post-operative and pre-operative values († $p<0.05$; One Way Repeated Measures ANOVA followed by Dunnett's post-hoc analysis) and from post-operative contralateral (■) values (* $p<0.05$; Student's t-test). No thermal hyperalgesia was seen on the contralateral side (■). **(B)** Paw withdrawal thresholds (PWT) from mechanical stimulation (von Frey filaments) showed significant reductions in post-operative compared to pre-operative values ipsilateral (O) to CCI († $p<0.05$; Friedman test on ranks followed be Dunn's post-hoc analysis) and between post-operative ipsilateral and contralateral values (* $p<0.05$; Wilcoxon test). No significant differences were seen in the contralateral side (■). **(C)** The suspended paw elevation time (SPET) to a cold water stimulus showed significant ipsilateral to CCI (O) differences between post-operative and pre-operative values († $p<0.05$; Friedman test on ranks followed be Dunn's post-hoc analysis) and from post-operative contralateral (■) values (* $p<0.05$; Wilcoxon test). No cold allodynia was observed on the contralateral side (■).

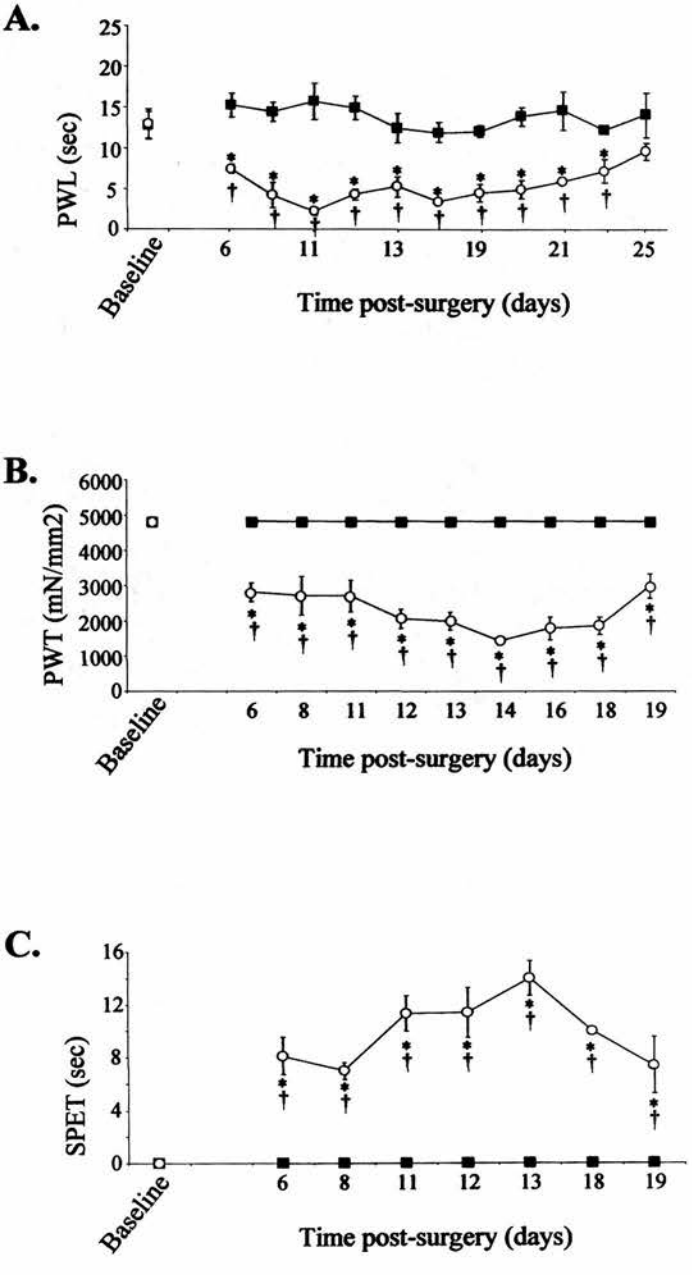
A.
PWL (sec)
25
20
15
10
5
0
Baseline
6
11
13
19
21
25
Time post-surgery (days)
B.
PWT (mN/mm2)
6000
5000
4000
3000
2000
1000
0
Baseline
6
8
11
12
13
14
16
18
19
Time post-surgery (days)
C.
SPET (sec)
16
12
8
4
0
Baseline
6
8
11
12
13
18
19
Time post-surgery (days)

Figure 4.2

Effects of the intrathecal administration of the p38 MAP kinase inhibitor SB 203580 and the p42/44 MAP kinase pathway inhibitor PD 098059 on nerve injury-induced thermal hyperalgesia and mechanical allodynia.

(A-D) Data show mean ± SEM responses prior to (baseline) and following intrathecal administration of SB 203580 (5nmol; n=6) or PD 098059 (2.5nmol; n=6). In all cases the animals were at the peak of behavioural reflex sensitisation as a result of CCI to the sciatic nerve, as determined by a significant reduction in ipsilateral (O) paw withdrawal latency from a noxious thermal stimuli (PWL; * $p<0.05$, Student's t-test, **A, C,**) or paw withdrawal threshold to mechanical stimuli (PWT; * $p<0.05$, Wilcoxon test, **B, D**) compared to contralateral withdrawal responses (■). Following intrathecal injection (shown by arrow), (**A**) SB 203580 or (**C**) PD 098059 significantly increased ipsilateral thermal paw withdrawal latencies in comparison to pre-injection ipsilateral values († $p<0.05$, One-Way Repeated Measures ANOVA followed by a Dunnett's test) with differences between ipsilateral and contralateral post-injection returning (* $p<0.05$, Student's t-test), while there was no significant alteration in the contralateral response. (**B**) SB 203580 and (**D**) PD 098059 show significantly increased ipsilateral mechanical paw withdrawal thresholds in comparison to pre-injection ipsilateral values († $p<0.05$, Friedman test on ranks followed by a Dunn's post-hoc test), again with differences between ipsilateral and contralateral post-injection returning (* $p<0.05$, Wilcoxon test), no significant alteration in the contralateral response was noted. Full recovery to pre-drug response levels was seen in each case.

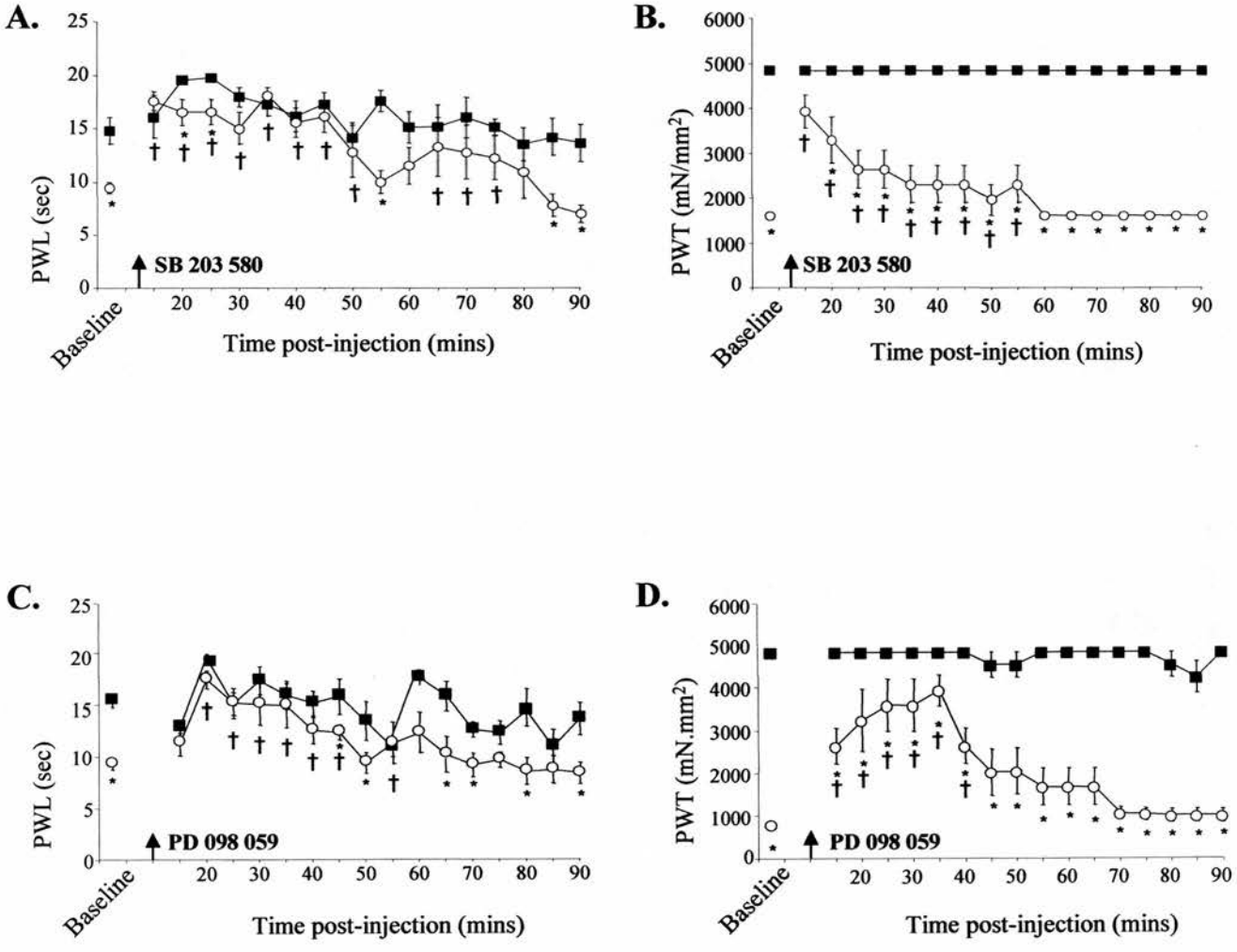
A.
PWL (sec)
SB 203 580
Baseline
Time post-injection (mins)
B.
PWT (mN/mm2)
SB 203 580
Baseline
Time post-injection (mins)
C.
PWL (sec)
PD 098 059
Baseline
Time post-injection (mins)
D.
PWT (mN.mm2)
PD 098 059
Baseline
Time post-injection (mins)

Figure 4.3

Effects of the intrathecal administration of the p42/44 MAP kinase pathway inhibitor U 0126 and its less active analogue U 0124 on nerve injury-induced thermal hyperalgesia and mechanical allodynia.

(A-D) Data show mean ± SEM responses prior to (baseline) and following intrathecal administration of either U 0126 (1.5nmol; n=8) or U 0124 (1.5nmol; n=6). In all cases the animals were at the peak of behavioural reflex sensitisation as a result of CCI to the sciatic nerve, as shown by a significant reduction in ipsilateral (O) paw withdrawal latency from a noxious thermal stimuli (PWL; * $p<0.05$, Student's t-test, **A**, **C**) or paw withdrawal threshold to mechanical stimuli (PWT; * $p<0.05$, Wilcoxon test, **B**, **D**) compared to contralateral withdrawal responses (■). Following intrathecal injection (shown by arrow), (**A**) U 0126 significantly increased ipsilateral thermal paw withdrawal latencies in comparison to pre-injection ipsilateral values († $p<0.05$, One-Way Repeated Measures ANOVA followed by a Dunnett's test) with differences between ipsilateral and contralateral post-injection returning (* $p<0.05$, Student's t-test), while there was no significant alteration in the contralateral response, while (**C**) U 0124 significantly increased ipsilateral thermal paw withdrawal latencies to a lesser extent than the active compound U 0126. (**B**) U 0126 significantly increased ipsilateral mechanical paw withdrawal thresholds in comparison to pre-injection ipsilateral values († $p<0.05$, Friedman test on ranks followed by a Dunn's post-hoc test), again with differences between ipsilateral and contralateral post-injection returning (* $p<0.05$, Wilcoxon test), no significant alteration in the contralateral response was noted. (**D**) U 0124, the less active analogue of U 0126, did not result in significant reversal of mechanical allodynia. Full recovery to pre-drug response levels was seen in each case.

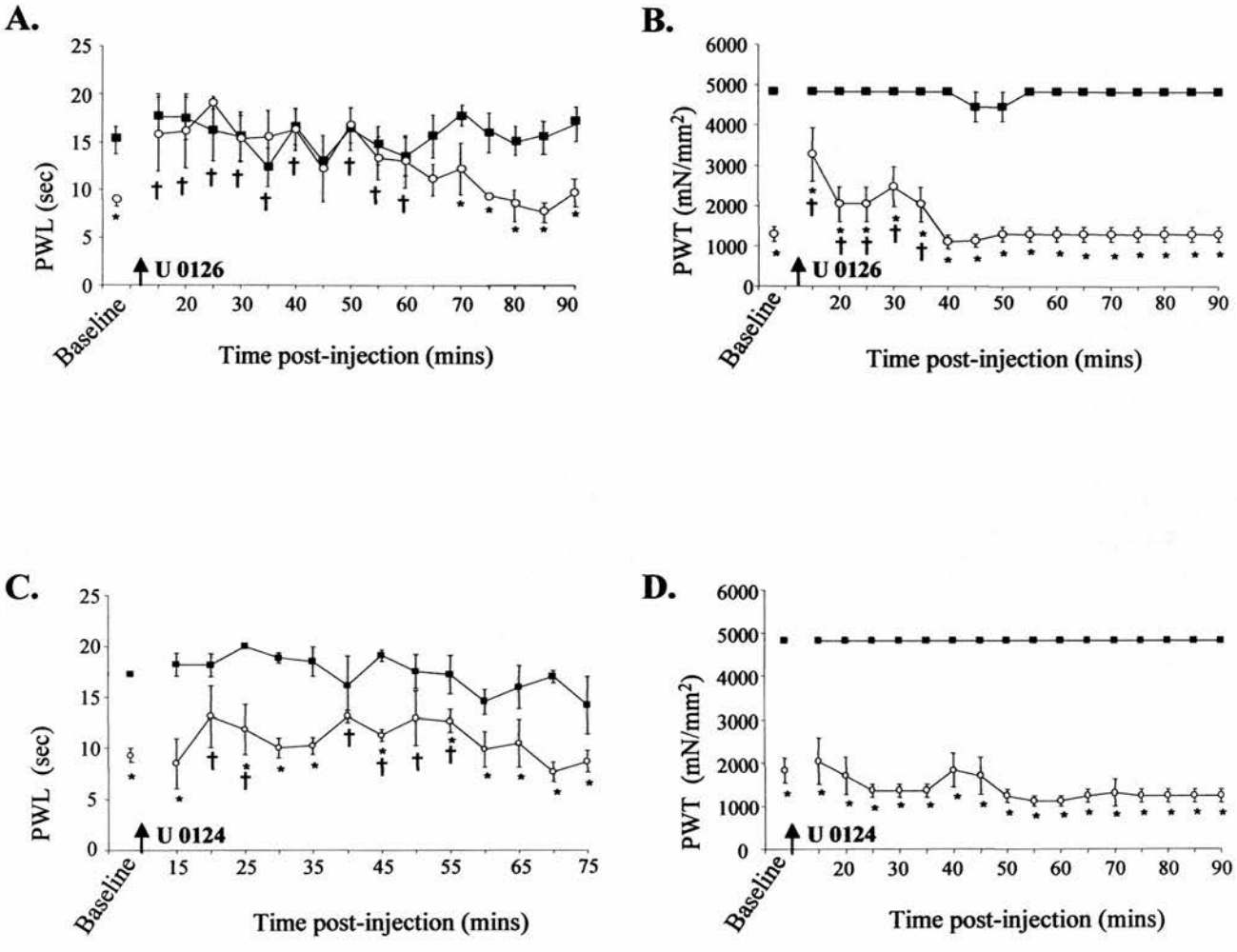
A.
PWL (sec)
U 0126
Baseline
Time post-injection (mins)
B.
PWT (mN/mm²)
U 0126
Baseline
Time post-injection (mins)
C.
PWL (sec)
U 0124
Baseline
Time post-injection (mins)
D.
PWT (mN/mm²)
U 0124
Baseline
Time post-injection (mins)

Figure 4.4

MAP kinase activation following experimental mononeuropathy (CCI) compared to naïve spinal cord.

Immunoblots showing the expression levels of phosphorylated p38 (phospho-p38), and phosphorylated p42/44 (phospho-p42/44), and corresponding pan-immunoreactivity for both kinases, pan-p38 and pan-p42/44 MAP kinase in spinal cord extracts of animals displaying peak behavioural reflex sensitisation following CCI, on the side ipsilateral (Ipsi; n=5) and contralateral (Con; n=5) to nerve injury and in naïve (n=5) animals. All tissue samples were taken at Day 12-14 following CCI when peak behavioural reflex sensitisation was seen in all animals. CCI alone caused an ipsilateral increase in the levels of activated phospho-p38 and phospho-p42/44 compared to the contralateral side and naïve animals. No significant alterations occurred in the overall levels of p38 (pan-p38) or p42/44 (pan-p42/44) as a result of nerve injury. The image shows a sample representation of MAP kinase activation following CCI compared to naïve animals.

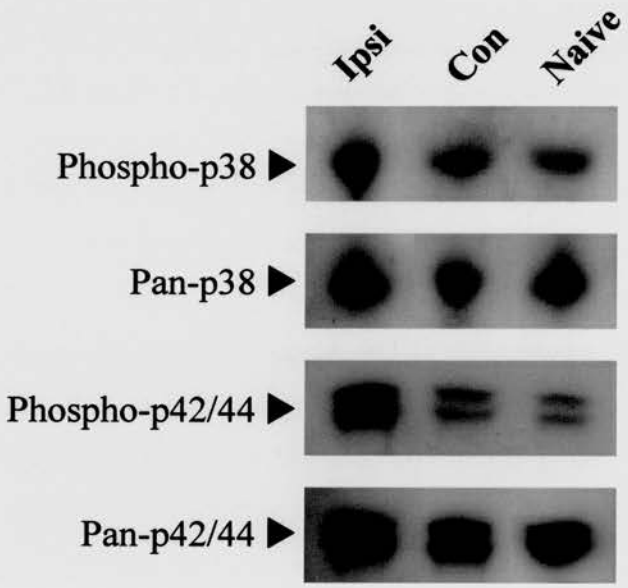
Ipsi
Con
Naive
Phospho-p38
Pan-p38
Phospho-p42/44
Pan-p42/44

Figure 4.5

Intrathecal administration of a glial inhibitor or the TNF-α receptor antagonist attenuates the behavioural reflex sensitisation that occurs following CCI.

(A-D) Data show mean ± SEM responses prior to (baseline) and following intrathecal administration of the glial inhibitor propentofylline (PPT; 0.5μmol; n=5) or the TNF-α receptor antagonist (WP9QY; 25μg; n=5). In all cases the animals were at the peak of behavioural reflex sensitisation as a result of CCI to the sciatic nerve, as demonstrated by a significant reduction in ipsilateral (O) paw withdrawal latency from a noxious thermal stimuli (PWL; * $p<0.05$, Student's t-test, **A, C**) or paw withdrawal threshold to mechanical stimuli (PWT; * $p<0.05$, Wilcoxon test, **B, D**) compared to contralateral withdrawal responses (■). Following intrathecal injection (shown by arrow), both (**A**) PPT and (**C**) WP9QY significantly increased ipsilateral thermal paw withdrawal latencies in comparison to pre-injection ipsilateral values († $p<0.05$, One-Way Repeated Measures ANOVA followed by a Dunnett's test) with significant differences between ipsilateral and contralateral post-injection returning (* $p<0.05$, Student's t-test), while there was no significant alteration in the contralateral response. (**B**) PPT and (**D**) WP9QY, significantly increased ipsilateral mechanical paw withdrawal thresholds in comparison to pre-injection ipsilateral values († $p<0.05$, Friedman test on ranks followed by a Dunn's post-hoc test), with differences between ipsilateral and contralateral post-injection shown (* $p<0.05$, Wilcoxon test). No significant alteration in the contralateral response was noted. Previous experiments have shown that intrathecal injection of the vehicle used had no effect on any behavioural reflex responses in CCI injured or naïve animals with all animals being of the same age, sex, weight and strain as to the animals used in this study and with all behavioural testing carried out in a similar manner it was felt unwarranted here to repeat such experiments again. Full recovery to pre-drug response levels was seen in both cases.

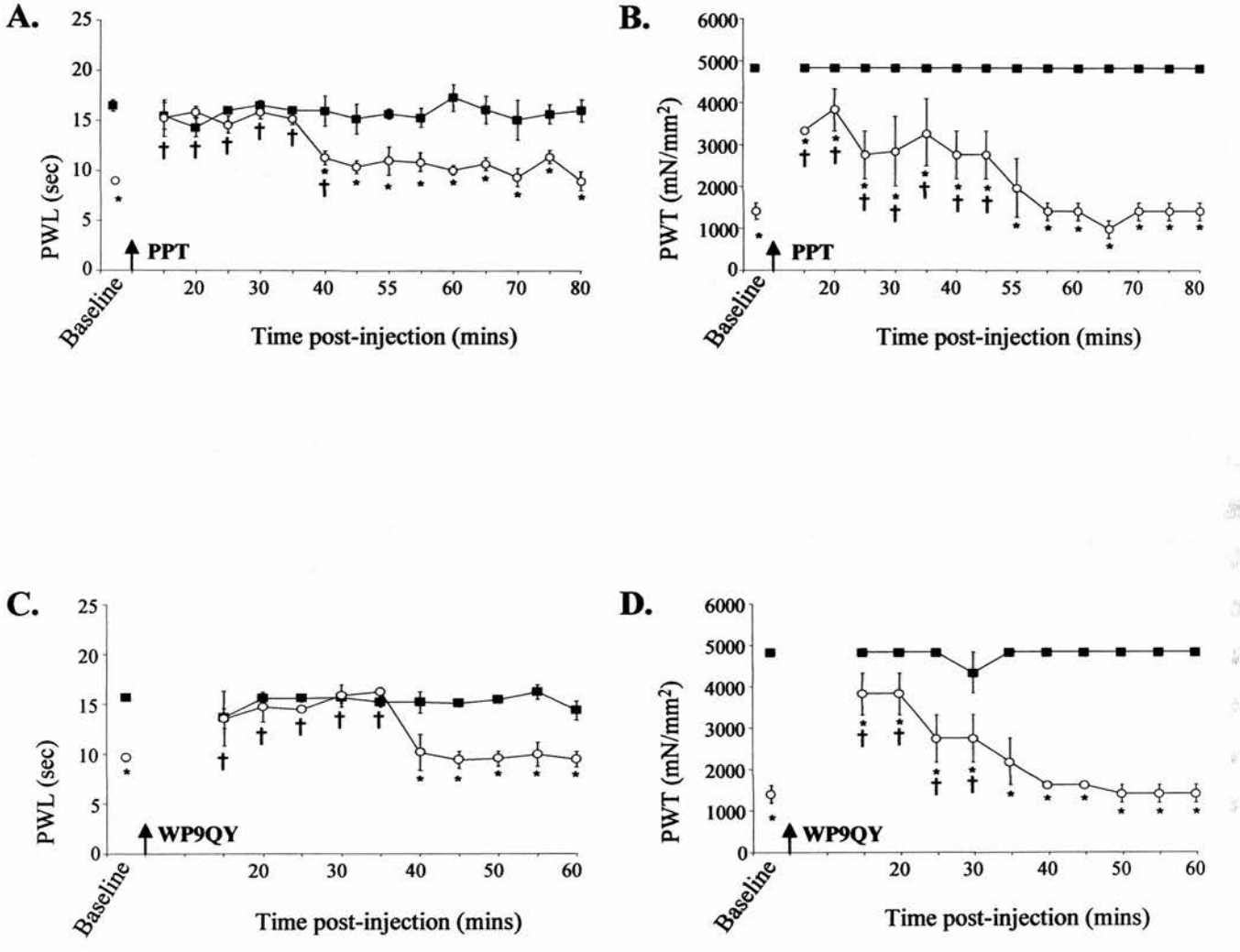
A.
PWL (sec)
PPT
Baseline
Time post-injection (mins)
B.
PWT (mN/mm²)
PPT
Baseline
Time post-injection (mins)
C.
PWL (sec)
WP9QY
Baseline
Time post-injection (mins)
D.
PWT (mN/mm²)
WP9QY
Baseline
Time post-injection (mins)

Figure 4.6

Inhibition of glia and TNF-α receptors suppresses the activation of p38 and p42/44 MAP kinases following CCI.

Immunoblots of spinal cord extracts show that incubation of the spinal cord with the glial inhibitor propentofylline (PPT; 10mM; n=5), an antagonist of the pro-inflammatory cytokine, TNF-α (WP9QY; 0.5mg/ml; n=5), or the inhibitor of TNF-α synthesis, thalidomide (200μM; n=5) to nerve injured spinal cords, all inhibited the activation of p38 (phospho-p38) and of p42/44 (phospho-p42/44) MAP kinase ipsilateral to CCI (samples taken at the peak of CCI-induced behavioural reflex sensitisation). No significant alterations occurred in the overall levels of p38 (pan-p38) or p42/44 (pan-p42/44) with any treatment. The incubation of the spinal cord with saline did not affect the activation of p38 (phospho-p38) or p42/44 (phospho-p42/44) MAP kinase observed ipsilateral to CCI nerve injury.

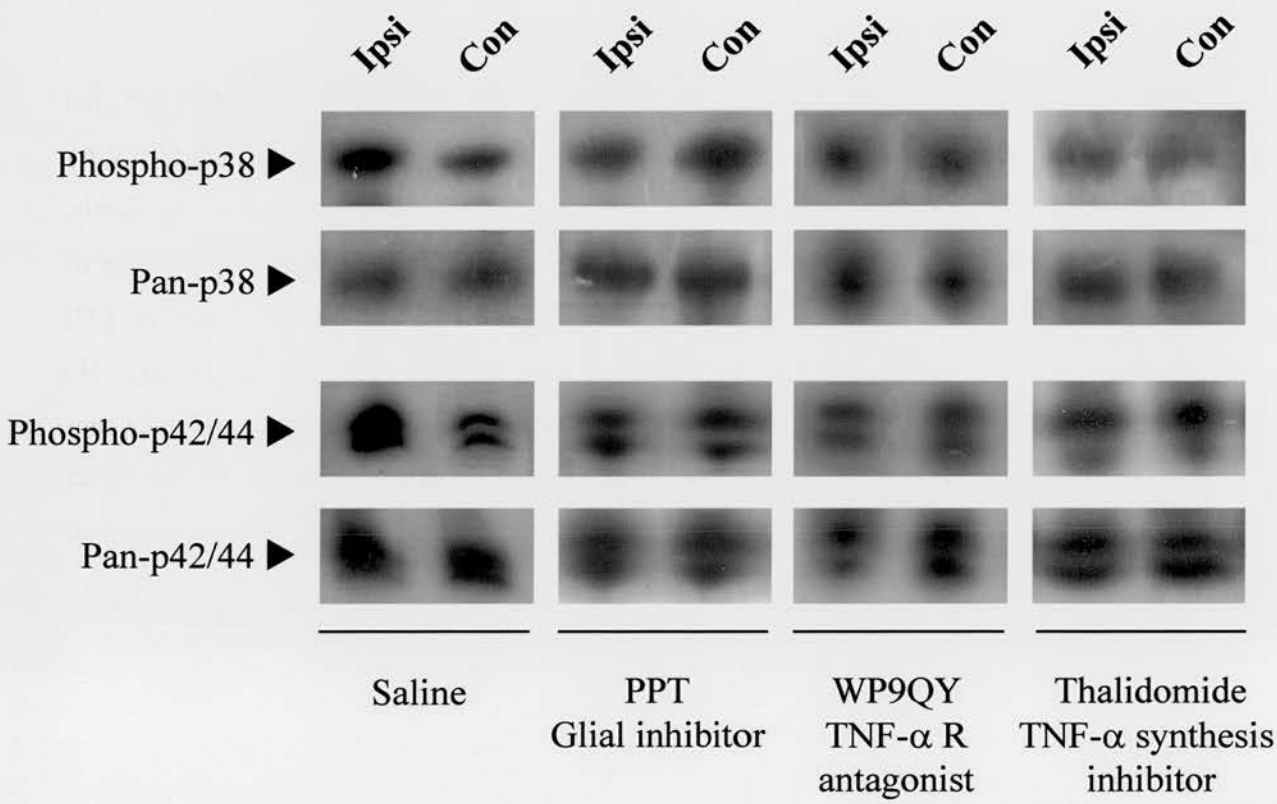
Ipsi
Con
Ipsi
Con
Ipsi
Con
Ipsi
Con
Phospho-p38 ▶
Pan-p38 ▶
Phospho-p42/44 ▶
Pan-p42/44 ▶
Saline
PPT
Glial inhibitor
WP9QY
TNF-α R
antagonist
Thalidomide
TNF-α synthesis
inhibitor

Figure 4.7

Intrathecal administration of either the $VPAC_2$ or NK_2 receptor antagonists reversed behavioural reflex sensitisation that occurs following CCI.

(A-D) Data show mean ± SEM responses prior to (baseline) and following intrathecal administration of the $VPAC_2$ (des(1-4), Arg^{16}]-Ro 25-1553; 0.1nmol; n=7) or NK_2 (SR 48968; 5nmol; n=5) receptor antagonists. In all cases the animals were at the peak of behavioural reflex sensitisation as a result of CCI, shown by a significant reduction in ipsilateral (O) paw withdrawal latency from a noxious thermal stimuli (PWL; * $p<0.05$, Student's t test, **A**, **C**) or paw withdrawal threshold to mechanical stimuli (PWT; * $p<0.05$, Wilcoxon test, **B**, **D**) compared to contralateral withdrawal responses (■). Following intrathecal injection (shown by arrow), both compounds (**A**) des(1-4), Arg^{16}]-Ro 25-1553 and (**C**) SR 48968 significantly increased ipsilateral thermal paw withdrawal latencies in comparison to pre-injection ipsilateral values († $p<0.05$, One-Way Repeated Measures ANOVA followed by a Dunnett's test) with significant differences between ipsilateral and contralateral post-injection returning (* $p<0.05$, Student's t-test), while there was no significant alteration in the contralateral response. (**B**) des(1-4), Arg^{16}]-Ro 25-1553 and (**D**) SR 48968, show significantly increased ipsilateral mechanical paw withdrawal thresholds in comparison to pre-injection ipsilateral values († $p<0.05$, Friedman test on ranks followed by a Dunn's post-hoc test), with differences between ipsilateral and contralateral post-injection shown (* $p<0.05$, Wilcoxon test), no significant alteration in the contralateral response was seen. Full recovery to pre-drug response levels was seen in each case.

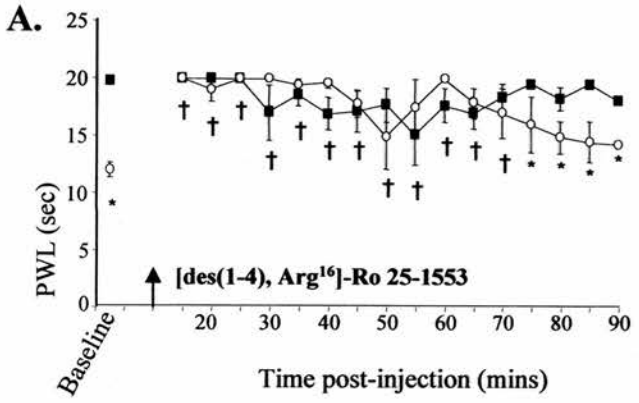
A.
PWL (sec)
[des(1-4), Arg16]-Ro 25-1553
Baseline
Time post-injection (mins)

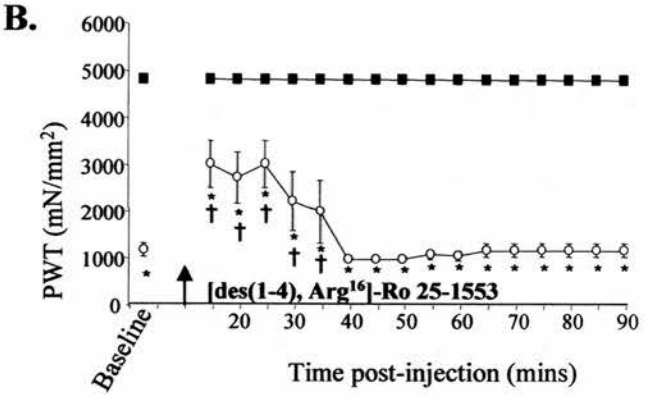
B.
PWT (mN/mm2)
[des(1-4), Arg16]-Ro 25-1553
Baseline
Time post-injection (mins)

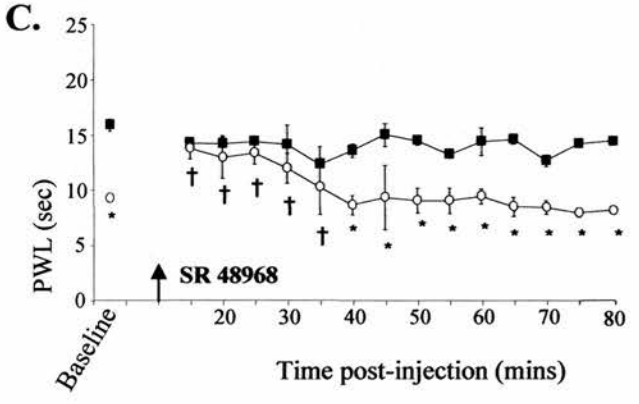
C.
PWL (sec)
SR 48968
Baseline
Time post-injection (mins)

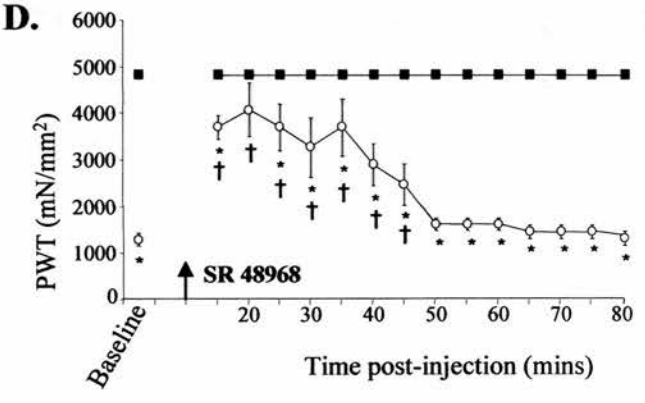
D.
PWT (mN/mm2)
SR 48968
Baseline
Time post-injection (mins)

Figure 4.8

$VPAC_2$, NK_2 and NMDA receptor antagonists can suppress activation of p38 and p42/44 MAP kinases following CCI.

Immunoblots of spinal cord extracts shows that incubation of the spinal cord with antagonists to the $VPAC_2$ ([des(1-4), Arg^{16}]-Ro 25-1553: 2μM; n=5), NK_2 (SR 48968; 100μM; n=5) and NMDA ((R)-CPP; 10μM; n=5) receptors suppressed the increased activation of p38 (phospho-p38) and of p42/44 (phospho-p42/44) MAP kinase ipsilateral to CCI (drugs incubation on the spinal cord at the peak of CCI-induced behavioural reflex sensitisation). No significant alterations occurred in the overall levels of p38 (pan-p38) or p42/44 (pan-p42/44) with any treatment. The incubation of the spinal cord with saline (0.9%; n=5) did not affect the activation of p38 (phospho-p38) or p42/44 (phospho-p42/44) MAP kinase observed ipsilateral to CCI nerve injury.

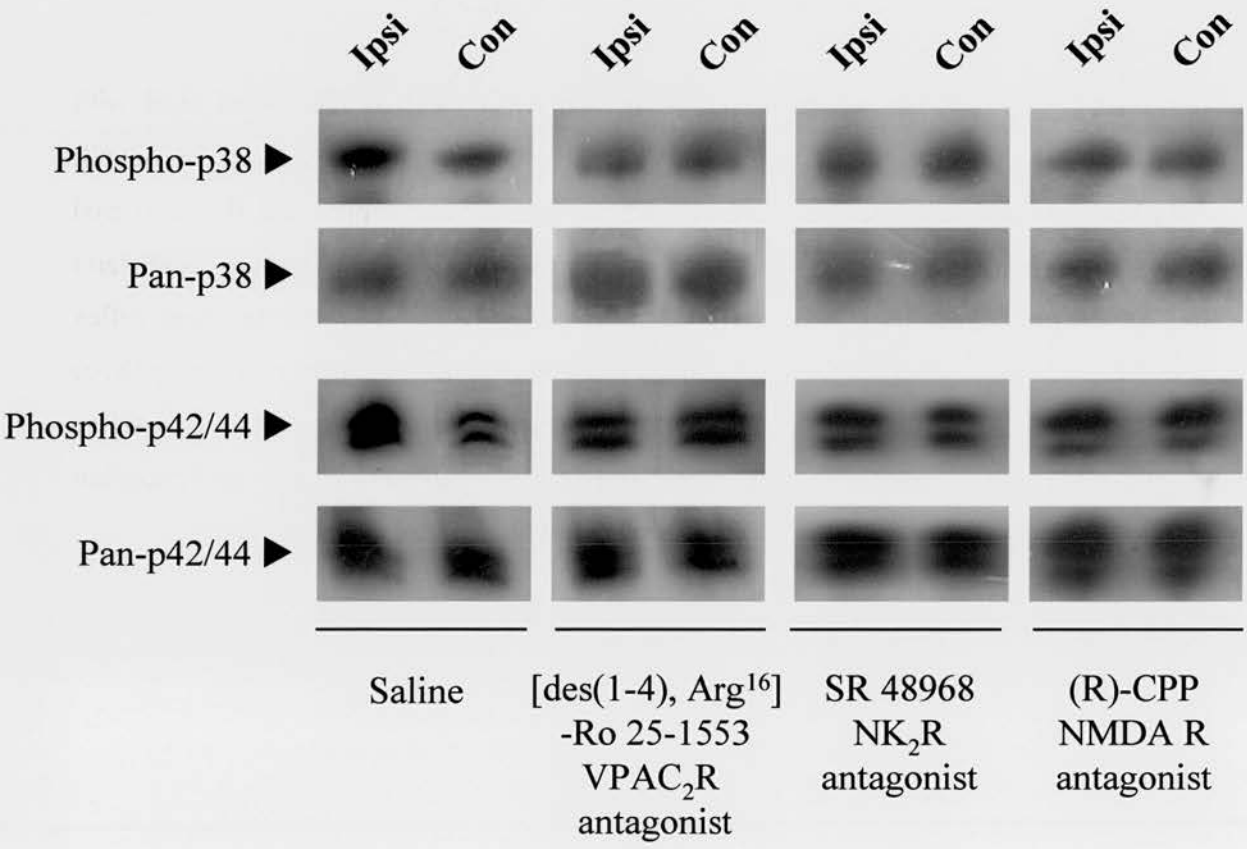
Ipsi
Con
Ipsi
Con
Ipsi
Con
Ipsi
Con
Phospho-p38 ▶
Pan-p38 ▶
Phospho-p42/44 ▶
Pan-p42/44 ▶
Saline
[des(1-4), Arg16] -Ro 25-1553 VPAC2R antagonist
SR 48968 NK2R antagonist
(R)-CPP NMDA R antagonist

Figure 4.9

Intrathecal administration of the $VPAC_2$ or the NK_2 receptor agonists in naïve animals results in behavioural reflex sensitisation that can be blocked by MAP kinase pathway inhibitors.

(A-D) Data represents bilateral mean hindpaw withdrawal latency ± SEM in response to a noxious heat stimulus prior to (baseline) and following intrathecal administration of (**A**) $VPAC_2$ (Ro 25-1553; 0.5nmol; n=6) or (**C**) NK_2 (GR 64349; 1.5nmol; n=6) receptor agonists or co-administration of (**B**) Ro 25-1553 with SB 203580 (a p38 MAP kinase inhibitor; 5nmol; n=6) or co-administration of (**D**) GR 64349 with U 0126 (a p42/44 MAP kinase pathway inhibitor; 1.5nmol; n=6). The single administration of both agonists caused behavioural sensitisation to thermal stimulation (**A**, **C**) in comparison to pre-injection values († $p<0.05$, One-Way Repeated Measures ANOVA followed by a Dunnett's test). The effects of Ro 25-1553 were blocked when it was co-administered with the p38 MAP kinase pathway inhibitor SB 203580 (**B**). Similarly, the effects of GR 64349 were blocked when co-administered with the p42/44 MAP kinase pathway inhibitor U 0126 (**D**). Full recovery to pre-drug responses was seen in each case.

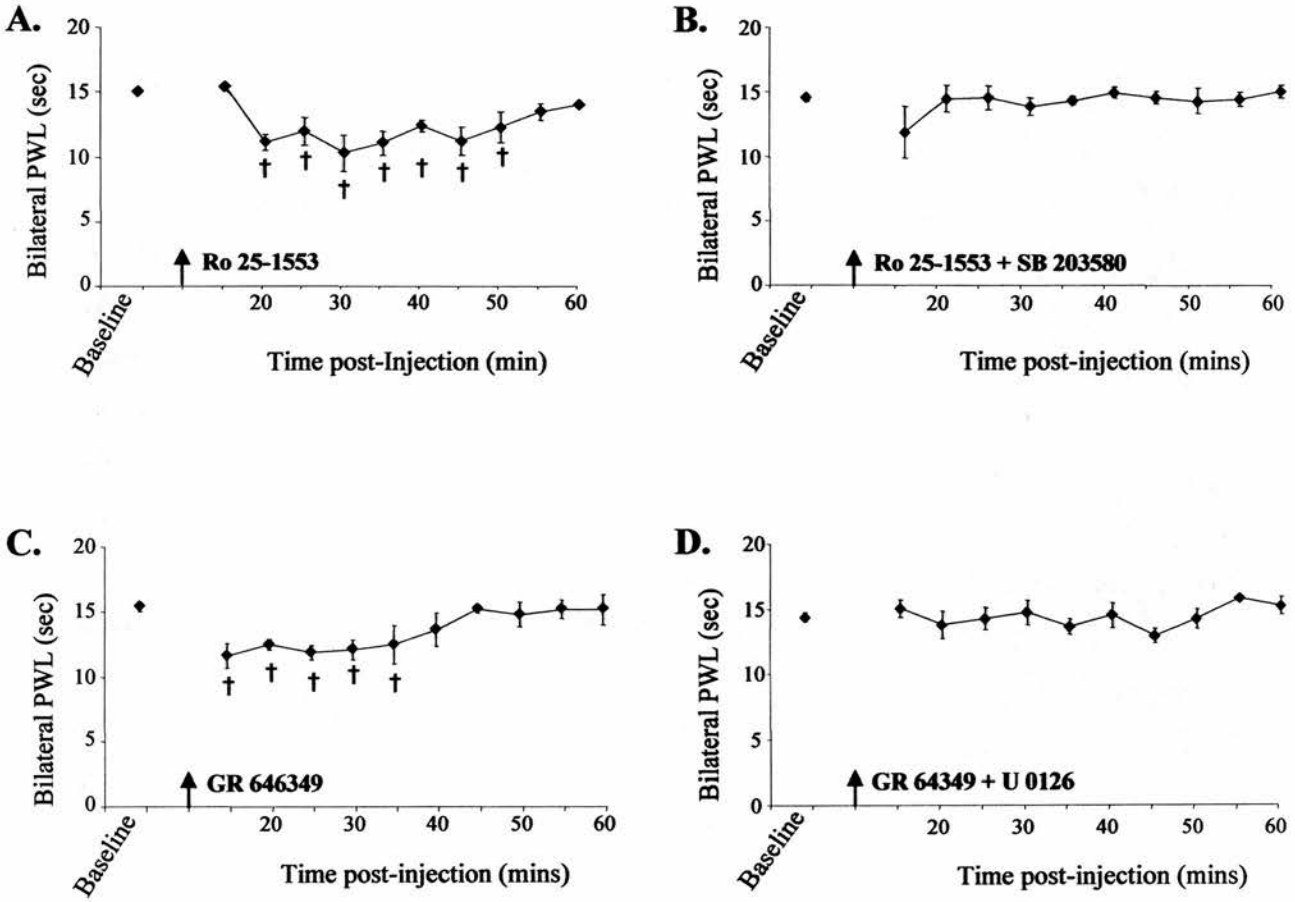
A.
Bilateral PWL (sec)
20
15
10
5
0
Ro 25-1553
Baseline
20
30
40
50
60
Time post-Injection (min)
B.
Bilateral PWL (sec)
Ro 25-1553 + SB 203580
Baseline
Time post-injection (mins)
C.
Bilateral PWL (sec)
GR 646349
Baseline
Time post-injection (mins)
D.
Bilateral PWL (sec)
GR 64349 + U 0126
Baseline
Time post-injection (mins)

Figure 4.10

Incubation of naïve spinal cords with $VPAC_2$ or the NK_2 receptor agonists caused activation of p38 and p42/44 MAP kinases that was suppressed by application with a glial inhibitor.

Immunoblots of naïve spinal cord extracts shows that incubation of the spinal cord with the $VPAC_2$ (Ro 25-1553; 30μM; n=5) and the NK_2 (GR 64349; 50μM; n=5) receptor agonists increased activation of p38 (phospho-p38) and of p42/44 (phospho-p42/44) MAP kinase. The $VPAC_2$ receptor agonist (Ro 25-1553) caused a relatively greater activation of p38 MAP kinase (phospho-p38) than did the NK_2 receptor agonist (GR 64349) compared to the application of saline. The NK_2 receptor agonist (GR 64349) was found to cause a relatively greater activation of p42/44 MAP kinase (phospho-p42/44) than did the $VPAC_2$ receptor agonist (Ro 25-1553), compared to the application of saline. The increased activation of p38 and p42/44 MAP kinases was prevented when the glial inhibitor propentofylline (PPT; 10mM; n=5 in each case) was co-incubated. Minimal levels of either phospho-p38 or phospho-p42/44 immunoreactivity were detected in controls where saline (0.9%; n=5) was incubated on the spinal cord instead. No significant alterations occurred in the overall levels of p38 (pan-p38) or p42/44 (pan-p42/44) with any treatment.

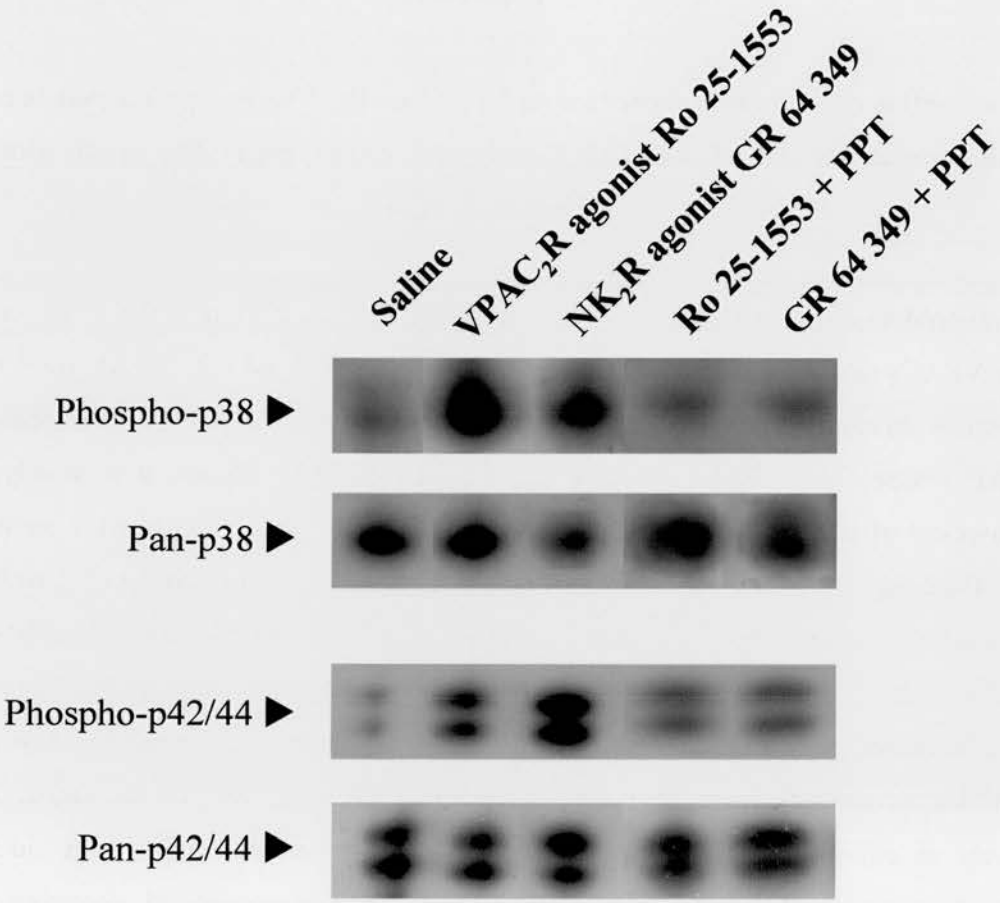
Saline
VPAC2R agonist Ro 25-1553
NK2R agonist GR 64 349
Ro 25-1553 + PPT
GR 64 349 + PPT
Phospho-p38 ▶
Pan-p38 ▶
Phospho-p42/44 ▶
Pan-p42/44 ▶

Table 4.1

Immunoblot densitometric ratio scores for phosphorylated:pan p38 and p42/44 MAP kinases in naïve spinal cord extracts or following CCI and incubation of naïve spinal cords with $VPAC_2$, NK_2 receptor agonists, saline, or with co-incubation of a glial inhibitor

Data presented show the immunoblot densitometric ratio scores for phosphorylated-p38:pan-p38 and phosphorylated-p42/44:pan-p42/44 (arbitrary density units; values are mean ± SEM) in **(A)** Spinal cord extracts of CCI nerve injured animals at the peak of behavioural reflex sensitisation ipsilateral (ipsi) and contralateral (con) to nerve injury (n=5) and naïve spinal cord (n=5; shown in Figure 4.3). The ratio of both phosphorylated -p38 and -p42/44 MAP kinases to pan-immunoreactivity was significantly increased ipsilateral to nerve injury when compared to contralateral and naïve samples (*$p<0.05$, Wilcoxon test). **(B)** Spinal cord extracts of naïve animals that have been incubated with agonists for the $VPAC_2$ receptor (Ro 25-1553; n=5) or the NK_2 receptor (GR 64349; n=5; shown in Figure 3.9). Both agonists resulted in significant increases in the ratio of both phosphorylated -p38 and -p42/44 MAP kinases to pan-immunoreactivity in naïve animals when compared to saline controls (*$p<0.05$, Wilcoxon test). Co-incubation of the $VPAC_2$ receptor agonist, Ro 25-1553 and the NK_2 receptor agonist, GR 64349 with the glial inhibitor propentofylline, PPT (n=5) blocked the increased phosphorylated p38 and p42/44 MAP kinases to levels that were not significantly different from saline controls.

A. Immunoblot densitometric ratio scores for phosphophorylated-p38:pan-p38 and phosphorylated-p42/44:pan-p42/44 (arbitrary density units)

MAP Kinase	*CCI Spinal Cord*		*Naïve Spinal Cord*
	Ipsi	***Con***	***Naïve***
p38	63.5 ± 5.7*	48.4 ± 6.2	44.6 ± 4.6
p42/44	56.1 ± 4.8*	35.9 ± 3.6	39.6 ± 7.1

B. Immunoblot densitometric ratio scores for phosphophorylated-p38:pan-p38 and phosphorylated-p42/44:pan-p42/44 (arbitrary density units)

MAP Kinase	*Saline*	*$VPAC_2$ receptor agonist*	*NK_2 receptor agonist*
p38	36.5 ± 4.2	60.7 ± 6.3*	53.2 ± 4.8*
p42/44	39.0 ± 7.3	67.1 ± 4.0*	94.4 ± 5.8*

MAP Kinase	*$VPAC_2$ receptor agonist and PPT*	*NK_2 receptor agonist and PPT*
p38	39.9 ± 5.3	43.3 ± 6.0
p42/44	34.8 ± 4.6	40.0 ± 5.7

Table 4.2

Immunoblot densitometric ratio scores for phosphorylated:pan p38 and p42/44 MAP kinases in spinal cord extracts following CCI and incubation of the spinal cord with the glial inhibitor, TNF-α receptor antagonist or TNF-α synthesis inhibitor or of the $VPAC_2$, NK_2 or NMDA receptor antagonists

Data presented shows the immunoblot densitometric ratio scores for phosphorylated-p38:pan-p38 and phosphorylated-p42/44:pan-p42/44 (arbitrary density units; values are mean ± SEM) in **(A)** Spinal cord extracts of CCI nerve injured animals at the peak of behavioural reflex sensitisation ipsilateral (ipsi) and contralateral (con) to nerve injury with either the glial inhibitor propentofylline, PPT (n=5), the TNF-α receptor antagonist WP9QY (n=5) or the TNF-α synthesis inhibitor, thalidomide (n=5), incubated on the spinal cord (shown in Figure 4.5). Each of these drugs prevented the ipsilateral increase in phosphorylated of p38 and p42/44 MAP kinases seen as a result of nerve injury when compared to saline controls (see **C** below). **(B)** Spinal cord extracts of CCI nerve injured animals at the peak of behavioural reflex sensitisation ipsilateral (ipsi) and contralateral (con) to nerve injury with either the $VPAC_2$ receptor antagonist, [des(1-4), Arg^{16}]-Ro 25-1553 (n=5), the NK_2 receptor antagonist, SR 48968 (n=5) or the NMDA receptor antagonist, (R)-CPP (n=5) incubated on the spinal cord (shown in Figure 4.5). The incubation of the spinal cord these drugs prevented the ipsilateral increase in phosphorylated of p38 and p42/44 MAP kinases seen as a result of nerve injury when compared to saline controls (see **C**). **(C)** Spinal cord extracts of CCI nerve injured animals at the peak of behavioural reflex sensitisation ipsilateral (ipsi) and contralateral (con) to nerve injury with saline incubated on the spinal cord (n=5; shown in Figure 4.5). The ratio of both phosphorylated -p38 and -p42/44 MAP kinases to pan-immunoreactivity was significantly increased ipsilateral to nerve injury when compared to contralateral (*$p<0.05$, Wilcoxon test).

Immunoblot densitometric ratio scores for phosphophorylated-p38:pan-p38 and phosphorylated-p42/44:pan-p42/44 (arbitrary density units)						
A	***Glial Inhibitor Propentofylline (PPT)***		***TNF-α R antagonist WP9QY***		***TNF-α synthesis inhibitor, thalidomide***	
MAP Kinase	***Ipsi***	***Con***	***Ipsi***	***Con***	***Ipsi***	***Con***
p38	37.4 ± 5.9	39.8 ± 4.7	40.3 ± 5.0	36.3 ± 7.5	41.5 ± 6.8	39.6 ± 4.8
p42/44	30.9 ± 4.3	38.3 ± 4.6	41.3 ± 8.3	34.8 ± 5.2	35.0 ± 6.2	45.9 ± 6.9
B	***$VPAC_2R$ antagonist [des(1-4), Arg16]-Ro 25-1553***		***NK_2 R antagonist SR 48968***		***NMDA R antagonist (R)-CPP***	
MAP Kinase	***Ipsi***	***Con***	***Ipsi***	***Con***	***Ipsi***	***Con***
p38	39.3 ± 7.3	35.8 ± 6.0	47.3 ± 5.5	45.6 ± 4.8	42.3 ± 7.6	44.1 ± 7.1
p42/44	39.7 ± 4.4	41.4 ± 5.0	37.9 ± 3.9	37.1 ± 5.2	39.6 ± 4.9	42.8 ± 4.3
C	***CCI with Saline***					
MAP Kinase	***Ipsi***		***Con***			
p38	63.5 ± 5.7*		48.4 ± 6.2			
p42/44	56.1 ± 4.8*		35.9 ± 3.6			

Table 4.3

The mean percent reversal of ipsilateral sensitisation in CCI injured animals following intrathecal administration of the $VPAC_1$, $VPAC_2$ or PAC_1 receptor antagonists or of the NK_1 and NK_2 receptor antagonists

Table presented shows the mean percent reversal of ipsilateral sensitisation from 15-30 min following intrathecal administration of each drug. Data represents mean percent reversal ± SEM from 15 - 30 min following intrathecal injection of each drug for measurements of thermal hyperalgesia and mechanical allodynia in animals at the peak of ipsilateral reflex sensitivity as a result of nerve injury. Drugs assessed were antagonists to the $VPAC_2$ (n=7), $VPAC_1$ (n=6) and PAC_1 (n=6) receptors (see figure 4.6 A+B for $VPAC_2$ receptor antagonist) and to NK_2 (n=5) and NK_1 (n=6) receptors (see figure 4.6 C+D for NK_2 receptor antagonist) for their effect on behavioural reflex sensitisation. Significant attenuation of thermal hyperalgesia was seen with the administration of $VPAC_2$, PAC_1 and NK_2 receptor antagonists ($*p < 0.05$, One Way Repeated Measures ANOVA followed by a Dunnett's test) when compared to pre-injection (baseline) ipsilateral values at each of the time points throughout this period. Significant attenuation of mechanical allodynia was seen with the administration of $VPAC_2$, PAC_1 and NK_1 and NK_2 receptor antagonists ($*p < 0.05$, Friedman test on ranks followed by a Dunn's post-hoc test) when compared to pre-injection (baseline) ipsilateral values at each of the time points throughout this period. No significant changes in contralateral responses were found at any time point.

Mean percent reversal of ipsilateral sensitisation from 15-30 min following intrathecal administration of each drug		
Drug	**Thermal hyperalgesia**	**Mechanical allodynia**
$VPAC_1R$ antagonist *[Ac-His^{1}, D-Phe^{2}, Lys^{15}, Arg^{16}, Leu^{17}]-VIP(3-7)GRF(8-27)*	8.3 ± 2.0	12.4 ± 4.6
$VPAC_2R$ antagonist *[des(1-4), Arg16]-Ro 25-1553*	93.6 ± 5.2 *	41.2 ± 6.1*
PAC_1R antagonist *$PACAP_{6-38}$*	27.6 ± 4.1*	19.5 ± 3.3*
NK_1R antagonist *RP 67580*	11.6 ± 4.8	22.9 ± 6.1*
NK_2R antagonist *SR 48968*	89.6 ± 4.3*	73.2 ± 6.5*

4.4 Discussion

This study was carried out to investigate activation of the p38 and p42/44 MAP kinases and involvement of the NK_2 and $VPAC_2$ peptidergic receptors and spinal glia in an experimental model of mononeuropathy. The model used in this study was a modification of the chronic constriction injury (CCI) model developed by Bennett and Xie (Bennett and Xie, 1988). This model relies on partial nerve damage rather than complete transection and produces a clinically relevant model with a combination of damaged and undamaged (hypersensitive) fibres. The pharmacological profile of this CCI model is similar to that seen in human neuropathic pain and the frequency of autotomy is lower in this model than following sciatic nerve transection (Attal et al., 1990; Bennett and Xie, 1988). All animals used in this study developed a robust increased sensitivity to previously innocuous mechanical and cold stimuli, indicating that CCI nerve injury resulted in the development of mechanical and cold allodynia in the affected hind limb, while also developing a marked reduction in response latency to a noxious heat stimulus. The CCI-induced behavioural reflex sensitisation described here is in agreement with previous reports using this CCI model (Dickinson et al., 1999). For all further investigations here using this CCI model, animals displaying peak behavioural reflex sensitisation following CCI nerve injury (ipsilateral to nerve injury) were used.

MAP kinase activation was shown here to be markedly enhanced in the spinal cord, following CCI nerve injury, as illustrated by an ipsilateral increased phosphorylation of both p38 and p42/44 MAP kinase when compared to the contralateral side and naïve controls. Previous findings from the laboratory illustrated that both p38 and p42/44 MAP kinase inhibitors (SB 203580 and PD 098059 respectively) attenuated the sensitisation of individual dorsal horn neurons as a result of mustard oil application, suggesting that both MAP kinases may contribute to the central sensitisation induced by nerve injury. Utilising this information, the present study investigated whether corresponding effects would be observed on nerve injury-induced behavioural reflex sensitisation. The results indicate that both p38 (SB 203580) and p42/44 (PD 098059 and U 0126) MAP kinase pathway inhibitors, when intrathecally administered, indeed clearly attenuate nerve

injury-induced behavioural reflex sensitisation. These findings are in agreement with other reports where intrathecal administration of the p38 (SB 203580) MAP kinase inhibitor, suppressed allodynia elicited by spinal nerve injury, blocked the hypersensitivity that occurs following the application of substance P and attenuated both formalin or Complete Freund's Adjuvant-induced inflammatory sensitisation (Jin et al., 2003; Svensson et al., 2003; Tsuda et al., 2004). The use of another inhibitor of p38 MAP kinase has also demonstrated antinociceptive effects in a model of diabetic neuropathy (Sweitzer et al., 2004). Equally inhibition of the p42/44 MAP kinase pathway through use of U 0126 has been reported to reduce hypersensitivity induced by capsaicin, by Complete Freund's Adjuvant-induced inflammation or by nerve transection (Dai et al., 2002; Ji et al., 2002a; Obata et al., 2003). The p42/44 MAP kinase pathway inhibitor PD 098059 has also recently been shown to reduce nociceptive behaviours in a model of chronic inflammatory articular pain (Cruz et al., 2005). Here using the CCI model of mononeuropathy, behavioural sensitisation was prevented with use of both the p38 and p42/44 MAP kinase inhibitors.

Non-neuronal, glial cell activation appears to be a key element in both the generation and maintenance of chronic pain states. Microglia and astrocytes have been shown to be activated following both, inflammation and peripheral nerve injury (Garrison et al., 1991; Hashizume et al., 2000; Sweitzer et al., 1999). Activated p38 and p42/44 MAP kinases have been localised to not only neurons but to astrocytes and microglia. Phosphorylation of p38 MAP kinase occurs in microglia following formalin-induced inflammation, nerve injury and axotomy (Jin et al., 2003; Kawasaki et al., 1997; Kim et al., 2002; Svensson et al., 2003; Tsuda et al., 2004), while phosphorylation of p42/44 MAP kinase occurs in addition to spinal neurons, in astrocytes and microglia following nerve injury (Ji et al., 1999; Ma and Quirion, 2002; Zhuang et al., 2005). It has been noted that CCI nerve injury is associated with activation of astrocytes, observed as an increased GFAP expression that is believed to involve a mechanism dependent on the NMDA receptor (Garrison et al., 1991; Garrison et al., 1994). However a similar increase in microglial activation has not been observed in this CCI nerve injury model (Colburn et al., 1997). It has yet to be determined if the increased activation of these MAP kinases corresponds to

glial activation (seen as increased GFAP expression) following nerve injury. As a first approach to this question, the present study assessed the effect of attenuating glial activation on both p38 and p42/44 MAP kinase activation.

Inhibiting glial function through use of the glial inhibitor, propentofylline and blocking the proinflammatory cytokine TNF-α released by active glial cells using the TNF-α receptor antagonist, WP9QY, both reversed behavioural reflex sensitisation following CCI nerve injury. Additionally the enhanced phosphorylation of p38 and p42/44 MAP kinases observed in the spinal cord as a result of nerve injury was seen to be prevented by the application (incubated on the spinal cord) of the same glial and TNF-α inhibitors, propentofylline and WP9QY and also by the inhibitor of TNF-α synthesis, thalidomide. Propentofylline, a non-selective inhibitor of glial activation has been reported to attenuate allodynia induced by nerve transection, as well as decreasing the formalin-induced behavioural response (Dorazil-Dudzik et al., 2004; Sweitzer et al., 2001b). In this study a more specific glial inhibitor, minocycline, which selectively blocks microglial activation (Tikka et al., 2001), and the TNF-α synthesis inhibitor thalidomide were not investigated for their effect on CCI induced behavioural sensitisation as minocycline has already been shown to prevent the activation of MAP kinase caused by NMDA receptor stimulation (Tikka and Koistinaho, 2001), and both compounds are known to attenuate behavioural sensitisation in different chronic pain models (George et al., 2000; Raghavendra et al., 2003a; Sommer et al., 1998a; Watkins and Maier, 2002).

It has been shown that expression of the pro-inflammatory cytokine TNF-α is upregulated following peripheral nerve injury in the spinal cord (Bartholdi and Schwab, 1997; DeLeo et al., 1997; Wagner and Myers, 1996). Indeed local application of TNF-α to afferents results in hyperalgesia and spontaneous activity in nociceptive afferent fibres (Sorkin et al., 1997; Sorkin and Doom, 2000). Blocking the TNF-α receptor 1 through use of a neutralising antibody was found to inhibit CCI nerve injury-induced behavioural sensitisation and an antagonist to TNF-α receptor 2 also attenuates behavioural sensitisation following nerve injury (Schafers et al., 2003; Sommer et al., 1998b; Winkelstein et al., 2001). TNF-α can activate p38 MAP kinase and inhibit glutamate

uptake, indeed blocking TNF-α results in reduction of nerve injury-induced p38 activation (Fine et al., 1996; Schafers et al., 2003; Svensson et al., 2005). Moreover thalidomide (which inhibits TNF-α synthesis; Sampaio et al., 1991) attenuates not only the behavioural sensitisation seen following nerve injury but also reduces the increased expression of TNF-α following CCI nerve injury (George et al., 2000; Sommer et al., 1998a). Together with the results presented here, these findings suggest that an increase in the expression or release of TNF-α may play a part in the sensitisation found in chronic pain states by activating either or both p38 and p42/44 MAP kinases in glial cells.

Another aspect of this study was looking at the involvement of the peptidergic receptors $VPAC_2$ and NK_2; firstly the neurokinin receptors, NK_1 and NK_2 whose ligands are SP and NKA respectively. Here the CCI nerve injury-induced behavioural sensitisation was prominently inhibited by the NK_2 receptor antagonist with only mechanical allodynia minimally inhibited by the NK_1 receptor antagonist. Correspondingly the CCI nerve injury-induced enhanced activation of p38 and p42/44 MAP kinase was reduced by incubation of the spinal cord with the NK_2 and also by the NMDA receptor antagonists. Secondly the peptidergic receptors for the excitatory peptide VIP, the $VPAC_2$, $VPAC_1$ and the closely related PAC_1 receptors were also assessed. The $VPAC_2$ receptor antagonist markedly inhibited the CCI nerve injury-induced behavioural sensitisation, while the $VPAC_1$ receptor antagonist had no effect on behavioural sensitisation and the PAC_1 receptor antagonist only modestly reversed the behavioural sensitisation. The $VPAC_2$ receptor antagonist used here has been shown to have a high affinity (with a 100-fold selectivity) for the $VPAC_2$ receptor, whereas the PAC_1 receptor antagonist, while highly selective for the $VPAC_1$ receptor, also has a moderately high affinity for the $VPAC_2$ receptor (Dickinson et al., 1997; Moreno et al., 2000), which may explain the modest reversal in behavioural sensitisation observed here by the PAC_1 receptor antagonist. The enhanced activation of p38 and p42/44 MAP kinase following CCI nerve injury was reduced by incubation of the spinal cord with the $VPAC_2$ receptor antagonist.

This study also revealed that agonist stimulation of spinal $VPAC_2$ receptors and to a lesser degree, NK_2 receptors, increases the activation of p38 MAP kinase, which was

prevented when the glial inhibitor propentofylline was co-applied. Accordingly, the $VPAC_2$ receptor agonist resulted in behavioural sensitisation in naïve animals that could be prevented by co-administration of the p38 MAP kinase inhibitor SB 203580. Agonist stimulation of NK_2 receptors resulted in the activation of p42/44 MAP kinase to a greater extent than that seen by $VPAC_2$ receptor stimulation; this increased activation was again blocked by co-applied propentofylline. The behavioural sensitisation induced in naïve animals by administration of the NK_2 receptor agonist was correspondingly attenuated by co-administration of the p42/44 MAP kinase inhibitor, U 0126. This suggests that p38 and p42/44 MAP kinase activation in the spinal cord may contribute to nerve injury-induced sensitisation and that spinal $VPAC_2$ and NK_2 receptors respectively may be important mediators of this injury-induced activation.

Glial cells express receptors for neurokinins, VIP and the excitatory amino acid glutamate, all of which are implicated in chronic pain states. Neurokinins are known to stimulate glial production of the pro-inflammatory cytokines IL-1 and TNF-α (Martin et al., 1992). There is an increased phosphorylation of p38 MAP kinase in microglia following the administration of SP, while Complete Freund's Adjuvant-induced inflammation results in upregulation of both the NK_1 receptor and p42/44 MAP kinase activation in the same dorsal horn neurons (Ji et al., 2002a; Svensson et al., 2003). NK_2 receptors are thought to be specifically involved in the hyperexcitability of dorsal horn neuron responses to noxious cutaneous stimuli (Fleetwood-Walker et al., 1990) and NK_2 receptor antagonists were found to be antinociceptive when administered following nerve injury (Coudore-Civiale et al., 1998; Fleetwood-Walker et al., 1990). Here the NK_2 receptor antagonist attenuated behavioural sensitisation following CCI nerve injury to a much greater extent than the NK_1 receptor antagonist. As a result, biochemical analysis focused on NK_2 receptors, which are located on spinal astrocytes, (also a site of p42/44 MAP kinase activation after nerve injury (Ma and Quirion, 2002). In addition to this the activation of p42/44 MAP kinase in the dorsal horn following C-fibre stimulation is known to involve neuronal NMDA receptors (Lever et al., 2003). It could be suggested that the activation of p42/44 MAP kinase seen in this CCI nerve injury model could partly be the result of glial NK_2 receptor activation that leads to pro-inflammatory

cytokine release and facilitation of the NMDA receptor's function. However with the current results it is not possible to exclude the idea that part of this phosphorylation of p42/44 MAP kinase as a result of NK_2 receptor activation may be occurring in neurons downstream of glial activation.

Following nerve injury, there is increased expression of the excitatory peptide VIP in small primary sensory neurons of the DRG, in conjunction with a decreased SP expression. These changes may represent a functional switch in peptides mediating central sensitisation of nociception. Indeed expression of the $VPAC_2$ receptor in the dorsal horn is increased following nerve injury, corresponding to the marked inhibitory effect of $VPAC_2$ receptor antagonists on neuropathic sensitisation (Dickinson and Fleetwood-Walker, 1999). $VPAC_2$ receptors along with the other VPAC and PAC receptor subtypes have been found to be expressed in astrocytes, VIP is capable of inducing TNF-α release (in cultured astrocytes) and PAC_1 receptor agonist stimulation of cultured astrocytes induces p44 MAP kinase activation and an injury-induced increase in TNF-α can be blocked by p38 MAP kinase inhibitors (Brenneman et al., 1990; Grimaldi and Cavallaro, 1999; Jaworski, 2000; Joo et al., 2004; Kim et al., 2000; Schafers et al., 2003). VIP acting through $VPAC_2$ receptors can result in a mixture of cytokines being released from astrocytes (including TNF-α) and can cause production of a neuroprotective factor and astrocytogenesis (Brenneman et al., 2003; Delgado et al., 2003; Zupan et al., 1998). Contrastingly VIP can inhibit TNFα production by injury or lipopolysaccharide (LPS)-activated microglia when acting through the $VPAC_1$ receptor (Kim et al., 2000; Zusev and Gozes, 2004). One would not expect such qualitatively different effects of $VPAC_1$ and $VPAC_2$ receptor activation (since their signalling pathways are very similar) unless the localisation of these receptors is distinctively different. In the present study the behavioural sensitisation caused by CCI nerve injury was attenuated by the selective $VPAC_2$ receptor antagonist, with little or no inhibition by PAC_1 or $VPAC_1$ receptor antagonists. The increased phosphorylation of p38 MAP kinase after CCI nerve injury was reduced by incubation of the spinal cord with the $VPAC_2$ receptor antagonist and to a lesser degree by the NK_2 receptor antagonist and applying a $VPAC_2$ receptor agonist to naïve tissue resulted in activation of p38 MAP kinase

(phosphorylation of p38 MAP kinase was induced to a smaller extent by the NK_2 receptor agonist). The corresponding behavioural study resulted in sensitisation in naïve animals upon administration of a $VPAC_2$ receptor agonist that was reversed when co-administered with the p38 MAP kinase inhibitor, SB 203580. Further experiments would have to be conducted to determine if the p38 MAP kinase activation response is in $VPAC_2$ receptor containing cells, however these findings suggest that the $VPAC_2$ receptors on spinal glial cells could play an important role in nerve injury-induced p38 MAP kinase activation.

To summarise, peripheral nerve damage can result in the development of chronic pain states that are highly resistant to classical analgesics. This current study reveals important new evidence to support the developing hypothesis that glial cells play a key role in spinal somatosensory processing. The results presented implicate the involvement of the $VPAC_2$, NK_2 and NMDA receptors in the activation of p38 and p42/44 MAP kinases following nerve injury, which contributes to the mechanism of sensitisation involved in the chronic neuropathic pain state.

5. Single point mutation of the SH3 domain of PSD-95 affects pain behaviours

5.1 Introduction

The Post Synaptic Density-95 protein (PSD-95) as reviewed in Chapter one (Section 1.7.3) belongs to the membrane associated guanylate kinases (MAGUK) family of proteins that can cluster ion channels on postsynaptic membranes at excitatory synapses and also interact with signalling molecules and the cytoskeleton (Sheng, 2001; Sheng and Kim, 2002). PSD-95 is an adapter protein with multiple protein interaction domains that can couple numerous proteins to for example the N-methyl-D-aspartate (NMDA) glutamate receptor as identified by *in vitro* studies (Husi et al., 2000; Husi and Grant, 2001). To reiterate, PSD-95 is comprised of three N-terminal PDZ (PSD-Dlg-ZO-1 homology) domains, an SH3 (Src homology 3) domain and a GK (guanylate kinase-like) domain in its C-terminal region (Figure 1.3). The importance of PSD-95 in plasticity was revealed with a mouse germline mutant construct that abrogated several domains of PSD-95, resulting in expression of a truncated form of PSD-95 lacking the PDZ 3, SH3 and GK domains, known as PSD-95^{PDZ1-2} (Migaud et al., 1998).

The PSD-95^{PDZ1-2} mutant mice exhibited altered forms of NMDA receptor-dependent forms of plasticity, such as learning, visual plasticity, cocaine sensitisation and neuropathic pain (Fagiolini et al., 2003; Garry et al., 2003; Migaud et al., 1998; Yao et al., 2004). Specifically the PSD-95^{PDZ1-2} mutants were found to have enhanced LTP (long-term potentiation) accompanied by severely impaired spatial learning (Migaud et al., 1998). Using the PSD-95^{PDZ1-2} mutant and wild type littermate mice, the functional impact of the mutant PSD-95 construct on neuropathic behavioural reflex sensitisation was assessed following nerve injury (CCI). In wild type mice, a progressive ipsilateral sensitisation was shown by a reduction in latency of withdrawal to a thermal stimulus and of threshold to a mechanical stimulus, along with an increased sensitivity to a cold stimulus when compared to pre-surgical and contralateral values (Garry et al., 2003). However for the homozygous PSD-95^{PDZ1-2} mutants, hyperalgesia and allodynia associated with this model of neuropathic pain were absent (Garry et al., 2003). This was consistent with a previous

report showing a delay in the onset of hyperalgesia and allodynia development following administration of a PSD-95 antisense reagent (Tao et al., 2001).

It was shown that the PSD-95^{PDZ1-2} mutant and wild type mice both developed normal inflammatory nociceptive behaviour following the injection of formalin that is both groups displayed the same early and late phase formalin responses, therefore suggesting the possibility that the requirement for PSD-95 may be selective for neuropathic rather than inflammatory sensitisation (Garry et al., 2003). This phenotype may have stemmed from functional loss of individual domains, the PDZ 3, SH3 or GK domains. This work raised the idea that individual domains of PSD-95 might themselves have discrete functions in different forms of sensitisation in different parts of the nervous system. This current study aims to assess the role of one of these domains, the SH3 domain.

SH3 domains were first identified as regions of sequence similarity between divergent signalling proteins such as the Src family of tyrosine kinases, the Crk adaptor protein and phospholipase C-γ (Mayer et al., 1988; Stahl et al., 1988). SH3 domains are found in many signalling and cytoskeleton associated molecules, and are established as modular protein interaction domains with a binding specificity for certain proline-rich motifs (Pawson and Scott, 1997). The human proteome is estimated to contain over 400 copies of SH3 domain–containing proteins spread among a diverse array of protein structures (Castagnoli et al., 2004). The majority of SH3 domains characterized to date recognize class I and/or class II peptides that share a core PXXP motif (Cohen et al., 1995; Erpel et al., 1995; Lim and Richards, 1994; Mayer, 2001; Mayer and Eck, 1995; Sparks et al., 1998). The importance of the SH3 domain in MAGUK function was revealed from mutational studies that resulted in cellular mis-localisation and a severe phenotype of neoplastic overgrowth of imaginal discs in Drosophila (Kohu et al., 2002; Woods et al., 1996). Knowledge of the consensus SH3 binding motif, PXXP, has helped in the identification of some of PSD-95's SH3 binding partners, which include: Pyk 2, a non-receptor tyrosine kinase (Huang et al., 2001; Seabold et al., 2003), Kainate KA2 receptor subunit (Garcia et al., 1998), Huntingtin protein (Sun et al., 2001), A-Kinase-anchoring Protein (AKAP) 79/150 (Colledge et al., 2000) and Mixed lineage kinase (MLK) 2 and 3 (Savinainen et al., 2001).

The SH3 domain has been structurally analysed by X-ray crystallographic studies of several proteins resulting in a prototypical SH3 domain structure (Borchert et al., 1994; Guruprasad et al., 1995; Musacchio et al., 1992; Musacchio et al., 1994; Noble et al., 1993), which confirmed the basis of the SH3 domain's interaction with proline-rich sequences (Erpel et al., 1995; Lim and Richards, 1994). Such X-ray crystallography studies also identified a key role played by tryptophan 470 in the SH3 domain of PSD-95, which was found to correspond to the highly conserved tryptophan residue found in the hydrophobic binding surface of SH3 domains that is thought to contribute to interaction with proline-containing peptides (Erpel et al., 1995; Lim and Richards, 1994). A mutant mouse construct was therefore generated by Seth Grant's group that carried a targeted mutation to tryptophan 470 in PSD-95 so that SH3 domain interactions with polyproline residues would be specifically disrupted whilst leaving the GK domain and all PDZ domains of PSD-95 and their interactions intact. The corresponding amino acid substitution of leucine to proline in the SH3 domain of the Drosophila homolog of PSD-95 (Discs large, Dlg) causes a severe mutant phenotype of loss of septate junctions and overproliferation of imaginal discs, suggesting that the mutation is effective at disrupting SH3 domain function and that such functions are of physiological importance (Woods et al., 1996). Using these PSD-95^{SH3W470L} mutant mice (and the wild type littermate mice as controls), we examined their behavioural response to a model of experimental mononeuropathy (CCI), to a model of persistent inflammation, Complete Freund's Adjuvant (CFA) and to formalin-induced responses, the aim of this was to characterise the pain state phenotype that may occur as a result of this mutation of the SH3 domain.

As noted in Chapter one (Section 1.4.2 and 1.7.3) NMDA receptors are crucially involved in sensitisation of spinal dorsal horn neurons (Coderre and Melzack, 1992a; Davies and Lodge, 1987; Dickenson and Sullivan, 1987a; Suzuki et al., 2001; Woolf and Thompson, 1991). The NMDA receptor has two principal subunits, NR1 and NR2, with the NR1 subunit being the core functional subunit of all NMDA receptor assemblies and NR2 subunit subtypes (A-D) determine the specific channel characteristics and engage in key interactions (Monyer et al., 1992). PSD-95 binds directly to the C-termini of the NMDA receptor subunits NR2A and NR2B via its PDZ domains (Chaplan et al., 1997). The

expression of the NMDA receptor subunits NR1, NR2A and NR2B was therefore also examined in the spinal cord. The family of MAGUK proteins expression in the spinal cord was also assessed to determine if this mutation of the SH3 domain altered overall levels of PSD-95 expression and also to see if any other MAGUK was compensating for the mutation in PSD-95 by altering its level of expression.

5.2 Generation of the PSD-95^{SH3W470L} mutant mouse

This mouse line carrying a targeted mutation into the SH3 domain of PSD-95, termed PSD-95^{SH3W470L} mutant was generated in Seth Grant's laboratory (Wellcome Trust Sanger Institute, Cambridgeshire, UK). As outlined above, tryptophan 470 of PSD-95 was found to correspond to the highly conserved tryptophan residue found in the hydrophobic binding surface of prototypical SH3 domains, which mediates interactions with proline-containing peptides (Erpel et al., 1995). This point was chosen to introduce a single amino acid mutation substituting leucine at this tryptophan site, thereby intending to selectively disrupt SH3 domain polyproline interactions. This single amino acid mutation that created the PSD-95^{SH3W470L} mutant mice used a gene targeting construct that was transfected into mouse embryonic stem (ES) cells. Homologous recombination into the PSD-95 locus was detected by genomic Southern blotting and PCR (polymerase chain reaction). Positive ES cells (i.e. carrying the targeted mutation) were injected into mouse blastocysts. Resulting chimeric offspring were crossed onto the MF1 background for subsequent studies. PSD-95^{SH3W470L} litters were genotyped (by PCR) and homozygotes were found to be fertile, show normal Mendelian transmission and no obvious seizure, tremor, ataxia or other overt neurological abnormality was observed. *[All of this work detailed in Section 5.2 was carried out by Seth Grant's laboratory].*

5.3 Methods

Throughout this study the experimenter was blinded to the genotype of the animals and only homozygous PSD-95^{SH3W470L} mutants and wild type littermate mice that were age matched were used. Animals of both sexes were used since post-hoc analysis revealed no

discernable differences in their responses in the case of either wildtype or mutant mice. As outlined in Chapter 3 the following methods were used in this study: adult PSD-95^{SH3W470L} mutant (n=6) and wild type littermate (n=6) mice underwent surgery for a model of experimental mononeuropathy, a unilateral chronic constriction injury to the sciatic nerve (CCI; Section 3.2.1). PSD-95^{SH3W470L} mutant (n=4) and wild type littermate (n=4) mice were used for the Complete Freund's adjuvant model of experimental persistent inflammation (CFA; Section 3.2.2). All animals were behaviourally tested (Section 3.4) prior to surgery/injection (to obtain baseline values) and post surgery (from day 4)/ post injection (from 30 minutes) until recovery (day 21 post surgery) from CCI and until 48 hours post injection of CFA. All animals were tested for signs of mechanical allodynia using calibrated Von Frey filaments (Section 3.4.2) and for signs of thermal hyperalgesia using the Hargreaves' thermal apparatus (Section 3.4.4). Adult PSD-95^{SH3W470L} mutant (n=9) and wild type littermate (n=8) mice that were used for intraplantar injection of formalin (1.5% solution: Section 3.2.3) were assessed for their formalin-induced behavioural response (Section 3.3), which consisted of flicking, flinching and licking of the affected hind-paw, until recovery (70 minutes post-injection).

The expression of NMDA receptor subunits and of the MAGUK family of proteins in the spinal cord was assessed in naïve PSD-95^{SH3W470L} mutant (n=2) and wild type littermate (n=3) mice by western immunoblot. Animals were terminally anaesthetised prior to and during dissection of all tissues and a laminectomy of the lumbar region of the mice was performed and spinal cord tissue was homogenised in standard Laemmli lysis buffer to prepare spinal cord extracts (Section 3.6.1). Extracts were then separated by electrophoresis and transferred to PVDF membranes, blocked and probed for NMDA receptor subunits (rabbit polyclonal anti-NR1, rabbit polyclonal anti-NR2A and rabbit polyclonal anti-NR2B) or for MAGUK proteins (mouse monoclonal anti-PSD-95, rabbit polyclonal anti-SAP-97, rabbit polyclonal anti-SAP-102 and rabbit polyclonal anti-PSD-93/Chapsyn 110) and for the ubiquitous housekeeping protein GAPDH and detected by peroxidase-linked secondary antibodies (goat-anti-mouse or goat-anti-rabbit) and enhanced chemiluminescence (Section 3.6.3). Densitometry was performed to measure quantitatively

the grey levels of positive protein bands and background grey levels relative to GAPDH (with the absolute numerical values derived being arbitrary; Section 3.8.2).

5.4 Results

5.4.1 Analysis of behavioural reflex changes in PSD-95^{SH3W470L} mutant and wild type littermate mice with chronic constriction injury to the sciatic nerve (CCI).

All PSD-95^{SH3W470L} mutant and wild type mice that underwent a unilateral CCI to the sciatic nerve appeared healthy and had no signs of weight loss and were handled without any distress being evident. During this study none of the PSD-95^{SH3W470L} mutant and wild type mice developed any signs of autotomy.

Thermal hyperalgesia ***(see Figure 5.1 A (wild type) and B (PSD-95^{SH3W470L} mutants))***

All animals were behaviourally tested for signs of thermal hyperalgesia, using the Hargreaves' thermal apparatus (Section 3.4.4). In analysing the behavioural reflex changes, the baseline (pre-surgical) paw withdrawal latency (PWL) was measured as ipsilateral, 8.9 ± 0.6 seconds in wild type and 8.0 ± 0.5 seconds in PSD-95^{SH3W470L} mutants and contralateral, 8.2 ± 0.5 seconds in wild type and 8.1 ± 0.6 seconds in PSD-95^{SH3W470L} mutants (mean ± SEM responses; n=6 in all groups). At all time points from the fourth day until the eighteenth day post-surgery, both wild type and PSD-95^{SH3W470L} mutants showed significantly reduced PWL ipsilateral to the injury as compared to the contralateral side ($p<0.05$ by Student's t-test) and a significant reduction in PWL was also seen between post-surgical and pre-surgery values ($p<0.05$; One Way Repeated Measures ANOVA followed by Dunnett's post-hoc analysis). No significant difference remained in the PWL from the nineteenth to the twenty-first day post-surgery, the animals were no longer tested after this time point. Both wild type and PSD-95^{SH3W470L} mutants reached a peak of thermal hyperalgesia between the thirteenth and fourteenth days post-surgery when the ipsilateral PWL was 5.0 ± 0.9 seconds in wild type and 4.7 ± 0.9 seconds in PSD-95^{SH3W470L} mutants and contralateral 8.1 ± 0.9 seconds in wild type and 8.2 ± 1.0 seconds in PSD-95^{SH3W470L} mutants (mean ± SEM responses). The contralateral PWL showed no significant reduction in its response.

Mechanical Allodynia ***(see Figure 5.1 C (wild type) and D (PSD-95^{SH3W470L} mutants))***

Wild type and PSD-95^{SH3W470L} mutant mice were tested for signs of mechanical allodynia using calibrated Von Frey filaments (Section 3.4.2). In assessing the behavioural reflex changes, the baseline (pre-surgical) paw withdrawal threshold (PWT) required to elicit a paw withdrawal response ipsilaterally was 602.6 ± 34.6 mN/mm^2 in wild type and 551.7 ± 37.2 mN/mm^2 in PSD-95^{SH3W470L} mutants and contralaterally was 616.6 ± 36.3 mN/mm^2 in wild type and 571.1 ± 35.0 mN/mm^2 in PSD-95^{SH3W470L} mutants (mean ± SEM response). At all time points from the fourth day until the eighteenth day post-surgery, both wild type and PSD-95^{SH3W470L} mutants demonstrated an increased sensitivity to mechanical stimuli with a significantly reduced PWT ipsilateral to the injury as compared to the contralateral side ($p<0.05$ Wilcoxon test) and a significant reduction in PWT was also seen between post-surgical and pre-surgery values ($p<0.05$; Friedman test on ranks followed by Dunn's post-hoc analysis). Again, consistent with results for thermal hyperalgesia there was no significant difference observed in the PWT from the nineteenth to the twenty-first day post-surgery and animals were no longer tested after this time point. Both wild type and PSD-95^{SH3W470L} mutants reached a peak of mechanical allodynia between the eighth and twelfth days post-surgery when the ipsilateral PWT was 318.2 ± 48.3 mN/mm^2 in wild type and 222.6 ± 17.0 mN/mm^2 in PSD-95^{SH3W470L} mutants and contralateral 449.9 ± 43.9 mN/mm^2 in wild type and 485.0 ± 58.5 mN/mm^2 in PSD-95^{SH3W470L} mutants (mean ± SEM response).

These results presented here for the development of both thermal hyperalgesia and mechanical allodynia ipsilateral to nerve injury, are in agreement with previous reports using this model of CCI in mice (Garry et al., 2003; Vogel et al., 2003).

5.4.2 Analysis of formalin-induced behavioural response in PSD-95^{SH3W470L} mutant and wild type littermate mice.

All PSD-95^{SH3W470L} mutant and wild type mice, where formalin was injected subcutaneously into the plantar surface of the hind paw, were allowed five minutes to recover before analysis began, which consisted of counting the number of flick/flinch responses per minute of the affected paw ***(see Figure 5.2)***.

The baseline (pre-injection) number of flick/flinch responses per minute was ipsilateral 0 ± 0 flick/flinches per minute in wild type and 0 ± 0 flick/flinches per minute in PSD-95^{SH3W470L} mutants and contralateral 0 ± 0 flick/flinches per minute in wild type and 0 ± 0 flick/flinches per minute in PSD-95^{SH3W470L} mutants (mean ± SEM response; n=9 PSD-95^{SH3W470L} mutants and n=8 wild type mice). There was no significant alteration between responses of wild type and PSD-95^{SH3W470L} mutant mice in the initial acute phase (first phase; 5-20 minutes post-injection of formalin), however in the late phase (second phase; 25-70 minutes post-injection), PSD-95^{SH3W470L} mutant mice had a significant reduction in responses, to 7.3 ± 0.5 flick/flinches per minute compared to wild type response of 14.9 ± 0.7 flick/flinches per minute, with contralateral values remaining at 0 ± 0 flick/flinches per minute in both PSD-95^{SH3W470L} mutants and wild type ($p<0.05$ Student's t-test; from 25-50 minutes post-injection). During the time points of 50-70 minutes post-injection no significant difference between PSD-95^{SH3W470L} mutants and wild type mice was noted. The animals were not assessed beyond 70 minutes post-injection as they had recovered from the formalin-induced behavioural response. Control animals were injected with an equal volume of saline (Section 3.2.3) and assessed for their response. In the case of both wild type and PSD-95^{SH3W470L} mutant mice no response to saline was observed at any time point (from 5-70 minutes post-injection).

5.4.3 Analysis of behavioural reflex responses in PSD-95^{SH3W470L} mutant and wild type littermate mice following the Complete Freund's Adjuvant model of persistent inflammation

All PSD-95^{SH3W470L} mutant and wild type mice injected with CFA showed signs of cutaneous inflammation within the first hour post-injection, showing an area of localised erythema and oedema of the injected paw that was present throughout testing and was similar between all animals.

Thermal Hyperalgesia ***(see Figure 5.3 A)***

All animals were behaviourally tested for signs of thermal hyperalgesia, using the Hargreaves' thermal apparatus (Section 3.4.4). In characterising the behavioural reflex changes, the baseline (pre-surgical) paw withdrawal latency (PWL) was measured as

ipsilateral, 8.9 ± 0.6 seconds in wild type and 8.0 ± 0.5 seconds in PSD-95^{SH3W470L} mutants and contralateral, 8.2 ± 0.5 seconds in wild type and 8.1 ± 0.6 seconds in PSD-95^{SH3W470L} mutants (mean ± SEM responses; n=4 in all groups). At 0-6 hours post-injection (no discernable difference from 0.5 to 6 hours) both wild type and PSD-95^{SH3W470L} mutants showed significantly reduced PWL ipsilateral to CFA, to values of 2.4 ± 0.4 seconds in wild type and 2.8 ± 0.4 seconds in PSD-95^{SH3W470L} mutants, with contralateral values of 9.1 ± 1.7 seconds in wild type and 6.9 ± 1.2 seconds in PSD-95^{SH3W470L} mutants (mean ± SEM response; $p<0.05$ by Student's t-test) and a significant reduction in PWL was also seen between post-injection and pre-injection values ($p<0.05$ by One Way Repeated Measures ANOVA followed by Dunnett's post-hoc analysis). At 24 hours post-injection only wild type mice still showed a significantly reduced PWL response ipsilateral to CFA, to 3.9 ± 0.7 seconds (with a now not significantly reduced response of 7.2 ± 0.5 seconds in PSD-95^{SH3W470L} mutants) as determined by Student's t-test ($p<0.05$; mean ± SEM response). This was compared to the contralateral response of 9.3 ± 0.6 seconds in wild type mice and 7.3 ± 0.5 seconds in PSD-95^{SH3W470L} mutants. PSD-95^{SH3W470L} mutants had a significantly greater ipsilateral thermal response latency following CFA when compared to the wild-type ipsilateral response as determined by Student's t-test ($p<0.05$; mean ± SEM response). Again at 48 hours post CFA injection a significant PWL reduction was only seen ipsilaterally in wild type mice, to 2.3 ± 0.1 seconds (with a response of 6.2 ± 0.6 seconds in PSD-95^{SH3W470L} mutants) compared to the contralateral values of 8.7 ± 1.1 seconds (6.6 ± 0.6 seconds in PSD-95^{SH3W470L} mutants; mean ± SEM response). Again the PSD-95^{SH3W470L} mutants mean thermal response latency ipsilateral to CFA was significantly greater than the ipsilateral values for the wild-type littermates as determined by Student's t-test ($p<0.05$; mean ± SEM response). At 24 and 48 hours post-injection a significant ipsilateral reduction in PWL was also seen between post-injection and pre-injection values in wild-type and at 48 hours in PSD-95^{SH3W470L} mutants both ipsilateral and contralateral to CFA injection ($p<0.05$ by One Way Repeated Measures ANOVA followed by Dunnett's post-hoc analysis. At all other time points the contralateral PWL responses showed no significant alterations. PSD-95^{SH3W470L} mutants and wild type mice both developed thermal hyperalgesia at the early stage of 0-6 hours post CFA injection, however this did not

continue in the PSD-95^{SH3W470L} mutants at 24 and 48 hours post CFA injection, but the behavioural reflex sensitivity continued in the wild type mice .

Mechanical Allodynia ***(see Figure 5.3 B)***

Wild type and PSD-95^{SH3W470L} mutant mice were tested for signs of mechanical allodynia using calibrated Von Frey filaments (Section 3.4.2). In determining the behavioural reflex changes, the baseline (pre-surgical) paw withdrawal threshold (PWT) required to elicit a paw withdrawal response ipsilaterally was 602.6 ± 34.6 mN/mm^2 in wild type and 551.7 ± 37.2 mN/mm^2 in PSD-95^{SH3W470L} mutants and contralaterally was 616.6 ± 36.3 mN/mm^2 in wild type and 571.1 ± 35.0 mN/mm^2 in PSD-95^{SH3W470L} mutants (mean ± SEM response). At 0-6 hours post-injection, both wild type and PSD-95^{SH3W470L} mutants demonstrated an increased sensitivity to mechanical stimuli with a significantly reduced PWT ipsilateral, 231.1 ± 65.3 mN/mm^2 in wild type and 318.19 ± 69.3 mN/mm^2 in PSD-95^{SH3W470L} mutants compared to the contralateral response of 441.0 ± 70.2 mN/mm^2 in wild type and 508.79 ± 55.1 mN/mm^2 in PSD-95^{SH3W470L} mutants ($p<0.05$ Wilcoxon test; mean ± SEM response). Significant reductions in PWT were also seen ipsilateral to CFA between post-injection and pre-injection values in both wild type and PSD-95^{SH3W470L} mutants ($p<0.05$ Friedman test on ranks followed by Dunn's post-hoc analysis), consistent with results observed for thermal hyperalgesia. At 24 hours post-injection only wild type mice showed significantly reduced ipsilateral PWT responses compared to contralateral controls (ipsilateral, 387.6 ± 52.2 mN/mm^2 in wild type and 381.6 ± 27.7 mN/mm^2 in PSD-95^{SH3W470L} mutants) as determined by Wilcoxon test ($p<0.05$; mean ± SEM response). Contralateral responses were 497.6 ± 81.1 mN/mm^2 and 387.6 ± 26.5 mN/mm^2 in PSD-95^{SH3W470L} mutants. At 24 hours post CFA injection a significant ipsilateral reduction in PWL was seen between post-injection and pre-injection values in wild-type and PSD-95^{SH3W470L} mutants ($p<0.05$ by One Way Repeated Measures ANOVA followed by Dunnett's post-hoc analysis. At 48 hours post CFA injection, no significant reduction could be seen in PWL ipsilateral to the stimulus in wild type mice or in PSD-95^{SH3W470L} mutants, with ipsilateral values of 326.9 ± 95.5.8 mN/mm^2 in wild type and 385.2 ± 33.2 mN/mm^2 in PSD-95^{SH3W470L} mutants (as determined by Wilcoxon test; $p<0.05$; mean ± SEM response). This compared to

contralateral values of 490.4 ± 98.6 mN/mm^2 in wild type and 254.9 ± 26.5 mN/mm^2 in PSD-95^{SH3W470L}.

5.4.4 NMDA receptor subunit and MAGUK expression in the spinal cord of PSD-95^{SH3W470L} mutant and wild type littermate mice

NMDA receptor subunits ***(see Figure 5.4 A and Table 5.1 A)***

The levels of NMDA receptor subunits, NR1, NR2A and NR2B expression in spinal cord extracts of naïve wild type and PSD-95^{SH3W470L} mutant mice were assessed by immunoblot. As compared by quantitative densitometry to the expression of GAPDH, the ubiquitous housekeeping protein, the level of NR1 expression was 66.8 ± 5.3% in PSD-95^{SH3W470L} mutants and 62.8 ± 3.8% in wild type, with NR2A expression 51.9 ± 2.1% in PSD-95^{SH3W470L} mutants and 45.0 ± 1.7% in wild type and NR2B expression 36.9 ± 3.4% in PSD-95^{SH3W470L} mutants and 37.4 ± 2.5% in wild type (mean ± SEM; percent of GAPDH expression; n= 2 PSD-95^{SH3W470L} mutants and n=3 wild type mice). These results show that the levels of expression of the NMDA receptor subunits were unaltered by the PSD-95^{SH3W470L} mutation, when compared to wild-type (levels were found to be not significantly different when assessed by Student's t-test).

MAGUK protein family ***(see Figure 5.4 B and Table 5.1 B)***

In naive wild type and PSD-95^{SH3W470L} mutant mice the expression of the four members of the MAGUK family of proteins (PSD-95, SAP-97, PSD-93/Chapsyn 110 and SAP-102) were assessed by immunoblot. The level of expression of PSD-95 was 74.5 ± 3.4% in PSD-95^{SH3W470L} mutants and 70.3 ± 3.2% in wild type, for SAP-97 expression was 76.1 ± 3.7% in PSD-95^{SH3W470L} mutants and 73.6 ± 3.9% in wild type, PSD-93 expression was 39.9 ± 0.4% in PSD-95^{SH3W470L} mutants and 41.2 ± 0.3% in wild type and SAP-102s expression was 71.7 ± 2.9% in PSD-95^{SH3W470L} mutants and 75.6 ± 2.6% in wild type (mean ± SEM; percent of GAPDH expression; n= 2 PSD-95^{SH3W470L} mutants and n=3 wild type mice). These findings demonstrate that the expression of MAGUKs in the spinal cord is unaltered by the PSD-95^{SH3W470L} mutation when compared to wild type (levels were found to be not significantly different between the two groups when assessed by Student's t-test).

Figure 5.1

Behavioural analysis of PSD-95^{SH3W470L} mutant and wild type littermate mice in a model of experimental mononeuropathy (CCI).

Data show mean ± SEM responses prior to surgery (baseline) and following the induction of a unilateral chronic constriction injury (CCI) to the sciatic nerve (post surgery). **(A and B)** In wild type (A) and PSD-95^{SH3W470L} mutant (B) mice (n=6 in both groups), paw withdrawal latency (PWL) from a noxious thermal stimulus (Hargreaves' thermal stimulator) ipsilateral to CCI (O) showed significant differences between post-operative and pre-operative values († $p<0.05$; One Way repeated-measures ANOVA followed by Dunnett's post hoc analysis) and from postoperative contralateral (■) values (* $p<0.05$ by Student's t-test). No thermal hyperalgesia was seen on the contralateral side (■) of either wild type (A) or PSD-95^{SH3W470L} mutant (B) mice. **(C and D)** Paw withdrawal thresholds (PWT) from mechanical stimulation (von Frey filaments) for both wild type (C) and PSD-95^{SH3W470L} mutant (D) mice showed significant reductions in post-operative compared to pre-operative values ipsilateral (O) to CCI († $p<0.05$; Friedman on ranks test followed by Dunn's post-hoc analysis) and between post-operative ipsilateral and contralateral values (* $p<0.05$; Wilcoxon test).

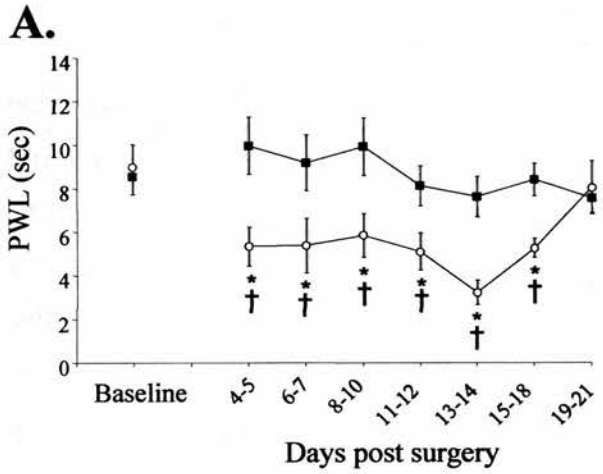
A.
PWL (sec)
14
12
10
8
6
4
2
0
Baseline
4-5
6-7
8-10
11-12
13-14
15-18
19-21
Days post surgery

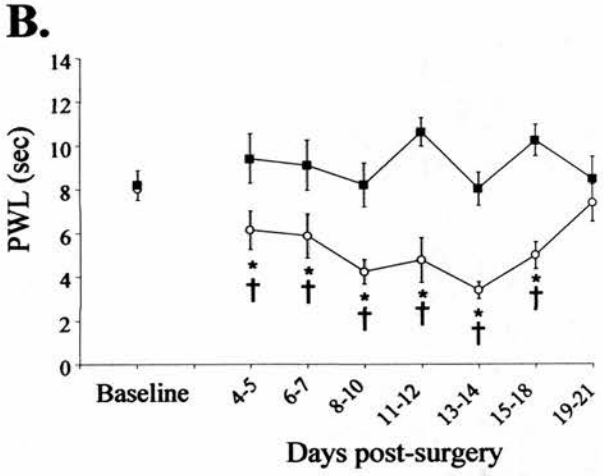
B.
PWL (sec)
14
12
10
8
6
4
2
0
Baseline
4-5
6-7
8-10
11-12
13-14
15-18
19-21
Days post-surgery

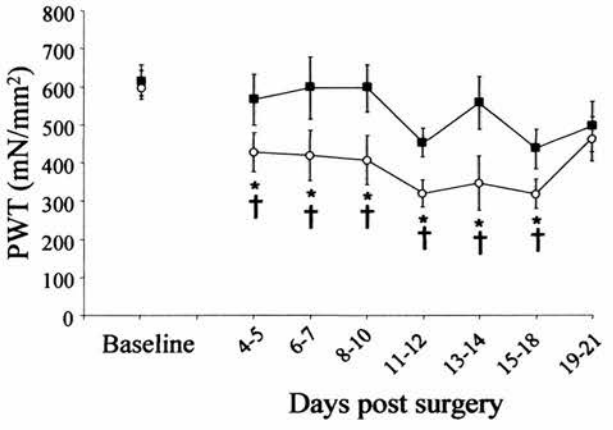
C.
PWT (mN/mm²)
800
700
600
500
400
300
200
100
0
Baseline
4-5
6-7
8-10
11-12
13-14
15-18
19-21
Days post surgery

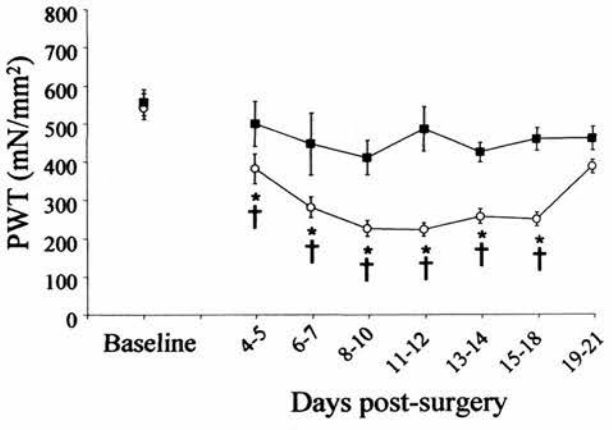
D.
PWT (mN/mm²)
800
700
600
500
400
300
200
100
0
Baseline
4-5
6-7
8-10
11-12
13-14
15-18
19-21
Days post-surgery

Figure 5.2

Behavioural analysis of PSD-95^{SH3W470L} mutant and wild type littermate mice following the intraplantar injection of formalin.

Data shows mean ± SEM number of paw flick/flinch responses per minute. There was no significant difference between responses of wild type (◆) and PSD-95^{SH3W470L} mutant (◇) mice (n=9 in PSD-95^{SH3W470L} mutants and n=8 in wild type mice) in the initial acute phase (5-20 minutes post-injection), however in the late (second; 25-70 minutes post-injection) phase of the formalin test, PSD-95^{SH3W470L} mutant (◇)mice showed a significant reduction in responses (* $p<0.05$ by Student's t-test).

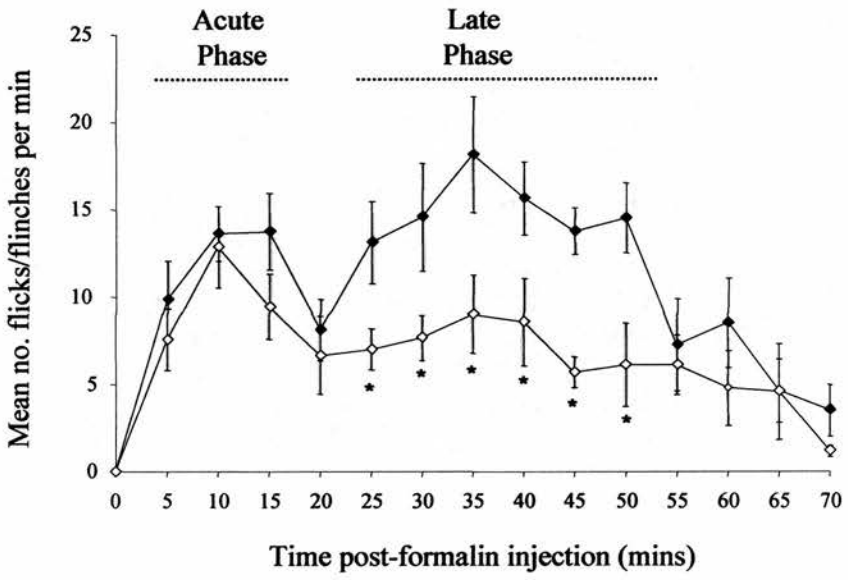
Acute
Phase
Late
Phase
Mean no. flicks/flinches per min
25
20
15
10
5
0
0
5
10
15
20
25
30
35
40
45
50
55
60
65
70
Time post-formalin injection (mins)

Figure 5.3

Behavioural analysis of PSD-95^{SH3W470L} mutant and wild type littermate mice following intraplantar injection of complete Freund's adjuvant.

Data show mean ± SEM responses prior to injection (baseline) and following the injection of complete Freund's adjuvant (CFA). **(A)** In wild type (WT, white) and PSD-95^{SH3W470L} mutant (SH3$^{-/-}$, grey) mice (n=4 in both groups), paw withdrawal latency (PWL) from a noxious thermal stimulus (Hargreaves' thermal stimulator) showed a significant ipsilateral (I) reduction in latency from contralateral (C) values at all time points in wild-type mice (white dotted) and only at the earliest time point in PSD-95^{SH3W470L} mutant mice (grey dotted; *$p<0.05$ by Student's t-test). Significant differences between pre- and post-injection values were determined by a-One Way repeated-measures ANOVA followed by Dunnett's post-hoc analysis († $p\leq0.05$). No thermal hyperalgesia was seen on the contralateral side of either wild type or PSD-95^{SH3W470L} mutant mice. At 24 and 48 hours post CFA a significant increase in PWL ipsilateral to CFA was seen in PSD-95^{SH3W470L} mutants when compared to the wild type ipsilateral response (♦$p<0.05$ by Student's t-test) indicating that sensitisation was attenuated in the mutant mice. **(B)** In wild-type (WT, white) and PSD-95^{SH3W470L} (SH3$^{-/-}$, grey), paw withdrawal thresholds (PWT) from mechanical stimulation (von Frey filaments) were significantly reduced between ipsilateral (I; white and grey) and contralateral (C; white dotted and grey dotted) paws (*$p<0.05$ by Wilcoxon test) at 0-6 hours post-injection. However, although a significant reduction was seen in wild-type mice at 24 hours, there was no significant ipsilateral reduction in the threshold required to elicit a response in PSD-95^{SH3W470L} mutants. No significant ipsilateral reduction in threshold was seen in either wild type or PSD-95^{SH3W470L} mutants at 48 hours post CFA injection. Significant differences between pre- and post-injection values were determined by Friedman on ranks test followed by Dunn's method post-hoc analysis († $p\leq0.05$).

A.

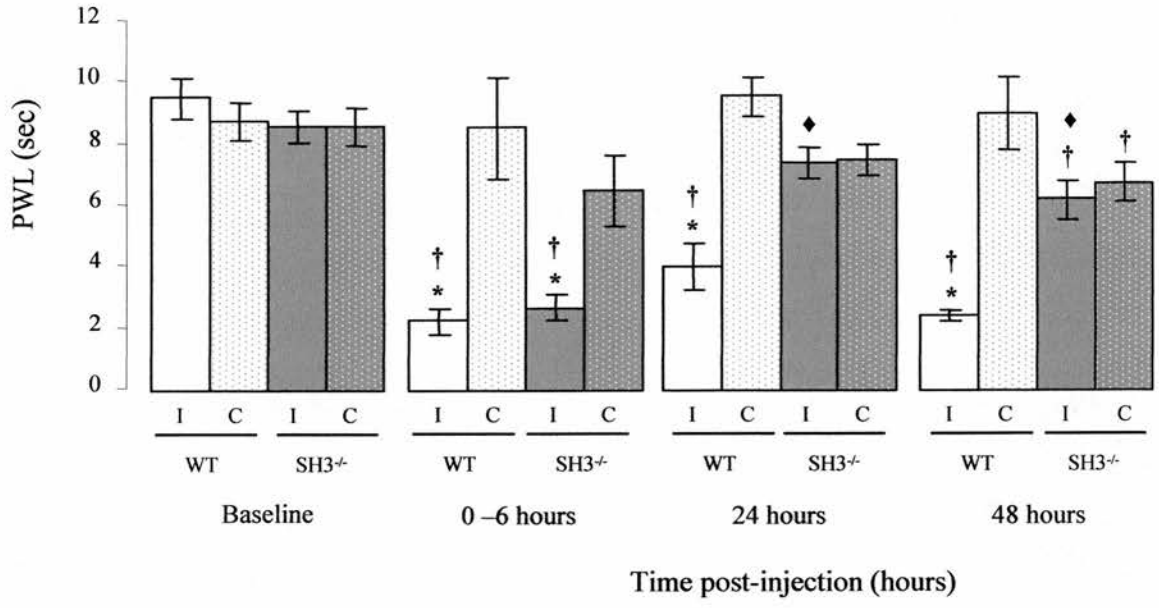
PWL (sec)
12
10
8
6
4
2
0
I C I C
WT SH3-/-
Baseline
0 –6 hours
24 hours
48 hours
Time post-injection (hours)

B.

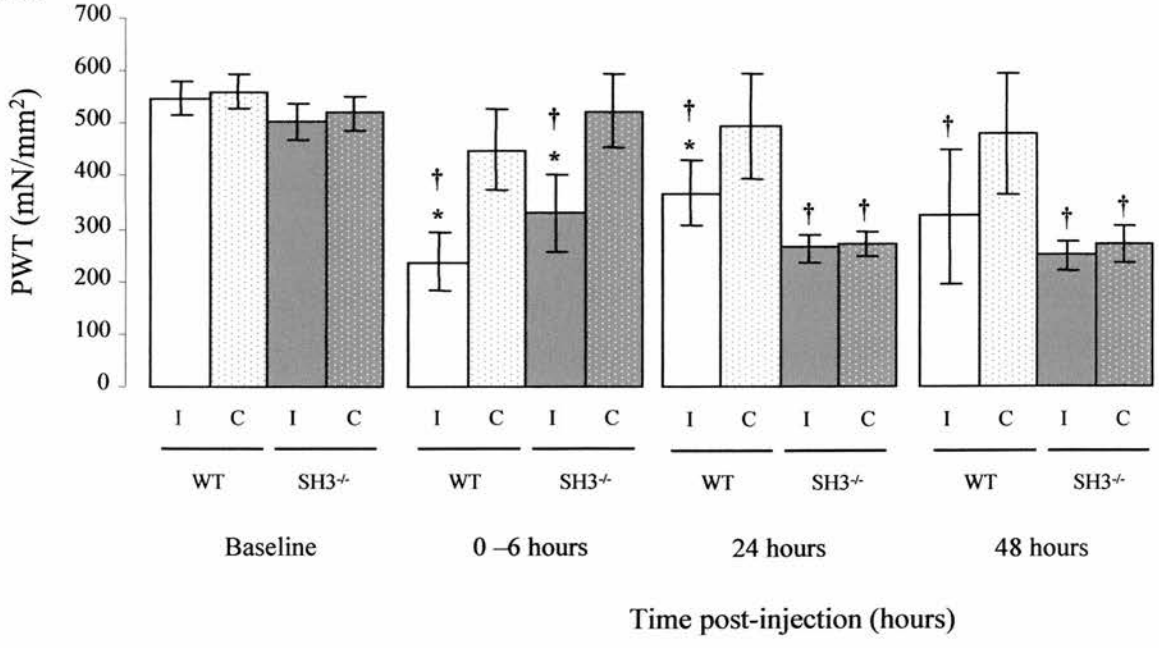
PWT (mN/mm2)
700
600
500
400
300
200
100
0
I C I C
WT SH3-/-
Baseline
0 –6 hours
24 hours
48 hours
Time post-injection (hours)

Figure 5.4

Expression of NMDA receptor subunits and MAGUK proteins in the spinal cord of PSD-95^{SH3W470L} mutant and wild type mice.

(A) Immunoblots of the NMDA receptor subunits NR1, NR2A and NR2B and the ubiquitous housekeeping enzyme GAPDH in spinal cord extracts of PSD-95^{SH3W470L} mutant (-/-; n=2) and wild type (n=3) mice. **(B)** Immunoblots of MAGUK proteins; PSD-95, SAP-97, PSD-93 and SAP-102 as well as GAPDH in spinal cord extracts of PSD-95^{SH3W470L} mutant (-/-; n=2) and wild type (n=3) mice.

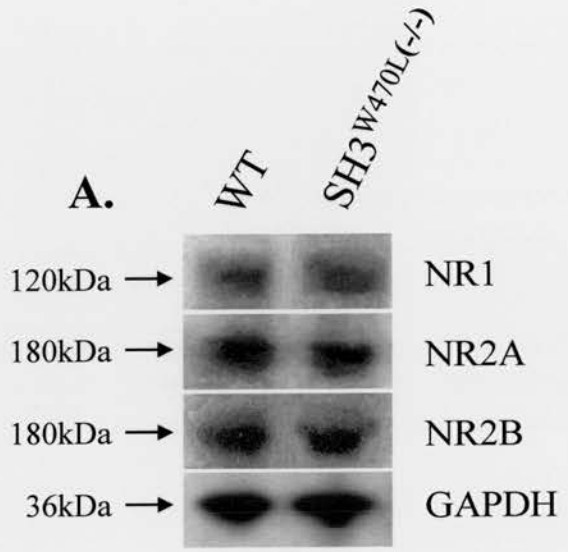
A.
WT
SH3 W470L(-/-)
120kDa
180kDa
180kDa
36kDa
NR1
NR2A
NR2B
GAPDH

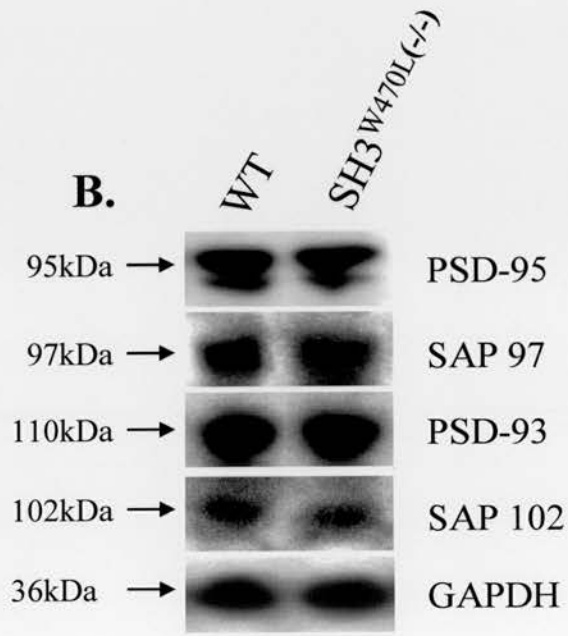
B.
WT
SH3 W470L(-/-)
95kDa
97kDa
110kDa
102kDa
36kDa
PSD-95
SAP 97
PSD-93
SAP 102
GAPDH

Table 5.1

The expression of NMDA receptor subunits and MAGUK proteins relative to GAPDH expression in spinal cord extracts.

Data shows the percent expression ± SEM as determined by densitometric analysis in wild type (n=3) and PSD-95^{SH3W470L} mutant (-/-; n=2) mice of **(A)** NMDA receptor subunits and **(B)** MAGUK proteins relative to GAPDH expression in spinal cord extracts. No significant differences were found (when assessed by Student's t-test) in the expression levels of the NMDA receptor subunits, NR1, NR2A and NR2B. The expression of the MAGUK proteins, PSD-95, SAP-97, PSD-93 and SAP-102 were also found to be not significantly different (when assessed by Student's t-test) between wild type and PSD-95^{SH3W470L} mutant (-/-) mice.

Protein	*Wild type*	*SH3W470L(-/-)*
A. Expression of NMDA Receptor subunits as a percentage of GAPDH expression in spinal cord extracts		
NR1	62.8 ± 3.8	66.8 ± 5.3
NR2A	45.0 ± 1.7	51.9 ± 2.1
NR2B	37.4 ± 2.5	36.9 ± 3.4
B. Expression of MAGUK proteins as a percentage of GAPDH expression in spinal cord extracts		
PSD-95	70.3 ± 3.2	74.5 ± 3.4
SAP-97	73.6 ± 3.9	76.1 ± 3.7
PSD-93	41.2 ± 0.3	39.9 ± 0.4
SAP-102	75.6 ± 2.6	71.7 ± 2.9

5.5 Discussion

Research into the role played by PSD-95 in the development of spinal nociception, utilising either antisense knockdown or mutant mice expressing a truncated form of PSD-95, (PSD-95^{PDZ1-2}) have established the importance of PSD-95 in nociceptive sensory processing (Garry et al., 2003; Tao et al., 2001). The present study was conducted to investigate the effect of a single point mutation to the SH3 domain of PSD-95 on the plasticity of spinal neuronal signalling involved in different pain states. The recent development of mice with a mutation in the SH3 domain of PSD-95 (PSD-$95^{SH3W470L}$ mutants) have, now allowed further investigation into the role of this domain in different pain states.

The PSD-$95^{SH3W470L}$ mutation was designed using available information from X-ray crystallographic studies on several SH3 domains (Borchert et al., 1994; Guruprasad et al., 1995; Musacchio et al., 1992; Musacchio et al., 1994; Noble et al., 1993), which identified tryptophan 470 in the SH3 domain of PSD-95 as a conserved residue in the hydrophobic binding surface of prototypical SH3 domains that mediates interaction with proline rich peptides (Erpel et al., 1995; Lim and Richards, 1994). However recent investigations into the structure of PSD-95's SH3 domain lead to the discovery of novel structural features of this SH3 domain. Unlike typical SH3 domains, PSD-95's SH3 domain is composed of discontinuous elements of sequence, divided by a large hinge region and the GK domain (Shin et al., 2000). The SH3 domain of PSD-95 was found to contain an extra β strand in its structure (six β strands (A-E) instead of five) and a large hinge region, which may occlude the peptide binding region, thus suggesting that ligands may bind in an atypical manner (McGee et al., 2001). The crystal structure of PSD-95 also revealed novel intramolecular interactions between the SH3 and GK domain which did not involve the polyproline binding site of the SH3 domain (Tavares et al., 2001). These studies suggest that the SH3 domain of PSD-95 has alternative surfaces for intra- and inter-molecular interactions, raising the possibility that this domain may contain multiple binding sites (McGee et al., 2001; Tavares et al., 2001; Yaffe, 2002).

The PSD-95^{SH3W470L} mutation, a highly specific mutation designed to interfere with particular protein-protein interactions, was shown here to not alter the expression of PSD-95 in the spinal cord or indeed of other members of the MAGUK family when compared to wild type littermates (Figure 5.4). As PSD-95 assembles with the NMDA receptor, thus coupling the receptor to distinct intracellular pathways that may mediate downstream changes, it was investigated whether the PSD-95^{SH3W470L} mutation altered the expression levels of NMDA receptor subunits. Expression of the NMDA receptor subunits was found to be unaffected by the PSD-95^{SH3W470L} mutation when compared to wild type littermates (Figure 5.4). Thus the PSD-95^{SH3W470L} mutation did not result in overall changes in levels of NMDA receptor subunit or MAGUK expression in the spinal cord, therefore suggesting that the phenotype displayed by this mutation may not have been the result of compensation by other MAGUK proteins but is likely to be due to the mutation itself.

PSD-95^{SH3W470L} mutants were found to develop the same behavioural reflex sensitivity to both thermal (Hargreaves' thermal stimulator) and mechanical (von Frey filaments) stimuli following peripheral nerve injury to that seen in wild type littermate mice. The PSD-95^{SH3W470L} mutants were tested to see if this mutation would disrupt sensitisation caused by inflammation using the intraplantar injection of formalin (Chaplan et al., 1997). The formalin test elicits a biphasic nociceptive response (Dubuisson and Dennis, 1977), consisting of an early intense response (first phase) and a more prolonged response (second phase). This biphasic response has been characterised by behavioural and electrophysiological measures (Chaplan et al., 1997; Coderre and Melzack, 1992b; Dickenson and Sullivan, 1987c; Dickenson and Sullivan, 1987b; Haley et al., 1990; Wheeler-Aceto and Cowan, 1991). There appeared to be no difference between PSD-95^{SH3W470L} mutant mice and wild type littermate responses in the first phase of the formalin test. However PSD-95^{SH3W470L} mutant mice had a greatly reduced second phase of the response compared to wild type littermates.

The first phase of the formalin response is considered to be of peripheral origin that is, a direct effect of formalin on peripheral nociceptive endings, where MAGUKs are generally thought not to be expressed (Garry et al., 2003; Tao et al., 2003a). This may explain the

findings presented here of an intact first phase response in both PSD-95^{SH3W470L} mutant and wild type littermate mice. The second phase of the formalin test appears to be driven by both ongoing peripheral activity (Dallel et al., 1995; Puig and Sorkin, 1996; Taylor et al., 1995) and by central sensitisation in the spinal cord (Chaplan et al., 1997; Coderre et al., 1990; Coderre and Melzack, 1992b; Dickenson and Sullivan, 1990; Haley et al., 1990; Villetti et al., 2003). This idea that the second phase of the formalin response may not be mediated by central sensitisation alone, may explain why the PSD-95^{SH3W470L} mutation resulted in a blunted response rather that a complete lack of second phase response.

PSD-95^{SH3W470L} mutants were assessed to see if their response to Complete Freund's Adjuvant as a model of persistent inflammation was attenuated by this single point mutation. PSD-95^{SH3W470L} mutants and wild type mice both developed the same ipsilateral behavioural reflex sensitivity to thermal and mechanical stimuli at the early stage of 0-6 hours post CFA injection. Interestingly this sensitivity does not continue in the PSD-95^{SH3W470L} mutants at the later stages of 24 and 48 hours post CFA injection unlike wild type mice which continued to display behavioural reflex sensitivity at these later times post CFA injection (up to 24 hours for mechanical allodynia in wild type).

Previous findings have reported the CFA response as having an acute phase (seen around 4 hours post injection), a subacute phase (represented by day 4 post injection) and a chronic phase (seen by day 14 post injection) (Parra et al., 2002; Raghavendra et al., 2004). Other reports have described a broadly similar profile of the CFA response involving behavioural sensitisation as early as 2-6 hours (Ji et al., 2002; Zhang et al., 2003) with recovery around day 5 post CFA injection (Zhang et al., 2003) and sensitisation to a thermal stimulus seen by 3 days but with recovery by 9 days post CFA injection (Molliver et al., 2005). The CFA inflammatory response seems to be quite variable perhaps depending on site of injection, however in most of these reports there seems to be an early onset of sensitisation followed by a sustained stage of sensitisation that can last up to 5-14 days post injection.

It has been suggested that in contrast to later times following CFA, the early time point of 6 hours may be a result of peripheral inflammation, as the use of a specific inhibitor (of p38

mitogen-activated protein (MAP) kinase), when administered into the intrathecal space via a catheter (at the level of L4) attenuated thermal hyperalgesia at 24 and 48 hours post CFA injection but had no effect at 6 hours post CFA injection and did not alter oedema or macrophage number in the inflamed skin, suggesting that intrathecal administration of the inhibitor did not alter peripheral inflammation (Ji et al., 2002). Here behavioural reflex sensitisation is seen ipsilaterally at 0-6 hours but not observed at the later times of 24 and 48 hours post CFA injection in PSD-95^{SH3W470L} mutants, the above report (Ji et al., 2002) suggests that the early stage of the CFA response may be of peripheral origin, which could explain why behavioural reflex sensitisation is still seen in PSD-95^{SH3W470L} mutants at this early time point in contrast to that at later times, which may be centrally mediated. The PSD-95^{SH3W470L} mutants here have highlighted the possibility of differences in the behavioural response as a result of CFA injection, at different stages of the response, by showing differences between the early and sustained stages.

However this does not explain why the PSD-95^{SH3W470L} mutation itself has lead to such a blunted inflammatory response. Due to previous findings of the persistence of the formalin response in PSD-95^{PDZ1-2} mutant mice, where the third PDZ, the SH3 and the GK domains are absent, an explanation for an attenuated inflammatory response here in the PSD-95^{SH3W470L} mutants might be explained by taking into account some novel structural features as outlined above of PSD-95's SH3 domain. The PSD-95^{SH3W470L} mutants have an SH3 domain with a mutation to its hydrophobic binding surface (the region containing the PXXP motif), which may prevent the intermolecular binding of the SH3 domain, thus resulting in disruption of the inflammatory response in these PSD-95^{SH3W470L} mutants. The PSD-95^{PDZ1-2} mutants show a formalin response equal to that of wild type, yet they lack PDZ 3, SH3 and GK domains (Garry et al., 2003). This could be explained by the possibility that although the SH3 domain intermolecular binding is prevented in the PSD-95^{PDZ1-2} mutation, so too is the intramolecular binding of the SH3 and GK domains in this mutation. However in the PSD-95^{SH3W470L} mutants, the intramolecular binding of the SH3 and GK domains was not thought to be targeted by the tryptophan 470 mutation. Indeed it has been reported that the mutation of tryptophan 470 of PSD-95 to phenylalanine or alanine (other nonpolar [hydrophobic] amino acids like tryptophan), did affect the

intermolecular interaction but did not abolish the intramolecular interaction (McGee and Bredt, 1999; Shin et al., 2000). This may suggest that the PSD-95^{SH3W470L} mutation is able to inhibit the inflammatory response through the mutation's prevention of intermolecular binding in the SH3 domain while maintaining the intramolecular binding of the SH3 and GK domains.

To summarize PSD-95^{PDZ1-2} mutant mice lack the expected sensory sensitisation following a peripheral nerve injury model while formalin-induced responses are entirely normal (Garry et al., 2003). In contrast PSD-95^{SH3W470L} mutant mice have intact neuropathic reflex behaviours and blunted inflammatory responses, suggesting that even different domains of the same molecule can contribute selectively to different pain states. It is striking that a single point mutation in a binding site of PSD-95 can have just as profound an effect on sensitised pain behaviours as domain deletions (Garry et al., 2003; Migaud et al., 1998) antisense ablation (Tao et al., 2003a) and complete null mutations (Tao et al., 2003b). The wider significance of this PSD-95^{SH3W470L} mutation may be in the design of novel analgesics that could act to prevent the sensitisation of specific pain states.

6. Investigation into the expression of PSD-95 and Pyk 2 in an experimental model of mononeuropathy, persistent inflammation and formalin-induced inflammation, focusing on their interaction in the experimental model of mononeuropathy

6.1 Introduction

As discussed previously (Section 1.7.3 and 5.1) PSD-95, a membrane associated guanylate kinase (MAGUK) is of critical importance for the development of nerve injury induced behavioural sensitization and is essential for spinal N-methyl-D-aspartate (NMDA) receptor-mediated thermal hyperalgesia (Garry et al., 2003; Tao et al., 2003). PSD-95 is composed of three N-terminal PDZ (PSD-Dlg-ZO-1 homology) domains, an SH3 (Src homology 3) domain and a GK (guanylate kinase-like) domain in its C-terminal region (see Figure 1.3). PSD-95 was first described, to be expressed in the spinal cord but not in peripheral nervous tissue, such as dorsal root ganglion by Tao et al. (Tao et al., 2001). PSD-95 immunoreactivity was found in the superficial dorsal horn of the spinal cord, with distribution in lamina I and outer lamina II, while Garry et al., showed expression of PSD-95 to be restricted to lamina II through β-galactosidase reporter gene staining of PSD-95 mutant mice (Garry et al., 2003; Tao et al., 2003). The localisation of PSD-95 to lamina I and lamina II is of interest as this distribution overlaps with that of the NMDA receptor subunits, in particular NR2B (Boyce et al., 1999; Garry et al., 2003; Tao et al., 2000). The superficial dorsal horn of the spinal cord is the primary area for processing noxious stimulation; it receives primary afferent termini from the periphery and descending fibers from supraspinal structures, in addition to receiving processes from the deep dorsal horn neurons (Rustioni and Weinberg, 1989). The fact that PSD-95 is localized to this area of the spinal cord advocates its potential importance in nociceptive processing.

The expression of spinal PSD-95 is not affected by spinal nerve axotomy or by dorsolateral funiculus lesions (Tao et al., 2000). It has recently been shown that spinal PSD-95 expression appeared similar between naïve animals and animals thirty minutes post complete Freund's adjuvant injection (Guo et al., 2004), although whether the

expression of PSD-95 is affected by other experimental pain models has yet to be clarified. The localization of PSD-95 expression in the spinal cord has been ascertained using the well established enzyme-mediated immunodetection (using the avidin–biotinylated horseradish peroxidase complex method; Tao et al., 2000) however this method makes it difficult to conduct a multiple staining approach to assess the possible association of PSD-95 with other antigens of interest. Immunofluoresence histochemistry allows for multiple staining of tissue and has been used to establish the expression of PSD-95 in the brain, however spinal PSD-95 has not been detected using this method thus far (Castejon et al., 2004; Seabold et al., 2003).

The investigations carried out in the previous chapter (Chapter 5) revealed the importance of a single domain of PSD-95, the SH3 domain, in the development of formalin- and CFA-induced behavioural responses. It would therefore be of interest to look at the possible interaction of PSD-95 with the binding partners of its SH3 domain as these interactions may play a specific and crucial role in pain signalling. As discussed previously SH3 domains (Section 1.7.3; Section 5.1) are protein interaction domains with a binding specificity for proline rich sequences containing a PXXP motif (Erpel et al., 1995; Lim and Richards, 1994; Mayer and Eck, 1995; Pawson and Scott, 1997). Until the turn of this century the only proline rich binding partner for a MAGUK SH3 domain identified was the kainaite subtype glutamate receptor subunit KA2 (Garcia et al., 1998). However the SH3 domain of PSD-95 can not be looked at in isolation, as recent investigations into its structure have revealed novel features, which show it to have an atypical binding specificity (McGee et al., 2001; Shin et al., 2000; Tavares et al., 2001). It was established that the SH3 domain and the GK domain form an integrated structural unit, that is the SH3 domain is composed of discontinuous elements of sequence, with four β strands (A-D) followed by a hinge region that separates β strands D and E, and the GK domain is inserted between β strands E and F (McGee et al., 2001; Tavares et al., 2001; see Figure 1.4). This shows the striking difference in structure of PSD-95's SH3 domain compared to typical SH3 domains, as it contains an extra β strand (six β strands (A-F) instead of five) and the large hinge region (McGee et al., 2001). The structural studies also illustrated novel intramolecular interactions between the SH3 and GK

domain, that do not involve the SH3 domain's proline binding site and that such intramolecular binding may be favoured over intermolecular binding (McGee and Bredt, 1999; Nix et al., 2000; Shin et al., 2000; Tavares et al., 2001). This research suggests that the SH3 domain of PSD-95 has alternative surfaces for intra- and inter-molecular interactions, raising the possibility that this domain may contain multiple binding sites (McGee et al., 2001; Tavares et al., 2001; Yaffe, 2002).

Understanding of the SH3 domain's structure may aid the identification of new binding partners for the SH3 domain. The KA2 subunit has been demonstrated to bind to both the SH3 and GK domains, interestingly binding and clustering of KA2 subunit is abolished when both SH3 and GK domains are mutated or deleted but if one domain is left intact clustering still occurs (Garcia et al., 1998). More recent investigations have identified more MAGUK SH3 domain binding partners that include: Mixed lineage kinases (MLK) 2 and 3, which have been identified to interact with PSD-95 in cultured cells and *in vivo* (Savinainen et al., 2001). The identification of MLK 2/3 as a specific binding partner of PSD-95's SH3 domain was carried out using PSD-95 GST-fusion protein constructs, that clearly identified MLK 2/3 binding to the SH3 or SH3-GK constructs but not the GK only construct (Savinainen et al., 2001). Another protein identified as a possible SH3 binding partner is A-Kinase-Anchoring Protein (AKAP) 79/150, again using GST-fusion protein constructs encompassing the domains of PSD-95 (Colledge et al., 2000). This work showed AKAP 79/150 binding to both the SH3 and GK domains, indeed mutating the SH3 proline-rich binding sequence did not affect the binding of AKAP 79/150, although interestingly disrupting the intramolecular binding of SH3 and GK domains diminished AKAP 79/150 binding (Colledge et al., 2000). Huntingtin protein, which is encoded by the huntingtin gene, has also been identified as an SH3 domain binding partner, when the huntingtin gene is defective a polyglutamine repeat in the protein huntingtin is expressed, which results in Huntington's disease, a fatal neurodegenerative disorder (Borrell-Pages et al., 2006). Huntingtin protein was identified as an SH3 domain binding partner through PSD-95 GST-fusion protein constructs, again that clearly identified huntingtin binding to the SH3 or SH3-GK constructs but not the GK only construct (Sun et al., 2001). Another binding partner of the SH3 domain identified

recently is Pyk 2, a non-receptor tyrosine kinase, which was shown to directly interact with PSD-95 in rat brain (independent of the presence of the NMDA receptor) and through GST-fusion protein constructs, Pyk 2 demonstrated binding to the SH3 domain only and not to the GK domain (Huang et al., 2001; Seabold et al., 2003).

As the research into SH3's binding partners outlined above had revealed that the KA2 subunit and AKAP 79/150 bound to both the SH3 and GK domains, it was decided not to focus on these proteins as they were not entirely SH3 domain specific. Since huntingtin, Pyk 2 and MLK 2/3 were illustrated to bind to the SH3 domain construct but not the GK domain construct it was therefore decided to focus on these proteins as they appeared to be SH3 domain specific. However due to time and technical (adequate antibody availability) limitations, only one of these proteins could be focused on, Pyk 2. This candidate was chosen based on its clearly identified direct interaction with PSD-95's SH3 domain, its potential role in NMDA receptor dependent plasticity (Huang et al., 2001) (and that of the subfamily of nonreceptor protein tyrosine kinases in synaptic plasticity (Huang and Hsu, 1999; O'Dell et al., 1991) and the possible involvement of Pyk 2 in the activation of mitogen-activated protein (MAP) kinases, including p42 and p44 MAP kinases (Blaukat et al., 1999), whose importance in the development of neuropathic pain sensitisation has been illustrated in Chapter four.

Protein tyrosine kinases can be sub-divided into receptor tyrosine kinases and non-receptor protein tyrosine kinases (which do not span the plasma membrane). Non-receptor protein tyrosine kinases have been classified into different subfamilies based on sequence similarity and distinct structural characteristics (Hanks and Quinn, 1991). To date there are nine subfamilies of non-receptor protein tyrosine kinases in addition to four protein tyrosine kinases that do not appear to belong to the classified subfamilies, one such subfamily is the focal adhesion family, which consists of the focal adhesion kinase (FAK) and the proline-rich tyrosine kinase (Pyk 2) (Neet and Hunter, 1996), another example of a subfamily is the Src family, which is comprised of nine protein tyrosine kinases and include for example, Src, Fyn, Lck and Lyn (Neet and Hunter, 1996). Src has been reported to be expressed in the DRG and in the spinal cord and is believed to

contribute to the development and maintenance of inflammatory-induced hypersensitivity (Guo et al., 2004; Igwe, 2003), additionally a recent report shows that nerve injury induces the activation of Src, Lck and Lyn in spinal microglia and when such activation is inhibited (through use of the Src-family tyrosine kinase inhibitor, PP2 ([4-amino-5-(4-chlorophenyl)-7-(t-butyl)pyrazolo[3,4-d]pyrimidine])) nerve injury-induced mechanical hypersensitivity was suppressed (Katsura et al., 2006). Here we will focus on Pyk 2, which is also known as CAK-β, CADTK, RAFTK and FAK2 (Avraham et al., 1995; Herzog et al., 1996; Lev et al., 1995; Sasaki et al., 1995; Yu et al., 1996) and is predominantly expressed in the central nervous system and cells derived from hematopoietic lineages, whereas its alternatively spliced isoform (Pyk 2-H) is specifically expressed in T and B lymphocytes, monocytes, and natural killer cells (Dikic et al., 1998; Lev et al., 1995). Pyk 2 has a molecular mass between 110-125 kDa and has a similar domain structure to that of FAK, while FAK is localized to focal adhesion sites in adherent cells, Pyk 2 is mainly diffused throughout the cytoplasm and is concentrated in the perinuclear region (Andreev et al., 1999).

Pyk 2 can be activated in response to various stimuli, such as depolarization, growth factor receptor activation that increase the intracellular calcium concentration, as well as by protein kinase C (PKC) activation (Lev et al., 1995; Park et al., 2000). Pyk 2 can also be activated in response to agonists of G-protein-coupled receptors such as bradykinin, L-α-lysophosphatidic acid (LPA; Dikic et al., 1996). Furthermore Pyk 2 can be activated in response to stress signals (such as tumor necrosis factor-α, changes in osmolarity) and in such cases can trigger activation of the JNK cascade (Tokiwa et al., 1996; Yu et al., 1996). Activation of Pyk 2 in response to an increase in intracellular free Ca^{2+} can be prevented by use of PKC inhibitors (Hiregowdara et al., 1997; Raja et al., 1997; Siciliano et al., 1996; Soltoff et al., 1998), although the exact mechanism of PKC's involvement is unclear. Upon activation of Pyk 2, autophosphorylation at Tyr402 (tyrosine402) and Tyr579/580 (tyrosine579/580) occurs, which allows for Pyk 2 to bind to the SH2 domain of Src (Dikic et al., 1996) leading to the activation of Src by relieving autoinhibition (Dikic et al., 1996; Thomas and Brugge, 1997; Xu et al., 1997). The phosphorylation of Pyk 2 in leading to the recruitment of Src can result in the activation of the MAPK

signalling cascade (Avraham et al., 1995; Lev et al., 1995), and furthermore, Src has a number of important substrates which have been identified to include the NMDA receptors (Wang and Salter, 1994; Yu et al., 1997; Zheng et al., 1998) (and $GABA_A$ receptors, Moss et al., 1995; voltage-gated K^+ channels, Holmes et al., 1996; Huang et al., 1993), whose response is enhanced by phosphorylation. Pyk 2 has also been shown to be associated with the ARF (ADP-ribosylation factor)-GAP protein, PAP (Pyk 2 C terminus-associated protein; Andreev et al., 1999) and with a novel family of Pyk 2-binding proteins designated Nirs (Pyk 2 N-terminal domain-interacting receptors; Lev et al., 1999), which are calcium-binding proteins that possess phosphatidylinositol transfer activity. Activation of Pyk 2 can also lead to tyrosine phosphorylation of the adapter protein Shc, focal contact proteins $p130^{cas}$ and paxillin (Astier et al., 1997; Lev et al., 1995; Li and Earp, 1997).

The purpose of this investigation is to illustrate for the first time the expression of Pyk 2 (both phosphorylated and pan [phosphorylation state-independent]) in the spinal cord and to assess any changes in Pyk 2 or PSD-95 protein expression that may occur following experimental models of mononeuropathy, persistent inflammation and formalin-induced inflammation. The interaction of PSD-95 with Pyk 2 will also be examined in the experimental model of mononeuropathy.

6.2 Methods

All experiments were carried out using adult male Wistar rats (180-250g). As outlined in Chapter three the following methods were used in this investigation: Animals (n=25) underwent surgery for a model of experimental mononeuropathy, a unilateral chronic constriction injury to the sciatic nerve (CCI; Section 3.2.1) and were behaviourally assessed (Section 3.4) prior to surgery (to obtain baseline values) and post surgery (from day 6) until recovery (day 19-25 post surgery) from CCI. Animals (n=8) that were used for a model of persistent inflammation were injected subcutaneously with complete Freund's adjuvant (CFA; Section 3.2.2) into the dorsum surface of the right hind paw. All animals were behaviourally assessed (Section 3.4) prior to injection (to obtain baseline values) and post injection from 0-2 hours until 5 days (120 hours) post injection. For both models, all animals were tested for signs of mechanical allodynia using calibrated Von Frey filaments (Section 3.4.2) and for signs of thermal hyperalgesia using the Hargreaves' thermal apparatus (Section 3.4.4) and in the case of CCI injured animals for cold allodynia (Section 3.4.3). Any effect of either CCI or CFA injury on behavioural reflexes were analysed as detailed in Section 3.8.1. Animals (n=8) that were used for the intraplantar injection of formalin (5% solution: Section 3.2.3) were assessed for their formalin-induced behavioural responses (Section 3.3), which consisted of flicking, flinching and licking of the affected hind-paw prior to injection until recovery (90 minutes post-injection), with any effect of formalin on the behavioural response analysed as detailed in Section 3.8.1.

The expression of PSD-95, Pyk 2 and [PTyr^{402}] Pyk 2 proteins in the spinal cord was assessed in CCI (n=8) and CFA (n=6) injured animals that displayed peak behavioural reflex sensitization and formalin (n=3) injured animals showing peak behavioural responses, in saline injected animals (n=3) and naïve (n=4) spinal cord and brain (n=2) samples. Animals were terminally anaesthetised prior to and during dissection of all tissues when a laminectomy of the spinal lumbar region was performed and spinal cord tissue was homogenised in Laemmli lysis buffer to prepare spinal cord extracts (Section 3.6.1). The proteins of prepared spinal cord extracts were then separated by

electrophoresis and transferred to PVDF membranes, blocked and probed for either mouse monoclonal anti-PSD-95, rabbit polyclonal anti-phosphorylated-[Tyr402]-Pyk 2 or rabbit polyclonal anti-Pyk 2 ('pan': phosphorylation state-independent) or for the ubiquitous housekeeping protein GAPDH, and detected by peroxidase-linked secondary antibodies (goat-anti-mouse or goat-anti-rabbit) and enhanced chemiluminescence (Section 3.6.4). Densitometry of spinal cord extracts immunoblots was performed to measure quantitatively the grey levels of positive protein bands and background grey levels relative to GAPDH (with the absolute numerical values derived being arbitrary; Section 3.8.2).

The expression of PSD-95 and Pan Pyk 2 in the spinal dorsal horn was assessed immunohistochemically in naïve (n=4) and CCI (n=6) nerve injured animals that displayed peak behavioural reflex sensitization (Section 3.7). All animals were terminally anaesthetised and transcardially perfused with a 4% paraformaldehyde fixative solution after which the spinal cord was removed and post-fixed (Section 3.7.1). Spinal cord sections were cut on a freezing microtome, washed, quenched and underwent an antigen retrieval step (sections treated with 3M Urea solution) prior to incubation with mouse monoclonal anti-PSD-95 and/or rabbit polyclonal anti-Pyk 2 ('pan': phosphorylation state-independent). Subsequently, sections were incubated with the appropriate fluorescent or peroxidase linked secondary antibody (and if necessary amplification reagent) before incubation with a nuclear marker (Section 3.7.2). All sections were examined using a Leica TCSNT Confocal system to acquire single optical section images at both low and higher (with x5 and x20 objective lens) magnification (Section 3.8.4). Images were analysed by measuring the mean fluorescent intensity in lamina I, II, III and IV of the ipsilateral and contralateral sides in CCI injured and naïve dorsal horns using Scion Image analysis, from 8-10 randomly selected sections from each of 4 naïve animals and of 6 CCI injured animals (Section 3.8.4). The total numbers of PSD-95 and Pan Pyk 2 immunopositive cells were counted in lamina I to III and the number of colocalised cells and non-colocalised cells that were either PSD-95 or Pan Pyk 2 immunopositive were measured using LCS-Lite software, from 6-8 randomly selected sections per 4 naïve animals and 6 CCI injured animals (Section 3.8.4).

6.3 Results

6.3.1 Analysis of the development of behavioural reflex sensitisation ipsilateral to sciatic nerve injury in the chronic constriction injury (CCI) model of experimental mononeuropathy.

All the nerve-injured animals showed the behavioural changes characteristic of the CCI model. All of the animals that underwent CCI surgery (Section 3.2.1) held the affected limb in a protective manner, keeping it held flexed with claws tightly clasped. The animals developed a limp gait and favoured the contralateral hind limb in locomotion. These abnormalities are thought to be indications of spontaneous pain (Attal et al., 1990). Apart from these changes post-operative animals appeared healthy, had no signs of weight loss and were handled without any distress being evident. During this study none of the animals developed any signs of autotomy.

Thermal Hyperalgesia ***[see Figure 4.1 A]***

All animals were behaviourally tested for signs of thermal hyperalgesia, using the Hargreaves' thermal apparatus (Section 3.4.4). Baseline (pre-surgical) paw withdrawal latency (PWL) was measured as ipsilateral, 12.9 ± 1.8 seconds and contralateral 12.8 ± 1.7 seconds (data show mean latency ± SEM responses). At all time points from the sixth day until the twenty fourth day post-surgery, all animals showed significantly reduced PWL ipsilateral to the injury as compared to the contralateral side ($p<0.05$ by Student's t-test) and a significant reduction in PWL was also seen between post-surgical and pre-surgery values ($p<0.05$; one way repeated measures ANOVA followed by Dunnetts post hoc analysis), no significant difference was observed in the PWL on the twenty fifth day post-surgery. For all animals the contralateral PWL did not show significant reductions in its response. All animals reached a peak of thermal hyperalgesia between the thirteenth and nineteenth days post-surgery when the ipsilateral PWL was 3.4 ± 0.1 seconds and contralateral was 11.9 ± 1.2 seconds (data show mean latency ± SEM responses). In addition to developing such a reduced ipsilateral response to a noxious heat stimulus, the animals also altered their response from a rapid flick of the hind paw returning to a resting posture (observed in pre-operative animals) to that of a flick where the animals

tended to hold the limb elevated for a longer period or shake and or lick the affected paw before returning to a resting posture (observed in post-operative animals).

Mechanical Allodynia *[see Figure 4.1 B]*

All animals were tested for signs of mechanical allodynia using calibrated Von Frey filaments (Section 3.4.2). The baseline (pre-surgical) paw withdrawal threshold (PWT) required to elicit a response was ipsilateral 4830.6 ± 0 mN/mm^2 and contralateral 4830.6 ± 0 mN/mm^2 (data show mean pressure ± SEM responses). At all time points from the sixth day until the nineteenth day post-surgery, all animals demonstrated an increased sensitivity to mechanical stimuli with a significantly reduced PWT ipsilateral to the injury as compared to the contralateral side ($p<0.05$ Wilcoxon test) and a significant reduction in PWT was also seen between post-surgical and pre-surgery values ($p<0.05$; Friedman test on ranks followed by Dunn's post hoc analysis). There was no significant reduction in the PWT response of the contralateral limb in all animals. Animals reached a peak of mechanical allodynia around the fourteenth day post-surgery when the ipsilateral PWT was 1429.0 ± 116.5 mN/mm^2 and contralateral was 4830.6 ± 43.9 mN/mm^2 (data show mean pressure ± SEM responses).

Cold Allodynia *[see Figure 4.1 C]*

All animals were tested for signs of cold allodynia by detecting the animal's response to iced water (4°C; Section 3.4.3), measuring the Suspended Paw Elevation Time (SPET) during a 20 second time period. Prior to surgery naïve rats showed no change in behaviour in response to iced water with both an ipsilateral and contralateral baseline SPET value of 0 ± 0 sec (data show mean ± SEM responses). At all time points from the sixth day until the nineteenth day post-surgery, all animals demonstrated an increased sensitivity to a cold stimulus with a significantly increased SPET value ipsilateral to the injury as compared to the contralateral side ($p<0.05$; Wilcoxon test) and a significant increase in SPET was also seen between post-surgical and pre-surgery values ($p<0.05$; Friedman test on ranks followed by Dunn's post-hoc analysis). There was no significant increase in the SPET response of the contralateral limb in all animals. Animals reached a peak of cold allodynia around the thirteenth day post-surgery when the ipsilateral SPET

was 14.0 ± 1.3 sec and contralateral remained unaffected at 0 ± 0 sec (data show mean ± SEM responses).

6.3.2 Analysis of the development of behavioural reflex sensitisation following the Complete Freund's Adjuvant (CFA) model of persistent inflammation.

All injured animals showed behavioural changes characteristic of the CFA model. All of the animals that underwent CFA injections (Section 3.2.2) showed signs of cutaneous inflammation within the first hour post-injection, demonstrated by an area of localized erythema and oedema around the site of injection in the affected hind paw, which remained present throughout testing and was similar between all animals. The animals, unlike the CCI nerve-injured animals, did not develop a limp gait or tend to favour the contralateral hind limb in locomotion. All post CFA injected animals appeared healthy, had no signs of weight loss and were handled without any distress being evident.

Thermal Hyperalgesia ***[see Figure 6.1 A]***

All CFA-injected animals were behaviourally tested for signs of thermal hyperalgesia, using the Hargreaves' thermal apparatus (Section 3.4.4). Baseline (pre-injection) paw withdrawal latency (PWL) was measured as ipsilateral, 16.1 ± 0.7 seconds and contralateral 16.9 ± 0.5 seconds (data show mean latency ± SEM responses). At all time points from the first two hours until forty eight hours post-injection, all animals showed significantly reduced PWL ipsilateral to the injury as compared to the contralateral side ($p<0.05$ by Student's t-test) and a significant reduction in PWL was also seen between post-surgical and pre-surgery values ($p<0.05$; one-way repeated measures ANOVA followed by Dunnetts post hoc analysis). No significant difference was observed in the PWL from seventy two to one hundred and twenty hours (days 3-5) post-injection, measured as ipsilateral 10.3 ± 0.4 seconds and contralateral 13.4 ± 1.5 seconds at 120 hours post injection (data show mean latency ± SEM responses). For all animals the contralateral PWL did not show significant reductions. All animals reached a peak of thermal hyperalgesia around twenty four/forty eight hours post-injection when the ipsilateral PWL was 7.4/7.4 ± 0.6 seconds and contralateral was 12.5/11.4 ± 1.2 seconds respectively (data show mean latency ± SEM responses).

Mechanical Allodynia ***[see Figure 6.1 B]***

All animals were tested for signs of mechanical allodynia using calibrated Von Frey filaments (Section 3.4.2). The baseline (pre-injection) paw withdrawal threshold (PWT) required to elicit a response was ipsilateral 4830.6 ± 0 mN/mm^2 and contralateral 4830.6 ± 0 mN/mm^2 (data show mean pressure ± SEM responses). At all time points from the first two hours until one hundred and twenty hours (day 5) post-injection, all animals demonstrated an increased sensitivity to mechanical stimuli with a significantly reduced PWT ipsilateral to the injury as compared to the contralateral side ($p<0.05$ Wilcoxon test) and from three-six hours until one hundred and twenty hours (day 5) post-injection a significant reduction in PWT was also seen between post-surgical and pre-surgery values ($p<0.05$; Friedman test on ranks followed by Dunn's post-hoc analysis). There was no significant reduction in the PWT response of the contralateral limb in all animals. Animals reached a peak of mechanical allodynia around forty eight/seventy two hours post-injection when the ipsilateral PWT was 1609.5 ± 433.8 mN/mm^2 at both time points and contralateral was 4329.6 ± 500.9 mN/mm^2 at both time points (data show mean pressure ± SEM responses).

6.3.3 Analysis of the formalin-induced behavioural response ***[see Figure 6.2]***

All animals were injected subcutaneously into the plantar surface of the hind paw and allowed five minutes to recover before analysis began, which consisted of counting the number of flick/flinch responses per minute of the affected paw. All animals developed the formalin-induced behavioural response of an initial acute phase (5-20 minutes post-injection) and a late phase (25-80 minutes post-injection), with all animals beginning to show signs of recovery around 90-95 minutes post-injection whereupon behavioural analysis was stopped. All animals had a significant increase in responses at all time points following formalin injection when compared to the pre-injection response ($p<0.05$; one-way repeated measures ANOVA followed by Dunnett's post-hoc analysis), with a maximal increase to 39.5 ± 4.1 (data show mean number of flicks/flinches per minute ± SEM).

6.3.4 The level of expression of PSD-95 Pyk 2 and [PTyr^{402}] Pyk 2 in the spinal cord of CCI, CFA and formalin-injured animals and in the spinal cord and brain of naïve animals

PSD-95 expression ***[see Figure 6.3 and Table 6.1]***

The level of PSD-95 protein expression was assessed in naïve brain and spinal cord and in CCI, CFA and formalin-injured spinal cord. The spinal cord extracts of CCI and CFA injured animals were taken at the peak of behavioural reflex sensitization and for formalin-injured animals at the peak of the late phase behavioural response. PSD-95 expression was significantly increased ipsilateral to CCI injury when compared to the contralateral side and naïve controls (data show percent ± SEM, percent expression of GAPDH, the ubiquitous housekeeping protein, as determined by densitometric analysis; $p<0.05$, Wilcoxon test). The respective values were 50 ± 2% (ipsilateral), 24 ± 6% (contralateral) and 23 ± 4% (naïve) with the absolute numerical values, derived from densitometry, being arbitrary. While there appeared to be some increase in the level of PSD-95 expression ipsilateral to formalin injury when compared to the contralateral, saline and naïve controls, this was not significant. The level of PSD-95 expression was not affected by CFA as no ipsilateral increase was observed when compared to the contralateral side, saline and naïve controls. The level of PSD-95 expression was similar in all cases between naïve and saline spinal cord and the contralateral side of injured spinal cord. The expression of PSD-95 in naïve brain is also shown, the expression of which can be seen to be greater than that observed in the spinal cord (see Table 6.1 for relative quantification).

Pan-Pyk 2 expression ***[see Figure 6.4 and Table 6.1]***

The level of Pan-Pyk 2 protein expression was assessed in naïve brain and spinal cord and in CCI, CFA and formalin-injured spinal cord. Again the spinal cord extracts of CCI and CFA-injured animals were taken at the peak of behavioural reflex sensitization and for formalin-injured animals at the peak of the late phase behavioural response. Pan-Pyk 2 expression was significantly increased ipsilateral to CCI injury when compared to the contralateral side and naïve controls (data show percent ± SEM, percent expression of

GAPDH, as determined by densitometric analysis; $p<0.05$, Wilcoxon test). The respective values were 31 ± 1% (ipsilateral), 24 ± 1% (contralateral) and 23 ± 1% (naïve) with the absolute numerical values, derived from densitometry, being arbitrary. Pan-Pyk 2 expression was unaltered by either CFA or formalin injury when the ipsilateral side was compared to the contralateral side, saline and naïve controls. Also the level of Pan-Pyk 2 expression did not differ between naïve and saline spinal cord and the contralateral side of injured spinal cord. The expression of Pan-Pyk 2 in naïve brain is also shown, the expression of which can be seen to be greater than that observed in the spinal cord (see Table 6.1 for relative quantification).

Phosphorylated Pyk 2 ([PTyr^{402}] Pyk 2) expression ***[see Figure 6.5 and Table 6.1]***

The level of [PTyr^{402}] Pyk 2 protein expression was assessed in naïve brain and spinal cord and in CCI, CFA and formalin-injured spinal cord. All injured spinal cord extracts were taken from animals at the peak of injury induced behavioural reflex sensitisation or in the late phase of the formalin behavioural response. Relative levels of [PTyr^{402}] Pyk 2 expression were not affected in any of the injury models explored here, the CCI, CFA or formalin models, when the ipsilateral side of each was compared to the contralateral side, saline and naïve controls. Again the level of [PTyr^{402}] Pyk 2 expression did not differ between naïve spinal cord and the contralateral side of injured spinal cord. The expression of [PTyr^{402}] Pyk 2 in naïve brain is also shown (see Table 6.1 for relative quantification).

6.3.5 Immunohistochemical analysis of the expression of PSD-95 and Pyk 2 in the spinal dorsal horn of naïve and CCI injured animals at low magnification.

PSD-95 expression ***[see Figure 6.6]***

The expression of PSD-95 was assessed in the dorsal horn of naïve and CCI-injured spinal cord by means of immunofluorescence histochemistry. All injured spinal cord sections were taken from animals at the peak of CCI injury-induced behavioural reflex sensitization. CCI resulted in a significant ipsilateral increase in the expression of PSD-95 (measured by the level of fluorescent staining intensity) in Lamina I and II when

compared to the contralateral side and naïve animals. Within the regions of interest in Lamina I and II (refer to section 3.8.4 and Figure 3.2), there was a significant ipsilateral increase in the mediolateral region to 112.8 ± 5.1 (mean fluorescence intensity in arbitrary absolute values ± SEM) when compared to the contralateral side 88.4 ± 4.7 ($p<0.05$, Student's paired t-test) and naïve animals 87.9 ± 2.3 ($p<0.05$, Student's unpaired t-test). There was also a significant ipsilateral increase in the intermediate region to 117.8 ± 5.0 and lateral region to 125.1 ± 5.7 (mean fluorescence intensity in arbitrary absolute values ± SEM) when compared to the contralateral side 85.2 ± 4.6; 93.4 ± 4.3, respectively ($p<0.05$, Student's paired t-test) and naïve animals 89.8 ± 1.9; 92.3 ± 2.6, respectively ($p<0.05$, Student's unpaired t-test). The expression of PSD-95 was not altered by CCI injury in either Lamina III or IV when the ipsilateral side was compared to the contralateral side or naïve animals.

Pyk 2 expression ***[see Figure 6.7]***

Immunofluorescence histochemical techniques were also utilized to assess the expression of Pyk 2 in the dorsal horn of naïve and CCI-injured spinal cord. All injured spinal cord sections were taken from animals at the peak of CCI injury-induced behavioural reflex sensitization. The expression of Pyk 2 was significantly increased (measured by the level of fluorescent staining intensity) ipsilateral to CCI injury in Lamina I and II when compared to the contralateral side and naïve animals. This increase was observed in the regions of interest in Lamina I and II (refer to section 3.8.4 and Figure 3.2), firstly with a significant ipsilateral increase in the mediolateral region to 74.3 ± 4.7 (mean fluorescence intensity in arbitrary absolute values ± SEM) when compared to the contralateral side, 62.6 ± 2.8 ($p<0.05$, Student's paired t-test) and naïve animals, 60.9 ± 1.5 ($p<0.05$, Students unpaired t-test). There was also a significant ipsilateral increase in the intermediate region to 74.5 ± 4.5 and lateral region, 77.8 ± 5.3 (mean fluorescence intensity in arbitrary absolute values ± SEM) when compared to the contralateral side 63.3 ± 2.9; 62.9 ± 3.3, respectively ($p<0.05$, Student's paired t-test) and naïve animals 61.2 ± 1.2; 60.2 ± 1.2, respectively ($p<0.05$, Student's unpaired t-test). Within Lamina III and IV the expression of Pyk 2 was not altered by CCI injury when the ipsilateral side was compared to the contralateral side or naïve animals.

6.3.6 Immunohistochemical analysis of the cellular expression of PSD-95 and Pyk 2 in the spinal dorsal horn of naïve and CCI-injured animals.

PSD-95 expression ***[see Figure 6.8 and 6.9]***

The number of PSD-95-immunopositive cells in the regions of interest (ROI) in the dorsal horn of naïve and CCI injured spinal cord (see Section 3.8.4) were counted from single optical section images from 6-8 randomly selected sections per 4 naïve animals and 6 CCI injured animals. The number of PSD-95-immunopositive cells were counted in lamina I, II and III using LCS-Lite software, where only cells that were associated with To-pro staining (nuclear marker) and whose intensity was at least twice background intensity were counted as immunopositive (refer to Section 3.8.4 and Figure 3.4). With regard to CCI-injured animals only spinal cord sections from animals at the peak of injury induced behavioural reflex sensitization were used for analysis. The number of PSD-95 immunopositive cells was increased ipsilateral to CCI injury when compared to the contralateral side and naïve animals. There was a significant increase in the number of PSD-95-immunopositive cells in Lamina I of the dorsal horn ipsilateral to injury to 541 ± 16 (total cell number per ROI ± SEM) when compared to the contralateral side 369 ± 12 ($p<0.05$; Student's paired t-test) and to naïve animals 361 ± 12 ($p<0.05$; students unpaired t-test). A significant increase in the number of PSD-95-immunopositive cells in Lamina II of the dorsal horn ipsilateral to injury was also noted, to 684 ± 18 (total cell number per ROI ± SEM) when compared to the contralateral side 407 ± 11 ($p<0.05$; student's paired t-test) and to naïve animals 379 ± 13 ($p<0.05$; Student's unpaired t-test). There was no difference in the number of PSD-95 immunopositive cells ipsilateral to CCI injury in Lamina III when compared to the contralateral side and naïve animals.

Pyk 2 expression ***[see Figure 6.10 and 6.11]***

The number of Pyk 2-immunopositive cells in the dorsal horn of naïve and CCI injured spinal cord were counted as above (also refer to Section 3.8.4). Animals at the peak of injury-induced behavioural reflex sensitization were used for CCI injury analysis. The number of Pyk 2 immunopositive cells increased ipsilateral to CCI injury when compared to the contralateral side and naïve animals. A significant increase in the number of Pyk 2-

immunopositive cells in lamina I of the dorsal horn ipsilateral to injury was noted, increasing to 521 ± 15 (total cell number per ROI ± SEM) when compared to the contralateral side 361 ± 12 ($p<0.05$; student's paired t-test) and naïve animals 378 ± 13 ($p<0.05$; Student's unpaired t-test). The number of Pyk 2-immunopositive cells in Lamina II of the dorsal horn significantly increased ipsilateral to injury to 700 ± 18 (total cell number per ROI ± SEM) when compared to the contralateral side 423 ± 12 ($p<0.05$; Student's paired t-test) and to naïve animals 402 ± 13 ($p<0.05$; Student's unpaired t-test). In Lamina III no significant difference in the number of Pyk 2-immunopositive cells ipsilateral to CCI injury was seen when compared to the contralateral side and naïve animals.

6.3.7 Immunohistochemical analysis of the colocalisation of PSD-95 and Pyk 2 in the spinal dorsal horn of naïve and CCI injured animals.

Colocalisation of PSD-95 with Pyk 2 ***[see Figure 6.12, 6.13 and 6.14]***

The colocalisation of PSD-95 with Pyk 2 in naïve and CCI injured animals in the spinal dorsal horn was assessed. Colocalisation was determined by profiling each cell using LCS-Lite software (refer to section 3.8.4 and Figure 3.4), whereby the intensity of each fluorochrome was measured in each cell and graphed, if the fluorochrome graph for PSD-95 and Pyk 2 overlapped in a cell that again showed To-pro staining and signal was at least twice background intensity for both PSD-95 and Pyk 2 the cell was counted as a colocalised cell. If the profile of the cell showed the intensities not to overlap then the cell was counted as a non-colocalised cell that was either PSD-95 or Pyk 2 immunopositive. The spinal cords of CCI-injured animals were taken at the peak of behavioural reflex sensitization. The total number of colocalised cells per ROI (Lamina I, II or III) was found to be increased ipsilateral to CCI injury when compared to the contralateral side and naïve animals. The increase in colocalisation was significant in Lamina I of the dorsal horn to 461 ± 13 (total number of colocalised cells per ROI ± SEM) when compared to the contralateral side 264 ± 9 ($p<0.05$; student's paired t-test) and to naïve animals 307 ± 10 ($p<0.05$; Student's unpaired t-test). A significant increase in the number of colocalised cells was also observed in Lamina II of the dorsal horn to

596 ± 15 (total number of colocalised cells per ROI ± SEM) when compared to the contralateral side 285 ± 8 ($p<0.05$; Student's paired t-test) and to naïve animals 295 ± 10 ($p<0.05$; Student's unpaired t-test). No ipsilateral increase in the number of colocalised cells was observed in Lamina III of the dorsal horn when compared to the contralateral side and naïve animals.

Non-Colocalised cells that were PSD-95-immunopositive ***[see Figure 6.13 and 6.15]***
While assessing the colocalisation of PSD-95 with Pyk 2 in naïve and CCI injured animals in the spinal dorsal horn, the number of cells that were not colocalised but PSD-95-immunopositive was also investigated, as described previously by the profiling of each individual cell using LCS Lite software (refer to Section 3.8.4 and Figure 3.4), whereby the intensity of each fluorochrome was measured in each cell and graphed, if the fluorochrome graph for PSD-95 and Pyk 2 showed the intensities not to overlap then the cell was counted as a non-colocalised cell that was either PSD-95 or Pyk 2-immunopositive. Again where each cell showed To-pro staining and signal was at least twice background intensity for both PSD-95 and Pyk 2. The total number of non-colocalised PSD-95-immunpositive cells was found to be increased ipsilateral to CCI injury when compared to the contralateral side and naïve animals. The increase in non-colocalised PSD-95-immunopositive cells was significant in Lamina I of the dorsal horn to 80 ± 2 (total number of non-colocalised PSD-95-immunopositive cells per ROI± SEM) when compared to 28 ± 1 on the contralateral side ($p<0.05$; student's paired t-test) and to 29 ± 1 in naïve animals ($p<0.05$; Student's unpaired t-test). The number of non-colocalised PSD-95-immunopositive cells was also significantly increased in Lamina II of the dorsal horn to 88 ± 2 (number of non-colocalised PSD-95 immunopositive cells per ROI ± SEM) when compared to 29 ± 1 on the contralateral side ($p<0.05$; student's paired t-test) and to 37 ± 2 in naïve animals ($p<0.05$; students unpaired t-test). A significant ipsilateral increase in the number of non-colocalised PSD-95 immunopositive cells was also noted in Lamina III of the dorsal horn to 47 ± 4 (number of non-colocalised PSD-95-immunopositive cells per ROI ± SEM) when compared to 32 ± 3 on the contralateral side ($p<0.05$; Student's paired t-test) and to 20 ± 2 in naïve animals ($p<0.05$; Student's unpaired t-test).

Non-Colocalised cells that were Pyk 2-immunopositive ***[see Figure 6.13 and 6.15]***

During the analysis of colocalisation of PSD-95 with Pyk 2 in naïve and CCI-injured animals in the spinal dorsal horn, the number of cells that were not colocalised but Pyk 2 immunopositive was also determined, as descirbed above (refer to Section 3.8.4 and Figure 3.4). An ipsilateral increase in the number of non-colocalised Pyk 2-immunopositive cells was found to be significant in Lamina II of the dorsal horn to 104 ± 2.7 (total number of non-colocalised Pyk 2-immunopositive cells per ROI ± SEM) when compared to 52 ± 2 on the contralateral side ($p<0.05$; Student's paired t-test) and to 54 ± 3 in naïve animals ($p<0.05$; Student's unpaired t-test). The number of non-colocalised Pyk 2-immunopositive cells was not significantly increased ipsilateral to CCI injury in either Lamina I or III of the dorsal horn when compared to the contralateral side and naïve animals.

Figure 6.1

The time course of development of thermal hyperalgesia and mechanical allodynia following intraplantar injection of complete Freund's adjuvant.

Data show mean ± SEM responses prior to injection (baseline) and following the injection of CFA (n=8). **(A)** Paw withdrawal latency (PWL) from a noxious thermal stimulus (Hargreaves' thermal stimulator) ipsilateral to CFA injection (O) showed significant differences between post-injection and pre-injection values († $p<0.05$; one-way repeated measures ANOVA followed by Dunnett's post-hoc analysis) and from post-injection contralateral (■) values (* $p<0.05$; Student's t-test). No thermal hyperalgesia was seen on the contralateral side (■). **(B)** Paw withdrawal thresholds (PWT) from mechanical stimulation (von Frey filaments) showed significant reductions in post-operative compared to pre-operative values ipsilateral (O) to CCI († $p<0.05$; Friedman test on ranks followed by Dunn's post hoc analysis) and between post-operative ipsilateral and contralateral values (* $p<0.05$; Wilcoxon test). No significant differences were seen in the contralateral side (■).

A.

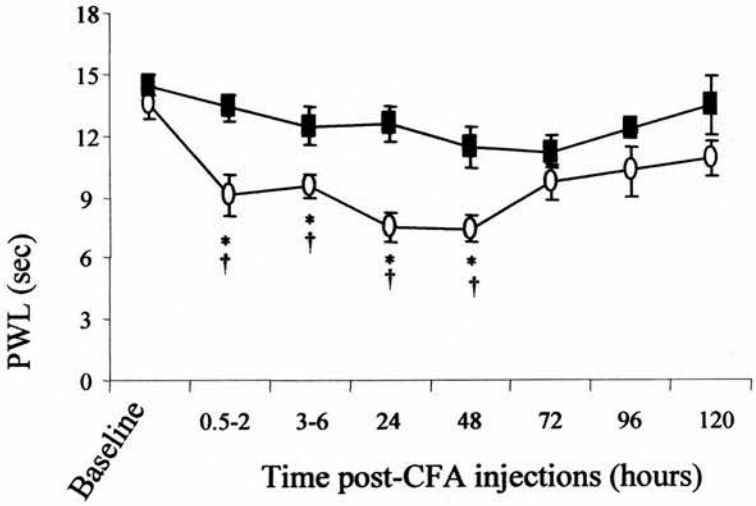
18
15
12
9
6
3
0
PWL (sec)
Baseline
0.5-2
3-6
24
48
72
96
120
Time post-CFA injections (hours)

B.

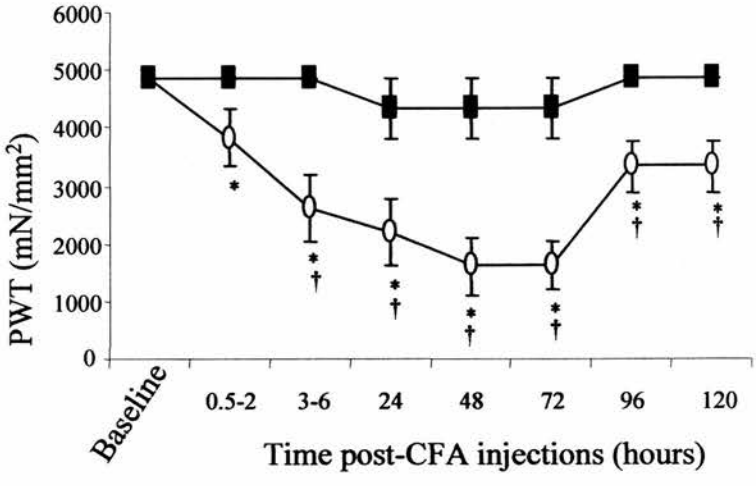
6000
5000
4000
3000
2000
1000
0
PWT (mN/mm²)
Baseline
0.5-2
3-6
24
48
72
96
120
Time post-CFA injections (hours)

Figure 6.2

The time course of development of the behavioural response following the intraplantar injection of formalin.

Data shows mean ± SEM number of paw flick/flinch responses per minute prior to injection and following the injection of formalin (n=8; ♦). All animals displayed both acute (5-20 minutes post-injection) and late (25-80 minutes post-injection) phases of the formalin test, with signs of recovery observed around 90-95 minutes post-injection. At all time points following formalin injection a significant increase in the number of flicks/flinches was observed when compared to pre-injection values (* $p<0.05$; one-way repeated measures ANOVA followed by Dunnett's post-hoc analysis).

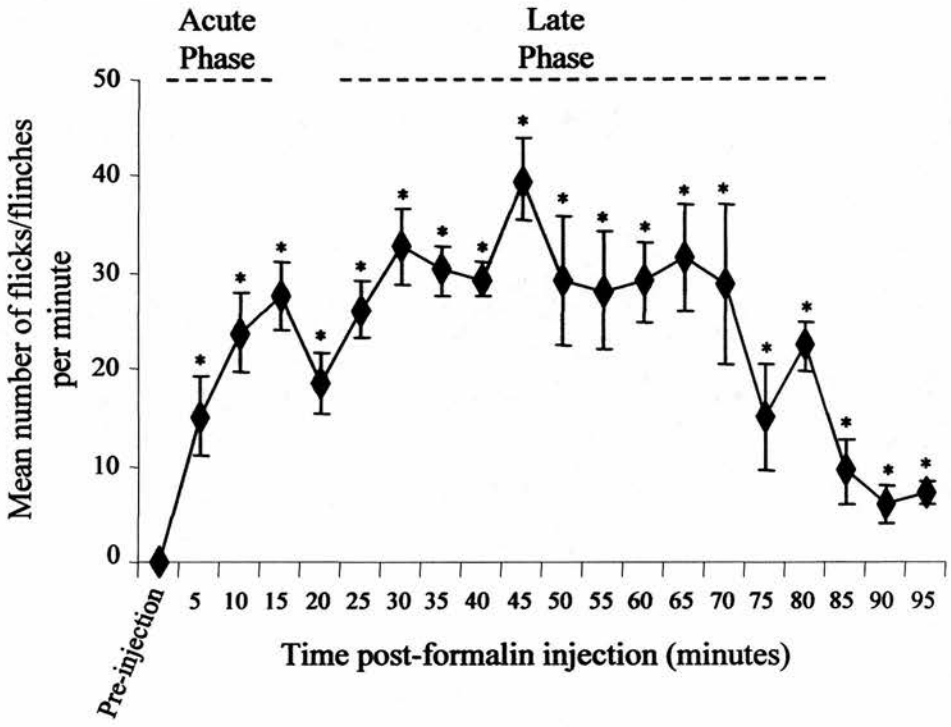
Acute
Phase
Late
Phase
Mean number of flicks/flinches per minute
50
40
30
20
10
0
Pre-injection
5 10 15 20 25 30 35 40 45 50 55 60 65 70 75 80 85 90 95
Time post-formalin injection (minutes)

Figure 6.3

The expression of PSD-95 in the spinal cord following CCI, CFA or Formalin compared to saline and naïve controls

Immunoblots showing the expression of PSD-95 and the ubiquitous housekeeping enzyme GAPDH following experimental mononeuropathy (CCI; n=8), complete Freund's adjuvant model of persistent inflammation (CFA; n=6) and formalin-induced inflammation (Formalin; n=3) compared to saline injected (Saline; n=3) and naïve spinal cord (n=4). Expression levels are from spinal cord extracts of animals displaying, peak behavioural reflex sensitisation following CCI and CFA, and peak late phase behavioural response to formalin on the side ipsilateral (Ipsi) and contralateral (Con) to injury and in saline injected animals ipsilateral (Ipsi) and contralateral (Con) to injection. Expression levels are also shown in spinal cord and brain (n=2) extracts of naïve animals. CCI resulted in a significant ipsilateral increase in the level of PSD-95, while formalin caused a modest but non-significant ipsilateral increase when compared to the contralateral side, saline injected and naïve animals (see Table 6.1 for relative quantification).

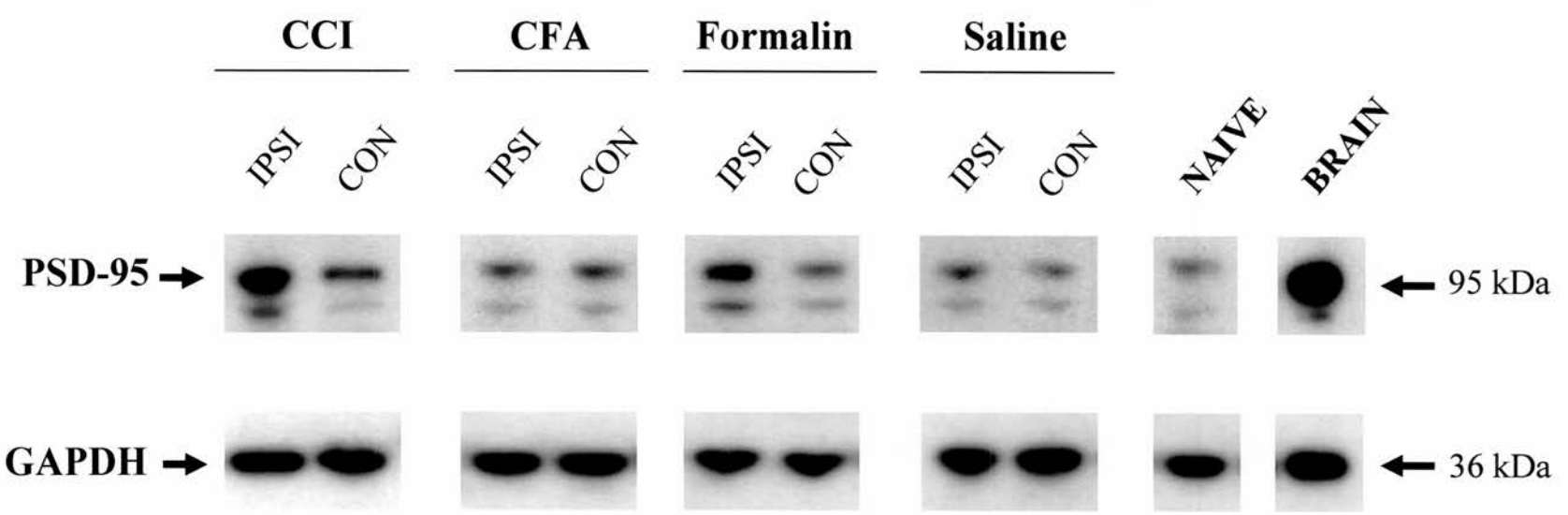
CCI
CFA
Formalin
Saline
IPSI
CON
IPSI
CON
IPSI
CON
IPSI
CON
NAIVE
BRAIN
PSD-95
95 kDa
GAPDH
36 kDa

Figure 6.4

The expression of Pan-Pyk 2 in the spinal cord following CCI, CFA or Formalin compared to saline and naïve controls

Immunoblots showing the expression of Pan-Pyk 2 and the ubiquitous housekeeping enzyme GAPDH following experimental mononeuropathy (CCI; n=8), complete Freund's adjuvant model of persistent inflammation (CFA; n=6) and formalin-induced inflammation (Formalin; n=3) compared to saline injected (Saline; n=3) and naïve spinal cord (n=4). Expression levels are from spinal cord extracts of animals displaying, peak behavioural reflex sensitisation following CCI and CFA, and peak late phase behavioural response to formalin on the side ipsilateral (Ipsi) and contralateral (Con) to injury and in saline injected animals ipsilateral (Ipsi) and contralateral (Con) to injection. Expression levels are also shown in spinal cord and brain (n=2) extracts of naïve animals. CCI alone resulted in a significant ipsilateral increase in the level of Pan-Pyk 2 when compared to the contralateral side, saline injected and naïve animals (see Table 6.1 for relative quantification).

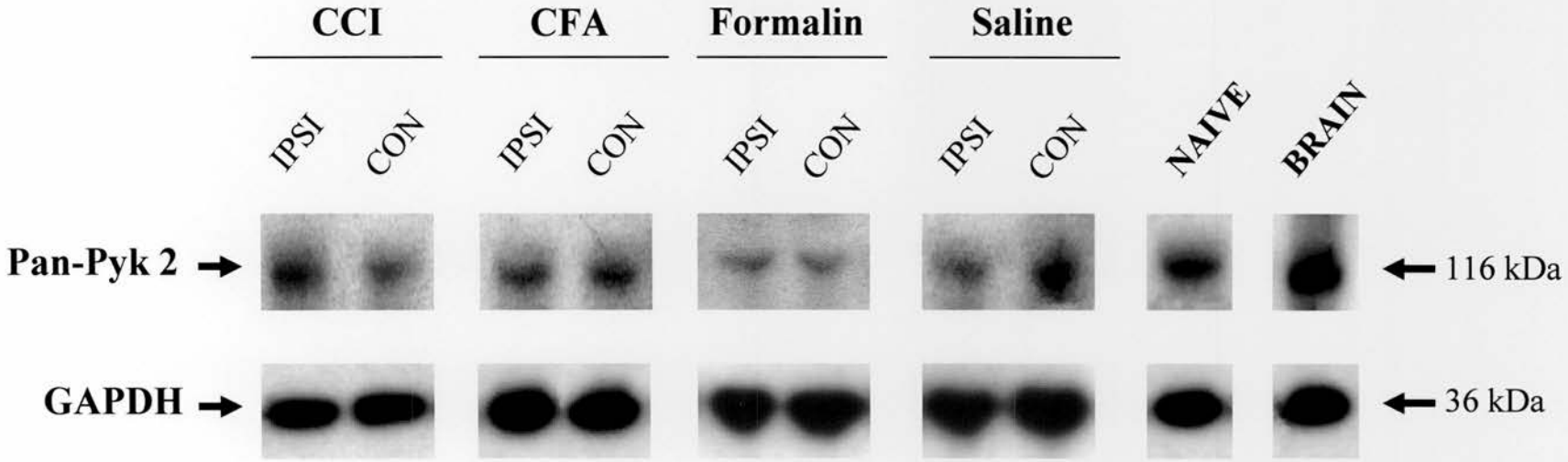
CCI
CFA
Formalin
Saline
IPSI
CON
IPSI
CON
IPSI
CON
IPSI
CON
NAIVE
BRAIN
Pan-Pyk 2
116 kDa
GAPDH
36 kDa

Figure 6.5

The expression of [PTyr^{402}] Pyk 2 in the spinal cord following CCI, CFA or Formalin compared to saline and naïve controls

Immunoblots showing the expression of phosphorylated Pyk 2 ([PTyr^{402}] Pyk 2) and the ubiquitous housekeeping enzyme GAPDH following experimental mononeuropathy (CCI; n=8), complete Freund's adjuvant model of persistent inflammation (CFA; n=6) and formalin-induced inflammation (Formalin; n=3) compared to saline injected (Saline; n=3) and naïve spinal cord (n=4). Expression levels are from spinal cord extracts of animals displaying, peak behavioural reflex sensitisation following CCI and CFA, and peak late phase behavioural response to formalin on the side ipsilateral (Ipsi) and contralateral (Con) to injury and in saline injected animals ipsilateral (Ipsi) and contralateral (Con) to injection. Expression levels are also shown in spinal cord and brain (n=2) extracts of naïve animals. [PTyr^{402}] Pyk 2 expression appears not to be altered by any of the models employed here when expression is compared to the contralateral side, saline injected and naïve animals (see Table 6.1 for relative quantification).

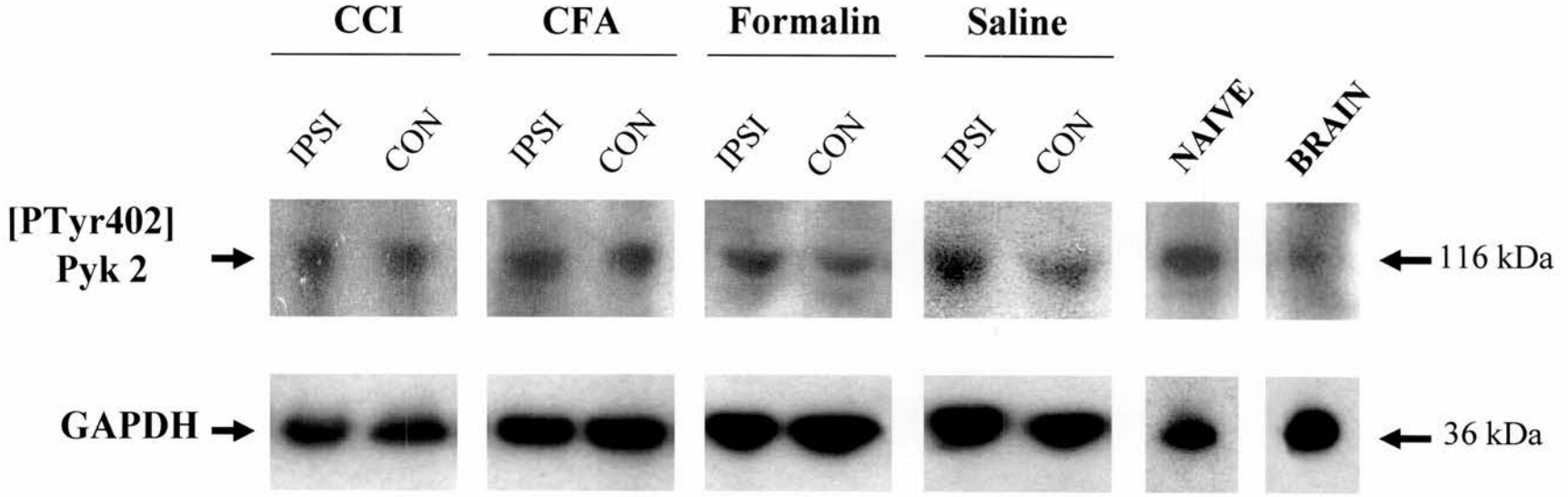
CCI
CFA
Formalin
Saline
IPSI
CON
IPSI
CON
IPSI
CON
IPSI
CON
NAIVE
BRAIN
[PTyr402]
Pyk 2
116 kDa
GAPDH
36 kDa

Figure 6.6

Immunofluoresecnce histochemistry for PSD-95 in the spinal dorsal horn following experimental mononeuropathy and in naïve controls.

(A) Low magnification images (x5 objective lens) illustrating the expression of PSD-95 (green) in the spinal dorsal horn following experimental mononeuropathy (CCI; n=6) compared to naïve (n=4) spinal cord. Expression of PSD-95 in spinal cord sections of animals that displayed peak behavioural reflex sensitization following CCI on the side ipsilateral (Ipsi) and contralateral (Con) to injury and from naïve animals. Following CCI there was an ipsilateral increase in the expression of PSD-95 when compared to the contralateral side and naïve animals. Scale bar 50μm, (L= Lateral edge of the dorsal horn). **(B)** The intensity of the fluorescent staining of PSD-95 was measured using Scion Image [refer to Section 3.8.4]. Data show the mean fluorescence intensity ± SEM (in arbitrary units). As a result of experimental mononeuropathy the expression of PSD-95 was significantly increased ipsilateral to injury when compared to the contralateral side (* $p<0.05$; Student's paired t-test) and naïve animals († $p<0.05$; Student's unpaired t-test). This significant increase was seen in Lamina I and II but not in Lamina III or IV of the dorsal horn.

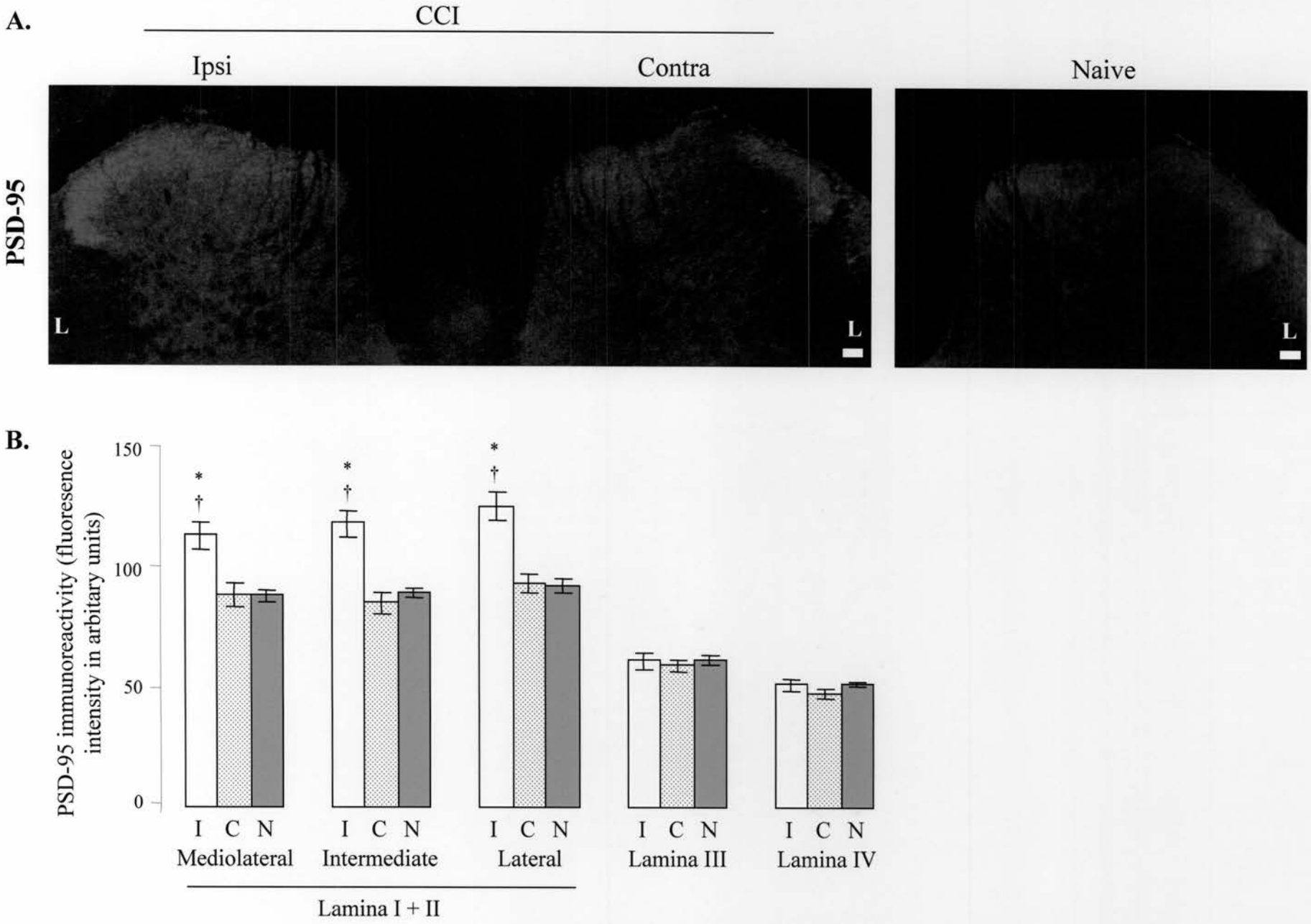
A.
CCI
Ipsi
Contra
Naive
PSD-95
L
L
L
B.
PSD-95 immunoreactivity (fluoresence intensity in arbitary units)
150
100
50
0
I C N
Mediolateral
Intermediate
Lateral
Lamina III
Lamina IV
Lamina I + II

Figure 6.7

Immunofluoresecnce histochemistry for Pan-Pyk 2 in the spinal dorsal horn following experimental mononeuropathy and in naïve controls.

(A) Low magnification images (x5 objective lens) illustrating the expression of Pan-Pyk 2 (red) in the spinal dorsal horn following experimental mononeuropathy (CCI; n=6) compared to naïve (n=4) spinal cord. Expression of Pan-Pyk 2 in spinal cord sections of animals that displayed peak behavioural reflex sensitization following CCI on the side ipsilateral (Ipsi) and contralateral (Con) to injury and from naïve animals. Following CCI there was an ipsilateral increase in the expression of Pan-Pyk 2 when compared to the contralateral side and naïve animals. Scale bar 50μm, (L= Lateral edge of the dorsal horn). **(B)** The intensity of the fluorescence staining of Pan-Pyk 2 was measured using Scion Image [refer to Section 3.8.4]. Data shows the mean fluorescence intensity ± SEM. (in arbitrary units). The expression of Pan-Pyk 2 as a result of experimental mononeuropathy was significantly increased ipsilateral to injury when compared to the contralateral side (* $p<0.05$; Student's paired t-test) and naïve animals († $p<0.05$; Student's unpaired t-test). This significant increase was seen in Lamina I and II but not in Lamina III or IV of the dorsal horn.

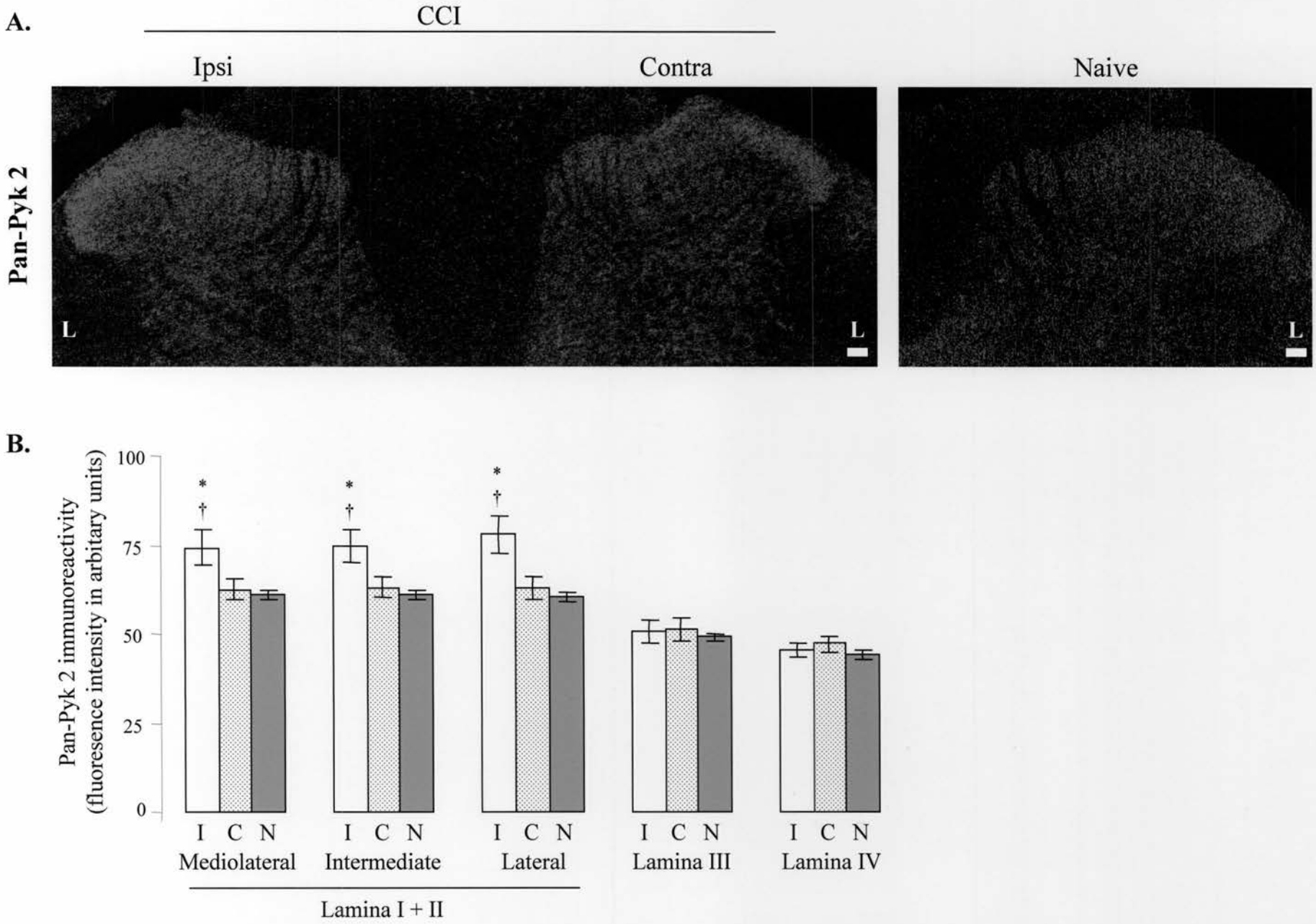
A.
CCI
Ipsi
Contra
Naive
Pan-Pyk 2
L
L
L
B.
Pan-Pyk 2 immunoreactivity
(fluoresence intensity in arbitary units)
100
75
50
25
0
*
†
I C N
Mediolateral
Intermediate
Lateral
Lamina III
Lamina IV
Lamina I + II

Figure 6.8

Immunofluoresecnce histochemistry for PSD-95 in the spinal cord, an example of high power images used for counting cells.

(A). Images taken at higher magnification (x20 objective lens) to show cells that are positive for PSD-95 immunofluorescent staining (green) in the spinal dorsal horn following experimental mononeuropathy (CCI; n=6) and in naïve (n=4) animals. The number of PSD-95-immunopositive cells was increased ipsilateral to CCI when compared to the contralateral side and naïve sections (see Figure 6.9 for graphs). Scale bar 25μm, (L= Lateral edge of the dorsal horn). **(B).** Inset image showing an example spinal cord with boundaries marked for Lamina I, II and III used in counting PSD-95 immunopositive cells (refer to Figure 3.4).

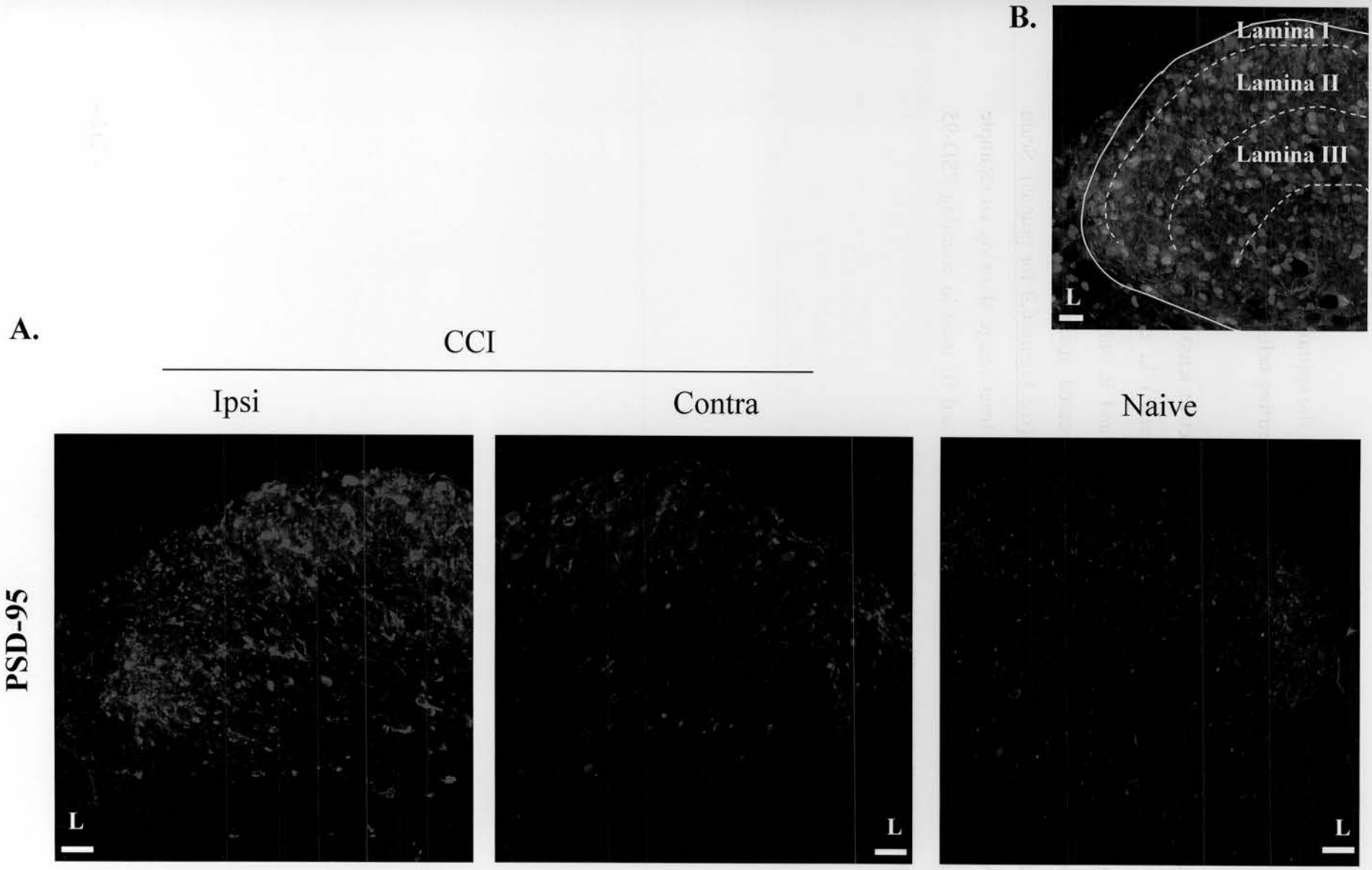
B.
Lamina I
Lamina II
Lamina III
L
A.
CCI
Ipsi
Contra
Naive
PSD-95
L
L
L

Figure 6.9

Gross quantification of numbers of PSD-95-immunopositive cells in the spinal dorsal horn following experimental mononeuropathy and in naïve controls.

PSD-95-immunopositive cells were counted in the ROI (Lamina I, II and III) in the dorsal horn of naïve (n=4) and following experimental mononeuropathy (CCI; n=6) spinal cords from single optical section images captured at higher magnification (x20 objective lens), using LCS-Lite software, where only cells that were associated with To-pro staining (nuclear marker) and whose intensity was at least twice background intensity were counted as immunopositive (refer to Section 3.8.4 and Figure 3.4). Data expressed as total cell number (of PSD-95-immunopositive cells) per ROI ± SEM. CCI resulted in a significant ipsilateral increase in the number of PSD-95-immunopositive cells when compared to the contralateral side (* $p<0.05$; Student's paired t-test) and to naïve animals († $p<0.05$; Student's unpaired t-test). This significant increase was seen in Lamina I **(A)** and Lamina II **(B)** but not in Lamina III **(C)** of the dorsal horn.

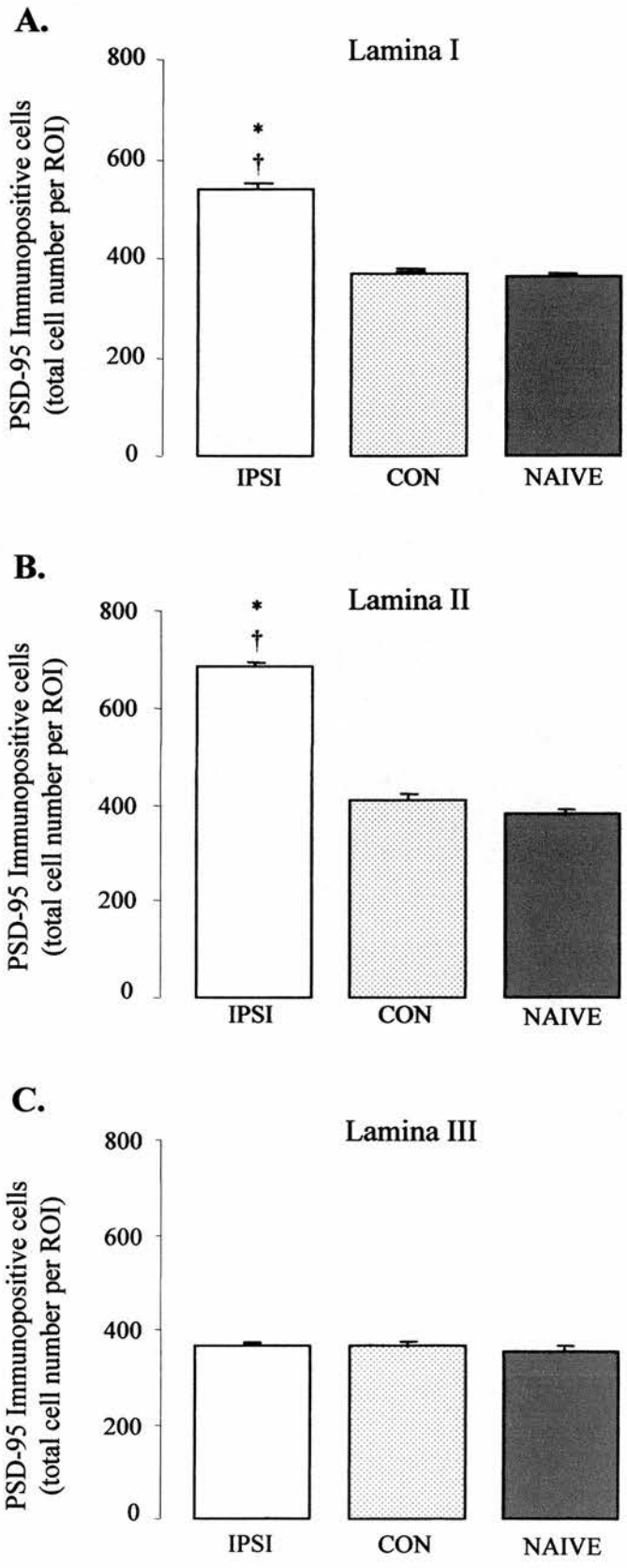
A.
Lamina I
PSD-95 Immunopositive cells
(total cell number per ROI)
800
600
400
200
0
*
†
IPSI
CON
NAIVE
B.
Lamina II
PSD-95 Immunopositive cells
(total cell number per ROI)
800
600
400
200
0
*
†
IPSI
CON
NAIVE
C.
Lamina III
PSD-95 Immunopositive cells
(total cell number per ROI)
800
600
400
200
0
IPSI
CON
NAIVE

Figure 6.10

Immunofluoresecnce histochemistry for Pan-Pyk 2 in the spinal cord, an example of high power images used for counting cells.

(A). Images taken at higher magnification (x20 objective lens) to show cells that are positive for Pan Pyk 2 fluorescent staining (red) in the spinal dorsal horn following experimental mononeuropathy (CCI; n=6) and in naïve (n=4) animals. The number of Pan-Pyk 2 immunopositive cells is increased ipsilateral to CCI when compared to the contralateral side and naïve sections (see Figure 6.11 for graphs). Scale bar 25μm, (L= Lateral edge of the dorsal horn). **(B).** Inset image showing an example spinal cord with boundaries marked for Lamina I, II and III used in counting Pan-Pyk 2 immunopositive cells (refer to Figure 3.4).

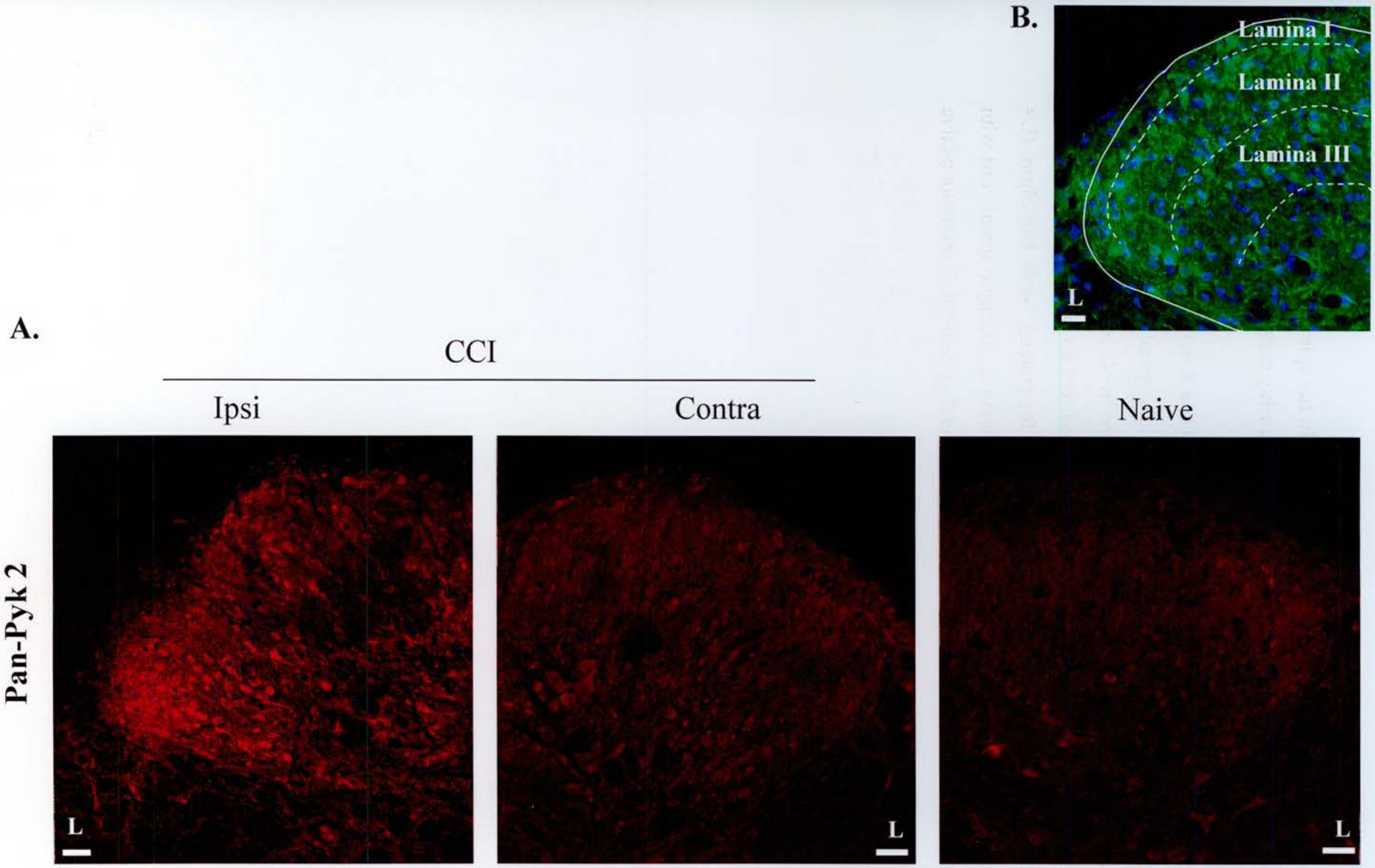
B.
Lamina I
Lamina II
Lamina III
L
A.
CCI
Ipsi
Contra
Naive
Pan-Pyk 2
L
L
L

Figure 6.11

Gross quantification of numbers of Pan-Pyk 2-immunopositive cells in the spinal dorsal horn following experimental mononeuropathy and in naïve controls.

Pan-Pyk 2-immunopositive cells were counted in the ROI (Lamina I, II and III) in the dorsal horn of naïve (n=4) and following experimental mononeuropathy (CCI; n=6) spinal cords from single optical section images captured at higher magnification (x20 objective lens), using LCS-Lite software, where only cells that were associated with To-pro staining (nuclear marker) and whose intensity was at least twice background intensity were counted as immunopositive (refer to Section 3.8.4 and Figure 3.4). Data expressed as total cell number (of Pan-Pyk 2-immunopositive cells) per ROI ± SEM. A significant ipsilateral increase in the number of Pan-Pyk 2-immunopositive cells occurred as a result of CCI when compared to the contralateral side (* $p<0.05$; student's paired t-test) and to naïve animals († $p<0.05$; students unpaired t-test). This significant increase was seen in Lamina I **(A)** and Lamina II **(B)** but not in Lamina III **(C)** of the dorsal horn.

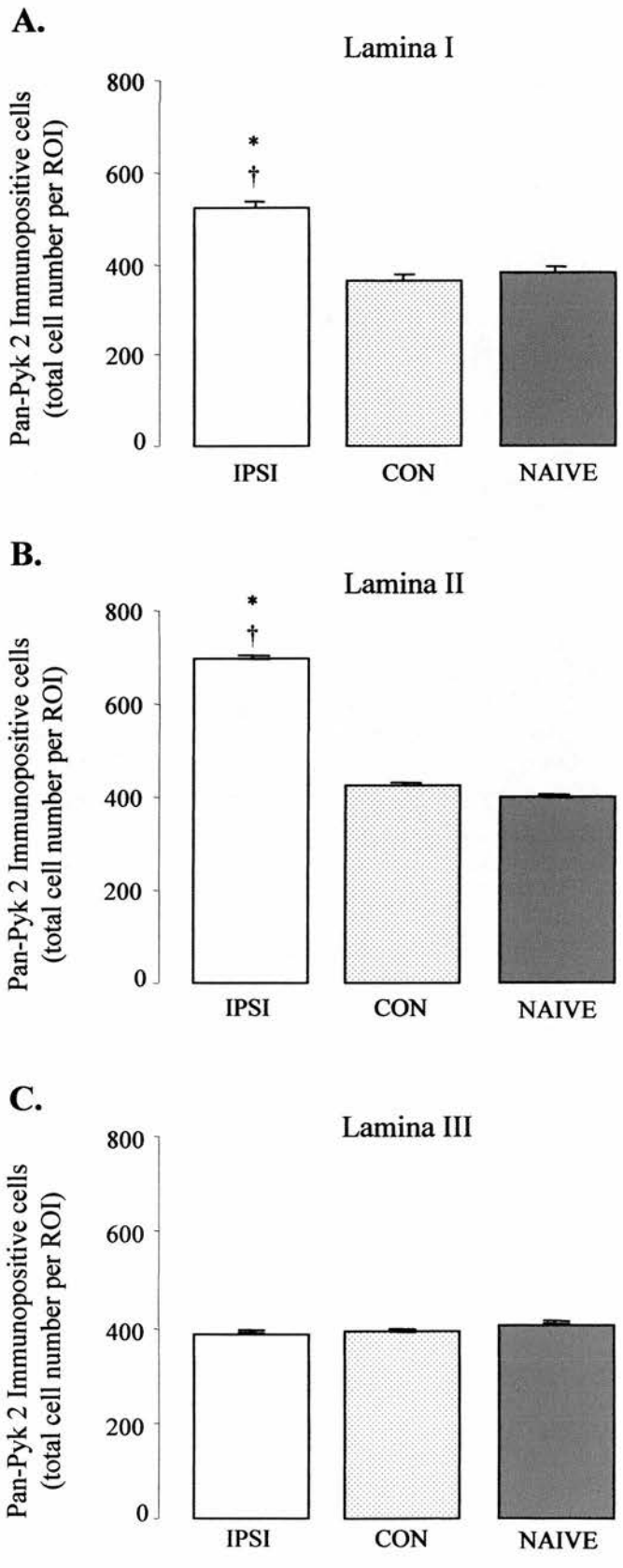
A.
Lamina I
Pan-Pyk 2 Immunopositive cells (total cell number per ROI)
800
600
400
200
0
*
†
IPSI
CON
NAIVE
B.
Lamina II
Pan-Pyk 2 Immunopositive cells (total cell number per ROI)
800
600
400
200
0
*
†
IPSI
CON
NAIVE
C.
Lamina III
Pan-Pyk 2 Immunopositive cells (total cell number per ROI)
800
600
400
200
0
IPSI
CON
NAIVE

Figure 6.12

Immunofluoresecnce histochemistry for colocalisation of PSD-95 with Pyk 2 in the spinal cord, an example of high power images used for counting colocalised cells.

(A) Single optical section images captured at higher magnification (x20 objective lens) to show the colocalisation of PSD-95-immunopositive cells (green) with Pyk 2-immunopositive cells (red) in the spinal dorsal horn following experimental mononeuropathy (CCI; n=6) and in naïve (n=4) animals. The number of colocalised cells per ROI was increased ipsilateral to CCI when compared to the contralateral side and naïve animals (see Figure 6.14 for graphs). (Scale bar 25μm; L= Lateral edge of the dorsal horn). The dashed line box indicates the origin of the magnified images in Figure 6.14, highlighting the region of interest (the box covers Lamina II and the edges of Lamina I and III), to show individual colocalised and non-colocalised cells. **(B)** Inset image showing an example spinal cord with boundaries marked for Lamina I, II and III used in counting the colocalisation of PSD-95-immunopositive cells with Pyk 2-immunopositive cells (refer to Figure 3.4).

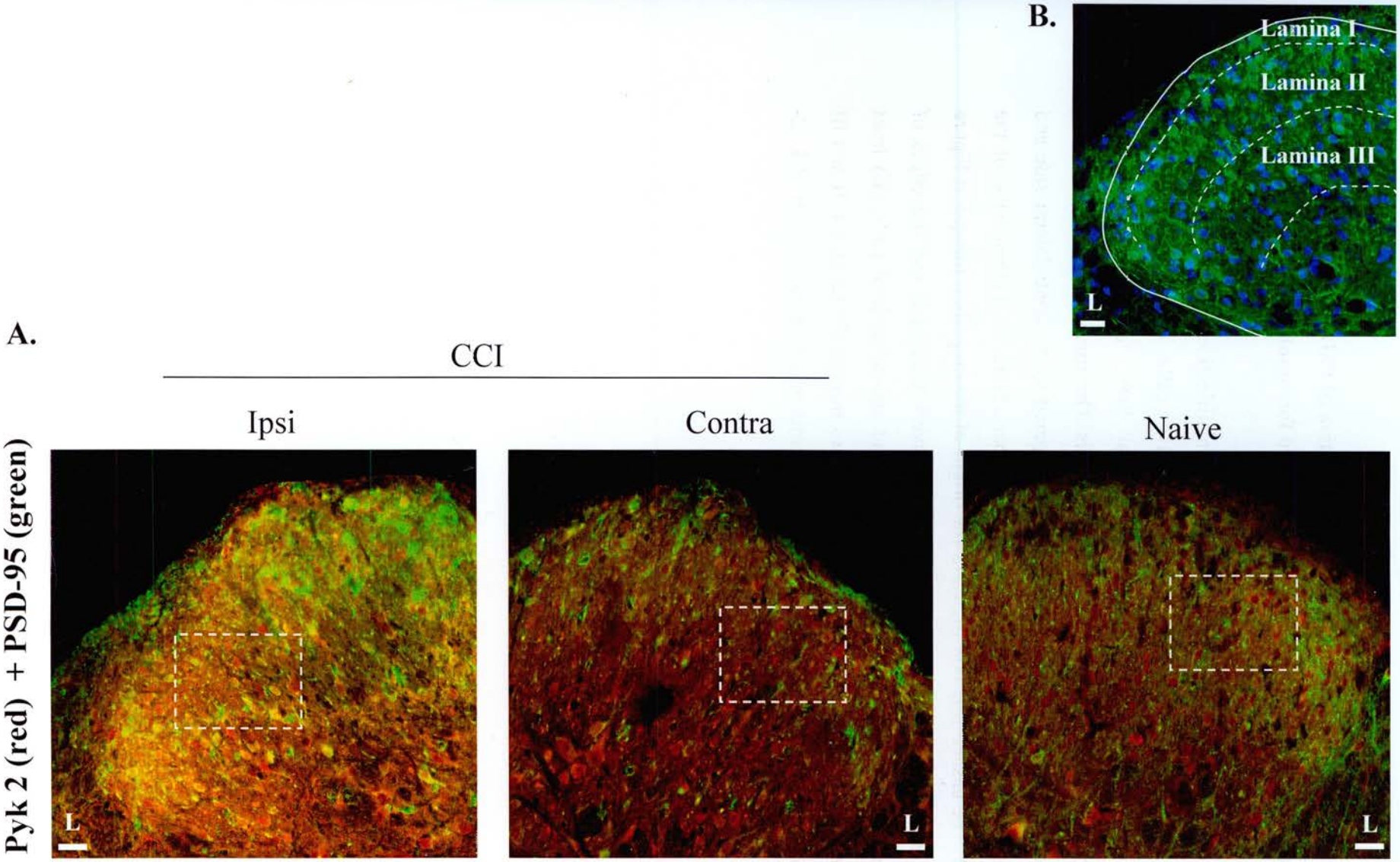
B.
Lamina I
Lamina II
Lamina III
L
A.
CCI
Ipsi
Contra
Naive
Pyk 2 (red) + PSD-95 (green)
L
L
L

Figure 6.13

Immunofluoresecnce histochemistry for colocalisation of PSD-95 with Pyk 2 in an example of a region of interest in the spinal cord

Single optical section images (slice width of 0.8μm) captured at higher magnification (x20 objective lens) using the Leica TCSNT Confocal system, illustrate the region of interest (part of ROI indicated in Figure 6.12 covering Lamina II) that was magnified from the images shown in Figure 6.12, indicated by a dashed line box. These images display colocalisation of PSD-95-immunopositive cells (green) with Pyk 2-immunopositive cells (red) in the spinal dorsal horn following experimental mononeuropathy (CCI; n=6) and in naïve (n=4) animals. Examples of cells that are colocalised are indicated by an arrowhead, cells that are Pyk 2-immunopositive but PSD-95-immunonegative are designated by a thin arrow, while cells that are PSD-95-immunopositive but Pyk 2-immunonegative are pointed out by a thick arrow. The number of colocalised cells per ROI was increased ipsilateral to CCI when compared to the contralateral side and naïve animals (see Figure 6.14 for graphs). The number of cells per ROI that are not colocalised but are either PSD-95- or Pyk 2-immunopositive was also increased ipsilateral to CCI when compared to the contralateral side and naïve sections (see Figure 6.16 for graphs). Scale bar 50μm, (L= Lateral edge of the dorsal horn).

Pyk 2 (red) + PSD-95 (green)

CCI

Ipsi Contra Naive

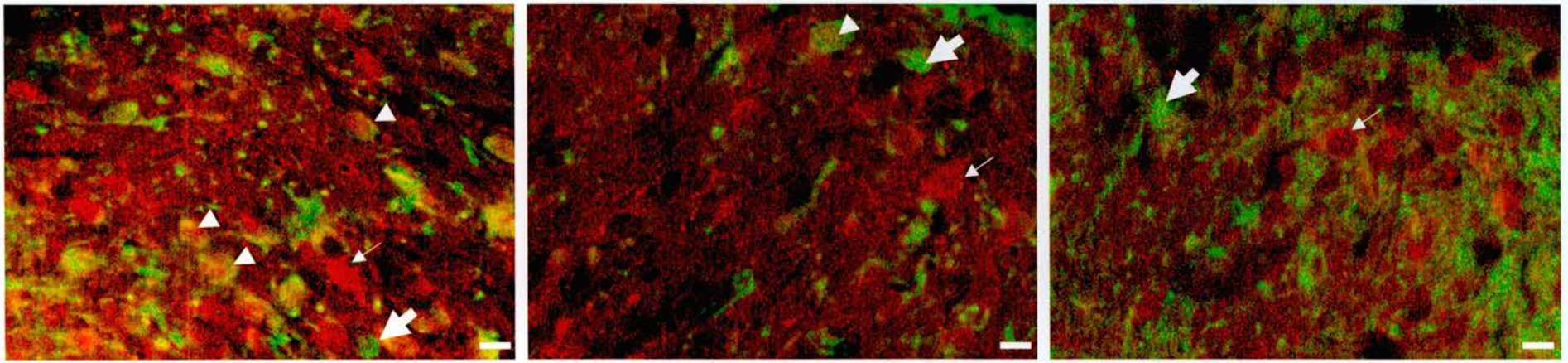

Figure 6.14

Gross quantification of numbers of cells where PSD-95 is colocalised with Pyk 2 in the spinal dorsal horn following experimental mononeuropathy and in naïve controls.

The number of cells that showed colocalisation of PSD-95 with Pyk 2 were counted in the ROI (Lamina I, II and III) following experimental mononeuropathy (CCI; n=6) and in naïve (n=4) spinal dorsal horns from single optical section images captured at higher magnification (x20 objective lens), using LCS-Lite software (refer to section 3.8.4 and Figure 3.4), whereby the intensity of each fluorochrome was measured in each cell and graphed, if the fluorochrome graph for PSD-95 and Pyk 2 overlapped in a cell that again showed To-pro staining and signal was at least twice background intensity for both PSD-95 and Pyk 2 the cell was counted as a colocalised cell. Data is expressed as total number of colocalised cells (colocalisation of PSD-95 with Pyk 2) per ROI ± SEM. A significant ipsilateral increase in the number of colocalised cells occurred as a result of CCI when compared to the contralateral side (* $p<0.05$; Student's paired t-test) and to naïve animals († $p<0.05$; Student's unpaired t-test). This significant increase was seen in Lamina I **(A)** and Lamina II **(B)** but not in Lamina III **(C)** of the dorsal horn.

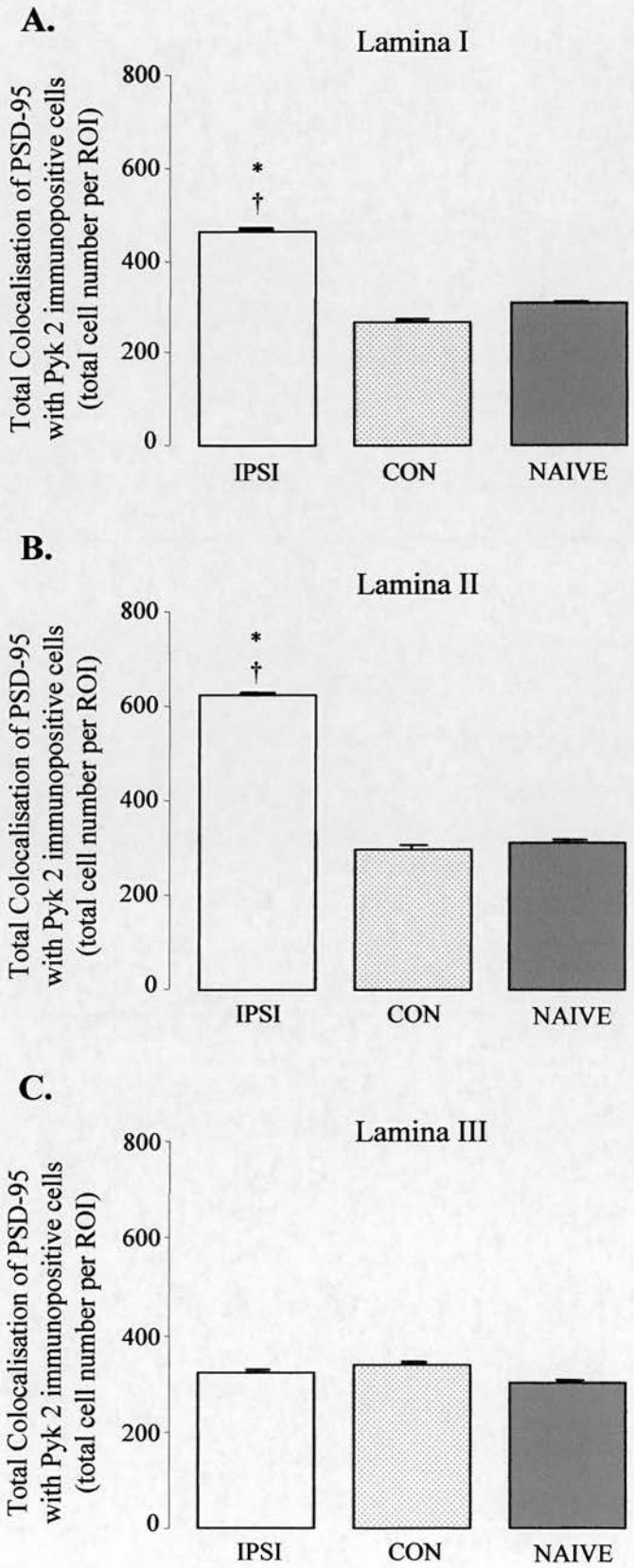
A.
Lamina I
Total Colocalisation of PSD-95 with Pyk 2 immunopositive cells (total cell number per ROI)
800
600
400
200
0
*
†
IPSI
CON
NAIVE
B.
Lamina II
Total Colocalisation of PSD-95 with Pyk 2 immunopositive cells (total cell number per ROI)
800
600
400
200
0
*
†
IPSI
CON
NAIVE
C.
Lamina III
Total Colocalisation of PSD-95 with Pyk 2 immunopositive cells (total cell number per ROI)
800
600
400
200
0
IPSI
CON
NAIVE

Figure 6.15

Gross quantification of numbers of cells where PSD-95 is not colocalised with Pyk 2 in the spinal dorsal horn following experimental mononeuropathy and in naïve controls.

The number of cells that did not show colocalisation of PSD-95 with Pyk 2 were counted in the ROI (Lamina I, II and III) following experimental mononeuropathy (CCI; n=6) and in naïve (n=4) spinal dorsal horns from single optical section images captured at higher magnification (x20 objective lens), using LCS-Lite software (refer to section 3.8.4 and Figure 3.4), whereby the intensity of each fluorochrome was measured in each cell and graphed, if the fluorochrome graph for PSD-95 and Pyk 2 showed the intensities not to overlap then the cell was counted as a non-colocalised cell that was either PSD-95 or Pyk 2-immunopositive. Again where each cell showed To-pro staining and signal was at least twice background intensity for both PSD-95 and Pyk 2. Data is expressed as total number of non-colocalised cells (that are either PSD-95 or Pyk 2-immunopositive) per ROI ± SEM. A significant ipsilateral increase in the number of non-colocalised cells that were PSD-95-immunopositive occurred as a result of CCI when compared to the contralateral side (* $p<0.05$; Student's paired t-test) and to naïve animals († $p<0.05$; Student's unpaired t-test) in Lamina I **(A)** Lamina II **(C)** and in Lamina III **(E)** of the dorsal horn. CCI also resulted in a significant ipsilateral increase in the number of non-colocalised cells that were Pyk 2-immunopositive when compared to the contralateral side (* $p<0.05$; Student's paired t-test) and to naïve animals († $p<0.05$; Student's unpaired t-test) in Lamina II **(D)** only, with no significance seen in Lamina I **(B)** and Lamina III **(F)** of the dorsal horn.

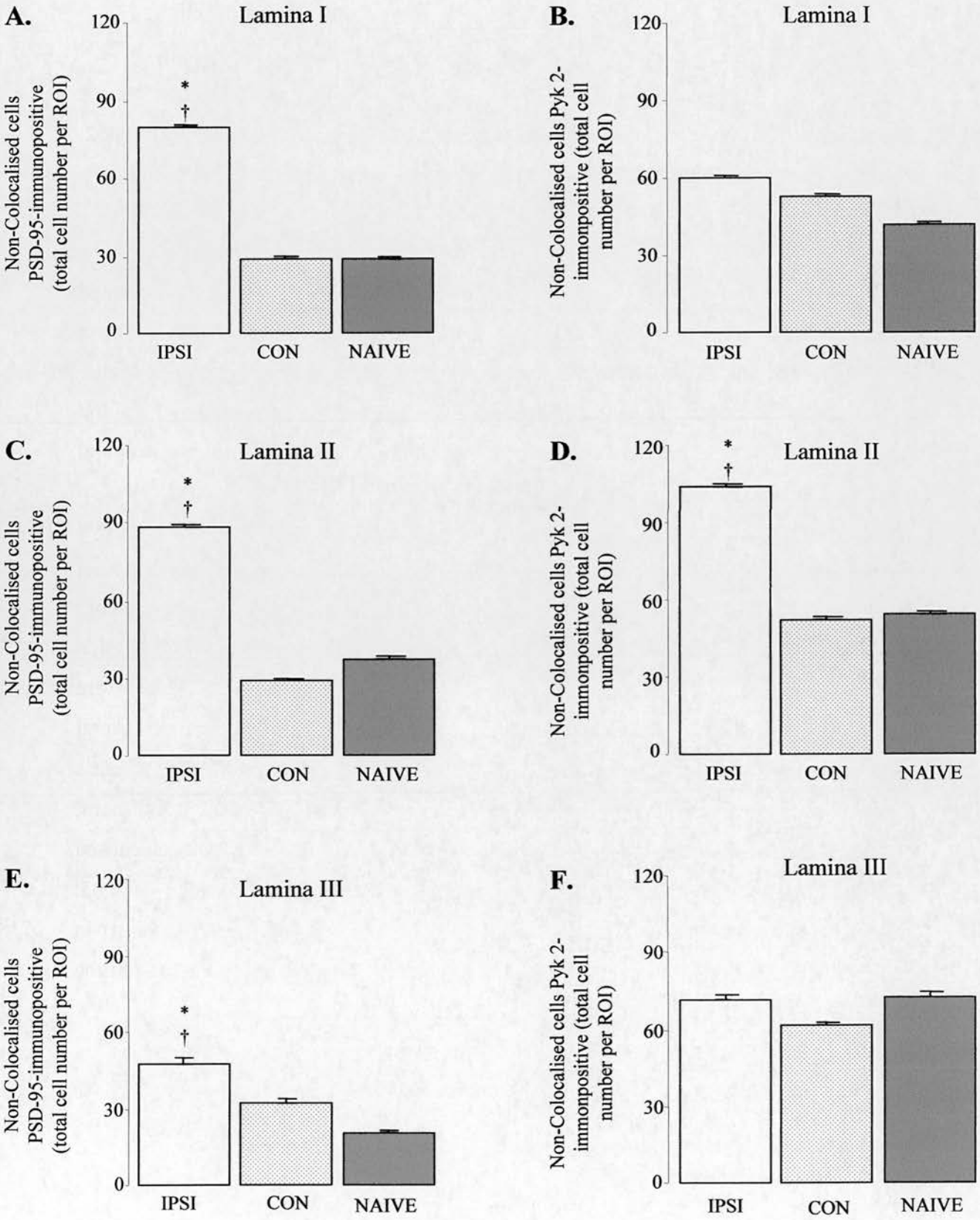
A.
Lamina I
Non-Colocalised cells PSD-95-immunopositive (total cell number per ROI)
120
90
60
30
0
*
†
IPSI
CON
NAIVE
B.
Lamina I
Non-Colocalised cells Pyk 2-immonpositive (total cell number per ROI)
120
90
60
30
0
IPSI
CON
NAIVE
C.
Lamina II
Non-Colocalised cells PSD-95-immunopositive (total cell number per ROI)
120
90
60
30
0
*
†
IPSI
CON
NAIVE
D.
Lamina II
Non-Colocalised cells Pyk 2-immonpositive (total cell number per ROI)
120
90
60
30
0
*
†
IPSI
CON
NAIVE
E.
Lamina III
Non-Colocalised cells PSD-95-immunopositive (total cell number per ROI)
120
90
60
30
0
*
†
IPSI
CON
NAIVE
F.
Lamina III
Non-Colocalised cells Pyk 2-immonpositive (total cell number per ROI)
120
90
60
30
0
IPSI
CON
NAIVE

Table 6.1

The effects of CCI, CFA or formalin challenges on spinal cord expression of PSD-95, Pan-Pyk 2 and [PTyr^{402}] Pyk 2 relative to GAPDH.

Data presented show the expression of Pan-Pyk 2, phosphorylated Pyk 2 ([PTyr^{402}] Pyk 2) and PSD-95 proteins as a percent of GAPDH expression in spinal cord and naïve brain extracts. Since all values are derived from densiometry with different antibodies and incubation conditions, the absolute numerical values, hence percentages calculated, are purely arbitrary. Meaningful comparisons can therefore only be made across treatments with the same antibody and not between antibodies. Data show the percent expression ± SEM as determined by densitometric analysis in spinal cord extracts of CCI (n=8), CFA (n=6) injured animals at the peak of behavioural reflex sensitization and of formalin-injured (n=3) animals at the peak of the late phase behavioural response and in saline injected (n=3) animals, in all cases ipsilateral (ipsi) and contralateral (con) to injury and in naïve brain (n=2) and spinal cord (n=4) [illustrated in Figure 6.4, 6.5 and 6.6]. The expression of Pan-Pyk 2 was found to be significantly increased ipsilateral to injury only following CCI when compared to contralateral and naïve samples (*$p<0.05$, Wilcoxon test). The expression of [PTyr^{402}] Pyk 2 was not affected by any of the injury models. The expression of PSD-95 was significantly increased ipsilateral to CCI injury when compared to contralateral and naïve samples (*$p<0.05$, Wilcoxon test), however the level of PSD-95 expression was not significantly altered by the other models presented here.

Expression of Pyk 2 and PSD-95 as a percent of GAPDH expression										
Protein	**Spinal Cord**									**Brain**
	CCI		CFA		Formalin		Saline			
	Ipsi	*Con*	*Ipsi*	*Con*	*Ipsi*	*Con*	*Ipsi*	*Con*	*Naïve*	*Naïve*
Pan-Pyk 2	31 ± 1	24 ± 1	23 ± 1	22 ± 1	23 ± 1	22 ± 1	20 ± 2	22 ± 3	23 ± 1	44 ± 8
[PTyr^{402}]-Pyk 2	23 ± 2	23 ± 2	25 ± 4	28 ± 4	28 ± 6	25 ± 1	24 ± 4	24 ± 5	25 ± 7	30 ± 6
PSD-95	50 ± 2	24 ± 6	24 ± 5	24 ± 5	34 ± 7	29 ± 6	25 ± 5	23 ± 5	23 ± 4	41 ± 8

6.4 Discussion

This study was conducted using three different models; the first was a unilateral chronic constriction injury (CCI) of the sciatic nerve model developed by Bennett and Xie (Bennett and Xie, 1988). As discussed in Chapter four (Section 4.4) all the animals that underwent CCI surgery developed an increased sensitivity to a previously innocuous mechanical and cold stimuli together with a marked reduction in latency response to a noxious heat stimulus. Maximal behavioural reflex sensitisation was reached around day thirteen to fourteen post surgery in all cases. For all the ensuing investigations using this CCI model only animals displaying peak behavioural reflex sensitisation following CCI nerve injury (ipsilateral to injury) were used. The injection of complete Freund's adjuvant (CFA) was used as a model of persistent inflammation. All animals developed a clear reduction in latency response to a noxious heat stimulus with maximal effect one to two days post injection, a striking sensitivity to a previously innocuous mechanical stimulus also developed, with greatest sensitivity seen two to three days post injection.

Earlier research has reported that the CFA challenge results in behavioural sensitization as early as two to six hours (Ji et al., 2002a; Ji et al., 2002b; Zhang et al., 2003) or three days post CFA injection (for thermal hyperalgesia) (Molliver et al., 2005), with recovery of behavioural reflex sensitisation observed around five or nine days post CFA injection (Molliver et al., 2005;Zhang et al., 2003). These findings are in agreement with the CFA model developed in this study where early sensitisation is observed at thirty minutes to two hours post injection and continues for two to three days post injection (with mechanical allodynia lasting longer). Recovery of thermal hyperalgesia occurs around four to five days post injection, however mechanical allodynia was still observed five days post injection, perhaps recovery would be seen a few days later (this was not characterized in this study). The slight variations in the timings of the CFA induced sensitisation could be due to the site of CFA injection and according to whether a saline:CFA solution or CFA alone is used for the injections in addition to the final volume injected.

Unlike the model of formalin-induced inflammation, the CFA model is not as well characterised to determine if each stage of the response is driven by periperhal activity and/or central sensitisation in the spinal cord. Intraplantar injection of formalin elicits a biphasic nociceptive response (Dubuisson and Dennis, 1977), that has been characterised by behavioural and electrophysiological measures to consist of an early intense response (first phase) and a more prolonged response (second phase) (Chaplan et al., 1997; Coderre and Melzack, 1992; Dickenson and Sullivan, 1987c; Dickenson and Sullivan, 1987b; Haley et al., 1990; Wheeler-Aceto and Cowan, 1991). As discussed in Chapter five (section 5.5) the first phase is considered to be of peripheral origin, with the second phase a result of both ongoing peripheral activity and central sensitisation in the spinal cord (Chaplan et al., 1997; Coderre et al., 1990; Coderre and Melzack, 1992; Dickenson and Sullivan, 1990; Haley et al., 1990; Villetti et al., 2003). In the subsequent analysis of the CFA model we used only animals displaying peak behavioural reflex sensitisation (ipsilateral to injection) and in the case of formalin induced inflammation, only animals that demonstrated peak second phase responses following injection.

As mentioned in Chapter one (section 1.4.2 and 1.7.3) NMDA receptors are critically involved in the mechanism of central sensitisation in the spinal cord (Davies and Lodge, 1987; Dickenson and Sullivan, 1987a; Suzuki et al., 2001; Woolf and Thompson, 1991), and the role of these receptors in chronic pain may be dependent upon the MAGUK proteins, two of which, PSD-95 and Chapsyn 110/PSD 93, have through genetic and antisense techniques been implicated in chronic pain states (Garry et al., 2003; Tao et al., 2003; Zhang et al., 2003). PSD-95 expression was shown here to be markedly enhanced in the spinal cord, following CCI nerve injury, as illustrated by an ipsilateral increase when compared to the contralateral side and naïve controls. However such an amplification of expression was not seen ipsilateral to CFA injection and although a modest increase was observed ipsilateral to formalin injection, this was not significant when compared to the contralateral side, saline and naïve controls. It must be noted that CCI-induced nerve-injury has a longer time course of sensitisation than either CFA or formalin-induced inflammation and whether this difference has an influence on detecting the involvement of PSD-95 cannot be ruled out. The level of expression of other

members of the MAGUK family was not looked at specifically in this study, but has been investigated by the lab (S.M. Fleetwood-Walker and colleagues, unpublished communication) and found to be unaltered in the spinal cord as a result of CCI injury. The findings presented here link with previous investigations that revealed the importance of PSD-95 in the development of nerve injury behavioural reflex sensitisation (Garry et al., 2003; Tao et al., 2001).

Since PSD-95 assembles with the NMDA receptor thereby coupling the receptor to diverse intracellular pathways that may mediate downstream changes, one of its signalling-associated binding partners was examined. Pyk 2 was chosen as outlined above and was not only shown to be expressed in the spinal cord but to display an ipsilateral increase following CCI nerve injury when compared to the contralateral side and naïve controls. This increase in expression was observed in 'pan-'(or phosphorylation state-independent) Pyk 2, whereas phosphorylated Pyk 2 ([PTyr^{402}] Pyk 2) remained unchanged by CCI nerve injury. Both [PTyr^{402}] Pyk 2 and pan-Pyk 2 were unaltered in their expression in the spinal cord ipsilateral to either CFA or formalin injection when compared to the contralateral side, saline and naïve controls. These findings demonstrate for the first time the potential involvement of this tyrosine kinase in CCI nerve injury. As to why the phosphorylated form of Pyk 2 was found to be unaltered could be explained by the fact that Pyk 2 is phosphorylated on multiple tyrosine residues which regulate both its enzymatic activity and pathway selectivity. Pyk 2 has four sites of tyrosine phosphorylation which include; Tyr402 (tyrosine402), an autophosphorylation site which also forms the binding site for SH2 domains of Src family kinases, Tyr881 (tyrosine881) the grb2-SH2 domain binding site, and two regulatory sites in the activation loop of the kinase domain Tyr579/580 (tyrosine579/580)(Avraham et al., 2000;Li et al., 1999). The site targeted by the anti-phosphorylated Pyk 2 antibody used in this study (Tyr402) appears to have remained unchanged in the models investigated.

Activation of Pyk 2 is thought to involve autophosphorylation at Tyr402, as well as transphosphorylation at the activation loop site Tyr580 and other sites, a pattern similar to the phosphorylation of FAK at homologous residues Tyr397 and Tyr577 (Salazar and

Rozengurt, 2001), but whether this sequential model of activation, as established for FAK, accounts for the activation of Pyk 2 is unclear. A recent report has shown that Pyk 2 is Ca^{++}-dependent at the activation loop site Tyr580, but not at Tyr402, following GPCR stimulation, suggesting that auto- and transphosphorylation sites differ in their response to Ca^{++}, thus proposing that Ca^{++}-independent signalling mechanisms may be responsible for autophosphorylation of Pyk 2 (Wu et al., 2006). It would be of interest to look at anti-phosphorylated Pyk 2 that targets Tyr^{580} site to see whether this site of phosphorylation differs in its response to the chronic pain states investigated here. Whether any of the other sites of phosphorylated Pyk 2 are altered remains to be determined. The increase observed in Pan-Pyk 2 expression, but not in [$pTyr^{402}$] Pyk 2 levels might suggest that the excess Pyk 2 expressed after CCI is not in an activated state, at least as monitored by Tyr^{402} phosphorylation.

For the remainder of this study it was decided to look at the interaction and expression of PSD-95 and Pan-Pyk 2 in the spinal dorsal horn following experimental mononeuropathy, due to their increased protein expression in the spinal cord in this model.

Immunohistochemical analysis to localise PSD-95 in the spinal cord involved the development of a new immunofluoresence staining technique, which proved to be challenging. This was partly due to the fixation process (of the tissue), which often alters the available immunoreactive antigenic epitopes or indeed results in their loss as a result of protein-protein and/or nucleic acid cross-linking (which is a special form of chemical modification involving the joining of two molecular components by covalent bonds). Fixation may induce a change in protein conformation or a change in accessibility of the residues encoding the antigenic epitope, thus masking the tissue antigenicity. An optimal antigen retrieval (AR) system was developed to give access to the antigenic epitopes, which involved the pretreating of fixed tissue with a heat-induced AR method, as cross-linkages between formalin and protein can be reversed by high temperature heating or strong alkaline treatment (Fraenkel-Conrat et al., 1947). AR alone was not the only modification required, suggesting that there were still antigens for which available

antigenic epitopes were still too sparse to be visualized after fixation. To resolve this dilemma, the combination of the optimised AR system (heat-treatment in a urea solution) and a signal amplification step was used. Signal amplification allows the signal to be enhanced so that the antigens that have been unmasked in the AR step can be visualized. A powerful amplification step, the ImmunoMax method (Merz et al., 2005) (the tyramine enhancement technique), using a biotinyl-tyramine amplification step whereby amplification is accomplished by covalent deposition of biotin molecules was employed (Merz et al., 2005). The combination of an AR step with this biotinylated tyramine enhancement step has been found to result in a 100-10,000 fold boost in sensitivity (compared to conventional avidin–biotinylated enzyme complex (ABC) procedures) (Merz et al., 2005). The development of this method (using both the AR and tyramine enhancement step) allowed for the visualization in the spinal cord of PSD-95 and of Pan-Pyk 2 (which only required the AR step).

Analysis involved capturing single optical sections of each spinal cord section at low magnification (x5 objective lens; captured image is 2000μm x 2000μm), which enabled both dorsal horns of the spinal cord to be captured in one image. Having one image with both dorsal horns intact ensured that any possible increase or decrease in fluorescent intensity found would be the result of the injury model and not due to any potential differences in capturing of the images were only one dorsal horn captured in each image. All images (at both low and high magnification) were captured using the Leica TCSNT Confocal system, which involves sequentially scanning the section with individual lasers to detect fluorescence in each channel ensuring that any possible spectral bleed-through is minimized thus producing an accurate merged image of fluorphore distribution (refer to Section 3.8.4). Single optical sections (optical width of 0.8μm) captured at higher magnification (x20 objective lens; captured image is 500μm x 500μm) were used to look at individual cell staining for either PSD-95 or Pyk 2 and of their colocalisation in the same cell in the regions of interest, namely Lamina I, II and III of the spinal dorsal horn (refer to Section 3.8.4). Colocalisation was determined using LCS-Lite software, where the intensity of each fluorochrome was measured in each cell and graphed, if the fluorochrome graph for PSD-95 and Pyk 2 overlapped in a cell that showed To-pro

(nuclear marker) staining and signal was at least twice background intensity for both PSD-95 and Pyk 2 the cell was counted as a colocalised cell, if the intensity of each fluorochrome graphed did not overlap then the cell was counted as a non-colocalised cell that was either PSD-95 or Pyk 2-immunopositive.

The intensity of both PSD-95 and Pyk 2 immunoreactivity was found to be markedly increased ipsilateral to nerve injury in lamina I and II of the dorsal spinal cord when compared to the contralateral side and naïve controls, with no difference observed in Lamina III or IV. Concurring with the intensity analysis, the number of immunopositive cells for both PSD-95 and Pyk 2 increased in lamina I and II with no alteration observed in lamina III ipsilateral to nerve injury when compared to the contralateral side and naïve controls. These findings are in agreement with the analysis of protein expression of both PSD-95 and Pyk 2 in the spinal cord as outlined before. The observations reiterate the importance of PSD-95 in the CCI nerve injury model and illustrate the potential significance of its binding partner Pyk 2 in this model. To investigate whether the increase in PSD-95 and Pyk 2 were occurring in the same cells and thereby possibly indicating an interaction of these two proteins, colocalisation analysis was conducted. PSD-95 and Pyk 2 were found to be colocalised in greater number in lamina I and II ipsilateral to injury but not in lamina III when compared to the contralteral side and naïve controls. These results point toward the possibility of PSD-95 and its binding partner Pyk 2 interacting both physically and functionally with a consequence of such an interaction being the potential activation of downstream signalling cascades.

While analyzing Pyk 2-immunopositive cells in Laminae I-III, a number of Pyk 2-immunopositive cells were noted in the deeper laminae of the spinal dorsal horn (Laminae IV-VI), which was not thought to differ as a result of nerve injury, although complete analysis was not conducted into the deeper laminae, additionally a number of Pyk 2-immunopositive cells were noted in the ventral horn of the spinal cord that did not appear to differ as a result of nerve injury. However for PSD-95 the number of immunopositive cells in the deeper laminae was far fewer and PSD-95-immunopositive cells were not observed in the ventral horn of the spinal cord, suggesting the expression

of PSD-95 is more restricted than that of Pyk 2 to the primary area for processing noxious stimulation in the spinal dorsal horn.

Following nerve-injury the colocalisation of PSD-95 with Pyk 2 increased in lamina I and II of the dorsal horn but not in lamina III, suggesting that these two proteins may physically interact in the superficial dorsal horn as a result of peripheral nerve injury. As a result of nerve injury 85% and 87% of PSD-95-immunopositive cells (ipsilateral to nerve injury) were also positive for Pyk 2 in lamina I and II respectively. CCI nerve injury-induced a greater number of PSD-95-immunopositive cells than the number of cells that were colocalised for PSD-95 and Pyk 2 in laminae I, II and III. Suggesting that in the PSD-95-immunopositive cells in laminae I, II and III that do not appear to contain Pyk 2, PSD-95 may be interacting with other binding partners, perhaps indicating that the nerve-injury enhanced expression of PSD-95 may lead only in part to interaction with Pyk 2, which is also enhanced in expression following nerve injury. It must be noted that limitation of the sensitivity of antibody detection can not be ruled out, therefore it could be suggested that a cell that appears not to express Pyk 2 may contain some functional Pyk 2 that was undetected here. While colocalisation of PSD-95 with Pyk 2 was increased in lamina I and II (with 88% and 85% of Pyk 2-positive cells colocalising with PSD-95 in lamina I and II respectively) as a result of CCI-induced nerve injury, the number of Pyk 2-immunopositive cells that did not colocalise with PSD-95 was significantly increased only in Lamina II ipsilateral to nerve injury. Possibly indicating that within Lamina II Pyk 2-positive cells that show no interaction with PSD-95, may have distinct roles independent of the NMDA/PSD-95 complexes. As there was no increase in the number of Pyk 2-immunopositive cells that did not colocalise with PSD-95 in Lamina I and III following nerve-injury, it could be suggested that within these laminae when Pyk 2 is expressed it may be especially involved with PSD-95 and thereby NMDA receptor function.

In conclusion this investigation has corroborated the importance of PSD-95 in the development of chronic pain as a result of peripheral nerve damage. This study also reveals new evidence that may point to an increased interaction of PSD-95 and Pyk 2

(pan) following peripheral nerve injury that could contribute to the mechanism involved in the development of a chronic neuropathic pain state. The factors regulating the association of PSD-95 with Pyk 2 need to be further explored to fully understand the role that PSD-95:Pyk 2 complexes might play in chronic pain states.

7. Summary and Conclusions

Chronic pain is a major health care problem; common sources of chronic pain include cancer pain, neuropathic pain, arthritic pain, back pain and headache. A recent survey established that chronic pain of moderate to severe intensity occurs in 19% of adult Europeans (Breivik et al., 2006). Chronic pain can seriously affect the daily activities, social and working lives of sufferers thereby resulting in a major socio-economic burden. Neuropathic pain is a form of chronic pain due to dysfunction in the peripheral or central nervous system, with associated symptoms including numbness, weakness, abnormal sensations and pain (Scadding, 1981). The chronic pain that develops manifests as hyperalgesia, allodynia and spontaneous pain. There are currently few viable options for the treatment of neuropathic pain conditions. Indeed, in the current situation, most patients have to undergo multiple drug therapy attempts in the hope of finding some treatment to alleviate their suffering. Classical opioid analgesics have often been reported to be ineffective (Arner and Meyerson, 1988; Bennett, 1994; Lee et al., 1994; Mao et al., 1995), frequently producing unwanted side effects. Indeed a drug can be considered successful if approximately 20-30% of the patient's respond (McQuay et al., 1996; McQuay et al., 1994), whereby responding means reporting less pain, not the eradication of the pain. One of the main problems experienced with currently available drugs to treat neuropathic pain are the side effects associated with them. For example, NMDA receptor antagonists (such as ketamine), which initially appeared promising in their therapeutic potential, exhibit toxicity, low safety margins and psychotropic side effects which limit their use.

Anticonvulsant drugs (such as carbamazepine) have been shown to attenuate painful diabetic neuropathy and trigeminal neuralgia (McCleane, 1999; Zakrzewska and Patsalos, 1992). Side effects associated with anticonvulsants include sedation and cerebellar symptoms, such as tremor and un-coordination (Jensen, 2002). Gabapentin, which is thought to target specific Ca^{++} channel subunits, is also currently used for the treatment of chronic pain conditions (Fink et al., 2000; Gustafsson et al., 2003). Although its exact mechanism of action is not fully understood, gabapentin has been reported to have some potential in the treatment of painful diabetic neuropathy and postherpetic neuralgia

(Backonja, 2000; Rice and Maton, 2001; Rowbotham et al., 1998). However the results can be contradictory with some studies failing to distinguish gabapentin from placebo (Gorson et al., 1999; Hemstreet and Lapointe, 2001). Some of the side effects associated with gabapentin include, dizziness, headache, peripheral oedema and sedation (Bosnjak et al., 2002; Rowbotham et al., 1998). Another drug used is pregabalin, which is a GABA analogue closely related to gabapentin. Pregabalin has mixed reports of success in the treatment of neuropathic pain. When tested alongside another drug, amitriptyline (a tricyclic anti-depressant), pregabalin was found not to be more effective than placebo while amitriptyline was found to be significantly better (2005). The associated side effects of pregabalin are similar to those of gabapentin, including mainly neuropsychological reactions (dizziness and drowsiness) and peripheral oedema.

Advances in the development of efficacious therapeutic treatments depend on progress in understanding the underlying mechanisms in chronic pain states. These mechanisms are complex, involving both peripheral and central changes that can persist long after the initial injury has healed. Here we used a modification of the chronic constriction injury (CCI) model of mononeuropathy developed by Bennett and Xie (Bennett and Xie, 1988), in which the sciatic nerve was exposed in the region of the trifurcation and four (in the rat) or three (in mice) chromic cat gut ligatures were tied loosely to constrict the peroneal and tibial nerves leaving the smallest sural nerve intact. This modification employs a partial nerve damage rather than complete transection thereby emphasising the contribution of both injured and non-injured inputs from the same peripheral fields. This animal model of mononeuropathy results in the development of increased sensitivity to previously innocuous mechanical and cold stimuli, showing that partial CCI nerve injury results in the development of mechanical and cold allodynia in the affected hind limb, while also developing a marked reduction in response latency to a noxious heat stimulus. Maximal behavioural reflex sensitisation occurred approximately ten to fourteen days following nerve-injury. The sub-cutaneous injection of complete Freund's adjuvant (CFA) was used as a model of persistent inflammation. As discussed previously, the CFA challenge has been reported to result in behavioural sensitization from as early as two to six hours Ji et al., 2002b; Zhang et al., 2003) or three days post-injection (Molliver et al., 2005), with

recovery of behavioural reflex sensitisation observed around five to nine days post-injection (Molliver et al., 2005; Zhang et al., 2003). Here, all animals developed a clear reduction in latency response to a noxious heat stimulus with maximal effect one to two days post injection, sensitivity to a previously innocuous mechanical stimulus also developed, with greatest sensitivity seen one to three days post injection. However the CFA model, unlike the model of formalin-induced inflammation, is not as well characterised as to whether each stage of the response is driven by peripheral activity and/or central sensitisation in the spinal cord. Intraplantar injection of formalin elicits a biphasic nociceptive response (Dubuisson and Dennis, 1977), that has been characterised by behavioural and electrophysiological measures to consist of an early intense response (first phase) and a more prolonged response (second phase) (Chaplan et al., 1997; Coderre and Melzack, 1992; Dickenson and Sullivan, 1987a; Haley et al., 1990; Wheeler-Aceto and Cowan, 1991). The first phase is considered to be of peripheral origin, with the second phase a result of both ongoing peripheral activity and central sensitisation in the spinal cord (Chaplan et al., 1997; Coderre et al., 1990; Dallel et al., 1995; Dickenson and Sullivan, 1990; Puig and Sorkin, 1996; Taylor et al., 1995). For all the ensuing investigations only animals displaying peak behavioural reflex sensitisation (ipsilateral to injury) following CCI nerve injury or CFA challenge and only animals that demonstrated peak second phase responses following formalin injection were used.

The work presented here utilises behavioural, pharmacological, biochemical and immunohistocehmical techniques to examine some of the mechanisms involved in the development and maintenance of neuropathic pain, while at times also looking at mechanistic differences between neuropathic and inflammatory chronic pain states. This thesis has been concerned with the role of p38 and p42/44 MAP kinase signalling pathway activation via the peptidergic NK_2 and $VPAC_2$ receptors and the ionotropic glutamate NMDA receptor, in addition to glial involvement of such activation in neuropathic pain states. The above techniques were also employed to investigate the association of the NMDA receptor complex adapter protein, PSD-95 with a downstream signalling partner Pyk 2, and to study the involvement of the SH3 domain of PSD-95 in the neuropathic pain state.

7.1 p38 and p42/44 MAP kinase activation in neuropathic pain

Long lasting changes in neuronal excitability can occur through activation of transcription factors via signalling pathways, for example, the MAP kinase signalling pathways, which are key mediators of transcriptional responses to extracellular signals (Whitmarsh, 2006; Hokfelt et al., 1994; Ji and Woolf, 2001). MAP kinase signalling can result in short-term modification of proteins via phosphorylation and long-term changes via activation of the transcription factor, CREB (cAMP response element binding protein; Xing et al., 1996) and is believed to be involved in the mechanisms of sensitisation in chronic pain states. Here, the involvement of p38 and p42/44 MAP kinases in mediating thermal hyperalgesia and mechanical allodynia was firstly examined by intrathecal injection of p38 and p42/44 MAP kinase pathway inhibitors (SB 203580 and (PD 98059 and U 0126), respectively) in animals with established neuropathic reflex sensitisation following nerve injury. Both p38 and p42/44 MAP kinase pathway inhibitors were found to attenuate the nerve injury-induced behavioural reflex sensitisation, these observations are consistent with previous reports indicating a role for MAP kinase signalling in the development and maintenance of behavioural reflex sensitisation in a number of chronic pain states (Cruz et al., 2005; Dai et al., 2002; Ji et al., 2002a; Jin et al., 2003; Obata et al., 2003; Svensson et al., 2003; Tsuda et al., 2004). To understand the role of these intracellular signalling cascades in chronic pain states we then looked at how these pathways are activated as a result of peripheral nerve injury.

Non-neuronal (glial) cell activation is currently viewed as a crucial component of the generation and maintenance of chronic pain states. Here we showed that inhibition of glial activation by use of the non-selective glial inhibitor, propentofylline (which can decrease the activation of both spinal astrocytes and microglia) or of the pro-inflammatory cytokine TNF-α (using the TNF-α receptor antagonist, WP9QY) alleviated nerve-injury-induced behavioural reflex sensitisation. Interestingly activated states of both p38 and p42/44 MAP kinases have been localised not only to neurons but also to astrocytes and microglia: Phosphorylation of p38 MAP kinase occurs in microglia following formalin-induced inflammation, nerve injury and axotomy (Jin et al., 2003;

Kawasaki et al., 1997; Kim et al., 2002; Svensson et al., 2003; Tsuda et al., 2004) and phosphorylation of p42/44 MAP kinase occurs (in addition to spinal neurons), in astrocytes and microglia following nerve injury (Ji et al., 1999; Ma and Quirion, 2002; Zhuang et al., 2005). Here we showed that the enhanced activation of p38 and p42/44 MAP kinases (revealed by their increased phosphorylation) in the spinal cord ipsilateral to nerve injury was prevented by spinal application of the same TNF-α and glial inhibitors used above (propentofylline, WP9QY) and by the TNF-α synthesis inhibitor, thalidomide. Our findings show agreement with other reports where propentofylline was reported to attenuate allodynia following spinal nerve transaction (Sweitzer et al., 2001) and reduce formalin-induced inflammatory pain by suppressing TNF-α (Dorazil-Dudzik et al., 2004). The expression of TNF-α in the spinal cord that is upregulated after peripheral nerve injury (Bartholdi and Schwab, 1997; DeLeo et al., 1997; Wagner and Myers, 1996) can be reduced through use of thalidomide (George et al., 2000), which has also been reported to be effective in delaying the development of behavioural reflex sensitisation induced by peripheral nerve injury (Sommer et al., 1998). It is possible that TNF-α, through its increased expression or release, may contribute to the sensitisation found in chronic pain states by inducing further activation of p38 and/or p42/44 MAP kinases in glial cells.

We examined the possibility of the involvement of the peptidergic NK_2 and $VPAC_2$ receptors in the activation of p38 and p42/44 MAP kinase pathways. Here we found that the NK_2 receptor antagonist prominently inhibited the nerve injury-induced behavioural reflex sensitisation (compared to the NK_1 receptor antagonist) and reduced the CCI nerve injury-induced activation of spinal p38 and p42/44 MAP kinases. The greater involvement of the NK_2 receptor in attenuating nerve-injury induced behavioural sensitisation agrees with work showing this receptor to be specifically involved in the hyperexcitability of dorsal horn neuron responses to noxious cutaneous stimuli (Fleetwood-Walker et al., 1990) and of the antinociceptive ability of the NK_2 receptor antagonist when administered following nerve injury (Coudore-Civiale et al., 1998). Additionally NK_2 receptors have been localised to spinal astrocytes, also a site of p42/44 MAP kinase activation following nerve injury (Ma and Quirion, 2002; Zerari et al.,

1998). We also showed that the nerve-injury induced activation of p38 and p42/44 MAP kinase was reduced by incubation of an NMDA receptor antagonist on the spinal cord. We then confirmed that agonist stimulation of NK_2 receptors resulted in activation of p42/44 MAP kinase (to a greater extent compared to $VPAC_2$ receptor stimulation) and that this could be blocked with co-application of the glial inhibitor, propentofylline. Focusing on the possible NK_2 receptor activation of p42/44 MAP kinase, we showed in parallel that the NK_2 receptor agonist induced a behavioural reflex sensitisation in naïve animals that could be attenuated by co-administration of the p42/44 MAP kinase inhibitor, U 0126. These findings suggest the possibility that activation of p42/44 MAP kinase as a result of glial NK_2 receptor activation in this model of mononeuropathy could lead not only to pro-inflammatory cytokine release but also to the facilitation of NMDA receptor function, while the involvement of any neuronal NK_2 receptors in such activation of p42/44 MAP kinase needs to be investigated.

The behavioural reflex sensitisation induced by nerve injury was also found to be attenuated by a selective $VPAC_2$ receptor antagonist, with little or no inhibition seen with PAC_1 or $VPAC_1$ receptor antagonists. Previous reports have indicated the importance of $VPAC_2$ receptors in neuropathic pain, showing increased expression of the $VPAC_2$ receptor in the dorsal horn following nerve injury and a marked inhibitory effect of $VPAC_2$ receptor antagonists on neuropathic sensitisation (Dickinson et al., 1999; Dickinson and Fleetwood-Walker, 1999). $VPAC_2$ receptors (along with the other VPAC and PAC receptor subtypes) have been found to be expressed in astrocytes (Brenneman et al., 1990; Grimaldi and Cavallaro, 1999; Jaworski, 2000). Having seen a greater activation of p42/44 MAP kinase by agonist stimulation of NK_2 receptors compared to $VPAC_2$ receptors, we found, in contrast, that agonist stimulation of $VPAC_2$ receptors increased the activation of p38 MAP kinase to a greater extent compared to NK_2 receptor stimulation. This response was again prevented by co-application of the glial inhibitor, propentofylline. We also showed that the increased activation of p38 MAP kinase following nerve injury was reduced by incubation of the spinal cord with the $VPAC_2$ receptor antagonist. The corresponding behavioural study showed behavioural sensitisation in naïve animals following administration of a $VPAC_2$ receptor agonist, a

response that was alleviated by co-administration of the p38 MAP kinase inhibitor, SB 203580. These findings suggest an involvement of glial $VPAC_2$ receptors in the spinal cord in the activation of p38 MAP kinase following nerve injury, although they do not show whether this activation occurs directly in $VPAC_2$ receptor-containing cells.

To further understand the mechanisms involved in the activation of p38 and/or p42/44 MAP kinases in glial cells, investigation into the localisation of these MAP kinase proteins could be conducted to see the involvement of glial NK_2 or $VPAC_2$ receptor-containing cells as against neuronal NK_2 or $VPAC_2$ receptor-containing cells in the activation of these proteins as a result of peripheral nerve-injury. The involvement of the pro-inflammatory cytokines, IL-1 and IL-6, also released by activated glia, were not specifically examined in this thesis and their involvement in the activation of p38 and/or p42/44 MAP kinases in glial cells cannot be ruled out. The activation of the MAP kinase signalling pathways in response to peripheral nerve injury appears to be an undeniably complex process involving multiple receptor mechanisms.

7.2 The SH3 domain of PSD-95 and its signalling partner Pyk 2 in chronic pain states

PSD-95 is a key adapter protein in the NMDA receptor complex that has been implicated in chronic pain states through genetic and antisense techniques (Garry et al., 2003; Tao et al., 2001). We examined here the expression of spinal PSD-95 in a number of chronic pain states and found an ipsilateral increase in protein levels following nerve injury, with no alteration in levels following either CFA or formalin-induced inflammation when compared to control. Of course it must be noted that CCI-induced nerve-injury has a longer time course of sensitisation than either CFA or formalin-induced inflammation and whether this difference has an influence on detecting the involvement of PSD-95 cannot be ruled out. Given the marked ipsilateral increase in PSD-95 expression as identified through Western immunoblotting, we utilised immunofluorescence techniques to localise the expression of PSD-95 in both naïve and nerve-injured animals. We show a marked ipsilateral increase in both the intensity of PSD-95 immunoreactivity and in the number of PSD-95-immunopositive cells in the spinal dorsal horn following nerve injury. The ipsilateral increase in PSD-95 expression appears to be restricted to the superficial dorsal horn (lamina I and lamina II), which is the main area for primary afferent termination and overlaps with the distribution of NMDA receptor subunits, in particular NR2B (Boyce et al., 1999; Garry et al., 2003; Tao et al., 2000), indicating the likely importance of PSD-95 in mediating neuropathic sensitisation. This specific localisation of PSD-95 to the superficial dorsal horn is in agreement with previous work, where PSD-95 was found to be mainly expressed in lamina I and II of the dorsal horn (Garry et al., 2003; Tao et al., 2000).

Mice expressing a truncated form of PSD-95 which lack PDZ 3, SH3 and GK domains, known as PSD-$95^{PDZ1\text{-}2}$ mutants, do not develop either hyperalgesia or allodynia as a result of peripheral nerve injury (Garry et al., 2003), indicating a central role for PSD-95 in mediating NMDA receptor-dependent plasticity. We investigated the effect of a single point mutation to the SH3 domain of PSD-95 in different chronic pain states. This PSD-$95^{SH3W470L}$ mutation is a single point mutation that targets the highly conserved tryptophan residue (tyrptophan 470) found in the hydrophobic binding surface of SH3 domains that is thought to be crucial for the interaction of SH3 domains with proline-rich

ligands. Thus this PSD-95^{SH3W470L} mutation is designed to specifically disrupt SH3 domain interactions with polyproline residues whilst leaving the GK domain and all PDZ domains of PSD-95 and their interactions intact. Adult PSD-95^{SH3W470L} mutant mice or wild-type littermates were utilised to determine any potential role of the SH3 domain in the development and maintenance of neuropathic behavioural reflex sensitisation. We found that PSD-95^{SH3W470L} mutants developed the same behavioural reflex sensitivity to both thermal and mechanical stimuli following peripheral nerve injury to that seen in wild type littermate mice. We examined the involvement of this mutation in the development of sensitisation following formalin-induced inflammation. As discussed above, the formalin test elicits a biphasic nociceptive response (Dubuisson and Dennis, 1977). We found no difference between PSD-95^{SH3W470L} mutant mice and wild type littermate responses in the first (acute) phase, but the PSD-95^{SH3W470L} mutant mice had a greatly reduced second (inflammatory) phase of the response compared to wild type littermates. We also investigated whether the PSD-95^{SH3W470L} mutation affected the behavioural sensitisation caused by CFA–induced inflammation and found that while both PSD-95^{SH3W470L} mutant and wild-type mice developed ipsilateral sensitivity 0-6 hours post-CFA, the mutant mice no longer displayed this behavioural sensitivity at 24 and 48 hours post-CFA, unlike the wild-type mice. These findings, of intact neuropathic behavioural reflex sensitisation and blunted inflammatory responses in PSD-95^{SH3W470L} mutant mice, suggest that within the one molecule of PSD-95, different domains may contribute selectively to different pain states.

As PSD-95, a member of the MAGUK family of proteins, assembles with the NMDA receptor, we examined whether this PSD-95^{SH3W470L} mutation altered the expression levels of NMDA receptor subunits in the mutant spinal cord. We found the expression of the NMDA receptor subunits was unaffected by the mutation when compared to wild type littermates. We found that this point specific mutation did not alter the expression of PSD-95 itself in the spinal cord. As members of the MAGUK family of proteins share a high degree of homology between their domains, it is possible that other MAGUKs present in the spinal cord might compensate in the regulation of the NMDA receptor pathway. However we found no alteration in the expression of Chapsyn110/PSD-93,

SAP-102 or SAP-97 in mutant spinal cord when compared to wild-type littermates. These findings show that the highly specific PSD-95^{SH3W470L} mutation did not result in overall changes in levels of NMDA receptor subunit or MAGUK expression in the spinal cord, thereby suggesting that the phenotype displayed by this mutation may not have been the result of compensation by other MAGUK proteins but is more likely due to interactions disrupted by the mutation itself.

To fully understand how this specific mutation of the SH3 domain (that leads to disruption of protein-protein interactions without altering the expression of PSD-95) can result in blunted inflammatory responses requires further research. It is possible that the PSD-95^{SH3W470L} mutation inhibits the inflammatory response through the resultant prevention of intermolecular binding of the SH3 domain while maintaining the intramolecular binding of the SH3 and GK domains. It would therefore be of interest to look at a point mutation of the intramolecular binding site of the SH3 domain, to examine the functional implication of disruption to intramolecular binding of the SH3 and GK domains while leaving the intermolecular binding site of SH3 intact. A small number of partners for the SH3 domain of PSD-95 have been identified to date. Indeed as new techniques are currently being developed to model the structure of multidomain proteins (Korkin et al., 2006), predictions of new theoretical binding partners will be made, which could then be assessed for their involvement in nerve injury-induced behavioural reflex sensitisation. It is possible that the identification of the binding partner(s) disrupted by this mutation may lead eventually to the design of a novel analgesic that could prevent sensitisation of specific pain states.

As these findings suggest the importance of the SH3 domain of PSD-95 in chronic pain states, the involvement of Pyk 2 (a signalling associated binding partner of PSD-95 that binds to the SH3 domain) was assessed. Spinal Pyk 2 expression in a number of chronic pain states was examined and we found an ipsilateral increase in Pan-Pyk 2 protein levels following nerve injury, with no alterations observed following either CFA or formalin-induced inflammation when compared to control. No alteration in levels of phosphorylated (i.e. activated) Pyk 2 expression was seen in any of the chronic pain

states explored here, which might suggest that the increased levels of Pyk 2 following nerve injury may not represent the enzyme in an activated state, as assessed by Tyr^{402} phosphorylation. Whether other phosphorylation sites on Pyk 2 are activated following nerve injury or indeed if the sensitivity of phosphorylated Tyr^{402} Pyk 2 antibody detection is limited cannot be ruled out. Focusing on Pan-Pyk 2, we found a marked ipsilateral increase in both the intensity of Pan-Pyk 2 immunoreactivity and in the number of Pan-Pyk 2 immunopositive cells following nerve injury in the spinal dorsal horn. The ipsilateral increase in expression of Pan-Pyk 2 following nerve-injury was found to be localised to the superficial dorsal horn, a pattern that overlaps with the distribution of PSD-95, thus suggesting a potential importance of Pyk 2 in the mechanisms underlying nerve-injury induced sensitisation.

The molecular interaction of Pyk 2 with PSD-95 was assessed in this model of peripheral nerve injury to identify if the increases in PSD-95 and Pyk 2 were occurring in the same cells. Following nerve-injury the colocalisation of PSD-95 and Pan-Pyk 2 was increased in lamina I and II of the dorsal horn but not in lamina III, suggesting that these two proteins may physically interact in the superficial dorsal horn as a result of peripheral nerve injury. Peripheral nerve injury induced a greater number of PSD-95 immunopositive cells than the number of cells that were colocalised for PSD-95 and Pan-Pyk 2. It is possible that in the PSD-95 immunopositive cells which do not appear to contain Pyk 2 (although the limitations of antibody sensitivity cannot be excluded), PSD-95 may interact with other binding partners, thereby suggesting the nerve-injury induced increase in PSD-95 may result in part in interaction with the increasingly expressed Pan-Pyk 2. In lamina II the number of Pan-Pyk 2 immunopositive cells that were not colocalised with PSD-95 was increased ipsilateral to nerve-injury, however there was no increase in the number of Pan-Pyk 2 only immunopositive cells in lamina I and III; this may suggest that in lamina II there are a number of Pyk 2-positive cells that do not interact with PSD-95 and may thereby have a distinct role independent of NMDA/PSD-95 complexes.

It would be of interest to identify the cells in the spinal dorsal horn in which PSD-95 colocalises with Pan-Pyk 2. It could be suggested that within lamina I and III these dorsal horn cells are projection neurons, which enter ascending spinal tracts and transmit sensory information to the brainstem, midbrain and thalamic nuclei, via the spinothalamic (STT), spinomesencephalic (SMT), spinocervical (SCT) tracts or of the postsynaptic dorsal column (PSDC). The cells that show colocalisation of PSD-95 and Pan-Pyk 2 in lamina II are more likely to be intrinsic interneurons, which have an extensive local integration, given the fact that very few lamina II neurons project to the brainstem (Giesler et al., 1976; Willis et al., 1979). As discussed above, non-neuronal cells are involved in the underlying mechanisms of central sensitisation, as to whether some of the PSD-95 and or Pyk 2 immunopositive cells are glial remains to be examined.

In conclusion, the findings of this study have highlighted a potential role for the SH3 domain of PSD-95 and its binding partners in the development of sensitisation in chronic pain states, leading to the possibility of a new molecular target being identified for the development of novel therapeutic agents. Additionally this thesis has illustrated the functional importance of glia in the activation of spinal signalling pathways involved in somatosensory processing, suggesting the possibility of targeting non-neuronal cells in future treatment of chronic pain. Further investigations to provide a clearer insight into these complex mechanisms involved in the development of chronic pain states may result in the development of new and efficacious therapeutic agents for the enduring problem of chronic pain.

Bibliography

(2005) Pregabalin: new drug. Very similar to gabapentin. Prescrire Int 14: 203-206.

Aanonsen LM, Wilcox GL (1986) Phencyclidine selectively blocks a spinal action of N-methyl-D-aspartate in mice. Neurosci Lett 67: 191-197.

Aanonsen LM, Wilcox GL (1987) Nociceptive action of excitatory amino acids in the mouse: effects of spinally administered opioids, phencyclidine and sigma agonists. J Pharmacol Exp Ther 243: 9-19.

Abe T, Sugihara H, Nawa H, Shigemoto R, Mizuno N, Nakanishi S (1992) Molecular characterization of a novel metabotropic glutamate receptor mGluR5 coupled to inositol phosphate/Ca2+ signal transduction. J Biol Chem 267: 13361-13368.

Akopian AN, Sivilotti L, Wood JN (1996) A tetrodotoxin-resistant voltage-gated sodium channel expressed by sensory neurons. Nature 379: 257-262.

Akopian AN, Souslova V, England S, Okuse K, Ogata N, Ure J, Smith A, Kerr BJ, McMahon SB, Boyce S, Hill R, Stanfa LC, Dickenson AH, Wood JN (1999) The tetrodotoxin-resistant sodium channel SNS has a specialized function in pain pathways. Nat Neurosci 2: 541-548.

Albuquerque C, Lee CJ, Jackson AC, MacDermott AB (1999) Subpopulations of GABAergic and non-GABAergic rat dorsal horn neurons express Ca2+-permeable AMPA receptors. Eur J Neurosci 11: 2758-2766.

Amaya F, Decosterd I, Samad TA, Plumpton C, Tate S, Mannion RJ, Costigan M, Woolf CJ (2000) Diversity of expression of the sensory neuron-specific TTX-resistant voltage-gated sodium ion channels SNS and SNS2. Mol Cell Neurosci 15: 331-342.

Andreev J, Simon JP, Sabatini DD, Kam J, Plowman G, Randazzo PA, Schlessinger J (1999) Identification of a new Pyk2 target protein with Arf-GAP activity. Mol Cell Biol 19: 2338-2350.

Angaut-Petit D (1975) The dorsal column system: II. Functional properties and bulbar relay of the postsynaptic fibres of the cat's fasciculus gracilis. Exp Brain Res 22: 471-493.

Aramori I, Nakanishi S (1992) Signal transduction and pharmacological characteristics of a metabotropic glutamate receptor, mGluR1, in transfected CHO cells. Neuron 8: 757-765.

Arimura A, Shioda S (1995) Pituitary adenylate cyclase activating polypeptide (PACAP) and its receptors: neuroendocrine and endocrine interaction. Front Neuroendocrinol 16: 53-88.

Arner S, Meyerson BA (1988) Lack of analgesic effect of opioids on neuropathic and idiopathic forms of pain. Pain 33: 11-23.

Astier A, Avraham H, Manie SN, Groopman J, Canty T, Avraham S, Freedman AS (1997) The related adhesion focal tyrosine kinase is tyrosine-phosphorylated after beta1-integrin stimulation in B cells and binds to p130cas. J Biol Chem 272: 228-232.

Attal N, Jazat F, Kayser V, Guilbaud G (1990) Further evidence for 'pain-related' behaviours in a model of unilateral peripheral mononeuropathy. Pain 41: 235-251.

Atweh SF, Kuhar MJ (1977) Autoradiographic localization of opiate receptors in rat brain. I. Spinal cord and lower medulla. Brain Res 124: 53-67.

Avraham H, Park SY, Schinkmann K, Avraham S (2000) RAFTK/Pyk2-mediated cellular signalling. Cell Signal 12: 123-133.

Avraham S, London R, Fu Y, Ota S, Hiregowdara D, Li J, Jiang S, Pasztor LM, White RA, Groopman JE, . (1995) Identification and characterization of a novel related adhesion focal tyrosine kinase (RAFTK) from megakaryocytes and brain. J Biol Chem 270: 27742-27751.

Backonja MM (2000) Anticonvulsants (antineuropathics) for neuropathic pain syndromes. Clin J Pain 16: S67-S72.

Bao L, Wang HF, Cai HJ, Tong YG, Jin SX, Lu YJ, Grant G, Hokfelt T, Zhang X (2002) Peripheral axotomy induces only very limited sprouting of coarse myelinated afferents into inner lamina II of rat spinal cord. Eur J Neurosci 16: 175-185.

Baranauskas G, Nistri A (1998) Sensitization of pain pathways in the spinal cord: cellular mechanisms. Prog Neurobiol 54: 349-365.

Baranowski AP, Priestley JV, McMahon SB (1994) The consequence of delayed versus immediate nerve repair on the properties of regenerating sensory nerve fibres in the adult rat. Neurosci Lett 168: 197-200.

Barber RP, Vaughn JE, Roberts E (1982) The cytoarchitecture of GABAergic neurons in rat spinal cord. Brain Res 238: 305-328.

Barbut D, Polak JM, Wall PD (1981) Substance P in spinal cord dorsal horn decreases following peripheral nerve injury. Brain Res 205: 289-298.

Bartholdi D, Schwab ME (1997) Expression of pro-inflammatory cytokine and chemokine mRNA upon experimental spinal cord injury in mouse: an in situ hybridization study. Eur J Neurosci 9: 1422-1438.

Basbaum AI, Fields HL (1984) Endogenous pain control systems: brainstem spinal pathways and endorphin circuitry. Annu Rev Neurosci 7: 309-338.

Basbaum AI, Gautron M, Jazat F, Mayes M, Guilbaud G (1991) The spectrum of fiber loss in a model of neuropathic pain in the rat: an electron microscopic study. Pain 47: 359-367.

Battaglia G, Rustioni A (1988) Coexistence of glutamate and substance P in dorsal root ganglion neurons of the rat and monkey. J Comp Neurol 277: 302-312.

Beltramo M, Bernardini N, Bertorelli R, Campanella M, Nicolussi E, Fredduzzi S, Reggiani A (2006) CB2 receptor-mediated antihyperalgesia: possible direct involvement of neural mechanisms. Eur J Neurosci 23: 1530-1538.

Bennett DL, Boucher TJ, Armanini MP, Poulsen KT, Michael GJ, Priestley JV, Phillips HS, McMahon SB, Shelton DL (2000) The glial cell line-derived neurotrophic factor family receptor components are differentially regulated within sensory neurons after nerve injury. J Neurosci 20: 427-437.

Bennett GJ, Xie YK (1988) A peripheral mononeuropathy in rat that produces disorders of pain sensation like those seen in man. Pain 33: 87-107.

Bennett GJ (1994) Neuropathic pain. In: Textbook of pain (Wall PD, Melzack R, eds), pp 201-224. Edinburgh: Churchill Livingstone.

Bergman E, Carlsson K, Liljeborg A, Manders E, Hokfelt T, Ulfhake B (1999) Neuropeptides, nitric oxide synthase and GAP-43 in B4-binding and RT97 immunoreactive primary sensory neurons: normal distribution pattern and changes after peripheral nerve transection and aging. Brain Res 832: 63-83.

Berthele A, Boxall SJ, Urban A, Anneser JM, Zieglgansberger W, Urban L, Tolle TR (1999) Distribution and developmental changes in metabotropic glutamate receptor messenger RNA expression in the rat lumbar spinal cord. Brain Res Dev Brain Res 112: 39-53.

Besse D, Lombard MC, Zajac JM, Roques BP, Besson JM (1990) Pre- and postsynaptic distribution of mu, delta and kappa opioid receptors in the superficial layers of the cervical dorsal horn of the rat spinal cord. Brain Res 521: 15-22.

Besson JM, Chaouch A (1987) Peripheral and spinal mechanisms of nociception. Physiol Rev 67: 67-186.

Bessou P, Perl ER (1969) Response of cutaneous sensory units with unmyelinated fibers to noxious stimuli. J Neurophysiol 32: 1025-1043.

Bessou P, Burgess PR, Perl ER, Taylor CB (1971) Dynamic properties of mechanoreceptors with unmyelinated (C) fibers. J Neurophysiol 34: 116-131.

Beyer C, Banas C, Gonzalez-Flores O, Komisaruk BR (1989) Blockage of substance P-induced scratching behavior in rats by the intrathecal administration of inhibitory amino acid agonists. Pharmacol Biochem Behav 34: 491-495.

Bezzi P, Carmignoto G, Pasti L, Vesce S, Rossi D, Rizzini BL, Pozzan T, Volterra A (1998) Prostaglandins stimulate calcium-dependent glutamate release in astrocytes. Nature 391: 281-285.

Bian D, Ossipov MH, Zhong C, Malan TP, Jr., Porreca F (1998) Tactile allodynia, but not thermal hyperalgesia, of the hindlimbs is blocked by spinal transection in rats with nerve injury. Neurosci Lett 241: 79-82.

Biella G, Panara C, Pecile A, Sotgiu ML (1991) Facilitatory role of calcitonin gene-related peptide (CGRP) on excitation induced by substance P (SP) and noxious stimuli in rat spinal dorsal horn neurons. An iontophoretic study in vivo. Brain Res 559: 352-356.

Black JA, Waxman SG (1996) Sodium channel expression: a dynamic process in neurons and non-neuronal cells. Dev Neurosci 18: 139-152.

Black JA, Cummins TR, Plumpton C, Chen YH, Hormuzdiar W, Clare JJ, Waxman SG (1999) Upregulation of a silent sodium channel after peripheral, but not central, nerve injury in DRG neurons. J Neurophysiol 82: 2776-2785.

Blaukat A, Ivankovic-Dikic I, Gronroos E, Dolfi F, Tokiwa G, Vuori K, Dikic I (1999) Adaptor proteins Grb2 and Crk couple Pyk2 with activation of specific mitogen-activated protein kinase cascades. J Biol Chem 274: 14893-14901.

Bleakman D, Rusin KI, Chard PS, Glaum SR, Miller RJ (1992) Metabotropic glutamate receptors potentiate ionotropic glutamate responses in the rat dorsal horn. Mol Pharmacol 42: 192-196.

Bolshakov VY, Carboni L, Cobb MH, Siegelbaum SA, Belardetti F (2000) Dual MAP kinase pathways mediate opposing forms of long-term plasticity at CA3-CA1 synapses. Nat Neurosci 3: 1107-1112.

Bond A, Lodge D (1995) Pharmacology of metabotropic glutamate receptor-mediated enhancement of responses to excitatory and inhibitory amino acids on rat spinal neurones in vivo. Neuropharmacology 34: 1015-1023.

Bonner TI, Affolter HU, Young AC, Young WS, III (1987) A cDNA encoding the precursor of the rat neuropeptide, neurokinin B. Brain Res 388: 243-249.

Borchert TV, Mathieu M, Zeelen JP, Courtneidge SA, Wierenga RK (1994) The crystal structure of human CskSH3: structural diversity near the RT-Src and n-Src loop. FEBS Lett 341: 79-85.

Borrell-Pages M, Zala D, Humbert S, Saudou F (2006) Huntington's disease: from huntingtin function and dysfunction to therapeutic strategies. Cell Mol Life Sci 63: 2642-2660.

Bortolotto ZA, Collingridge GL (1998) Involvement of calcium/calmodulin-dependent protein kinases in the setting of a molecular switch involved in hippocampal LTP. Neuropharmacology 37: 535-544.

Bosnjak S, Jelic S, Susnjar S, Luki V (2002) Gabapentin for relief of neuropathic pain related to anticancer treatment: a preliminary study. J Chemother 14: 214-219.

Boucher TJ, McMahon SB (2001) Neurotrophic factors and neuropathic pain. Curr Opin Pharmacol 1: 66-72.

Boyce S, Wyatt A, Webb JK, O'Donnell R, Mason G, Rigby M, Sirinathsinghji D, Hill RG, Rupniak NM (1999) Selective NMDA NR2B antagonists induce antinociception without motor dysfunction: correlation with restricted localisation of NR2B subunit in dorsal horn. Neuropharmacology 38: 611-623.

Braz JM, Nassar MA, Wood JN, Basbaum AI (2005) Parallel "pain" pathways arise from subpopulations of primary afferent nociceptor. Neuron 47: 787-793.

Breivik H, Collett B, Ventafridda V, Cohen R, Gallacher D (2006) Survey of chronic pain in Europe: prevalence, impact on daily life, and treatment. Eur J Pain 10: 287-333.

Brenneman DE, Nicol T, Warren D, Bowers LM (1990) Vasoactive intestinal peptide: a neurotrophic releasing agent and an astroglial mitogen. J Neurosci Res 25: 386-394.

Brenneman DE, Phillips TM, Hauser J, Hill JM, Spong CY, Gozes I (2003) Complex array of cytokines released by vasoactive intestinal peptide. Neuropeptides 37: 111-119.

Brown AG, Iggo A (1967) A quantitative study of cutaneous receptors and afferent fibres in the cat and rabbit. J Physiol 193: 707-733.

Brown AG (1981) Organization in the spinal cord: the anatomy and physiology of identified neurones. Berlin: Springer-Verlag.

Brown AG, Brown PB, Fyffe RE, Pubols LM (1983) Receptive field organization and response properties of spinal neurones with axons ascending the dorsal columns in the cat. J Physiol 337: 575-588.

Brown JL, Liu H, Maggio JE, Vigna SR, Mantyh PW, Basbaum AI (1995) Morphological characterization of substance P receptor-immunoreactive neurons in the rat spinal cord and trigeminal nucleus caudalis. J Comp Neurol 356: 327-344.

Brown PB, Fuchs JL (1975) Somatotopic representation of hindlimb skin in cat dorsal horn. J Neurophysiol 38: 1-9.

Budai D, Wilcox GL, Larson AA (1992) Enhancement of NMDA-evoked neuronal activity by glycine in the rat spinal cord in vivo. Neurosci Lett 135: 265-268.

Burgess PR, Perl ER (1967) Myelinated afferent fibres responding specifically to noxious stimulation of the skin. J Physiol 190: 541-562.

Burgess PR, Perl ER (1973) Cutaneous mechanoreceptors and nociceptors. In: Handbook of sensory physiology (Iggo A, ed), pp 29-78. Berlin: Springer-Verlag.

Cahill CM, Coderre TJ (2002) Attenuation of hyperalgesia in a rat model of neuropathic pain after intrathecal pre- or post-treatment with a neurokinin-1 antagonist. Pain 95: 277-285.

Calejesan AA, Ch'ang MH, Zhuo M (1998) Spinal serotonergic receptors mediate facilitation of a nociceptive reflex by subcutaneous formalin injection into the hindpaw in rats. Brain Res 798: 46-54.

Calejesan AA, Kim SJ, Zhuo M (2000) Descending facilitatory modulation of a behavioral nociceptive response by stimulation in the adult rat anterior cingulate cortex. Eur J Pain 4: 83-96.

Cameron AA, Cliffer KD, Dougherty PM, Willis WD, Carlton SM (1991) Changes in lectin, GAP-43 and neuropeptide staining in the rat superficial dorsal horn following experimental peripheral neuropathy. Neurosci Lett 131: 249-252.

Cameron AA, Cliffer KD, Dougherty PM, Garrison CJ, Willis WD, Carlton SM (1997) Time course of degenerative and regenerative changes in the dorsal horn in a rat model of peripheral neuropathy. J Comp Neurol 379: 428-442.

Cao CQ, Djouhri L, Brown AG (1993) Lumbosacral spinal neurons in the cat that are candidates for being activated by collaterals from the spinocervical tract. Neuroscience 57: 153-165.

Carlton SM, Dougherty PM, Pover CM, Coggeshall RE (1991) Neuroma formation and numbers of axons in a rat model of experimental peripheral neuropathy. Neurosci Lett 131: 88-92.

Carlton SM, Coggeshall RE (1996) Stereological analysis of galanin and CGRP synapses in the dorsal horn of neuropathic primates. Brain Res 711: 16-25.

Carlton SM, Du J, Davidson E, Zhou S, Coggeshall RE (2001) Somatostatin receptors on peripheral primary afferent terminals: inhibition of sensitized nociceptors. Pain 90: 233-244.

Carlton SM (2002) Localization of CaMKIIalpha in rat primary sensory neurons: increase in inflammation. Brain Res 947: 252-259.

Carroll P, Lewin GR, Koltzenburg M, Toyka KV, Thoenen H (1998) A role for BDNF in mechanosensation. Nat Neurosci 1: 42-46.

Carter MS, Krause JE (1990) Structure, expression, and some regulatory mechanisms of the rat preprotachykinin gene encoding substance P, neurokinin A, neuropeptide K, and neuropeptide gamma. J Neurosci 10: 2203-2214.

Castagnoli L, Costantini A, Dall'Armi C, Gonfloni S, Montecchi-Palazzi L, Panni S, Paoluzi S, Santonico E, Cesareni G (2004) Selectivity and promiscuity in the interaction network mediated by protein recognition modules. FEBS Lett 567: 74-79.

Castane A, Celerier E, Martin M, Ledent C, Parmentier M, Maldonado R, Valverde O (2006) Development and expression of neuropathic pain in CB1 knockout mice. Neuropharmacology 50: 111-122.

Castejon OJ, Fuller L, Dailey ME (2004) Localization of synapsin-I and PSD-95 in developing postnatal rat cerebellar cortex. Brain Res Dev Brain Res 151: 25-32.

Cervero F, Iggo A, Ogawa H (1976) Nociceptor-driven dorsal horn neurones in the lumbar spinal cord of the cat. Pain 2: 5-24.

Cervero F, Molony V, Iggo A (1979) Supraspinal linkage of substantia gelatinosa neurones: effects of descending impulses. Brain Res 175: 351-355.

Cervero F, Iggo A (1980) The substantia gelatinosa of the spinal cord: a critical review. Brain 103: 717-772.

Cervero F (1983) Somatic and visceral inputs to the thoracic spinal cord of the cat: effects of noxious stimulation of the biliary system. J Physiol 337: 51-67.

Chacur M, Milligan ED, Gazda LS, Armstrong C, Wang H, Tracey KJ, Maier SF, Watkins LR (2001) A new model of sciatic inflammatory neuritis (SIN): induction of unilateral and bilateral mechanical allodynia following acute unilateral peri-sciatic immune activation in rats. Pain 94: 231-244.

Chaouch A, Menetrey D, Binder D, Besson JM (1983) Neurons at the origin of the medial component of the bulbopontine spinoreticular tract in the rat: an anatomical study using horseradish peroxidase retrograde transport. J Comp Neurol 214: 309-320.

Chaplan SR, Malmberg AB, Yaksh TL (1997) Efficacy of spinal NMDA receptor antagonism in formalin hyperalgesia and nerve injury evoked allodynia in the rat. J Pharmacol Exp Ther 280: 829-838.

Chen L, Huang LY (1992) Protein kinase C reduces Mg2+ block of NMDA-receptor channels as a mechanism of modulation. Nature 356: 521-523.

Chiang CY, Park SJ, Kwan CL, Hu JW, Sessle BJ (1998) NMDA receptor mechanisms contribute to neuroplasticity induced in caudalis nociceptive neurons by tooth pulp stimulation. J Neurophysiol 80: 2621-2631.

Choi Y, Yoon YW, Na HS, Kim SH, Chung JM (1994) Behavioral signs of ongoing pain and cold allodynia in a rat model of neuropathic pain. Pain 59: 369-376.

Christensen BN, Perl ER (1970) Spinal neurons specifically excited by noxious or thermal stimuli: marginal zone of the dorsal horn. J Neurophysiol 33: 293-307.

Chung K, Chung JM (2001) Sympathetic sprouting in the dorsal root ganglion after spinal nerve ligation: evidence of regenerative collateral sprouting. Brain Res 895: 204-212.

Ciabarra AM, Sullivan JM, Gahn LG, Pecht G, Heinemann S, Sevarino KA (1995) Cloning and characterization of chi-1: a developmentally regulated member of a novel class of the ionotropic glutamate receptor family. J Neurosci 15: 6498-6508.

Clark AR, Dean JL, Saklatvala J (2003) Post-transcriptional regulation of gene expression by mitogen-activated protein kinase p38. FEBS Lett 546: 37-44.

Clatworthy AL, Illich PA, Castro GA, Walters ET (1995) Role of peri-axonal inflammation in the development of thermal hyperalgesia and guarding behavior in a rat model of neuropathic pain. Neurosci Lett 184: 5-8.

Coderre TJ, Vaccarino AL, Melzack R (1990) Central nervous system plasticity in the tonic pain response to subcutaneous formalin injection. Brain Res 535: 155-158.

Coderre TJ, Melzack R (1992) The contribution of excitatory amino acids to central sensitization and persistent nociception after formalin-induced tissue injury. J Neurosci 12: 3665-3670.

Coderre TJ, Yashpal K (1994) Intracellular messengers contributing to persistent nociception and hyperalgesia induced by L-glutamate and substance P in the rat formalin pain model. Eur J Neurosci 6: 1328-1334.

Coggeshall RE, Applebaum ML, Fazen M, Stubbs TB, III, Sykes MT (1975) Unmyelinated axons in human ventral roots, a possible explanation for the failure of dorsal rhizotomy to relieve pain. Brain 98: 157-166.

Coggeshall RE, Dougherty PM, Pover CM, Carlton SM (1993) Is large myelinated fiber loss associated with hyperalgesia in a model of experimental peripheral neuropathy in the rat? Pain 52: 233-242.

Coggeshall RE, Carlton SM (1997) Receptor localization in the mammalian dorsal horn and primary afferent neurons. Brain Res Brain Res Rev 24: 28-66.

Cohen GB, Ren R, Baltimore D (1995) Modular binding domains in signal transduction proteins. Cell 80: 237-248.

Colburn RW, DeLeo JA, Rickman AJ, Yeager MP, Kwon P, Hickey WF (1997) Dissociation of microglial activation and neuropathic pain behaviors following peripheral nerve injury in the rat. J Neuroimmunol 79: 163-175.

Colburn RW, Rickman AJ, DeLeo JA (1999) The effect of site and type of nerve injury on spinal glial activation and neuropathic pain behavior. Exp Neurol 157: 289-304.

Colledge M, Dean RA, Scott GK, Langeberg LK, Huganir RL, Scott JD (2000) Targeting of PKA to glutamate receptors through a MAGUK-AKAP complex. Neuron 27: 107-119.

Collingridge GL, Kehl SJ, McLennan H (1983) Excitatory amino acids in synaptic transmission in the Schaffer collateral-commissural pathway of the rat hippocampus. J Physiol 334: 33-46.

Coudore-Civiale MA, Courteix C, Eschalier A, Fialip J (1998) Effect of tachykinin receptor antagonists in experimental neuropathic pain. Eur J Pharmacol 361: 175-184.

Courteix C, Lavarenne J, Eschalier A (1993) RP-67580, a specific tachykinin NK1 receptor antagonist, relieves chronic hyperalgesia in diabetic rats. Eur J Pharmacol 241: 267-270.

Craig AD, Kniffki KD (1985) Spinothalamic lumbosacral lamina I cells responsive to skin and muscle stimulation in the cat. J Physiol 365: 197-221.

Cruz CD, Neto FL, Castro-Lopes J, McMahon SB, Cruz F (2005) Inhibition of ERK phosphorylation decreases nociceptive behaviour in monoarthritic rats. Pain 116: 411-419.

Cruz L, Basbaum AI (1985) Multiple opioid peptides and the modulation of pain: immunohistochemical analysis of dynorphin and enkephalin in the trigeminal nucleus caudalis and spinal cord of the cat. J Comp Neurol 240: 331-348.

Cull-Candy S, Brickley S, Farrant M (2001) NMDA receptor subunits: diversity, development and disease. Curr Opin Neurobiol 11: 327-335.

Cummins TR, Waxman SG (1997) Downregulation of tetrodotoxin-resistant sodium currents and upregulation of a rapidly repriming tetrodotoxin-sensitive sodium current in small spinal sensory neurons after nerve injury. J Neurosci 17: 3503-3514.

Curtis DR, PHILLIS JW, Watkins JC (1959) The depression of spinal neurones by gamma-amino-n-butyric acid and beta-alanine. J Physiol 146: 185-203.

Curtis DR, Lodge D, Brand SJ (1977) GABA and spinal afferent terminal excitability in the cat. Brain Res 130: 360-363.

Dai Y, Iwata K, Fukuoka T, Kondo E, Tokunaga A, Yamanaka H, Tachibana T, Liu Y, Noguchi K (2002) Phosphorylation of extracellular signal-regulated kinase in primary afferent neurons by noxious stimuli and its involvement in peripheral sensitization. J Neurosci 22: 7737-7745.

Dallel R, Raboisson P, Clavelou P, Saade M, Woda A (1995) Evidence for a peripheral origin of the tonic nociceptive response to subcutaneous formalin. Pain 61: 11-16.

Dalsgaard CJ, Haegerstrand A, Theodorsson-Norheim E, Brodin E, Hokfelt T (1985) Neurokinin A-like immunoreactivity in rat primary sensory neurons; coexistence with substance P. Histochemistry 83: 37-39.

Davies J, Evans RH, Francis AA, Watkins JC (1979) Excitatory amino acid receptors and synaptic excitation in the mammalian central nervous system. J Physiol (Paris) 75: 641-654.

Davies SN, Lodge D (1987) Evidence for involvement of N-methylaspartate receptors in 'wind-up' of class 2 neurones in the dorsal horn of the rat. Brain Res 424: 402-406.

De Biasi S, Rustioni A (1988) Glutamate and substance P coexist in primary afferent terminals in the superficial laminae of spinal cord. Proc Natl Acad Sci U S A 85: 7820-7824.

De Blasi A, Conn PJ, Pin J, Nicoletti F (2001) Molecular determinants of metabotropic glutamate receptor signaling. Trends Pharmacol Sci 22: 114-120.

Decosterd I, Woolf CJ (2000) Spared nerve injury: an animal model of persistent peripheral neuropathic pain. Pain 87: 149-158.

Decosterd I, Ji RR, Abdi S, Tate S, Woolf CJ (2002) The pattern of expression of the voltage-gated sodium channels Na(v)1.8 and Na(v)1.9 does not change in uninjured primary sensory neurons in experimental neuropathic pain models. Pain 96: 269-277.

DeLeo JA, Colburn RW, Rickman AJ (1997) Cytokine and growth factor immunohistochemical spinal profiles in two animal models of mononeuropathy. Brain Res 759: 50-57.

DeLeo JA, Yezierski RP (2001) The role of neuroinflammation and neuroimmune activation in persistent pain. Pain 90: 1-6.

Delgado M, Leceta J, Ganea D (2003) Vasoactive intestinal peptide and pituitary adenylate cyclase-activating polypeptide inhibit the production of inflammatory mediators by activated microglia. J Leukoc Biol 73: 155-164.

Derkach V, Barria A, Soderling TR (1999) Ca2+/calmodulin-kinase II enhances channel conductance of alpha-amino-3-hydroxy-5-methyl-4-isoxazolepropionate type glutamate receptors. Proc Natl Acad Sci U S A 96: 3269-3274.

Derkinderen P, Enslen H, Girault JA (1999) The ERK/MAP-kinases cascade in the nervous system. Neuroreport 10: R24-R34.

Desmeules JA, Kayser V, Weil-Fuggaza J, Bertrand A, Guilbaud G (1995) Influence of the sympathetic nervous system in the development of abnormal pain-related behaviours in a rat model of neuropathic pain. Neuroscience 67: 941-951.

Devor M, Janig W, Michaelis M (1994) Modulation of activity in dorsal root ganglion neurons by sympathetic activation in nerve-injured rats. J Neurophysiol 71: 38-47.

Devor M, Seltzer Z (1999) Pathophysiology of damaged nerves in relation to chronic pain. In: Textbook of Pain (Wall PD, Melzack R, eds), pp 129-164. London: Churchill Livingstone.

Dib-Hajj SD, Fjell J, Cummins TR, Zheng Z, Fried K, LaMotte R, Black JA, Waxman SG (1999) Plasticity of sodium channel expression in DRG neurons in the chronic constriction injury model of neuropathic pain. Pain 83: 591-600.

Dickenson AH, Sullivan AF (1987) Subcutaneous formalin-induced activity of dorsal horn neurones in the rat: differential response to an intrathecal opiate administered pre or post formalin. Pain 30: 349-360.

Dickenson AH, Sullivan AF (1987) Evidence for a role of the NMDA receptor in the frequency dependent potentiation of deep rat dorsal horn nociceptive neurones following C fibre stimulation. Neuropharmacology 26: 1235-1238.

Dickenson AH, Sullivan AF (1987) Peripheral origins and central modulation of subcutaneous formalin-induced activity of rat dorsal horn neurones. Neurosci Lett 83: 207-211.

Dickenson AH, Sullivan AF (1990) Differential effects of excitatory amino acid antagonists on dorsal horn nociceptive neurones in the rat. Brain Res 506: 31-39.

Dickenson AH, Aydar E (1991) Antagonism at the glycine site on the NMDA receptor reduces spinal nociception in the rat. Neurosci Lett 121: 263-266.

Dickinson T, Fleetwood-Walker SM, Mitchell R, Lutz EM (1997) Evidence for roles of vasoactive intestinal polypeptide (VIP) and pituitary adenylate cyclase activating polypeptide (PACAP) receptors in modulating the responses of rat dorsal horn neurons to sensory inputs. Neuropeptides 31: 175-185.

Dickinson T, Fleetwood-Walker SM (1999) VIP and PACAP: very important in pain? Trends Pharmacol Sci 20: 324-329.

Dickinson T, Mitchell R, Robberecht P, Fleetwood-Walker SM (1999) The role of VIP/PACAP receptor subtypes in spinal somatosensory processing in rats with an experimental peripheral mononeuropathy. Neuropharmacology 38: 167-180.

Dickson L, Aramori I, McCulloch J, Sharkey J, Finlayson K (2006) A systematic comparison of intracellular cyclic AMP and calcium signalling highlights complexities in human VPAC/PAC receptor pharmacology. Neuropharmacology 51: 1086-1098.

Dikic I, Tokiwa G, Lev S, Courtneidge SA, Schlessinger J (1996) A role for Pyk2 and Src in linking G-protein-coupled receptors with MAP kinase activation. Nature 383: 547-550.

Dikic I, Dikic I, Schlessinger J (1998) Identification of a new Pyk2 isoform implicated in chemokine and antigen receptor signaling. J Biol Chem 273: 14301-14308.

Ding YQ, Shigemoto R, Takada M, Ohishi H, Nakanishi S, Mizuno N (1996) Localization of the neuromedin K receptor (NK3) in the central nervous system of the rat. J Comp Neurol 364: 290-310.

Dogrul A, Ossipov MH, Lai J, Malan TP, Jr., Porreca F (2000) Peripheral and spinal antihyperalgesic activity of SIB-1757, a metabotropic glutamate receptor (mGLUR(5)) antagonist, in experimental neuropathic pain in rats. Neurosci Lett 292: 115-118.

Dorazil-Dudzik M, Mika J, Schafer MK, Li Y, Obara I, Wordliczek J, Przewlocka B (2004) The effects of local pentoxifylline and propentofylline treatment on formalin-induced pain and tumor necrosis factor-alpha messenger RNA levels in the inflamed tissue of the rat paw. Anesth Analg 98: 1566-73, table.

Doubell TP, McCulloch J (1999) The dorsal horn: state-dependent sensory processing, plasticity and the generation of pain. In: Textbook of Pain (Melzack R, Wall PD, eds), pp 165-182. London: Churchill Livingstone.

Dougherty PM, Palecek J, Paleckova V, Sorkin LS, Willis WD (1992) The role of NMDA and non-NMDA excitatory amino acid receptors in the excitation of primate spinothalamic tract neurons by mechanical, chemical, thermal, and electrical stimuli. J Neurosci 12: 3025-3041.

Drew LJ, Harris J, Millns PJ, Kendall DA, Chapman V (2000) Activation of spinal cannabinoid 1 receptors inhibits C-fibre driven hyperexcitable neuronal responses and increases [35S]GTPgammaS binding in the dorsal horn of the spinal cord of noninflamed and inflamed rats. Eur J Neurosci 12: 2079-2086.

Dubner R, Bennett GJ (1983) Spinal and trigeminal mechanisms of nociception. Annu Rev Neurosci 6: 381-418.

Dubuisson D, Dennis SG (1977) The formalin test: a quantitative study of the analgesic effects of morphine, meperidine, and brain stem stimulation in rats and cats. Pain 4: 161-174.

Duggan AW, Johnston GA (1970) Glutamate and related amino acids in cat spinal roots, dorsal root ganglia and peripheral nerves. J Neurochem 17: 1205-1208.

Duggan AW, Griersmith BT (1979) Inhibition of the spinal transmission of nociceptive information by supraspinal stimulation in the cat. Pain 6: 149-161.

Duggan AW, North RA (1983) Electrophysiology of opioids. Pharmacol Rev 35: 219-281.

Duggan AW, Hendry IA, Morton CR, Hutchison WD, Zhao ZQ (1988) Cutaneous stimuli releasing immunoreactive substance P in the dorsal horn of the cat. Brain Res 451: 261-273.

Duggan AW, Hope PJ, Jarrott B, Schaible HG, Fleetwood-Walker SM (1990) Release, spread and persistence of immunoreactive neurokinin A in the dorsal horn of the cat following noxious cutaneous stimulation. Studies with antibody microprobes. Neuroscience 35: 195-202.

Duggan AW, Furmidge LJ (1994) Probing the brain and spinal cord with neuropeptides in pathways related to pain and other functions. Front Neuroendocrinol 15: 275-300.

Duggan AW, Riley RC, Mark MA, MacMillan SJ, Schaible HG (1995) Afferent volley patterns and the spinal release of immunoreactive substance P in the dorsal horn of the anaesthetized spinal cat. Neuroscience 65: 849-858.

Dun NJ, Miyazaki T, Tang H, Dun EC (1996) Pituitary adenylate cyclase activating polypeptide immunoreactivity in the rat spinal cord and medulla: implication of sensory and autonomic functions. Neuroscience 73: 677-686.

Erpel T, Superti-Furga G, Courtneidge SA (1995) Mutational analysis of the Src SH3 domain: the same residues of the ligand binding surface are important for intra- and intermolecular interactions. EMBO J 14: 963-975.

Fagiolini M, Katagiri H, Miyamoto H, Mori H, Grant SG, Mishina M, Hensch TK (2003) Separable features of visual cortical plasticity revealed by N-methyl-D-aspartate receptor 2A signaling. Proc Natl Acad Sci U S A 100: 2854-2859.

Fang L, Wu J, Lin Q, Willis WD (2002) Calcium-calmodulin-dependent protein kinase II contributes to spinal cord central sensitization. J Neurosci 22: 4196-4204.

Faris PL, Komisaruk BR, Watkins LR, Mayer DJ (1983) Evidence for the neuropeptide cholecystokinin as an antagonist of opiate analgesia. Science 219: 310-312.

Farquhar-Smith WP, Egertova M, Bradbury EJ, McMahon SB, Rice AS, Elphick MR (2000) Cannabinoid CB(1) receptor expression in rat spinal cord. Mol Cell Neurosci 15: 510-521.

Fine SM, Angel RA, Perry SW, Epstein LG, Rothstein JD, Dewhurst S, Gelbard HA (1996) Tumor necrosis factor alpha inhibits glutamate uptake by primary human astrocytes. Implications for pathogenesis of HIV-1 dementia. J Biol Chem 271: 15303-15306.

Fink K, Meder W, Dooley DJ, Gothert M (2000) Inhibition of neuronal Ca(2+) influx by gabapentin and subsequent reduction of neurotransmitter release from rat neocortical slices. Br J Pharmacol 130: 900-906.

Finley JC, Maderdrut JL, Roger LJ, Petrusz P (1981) The immunocytochemical localization of somatostatin-containing neurons in the rat central nervous system. Neuroscience 6: 2173-2192.

Fitzgerald M, Lynn B (1977) The sensitization of high threshold mechanoreceptors with myelinated axons by repeated heating. J Physiol 265: 549-563.

Fitzgerald M, Wall PD, Goedert M, Emson PC (1985) Nerve growth factor counteracts the neurophysiological and neurochemical effects of chronic sciatic nerve section. Brain Res 332: 131-141.

Fleetwood-Walker SM, Hope PJ, Mitchell R, El Yassir N, Molony V (1988) The influence of opioid receptor subtypes on the processing of nociceptive inputs in the spinal dorsal horn of the cat. Brain Res 451: 213-226.

Fleetwood-Walker SM, Hope PJ, Mitchell R (1988) Antinociceptive actions of descending dopaminergic tracts on cat and rat dorsal horn somatosensory neurones. J Physiol 399: 335-348.

Fleetwood-Walker SM, Mitchell R, Hope PJ, El Yassir N, Molony V, Bladon CM (1990) The involvement of neurokinin receptor subtypes in somatosensory processing in the superficial dorsal horn of the cat. Brain Res 519: 169-182.

Fleetwood-Walker SM, Parker RM, Munro FE, Young MR, Hope PJ, Mitchell R (1993) Evidence for a role of tachykinin NK2 receptors in mediating brief nociceptive inputs to rat dorsal horn (laminae III-V) neurons. Eur J Pharmacol 242: 173-181.

Foong FW, Duggan AW (1986) Brain-stem areas tonically inhibiting dorsal horn neurones: studies with microinjection of the GABA analogue piperidine-4-sulphonic acid. Pain 27: 361-371.

Fox A, Kesingland A, Gentry C, McNair K, Patel S, Urban L, James I (2001) The role of central and peripheral Cannabinoid1 receptors in the antihyperalgesic activity of cannabinoids in a model of neuropathic pain. Pain 92: 91-100.

Fraenkel-Conrat H, Brandon BA, Olcott HS (1947) The reaction of formaldehyde with proteins IV participation of indole groups. J Biol Chemistry 168: 99-118.

Fried K, Govrin-Lippmann R, Devor M (1993) Close apposition among neighbouring axonal endings in a neuroma. J Neurocytol 22: 663-681.

Fuji K, Senba E, Ueda Y, Tohyama M (1983) Vasoactive intestinal polypeptide (VIP)-containing neurons in the spinal cord of the rat and their projections. Neurosci Lett 37: 51-55.

Fukuoka T, Kondo E, Dai Y, Hashimoto N, Noguchi K (2001) Brain-derived neurotrophic factor increases in the uninjured dorsal root ganglion neurons in selective spinal nerve ligation model. J Neurosci 21: 4891-4900.

Furuyama T, Kiyama H, Sato K, Park HT, Maeno H, Takagi H, Tohyama M (1993) Region-specific expression of subunits of ionotropic glutamate receptors (AMPA-type, KA-type and NMDA receptors) in the rat spinal cord with special reference to nociception. Brain Res Mol Brain Res 18: 141-151.

Galan A, Lopez-Garcia JA, Cervero F, Laird JM (2002) Activation of spinal extracellular signaling-regulated kinase-1 and -2 by intraplantar carrageenan in rodents. Neurosci Lett 322: 37-40.

Garcia EP, Mehta S, Blair LA, Wells DG, Shang J, Fukushima T, Fallon JR, Garner CC, Marshall J (1998) SAP90 binds and clusters kainate receptors causing incomplete desensitization. Neuron 21: 727-739.

Gardoni F, Schrama LH, van Dalen JJ, Gispen WH, Cattabeni F, Di Luca M (1999) AlphaCaMKII binding to the C-terminal tail of NMDA receptor subunit NR2A and its modulation by autophosphorylation. FEBS Lett 456: 394-398.

Garner CC, Nash J, Huganir RL (2000) PDZ domains in synapse assembly and signalling. Trends Cell Biol 10: 274-280.

Garrison CJ, Dougherty PM, Kajander KC, Carlton SM (1991) Staining of glial fibrillary acidic protein (GFAP) in lumbar spinal cord increases following a sciatic nerve constriction injury. Brain Res 565: 1-7.

Garrison CJ, Dougherty PM, Carlton SM (1994) GFAP expression in lumbar spinal cord of naive and neuropathic rats treated with MK-801. Exp Neurol 129: 237-243.

Garry EM, Moss A, Delaney A, O'Neill F, Blakemore J, Bowen J, Husi H, Mitchell R, Grant SG, Fleetwood-Walker SM (2003) Neuropathic sensitization of behavioral reflexes and spinal NMDA receptor/CaM kinase II interactions are disrupted in PSD-95 mutant mice. Curr Biol 13: 321-328.

Gasser HS (1950) Unmedullated fibers originating in dorsal root ganglia. J Gen Physiol 33: 651-690.

Gautron M, Jazat F, Ratinahirana H, Hauw JJ, Guilbaud G (1990) Alterations in myelinated fibres in the sciatic nerve of rats after constriction: possible relationships between the presence of abnormal small myelinated fibres and pain-related behaviour. Neurosci Lett 111: 28-33.

Gazda LS, Milligan ED, Hansen MK, Twining CM, Poulos NM, Chacur M, O'Connor KA, Armstrong C, Maier SF, Watkins LR, Myers RR (2001) Sciatic inflammatory neuritis (SIN): behavioral allodynia is paralleled by peri-sciatic proinflammatory cytokine and superoxide production. J Peripher Nerv Syst 6: 111-129.

George A, Marziniak M, Schafers M, Toyka KV, Sommer C (2000) Thalidomide treatment in chronic constrictive neuropathy decreases endoneurial tumor necrosis factor-alpha, increases interleukin-10 and has long-term effects on spinal cord dorsal horn met-enkephalin. Pain 88: 267-275.

Gerber G, Randic M (1989) Excitatory amino acid-mediated components of synaptically evoked input from dorsal roots to deep dorsal horn neurons in the rat spinal cord slice. Neurosci Lett 106: 211-219.

Gibson SJ, Polak JM, Bloom SR, Wall PD (1981) The distribution of nine peptides in rat spinal cord with special emphasis on the substantia gelatinosa and on the area around the central canal (lamina X). J Comp Neurol 201: 65-79.

Gibson SJ, Polak JM, Anand P, Blank MA, Morrison JF, Kelly JS, Bloom SR (1984) The distribution and origin of VIP in the spinal cord of six mammalian species. Peptides 5: 201-207.

Giesler GJ, Menetrey D, Guilbaud G, Besson JM (1976) Lumbar cord neurons at the origin of the spinothalamic tract in the rat. Brain Res 118: 320-324.

Giesler GJ, Jr., Menetrey D, Basbaum AI (1979) Differential origins of spinothalamic tract projections to medial and lateral thalamus in the rat. J Comp Neurol 184: 107-126.

Giesler GJ, Jr., Nahin RL, Madsen AM (1984) Postsynaptic dorsal column pathway of the rat. I. Anatomical studies. J Neurophysiol 51: 260-275.

Gilbert AK, Franklin KB (2001) GABAergic modulation of descending inhibitory systems from the rostral ventromedial medulla (RVM). Dose-response analysis of nociception and neurological deficits. Pain 90: 25-36.

Gillespie CS, Sherman DL, Fleetwood-Walker SM, Cottrell DF, Tait S, Garry EM, Wallace VC, Ure J, Griffiths IR, Smith A, Brophy PJ (2000) Peripheral demyelination and neuropathic pain behavior in periaxin-deficient mice. Neuron 26: 523-531.

Gillette RG, Kramis RC, Roberts WJ (1994) Sympathetic activation of cat spinal neurons responsive to noxious stimulation of deep tissues in the low back. Pain 56: 31-42.

Girault JA, Costa A, Derkinderen P, Studler JM, Toutant M (1999) FAK and PYK2/CAKbeta in the nervous system: a link between neuronal activity, plasticity and survival? Trends Neurosci 22: 257-263.

Glazer EJ, Basbaum AI (1981) Immunohistochemical localization of leucine-enkephalin in the spinal cord of the cat: enkephalin-containing marginal neurons and pain modulation. J Comp Neurol 196: 377-389.

Gorson KC, Schott C, Herman R, Ropper AH, Rand WM (1999) Gabapentin in the treatment of painful diabetic neuropathy: a placebo controlled, double blind, crossover trial. J Neurol Neurosurg Psychiatry 66: 251-252.

Grant SG, Marshall MC, Page KL, Cumiskey MA, Armstrong JD (2005) Synapse proteomics of multiprotein complexes: en route from genes to nervous system diseases. Hum Mol Genet 14 Spec No. 2: R225-R234.

Greenamyre JT, Young AB, Penney JB (1984) Quantitative autoradiographic distribution of L-[3H]glutamate-binding sites in rat central nervous system. J Neurosci 4: 2133-2144.

Grimaldi M, Cavallaro S (1999) Functional and molecular diversity of PACAP/VIP receptors in cortical neurons and type I astrocytes. Eur J Neurosci 11: 2767-2772.

Guilbaud G, Caille D, Besson JM, Benelli G (1977) Single units activities in ventral posterior and posterior group thalamic nuclei during nociceptive and non nociceptive stimulations in the cat. Arch Ital Biol 115: 38-56.

Guilbaud G, Gautron M, Jazat F, Ratinahirana H, Hassig R, Hauw JJ (1993) Time course of degeneration and regeneration of myelinated nerve fibres following chronic loose ligatures of the rat sciatic nerve: can nerve lesions be linked to the abnormal pain-related behaviours? Pain 53: 147-158.

Guo W, Wei F, Zou S, Robbins MT, Sugiyo S, Ikeda T, Tu JC, Worley PF, Dubner R, Ren K (2004) Group I metabotropic glutamate receptor NMDA receptor coupling and signaling cascade mediate spinal dorsal horn NMDA receptor 2B tyrosine phosphorylation associated with inflammatory hyperalgesia. J Neurosci 24: 9161-9173.

Guruprasad L, Dhanaraj V, Timm D, Blundell TL, Gout I, Waterfield MD (1995) The crystal structure of the N-terminal SH3 domain of Grb2. J Mol Biol 248: 856-866.

Gustafsson H, Flood K, Berge OG, Brodin E, Olgart L, Stiller CO (2003) Gabapentin reverses mechanical allodynia induced by sciatic nerve ischemia and formalin-induced nociception in mice. Exp Neurol 182: 427-434.

Habler HJ, Janig W, Koltzenburg M (1987) Activation of unmyelinated afferents in chronically lesioned nerves by adrenaline and excitation of sympathetic efferents in the cat. Neurosci Lett 82: 35-40.

Haley JE, Sullivan AF, Dickenson AH (1990) Evidence for spinal N-methyl-D-aspartate receptor involvement in prolonged chemical nociception in the rat. Brain Res 518: 218-226.

Hama AT, Unnerstall JR, Siegan JB, Sagen J (1995) Modulation of NMDA receptor expression in the rat spinal cord by peripheral nerve injury and adrenal medullary grafting. Brain Res 687: 103-113.

Hanks SK, Quinn AM (1991) Protein kinase catalytic domain sequence database: identification of conserved features of primary structure and classification of family members. Methods Enzymol 200: 38-62.

Hargreaves K, Dubner R, Brown F, Flores C, Joris J (1988) A new and sensitive method for measuring thermal nociception in cutaneous hyperalgesia. Pain 32: 77-88.

Harmar T, Lutz E (1994) Multiple receptors for PACAP and VIP. Trends Pharmacol Sci 15: 97-99.

Hashimoto H, Ishihara T, Shigemoto R, Mori K, Nagata S (1993) Molecular cloning and tissue distribution of a receptor for pituitary adenylate cyclase-activating polypeptide. Neuron 11: 333-342.

Hashimoto H, Ogawa N, Hagihara N, Yamamoto K, Imanishi K, Nogi H, Nishino A, Fujita T, Matsuda T, Nagata S, Baba A (1997) Vasoactive intestinal polypeptide and pituitary adenylate cyclase-activating polypeptide receptor chimeras reveal domains that determine specificity of vasoactive intestinal polypeptide binding and activation. Mol Pharmacol 52: 128-135.

Hashizume H, DeLeo JA, Colburn RW, Weinstein JN (2000) Spinal glial activation and cytokine expression after lumbar root injury in the rat. Spine 25: 1206-1217.

Hayashi Y, Shi SH, Esteban JA, Piccini A, Poncer JC, Malinow R (2000) Driving AMPA receptors into synapses by LTP and CaMKII: requirement for GluR1 and PDZ domain interaction. Science 287: 2262-2267.

Hayes AG, Tyers MB (1979) Effects of intrathecal and intracerebroventricular injections of substance P on nociception in the rat and mouse [proceedings]. Br J Pharmacol 66: 488P.

Heinz M, Schafer K, Braun HA (1990) Analysis of facial cold receptor activity in the rat. Brain Res 521: 289-295.

Helke CJ, Charlton CG, Wiley RG (1986) Studies on the cellular localization of spinal cord substance P receptors. Neuroscience 19: 523-533.

Hemstreet B, Lapointe M (2001) Evidence for the use of gabapentin in the treatment of diabetic peripheral neuropathy. Clin Ther 23: 520-531.

Henley JM (1993) Localization of AMPA receptor subunits in rat CNS using anti-peptide antibodies. Neuroreport 4: 334-336.

Henry JL (1976) Effects of substance P on functionally identified units in cat spinal cord. Brain Res 114: 439-451.

Henry JL, Salter MW (1987) Neurokinin A excites nociceptive and non-nociceptive dorsal horn neurones in the cat spinal cord. In: Substance P and Neurokinins (Henry JL, Couture R, Cuello AC, Pelletier G, Quirion R, Regoli D, eds), pp 279-281. New York: Springer.

Heppenstall PA, Fleetwood-Walker SM (1997) Glycine receptor regulation of neurokinin1 receptor function in rat dorsal horn neurones. Neuroreport 8: 3109-3112.

Herkenham M, Groen BG, Lynn AB, De Costa BR, Richfield EK (1991) Neuronal localization of cannabinoid receptors and second messengers in mutant mouse cerebellum. Brain Res 552: 301-310.

Herzberg U, Eliav E, Bennett GJ, Kopin IJ (1997) The analgesic effects of R(+)-WIN 55,212-2 mesylate, a high affinity cannabinoid agonist, in a rat model of neuropathic pain. Neurosci Lett 221: 157-160.

Herzog H, Nicholl J, Hort YJ, Sutherland GR, Shine J (1996) Molecular cloning and assignment of FAK2, a novel human focal adhesion kinase, to 8p11.2-p22 by nonisotopic in situ hybridization. Genomics 32: 484-486.

Hewitt DJ, McDonald M, Portenoy RK, Rosenfeld B, Passik S, Breitbart W (1997) Pain syndromes and etiologies in ambulatory AIDS patients. Pain 70: 117-123.

Hide I, Tanaka M, Inoue A, Nakajima K, Kohsaka S, Inoue K, Nakata Y (2000) Extracellular ATP triggers tumor necrosis factor-alpha release from rat microglia. J Neurochem 75: 965-972.

Hill R (2000) NK1 (substance P) receptor antagonists--why are they not analgesic in humans? Trends Pharmacol Sci 21: 244-246.

Hiregowdara D, Avraham H, Fu Y, London R, Avraham S (1997) Tyrosine phosphorylation of the related adhesion focal tyrosine kinase in megakaryocytes upon stem cell factor and phorbol myristate acetate stimulation and its association with paxillin. J Biol Chem 272: 10804-10810.

Hocking G, Cousins MJ (2003) Ketamine in chronic pain management: an evidence-based review. Anesth Analg 97: 1730-1739.

Hokfelt T, Kellerth JO, Nilsson G, Pernow B (1975) Experimental immunohistochemical studies on the localization and distribution of substance P in cat primary sensory neurons. Brain Res 100: 235-252.

Hokfelt T, Elde R, Johansson O, Luft R, Nilsson G, Arimura A (1976) Immunohistochemical evidence for separate populations of somatostatin-containing and substance P-containing primary afferent neurons in the rat. Neuroscience 1: 131-136.

Hokfelt T, Elfvin LG, Schultzberg M, Goldstein M, Nilsson G (1977) On the occurrence of substance P-containing fibers in sympathetic ganglia: immunohistochemical evidence. Brain Res 132: 29-41.

Hokfelt T, Lundberg JM, Schultzberg M, Johansson O, Skirboll L, Anggard A, Fredholm B, Hamberger B, Pernow B, Rehfeld J, Goldstein M (1980) Cellular localization of peptides in neural structures. Proc R Soc Lond B Biol Sci 210: 63-77.

Hokfelt T, Zhang X, Verge V, Villar M, Elde R, Bartfai T, Xu XJ, Wiesenfeld-Hallin Z (1993) Coexistence and interaction of neuropeptides with substance P in primary sensory neurons, with special reference to galanin. Regul Pept 46: 76-80.

Hokfelt T, Zhang X, Wiesenfeld-Hallin Z (1994) Messenger plasticity in primary sensory neurons following axotomy and its functional implications. Trends Neurosci 17: 22-30.

Holmes TC, Fadool DA, Levitan IB (1996) Tyrosine phosphorylation of the Kv1.3 potassium channel. J Neurosci 16: 1581-1590.

Hope PJ, Jarrott B, Schaible HG, Clarke RW, Duggan AW (1990) Release and spread of immunoreactive neurokinin A in the cat spinal cord in a model of acute arthritis. Brain Res 533: 292-299.

Hosoya M, Onda H, Ogi K, Masuda Y, Miyamoto Y, Ohtaki T, Okazaki H, Arimura A, Fujino M (1993) Molecular cloning and functional expression of rat cDNAs encoding the receptor for pituitary adenylate cyclase activating polypeptide (PACAP). Biochem Biophys Res Commun 194: 133-143.

Hua XY, Boublik JH, Spicer MA, Rivier JE, Brown MR, Yaksh TL (1991) The antinociceptive effects of spinally administered neuropeptide Y in the rat: systematic studies on structure-activity relationship. J Pharmacol Exp Ther 258: 243-248.

Huang CC, Hsu KS (1999) Protein tyrosine kinase is required for the induction of long-term potentiation in the rat hippocampus. J Physiol 520 Pt 3: 783-796.

Huang WJ, Wang BR, Yao LB, Huang CS, Wang X, Zhang P, Jiao XY, Duan XL, Chen BF, Ju G (2000) Activity of p44/42 MAP kinase in the caudal subnucleus of trigeminal spinal nucleus is increased following perioral noxious stimulation in the mouse. Brain Res 861: 181-185.

Huang XY, Morielli AD, Peralta EG (1993) Tyrosine kinase-dependent suppression of a potassium channel by the G protein-coupled m1 muscarinic acetylcholine receptor. Cell 75: 1145-1156.

Huang Y, Lu W, Ali DW, Pelkey KA, Pitcher GM, Lu YM, Aoto H, Roder JC, Sasaki T, Salter MW, MacDonald JF (2001) CAKbeta/Pyk2 kinase is a signaling link for induction of long-term potentiation in CA1 hippocampus. Neuron 29: 485-496.

Hughes DI, Scott DT, Todd AJ, Riddell JS (2003) Lack of evidence for sprouting of Abeta afferents into the superficial laminas of the spinal cord dorsal horn after nerve section. J Neurosci 23: 9491-9499.

Hunt SP, Kelly JS, Emson PC, Kimmel JR, Miller RJ, Wu JY (1981) An immunohistochemical study of neuronal populations containing neuropeptides or gamma-aminobutyrate within the superficial layers of the rat dorsal horn. Neuroscience 6: 1883-1898.

Husi H, Ward MA, Choudhary JS, Blackstock WP, Grant SG (2000) Proteomic analysis of NMDA receptor-adhesion protein signaling complexes. Nat Neurosci 3: 661-669.

Husi H, Grant SG (2001) Isolation of 2000-kDa complexes of N-methyl-D-aspartate receptor and postsynaptic density 95 from mouse brain. J Neurochem 77: 281-291.

Hwang SJ, Pagliardini S, Rustioni A, Valtschanoff JG (2001) Presynaptic kainate receptors in primary afferents to the superficial laminae of the rat spinal cord. J Comp Neurol 436: 275-289.

Hylden JL, Wilcox GL (1981) Intrathecal substance P elicits a caudally-directed biting and scratching behavior in mice. Brain Res 217: 212-215.

Ibuki T, Hama AT, Wang XT, Pappas GD, Sagen J (1997) Loss of GABA-immunoreactivity in the spinal dorsal horn of rats with peripheral nerve injury and promotion of recovery by adrenal medullary grafts. Neuroscience 76: 845-858.

Iggo A (1959) Cutaneous heat and cold receptors with slowly conducting (C) afferent fibres. Q J Exp Physiol Cogn Med Sci 44: 362-370.

Iggo A (1969) Cutaneous thermoreceptors in primates and sub-primates. J Physiol 200: 403-430.

Iggo A, Ramsey RL (1974) Proceedings: Dorsal horn neurons excited by cutaneous cold receptors in primates. J Physiol 242: 132P-133P.

Igwe OJ (2003) c-Src kinase activation regulates preprotachykinin gene expression and substance P secretion in rat sensory ganglia. Eur J Neurosci 18: 1719-1730.

Impey S, Obrietan K, Storm DR (1999) Making new connections: role of ERK/MAP kinase signaling in neuronal plasticity. Neuron 23: 11-14.

Ishihara T, Shigemoto R, Mori K, Takahashi K, Nagata S (1992) Functional expression and tissue distribution of a novel receptor for vasoactive intestinal polypeptide. Neuron 8: 811-819.

Jahr CE, Jessell TM (1985) Synaptic transmission between dorsal root ganglion and dorsal horn neurons in culture: antagonism of monosynaptic excitatory postsynaptic potentials and glutamate excitation by kynurenate. J Neurosci 5: 2281-2289.

Jaworski DM (2000) Expression of pituitary adenylate cyclase-activating polypeptide (PACAP) and the PACAP-selective receptor in cultured rat astrocytes, human brain tumors, and in response to acute intracranial injury. Cell Tissue Res 300: 219-230.

Jensen TS (2002) Anticonvulsants in neuropathic pain: rationale and clinical evidence. Eur J Pain 6 Suppl A: 61-68.

Jessell T, Tsunoo A, Kanazawa I, Otsuka M (1979) Substance P: depletion in the dorsal horn of rat spinal cord after section of the peripheral processes of primary sensory neurons. Brain Res 168: 247-259.

Jessell TM, Yoshioka K, Jahr CE (1986) Amino acid receptor-mediated transmission at primary afferent synapses in rat spinal cord. J Exp Biol 124: 239-258.

Ji RR, Baba H, Brenner GJ, Woolf CJ (1999) Nociceptive-specific activation of ERK in spinal neurons contributes to pain hypersensitivity. Nat Neurosci 2: 1114-1119.

Ji RR, Woolf CJ (2001) Neuronal plasticity and signal transduction in nociceptive neurons: implications for the initiation and maintenance of pathological pain. Neurobiol Dis 8: 1-10.

Ji RR, Samad TA, Jin SX, Schmoll R, Woolf CJ (2002) p38 MAPK activation by NGF in primary sensory neurons after inflammation increases TRPV1 levels and maintains heat hyperalgesia. Neuron 36: 57-68.

Ji RR, Befort K, Brenner GJ, Woolf CJ (2002) ERK MAP kinase activation in superficial spinal cord neurons induces prodynorphin and NK-1 upregulation and contributes to persistent inflammatory pain hypersensitivity. J Neurosci 22: 478-485.

Ji RR, Kohno T, Moore KA, Woolf CJ (2003) Central sensitization and LTP: do pain and memory share similar mechanisms? Trends Neurosci 26: 696-705.

Ji RR, Kohno T, Moore KA, Woolf CJ (2003) Central sensitization and LTP: do pain and memory share similar mechanisms? Trends Neurosci 26: 696-705.

Jia H, Rustioni A, Valtschanoff JG (1999) Metabotropic glutamate receptors in superficial laminae of the rat dorsal horn. J Comp Neurol 410: 627-642.

Jin SX, Zhuang ZY, Woolf CJ, Ji RR (2003) p38 mitogen-activated protein kinase is activated after a spinal nerve ligation in spinal cord microglia and dorsal root ganglion neurons and contributes to the generation of neuropathic pain. J Neurosci 23: 4017-4022.

Joo KM, Chung YH, Kim MK, Nam RH, Lee BL, Lee KH, Cha CI (2004) Distribution of vasoactive intestinal peptide and pituitary adenylate cyclase-activating polypeptide receptors (VPAC1, VPAC2, and PAC1 receptor) in the rat brain. J Comp Neurol 476: 388-413.

Ju G, Hokfelt T, Brodin E, Fahrenkrug J, Fischer JA, Frey P, Elde RP, Brown JC (1987) Primary sensory neurons of the rat showing calcitonin gene-related peptide immunoreactivity and their relation to substance P-, somatostatin-, galanin-, vasoactive intestinal polypeptide- and cholecystokinin-immunoreactive ganglion cells. Cell Tissue Res 247: 417-431.

Kajander KC, Bennett GJ (1992) Onset of a painful peripheral neuropathy in rat: a partial and differential deafferentation and spontaneous discharge in A beta and A delta primary afferent neurons. J Neurophysiol 68: 734-744.

Kajander KC, Wakisaka S, Bennett GJ (1992) Spontaneous discharge originates in the dorsal root ganglion at the onset of a painful peripheral neuropathy in the rat. Neurosci Lett 138: 225-228.

Kajander KC, Xu J (1995) Quantitative evaluation of calcitonin gene-related peptide and substance P levels in rat spinal cord following peripheral nerve injury. Neurosci Lett 186: 184-188.

Kajander KC, Pollock CH, Berg H (1996) Evaluation of hindpaw position in rats during chronic constriction injury (CCI) produced with different suture materials. Somatosens Mot Res 13: 95-101.

Kanazawa I, Ogawa T, Kimura S, Munekata E (1984) Regional distribution of substance P, neurokinin alpha and neurokinin beta in rat central nervous system. Neurosci Res 2: 111-120.

Kar S, Quirion R (1992) Quantitative autoradiographic localization of [125I]neuropeptide Y receptor binding sites in rat spinal cord and the effects of neonatal capsaicin, dorsal rhizotomy and peripheral axotomy. Brain Res 574: 333-337.

Kar S, Quirion R (1995) Neuropeptide receptors in developing and adult rat spinal cord: an in vitro quantitative autoradiography study of calcitonin gene-related peptide, neurokinins, mu-opioid, galanin, somatostatin, neurotensin and vasoactive intestinal polypeptide receptors. J Comp Neurol 354: 253-281.

Kashiba H, Uchida Y, Senba E (2001) Difference in binding by isolectin B4 to trkA and c-ret mRNA-expressing neurons in rat sensory ganglia. Brain Res Mol Brain Res 95: 18-26.

Katsura H, Obata K, Mizushima T, Sakurai J, Kobayashi K, Yamanaka H, Dai Y, Fukuoka T, Sakagami M, Noguchi K (2006) Activation of Src-family kinases in spinal microglia contributes to mechanical hypersensitivity after nerve injury. J Neurosci 26: 8680-8690.

Kauppila T, Kontinen VK, Pertovaara A (1998) Influence of spinalization on spinal withdrawal reflex responses varies depending on the submodality of the test stimulus and the experimental pathophysiological condition in the rat. Brain Res 797: 234-242.

Kawasaki H, Morooka T, Shimohama S, Kimura J, Hirano T, Gotoh Y, Nishida E (1997) Activation and involvement of p38 mitogen-activated protein kinase in glutamate-induced apoptosis in rat cerebellar granule cells. J Biol Chem 272: 18518-18521.

Kenney AM, Kocsis JD (1998) Peripheral axotomy induces long-term c-Jun amino-terminal kinase-1 activation and activator protein-1 binding activity by c-Jun and junD in adult rat dorsal root ganglia In vivo. J Neurosci 18: 1318-1328.

Kerchner GA, Wang GD, Qiu CS, Huettner JE, Zhuo M (2001) Direct presynaptic regulation of GABA/glycine release by kainate receptors in the dorsal horn: an ionotropic mechanism. Neuron 32: 477-488.

Kerchner GA, Wilding TJ, Li P, Zhuo M, Huettner JE (2001) Presynaptic kainate receptors regulate spinal sensory transmission. J Neurosci 21: 59-66.

Kerr BJ, Souslova V, McMahon SB, Wood JN (2001) A role for the TTX-resistant sodium channel Nav 1.8 in NGF-induced hyperalgesia, but not neuropathic pain. Neuroreport 12: 3077-3080.

Kerr RC, Maxwell DJ, Todd AJ (1998) GluR1 and GluR2/3 subunits of the AMPA-type glutamate receptor are associated with particular types of neurone in laminae I-III of the spinal dorsal horn of the rat. Eur J Neurosci 10: 324-333.

Kidd BL, Urban LA (2001) Mechanisms of inflammatory pain. Br J Anaesth 87: 3-11.

Kim E, Naisbitt S, Hsueh YP, Rao A, Rothschild A, Craig AM, Sheng M (1997) GKAP, a novel synaptic protein that interacts with the guanylate kinase-like domain of the PSD-95/SAP90 family of channel clustering molecules. J Cell Biol 136: 669-678.

Kim HJ, Na HS, Sung B, Hong SK (1998) Amount of sympathetic sprouting in the dorsal root ganglia is not correlated to the level of sympathetic dependence of neuropathic pain in a rat model. Neurosci Lett 245: 21-24.

Kim JH, Lee HK, Takamiya K, Huganir RL (2003) The role of synaptic GTPase-activating protein in neuronal development and synaptic plasticity. J Neurosci 23: 1119-1124.

Kim KJ, Yoon YW, Chung JM (1997) Comparison of three rodent neuropathic pain models. Exp Brain Res 113: 200-206.

Kim SH, Chung JM (1991) Sympathectomy alleviates mechanical allodynia in an experimental animal model for neuropathy in the rat. Neurosci Lett 134: 131-134.

Kim SH, Chung JM (1992) An experimental model for peripheral neuropathy produced by segmental spinal nerve ligation in the rat. Pain 50: 355-363.

Kim SH, Na HS, Sheen K, Chung JM (1993) Effects of sympathectomy on a rat model of peripheral neuropathy. Pain 55: 85-92.

Kim SY, Bae JC, Kim JY, Lee HL, Lee KM, Kim DS, Cho HJ (2002) Activation of p38 MAP kinase in the rat dorsal root ganglia and spinal cord following peripheral inflammation and nerve injury. Neuroreport 13: 2483-2486.

Kim WK, Kan Y, Ganea D, Hart RP, Gozes I, Jonakait GM (2000) Vasoactive intestinal peptide and pituitary adenylyl cyclase-activating polypeptide inhibit tumor necrosis factor-alpha production in injured spinal cord and in activated microglia via a cAMP-dependent pathway. J Neurosci 20: 3622-3630.

King AE, Lopez-Garcia JA (1993) Excitatory amino acid receptor-mediated neurotransmission from cutaneous afferents in rat dorsal horn in vitro. J Physiol 472: 443-457.

Kistner U, Garner CC, Linial M (1995) Nucleotide binding by the synapse associated protein SAP90. FEBS Lett 359: 159-163.

Kleckner NW, Dingledine R (1988) Requirement for glycine in activation of NMDA-receptors expressed in Xenopus oocytes. Science 241: 835-837.

Knyihar-Csillik E, Kreutzberg GW, Raivich G, Csillik B (1991) Vasoactive intestinal polypeptide in dorsal root terminals of the rat spinal cord is regulated by the axoplasmic transport in the peripheral nerve. Neurosci Lett 131: 83-87.

Knyihar-Csillik E, Kreutzberg GW, Csillik B (1993) Fine structural correlates of VIP-like immunoreactivity in the upper spinal dorsal horn after peripheral axotomy: possibilities of a neuro-glial translocation of a neuropeptide. Acta Histochem 94: 1-12.

Kohama I, Ishikawa K, Kocsis JD (2000) Synaptic reorganization in the substantia gelatinosa after peripheral nerve neuroma formation: aberrant innervation of lamina II neurons by Abeta afferents. J Neurosci 20: 1538-1549.

Kohu K, Ogawa F, Akiyama T (2002) The SH3, HOOK and guanylate kinase-like domains of hDLG are important for its cytoplasmic localization. Genes Cells 7: 707-715.

Kolhekar R, Meller ST, Gebhart GF (1994) N-methyl-D-aspartate receptor-mediated changes in thermal nociception: allosteric modulation at glycine and polyamine recognition sites. Neuroscience 63: 925-936.

Koltzenburg M, Wall PD, McMahon SB (1999) Does the right side know what the left is doing? Trends Neurosci 22: 122-127.

Komiyama NH, Watabe AM, Carlisle HJ, Porter K, Charlesworth P, Monti J, Strathdee DJ, O'Carroll CM, Martin SJ, Morris RG, O'Dell TJ, Grant SG (2002) SynGAP regulates ERK/MAPK signaling, synaptic plasticity, and learning in the complex with postsynaptic density 95 and NMDA receptor. J Neurosci 22: 9721-9732.

Korenman EM, Devor M (1981) Ectopic adrenergic sensitivity in damaged peripheral nerve axons in the rat. Exp Neurol 72: 63-81.

Korkin D, Davis FP, Alber F, Luong T, Shen MY, Lucic V, Kennedy MB, Sali A (2006) Structural modeling of protein interactions by analogy: application to PSD-95. PLoS Comput Biol 2: e153.

Kornau HC, Schenker LT, Kennedy MB, Seeburg PH (1995) Domain interaction between NMDA receptor subunits and the postsynaptic density protein PSD-95. Science 269: 1737-1740.

Krause JE, Chirgwin JM, Carter MS, Xu ZS, Hershey AD (1987) Three rat preprotachykinin mRNAs encode the neuropeptides substance P and neurokinin A. Proc Natl Acad Sci U S A 84: 881-885.

Kuraishi Y, Hirota N, Sato Y, Hanashima N, Takagi H, Satoh M (1989) Stimulus specificity of peripherally evoked substance P release from the rabbit dorsal horn in situ. Neuroscience 30: 241-250.

La Rana G, Russo R, Campolongo P, Bortolato M, Mangieri RA, Cuomo V, Iacono A, Raso GM, Meli R, Piomelli D, Calignano A (2006) Modulation of neuropathic and inflammatory pain by the endocannabinoid transport inhibitor AM404 [N-(4-hydroxyphenyl)-eicosa-5,8,11,14-tetraenamide]. J Pharmacol Exp Ther 317: 1365-1371.

Laing I, Todd AJ, Heizmann CW, Schmidt HH (1994) Subpopulations of GABAergic neurons in laminae I-III of rat spinal dorsal horn defined by coexistence with classical transmitters, peptides, nitric oxide synthase or parvalbumin. Neuroscience 61: 123-132.

Laird JM, Hargreaves RJ, Hill RG (1993) Effect of RP 67580, a non-peptide neurokinin1 receptor antagonist, on facilitation of a nociceptive spinal flexion reflex in the rat. Br J Pharmacol 109: 713-718.

Laird JM, Bennett GJ (1993) An electrophysiological study of dorsal horn neurons in the spinal cord of rats with an experimental peripheral neuropathy. J Neurophysiol 69: 2072-2085.

Laird JM, Souslova V, Wood JN, Cervero F (2002) Deficits in visceral pain and referred hyperalgesia in Nav1.8 (SNS/PN3)-null mice. J Neurosci 22: 8352-8356.

Laube B, Hirai H, Sturgess M, Betz H, Kuhse J (1997) Molecular determinants of agonist discrimination by NMDA receptor subunits: analysis of the glutamate binding site on the NR2B subunit. Neuron 18: 493-503.

Le Greves P, Nyberg F, Terenius L, Hokfelt T (1985) Calcitonin gene-related peptide is a potent inhibitor of substance P degradation. Eur J Pharmacol 115: 309-311.

Ledeboer A, Sloane EM, Milligan ED, Frank MG, Mahony JH, Maier SF, Watkins LR (2005) Minocycline attenuates mechanical allodynia and proinflammatory cytokine expression in rat models of pain facilitation. Pain 115: 71-83.

Lee SH, Kayser V, Desmeules J, Guilbaud G (1994) Differential action of morphine and various opioid agonists on thermal allodynia and hyperalgesia in mononeuropathic rats. Pain 57: 233-240.

Leem JW, Willis WD, Chung JM (1993) Cutaneous sensory receptors in the rat foot. J Neurophysiol 69: 1684-1699.

Leem JW, Choi EJ, Park ES, Paik KS (1996) N-methyl-D-aspartate (NMDA) and non-NMDA glutamate receptor antagonists differentially suppress dorsal horn neuron responses to mechanical stimuli in rats with peripheral nerve injury. Neurosci Lett 211: 37-40.

Lekan HA, Carlton SM, Coggeshall RE (1996) Sprouting of A beta fibers into lamina II of the rat dorsal horn in peripheral neuropathy. Neurosci Lett 208: 147-150.

Lerma J, Paternain AV, Rodriguez-Moreno A, Lopez-Garcia JC (2001) Molecular physiology of kainate receptors. Physiol Rev 81: 971-998.

Lev S, Moreno H, Martinez R, Canoll P, Peles E, Musacchio JM, Plowman GD, Rudy B, Schlessinger J (1995) Protein tyrosine kinase PYK2 involved in Ca(2+)-induced regulation of ion channel and MAP kinase functions. Nature 376: 737-745.

Lev S, Hernandez J, Martinez R, Chen A, Plowman G, Schlessinger J (1999) Identification of a novel family of targets of PYK2 related to Drosophila retinal degeneration B (rdgB) protein. Mol Cell Biol 19: 2278-2288.

Lever IJ, Malcangio M (2002) CB(1) receptor antagonist SR141716A increases capsaicin-evoked release of Substance P from the adult mouse spinal cord. Br J Pharmacol 135: 21-24.

Lever IJ, Pezet S, McMahon SB, Malcangio M (2003) The signaling components of sensory fiber transmission involved in the activation of ERK MAP kinase in the mouse dorsal horn. Mol Cell Neurosci 24: 259-270.

Levine JD, Fields HL, Basbaum AI (1993) Peptides and the primary afferent nociceptor. J Neurosci 13: 2273-2286.

Li P, Wilding TJ, Kim SJ, Calejesan AA, Huettner JE, Zhuo M (1999) Kainate-receptor-mediated sensory synaptic transmission in mammalian spinal cord. Nature 397: 161-164.

Li X, Earp HS (1997) Paxillin is tyrosine-phosphorylated by and preferentially associates with the calcium-dependent tyrosine kinase in rat liver epithelial cells. J Biol Chem 272: 14341-14348.

Li X, Dy RC, Cance WG, Graves LM, Earp HS (1999) Interactions between two cytoskeleton-associated tyrosine kinases: calcium-dependent tyrosine kinase and focal adhesion tyrosine kinase. J Biol Chem 274: 8917-8924.

Lichtman AH, Martin BR (1997) The selective cannabinoid antagonist SR 141716A blocks cannabinoid-induced antinociception in rats. Pharmacol Biochem Behav 57: 7-12.

Light AR, Perl ER (1979) Reexamination of the dorsal root projection to the spinal dorsal horn including observations on the differential termination of coarse and fine fibers. J Comp Neurol 186: 117-131.

Lim G, Sung B, Ji RR, Mao J (2003) Upregulation of spinal cannabinoid-1-receptors following nerve injury enhances the effects of Win 55,212-2 on neuropathic pain behaviors in rats. Pain 105: 275-283.

Lim WA, Richards FM (1994) Critical residues in an SH3 domain from Sem-5 suggest a mechanism for proline-rich peptide recognition. Nat Struct Biol 1: 221-225.

Lima D, Coimbra A (1986) A Golgi study of the neuronal population of the marginal zone (lamina I) of the rat spinal cord. J Comp Neurol 244: 53-71.

Lima D, Coimbra A (1989) Morphological types of spinomesencephalic neurons in the marginal zone (lamina I) of the rat spinal cord, as shown after retrograde labelling with cholera toxin subunit B. J Comp Neurol 279: 327-339.

Lima D, Mendes-Ribeiro JA, Coimbra A (1991) The spino-latero-reticular system of the rat: projections from the superficial dorsal horn and structural characterization of marginal neurons involved. Neuroscience 45: 137-152.

Lindsay RM, Harmar AJ (1989) Nerve growth factor regulates expression of neuropeptide genes in adult sensory neurons. Nature 337: 362-364.

Liu Y, Zhang GY, Yan JZ, Xu TL (2005) Suppression of Pyk2 attenuated the increased tyrosine phosphorylation of NMDA receptor subunit 2A after brain ischemia in rat hippocampus. Neurosci Lett 379: 55-58.

Loh L, Nathan PW (1978) Painful peripheral states and sympathetic blocks. J Neurol Neurosurg Psychiatry 41: 664-671.

Lucifora S, Willcockson HH, Lu CR, Darstein M, Phend KD, Valtschanoff JG, Rustioni A (2006) Presynaptic low- and high-affinity kainate receptors in nociceptive spinal afferents. Pain 120: 97-105.

Lundberg JM, Terenius L, Hokfelt T, Goldstein M (1983) High levels of neuropeptide Y in peripheral noradrenergic neurons in various mammals including man. Neurosci Lett 42: 167-172.

Luo L, Wiesenfeld-Hallin Z (1995) Effects of intrathecal local anesthetics on spinal excitability and on the development of autotomy. Pain 63: 173-179.

Luo ZD, Chaplan SR, Scott BP, Cizkova D, Calcutt NA, Yaksh TL (1999) Neuronal nitric oxide synthase mRNA upregulation in rat sensory neurons after spinal nerve ligation: lack of a role in allodynia development. J Neurosci 19: 9201-9208.

Lutz EM, Sheward WJ, West KM, Morrow JA, Fink G, Harmar AJ (1993) The VIP2 receptor: molecular characterisation of a cDNA encoding a novel receptor for vasoactive intestinal peptide. FEBS Lett 334: 3-8.

Lynn B, Carpenter SE (1982) Primary afferent units from the hairy skin of the rat hind limb. Brain Res 238: 29-43.

Lynn B (1994) The fibre composition of cutaneous nerves and the classification and response properties of cutaneous afferents, with particular reference to nociception. Pain Reviews 1: 172-183.

Ma W, Bisby MA (1997) Differential expression of galanin immunoreactivities in the primary sensory neurons following partial and complete sciatic nerve injuries. Neuroscience 79: 1183-1195.

Ma W, Quirion R (2002) Partial sciatic nerve ligation induces increase in the phosphorylation of extracellular signal-regulated kinase (ERK) and c-Jun N-terminal kinase (JNK) in astrocytes in the lumbar spinal dorsal horn and the gracile nucleus. Pain 99: 175-184.

Macdonald RL, Nowak LM (1981) Substance P and somatostatin actions on spinal cord neurons in primary dissociated cell culture. Adv Biochem Psychopharmacol 28: 159-173.

Maggi CA, Patacchini R, Rovero P, Giachetti A (1993) Tachykinin receptors and tachykinin receptor antagonists. J Auton Pharmacol 13: 23-93.

Maleki J, LeBel AA, Bennett GJ, Schwartzman RJ (2000) Patterns of spread in complex regional pain syndrome, type I (reflex sympathetic dystrophy). Pain 88: 259-266.

Malmberg AB, Chen C, Tonegawa S, Basbaum AI (1997) Preserved acute pain and reduced neuropathic pain in mice lacking PKCgamma. Science 278: 279-283.

Mantyh PW, Rogers SD, Ghilardi JR, Maggio JE, Mantyh CR, Vigna SR (1996) Differential expression of two isoforms of the neurokinin-1 (substance P) receptor in vivo. Brain Res 719: 8-13.

Mantyh PW, Rogers SD, Honore P, Allen BJ, Ghilardi JR, Li J, Daughters RS, Lappi DA, Wiley RG, Simone DA (1997) Inhibition of hyperalgesia by ablation of lamina I spinal neurons expressing the substance P receptor. Science 278: 275-279.

Mao J, Price DD, Mayer DJ, Lu J, Hayes RL (1992) Intrathecal MK-801 and local nerve anesthesia synergistically reduce nociceptive behaviors in rats with experimental peripheral mononeuropathy. Brain Res 576: 254-262.

Mao J, Price DD, Hayes RL, Lu J, Mayer DJ (1992) Differential roles of NMDA and non-NMDA receptor activation in induction and maintenance of thermal hyperalgesia in rats with painful peripheral mononeuropathy. Brain Res 598: 271-278.

Mao J, Coghill RC, Kellstein DE, Frenk H, Mayer DJ (1992) Calcitonin gene-related peptide enhances substance P-induced behaviors via metabolic inhibition: in vivo evidence for a new mechanism of neuromodulation. Brain Res 574: 157-163.

Mao J, Price DD, Hayes RL, Lu J, Mayer DJ, Frenk H (1993) Intrathecal treatment with dextrorphan or ketamine potently reduces pain-related behaviors in a rat model of peripheral mononeuropathy. Brain Res 605: 164-168.

Mao J, Price DD, Mayer DJ (1995) Experimental mononeuropathy reduces the antinociceptive effects of morphine: implications for common intracellular mechanisms involved in morphine tolerance and neuropathic pain. Pain 61: 353-364.

Marinissen MJ, Gutkind JS (2001) G-protein-coupled receptors and signaling networks: emerging paradigms. Trends Pharmacol Sci 22: 368-376.

Martin FC, Charles AC, Sanderson MJ, Merrill JE (1992) Substance P stimulates IL-1 production by astrocytes via intracellular calcium. Brain Res 599: 13-18.

Marvizon JC, Martinez V, Grady EF, Bunnett NW, Mayer EA (1997) Neurokinin 1 receptor internalization in spinal cord slices induced by dorsal root stimulation is mediated by NMDA receptors. J Neurosci 17: 8129-8136.

Matzner O, Devor M (1994) Hyperexcitability at sites of nerve injury depends on voltage-sensitive Na+ channels. J Neurophysiol 72: 349-359.

Maves TJ, Gebhart GF, Meller ST (1995) Continuous infusion of acidified saline around the rat sciatic nerve produces thermal hyperalgesia. Neurosci Lett 194: 45-48.

Mayer BJ, Hamaguchi M, Hanafusa H (1988) A novel viral oncogene with structural similarity to phospholipase C. Nature 332: 272-275.

Mayer BJ, Eck MJ (1995) SH3 domains. Minding your p's and q's. Curr Biol 5: 364-367.

Mayer BJ (2001) SH3 domains: complexity in moderation. J Cell Sci 114: 1253-1263.

McCleane GJ (1999) Intravenous infusion of phenytoin relieves neuropathic pain: a randomized, double-blinded, placebo-controlled, crossover study. Anesth Analg 89: 985-988.

McGaraughty S, Heinricher MM (2002) Microinjection of morphine into various amygdaloid nuclei differentially affects nociceptive responsiveness and RVM neuronal activity. Pain 96: 153-162.

McGee AW, Bredt DS (1999) Identification of an intramolecular interaction between the SH3 and guanylate kinase domains of PSD-95. J Biol Chem 274: 17431-17436.

McGee AW, Dakoji SR, Olsen O, Bredt DS, Lim WA, Prehoda KE (2001) Structure of the SH3-guanylate kinase module from PSD-95 suggests a mechanism for regulated assembly of MAGUK scaffolding proteins. Mol Cell 8: 1291-1301.

McGee AW, Topinka JR, Hashimoto K, Petralia RS, Kakizawa S, Kauer FW, Aguilera-Moreno A, Wenthold RJ, Kano M, Bredt DS (2001) PSD-93 knock-out mice reveal that neuronal MAGUKs are not required for development or function of parallel fiber synapses in cerebellum. J Neurosci 21: 3085-3091.

McLachlan EM, Janig W, Devor M, Michaelis M (1993) Peripheral nerve injury triggers noradrenergic sprouting within dorsal root ganglia. Nature 363: 543-546.

McMahon SB, Wall PD (1983) A system of rat spinal cord lamina 1 cells projecting through the contralateral dorsolateral funiculus. J Comp Neurol 214: 217-223.

McMahon SB, Wall PD, Granum SL, Webster KE (1984) The effects of capsaicin applied to peripheral nerves on responses of a group of lamina I cells in adult rats. J Comp Neurol 227: 393-400.

McQuay H, Carroll D, Moore A (1996) Variation in the placebo effect in randomised controlled trials of analgesics: all is as blind as it seems. Pain 64: 331-335.

McQuay HJ, Carroll D, Jadad AR, Glynn CJ, Jack T, Moore RA, Wiffeh PJ (1994) Dextromethorphan for the treatment of neuropathic pain: a double-blind randomised controlled crossover trial with integral n-of-1 design. Pain 59: 127-133.

MEHLER WR, FEFERMAN ME, NAUTA WJ (1960) Ascending axon degeneration following anterolateral cordotomy. An experimental study in the monkey. Brain 83: 718-750.

Meller ST, Pechman PS, Gebhart GF, Maves TJ (1992) Nitric oxide mediates the thermal hyperalgesia produced in a model of neuropathic pain in the rat. Neuroscience 50: 7-10.

Meller ST, Dykstra C, Grzybycki D, Murphy S, Gebhart GF (1994) The possible role of glia in nociceptive processing and hyperalgesia in the spinal cord of the rat. Neuropharmacology 33: 1471-1478.

Melzack R, Wall PD (1965) Pain mechanisms: a new theory. Science 150: 971-979.

Mendell LM (1966) Physiological properties of unmyelinated fiber projection to the spinal cord. Exp Neurol 16: 316-332.

Mendell LM, Munson JB, Arvanian VL (2001) Neurotrophins and synaptic plasticity in the mammalian spinal cord. J Physiol 533: 91-97.

Menetrey D, Chaouch A, Besson JM (1980) Location and properties of dorsal horn neurons at origin of spinoreticular tract in lumbar enlargement of the rat. J Neurophysiol 44: 862-877.

Menetrey D, Besson JM (1981) Electrophysiology and location of dorsal horn neurones in the rat, including cells at the origin of the spinoreticular and spinothalamic tracts. In: Spinal Cord Sensation (Brown AG, Rethelyi M, eds), pp 179-188. Edinburgh: Scottish Academic Press.

Menetrey D, Chaouch A, Binder D, Besson JM (1982) The origin of the spinomesencephalic tract in the rat: an anatomical study using the retrograde transport of horseradish peroxidase. J Comp Neurol 206: 193-207.

Merskey H, Bogduk N (1994) Classification of chronic pain: IASP pain terminology. In: IASP task force on taxonomy (Merskey H, Bogduk N, eds), pp 209-214. IASP Press.

Merz, H., Malisius, R, Mannweiler, S, Zhou, R, Hartmann, W, Orscheschek, K, Moubayed, P, and Feller, A. C. Immunomax - a maximized immunohistochemical method for the retrieval and enhancement of hidden antigens. Lab.Invest 73, 149. 2005.
Ref Type: Pamphlet

Michaelis M, Devor M, Janig W (1996) Sympathetic modulation of activity in rat dorsal root ganglion neurons changes over time following peripheral nerve injury. J Neurophysiol 76: 753-763.

Migaud M, Charlesworth P, Dempster M, Webster LC, Watabe AM, Makhinson M, He Y, Ramsay MF, Morris RG, Morrison JH, O'Dell TJ, Grant SG (1998) Enhanced long-term potentiation and impaired learning in mice with mutant postsynaptic density-95 protein. Nature 396: 433-439.

Miletic V, Tan H (1988) Iontophoretic application of calcitonin gene-related peptide produces a slow and prolonged excitation of neurons in the cat lumbar dorsal horn. Brain Res 446: 169-172.

Millan MJ (1999) The induction of pain: an integrative review. Prog Neurobiol 57: 1-164.

Milligan ED, Twining C, Chacur M, Biedenkapp J, O'Connor K, Poole S, Tracey K, Martin D, Maier SF, Watkins LR (2003) Spinal glia and proinflammatory cytokines mediate mirror-image neuropathic pain in rats. J Neurosci 23: 1026-1040.

Mizushima T, Obata K, Yamanaka H, Dai Y, Fukuoka T, Tokunaga A, Mashimo T, Noguchi K (2005) Activation of p38 MAPK in primary afferent neurons by noxious stimulation and its involvement in the development of thermal hyperalgesia. Pain 113: 51-60.

Mohamed, S. S. and Carr, D. B. Pain During Herpes Zoster (Shingles) and Long After. 1-4. 1994. Pain Clinical Updates.
Ref Type: Pamphlet

Molander C, Xu Q, Grant G (1984) The cytoarchitectonic organization of the spinal cord in the rat. I. The lower thoracic and lumbosacral cord. J Comp Neurol 230: 133-141.

Moller K, Zhang YZ, Hakanson R, Luts A, Sjolund B, Uddman R, Sundler F (1993) Pituitary adenylate cyclase activating peptide is a sensory neuropeptide: immunocytochemical and immunochemical evidence. Neuroscience 57: 725-732.

Molliver DC, Lindsay J, Albers KM, Davis BM (2005) Overexpression of NGF or GDNF alters transcriptional plasticity evoked by inflammation. Pain 113: 277-284.

Monaghan DT, Cotman CW (1985) Distribution of N-methyl-D-aspartate-sensitive L-[3H]glutamate-binding sites in rat brain. J Neurosci 5: 2909-2919.

Monyer H, Sprengel R, Schoepfer R, Herb A, Higuchi M, Lomeli H, Burnashev N, Sakmann B, Seeburg PH (1992) Heteromeric NMDA receptors: molecular and functional distinction of subtypes. Science 256: 1217-1221.

Moreno D, Gourlet P, De Neef P, Cnudde J, Waelbroeck M, Robberecht P (2000) Development of selective agonists and antagonists for the human vasoactive intestinal polypeptide VPAC(2) receptor. Peptides 21: 1543-1549.

Mori H, Mishina M (1995) Structure and function of the NMDA receptor channel. Neuropharmacology 34: 1219-1237.

Moriyoshi K, Masu M, Ishii T, Shigemoto R, Mizuno N, Nakanishi S (1991) Molecular cloning and characterization of the rat NMDA receptor. Nature 354: 31-37.

Morris RG, Anderson E, Lynch GS, Baudry M (1986) Selective impairment of learning and blockade of long-term potentiation by an N-methyl-D-aspartate receptor antagonist, AP5. Nature 319: 774-776.

Morton CR, Johnson SM, Duggan AW (1983) Lateral reticular regions and the descending control of dorsal horn neurones of the cat: selective inhibition by electrical stimulation. Brain Res 275: 13-21.

Morton CR, Hutchison WD (1990) Morphine does not reduce the intraspinal release of calcitonin gene-related peptide in the cat. Neurosci Lett 117: 319-324.

Moss SJ, Gorrie GH, Amato A, Smart TG (1995) Modulation of GABAA receptors by tyrosine phosphorylation. Nature 377: 344-348.

Moussaoui SM, Hermans E, Mathieu AM, Bonici B, Clerc F, Guinet F, Garret C, Laduron PM (1992) Polyclonal antibodies against the rat NK1 receptor: characterization and localization in the spinal cord. Neuroreport 3: 1073-1076.

Mulderry PK, Lindsay RM (1990) Rat dorsal root ganglion neurons in culture express vasoactive intestinal polypeptide (VIP) independently of nerve growth factor. Neurosci Lett 108: 314-320.

Munro FE, Fleetwood-Walker SM, Parker RM, Mitchell R (1993) The effects of neurokinin receptor antagonists on mustard oil-evoked activation of rat dorsal horn neurons. Neuropeptides 25: 299-305.

Munro FE, Fleetwood-Walker SM, Mitchell R (1994) Evidence for a role of protein kinase C in the sustained activation of rat dorsal horn neurons evoked by cutaneous mustard oil application. Neurosci Lett 170: 199-202.

Murase K, Nedeljkov V, Randic M (1982) The actions of neuropeptides on dorsal horn neurons in the rat spinal cord slice preparation: an intracellular study. Brain Res 234: 170-176.

Musacchio A, Noble M, Pauptit R, Wierenga R, Saraste M (1992) Crystal structure of a Src-homology 3 (SH3) domain. Nature 359: 851-855.

Musacchio A, Saraste M, Wilmanns M (1994) High-resolution crystal structures of tyrosine kinase SH3 domains complexed with proline-rich peptides. Nat Struct Biol 1: 546-551.

Myers RR, Yamamoto T, Yaksh TL, Powell HC (1993) The role of focal nerve ischemia and Wallerian degeneration in peripheral nerve injury producing hyperesthesia. Anesthesiology 78: 308-316.

Na HS, Leem JW, Chung JM (1993) Abnormalities of mechanoreceptors in a rat model of neuropathic pain: possible involvement in mediating mechanical allodynia. J Neurophysiol 70: 522-528.

Nagy JI, Hunt SP (1982) Fluoride-resistant acid phosphatase-containing neurones in dorsal root ganglia are separate from those containing substance P or somatostatin. Neuroscience 7: 89-97.

Nahin RL, Ren K, De Leon M, Ruda M (1994) Primary sensory neurons exhibit altered gene expression in a rat model of neuropathic pain. Pain 58: 95-108.

Naim M, Spike RC, Watt C, Shehab SA, Todd AJ (1997) Cells in laminae III and IV of the rat spinal cord that possess the neurokinin-1 receptor and have dorsally directed dendrites receive a major synaptic input from tachykinin-containing primary afferents. J Neurosci 17: 5536-5548.

Narita M, Dun SL, Dun NJ, Tseng LF (1996) Hyperalgesia induced by pituitary adenylate cyclase-activating polypeptide in the mouse spinal cord. Eur J Pharmacol 311: 121-126.

Nasstrom J, Karlsson U, Post C (1992) Antinociceptive actions of different classes of excitatory amino acid receptor antagonists in mice. Eur J Pharmacol 212: 21-29.

Nawa H, Kotani H, Nakanishi S (1984) Tissue-specific generation of two preprotachykinin mRNAs from one gene by alternative RNA splicing. Nature 312: 729-734.

Neet K, Hunter T (1996) Vertebrate non-receptor protein-tyrosine kinase families. Genes Cells 1: 147-169.

Neugebauer V, Lucke T, Schaible HG (1993) N-methyl-D-aspartate (NMDA) and non-NMDA receptor antagonists block the hyperexcitability of dorsal horn neurons during development of acute arthritis in rat's knee joint. J Neurophysiol 70: 1365-1377.

Niethammer M, Kim E, Sheng M (1996) Interaction between the C terminus of NMDA receptor subunits and multiple members of the PSD-95 family of membrane-associated guanylate kinases. J Neurosci 16: 2157-2163.

Nishi M, Hinds H, Lu HP, Kawata M, Hayashi Y (2001) Motoneuron-specific expression of NR3B, a novel NMDA-type glutamate receptor subunit that works in a dominant-negative manner. J Neurosci 21: RC185.

Nishiyama T (2000) Interaction among NMDA receptor-, NMDA glycine site- and AMPA receptor antagonists in spinally mediated analgesia. Can J Anaesth 47: 693-698.

Nix SL, Chishti AH, Anderson JM, Walther Z (2000) hCASK and hDlg associate in epithelia, and their src homology 3 and guanylate kinase domains participate in both intramolecular and intermolecular interactions. J Biol Chem 275: 41192-41200.

Noble ME, Musacchio A, Saraste M, Courtneidge SA, Wierenga RK (1993) Crystal structure of the SH3 domain in human Fyn; comparison of the three-dimensional structures of SH3 domains in tyrosine kinases and spectrin. EMBO J 12: 2617-2624.

Noguchi K, Senba E, Morita Y, Sato M, Tohyama M (1989) Prepro-VIP and preprotachykinin mRNAs in the rat dorsal root ganglion cells following peripheral axotomy. Brain Res Mol Brain Res 6: 327-330.

Noguchi K, Senba E, Morita Y, Sato M, Tohyama M (1990) Alpha-CGRP and beta-CGRP mRNAs are differentially regulated in the rat spinal cord and dorsal root ganglion. Brain Res Mol Brain Res 7: 299-304.

Noguchi K, De Leon M, Nahin RL, Senba E, Ruda MA (1993) Quantification of axotomy-induced alteration of neuropeptide mRNAs in dorsal root ganglion neurons with special reference to neuropeptide Y mRNA and the effects of neonatal capsaicin treatment. J Neurosci Res 35: 54-66.

Novakovic SD, Tzoumaka E, McGivern JG, Haraguchi M, Sangameswaran L, Gogas KR, Eglen RM, Hunter JC (1998) Distribution of the tetrodotoxin-resistant sodium channel PN3 in rat sensory neurons in normal and neuropathic conditions. J Neurosci 18: 2174-2187.

O'Brien RJ, Lau LF, Huganir RL (1998) Molecular mechanisms of glutamate receptor clustering at excitatory synapses. Curr Opin Neurobiol 8: 364-369.

O'Dell TJ, Kandel ER, Grant SG (1991) Long-term potentiation in the hippocampus is blocked by tyrosine kinase inhibitors. Nature 353: 558-560.

Obata K, Yamanaka H, Dai Y, Tachibana T, Fukuoka T, Tokunaga A, Yoshikawa H, Noguchi K (2003) Differential activation of extracellular signal-regulated protein kinase in primary afferent neurons regulates brain-derived neurotrophic factor expression after peripheral inflammation and nerve injury. J Neurosci 23: 4117-4126.

Obata K, Yamanaka H, Dai Y, Mizushima T, Fukuoka T, Tokunaga A, Noguchi K (2004) Differential activation of MAPK in injured and uninjured DRG neurons following chronic constriction injury of the sciatic nerve in rats. Eur J Neurosci 20: 2881-2895.

Obata K, Yamanaka H, Kobayashi K, Dai Y, Mizushima T, Katsura H, Fukuoka T, Tokunaga A, Noguchi K (2004) Role of mitogen-activated protein kinase activation in injured and intact primary afferent neurons for mechanical and heat hypersensitivity after spinal nerve ligation. J Neurosci 24: 10211-10222.

Ochoa J, Torebjork E (1989) Sensations evoked by intraneural microstimulation of C nociceptor fibres in human skin nerves. J Physiol 415: 583-599.

Ogawa T, Kanazawa I, Kimura S (1985) Regional distribution of substance P, neurokinin alpha and neurokinin beta in rat spinal cord, nerve roots and dorsal root ganglia, and the effects of dorsal root section or spinal transection. Brain Res 359: 152-157.

Ohba T, Ishino M, Aoto H, Sasaki T (1998) Interaction of two proline-rich sequences of cell adhesion kinase beta with SH3 domains of p130Cas-related proteins and a GTPase-activating protein, Graf. Biochem J 330 (Pt 3): 1249-1254.

Okamoto M, Baba H, Goldstein PA, Higashi H, Shimoji K, Yoshimura M (2001) Functional reorganization of sensory pathways in the rat spinal dorsal horn following peripheral nerve injury. J Physiol 532: 241-250.

Oku R, Satoh M, Fujii N, Otaka A, Yajima H, Takagi H (1987) Calcitonin gene-related peptide promotes mechanical nociception by potentiating release of substance P from the spinal dorsal horn in rats. Brain Res 403: 350-354.

Oliveras JL, Besson JM, Guilbaud G, Liebeskind JC (1974) Behavioral and electrophysiological evidence of pain inhibition from midbrain stimulation in the cat. Exp Brain Res 20: 32-44.

Omana-Zapata I, Khabbaz MA, Hunter JC, Clarke DE, Bley KR (1997) Tetrodotoxin inhibits neuropathic ectopic activity in neuromas, dorsal root ganglia and dorsal horn neurons. Pain 72: 41-49.

Onda A, Hamba M, Yabuki S, Kikuchi S (2002) Exogenous tumor necrosis factor-alpha induces abnormal discharges in rat dorsal horn neurons. Spine 27: 1618-1624.

Ossipov MH, Zhang ET, Carvajal C, Gardell L, Quirion R, Dumont Y, Lai J, Porreca F (2002) Selective mediation of nerve injury-induced tactile hypersensitivity by neuropeptide Y. J Neurosci 22: 9858-9867.

Otten U, Goedert M, Mayer N, Lembeck F (1980) Requirement of nerve growth factor for development of substance P-containing sensory neurones. Nature 287: 158-159.

Palecek J, Dougherty PM, Kim SH, Paleckova V, Lekan H, Chung JM, Carlton SM, Willis WD (1992) Responses of spinothalamic tract neurons to mechanical and thermal stimuli in an experimental model of peripheral neuropathy in primates. J Neurophysiol 68: 1951-1966.

Park SY, Avraham H, Avraham S (2000) Characterization of the tyrosine kinases RAFTK/Pyk2 and FAK in nerve growth factor-induced neuronal differentiation. J Biol Chem 275: 19768-19777.

Parra MC, Nguyen TN, Hurley RW, Hammond DL (2002) Persistent inflammatory nociception increases levels of dynorphin 1-17 in the spinal cord, but not in supraspinal nuclei involved in pain modulation. J Pain 3: 330-336.

Passafaro M, Sala C, Niethammer M, Sheng M (1999) Microtubule binding by CRIPT and its potential role in the synaptic clustering of PSD-95. Nat Neurosci 2: 1063-1069.

Pawson T, Scott JD (1997) Signaling through scaffold, anchoring, and adaptor proteins. Science 278: 2075-2080.

Pekny M (2001) Astrocytic intermediate filaments: lessons from GFAP and vimentin knock-out mice. Prog Brain Res 132: 23-30.

Perl ER (1984) Characterization of nociceptors and their activation of neurons in the superficial dorsal horn: first steps for the sensation of pain. In: Advances in Pain Research and Therapy (Kruger L, Liebeskind JC, eds), pp 23-51. New York: Raven Press.

Pertwee RG (1997) Pharmacology of cannabinoid CB1 and CB2 receptors. Pharmacol Ther 74: 129-180.

Pertwee RG (1998) Pharmacological, physiological and clinical implications of the discovery of cannabinoid receptors. Biochem Soc Trans 26: 267-272.

Petruska JC, Napaporn J, Johnson RD, Gu JG, Cooper BY (2000) Subclassified acutely dissociated cells of rat DRG: histochemistry and patterns of capsaicin-, proton-, and ATP-activated currents. J Neurophysiol 84: 2365-2379.

Picard P, Boucher S, Regoli D, Gitter BD, Howbert JJ, Couture R (1993) Use of non-peptide tachykinin receptor antagonists to substantiate the involvement of NK1 and NK2 receptors in a spinal nociceptive reflex in the rat. Eur J Pharmacol 232: 255-261.

Pin JP, Duvoisin R (1995) The metabotropic glutamate receptors: structure and functions. Neuropharmacology 34: 1-26.

Polgar E, Puskar Z, Watt C, Matesz C, Todd AJ (2002) Selective innervation of lamina I projection neurones that possess the neurokinin 1 receptor by serotonin-containing axons in the rat spinal cord. Neuroscience 109: 799-809.

Polgar E, Hughes DI, Riddell JS, Maxwell DJ, Puskar Z, Todd AJ (2003) Selective loss of spinal GABAergic or glycinergic neurons is not necessary for development of thermal hyperalgesia in the chronic constriction injury model of neuropathic pain. Pain 104: 229-239.

Popratiloff A, Weinberg RJ, Rustioni A (1996) AMPA receptor subunits underlying terminals of fine-caliber primary afferent fibers. J Neurosci 16: 3363-3372.

Porreca F, Burgess SE, Gardell LR, Vanderah TW, Malan TP, Jr., Ossipov MH, Lappi DA, Lai J (2001) Inhibition of neuropathic pain by selective ablation of brainstem medullary cells expressing the mu-opioid receptor. J Neurosci 21: 5281-5288.

Powell JJ, Todd AJ (1992) Light and electron microscope study of GABA-immunoreactive neurones in lamina III of rat spinal cord. J Comp Neurol 315: 125-136.

Price DD, Dubner R, Hu JW (1976) Trigeminothalamic neurons in nucleus caudalis responsive to tactile, thermal, and nociceptive stimulation of monkey's face. J Neurophysiol 39: 936-953.

Price DD, Hayes RL, Ruda M, Dubner R (1978) Spatial and temporal transformations of input to spinothalamic tract neurons and their relation to somatic sensations. J Neurophysiol 41: 933-947.

Procter MJ, Houghton AK, Faber ES, Chizh BA, Ornstein PL, Lodge D, Headley PM (1998) Actions of kainate and AMPA selective glutamate receptor ligands on nociceptive processing in the spinal cord. Neuropharmacology 37: 1287-1297.

Puig S, Sorkin LS (1996) Formalin-evoked activity in identified primary afferent fibers: systemic lidocaine suppresses phase-2 activity. Pain 64: 345-355.

Quirion R, Shults CW, Moody TW, Pert CB, Chase TN, O'Donohue TL (1983) Autoradiographic distribution of substance P receptors in rat central nervous system. Nature 303: 714-716.

Quirion R, Davey PT (1988) Multiple neurokinin receptors: Recent Developments. Regulatory Peptides 22: 18-25.

Rabert D, Xiao Y, Yiangou Y, Kreder D, Sangameswaran L, Segal MR, Anthony HC, Birch R, Anand P (2004) Plasticity of gene expression in injured human dorsal root ganglia revealed by GeneChip oligonucleotide microarrays. J Clin Neurosci 11: 289-299.

Raghavendra V, Tanga F, DeLeo JA (2003) Inhibition of microglial activation attenuates the development but not existing hypersensitivity in a rat model of neuropathy. J Pharmacol Exp Ther 306: 624-630.

Raghavendra V, Tanga F, Rutkowski MD, DeLeo JA (2003) Anti-hyperalgesic and morphine-sparing actions of propentofylline following peripheral nerve injury in rats: mechanistic implications of spinal glia and proinflammatory cytokines. Pain 104: 655-664.

Raghavendra V, Tanga FY, DeLeo JA (2004) Complete Freunds adjuvant-induced peripheral inflammation evokes glial activation and proinflammatory cytokine expression in the CNS. Eur J Neurosci 20: 467-473.

Raingeaud J, Gupta S, Rogers JS, Dickens M, Han J, Ulevitch RJ, Davis RJ (1995) Pro-inflammatory cytokines and environmental stress cause p38 mitogen-activated protein kinase activation by dual phosphorylation on tyrosine and threonine. J Biol Chem 270: 7420-7426.

Raja S, Avraham S, Avraham H (1997) Tyrosine phosphorylation of the novel protein-tyrosine kinase RAFTK during an early phase of platelet activation by an integrin glycoprotein IIb-IIIa-independent mechanism. J Biol Chem 272: 10941-10947.

Ramer MS, French GD, Bisby MA (1997) Wallerian degeneration is required for both neuropathic pain and sympathetic sprouting into the DRG. Pain 72: 71-78.

Ramer MS, Bisby MA (1997) Rapid sprouting of sympathetic axons in dorsal root ganglia of rats with a chronic constriction injury. Pain 70: 237-244.

Randic M, Miletic V (1978) Depressant actions of methionine-enkephalin and somatostatin in cat dorsal horn neurones activated by noxious stimuli. Brain Res 152: 196-202.

Rasminsky M (1978) Ectopic generation of impulses and cross-talk in spinal nerve roots of "dystrophic" mice. Ann Neurol 3: 351-357.

Reeve AJ, Patel S, Fox A, Walker K, Urban L (2000) Intrathecally administered endotoxin or cytokines produce allodynia, hyperalgesia and changes in spinal cord neuronal responses to nociceptive stimuli in the rat. Eur J Pain 4: 247-257.

Regoli D, Drapeau G, Dion S, D'Orleans-Juste P (1987) Pharmacological receptors for substance P and neurokinins. Life Sci 40: 109-117.

Regoli D, Boudon A, Fauchere JL (1994) Receptors and antagonists for substance P and related peptides. Pharmacol Rev 46: 551-599.

Reichling DB, Basbaum AI (1990) Contribution of brainstem GABAergic circuitry to descending antinociceptive controls: I. GABA-immunoreactive projection neurons in the periaqueductal gray and nucleus raphe magnus. J Comp Neurol 302: 370-377.

Rethelyi M, Light AR, Perl ER (1983) Synapses made by nociceptive lamina I and II neurones. In: Advances in Pain Research and Therapy (Bonica JJ, Lindbloom U, Iggo A, eds), pp 111-118. New York: Raven Press.

REXED B (1952) The cytoarchitectonic organization of the spinal cord in the cat. J Comp Neurol 96: 414-495.

Ribeiro RA, Vale ML, Ferreira SH, Cunha FQ (2000) Analgesic effect of thalidomide on inflammatory pain. Eur J Pharmacol 391: 97-103.

Rice AS, Maton S (2001) Gabapentin in postherpetic neuralgia: a randomised, double blind, placebo controlled study. Pain 94: 215-224.

Richardson JD, Aanonsen L, Hargreaves KM (1998) Antihyperalgesic effects of spinal cannabinoids. Eur J Pharmacol 345: 145-153.

Robson P (2001) Therapeutic aspects of cannabis and cannabinoids. Br J Psychiatry 178: 107-115.

Romorini S, Piccoli G, Jiang M, Grossano P, Tonna N, Passafaro M, Zhang M, Sala C (2004) A functional role of postsynaptic density-95-guanylate kinase-associated protein complex in regulating Shank assembly and stability to synapses. J Neurosci 24: 9391-9404.

Romualdi P, Lesa G, Cox BM, Ferri S (1990) Distribution and characterization of VIP-related peptides in the rat spinal cord. Neuropeptides 16: 219-225.

Rowbotham M, Harden N, Stacey B, Bernstein P, Magnus-Miller L (1998) Gabapentin for the treatment of postherpetic neuralgia: a randomized controlled trial. JAMA 280: 1837-1842.

Roza C, Laird JM, Souslova V, Wood JN, Cervero F (2003) The tetrodotoxin-resistant Na+ channel Nav1.8 is essential for the expression of spontaneous activity in damaged sensory axons of mice. J Physiol 550: 921-926.

Rustioni A, Weinberg RJ (1989) The somatosensory system. In *Handbook of Chemical Neuroanatomy*. Elsevier, Amsterdam.

Salazar EP, Rozengurt E (2001) Src family kinases are required for integrin-mediated but not for G protein-coupled receptor stimulation of focal adhesion kinase autophosphorylation at Tyr-397. J Biol Chem 276: 17788-17795.

Salio C, Fischer J, Franzoni MF, Mackie K, Kaneko T, Conrath M (2001) CB1-cannabinoid and mu-opioid receptor co-localization on postsynaptic target in the rat dorsal horn. Neuroreport 12: 3689-3692.

Salt TE, Crozier CS, Hill RG (1982) The effects of capsaicin pre-treatment on the responses of single neurones to sensory stimuli in the trigeminal nucleus caudalis of the rat: evidence against a role for substance P as the neurotransmitter serving thermal nociception. Neuroscience 7: 1141-1148.

Salt TE, Hill RG (1983) Neurotransmitter candidates of somatosensory primary afferent fibres. Neuroscience 10: 1083-1103.

Sammons MJ, Raval P, Davey PT, Rogers D, Parsons AA, Bingham S (2000) Carrageenan-induced thermal hyperalgesia in the mouse: role of nerve growth factor and the mitogen-activated protein kinase pathway. Brain Res 876: 48-54.

Sampaio EP, Sarno EN, Galilly R, Cohn ZA, Kaplan G (1991) Thalidomide selectively inhibits tumor necrosis factor alpha production by stimulated human monocytes. J Exp Med 173: 699-703.

Sandkuhler J, Liu X (1998) Induction of long-term potentiation at spinal synapses by noxious stimulation or nerve injury. Eur J Neurosci 10: 2476-2480.

Sandkuhler J (2000) Learning and memory in pain pathways. Pain 88: 113-118.

Sasaki H, Nagura K, Ishino M, Tobioka H, Kotani K, Sasaki T (1995) Cloning and characterization of cell adhesion kinase beta, a novel protein-tyrosine kinase of the focal adhesion kinase subfamily. J Biol Chem 270: 21206-21219.

Sato K, Kiyama H, Park HT, Tohyama M (1993) AMPA, KA and NMDA receptors are expressed in the rat DRG neurones. Neuroreport 4: 1263-1265.

Satoh O, Omote K (1996) Roles of monoaminergic, glycinergic and GABAergic inhibitory systems in the spinal cord in rats with peripheral mononeuropathy. Brain Res 728: 27-36.

Savinainen A, Garcia EP, Dorow D, Marshall J, Liu YF (2001) Kainate receptor activation induces mixed lineage kinase-mediated cellular signaling cascades via post-synaptic density protein 95. J Biol Chem 276: 11382-11386.

Sawada M, Kondo N, Suzumura A, Marunouchi T (1989) Production of tumor necrosis factor-alpha by microglia and astrocytes in culture. Brain Res 491: 394-397.

Scadding JW (1981) Development of ongoing activity, mechanosensitivity, and adrenaline sensitivity in severed peripheral nerve axons. Exp Neurol 73: 345-364.

Scadding JW (1984) Peripheral neuropathies. In: Textbook of Pain (Wall PD, Melzack R, eds), pp 413-425. Edinburgh: Churchill Livingstone.

Schafers M, Svensson CI, Sommer C, Sorkin LS (2003) Tumor necrosis factor-alpha induces mechanical allodynia after spinal nerve ligation by activation of p38 MAPK in primary sensory neurons. J Neurosci 23: 2517-2521.

Scherer SS, Xu YT, Roling D, Wrabetz L, Feltri ML, Kamholz J (1994) Expression of growth-associated protein-43 kD in Schwann cells is regulated by axon-Schwann cell interactions and cAMP. J Neurosci Res 38: 575-589.

Schmalbruch H (1986) Fiber composition of the rat sciatic nerve. Anat Rec 215: 71-81.

Schmidt R, Schmelz M, Forster C, Ringkamp M, Torebjork E, Handwerker H (1995) Novel classes of responsive and unresponsive C nociceptors in human skin. J Neurosci 15: 333-341.

Schouenborg J, Sjolund BH (1983) Activity evoked by A- and C-afferent fibers in rat dorsal horn neurons and its relation to a flexion reflex. J Neurophysiol 50: 1108-1121.

Seabold GK, Burette A, Lim IA, Weinberg RJ, Hell JW (2003) Interaction of the tyrosine kinase Pyk2 with the N-methyl-D-aspartate receptor complex via the Src homology 3 domains of PSD-95 and SAP102. J Biol Chem 278: 15040-15048.

Sebert ME, Shooter EM (1993) Expression of mRNA for neurotrophic factors and their receptors in the rat dorsal root ganglion and sciatic nerve following nerve injury. J Neurosci Res 36: 357-367.

Seger R, Krebs EG (1995) The MAPK signaling cascade. FASEB J 9: 726-735.

Seltzer Z, Devor M (1979) Ephaptic transmission in chronically damaged peripheral nerves. Neurology 29: 1061-1064.

Seltzer Z, Dubner R, Shir Y (1990) A novel behavioral model of neuropathic pain disorders produced in rats by partial sciatic nerve injury. Pain 43: 205-218.

Shadiack AM, Sun Y, Zigmond RE (2001) Nerve growth factor antiserum induces axotomy-like changes in neuropeptide expression in intact sympathetic and sensory neurons. J Neurosci 21: 363-371.

Shehab SA, Atkinson ME (1986) Vasoactive intestinal polypeptide increases in areas of the dorsal horn of the spinal cord from which other neuropeptides are depleted following peripheral axotomy. Exp Brain Res 62: 422-430.

Shehab SA, Spike RC, Todd AJ (2003) Evidence against cholera toxin B subunit as a reliable tracer for sprouting of primary afferents following peripheral nerve injury. Brain Res 964: 218-227.

Sheng M (1996) PDZs and receptor/channel clustering: rounding up the latest suspects. Neuron 17: 575-578.

Sheng M, Kim E (1996) Ion channel associated proteins. Curr Opin Neurobiol 6: 602-608.

Sheng M (2001) Molecular organization of the postsynaptic specialization. Proc Natl Acad Sci U S A 98: 7058-7061.

Sheng M, Kim MJ (2002) Postsynaptic signaling and plasticity mechanisms. Science 298: 776-780.

Sherrington CS (1906) The integrative action of the nervous system. New York: Scribner.

Shin H, Hsueh YP, Yang FC, Kim E, Sheng M (2000) An intramolecular interaction between Src homology 3 domain and guanylate kinase-like domain required for channel clustering by postsynaptic density-95/SAP90. J Neurosci 20: 3580-3587.

Shir Y, Seltzer Z (1991) Effects of sympathectomy in a model of causalgiform pain produced by partial sciatic nerve injury in rats. Pain 45: 309-320.

Shivers BD, Gorcs TJ, Gottschall PE, Arimura A (1991) Two high affinity binding sites for pituitary adenylate cyclase-activating polypeptide have different tissue distributions. Endocrinology 128: 3055-3065.

Siciliano JC, Toutant M, Derkinderen P, Sasaki T, Girault JA (1996) Differential regulation of proline-rich tyrosine kinase 2/cell adhesion kinase beta (PYK2/CAKbeta) and pp125(FAK) by glutamate and depolarization in rat hippocampus. J Biol Chem 271: 28942-28946.

Silva AJ, Stevens CF, Tonegawa S, Wang Y (1992) Deficient hippocampal long-term potentiation in alpha-calcium-calmodulin kinase II mutant mice. Science 257: 201-206.

Simone DA, Kajander KC (1996) Excitation of rat cutaneous nociceptors by noxious cold. Neurosci Lett 213: 53-56.

Simone DA, Kajander KC (1997) Responses of cutaneous A-fiber nociceptors to noxious cold. J Neurophysiol 77: 2049-2060.

Sivilotti L, Woolf CJ (1994) The contribution of GABAA and glycine receptors to central sensitization: disinhibition and touch-evoked allodynia in the spinal cord. J Neurophysiol 72: 169-179.

Sloane, E. M., Langer, S. E., Milligan, E. D., Wieseler-Frank, J., Mahony, J. H., Levkoff, L., Cruz, P., Flotte, T. R., Leinwant, L., Maier, S. F., and Watkins, L. R. Chronic constriction injury induced pathological pain states are controlled long term via intrathecal administration of a non-viral vector (NVV) encoding the anti-inflammatory cytokine IL-10. Proc.Am.Pain Soc. 2004. Ref Type: Conference Proceeding

Smith GD, Seckl JR, Harmar AJ (1993) Distribution of neuropeptides in dorsal root ganglia of the rat; substance P, somatostatin and calcitonin gene-related peptide. Neurosci Lett 153: 5-8.

Smith GD, Wiseman J, Harrison SM, Elliott PJ, Birch PJ (1994) Pre treatment with MK-801, a non-competitive NMDA antagonist, prevents development of mechanical hyperalgesia in a rat model of chronic neuropathy, but not in a model of chronic inflammation. Neurosci Lett 165: 79-83.

Smith PB, Martin BR (1992) Spinal mechanisms of delta 9-tetrahydrocannabinol-induced analgesia. Brain Res 578: 8-12.

Snider WD, McMahon SB (1998) Tackling pain at the source: new ideas about nociceptors. Neuron 20: 629-632.

Soltoff SP, Avraham H, Avraham S, Cantley LC (1998) Activation of P2Y2 receptors by UTP and ATP stimulates mitogen-activated kinase activity through a pathway that involves related adhesion focal tyrosine kinase and protein kinase C. J Biol Chem 273: 2653-2660.

Sommer C, Marziniak M, Myers RR (1998) The effect of thalidomide treatment on vascular pathology and hyperalgesia caused by chronic constriction injury of rat nerve. Pain 74: 83-91.

Sommer C, Schmidt C, George A (1998) Hyperalgesia in experimental neuropathy is dependent on the TNF receptor 1. Exp Neurol 151: 138-142.

Sorkin LS, Xiao WH, Wagner R, Myers RR (1997) Tumour necrosis factor-alpha induces ectopic activity in nociceptive primary afferent fibres. Neuroscience 81: 255-262.

Sorkin LS, Doom CM (2000) Epineurial application of TNF elicits an acute mechanical hyperalgesia in the awake rat. J Peripher Nerv Syst 5: 96-100.

Sotgiu ML, Biella G (2000) Differential effects of MK-801, a N-methyl-D-aspartate non-competitive antagonist, on the dorsal horn neuron hyperactivity and hyperexcitability in neuropathic rats. Neurosci Lett 283: 153-156.

Sotgui ML (1993) Descending influence on dorsal horn neuronal hyperactivity in a rat model of neuropathic pain. Neuroreport 4: 21-24.

Sparks AB, Rider JE, Kay BK (1998) Mapping the specificity of SH3 domains with phage-displayed random-peptide libraries. Methods Mol Biol 84: 87-103.

Spengler D, Waeber C, Pantaloni C, Holsboer F, Bockaert J, Seeburg PH, Journot L (1993) Differential signal transduction by five splice variants of the PACAP receptor. Nature 365: 170-175.

Stahl ML, Ferenz CR, Kelleher KL, Kriz RW, Knopf JL (1988) Sequence similarity of phospholipase C with the non-catalytic region of src. Nature 332: 269-272.

Stanfa LC, Dickenson AH (1999) The role of non-N-methyl-D-aspartate ionotropic glutamate receptors in the spinal transmission of nociception in normal animals and animals with carrageenan inflammation. Neuroscience 93: 1391-1398.

Strack S, Colbran RJ (1998) Autophosphorylation-dependent targeting of calcium/ calmodulin-dependent protein kinase II by the NR2B subunit of the N-methyl- D-aspartate receptor. J Biol Chem 273: 20689-20692.

Sucher NJ, Akbarian S, Chi CL, Leclerc CL, Awobuluyi M, Deitcher DL, Wu MK, Yuan JP, Jones EG, Lipton SA (1995) Developmental and regional expression pattern of a novel NMDA receptor-like subunit (NMDAR-L) in the rodent brain. J Neurosci 15: 6509-6520.

Sun RQ, Lawand NB, Willis WD (2003) The role of calcitonin gene-related peptide (CGRP) in the generation and maintenance of mechanical allodynia and hyperalgesia in rats after intradermal injection of capsaicin. Pain 104: 201-208.

Sun Y, Savanenin A, Reddy PH, Liu YF (2001) Polyglutamine-expanded huntingtin promotes sensitization of N-methyl-D-aspartate receptors via post-synaptic density 95. J Biol Chem 276: 24713-24718.

Sung B, Na HS, Kim YI, Yoon YW, Han HC, Nahm SH, Hong SK (1998) Supraspinal involvement in the production of mechanical allodynia by spinal nerve injury in rats. Neurosci Lett 246: 117-119.

Suzuki R, Matthews EA, Dickenson AH (2001) Comparison of the effects of MK-801, ketamine and memantine on responses of spinal dorsal horn neurones in a rat model of mononeuropathy. Pain 91: 101-109.

Svensson CI, Marsala M, Westerlund A, Calcutt NA, Campana WM, Freshwater JD, Catalano R, Feng Y, Protter AA, Scott B, Yaksh TL (2003) Activation of p38 mitogen-activated protein kinase in spinal microglia is a critical link in inflammation-induced spinal pain processing. J Neurochem 86: 1534-1544.

Svensson CI, Schafers M, Jones TL, Powell H, Sorkin LS (2005) Spinal blockade of TNF blocks spinal nerve ligation-induced increases in spinal P-p38. Neurosci Lett 379: 209-213.

Sweatt JD (2001) The neuronal MAP kinase cascade: a biochemical signal integration system subserving synaptic plasticity and memory. J Neurochem 76: 1-10.

Sweitzer S, Martin D, DeLeo JA (2001) Intrathecal interleukin-1 receptor antagonist in combination with soluble tumor necrosis factor receptor exhibits an anti-allodynic action in a rat model of neuropathic pain. Neuroscience 103: 529-539.

Sweitzer SM, Colburn RW, Rutkowski M, DeLeo JA (1999) Acute peripheral inflammation induces moderate glial activation and spinal IL-1beta expression that correlates with pain behavior in the rat. Brain Res 829: 209-221.

Sweitzer SM, Schubert P, DeLeo JA (2001) Propentofylline, a glial modulating agent, exhibits antiallodynic properties in a rat model of neuropathic pain. J Pharmacol Exp Ther 297: 1210-1217.

Sweitzer SM, Medicherla S, Almirez R, Dugar S, Chakravarty S, Shumilla JA, Yeomans DC, Protter AA (2004) Antinociceptive action of a p38alpha MAPK inhibitor, SD-282, in a diabetic neuropathy model. Pain 109: 409-419.

Swett JE, Woolf CJ (1985) The somatotopic organization of primary afferent terminals in the superficial laminae of the dorsal horn of the rat spinal cord. J Comp Neurol 231: 66-77.

Takasaki W, Kajino Y, Kajino K, Murali R, Greene MI (1997) Structure-based design and characterization of exocyclic peptidomimetics that inhibit TNF alpha binding to its receptor. Nat Biotechnol 15: 1266-1270.

Takeuchi M, Hata Y, Hirao K, Toyoda A, Irie M, Takai Y (1997) SAPAPs. A family of PSD-95/SAP90-associated proteins localized at postsynaptic density. J Biol Chem 272: 11943-11951.

Takuma K, Matsuda T, Hashimoto H, Kitanaka J, Asano S, Kishida Y, Baba A (1996) Role of Na(+)-Ca2+ exchanger in agonist-induced Ca2+ signaling in cultured rat astrocytes. J Neurochem 67: 1840-1845.

Tal M, Bennett GJ (1993) Dextrorphan relieves neuropathic heat-evoked hyperalgesia in the rat. Neurosci Lett 151: 107-110.

Tao F, Tao YX, Gonzalez JA, Fang M, Mao P, Johns RA (2001) Knockdown of PSD-95/SAP90 delays the development of neuropathic pain in rats. Neuroreport 12: 3251-3255.

Tao F, Tao YX, Mao P, Johns RA (2003) Role of postsynaptic density protein-95 in the maintenance of peripheral nerve injury-induced neuropathic pain in rats. Neuroscience 117: 731-739.

Tao YX, Huang YZ, Mei L, Johns RA (2000) Expression of PSD-95/SAP90 is critical for N-methyl-D-aspartate receptor-mediated thermal hyperalgesia in the spinal cord. Neuroscience 98: 201-206.

Tao YX, Rumbaugh G, Wang GD, Petralia RS, Zhao C, Kauer FW, Tao F, Zhuo M, Wenthold RJ, Raja SN, Huganir RL, Bredt DS, Johns RA (2003) Impaired NMDA receptor-mediated postsynaptic function and blunted NMDA receptor-dependent persistent pain in mice lacking postsynaptic density-93 protein. J Neurosci 23: 6703-6712.

Tate S, Benn S, Hick C, Trezise D, John V, Mannion RJ, Costigan M, Plumpton C, Grose D, Gladwell Z, Kendall G, Dale K, Bountra C, Woolf CJ (1998) Two sodium channels contribute to the TTX-R sodium current in primary sensory neurons. Nat Neurosci 1: 653-655.

Tavares GA, Panepucci EH, Brunger AT (2001) Structural characterization of the intramolecular interaction between the SH3 and guanylate kinase domains of PSD-95. Mol Cell 8: 1313-1325.

Taylor BK, Peterson MA, Basbaum AI (1995) Persistent cardiovascular and behavioral nociceptive responses to subcutaneous formalin require peripheral nerve input. J Neurosci 15: 7575-7584.

Theodorsson-Norheim E, Hemsen A, Brodin E, Lundberg JM (1987) Sample handling techniques when analyzing regulatory peptides. Life Sci 41: 845-848.

Thoenen H (1991) The changing scene of neurotrophic factors. Trends Neurosci 14: 165-170.

Thomas SM, Brugge JS (1997) Cellular functions regulated by Src family kinases. Annu Rev Cell Dev Biol 13: 513-609.

Tian D, Litvak V, Lev S (2000) Cerebral ischemia and seizures induce tyrosine phosphorylation of PYK2 in neurons and microglial cells. J Neurosci 20: 6478-6487.

Tikka T, Fiebich BL, Goldsteins G, Keinanen R, Koistinaho J (2001) Minocycline, a tetracycline derivative, is neuroprotective against excitotoxicity by inhibiting activation and proliferation of microglia. J Neurosci 21: 2580-2588.

Tikka TM, Koistinaho JE (2001) Minocycline provides neuroprotection against N-methyl-D-aspartate neurotoxicity by inhibiting microglia. J Immunol 166: 7527-7533.

Todd AJ, Lewis SG (1986) The morphology of Golgi-stained neurons in lamina II of the rat spinal cord. J Anat 149: 113-119.

Todd AJ (1988) Electron microscope study of Golgi-stained cells in lamina II of the rat spinal dorsal horn. J Comp Neurol 275: 145-157.

Todd AJ, McKenzie J (1989) GABA-immunoreactive neurons in the dorsal horn of the rat spinal cord. Neuroscience 31: 799-806.

Todd AJ, Sullivan AC (1990) Light microscope study of the coexistence of GABA-like and glycine-like immunoreactivities in the spinal cord of the rat. J Comp Neurol 296: 496-505.

Todd AJ, McGill MM, Shehab SA (2000) Neurokinin 1 receptor expression by neurons in laminae I, III and IV of the rat spinal dorsal horn that project to the brainstem. Eur J Neurosci 12: 689-700.

Todd AJ (2002) Anatomy of primary afferents and projection neurones in the rat spinal dorsal horn with particular emphasis on substance P and the neurokinin 1 receptor. Exp Physiol 87: 245-249.

Tokiwa G, Dikic I, Lev S, Schlessinger J (1996) Activation of Pyk2 by stress signals and coupling with JNK signaling pathway. Science 273: 792-794.

Tolle TR, Berthele A, Zieglgansberger W, Seeburg PH, Wisden W (1993) The differential expression of 16 NMDA and non-NMDA receptor subunits in the rat spinal cord and in periaqueductal gray. J Neurosci 13: 5009-5028.

Tong YG, Wang HF, Ju G, Grant G, Hokfelt T, Zhang X (1999) Increased uptake and transport of cholera toxin B-subunit in dorsal root ganglion neurons after peripheral axotomy: possible implications for sensory sprouting. J Comp Neurol 404: 143-158.

Torebjork HE, Ochoa JL (1980) Specific sensations evoked by activity in single identified sensory units in man. Acta Physiol Scand 110: 445-447.

Tsuda M, Mizokoshi A, Shigemoto-Mogami Y, Koizumi S, Inoue K (2004) Activation of p38 mitogen-activated protein kinase in spinal hyperactive microglia contributes to pain hypersensitivity following peripheral nerve injury. Glia 45: 89-95.

Tu JC, Xiao B, Naisbitt S, Yuan JP, Petralia RS, Brakeman P, Doan A, Aakalu VK, Lanahan AA, Sheng M, Worley PF (1999) Coupling of mGluR/Homer and PSD-95 complexes by the Shank family of postsynaptic density proteins. Neuron 23: 583-592.

Ullstrom M, Parker D, Svensson E, Grillner S (1999) Neuropeptide-mediated facilitation and inhibition of sensory inputs and spinal cord reflexes in the lamprey. J Neurophysiol 81: 1730-1740.

Verge VM, Richardson PM, Wiesenfeld-Hallin Z, Hokfelt T (1995) Differential influence of nerve growth factor on neuropeptide expression in vivo: a novel role in peptide suppression in adult sensory neurons. J Neurosci 15: 2081-2096.

Villar MJ, Cortes R, Theodorsson E, Wiesenfeld-Hallin Z, Schalling M, Fahrenkrug J, Emson PC, Hokfelt T (1989) Neuropeptide expression in rat dorsal root ganglion cells and spinal cord after peripheral nerve injury with special reference to galanin. Neuroscience 33: 587-604.

Villar MJ, Wiesenfeld-Hallin Z, Xu XJ, Theodorsson E, Emson PC, Hokfelt T (1991) Further studies on galanin-, substance P-, and CGRP-like immunoreactivities in primary sensory neurons and spinal cord: effects of dorsal rhizotomies and sciatic nerve lesions. Exp Neurol 112: 29-39.

Villetti G, Bergamaschi M, Bassani F, Bolzoni PT, Maiorino M, Pietra C, Rondelli I, Chamiot-Clerc P, Simonato M, Barbieri M (2003) Antinociceptive activity of the N-methyl-D-aspartate receptor antagonist N-(2-Indanyl)-glycinamide hydrochloride (CHF3381) in experimental models of inflammatory and neuropathic pain. J Pharmacol Exp Ther 306: 804-814.

Vitkovic L, Bockaert J, Jacque C (2000) "Inflammatory" cytokines: neuromodulators in normal brain? J Neurochem 74: 457-471.

Vogel C, Mossner R, Gerlach M, Heinemann T, Murphy DL, Riederer P, Lesch KP, Sommer C (2003) Absence of thermal hyperalgesia in serotonin transporter-deficient mice. J Neurosci 23: 708-715.

Wagner R, Myers RR (1996) Schwann cells produce tumor necrosis factor alpha: expression in injured and non-injured nerves. Neuroscience 73: 625-629.

Wakisaka S, Kajander KC, Bennett GJ (1991) Increased neuropeptide Y (NPY)-like immunoreactivity in rat sensory neurons following peripheral axotomy. Neurosci Lett 124: 200-203.

Walczak JS, Pichette V, Leblond F, Desbiens K, Beaulieu P (2005) Behavioral, pharmacological and molecular characterization of the saphenous nerve partial ligation: a new model of neuropathic pain. Neuroscience 132: 1093-1102.

Walker K, Reeve A, Bowes M, Winter J, Wotherspoon G, Davis A, Schmid P, Gasparini F, Kuhn R, Urban L (2001) mGlu5 receptors and nociceptive function II. mGlu5 receptors functionally expressed on peripheral sensory neurones mediate inflammatory hyperalgesia. Neuropharmacology 40: 10-19.

Wall PD (1960) Cord cells responding to touch, damage, and temperature of skin. J Neurophysiol 23: 197-210.

Wallace VC, Cottrell DF, Brophy PJ, Fleetwood-Walker SM (2003) Focal lysolecithin-induced demyelination of peripheral afferents results in neuropathic pain behavior that is attenuated by cannabinoids. J Neurosci 23: 3221-3233.

Wang YT, Salter MW (1994) Regulation of NMDA receptors by tyrosine kinases and phosphatases. Nature 369: 233-235.

Warden MK, Young WS, III (1988) Distribution of cells containing mRNAs encoding substance P and neurokinin B in the rat central nervous system. J Comp Neurol 272: 90-113.

Watkins JC, Evans RH (1981) Excitatory amino acid transmitters. Annu Rev Pharmacol Toxicol 21: 165-204.

Watkins LR, Martin D, Ulrich P, Tracey KJ, Maier SF (1997) Evidence for the involvement of spinal cord glia in subcutaneous formalin induced hyperalgesia in the rat. Pain 71: 225-235.

Watkins LR, Hansen MK, Nguyen KT, Lee JE, Maier SF (1999) Dynamic regulation of the proinflammatory cytokine, interleukin-1beta: molecular biology for non-molecular biologists. Life Sci 65: 449-481.

Watkins LR, Milligan ED, Maier SF (2001) Glial activation: a driving force for pathological pain. Trends Neurosci 24: 450-455.

Watkins LR, Milligan ED, Maier SF (2001) Spinal cord glia: new players in pain. Pain 93: 201-205.

Watkins LR, Maier SF (2002) Beyond neurons: evidence that immune and glial cells contribute to pathological pain states. Physiol Rev 82: 981-1011.

Watkins LR, Maier SF (2003) Glia: a novel drug discovery target for clinical pain. Nat Rev Drug Discov 2: 973-985.

Waxman SG (1999) The molecular pathophysiology of pain: abnormal expression of sodium channel genes and its contributions to hyperexcitability of primary sensory neurons. Pain Suppl 6: S133-S140.

Waxman SG, Dib-Hajj S, Cummins TR, Black JA (1999) Sodium channels and pain. Proc Natl Acad Sci U S A 96: 7635-7639.

Waxman SG, Cummins TR, Dib-Hajj S, Fjell J, Black JA (1999) Sodium channels, excitability of primary sensory neurons, and the molecular basis of pain. Muscle Nerve 22: 1177-1187.

Waxman SG, Cummins TR, Dib-Hajj SD, Black JA (2000) Voltage-gated sodium channels and the molecular pathogenesis of pain: a review. J Rehabil Res Dev 37: 517-528.

Wheeler-Aceto H, Cowan A (1991) Standardization of the rat paw formalin test for the evaluation of analgesics. Psychopharmacology (Berl) 104: 35-44.

Whitmarsh AJ (2006) Regulation of gene transcription by mitogen-activated protein kinase signaling pathways. Biochim Biophys Acta.

Widmann C, Gibson S, Jarpe MB, Johnson GL (1999) Mitogen-activated protein kinase: conservation of a three-kinase module from yeast to human. Physiol Rev 79: 143-180.

Wiesenfeld-Hallin Z (1985) Intrathecal somatostatin modulates spinal sensory and reflex mechanisms: behavioral and electrophysiological studies in the rat. Neurosci Lett 62: 69-74.

Wiesenfeld-Hallin Z, Xu XJ, Hakanson R, Feng DM, Folkers K, Kristensson K, Villar MJ, Fahrenkrug J, Hokfelt T (1991) On the role of substance P, galanin, vasoactive intestinal peptide, and calcitonin gene-related peptide in mediation of spinal reflex excitability in rats with intact and sectioned peripheral nerves. Ann N Y Acad Sci 632: 198-211.

Wiesenfeld-Hallin Z, Xu XJ, Hakanson R, Feng DM, Folkers K (1991) Low-dose intrathecal morphine facilitates the spinal flexor reflex by releasing different neuropeptides in rats with intact and sectioned peripheral nerves. Brain Res 551: 157-162.

Wiesenfeld-Hallin Z, Xu XJ (1996) Plasticity of messenger function in primary afferents following nerve injury--implications for neuropathic pain. Prog Brain Res 110: 113-124.

Willis WD, Haber LH, Martin RF (1977) Inhibition of spinothalamic tract cells and interneurons by brain stem stimulation in the monkey. J Neurophysiol 40: 968-981.

Willis WD, Kenshalo DR, Jr., Leonard RB (1979) The cells of origin of the primate spinothalamic tract. J Comp Neurol 188: 543-573.

Willis WD, Coggeshall RE (1991) Sensory Mechanisms of the Spinal Cord. New York and London: Plenum Press.

Wilson JA, Garry EM, Anderson HA, Rosie R, Colvin LA, Mitchell R, Fleetwood-Walker SM (2005) NMDA receptor antagonist treatment at the time of nerve injury prevents injury-induced changes in spinal NR1 and NR2B subunit expression and increases the sensitivity of residual pain behaviours to subsequently administered NMDA receptor antagonists. Pain 117: 421-432.

Wilson P, Kitchener PD (1996) Plasticity of cutaneous primary afferent projections to the spinal dorsal horn. Prog Neurobiol 48: 105-129.

Winkelstein BA, Rutkowski MD, Sweitzer SM, Pahl JL, DeLeo JA (2001) Nerve injury proximal or distal to the DRG induces similar spinal glial activation and selective cytokine expression but differential behavioral responses to pharmacologic treatment. J Comp Neurol 439: 127-139.

Winkelstein BA, DeLeo JA (2002) Nerve root injury severity differentially modulates spinal glial activation in a rat lumbar radiculopathy model: considerations for persistent pain. Brain Res 956: 294-301.

Wisden W, Seeburg PH (1993) Mammalian ionotropic glutamate receptors. Curr Opin Neurobiol 3: 291-298.

Woda A, Pionchon P (2000) A unified concept of idiopathic orofacial pain: pathophysiologic features. J Orofac Pain 14: 196-212.

Woods DF, Hough C, Peel D, Callaini G, Bryant PJ (1996) Dlg protein is required for junction structure, cell polarity, and proliferation control in Drosophila epithelia. J Cell Biol 134: 1469-1482.

Woolf CJ, Wall PD (1982) Chronic peripheral nerve section diminishes the primary afferent A-fibre mediated inhibition of rat dorsal horn neurones. Brain Res 242: 77-85.

Woolf CJ, Fitzgerald M (1983) The properties of neurones recorded in the superficial dorsal horn of the rat spinal cord. J Comp Neurol 221: 313-328.

Woolf CJ, Thompson SW (1991) The induction and maintenance of central sensitization is dependent on N-methyl-D-aspartic acid receptor activation; implications for the treatment of post-injury pain hypersensitivity states. Pain 44: 293-299.

Woolf CJ, Shortland P, Coggeshall RE (1992) Peripheral nerve injury triggers central sprouting of myelinated afferents. Nature 355: 75-78.

Woolf CJ, Doubell TP (1994) The pathophysiology of chronic pain--increased sensitivity to low threshold A beta-fibre inputs. Curr Opin Neurobiol 4: 525-534.

Woolf CJ (1996) Windup and central sensitization are not equivalent. Pain 66: 105-108.

Woolf CJ, Costigan M (1999) Transcriptional and posttranslational plasticity and the generation of inflammatory pain. Proc Natl Acad Sci U S A 96: 7723-7730.

Woolf CJ, Mannion RJ (1999) Neuropathic pain: aetiology, symptoms, mechanisms, and management. Lancet 353: 1959-1964.

Woolf CJ, Salter MW (2000) Neuronal plasticity: increasing the gain in pain. Science 288: 1765-1769.

Wu SS, Jacamo RO, Vong SK, Rozengurt E (2006) Differential regulation of Pyk2 phosphorylation at Tyr-402 and Tyr-580 in intestinal epithelial cells: roles of calcium, Src, Rho kinase, and the cytoskeleton. Cell Signal 18: 1932-1940.

Xia Z, Dudek H, Miranti CK, Greenberg ME (1996) Calcium influx via the NMDA receptor induces immediate early gene transcription by a MAP kinase/ERK-dependent mechanism. J Neurosci 16: 5425-5436.

Xie Y, Zhang J, Petersen M, LaMotte RH (1995) Functional changes in dorsal root ganglion cells after chronic nerve constriction in the rat. J Neurophysiol 73: 1811-1820.

Xie YK, Xiao WH (1990) Electrophysiological evidence for hyperalgesia in the peripheral neuropathy. Sci China B 33: 663-672.

Xing J, Ginty DD, Greenberg ME (1996) Coupling of the RAS-MAPK pathway to gene activation by RSK2, a growth factor-regulated CREB kinase. Science 273: 959-963.

Xu J, Pollock CH, Kajander KC (1996) Chromic gut suture reduces calcitonin-gene-related peptide and substance P levels in the spinal cord following chronic constriction injury in the rat. Pain 64: 503-509.

Xu W, Harrison SC, Eck MJ (1997) Three-dimensional structure of the tyrosine kinase c-Src. Nature 385: 595-602.

Xu XJ, Wiesenfeld-Hallin Z, Villar MJ, Fahrenkrug J, Hokfelt T (1990) On the Role of Galanin, Substance P and Other Neuropeptides in Primary Sensory Neurons of the Rat: Studies on Spinal Reflex Excitability and Peripheral Axotomy. Eur J Neurosci 2: 733-743.

Xu XJ, Maggi CA, Wiesenfeld-Hallin Z (1991) On the role of NK-2 tachykinin receptors in the mediation of spinal reflex excitability in the rat. Neuroscience 44: 483-490.

Yaffe MB (2002) MAGUK SH3 domains--swapped and stranded by their kinases? Structure (Camb) 10: 3-5.

Yaksh TL (1981) Spinal opiate analgesia: characteristics and principles of action. Pain 11: 293-346.

Yaksh TL, Abay EO, Go VL (1982) Studies on the location and release of cholecystokinin and vasoactive intestinal peptide in rat and cat spinal cord. Brain Res 242: 279-290.

Yaksh TL (1986) Spinal afferent processing. Kluwer Academic Publishing.

Yaksh TL, Michener SR, Bailey JE, Harty GJ, Lucas DL, Nelson DK, Roddy DR, Go VL (1988) Survey of distribution of substance P, vasoactive intestinal polypeptide, cholecystokinin, neurotensin, Met-enkephalin, bombesin and PHI in the spinal cord of cat, dog, sloth and monkey. Peptides 9: 357-372.

Yamakura T, Shimoji K (1999) Subunit- and site-specific pharmacology of the NMDA receptor channel. Prog Neurobiol 59: 279-298.

Yamauchi J, Nagao M, Kaziro Y, Itoh H (1997) Activation of p38 mitogen-activated protein kinase by signaling through G protein-coupled receptors. Involvement of Gbetagamma and Galphaq/11 subunits. J Biol Chem 272: 27771-27777.

Yao WD, Gainetdinov RR, Arbuckle MI, Sotnikova TD, Cyr M, Beaulieu JM, Torres GE, Grant SG, Caron MG (2004) Identification of PSD-95 as a regulator of dopamine-mediated synaptic and behavioral plasticity. Neuron 41: 625-638.

Yashpal K, Henry JL (1984) Substance p analogue blocks sp-induced facilitation of a spinal nociceptive reflex. Brain Res Bull 13: 597-600.

Yashpal K, Dam TV, Quirion R (1990) Quantitative autoradiographic distribution of multiple neurokinin binding sites in rat spinal cord. Brain Res 506: 259-266.

Yashpal K, Dam TV, Quirion R (1991) Effects of dorsal rhizotomy on neurokinin receptor sub-types in the rat spinal cord: a quantitative autoradiographic study. Brain Res 552: 240-247.

Yashpal K, Hui-Chan CW, Henry JL (1996) SR 48968 specifically depresses neurokinin A- vs. substance P-induced hyperalgesia in a nociceptive withdrawal reflex. Eur J Pharmacol 308: 41-48.

Yin KJ (1995) Distribution of somatostatin mRNA containing neurons in the primary pain relaying nuclei of the rat. Anat Rec 241: 579-584.

Yoon YW, Sung B, Chung JM (1998) Nitric oxide mediates behavioral signs of neuropathic pain in an experimental rat model. Neuroreport 9: 367-372.

Young AB, Fagg GE (1990) Excitatory amino acid receptors in the brain: membrane binding and receptor autoradiographic approaches. Trends Pharmacol Sci 11: 126-133.

Young MR, Fleetwood-Walker SM, Mitchell R, Dickinson T (1995) The involvement of metabotropic glutamate receptors and their intracellular signalling pathways in sustained nociceptive transmission in rat dorsal horn neurons. Neuropharmacology 34: 1033-1041.

Young MR, Fleetwood-Walker SM, Dickinson T, Blackburn-Munro G, Sparrow H, Birch PJ, Bountra C (1997) Behavioural and electrophysiological evidence supporting a role for group I metabotropic glutamate receptors in the mediation of nociceptive inputs to the rat spinal cord. Brain Res 777: 161-169.

Young MR, Blackburn-Munro G, Dickinson T, Johnson MJ, Anderson H, Nakalembe I, Fleetwood-Walker SM (1998) Antisense ablation of type I metabotropic glutamate receptor mGluR1 inhibits spinal nociceptive transmission. J Neurosci 18: 10180-10188.

Yu H, Li X, Marchetto GS, Dy R, Hunter D, Calvo B, Dawson TL, Wilm M, Anderegg RJ, Graves LM, Earp HS (1996) Activation of a novel calcium-dependent protein-tyrosine kinase. Correlation with c-Jun N-terminal kinase but not mitogen-activated protein kinase activation. J Biol Chem 271: 29993-29998.

Yu XM, Askalan R, Keil GJ, Salter MW (1997) NMDA channel regulation by channel-associated protein tyrosine kinase Src. Science 275: 674-678.

Yung KK (1998) Localization of glutamate receptors in dorsal horn of rat spinal cord. Neuroreport 9: 1639-1644.

Zakrzewska JM, Patsalos PN (1992) Drugs used in the management of trigeminal neuralgia. Oral Surg Oral Med Oral Pathol 74: 439-450.

Zerari F, Dery O, Fischer J, Frobert Y, Couraud JY, Conrath M (1995) Ultrastructural study of substance P receptors in the dorsal horn of the rat spinal cord using monoclonal anti-complementary peptide antibody. J Chem Neuroanat 9: 65-77.

Zerari F, Karpitskiy V, Krause J, Descarries L, Couture R (1997) Immunoelectron microscopic localization of NK-3 receptor in the rat spinal cord. Neuroreport 8: 2661-2664.

Zerari F, Karpitskiy V, Krause J, Descarries L, Couture R (1998) Astroglial distribution of neurokinin-2 receptor immunoreactivity in the rat spinal cord. Neuroscience 84: 1233-1246.

Zhang B, Tao F, Liaw WJ, Bredt DS, Johns RA, Tao YX (2003) Effect of knock down of spinal cord PSD-93/chapsin-110 on persistent pain induced by complete Freund's adjuvant and peripheral nerve injury. Pain 106: 187-196.

Zhang C, Yang SW, Guo YG, Qiao JT, Dafny N (1997) Locus coeruleus stimulation modulates the nociceptive response in parafascicular neurons: an analysis of descending and ascending pathways. Brain Res Bull 42: 273-278.

Zhang ET, Han ZS, Craig AD (1996) Morphological classes of spinothalamic lamina I neurons in the cat. J Comp Neurol 367: 537-549.

Zhang J, Hoffert C, Vu HK, Groblewski T, Ahmad S, O'Donnell D (2003) Induction of CB2 receptor expression in the rat spinal cord of neuropathic but not inflammatory chronic pain models. Eur J Neurosci 17: 2750-2754.

Zhang JM, Song XJ, LaMotte RH (1997) An in vitro study of ectopic discharge generation and adrenergic sensitivity in the intact, nerve-injured rat dorsal root ganglion. Pain 72: 51-57.

Zhang Q, Shi TJ, Ji RR, Zhang YZ, Sundler F, Hannibal J, Fahrenkrug J, Hokfelt T (1995) Expression of pituitary adenylate cyclase-activating polypeptide in dorsal root ganglia following axotomy: time course and coexistence. Brain Res 705: 149-158.

Zhang X, Verge VM, Wiesenfeld-Hallin Z, Piehl F, Hokfelt T (1993) Expression of neuropeptides and neuropeptide mRNAs in spinal cord after axotomy in the rat, with special reference to motoneurons and galanin. Exp Brain Res 93: 450-461.

Zhang X, Nicholas AP, Hokfelt T (1993) Ultrastructural studies on peptides in the dorsal horn of the spinal cord--I. Co-existence of galanin with other peptides in primary afferents in normal rats. Neuroscience 57: 365-384.

Zhang X, Wiesenfeld-Hallin Z, Hokfelt T (1994) Effect of peripheral axotomy on expression of neuropeptide Y receptor mRNA in rat lumbar dorsal root ganglia. Eur J Neurosci 6: 43-57.

Zhang X, Bean AJ, Wiesenfeld-Hallin Z, Xu XJ, Hokfelt T (1995) Ultrastructural studies on peptides in the dorsal horn of the rat spinal cord--III. Effects of peripheral axotomy with special reference to galanin. Neuroscience 64: 893-915.

Zhang X, Bean AJ, Wiesenfeld-Hallin Z, Hokfelt T (1995) Ultrastructural studies on peptides in the dorsal horn of the rat spinal cord--IV. Effects of peripheral axotomy with special reference to neuropeptide Y and vasoactive intestinal polypeptide/peptide histidine isoleucine. Neuroscience 64: 917-941.

Zhang YZ, Sjolund B, Moller K, Hakanson R, Sundler F (1993) Pituitary adenylate cyclase activating peptide produces a marked and long-lasting depression of a C-fibre-evoked flexion reflex. Neuroscience 57: 733-737.

Zheng F, Gingrich MB, Traynelis SF, Conn PJ (1998) Tyrosine kinase potentiates NMDA receptor currents by reducing tonic zinc inhibition. Nat Neurosci 1: 185-191.

Zhou S, Bonasera L, Carlton SM (1996) Peripheral administration of NMDA, AMPA or KA results in pain behaviors in rats. Neuroreport 7: 895-900.

Zhuang ZY, Gerner P, Woolf CJ, Ji RR (2005) ERK is sequentially activated in neurons, microglia, and astrocytes by spinal nerve ligation and contributes to mechanical allodynia in this neuropathic pain model. Pain 114: 149-159.

Zhuang ZY, Wen YR, Zhang DR, Borsello T, Bonny C, Strichartz GR, Decosterd I, Ji RR (2006) A peptide c-Jun N-terminal kinase (JNK) inhibitor blocks mechanical allodynia after spinal nerve ligation: respective roles of JNK activation in primary sensory neurons and spinal astrocytes for neuropathic pain development and maintenance. J Neurosci 26: 3551-3560.

Zhuo M, Gebhart GF (1990) Characterization of descending inhibition and facilitation from the nuclei reticularis gigantocellularis and gigantocellularis pars alpha in the rat. Pain 42: 337-350.

Zieglgansberger W, Tulloch IF (1979) Effects of substance P on neurones in the dorsal horn of the spinal cord of the cat. Brain Res 166: 273-282.

Zieglgansberger W, Sutor B (1983) Responses of substantia gelatinosa neurons to putative neurotransmitters in an in vitro preparation of the adult rat spinal cord. Brain Res 279: 316-320.

Zupan V, Hill JM, Brenneman DE, Gozes I, Fridkin M, Robberecht P, Evrard P, Gressens P (1998) Involvement of pituitary adenylate cyclase-activating polypeptide II vasoactive intestinal peptide 2 receptor in mouse neocortical astrocytogenesis. J Neurochem 70: 2165-2173.

Zusev M, Gozes I (2004) Differential regulation of activity-dependent neuroprotective protein in rat astrocytes by VIP and PACAP. Regul Pept 123: 33-41.

Appendix: Publications arising from research

A. Delaney, E.M. Garry, G. Blackburn-Munro, R. Mitchell, S.M. Fleetwood-Walker (2003) Activation and role of p42/44 map kinases by $VPAC_2$ receptors in the spinal dorsal horn following neuropathic nerve damage. [Abstract] Society for Neuroscience 33rd Annual Meeting, Program No. 382.4. 2003 Abstract Viewer/Itinerary Planner Online: Society for Neuroscience.

E.M. Garry[1], A. Delaney[1], G. Blackburn-Munro, T. Dickinson, A. Moss, I. Nakalembe, R. Rosie, P. Robberecht, R. Mitchell, and S.M. Fleetwood-Walker (2005) Activation of p38 and p42/44 MAP kinase in neuropathic pain: Involvement of $VPAC_2$ and NK_2 receptors and mediation by spinal glia. Mol. Cell. Neuroscience 30(4):523-37
([1] Contributed equally to this work as joint first authors)

E.M. Garry, A. Delaney, H.A. Anderson, E.C. Sirinathsinghji, R.H. Clapp, W.J. Martin, P.R. Kinchington, D.L. Krah, C. Abaddie & S.M.Fleetwood-Walker (2005) Varicella zoster virus induces neuropathic changes in rat dorsal root ganglia and behavioral reflex sensitisation that is attenuated by gabapentin or sodium channel blocking drugs. Pain 118(1-2):97-111.

E.M. Garry, A Moss, R Rosie, A. Delaney, R Mitchell & SM Fleetwood-Walker (2003) Specific involvement in neuropathic pain of AMPA receptors and adapter proteins for the GluR2 subunit. Molecular and Cellular Neuroscience 24 (1): 10.

E.M. Garry, A. Moss, A. Delaney, F. O'Neill, J. Blakemore, J. Bowen, H. Husi, R. Mitchell, S.G.N. Grant & S.M. Fleetwood-Walker (2003) Neuropathic sensitization of behavioural reflexes and spinal NMDA receptor/Cam Kinase II interactions are disrupted in PSD-95 mutant mice. Current Biology 13: 321.

Abstract

Society for Neuroscience 33rd Annual Conference, New Orleans, USA, 2003

Activation and role of p42/44 MAP kinases by $VPAC_2$ receptors in the spinal dorsal horn following neuropathic nerve damage

A Delaney[1], E M Garry[1], G. Blackburn-Munro[3], R Mitchell[2] and S M Fleetwood-Walker[1]

[1]Dept. Preclinical Veterinary Sciences, R (D) SVS, Summerhall, 2MRC Membrane and Adapter Proteins Co-op, [2] Membrane Biology Group, School of Biomedical and Clinical Laboratory Sciences, University of Edinburgh, [3] NeuroSearch AG, Copenhagen, Denmark.

Neuropathic pain is a pervasive clinical condition in need of novel targets for therapeutic treatment. Stimulation of peripheral nociceptive inputs causes downstream activation of kinases in the spinal dorsal horn which can facilitate dorsal horn neuron (DHN) responsiveness and contribute to the behavioural hyperalgesia observed in animal models of chronic pain. Here, using the CCI model of neuropathic pain we examine the roles of the p42/44 extracellular signal-regulated kinases (ERKs) and their activation by the $VPAC_2$ receptor, the expression of which we have previously shown to be increased in neuropathic pain. Electrophysiology at the level of single dorsal horn neurons revealed the ability of the ERK inhibitor, PD 098059, to block the sensitisation of responsiveness following mustard oil stimulation, confirming the role of ERKs in this neuropathic model. Intrathecal injection of the same compound showed a reversal of the hyperalgesic and allodynic behaviours that develop following CCI. In addition, protein levels of phosphorylated p42/44 ERK were increased ipsilateral to CCI injury and following topical application of a $VPAC_2$ receptor agonist while pan p42/44 ERK levels remained unaltered. Furthermore, a specific $VPAC_2$ receptor antagonist inhibited the sensitisation following nerve injury, but showed no effects following inflammatory stimulation. This is consistent with evidence that VIP expression in DRG is induced in neuropathic, but not inflammatory pain states. The regulation of the ERKs by the neuropathic-specific $VPAC_2$ receptor serves to isolate a specific signalling pathway that could represent a novel therapeutic target.

ELSEVIER

MCN Molecular and Cellular Neuroscience

www.elsevier.com/locate/ymcne
Mol. Cell. Neurosci. 30 (2005) 523 – 537

Activation of p38 and p42/44 MAP kinase in neuropathic pain: Involvement of $VPAC_2$ and NK_2 receptors and mediation by spinal glia

E.M. Garry,[a,1] A. Delaney,[a,1] G. Blackburn-Munro,[a,2] T. Dickinson,[a,3] A. Moss,[a,4] I. Nakalembe,[a,5] D.C. Robertson,[a] R. Rosie,[a] P. Robberecht,[b] R. Mitchell,[c] and S.M. Fleetwood-Walker [a,*]

[a]*Centre for Neuroscience, Division of Veterinary Biomedical Sciences, University of Edinburgh, EH9 1QH, UK*
[b]*Department of Biological Chemistry and Nutrition, Faculty of Medicine, Université Libre de Bruxelles, Brussels, Belgium*
[c]*Centre for Integrative Physiology, Membrane Biology Group, School of Biomedical and Clinical Laboratory Sciences, University of Edinburgh, EH8 9XD, UK*

Received 22 April 2005; revised 22 August 2005; accepted 26 August 2005
Available online 3 October 2005

Activation of intracellular signaling pathways involving p38 and p42/44 MAP kinases may contribute importantly to synaptic plasticity underlying spinal neuronal sensitization. Inhibitors of p38 or p42/44 pathways moderately attenuated responses of dorsal horn neurons evoked by mustard oil but not brush and alleviated the behavioral reflex sensitization seen following nerve injury. Activation of p38 and p42/44 MAP kinases in spinal cord ipsilateral to constriction injury was reduced by antagonists of NMDA, $VPAC_2$ and NK_2 (but not related) receptors, the glial inhibitor propentofylline and inhibitors of TNF-α. A $VPAC_2$ receptor agonist enhanced p38 phosphorylation and caused behavioral reflex sensitization in naïve animals that could be blocked by co-administration of p38 inhibitor. Conversely, an NK_2 receptor agonist activated p42/44 and caused behavioral sensitization that could be prevented by co-administration of p42/44 inhibitor. Thus, spinal p38 and p42/44 MAP kinases are activated in neuropathic pain states by mechanisms involving $VPAC_2$, NK_2, NMDA receptors and glial cytokine production.

Introduction

Peripheral nerve damage can result in chronic neuropathic pain that is resistant to current analgesic treatments. The p38 and p42/44 (ERK1/2) classes of mitogen-activated protein (MAP) kinases are thought to participate in chronic pain mechanisms. Phosphorylation of p38 MAP kinase is induced in the ipsilateral superficial dorsal horn of the spinal cord and dorsal root ganglia following peripheral nerve injury or inflammation, and inhibition prevents behavioral sensitization (Kim et al., 2002; Svensson et al., 2003; Jin et al., 2003; Ji et al., 2002a). Inflammation or C-fiber stimulation also induces phosphorylation of p44/42 MAP kinase in the trigeminal nucleus and the superficial dorsal horn and behavioral sensitization that is reversed by p42/44 MAP kinase inhibition (Huang et al., 2000; Ji et al., 1999, 2002a). Furthermore, these kinases are expressed not only in neurons but also in spinal glial cells, with sensory stimulus-induced activation of p38 and p42/44 MAP kinases being differentially localized to microglia and astrocytes, respectively (Jin et al., 2003; Ma and Quirion, 2002).

The MAP kinases can be activated by Ca^{2+}-permeable ionotropic receptors such as the NMDA receptor (Xia et al., 1996; Kawasaki et al., 1997) and by a variety of G-protein-coupled receptors (GPCRs) (Marinissen and Gutkind, 2001; Yamauchi et al., 1997). Such GPCRs in spinal cord include neurokinin (NK) and vasoactive intestinal polypeptide (VIP) receptors, both of which are prominently involved in nociception and hyperalgesia (Coderre and

Abbreviations: MAP kinase, mitogen-activated protein kinase; TNF-α, tumor necrosis factor-α; PPT, propentofylline; VIP, vasoactive intestinal polypeptide; PACAP, pituitary adenylate cyclase-activating peptide; CCI, chronic constriction injury.

* Corresponding author. Fax: +44 131 650 6576.
E-mail address: sfw@vet.ed.ac.uk (S.M. Fleetwood-Walker).

[1] Contributed equally to this work as joint first authors.

[2] Current address: NeuroSearch A/S, 93 Pederstrupvej, #DK-2750, Ballerup, Denmark.

[3] Current address: Department of Pharmacology, Quintiles Scotland Ltd., Heriot-Watt University Research Park, Edinburgh EH14 4AP, Scotland.

[4] Current address: Department of Anatomy and Developmental Biology, University College London, WC1E 6BT, UK.

[5] Current address: Department of Physiological Science, Faculty of Veterinary Medicine, Makerere University, Kampala, PO Box 7062, Uganda.

Available online on ScienceDirect (www.sciencedirect.com).

1044-7431/$ - see front matter © 2005 Elsevier Inc. All rights reserved.
doi:10.1016/j.mcn.2005.08.016

Melzack, 1992; Laird et al., 1993; Dickinson and Fleetwood-Walker, 1999). Neurokinin A (NKA), the endogenous ligand for NK_2 receptors, is localized to unmyelinated C-fibers, can produce spinal hyperexcitability and is depleted following nerve transection (Dalsgaard et al., 1985; Hökfelt et al., 1994; Ogawa et al., 1985; Xu et al., 1991). Furthermore, dorsal horn neuron excitability and sensitization following nerve injury can also be blocked by NK_2 receptor antagonists (Yashpal et al., 1996; Fleetwood-Walker et al., 1990; Coudoré-Civiale et al., 1998). NK_2 receptor binding sites are present in spinal cord (Quirion and Dam, 1988), where a substantial proportion is thought to be located on astrocytes (Zerari et al., 1998). The $VPAC_2$ receptor, a target for VIP, is normally present in spinal cord at low levels, but the expression of VIP in fine afferents and the $VPAC_2$ receptor in dorsal horn are increased following nerve injury (Nahin et al., 1994; Dickinson et al., 1999) that corresponds to the marked inhibitory effect of $VPAC_2$ receptor antagonists on neuropathic sensitization (Dickinson and Fleetwood-Walker, 1999; Dickinson et al., 1999). VIP and $VPAC_2$ receptors have been associated with glial regulation in spinal and other regions (Knyihár-Csillik et al., 1993; Brenneman et al., 1990).

It is becoming increasingly apparent that glial cells, namely astrocytes and microglia, are important in the generation and maintenance of chronic pain states (Watkins and Maier, 2002; Garrison et al., 1991). Glial activation in the spinal cord parallels the development of pain behaviors (Honore et al., 2000) and glial inhibitors such as fluorocitrate and minocycline attenuate allodynia and hyperalgesia in various nerve injury models (Watkins and Maier, 2002). Also, inhibitors of the synthesis and action of glially generated pro-inflammatory cytokine tumor necrosis factor-α (TNF-α), including propentofylline (PPT) and thalidomide, are analgesic in chronic pain states (Raghavendra et al., 2003a; George et al., 2000, Sommer et al., 1998a).

Here, we examined the activation of p38 and p42/44 MAP kinases in the spinal cord following nerve injury, their functional role in behavioral reflex sensitization and the contribution made by NK_2, $VPAC_2$ and NMDA receptors as well as spinal glial cells to these effects.

Results

Single dorsal horn neuronal responses to sensory stimulation are reduced by inhibitors of the MAP kinase pathway

Spinal MAP kinases are activated in response to noxious cutaneous stimuli and following C-fiber and noxious stimulation (Ji et al., 1999, 2002a; Galan et al., 2002). To investigate whether MAP kinases play a particular role in mechanisms of neuropathic sensitization, we examined the effects of MAP kinase inhibitors on brush and mustard oil-evoked responses of single dorsal horn neurons (DHNs) in neuropathic compared to control animals. Brush will activate low threshold mechanoreceptors, and mustard oil will activate high threshold polymodal nociceptors. CCI animals were used at the peak of injury-induced behavioral sensitivity and were compared with naïve animals. In parallel studies, the non-noxious 0.5-g and the noxious 25-g responses were increased from 3.8 ± 0.8 to 14.8 ± 4.2 action potentials per second and from 11.7 ± 1.8 to 22.8 ± 3.9 action potentials per second, respectively. We showed that following CCI, there was sensitization in both sensory ranges corresponding to the brush and mustard oil responses investigated here. We examined any differential effect on responses to sensory stimulation with the C-fiber selective algogen mustard oil compared to innocuous brush stimulation. In all of the DHNs studied, activation occurred in response to either innocuous brush or noxious mustard oil stimuli. The duration over which these ongoing stimuli were applied was typically about 50 min, and the firing rates reported here were generally well maintained through that period. These were recorded from depths previously characterized as corresponding to location in laminae III–V (Moss et al., 2002).

Ionophoresis of the p38 MAP kinase inhibitor SB 203580 (100 μM in 0.3% dimethylformamide/H_2O) had no significant effects on innocuous brush-evoked activity at currents up to 60 nA in either naïve (13 ± 12%, $n = 12$, Fig. 1a) or neuropathic rats (5 ± 6%, $n = 12$, Fig. 1c). In naïve animals, SB 203580 consistently caused a partial inhibition of mustard oil-evoked activity at 30–40 nA (by 38 ± 6%; paired t test, $P < 0.05$; $n = 11$, Fig. 1b), while there was often a much greater inhibition of neuronal responses in 6 out of 10 neurons from neuropathic animals at the lower current of 20 nA (by 58 ± 10%; paired t test, $P < 0.05$; $n = 10$, Fig. 1d). The remaining neurons were inhibited to a similar extent to those in naïve animals. Correspondingly, in naïve animals, following intravenous injection of SB 203580 (0.5–0.75 mg/kg), while neuronal activity due to brush stimulation of the peripheral receptive field was unchanged (increasing by only 2 ± 3%; $n = 3$), the mustard oil-evoked activity of these neurons was significantly reduced (by 45 ± 10% (paired t test, $P < 0.01$; $n = 6$). Administration of vehicle had no effect on either brush-evoked (6 ± 7% inhibition; $n = 4$) or mustard oil-evoked (1 ± 2% inhibition; $n = 4$) activation of DHNs.

Ionophoresis of the p42/44 MAP kinase pathway inhibitor PD 98059 (50 μM in 0.3% dimethylformamide/H_2O) had minimal effects on innocuous brush-evoked activity at currents up to 50 nA in naïve rats (8 ± 6% inhibition; $n = 8$, Fig. 2a), while there was moderate inhibition at low currents in neuropathic rats (46 ± 13%, paired t test, $P < 0.05$; $n = 7$, Fig. 2c). PD 98059 caused moderate but statistically significant reductions in mustard oil neuronal responses in naïve rats (paired t test, $P < 0.05$ in each case; Fig. 2b) which appeared to be greater in neuropathic rats (Fig. 2d). Although effects were generally more modest than those with the p38 inhibitor, the percentage inhibition of mustard oil-induced firing at low currents of PD 98059 (such as 20 nA) appeared to be consistently greater in neuropathic than in naïve animals (47 ± 8% and 26 ± 11%, respectively, $n = 6$). Neither of the kinase inhibitors affected spontaneous firing of neurons from naïve or neuropathic animals. Also, there was no discernible change in neuronal activity following the ejection of either saline or vehicle at currents up to 50 nA. These results indicate that both p38 and p42/44 MAP kinases may play a role in maintained activity of dorsal horn neurons following prolonged noxious stimulation but have minimal effects on innocuous transmission and suggest that both contribute to the central sensitization brought about by nerve injury.

Intrathecal injections of p38 or p42/44 MAP kinase pathway inhibitors attenuate neuropathic reflex sensitization following CCI

Since p38 and p42/44 MAP kinase pathway inhibitors affected single dorsal horn neuron responses to sensory stimulation, we next asked whether corresponding effects were observed on reflex pain behavior. Intrathecal administration of the p38 MAP kinase inhibitor SB 203580 (5 nmol in 0.3% dimethylformamide/saline, doses of 0.5 nmol and 20 nmol were also injected to investigate dose–response relationships) in rats at the peak of the ipsilateral

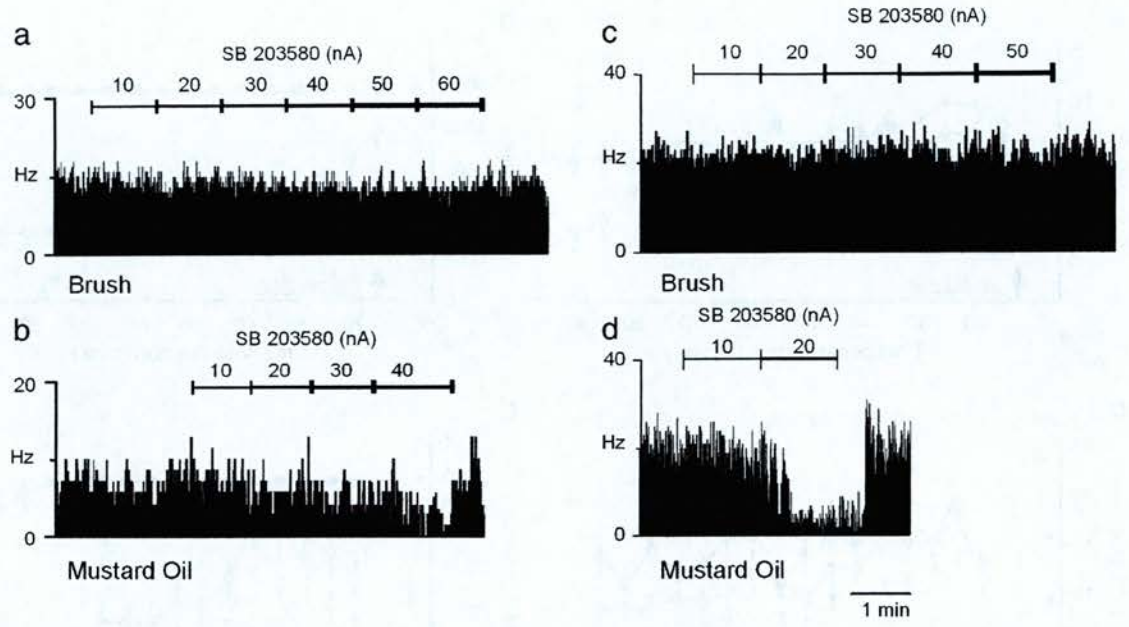

Fig. 1. Effects of ionophoretically applied SB 203580 (a p38 MAP kinase inhibitor) on evoked activity in spinal dorsal horn neurons. Records show typical examples of the effects of SB 203580 on the firing of individual neurons, driven by either continuous motorized brush (a) and (c) or mustard oil (b) or (d) applied to the cutaneous receptive field. Neuronal firing is displayed as action potentials per second (Hz), plotted against time. Brush-evoked firing was unaffected by SB 203580 at ionophoretic currents up to 60 nA in both naïve animals (a) and animals with established ipsilateral sensitization of behavioral reflexes following CCI (c). Mustard oil-evoked firing in naïve animals was inhibited in a current-dependent manner by SB 203580 ionophoresis (b), while that in CCI animals appeared to be reduced to a greater extent at lower currents (d). Full recovery after cessation of ionophoresis was seen in each case. Ionophoresis of SB 203580 at currents up to 60 nA had no apparent effect on spontaneous firing in naïve or CCI animals (data not shown). Vehicle or saline ejection at currents up to 60 nA had no effect on any neuronal activity (data not shown).

reflex sensitization following CCI caused a significant reversal of thermal hyperalgesia for 75 min post-injection (Fig. 3a) and of mechanical allodynia for 55 min post-injection (Fig. 3b). Similarly, intrathecal administration of the p42/44 MAP kinase pathway inhibitor PD 98059 (2.5 nmol in 0.3% dimethylformamide/saline, doses of 0.5 nmol and 7.5 nmol were also injected to investigate

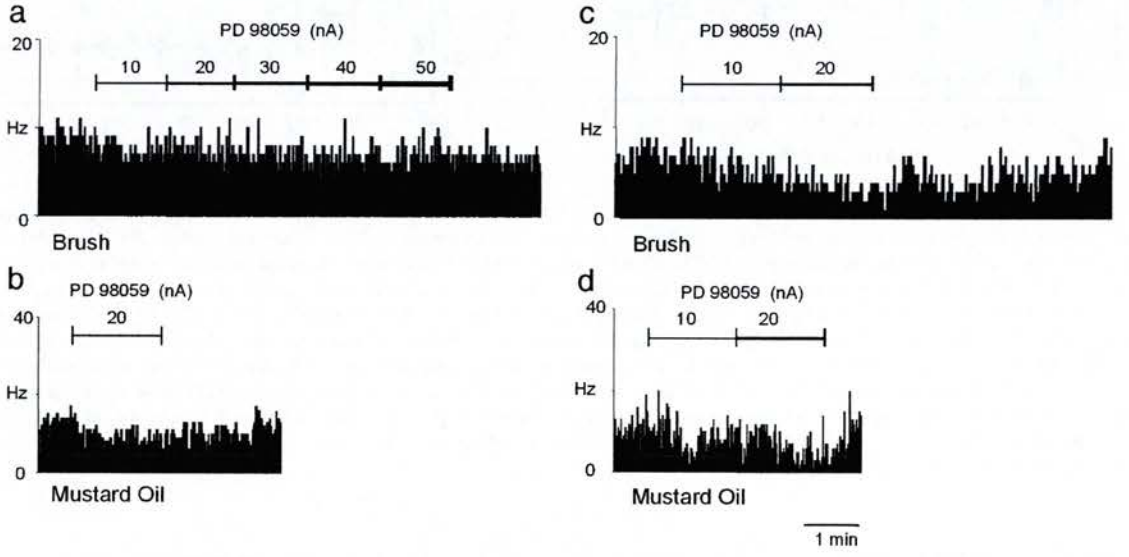

Fig. 2. Effects of ionophoretically applied PD 98059 (an inhibitor of the p42/44 MAP kinase pathway) on evoked activity in spinal dorsal horn neurons. Records show typical examples of the effects of PD 98059 on the ongoing firing of individual neurons, displayed as action potentials per second (Hz), plotted against time. Brush-evoked firing was unaffected by PD 98059 at ionophoretic currents up to 50 nA in naïve animals (a) but was moderately inhibited at low currents in animals with established ipsilateral sensitization of behavioral reflexes following CCI (c). Mustard oil-evoked activity in naïve animals was moderately inhibited by PD 98059 ionophoresis at low currents (b), while that in CCI animals appeared to be reduced to a greater extent at similar currents (d). Full recovery after cessation of ionophoresis was seen in each case. Ionophoresis of PD 98059 at currents up to 50 nA had no apparent effect on spontaneous firing in naïve or CCI animals (data not shown). Vehicle or saline ejection at currents up to 50 nA had no effect on any neuronal activity (data not shown).

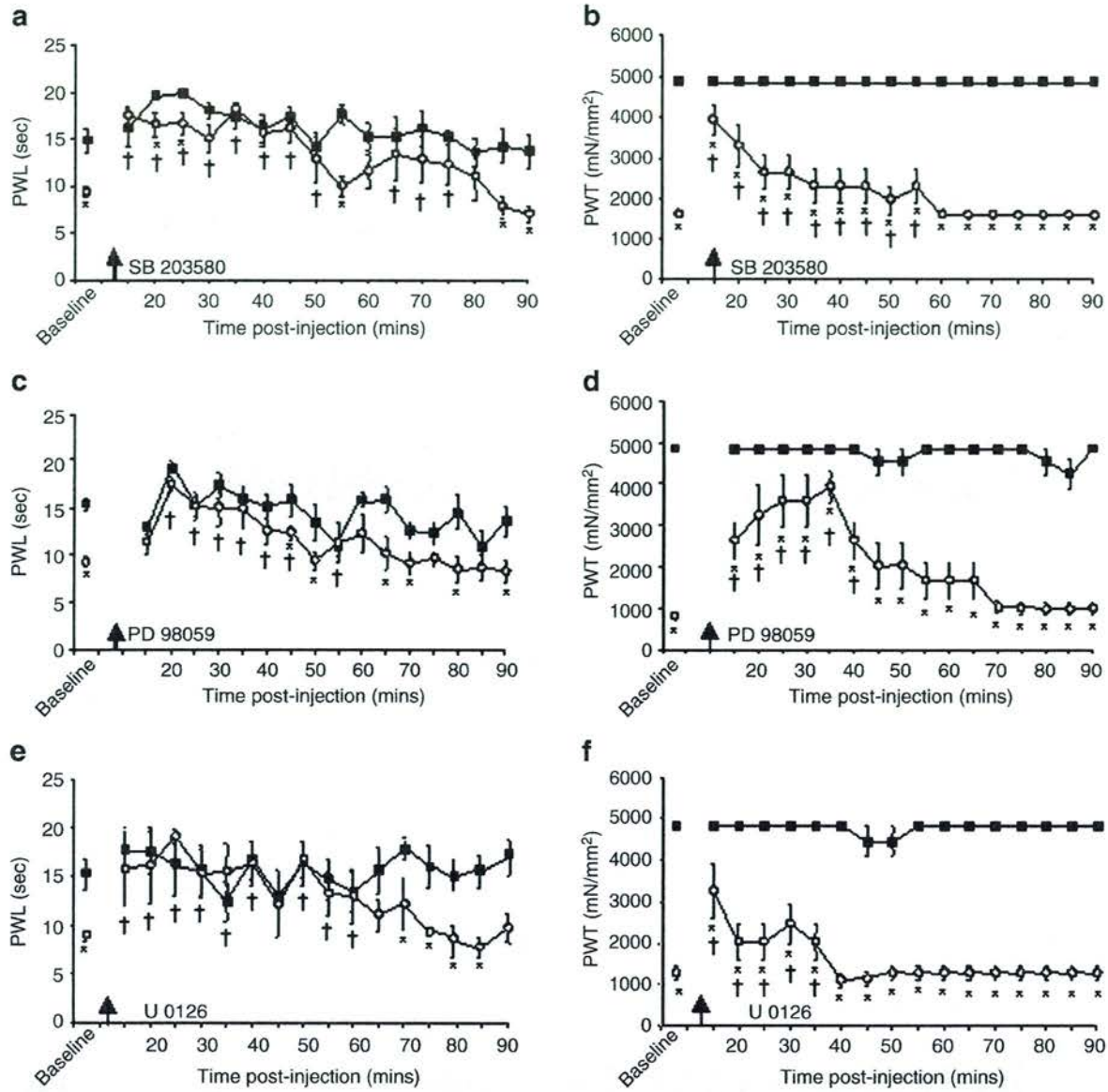

Fig. 3. Effects of the intrathecal administration of the p38 inhibitor SB 203580 and the p42/44 MAP kinase pathway inhibitors PD 98059 and U 0126 on nerve injury-induced thermal hyperalgesia and mechanical allodynia. Data represent the average hindlimb withdrawal latency (PWL; seconds) to noxious heat (a, c, e) and withdrawal threshold to mechanical stimuli (PWT; mN/mm^2; b, d, f) ± SEM before or following the intrathecal injection of either SB 203580 (5 nmol, a, b; $n = 6$), PD 98059 (2.5 nmol, c, d; $n = 6$) or U 0126 (1.5 nmol, e, f, $n = 8$). Rats were at the peak of ipsilateral reflex sensitization, as determined by a significant reduction in ipsilateral paw withdrawal latency to thermal stimuli (PWL; $^*P < 0.05$, Student's t test, a, c, e) or paw withdrawal threshold to mechanical stimuli (PWT; $^*P < 0.05$, Wilcoxon test, b, d, f; ○) compared to contralateral withdrawal responses (■). Following intrathecal injection (at arrow), SB 203580 (a), PD 98059 (c) and U 0126 (e) significantly increased ipsilateral thermal paw withdrawal latencies in comparison to pre-injection ipsilateral values ($^\dagger P < 0.05$, one-way repeated measures ANOVA followed by a Dunnett's test), while there was no significant alteration in the contralateral response. Graphs (b, d and f) show that the corresponding kinase inhibitors significantly increased ipsilateral mechanical paw withdrawal thresholds in comparison to pre-injection ipsilateral values ($^\dagger P < 0.05$, Friedman test followed by a Dunn's post-hoc test), while there was no significant alteration in the contralateral response. Full recovery to pre-drug response levels was seen in each case.

dose–response relationships) caused a significant reversal of thermal hyperalgesia for up to 55 min post-injection (Fig. 3c) and reversed the mechanical allodynia response for 40 min (Fig. 3d). A further p42/44 MAP kinase pathway inhibitor U 0126 (1.5 nmol in 0.3% dimethylformamide/saline) caused a significant inhibition of thermal hyperalgesia for 60 min post-injection (Fig. 3e) with a briefer (35 min) effect on mechanical allodynia (Fig. 3f). Full recovery to pre-injection response levels was documented in each case within the 90-min post-drug recording period of the experiment. An inactive analogue U 0124 at the same dose had minimal effects with the mean percent reversal of reflex sensitization over the first 35 min of drug administration being 9.7 ± 2.0% and 8.8% ± 4.3 for mechanical allodynia and thermal hyperalgesia, respectively (mean% ± SEM; $n = 7$). None of the compounds

tested had any significant effects on the contralateral hindpaw nor when administered to naïve animals (data not shown). These data indicate that either p38 or p42/44 MAP kinase pathway inhibition can alleviate peripheral nerve injury-induced sensitization. Intrathecal administration of a low dose (0.5 nmol) of SB 203580 caused no significant reversal of either thermal hyperalgesia (contralateral 16.4 ± 1.2 s; ipsilateral 9.3 ± 0.3 s) or mechanical allodynia (contralateral 4830.6 ± 0.0 mN/mm^2; ipsilateral 1188.4 ± 210.6 mN/mm^2). A higher dose (20 nmol) of SB 203580 caused a similar reversal of thermal hyperalgesia (contralateral 16.7 ± 0.8 s, ipsilateral 15.4 ± 2.2 s) and a moderately longer reversal (65 min) of mechanical allodynia (contralateral 4830.6 ± 0.0 mN/mm^2, ipsilateral 3828.7 ± 572.7 mN/mm^2) as was seen for the 5 nmol dose presented in Figs. 3a and b. Intrathecal administration of a low dose (0.5 nmol) of PD 98059 did not affect thermal hyperalgesia (contralateral 15.8 ± 0.9 s, ipsilateral 8.6 ± 1.8 s) or mechanical allodynia (contralateral 4830.6 ± 0.0 mN/mm^2, ipsilateral 1451.6 ± 141.3 mN/mm^2). A high dose (7.5 nmol) of PD 98059 caused a similar reversal of thermal hyperalgesia (contralateral 15.9 ± 1.7 s, ipsilateral 16.2 ± 3.0 s) for a longer time of 65 min and mechanical allodynia (contralateral 4830.6 ± 0.0 mN/mm^2, ipsilateral 3703.4 ± 501.3 mN/mm^2) for 40 min post-injection as was seen for the 2.5 nmol dose presented in Figs. 3c and d. These observations indicate that the partial inhibitory effects of the MAP kinase inhibitors were essentially of maximal magnitude at the doses shown in Fig. 3, but that some increases in the duration of effects were seen at higher doses.

The glial inhibitor propentofylline and the TNF-α inhibitor WP9QY both attenuate neuropathic reflex sensitization following CCI

Glial activation is now known to be involved in the genesis and maintenance of chronic pain (Watkins and Maier, 2002). We examined the effects of disrupting the function of both astrocytes and microglia using propentofylline (PPT). Glial release of TNF-α also contributes to chronic pain (Sommer et al., 1998a,b), thus we also examined any effects of the TNF-α receptor antagonist WP9QY following CCI-induced peak sensitivity. Intrathecal injection of PPT (0.5 μmol in saline and 1.5 μmol in saline; Figs. 4a, b) or WP9QY (0.025 mg in saline; Figs. 4c, d) reversed thermal hyperalgesia for 35–40 min and mechanical allodynia for 30–40 min. The higher dose (1.5 μmol) of PPT reversed thermal hyperalgesia for slightly longer (50 min) post-injection and reversed mechanical allodynia for the same amount of time (40 min) post-injection. Full recovery to pre-injection response levels was documented within 60 min post-drug in each case. These results suggest that both astrocytes and microglia could be involved in nerve injury-induced sensitization.

Involvement of specific receptors for afferent neuropeptide transmitters in behavioral reflex sensitization following nerve injury

In rats with established thermal hyperalgesia and mechanical allodynia following CCI, we intrathecally injected selective antagonists for $VPAC_1$ (0.1 nmol [Ac-His^1, D-Phe^2, Lys^{15}, Arg^{16}, Leu^{17}]-VIP (3–7) GRF (8–27)), $VPAC_2$ (0.1 nmol [des (1–4), Arg^{16}]-Ro 25–1553) and PAC_1 (0.1 nmol $PACAP_{6-38}$) receptors and for NK_1 (5 mol RP 67580) and NK_2 (5 nmol SR 48968) receptors. Although these agents had no significant effects on withdrawal responses in naïve animals or contralateral to CCI, $VPAC_2$ receptor and NK_2 receptor antagonists demonstrated marked antinociceptive effects on sensitized thermal and mechanical responses ipsilateral to CCI (Fig. 5, Table 1). Under identical conditions, the selective antagonists of $VPAC_1$, PAC_1 and NK_1 receptors caused only minor or no significant attenuation of such sensitized responses (Table 1). The PAC_1 receptor-selective antagonist is known to also have significant affinity for $VPAC_2$ receptors (Dickinson et al., 1999). These data emphasize the importance of $VPAC_2$ and NK_2 receptors in central sensitization following CCI.

Assessment of the effects of $VPAC_2$, NK_2 and NMDA receptor antagonists and glial inhibitors on MAP kinase activation

Following CCI, we found increases in the levels of phosphorylated (active) p38 (Fig. 6a) and phosphorylated (active) p42/44 (Fig. 5b) in the ipsilateral spinal cord in comparison to the contralateral spinal cord and naïve animals. The activation of p38 and p42/44 MAP kinases can occur via a number of routes. For example, NMDA and neurokinin 1 (NK_1) receptor stimulation can activate p38 and p42/44 MAP kinase elsewhere (Kawasaki et al., 1997; Fiebich et al., 2000; Svensson et al., 2003; Sweatt, 2001). In addition, antagonists of NMDA, NK_2 and $VPAC_2$ receptors block CCI-induced reflex sensitization (Fig. 5, Table 1; Mao et al., 1993; Coudoré-Civiale et al., 1998; Dickinson et al., 1999). Here, we further found that the enhanced activation (phosphorylation) of both p38 and p42/44 MAP kinase that occurred following CCI could be reduced by topical spinal application of NMDA, NK_2 and $VPAC_2$ receptor antagonists ((R)-CPP, SR 48968 and [des (1–4), Arg^{16}]-Ro 25–1553, respectively), but not saline vehicle (Figs. 6c, d and Table 2).

Glial cells are known to express p38 and p42/44 MAP kinases, so we examined any effects of glial blockade on MAP kinase activation. We show that the functional inhibitor of glia, PPT, as well as the TNF-α receptor antagonist WP9QY and the TNF-α synthesis inhibitor thalidomide could suppress increases in activation of p38 (Fig. 6c, Table 2) and p42/44 (Fig. 6d, Table 2) MAP kinases that occurred following CCI. There was no change in the overall (pan) levels of p38 or p42/44 MAP kinase following administration of these reagents (Figs. 6c and d, lower panels).

Activation of $VPAC_2$ and NK_2 receptors increases phosphorylation of p38 and p42/44 MAP kinases and causes behavioral reflex sensitization that is blocked by a glial inhibitor

Immunoblot analysis of naïve spinal cord following the topical application of the selective $VPAC_2$ receptor agonist Ro 25–1553 revealed a marked increase in the level of phosphorylated p38 MAP kinase in comparison to saline treatment (Fig. 7a, Table 3), while there was a lesser, but still significant activation of p38 MAP kinase following application of the NK_2 receptor agonist GR 64349 (Fig. 7a, Table 3).

Conversely, there was a much greater increase in levels of phosphorylated p42/44 MAP kinase following application of the NK_2 receptor agonist, GR 64349 than seen for $VPAC_2$ receptor agonist stimulation, although both were statistically significant (Fig. 7b, Table 3). Both $VPAC_2$ receptor and NK_2 receptor agonist-induced increases of either MAP kinase could be

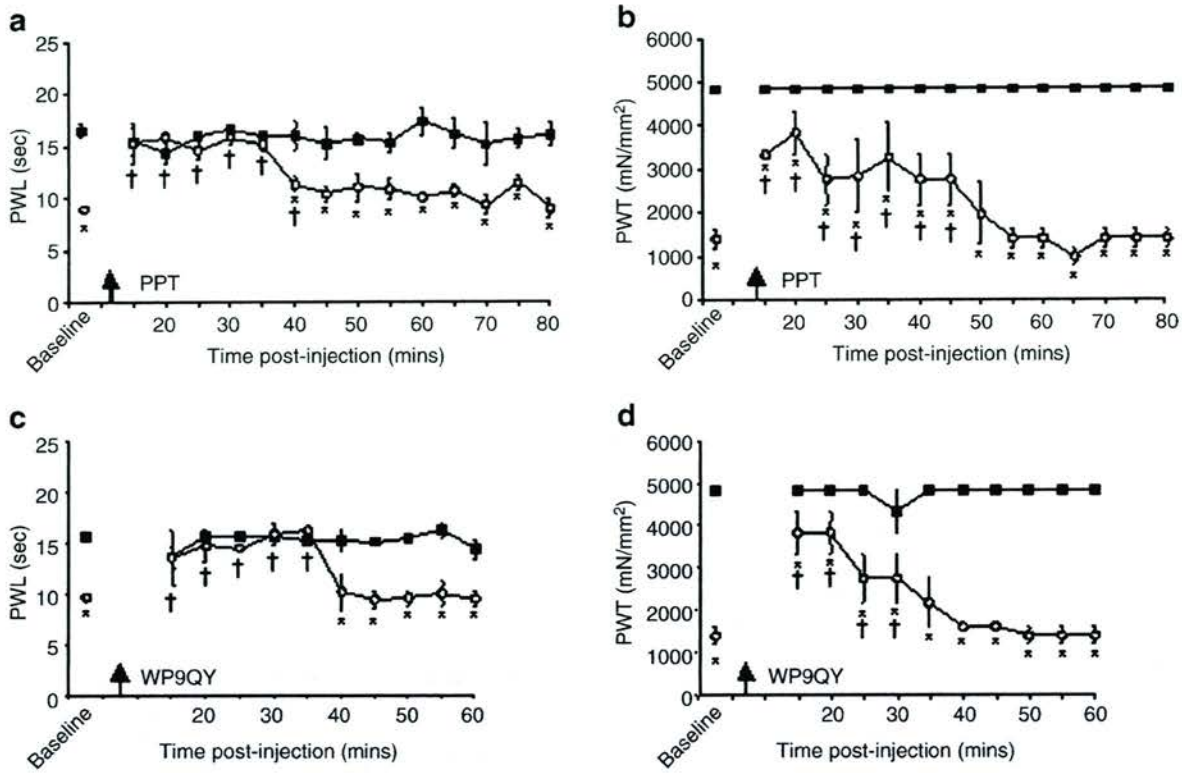

Fig. 4. The glial inhibitor propentofylline and the TNF-α receptor antagonist WP9QY reverse the behavioral sensitization that occurs following CCI. Data represent the average hindlimb withdrawal latency (PWL; seconds) to noxious heat (a, c) and withdrawal threshold to mechanical stimuli (PWT; mN/mm^2; b, d) ± SEM before or following the intrathecal injection of either propentofylline (0.5 μmol, PPT; a, b; $n = 5$) or WP9QY (0.025 mg, c, d; $n = 5$). Rats were used at the peak of ipsilateral reflex sensitization, as determined by a significant reduction in ipsilateral paw withdrawal latency to thermal stimuli (PWT; $^{*}P < 0.05$, Student's t test, a, c) or paw withdrawal threshold to mechanical stimuli (PWT; $^{*}P < 0.05$ Wilcoxon test, b, d; ○) compared to contralateral withdrawal responses (■). Both compounds significantly increased ipsilateral thermal paw withdrawal latencies (a, c) in comparison to pre-injection ipsilateral values ($^{\dagger}P < 0.05$, one-way repeated measures ANOVA followed by a Dunnett's test), while there was no significant alteration in the contralateral response. Similarly, both compounds significantly increased ipsilateral mechanical paw withdrawal thresholds in comparison to pre-injection values ($^{\dagger}P < 0.05$, Friedman test followed by a Dunn's post-hoc test), while there was no significant alteration in the contralateral response. Full recovery to pre-drug response levels was seen in each case.

reduced to saline control levels when agonists were co-administered with the glial inhibitor PPT (Figs. 7a and b, Table 3). Overall (pan) levels of either p38 or p42/44 MAP kinase did not significantly differ between any of the drug-treated groups (Figs. 7a and b).

To establish that agonist-induced responses in p38 or p42/44 phosphorylation were reflected in functional alterations of spinal responsiveness, we performed intrathecal injections with combinations of receptor agonist/kinase antagonist. For these experiments, we selected the receptor agonists that had caused the greatest change in either p38 or p42/44 phosphorylation. In naïve animals, intrathecal administration of the $VPAC_2$ receptor agonist Ro 25–1553 (0.5 nmol) caused bilateral behavioral sensitization to thermal stimuli (Fig. 7c) and mechanical stimuli (data not shown) that was abolished when Ro 25–1553 was co-administered with the p38 MAP kinase inhibitor, SB 203580 (5 nmol) (Fig. 7d). Similarly, the NK_2 receptor agonist GR 64349 produced bilateral behavioral sensitization to thermal stimuli (Fig. 7e) and mechanical stimuli (data not shown) that was blocked when GR 64349 (1.5 nmol) was co-administered with the p42/44 MAP kinase pathway inhibitor U 0126 (1.5 nmol) (Fig. 7f).

Discussion

The present data indicate that both p38 and p42/44 MAP kinases play an important role in mediating nociceptive afferent inputs at the spinal dorsal horn level. We show that p38 and p42/44 inhibitors attenuate the sensitization of individual dorsal horn neurons resulting from mustard oil application and inhibit the thermal and mechanical behavioral reflex sensitization that occurs following peripheral nerve constriction injury (CCI). The anti-nociceptive effects of MAP kinase pathway inhibitors were of rapid onset, probably on account of their delivery to the close proximity of the site of action by the ionophoretic technique, thereby minimizing diffusion distances. Additionally, inhibition of glial activation (propentofylline) or of TNF-α (using WP9QY or the synthesis inhibitor, thalidomide) reverses CCI-induced behavioral reflex sensitization. Furthermore, the enhanced phosphorylation of p38 and p42/44 MAP kinase that occurs in the ipsilateral spinal cord following CCI can be prevented by spinal application of the same TNF-α and glial inhibitors. The CCI-induced behavioral sensitization was prominently inhibited by $VPAC_2$ and NK_2 receptor antagonists, but only minimally by $VPAC_1$,

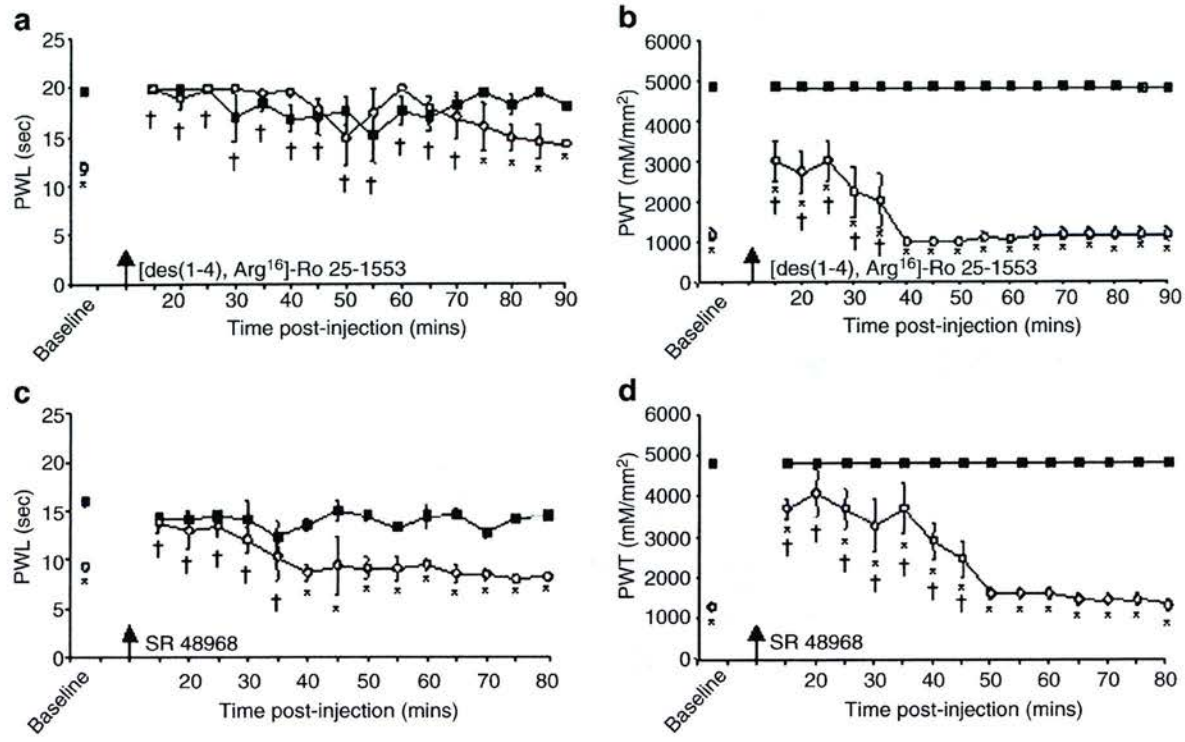

Fig. 5. $VPAC_2$ and NK_2 receptor antagonists reverse the behavioral sensitization that occurs following CCI. Data represent the average hindlimb withdrawal latency (PWL; seconds) to noxious heat (a, c) and withdrawal threshold to mechanical stimuli (PWT; mN/mm^2; b, d) ± SEM before or following the intrathecal injection of either a $VPAC_2$ receptor antagonist (0.1 nmol [des (1–4), Arg^{16}]-Ro 25–1553; a, b; $n = 7$) or an NK_2 receptor antagonist (5 nmol SR 48968; c, d; $n = 5$). Rats were used at the peak of ipsilateral reflex sensitization, as determined by a significant reduction in ipsilateral paw withdrawal latency to thermal stimuli (PWT; $^*P < 0.05$, Student's t test, a, c) or paw withdrawal threshold to mechanical stimuli (PWT; $^*P < 0.05$ Wilcoxon test, b, d; ○) compared to contralateral withdrawal responses (■). Both compounds significantly increased ipsilateral thermal paw withdrawal latencies (a, c) ($^\dagger P < 0.05$, one-way repeated measures ANOVA followed by a Dunnett's test) and ipsilateral mechanical paw withdrawal thresholds ($^\dagger P < 0.05$, Friedman test followed by a Dunn's post-hoc test) in comparison to pre-injection ipsilateral values. There was no significant alteration in the contralateral response. Full recovery to pre-drug response levels was seen in each case.

PAC_1 and NK_1 receptor antagonists. Correspondingly, the CCI-induced p38 and p42/44 phosphorylation is reduced by spinal application of $VPAC_2$ and NK_2 receptor antagonists and also by a blocker of the NMDA receptor, which is implicated in mechanisms of central sensitization. Agonist stimulation of spinal $VPAC_2$ (and to a lesser extent, NK_2) receptors increases the phosphorylation of p38 MAP kinase; a response that was inhibited by the glial inhibitor propentofylline. In addition, behavioral sensitization induced by a $VPAC_2$ receptor agonist in naïve rats was prevented when the p38 inhibitor SB 203580 was co-administered. Finally, agonist stimulation of NK_2 receptors induced phosphorylation of p42/44 MAP kinase to a greater extent than the $VPAC_2$ receptor agonist, and this again could be prevented by propentofylline. Correspondingly, the NK_2 receptor agonist-induced sensitization of behavioral responses in naïve rats was inhibited by co-administration of the p42/44 MAP kinase inhibitor U 0126. These results suggest that p38 and p42/44 activation in the spinal cord contributes to neuropathic sensitization, that spinal $VPAC_2$ receptors and NK_2 receptors are significant mediators of the p38 and p42/44 activation respectively, and that glial activation and TNF-α action may be important in both cases.

Table 1
Mean % reversal of ipsilateral sensitisation from 15 to 30 min following drug administration

Compound	Thermal hyperalgesia	Mechanical allodynia
$VPAC_1R$ antagonist	8.3 ± 2.0	12.4 ± 4.6
$VPAC_2R$ antagonist	93.6 ± 5.2*	41.2 ± 6.1*
PAC_1R antagonist	27.6 ± 4.1*	19.5 ± 3.3*
RP 67580 NK_1R antagonist	11.6 ± 4.8	22.9 ± 6.1*
SR 48968 NK_2R antagonist	89.6 ± 4.3*	73.2 ± 6.5*

Summary of the effects of intrathecal administration of $VPAC_2$, $VPAC_1$, PAC_1, NK_2 and NK_1 receptor antagonists on pain-related behavioral reflex responses. Data represent mean percent reversal ± SEM from 15 to 30 min following intrathecal injection of each compound for measurements of thermal hyperalgesia and mechanical allodynia in rats at the peak of ipsilateral reflex sensitivity. *Indicates a significantly attenuated ipsilateral thermal hyperalgesia ($P < 0.05$, one-way ANOVA followed by a Dunnett's test) or mechanical allodynia ($P < 0.05$, Kruskal–Wallis ANOVA followed by a Dunn's test) in comparison to pre-injection ipsilateral values at each of the time points throughout this period. There were no significant changes in contralateral responses at any time.

MAP kinases are known to be phosphorylated in sensory afferents and in the spinal cord following selective C-fiber stimulation or noxious stimulation (Ji et al., 1999, 2002a,b; Galan et al., 2002; Kim et al., 2002; Obata et al., 2003, 2004; Mizushima et al., 2005). Here, the increased responsiveness of dorsal horn neurons bought about by mustard oil stimulation of C-fibers and CCI-induced reflex sensitization could be reduced by inhibitors of either p38 or p42/44 pathways. These findings are in agreement with others

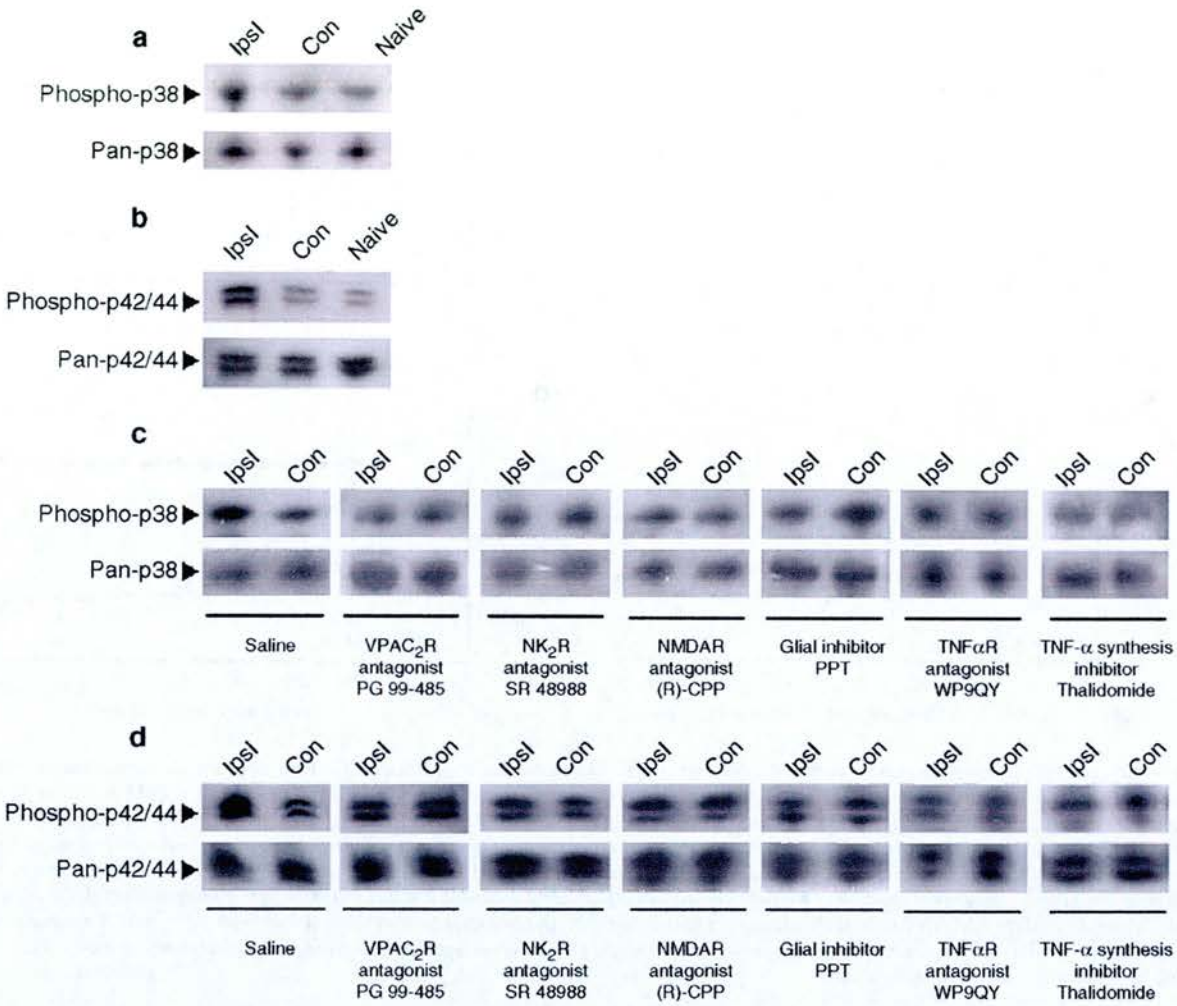

Fig. 6. Phospho-specific immunoblot evidence that $VPAC_2$, NK_2 and NMDA receptor antagonists and glial inhibitors can suppress activation of MAP kinases following CCI. Immunoblots from spinal cord samples at the peak of CCI-induced behavioral sensitization ($n = 5$) or naïve ($n = 5$) animals showing the expression levels of activated phospho-p38 (a) or phospho-p42/44 (b) (together with corresponding pan immunoreactivity for the kinases) on the side ipsilateral (ipsi) to CCI in comparison to the contralateral (con) side and naïve levels. CCI alone (CCI) caused an increase in the levels of activated phospho-p38 (a) and phospho-p42/44 (b) in the ipsilateral spinal cord compared to the contralateral side and naïve spinal samples. Topical application of antagonists to the $VPAC_2$ ([des (1–4), Arg^{16}]-Ro 25–1553), NK_2 (SR 48968) and NMDA ((R)-CPP) receptors to CCI spinal cords could all suppress the increased activation of both p38 (c) and p42/44 (d) MAP kinases, whereas saline vehicle had no effect. Similarly, topical application of the glial inhibitor propentofylline (PPT), an antagonist of the pro-inflammatory cytokine, TNF-α (WP9QY) and the inhibitor of TNF-α synthesis, thalidomide, could all inhibit p38 (a) and p42/44 (b) MAP kinase activation ipsilateral to CCI. No significant alterations occurred in the overall levels of p38 (pan-p38) or p42/44 (pan-p42/44) with any treatment (lower panels).

where p38 MAP kinase inhibition by intrathecal SB 203580 can suppress spinal nerve injury-induced allodynia, the hypersensitivity that occurs following substance P application and formalin- or Complete Freund's Adjuvant (CFA)-induced inflammation (Tsuda et al., 2004; Jin et al., 2003; Svensson et al., 2003). Similarly, inhibition of the p42/44 MAP kinase pathway with U 0126 reduces capsaicin-, inflammation- and nerve transection-induced hypersensitivity (Obata et al., 2003; Dai et al., 2002; Ji et al., 2002a).

Non-neuronal (glial) cell activation is now seen as a crucial component of the generation and maintenance of chronic pain states. Microglia and astrocytes can be activated in response to inflammation and peripheral nerve injury (Sweitzer et al., 1999; Hashizume et al., 2000; Garrison et al., 1991). Formalin, axotomy and nerve injury can activate p38 MAP kinase in microglia (Kim et al., 2002; Kawasaki et al., 1997; Jin et al., 2003; Svensson et al., 2003; Tsuda et al., 2004), and phosphorylation of p42/44 MAP kinase occurs in spinal neurons following peripheral inflammation and in astrocytes after partial nerve ligation (Ji et al., 1999; Ma and Quirion, 2002). It is now known that p42/44 is activated not only in neurons but also in microglia and astrocytes following nerve injury (Zhuang et al., 2005). The non-selective glial inhibitor propentofylline (which can decrease the activation of both spinal astrocytes and microglia) attenuates allodynia following spinal nerve transection (Sweitzer et al., 2001) and reduces formalin-induced inflammatory pain by suppressing TNF-α (Dorazil-Dudzik et al., 2004). Here, intrathecal propentofylline reversed the CCI-induced behavioral reflex sensitization. Minocycline, a blocker of microglial activation (Tikka et al., 2001) can inhibit MAP kinase activation caused by NMDA receptor stimulation (Tikka and Koistinaho, 2001) and prevent the development of pain behaviors

Table 2
Immunoblot densitometric ratio scores for phospho-p38:pan-p38 and phospho-p42/44:pan-p42/44 (arbitrary density units)

Treatment	CCI with saline		$VPAC_2$ receptor antagonist [des (1–4), Arg^{16}]-Ro 25–1553		NK_2 receptor antagonist SR 48968	
MAP kinase	Ipsi	Con	Ipsi	Con	Ipsi	Con
p38	63.5 ± 5.7*	48.4 ± 6.2	39.3 ± 7.3	35.8 ± 6.0	47.3 ± 5.5	45.6 ± 4.8
p42/44	56.1 ± 4.8*	35.9 ± 3.6	39.7 ± 4.4	41.4 ± 5.0	37.9 ± 3.9	37.1 ± 5.2
Treatment	NMDA receptor antagonist (R)-CPP		Glial inhibitor PPT		TNF-α receptor antagonist WP9QY	
MAP kinase	Ipsi	Con	Ipsi	Con	Ipsi	Con
p38	42.3 ± 7.6	44.1 ± 7.1	37.4 ± 5.9	39.8 ± 4.7	40.3 ± 5.0	36.3 ± 7.5
p42/44	39.6 ± 4.9	42.8 ± 4.3	30.9 ± 4.3	38.3 ± 4.6	41.3 ± 8.3	34.8 ± 5.2
Treatment	TNF-α synthesis inhibitor thalidomide		No treatment			
MAP kinase	Ipsi	Con	Naïve spinal cord			
p38	41.5 ± 6.8	39.6 ± 4.8	44.6 ± 4.6			
p42/44	35.0 ± 6.2	45.9 ± 6.9	39.6 ± 7.1			

Values are mean ± SEM values ($n = 5$) derived from quantitative densitometry of co-processed immunoblots (shown in Figs. 6c and d). p42/44 represents the mean value from the densitometric analysis of p42 and p44. Statistically significant differences in the ratio of phospho to pan immunoreactivity compared to the contralateral, uninjured side in saline controls are shown as $*P < 0.05$ by Wilcoxon test. The levels of p38 expression and p42/44 expression in naïve animals were not significantly different from those on the contralateral side of CCI animals treated with saline or indeed, with any other drugs.

following nerve injury (Raghavendra et al., 2003b). Astrocyte activation (in terms of increased GFAP expression) can occur following CCI and is thought to involve NMDA receptors (Garrison et al., 1994), although no microglial activation has been reported in this model (Colburn et al., 1997). The MAP kinase activation response following nerve injury may not however correspond directly to the classical astrocyte activation (GFAP expression) response. Nevertheless, minocycline or the inhibitor of TNF-α synthesis, thalidomide, is already known to be effective in reducing sensitization in various chronic pain models (Watkins and Maier, 2002; Raghavendra et al., 2003b; George et al., 2000; Sommer et al., 1998a), suggesting that increased TNF-α expression or release may contribute to sustained pain processing by further activation of p38 and/or p42/44 MAP kinases in glial cells.

Pro-inflammatory cytokines including TNF-α can be released from astrocytes and microglia in the CNS (Sawada et al., 1989), and spinal expression of TNF-α is upregulated after peripheral nerve injury (De Leo et al., 1997; Bartholdi and Schwab, 1997; Wagner and Myers, 1996). Local application of TNF-α to afferents induces pain and spontaneous activity in nociceptive fibers (Sorkin and Doom, 2000; Sorkin et al., 1997). Neutralizing antibody blockade of the TNF-α receptor 1 (TNRF1) can block CCI-induced pain in mice (Sommer et al., 1998b), and a TNF-α antagonist can attenuate nerve injury-induced allodynia behavior (Schäfers et al., 2003; Winkelstein et al., 2001). TNF-α activates p38 MAP kinase and inhibits glutamate uptake (Schäfers et al., 2003; Fine et al., 1996); both actions consistent with sensitization, while TNF-α blockade can reduce nerve injury-induced p38 activation (Svensson et al., 2005). Furthermore, thalidomide, which inhibits the synthesis of TNF-α (Sampaio et al., 1991), prevents behavioral sensitization following nerve injury (Sommer et al., 1998a) and reduces the CCI-induced increase in spinal TNF-α expression (George et al., 2000).

A variety of neurotransmitter receptors are expressed in glia as well as neurons. Neurokinins can stimulate glial production of IL-1 and TNF-α (Martin et al., 1992), and intrathecally applied substance P (SP) causes increased phosphorylation of p38 MAP kinase in microglia (Svensson et al., 2003). CFA-induced inflammation upregulates both NK_1 receptor and p42/44 MAP kinase activation in the same dorsal horn neurons (Ji et al., 2002a). However, NK_2 receptors have also been specifically implicated in NKA-induced enhancement of dorsal horn neuron responses to noxious cutaneous stimuli (Fleetwood-Walker et al., 1990). NK_2 receptor antagonists are antinociceptive when administered intrathecally following CCI (Coudoré-Civiale et al., 1998), and a non-peptide NK_2 receptor antagonist reduced sensitization of thermal and mechanical responses to a greater extent here than an NK_1 receptor antagonist of similar potency. The activation of p42/44 in dorsal horn following C-fiber stimulation is known to involve neuronal NMDA receptors (Lever et al., 2003). NK_2 receptors are located on spinal astrocytes (Zerari et al., 1998), also a site of p42/44 MAP kinase activation following nerve injury (Ma and Quirion, 2002), so the activation of p42/44 MAP kinase seen here could partly be the result of glial NK_2 receptor activation leading to cytokine release and facilitation of NMDA receptor function. It is not possible to exclude that at least part of the MAP kinase phosphorylation resulting from NK_2 receptor activation may be occurring indirectly in neurons downstream of glial activation. This may be consistent with the sensitivity of the MAP kinase response to the NMDA receptor antagonist since the relevant NMDA receptors may be neuronally located.

$VPAC_2$ receptors are also important in neuropathic pain (Dickinson and Fleetwood-Walker, 1999; Dickinson et al., 1999, 1997). The expression of the $VPAC_2$ receptor ligand vasoactive intestinal polypeptide (VIP) in small DRG cells (and decreased expression of SP) following nerve injury may represent a functional switch in the central mediation of nociception. VIP can also be expressed in spinal glial cells, and this is increased following nerve damage (Brenneman et al., 1990; Knyihár-Csillik et al., 1993). All subtypes of VIP receptor, including $VPAC_2$, have been reported in astrocytes (Grimaldi and Cavallaro, 1999; Jaworski, 2000; Joo et al., 2004), and p44 MAP kinase activation is reported to be induced by application of the broad-spectrum agonist PACAP in cultured astrocytes (Moroo et al., 1998). VIP is reported to elicit TNF-α release from cultured astrocytes, and injury-induced upregulation of TNF-α can be blocked by a $VPAC_1$ receptor agonist and p38 MAP kinase antagonists (Brenneman et al., 1990; Kim et al., 2000;

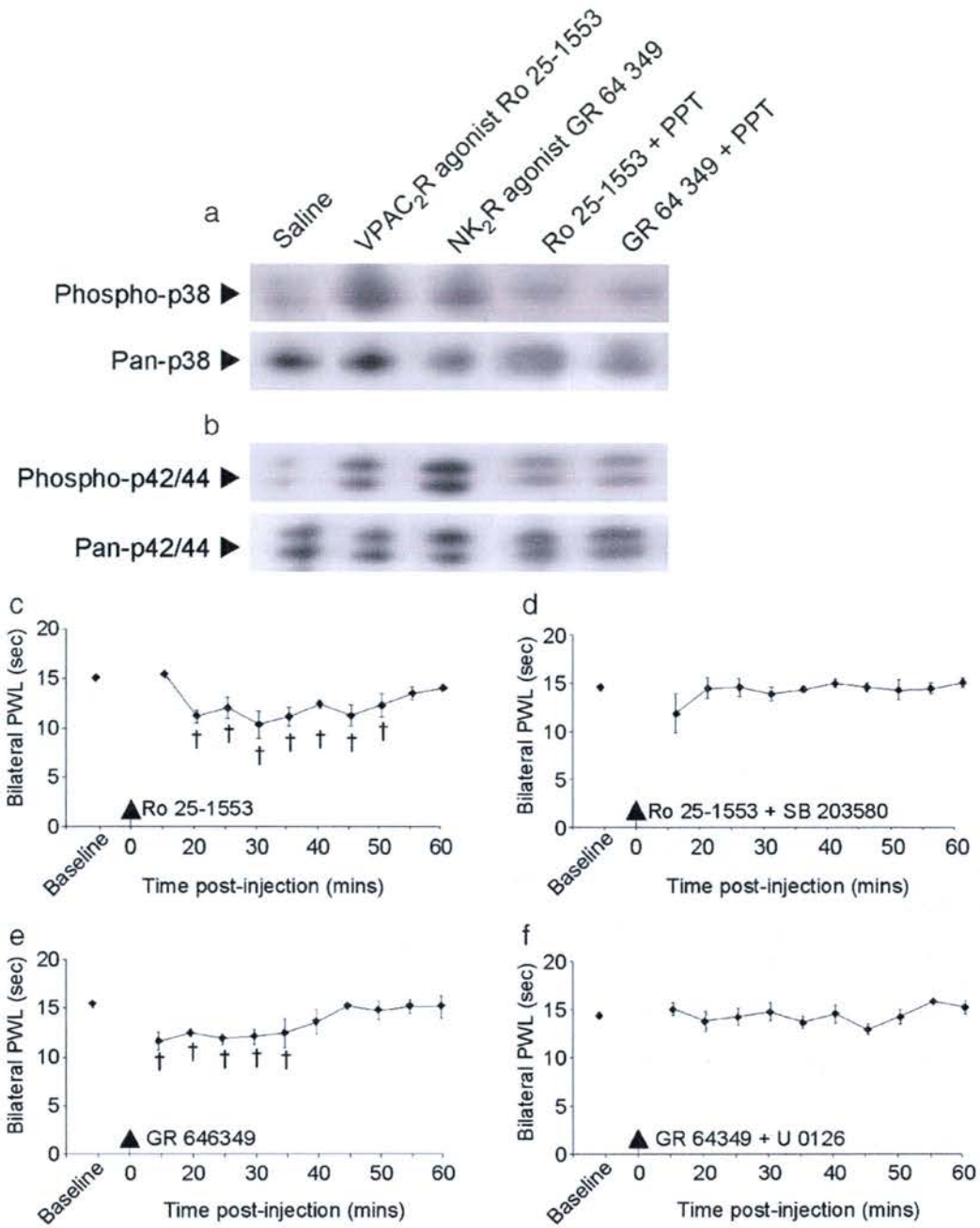

Fig. 7. Topical spinal application of $VPAC_2$ and NK_2 receptor agonists in naïve animals causes increased phosphorylation of p38 and p42/44 MAP kinase and behavioral reflex sensitization that can by blocked by MAP kinase and glial inhibitors. (a, b) Immunoblots from naïve spinal cord samples (n = 5 per treatment) following the topical application of either saline, Ro 25–1553 ($VPAC_2$ receptor agonist), GR 64349 (NK_2 receptor agonist), or either Ro 25–1553 or GR 64349 co-administered with propentofylline (PPT; glial inhibitor). Upper blots in panels (a) and (b) show the levels of immunoreactivity for activated (phosphorylated) 'phospho-p38' (a) and activated (phosphorylated) 'phospho-p42/44' (b). Lower panels show overall 'pan' levels for p38 (a) and p42/44 (b). In panel (a), $VPAC_2$ receptor agonist caused a relatively greater activation of p38 MAP kinase than did the NK_2 receptor agonist compared to saline, and both of these responses were prevented when agonists were co-administered with PPT. In panel (b), NK_2 receptor agonist caused a relatively greater activation of p42/44 MAP kinase than did the $VPAC_2$ receptor agonist, compared to saline, and both of these responses were prevented when PPT was co-applied. Minimal levels of phospho-p38 or phospho-p42/44 immunoreactivity were detected in controls where the saline vehicle control was topically applied instead. (c–f) Data represent bilateral hindpaw withdrawal latency (seconds) to noxious heat before and following the intrathecal injection of the $VPAC_2$ receptor agonist Ro 25–1553 alone (0.5 nmol) (c) or when co-administered with SB 203580 (5 nmol), (d) or the NK_2 receptor agonist GR 64349 alone (1.5 nmol), (e) or when co-administered with U 0126 (1.5 nmol) (f). Both agonists caused behavioral sensitization to thermal stimulation when administered alone (c, e) in comparison to pre-injection ipsilateral values ($^{\dagger}P < 0.05$, one-way repeated measures ANOVA followed by a Dunnett's test). The effects of Ro 25–1553 were blocked when it was co-administered with the p38 MAP kinase inhibitor SB 203580 (d). Similarly, the effects of GR 64349 were blocked when co-administered with the p42/44 MAP kinase pathway inhibitor U 0126 (f).

Table 3
Immunoblot densitometric ratio scores for phospho-p38:pan-p38 and phospho-p42/44:pan-p42/44 (arbitrary density units)

Treatment	Saline	$VPAC_2$ receptor agonist Ro 25–1553	NK_2 receptor agonist GR 646349	Ro 25–1553+PPT	GR 646349+PPT
p38 MAP kinase	36.5 ± 4.2	60.7 ± 6.3*	53.2 ± 4.8*	39.9 ± 5.3	43.3 ± 6.0
p42/44 MAP kinase	39.0 ± 7.3	67.1 ± 4.0*	94.4 ± 5.8*	34.8 ± 4.6	40.0 ± 5.7

Values are mean ± SEM values ($n = 5$) derived from quantitative densitometry of co-processed immunoblots (shown in Figs. 7a and b). Statistically significant differences in the ratio of phospho to pan immunoreactivity compared to saline controls are shown as $*P < 0.05$ by Wilcoxon test.

Schäfers et al., 2003). Acting through $VPAC_2$ receptors, VIP releases a mixture of cytokines, including TNF-α, from astrocytes to cause production of a neuroprotective factor and astrocytogenesis (Brenneman et al., 2003; Zusev and Gozes, 2004; Zupan et al., 1998). In contrast, VIP can inhibit TNF-α production (Delgado et al., 2003) by injury- or lipopolysaccharide-activated microglia but, in this case, via $VPAC_1$ receptors (Kim et al., 2000). Here, the behavioral reflex sensitization to thermal and mechanical stimuli following CCI was reduced by a highly selective $VPAC_2$ receptor antagonist, but only to little or no extent by PAC_1 or $VPAC_1$ receptor antagonists. Correspondingly, the p38 MAP kinase activation seen following nerve injury could be reduced to basal levels with topical spinal application of a $VPAC_2$ receptor antagonist and to a lesser extent by NK_2 receptor antagonist. Also, p38 MAP kinase phosphorylation could be evoked in naïve animals by the topical application of a $VPAC_2$ receptor agonist (and less so by an NK_2 receptor agonist), while the corresponding behavioral sensitization was inhibited by co-administration of the p38 MAP kinase inhibitor, SB 203580. Although our data do not specify that the p38 activation response is directly within $VPAC_2$ receptor-containing cells, taken together, these findings suggest that $VPAC_2$ receptors on spinal glial cells play a significant role in nerve injury-induced p38 activation and spinal sensitization.

In conclusion, it is clear that glia no longer can be viewed as playing a solely supportive role for spinal neurons. The present data add to an increasing body of evidence for the functional importance of glia in spinal somatosensory processing. These studies implicate $VPAC_2$, NK_2 and NMDA receptors in leading to the activation of p38 and p42/44 MAP kinases in spinal glial cells following afferent nerve injury and thereby contributing significantly to the mechanisms of sensitization underlying chronic neuropathic pain.

Experimental methods

All experiments were performed in accordance with the UK Animals (Scientific Procedures) Act, 1986.

Drugs

All drugs were purchased from Merck Biosciences (Nottingham, UK) unless otherwise stated and were administered in vehicle of 0–0.3% dimethylformamide (DMF) in deionized water for ionophoresis and in saline for other experiments. Previous experiments established that these vehicles had no discernable effect on neuronal firing, behavioral or biochemical responses. Drugs included the p38 inhibitor SB 203580, the p42/44 MAP kinase pathway inhibitors PD 98059 and U 0126 and its inactive analogue U 0124, the TNF-α receptor antagonist WP9QY (Takasaki et al., 1997), the TNF-α synthesis inhibitor thalidomide and the glial inhibitor propentofylline, PPT (Sigma-Aldrich, Poole, Dorset), the selective $VPAC_1$ receptor antagonist ([Ac-His^1, D-Phe^2, Lys^{15}, Arg^{16}, Leu^{17}]-VIP (3–7) GRF (8–27), gift from P. Robberecht), the selective $VPAC_2$ receptor antagonist, des (1–4), Arg^{16}-Ro25–1553 (gift from P, Robberecht), the selective $VPAC_2$ receptor agonist, Ro 25–1553 (gift from P. Robberecht), the selective PAC_1 receptor antagonist, PACAP 6–38 (Bachem UK Ltd., St. Helens, Merseyside), the selective NK_1 receptor antagonist, RP 65780 (gift from C Garret, Rhone-Poulenc Rorer), the selective NK_2 receptor antagonist, SR 48968 (gift from X. Emonds-Alt, Sanofi Recherche), the selective NK_2 receptor agonist GR 646349 (gift from P. Birch, Glaxo, Smith-Kline) and the selective NMDA receptor antagonist (R)-CPP (Tocris, Avonmouth, UK).

Antibodies

The following reagents were used: rabbit polyclonal antibodies specific to phospho-[Thr180/Tyr182]-p38 MAP kinase (1:250, Cell Signalling Technology Inc., Beverly, MA) and p38 MAP kinase ('pan': phosphorylation state-independent; 1:500, Cell Signalling), or phospho-[Thr1202/Tyr204]-p42/44 MAP kinase (1:250, Cell Signalling) and p42/44 MAP kinase ('pan': phosphorylation state-independent; 1:500, Cell Signalling), the housekeeping enzyme glyceraldehyde-3-phosphate dehydrogenase (GAPDH, 1:750, Chemicon International Ltd., Harrow, UK).

Methods

Chronic constriction injury

Adult male Wistar rats (250–320 g, Charles River, Kent, UK) were anesthetized with sodium pentobarbital (Sagatal 0.36 mg/kg, i.p.; Rhône Merieux, Essex, UK) and supplemented with halothane/O_2 (Zeneca, Cheshire, UK). Under aseptic conditions, a unilateral chronic constriction injury (CCI; Bennett and Xie (1988)) was induced as described previously (Garry et al., 2003).

Behavioral testing of neuropathic rats

Quantitative sensory reflex testing of mechanical allodynia and thermal hyperalgesia was performed to ensure each rat had developed maximal behavioral sensitization (typically 10–14 days post-surgery).

The latency of withdrawal (seconds) for thermal hyperalgesia was assessed with a Hargreaves' thermal stimulator (Linton Instrumentation, Diss, UK) for the uninjured contralateral and injured ipsilateral paw and recorded as the paw withdrawal latency (PWL). Mechanical allodynia was assessed with calibrated Semmes–Weinstein von Frey filaments (Stoelting, Wood Dale, Illinois, USA), and the indentation pressure (mN/mm^2) required to elicit a response in each hindpaw was recorded as the paw withdrawal threshold (PWT), as described previously (Moss et al.,

2002). Only animals with fully established maximal ipsilateral behavioral sensitization were used in the electrophysiology, intrathecal and immunoblotting experiments.

Electrophysiological recordings

Under initial halothane anesthesia, the jugular vein and trachea were cannulated in naïve control ($n = 8$) or neuropathic rats ($n = 7$). Animals were then anesthetized using intravenous α-chloralose (60 mg/kg) and urethane (1.2 mg/kg), with supplementary doses of α-chloralose given as required, enabling a laminectomy (segments L3–L6) to be performed, as described previously (Moss et al., 2002; Dickinson et al., 1997). Extracellular recordings were made from multireceptive single neurons located in laminae III–V of the spinal cord (ipsilateral to the nerve injury in neuropathic animals and from both sides of the cord in naïve rats), as described previously (Moss et al., 2002).

To investigate the involvement of the p38 and p42/44 MAP kinases in the processing of somatosensory information at the spinal cord level, the effects of the p38 inhibitor SB 203580 and the p42/44 inhibitor PD 98059 were examined on sustained sensory inputs in both normal and neuropathic animals. The inhibitors were applied by ionophoresis at increasing currents from 10 to 60 nA, over a set period of time, until clear effects were seen. The mean percentage inhibition was calculated through the 30-s period encompassing the maximal change from control, pre-drug firing levels.

Sustained innocuous inputs were produced by means of a motorized, rotating brush, giving a steady neuronal firing rate of 10–35 Hz. Also, a sustained noxious input was produced by hindpaw topical application of the C-fiber selective chemical algogen mustard oil. This irritant was repeatedly applied over an area of approximately 2 cm^2 and after 2–5 applications, separated by 5-min intervals, steady elevated firing rates were observed (9–30 Hz).

Intrathecal injections

For intrathecal injections, all drugs were administered at a volume of 50 μl in saline using a 25-gauge needle microsyringe (BD Biosciences, Oxford, UK), as described previously (Moss et al., 2002; Garry et al., 2003). The effects of intrathecal injection of the p38 MAP kinase inhibitor SB 203580 and the p42/44 MAP kinase pathway inhibitors PD 98059, U 0126 and its inactive analogue U 0124, the TNF-α receptor antagonist WP9QY and propentofylline (PPT) and selective antagonists of $VPAC_1$, $VPAC_2$, PAC_1, NK_1 and NK_2 receptors were examined in animals ($n = 6–8$ per drug) that had undergone chronic constriction injury and were at the peak of neuropathic behavioral reflex sensitization. We also assessed the effects of the intrathecal injection of a selective $VPAC_2$ receptor agonist, Ro 25–1553 or an NK_2 receptor agonist GR 64349 on the behavioral reflexes of naïve animals. In addition, we examined the effects of Ro 25–1553 co-administration with the p38 MAP kinase inhibitor SB 203580, or GR 64349 co-administration with the p42/44 pathway inhibitor U 0126 in naïve animals. Baseline measurements were recorded for thermal hyperalgesia (Hargreaves' test) and mechanical allodynia (von Frey filament test) immediately prior to injection. Then animals were briefly anesthetized with halothane and O_2 and intrathecally injected at the L5 level of the spinal cord with drug or vehicle controls. Testing began 15 min following injection (to allow for anesthetic recovery) and was performed at 5-min intervals for both tests until readings returned to baseline levels.

Immunoblotting

Tissue

In naïve animals, prior to removal of L3–6 spinal segments, the cord was treated (as described previously, Garry et al., 2003) with either saline control, the agonists for $VPAC_2$ receptor, Ro 25–1553 (30 μM) or NK_2 receptor, GR 64349 (50 μM) and either Ro 25–1553 or GR 64349 in combination with the glial inhibitor PPT (10 mM in saline; $n = 5$ per drug). In nerve-injured animals prior to the removal of L3–6 spinal segments, the cord was treated with either saline control, the $VPAC_2$ receptor antagonist ([des (1–4), Arg^{16}]-Ro 25–1553), the NMDA receptor antagonist ((R)-CPP; 10 μM in saline), PPT, a TNF-α receptor antagonist (WP9QY; 0.5 mg/ml) or the TNF-α synthesis inhibitor, thalidomide; 200 μM in 0.3% dimethylformamide/saline ($n = 5$ per drug). All drugs were left in contact with the cord for 30 min, then the spinal tissue (L3–6) was removed and hemisected to separate ipsilateral and contralateral sides, and samples were prepared for immunoblotting as described previously (Moss et al., 2002). Untreated CCI and naïve spinal cords ($n = 5$ per group) were prepared in parallel as a comparison. Homogenization was in standard Laemmli buffer and denatured at 100°C for 5 min. Extracts were separated by electrophoresis on pre-cast 10% polyacrylamide gels (BioRad, Hemel Hempstead, UK), transferred to PVDF membrane and blocked overnight at 4°C in 4% Marvel, 0.1% Tween-20. Blots were probed with rabbit polyclonal antibodies specific to [Thr180/Tyr182] phospho-p38 MAP kinase (1:250) and pan p38 MAP kinase ('pan': phosphorylation state-independent) (1:500), or [Thr1202/Tyr204] phospho-p42/44 MAP kinase (1:250, Cell Signalling) and pan p42/44 MAP kinase ('pan': phosphorylation state-independent) (1:500) and immunoreactive bands were detected by peroxidase-linked secondary antibody-enhanced chemiluminescence.

Blots were also probed for the ubiquitous housekeeping enzyme glyceraldehyde-3-phosphate dehydrogenase (GAPDH, 1:750, Chemicon) for protein level normalization. Relative levels of GAPDH between samples were similar to those of both pan p38 and pan p42/44 (data not shown). Densitometry was performed using 'Scan Analysis' software whereby grey levels of positive protein bands and background grey levels were quantitatively measured. The grey levels of the phosphorylated form of both p38 and p42/44 MAP kinases were meaned and calculated as densitometric ratios against pan MAP kinase levels.

Acknowledgments

This work was supported by The Wellcome Trust (S.F-W, EG and RM), the MRC (RM), BJA/RCA (DR), the MRC for the award of Studentships to AM and AD and The World Bank for supporting a studentship for IN. We thank the staff at the Medical Faculty Animal Area (MFAA) facilities for the animal husbandry.

References

Bartholdi, D., Schwab, M.E., 1997. Expression of pro-inflammatory cytokine and chemokine mRNA upon experimental spinal cord injury in mouse: an in situ hybridization study. Eur. J. Neurosci. 9, 1422–1438.

Bennett, G.J., Xie, Y.K., 1988. A peripheral mononeuropathy in rat that produces disorders of pain sensation like those seen in man. Pain 33, 87–107.

Brenneman, D.E., Nicol, T., Warren, D., Bowers, L.M., 1990. Vasoactive intestinal peptide: a neurotrophic releasing agent and an astroglial mitogen. J. Neurosci. Res. 25, 386–394.

Brenneman, D.E., Phillips, T.M., Hauser, J., Hill, J.M., Spong, C.Y., Gozes, I., 2003. Complex array of cytokines released by vasoactive intestinal peptide. Neuropeptides 37, 111–119.

Coderre, T.J., Melzack, R., 1992. The contribution of excitatory amino acids to central sensitisation and persistent nociception after formalin-induced tissue injury. J. Neurosci. 12, 3665–3670.

Colburn, R.W., DeLeo, J.A., Rickman, A.J., Yeager, M.P., Kwon, P., Hickey, W.F., 1997. Dissociation of microglial activation and neuropathic pain behaviors following peripheral nerve injury in the rat. J. Neuroimmunol. 79, 163–175.

Coudoré-Civiale, M.A., Courteix, C., Eschalier, A., Fialip, J., 1998. Effect of tachykinin receptor antagonists in experimental neuropathic pain. Eur. J. Pharmacol. 361, 175–184.

Dai, Y., Iwata, K., Fukuoka, T., Kondo, E., Tokunaga, A., Yamanaka, H., Tachibana, T., Liu, Y., Noguchi, K., 2002. Phosphorylation of extracellular signal-regulated kinase in primary afferent neurons by noxious stimuli and its involvement in peripheral sensitization. J. Neurosci. 22, 7737–7745.

Dalsgaard, C.J., Haegerstrand, A., Theodorsson-Norheim, E., Brodin, E., Hökfelt, T., 1985. Neurokinin A-like immunoreactivity in rat primary sensory neurons; coexistence with substance P. Histochemistry 83, 37–39.

De Leo, J.A., Colburn, R.W., Rickman, A.J., 1997. Cytokine and growth factor immunohistochemical spinal profiles in two animal models of mononeuropathy. Brain Res. 759, 50–57.

Delgado, M., Leceta, J., Ganea, D., 2003. Vasoactive intestinal peptide and pituitary adenylate cyclase-activating polypeptide inhibit the production of inflammatory mediators by activated microglia. J. Leukocyte Biol. 73 (1), 155–164.

Dickinson, T., Fleetwood-Walker, S.M., 1999. VIP and PACAP: very important in pain? Trends Pharmacol. Sci. 20, 324–329.

Dickinson, T., Fleetwood-Walker, S.M., Mitchell, R., Lutz, E.M., 1997. Evidence for roles of vasoactive intestinal polypeptide (VIP) and pituitary adenylate cyclase activating polypeptide (PACAP) receptors in modulating the responses of rat dorsal horn neurons to sensory inputs. Neuropeptides 31, 175–185.

Dickinson, T., Mitchell, R., Robberecht, P., Fleetwood-Walker, S.M., 1999. The role of VIP/PACAP receptor subtypes in spinal somatosensory processing in rats with an experimental peripheral mononeuropathy. Neuropharmacology 38, 167–180.

Dorazil-Dudzik, M., Mika, J., Schafer, M.K., Li, Y., Obara, I., Wordliczek, J., Przewlocka, B., 2004. The effects of local pentoxifylline and propentofylline treatment on formalin-induced pain and tumor necrosis factor-alpha messenger RNA levels in the inflamed tissue of the rat paw. Anesth. Analg. 98, 1566–1573.

Fiebich, B.L., Schleicher, S., Butcher, R.D., Craig, A., Lieb, K., 2000. The neuropeptide substance P activates p38 mitogen-activated protein kinase resulting in IL-6 expression independently from NF-κB. J. Immunol. 165, 5606–5611.

Fine, S.M., Angel, R.A., Perry, S.W., Epstein, L.G., Rothstein, J.D., Dewhurst, S., Gelbard, H.A., 1996. Tumor necrosis factor alpha inhibits glutamate uptake by primary human astrocytes. Implications for pathogenesis of HIV-1 dementia. J. Biol. Chem. 271, 15303–15306.

Fleetwood-Walker, S.M., Mitchell, R., Hope, P.J., El-Yassir, N., Molony, V., Bladon, C.M., 1990. The involvement of neurokinin receptor subtypes in somatosensory processing in the superficial dorsal horn of the cat. Brain Res. 519, 169–182.

Galan, A., Lopez-Garcia, J.A., Cervero, F., Laird, J.M., 2002. Activation of spinal extracellular signaling-regulated kinase-1 and -2 by intraplantar carrageenan in rodents. Neurosci. Lett. 322, 37–40.

Garrison, C.J., Dougherty, P.M., Kajander, K.C., Carlton, S.M., 1991. Staining of glial fibrillary acidic protein (GFAP) in lumbar spinal cord increases following a sciatic nerve constriction injury. Brain Res. 565, 1–7.

Garrison, C.J., Dougherty, P.M., Carlton, S.M., 1994. GFAP expression in lumbar spinal cord of naïve and neuropathic rats treated with MK-801. Exp. Neurol. 129, 237–243.

Garry, E.M., Moss, A., Rosie, R., Delaney, A., Mitchell, R., Fleetwood-Walker, S.M., 2003. Specific involvement in neuropathic pain of AMPA receptors and adapter proteins for the GluR2 subunit. Mol. Cell. Neurosci. 24, 10–22.

George, A., Marziniak, M., Schafers, M., Toyka, K.V., Sommer, C., 2000. Thalidomide treatment in chronic constrictive neuropathy decreases endoneurial tumor necrosis factor-alpha, increases interleukin-10 and has long-term effects on spinal cord dorsal horn met-enkephalin. Pain 88, 267–275.

Grimaldi, M., Cavallaro, S., 1999. Functional and molecular diversity of PACAP/VIP receptors in cortical neurons and type I astrocytes. Eur. J. Neurosci. 11, 2767–2772.

Hashizume, H., DeLeo, J.A., Colburn, R.W., Weinstein, J.N., 2000. Spinal glial activation and cytokine expression after lumbar root injury in the rat. Spine 25, 1206–1217.

Hökfelt, T., Zhang, X., Wiesenfeld-Hallin, Z., 1994. Messenger plasticity in primary sensory neurons following axotomy and its functional implications. Trends Neurosci. 17, 22–30.

Honore, P., Rogers, S.D., Schwei, M.J., Salak-Johnson, J.L., Luger, N.M., Sabino, M.C., Clohisy, D.R., Mantyh, P.W., 2000. Murine models of inflammatory, neuropathic and cancer pain each generates a unique set of neurochemical changes in the spinal cord and sensory neurons. Neuroscience 98, 585–598.

Huang, W.J., Wang, B.R., Yao, L.B., Huang, C.S., Wang, X., Zhang, P., Jiao, X.Y., Duan, X.L., Chen, B.F., Ju, G., 2000. Activity of p44/42 MAP kinase in the caudal subnucleus of trigeminal spinal nucleus is increased following perioral noxious stimulation in the mouse. Brain Res. 861, 181–185.

Jaworski, D.M., 2000. Expression of pituitary adenylate cyclase-activating polypeptide (PACAP) and the PACAP-selective receptor in cultured rat astrocytes, human brain tumors, and in response to acute intracranial injury. Cell Tissue Res. 300, 219–230.

Ji, R.R., Baba, H., Brenner, G.J., Woolf, C.J., 1999. Nociceptive-specific activation of ERK in spinal neurons contributes to pain hypersensitivity. Nat. Neurosci. 2, 1114–1119.

Ji, R.R., Befort, K., Brenner, G.J., Woolf, C.J., 2002a. ERK MAP kinase activation in superficial spinal cord neurons induces prodynorphin and NK-1 upregulation and contributes to persistent inflammatory pain hypersensitivity. J. Neurosci. 22, 478–485.

Ji, R.R., Samad, T.A., Jin, S.X., Schmoll, R., Woolf, C.J., 2002b. p38 MAP activation by NGF in primary sensory neurons after inflammation increases TRPV1 levels and maintains heat hyperalgesia. Neuron 36, 57–66.

Jin, S.X., Zhuang, Z.Y., Woolf, C.J., Ji, R.R., 2003. p38 mitogen-activated protein kinase is activated after a spinal nerve ligation in spinal cord microglia and dorsal root ganglion neurons and contributes to the generation of neuropathic pain. J. Neurosci. 23, 4017–4022.

Joo, K.M., Chung, Y.H., Kim, M.K., Nam, R.H., Lee, B.L., Lee, K.H., Cha, C.I., 2004. Distribution of vasoactive intestinal polypeptide and pituitary adenylate cyclase-activating polypeptide receptors (VPAC1, VPAC2, and PAC1 receptor) in the rat brain. J. Comp. Neurol. 476, 388–413.

Kawasaki, H., Morooka, T., Shimohama, S., Kimura, J., Hirano, T., Gotoh, Y., Nishida, E., 1997. Activation and involvement of p38 mitogen-activated protein kinase in glutamate-induced apoptosis in rat cerebellar granule cells. J. Biol. Chem. 272 (30), 18518–18521.

Kim, W.K., Kan, Y., Ganea, D., Hart, R.P., Gozes, I., Jonakait, G.M., 2000. Vasoactive intestinal peptide and pituitary adenylyl cyclase-activating polypeptide inhibit tumor necrosis factor-alpha production in injured spinal cord and in activated microglia via a cAMP-dependent pathway. J. Neurosci. 20 (10), 3622–3630.

Kim, S.Y., Bae, J.C., Kim, J.Y., Lee, H.L., Lee, K.M., Kim, D.S., Cho, H.J., 2002. Activation of p38 MAP kinase in the rat dorsal root ganglia and

spinal cord following peripheral inflammation and nerve injury. NeuroReport 13 (18), 2483–2486.

Knyihár-Csillik, E., Kreutzberg, G.W., Csillik, B., 1993. Fine structural correlates of VIP-like immunoreactivity in the upper spinal dorsal horn after peripheral axotomy: possibilities of a neuro-glial translocation of a neuropeptide. Acta Histochem. 94 (1), 1–12.

Laird, J.M.A., Hargreaves, R.J., Hill, R.G., 1993. Effect of RP 67580, a non-peptide neurokinin1 receptor antagonist on facilitation of a nociceptive spinal flexion reflex in the rat. Br. J. Pharmacol. 109, 713–718.

Lever, I.J., Pezet, S., McMahon, S.B., Malcangio, M., 2003. The signaling components of sensory fibre transmission involved in the activation of ERK MAP kinase in the mouse dorsal horn. Mol. Cell. Neurosci. 24 (2), 259–270.

Ma, W., Quirion, R., 2002. Partial sciatic nerve ligation induces increase in the phosphorylation of extracellular signal-regulated kinase (ERK) and c-Jun N-terminal kinase (JNK) in astrocytes in the lumbar spinal dorsal horn and the gracile nucleus. Pain 99 (1–2), 175–184.

Mao, J., Price, D.D., Hayes, R.L., Lu, J., Mayer, D.J., Frenk, H., 1993. Intrathecal treatment with dextrorphan or ketamine potently reduces pain-related behaviors in a rat model of peripheral mononeuropathy. Brain Res. 605 (1), 164–168.

Marinissen, M.J., Gutkind, J.S., 2001. G-protein-coupled receptors and signaling networks: emerging paradigms. Trends Pharmacol. Sci. 22 (7), 368–376.

Martin, F.C., Charles, A.C., Sanderson, M.J., Merrill, J.E., 1992. Substance P stimulates IL-1 production by astrocytes via intracellular calcium. Brain Res. 599 (1), 13–18.

Mizushima, T., Obata, K., Yamanaka, H., Dai, Y., Fukuoka, T., Tokunaga, A., Mashimo, T., Noguchi, K., 2005. Activation of p38 MAPK in primary afferent neurons by noxious stimulation and its involvement in the development of thermal hyperalgesia. Pain 113, 51–60.

Moroo, I., Tatsuno, I., Uchida, D., Tanaka, T., Saito, J., Saito, Y., Hirai, A., 1998. Pituitary adenylate cyclase activating polypeptide (PACAP) stimulates mitogen-activated protein kinase (MAPK) in cultured rat astrocytes. Brain Res. 795 (1–2), 191–196.

Moss, A., Blackburn-Munro, G., Garry, E.M., Blakemore, J.A., Dickinson, T., Rosie, R., Mitchell, R., Fleetwood-Walker, S.M., 2002. A role of the ubiquitin-proteasome system in neuropathic pain. J. Neurosci. 22 (4), 1363–1372.

Nahin, R.L., Ren, K., De León, M., Ruda, M., 1994. Primary sensory neurons exhibit altered gene expression in a rat model of neuropathic pain. Pain 58, 95–108.

Obata, K., Yamanaka, H., Dai, Y., Tachibana, T., Fukuoka, T., Tokunaga, A., Yoshikawa, H., Noguchi, K., 2003. Differential activation of extracellular signal-regulated protein kinase in primary afferent neurons regulates brain-derived neurotrophic factor expression after peripheral inflammation and nerve injury. J. Neurosci. 23 (10), 4117–4126.

Obata, K., Yamanaka, H., Dai, Y., Mizushima, T., Fukuoka, T., Tokunaga, A., Noguchi, K., 2004. Differential activation of MAPK in inured and uninjured DRG neurons following chronic constriction injury of the sciatic nerve in rats. Eur. J. Neurosci. 20, 2881–2895.

Ogawa, T., Kanazawa, I., Kimura, S., 1985. Regional distribution of substance P, neurokinin alpha and neurokinin beta in rat spinal cord, nerve roots and dorsal root ganglia, and the effects of dorsal root section or spinal transection. Brain Res. 359 (1–2), 152–157.

Quirion, R., Dam, T.-V., 1988. Multiple tachykinin receptors: recent developments. Regul. Pept. 22, 18–25.

Raghavendra, V., Flobert Tanga, F., Rutkowski, M.D., DeLeo, J.A., 2003a. Anti-hyperalgesic and morphine-sparing actions of propentofylline following peripheral nerve injury in rats: mechanistic implications of spinal glia and proinflammatory cytokines. Pain 104 (3), 655–664.

Raghavendra, V., Tanga, F., DeLeo, J.A., 2003b. Inhibition of microglial activation attenuates the development but not existing hypersensitivity in a rat model of neuropathy. J. Pharmacol. Exp. Ther. 306 (2), 624–630.

Sampaio, E.P., Sarno, E.N., Galilly, R., Cohn, Z.A., Kaplan, G., 1991. Thalidomide selectively inhibits tumor necrosis factor alpha production by stimulated human monocytes. J. Exp. Med. 173, 699–703.

Sawada, M., Kondo, N., Suzumura, A., Marunouchi, T., 1989. Production of tumor necrosis factor—αby microglia and astrocytes in culture. Brain Res. 491, 394–397.

Schäfers, M., Svensson, C.I., Sommer, C., Sorkin, L.S., 2003. Tumor necrosis factor-alpha induces mechanical allodynia after spinal nerve ligation by activation of p38 MAPK in primary sensory neurons. J. Neurosci. 23 (7), 2517–2521.

Sommer, C., Marziniak, M., Myers, R.R., 1998a. The effect of thalidomide treatment on vascular pathology and hyperalgesia caused by chronic constriction injury of rat nerve. Pain 74, 83–91.

Sommer, C., Schmidt, C., George, A., 1998b. Hyperalgesia in experimental neuropathy is dependent on the TNF receptor 1. Exp. Neurol. 151 (1), 138–142.

Sorkin, L.S., Doom, C.M., 2000. Epineurial application of TNF elicits an acute mechanical hyperalgesia in the awake rat. J. Peripher. Nerv. Syst. 5 (2), 96–100.

Sorkin, L.S., Xiao, W.H., Wagner, R., Myers, R.R., 1997. Tumour necrosis factor-alpha induces ectopic activity in nociceptive primary afferent fibres. Neuroscience 81 (1), 255–262.

Svensson, C.I., Marsala, M., Westerlund, A., Calcutt, N.A., Campana, W.M., Freshwater, J.D., Catalano, R., Feng, Y., Protter, A.A., Scott, B., Yaksh, T.L., 2003. Activation of p38 mitogen-activated protein kinase in spinal microglia is a critical link in inflammation-induced spinal pain processing. J. Neurochem. 86 (6), 1534–1544.

Svensson, C.I., Schafers, M., Jones, T.L., Powell, H., Sorkin, L.S., 2005. Spinal blockade of TNF blocks spinal nerve ligation-induced increases in spinal P-p38. Neurosci. Lett. 379 (3), 209–213.

Sweatt, J.D., 2001. The neuronal MAP kinase cascade: a biochemical signal integration system subserving synaptic plasticity and memory. J. Neurochem. 76, 1–10.

Sweitzer, S.M., Colburn, R.W., Rutkowski, M., DeLeo, J.A., 1999. Acute peripheral inflammation induces moderate glial activation and spinal IL-1beta expression that correlates with pain behavior in the rat. Brain Res. 829 (1–2), 209–221.

Sweitzer, S.M., Schubert, P., DeLeo, J.A., 2001. Propentofylline, a glial modulating agent, exhibits antiallodynic properties in a rat model of neuropathic pain. J. Pharmacol. Exp. Ther. 297 (3), 1210–1217.

Takasaki, W., Kajino, Y., Kajino, K., Murali, R., Greene, M.I., 1997. Structure-based design and characterization of exocyclic peptidomimetics that inhibit TNF alpha binding to its receptor. Nat. Biotechnol. 15, 1266–1270.

Tikka, T.M., Koistinaho, J.E., 2001. Minocycline provides neuroprotection against *N*-methyl-D-aspartate neurotoxicity by inhibiting microglia. J. Immunol. 166, 7527–7533.

Tikka, T., Fiebich, B.L., Goldsteins, G., Keinanen, R., Koistinaho, J., 2001. Minocycline, a tetracycline derivative, is neuroprotective against excitotoxicity by inhibiting activation and proliferation of microglia. J. Neurosci. 21, 2580–2588.

Tsuda, M., Mizokoshi, A., Shigemoto-Mogami, Y., Koizumi, S., Inoue, K., 2004. Activation of p38 mitogen-activated protein kinase in spinal hyperactive microglia contributes to pain hypersensitivity following peripheral nerve injury. Glia 45, 89–95.

Wagner, R., Myers, R.R., 1996. Schwann cells produce TNF-alpha: expression in injured and non-injured nerves. Neuroscience 73, 625–629.

Watkins, L.R., Maier, S.F., 2002. Beyond neurons: evidence that immune and glial cells contribute to pathological pain states. Physiol. Rev. 82, 981–1011.

Winkelstein, B.A., Rutkowski, M.D., Sweitzer, S.M., Pahl, J.L., DeLeo, J.A., 2001. Nerve injury proximal or distal to the DRG induces similar spinal glial activation and selective cytokine expression but differential behavioral responses to pharmacologic treatment. J. Comp. Neurol. 439, 127–139.

Xia, Z., Miranti, C.K., Greenberg, M.E., 1996. Calcium influx via the NMDA receptor induces immediate early gene transcription by a MAP kinase/ERK-dependent mechanism. J. Neurosci. 16, 5425–5436.

Xu, X.J., Maggi, C.A., Wiesenfeld-Hallin, Z., 1991. On the role of NK-2 tachykinin receptors in the mediation of spinal reflex excitability in the rat. Neuroscience 44, 483–490.

Yamauchi, J.J., Nagao, M., Kaziro, Y., Itoh, H., 1997. Activation of p38 mitogen-activated protein kinase by signalling through G protein-coupled receptors—involvement of G beta gamma and G alpha (q/11) subunits. J. Biol. Chem. 272, 27771–27777.

Yashpal, K., Hui-Chan, C.W., Henry, J.L., 1996. SR 48968 specifically depresses neurokinin A- vs. substance P-induced hyperalgesia in a nociceptive withdrawal reflex. Eur. J. Pharmacol. 308, 41–48.

Zerari, F., Karpitskiy, V., Krause, J., Descarries, L., Couture, R., 1998. Astroglial distribution of neurokinin-2 receptor immunoreactivity in the rat spinal cord. Neuroscience 84, 1233–1246.

Zhuang, Z.-Y., Gerner, P., Woolf, C.J., Ji, R.-R., 2005. ERK is sequentially activated in neurons, microglia, and astrocytes by spinal nerve ligation and contributes to mechanical allodynia in this neuropathic pain model. Pain 114 (1–2), 149–159.

Zupan, V., Hill, J.M., Brenneman, D.E., Gozes, I., Fridkin, M., Robberecht, P., Evrard, P., Gressens, P., 1998. Involvement of pituitary adenylate cyclase-activating polypeptide II vasoactive intestinal polypeptide 2 receptor in mouse neocortical astrocytrogenesis. J. Neurochem. 70, 2165–2173.

Zusev, M., Gozes, I., 2004. Differential regulation of activity-dependent neuroprotective protein in rat astrocytes by VIP and PACAP. Regul. Pept. 123, 33–41.

Pain 118 (2005) 97–111

PAIN

www.elsevier.com/locate/pain

Varicella zoster virus induces neuropathic changes in rat dorsal root ganglia and behavioral reflex sensitisation that is attenuated by gabapentin or sodium channel blocking drugs

Emer M. Garry[a], Ada Delaney[a], Heather A. Anderson[a], Eva C. Sirinathsinghji[a], Rachel H. Clapp[a], William J. Martin[b], Paul R. Kinchington[c], David L. Krah[d], Catherine Abbadie[b], Susan M. Fleetwood-Walker[a,*]

[a]*Division of Veterinary Biomedical Sciences, Centre for Neuroscience Research, University of Edinburgh, Summerhall, Edinburgh EH9 1QH, UK*
[b]*Department of Pharmacology, RY80Y-140, Merck Research Laboratories, P.O. Box 2000, Rahway, NJ 07065, USA*
[c]*Departments of Ophthalmology and Molecular Genetics and Biochemistry, 1020 EEI, University of Pittsburgh, Pittsburgh, PA 15213, USA*
[d]*Vaccine and Biologics Research, Merck Research Laboratories, 770 Sumneytown Pike, West Point, PA 19486, USA*

Received 29 November 2004; received in revised form 22 July 2005; accepted 1 August 2005

Abstract

Reactivation of latent varicella zoster virus (VZV) within sensory trigeminal and dorsal root ganglia (DRG) neurons produces shingles (zoster), often accompanied by a chronic neuropathic pain state, post-herpetic neuralgia (PHN). PHN persists despite latency of the virus within human sensory ganglia and is often unresponsive to current analgesic or antiviral agents. To study the basis of varicella zoster-induced pain, we have utilised a recently developed model of chronic VZV infection in rodents. Immunohistochemical analysis of DRG following VZV infection showed the presence of a viral immediate early gene protein (IE62) co-expressed with markers of A- (neurofilament-200; NF-200) and C- (peripherin) afferent sensory neurons. There was increased expression of neuropeptide Y (NPY) in neurons co-expressing NF-200. In addition, there was an increased expression of $\alpha 2\delta 1$ calcium channel, $Na_v1.3$ and $Na_v1.8$ sodium channels, the neuropeptide galanin and the nerve injury marker, Activating Transcription Factor-3 (ATF-3) as determined by Western blotting in DRG of VZV-infected rats. VZV infection induced increased behavioral reflex responsiveness to both noxious thermal and mechanical stimuli ipsilateral to injection (lasting up to 10 weeks post-infection) that is mediated by spinal NMDA receptors. These changes were reversed by systemic administration of gabapentin or the sodium channel blockers, mexiletine and lamotrigine, but not by the non-steroidal anti-inflammatory agent, diclofenac. This is the first time that the profile of VZV infection-induced phenotypic changes in DRG has been shown in rodents and reveals that this profile appears to be broadly similar (but not identical) to changes in other neuropathic pain models.

Keywords: Post-herpetic neuralgia; Varicella zoster virus; Dorsal root ganglia; Sodium channels; Neuropeptide Y; Galanin; Gabapentin

1. Introduction

Chronic pain arising from nerve injury is difficult to treat. New effective pain-killers are urgently needed. Varicella zoster virus (VZV) is a neurotropic human herpesvirus that remains latent in sensory ganglia following primary infection (chickenpox or varicella; Cohrs et al., 2004). Virus reactivation produces localised skin lesions, shingles (zoster) at sites innervated by the affected sensory ganglia (Arvin, 1996; Cohrs et al., 2004). Following lesion resolution, post-herpetic neuralgia (PHN) can persist (Cohrs et al., 2004). Predisposition to PHN is not understood, although it is a major cause of morbidity and is unresponsive to current analgesics (Bowsher, 1995; Tenser, 2001). PHN is characterized by the development of hyperalgesia (a facilitated behavioral response to painful stimuli), mechanical allodynia (the perception of innocuous

* Corresponding author. Tel.: +44 131 650 6091; fax: +44 131 650 6576.
E-mail address: s.m.fleetwood-walker@ed.ac.uk (S.M. Fleetwood-Walker).

0304-3959/$20.00
doi:10.1016/j.pain.2005.08.003

stimuli as painful), and spontaneous pain, all features of neuropathic pain (Rowbotham and Fields, 1996).

Investigation of the neural mechanisms underlying PHN has been facilitated by the introduction of a rat model of VZV persistent infection (Sadzot-Delvaux et al., 1990) with striking reflex pain behaviours (Fleetwood-Walker et al., 1999). At least five VZV-encoded transcripts and proteins (genes 4, 21, 29, 62 and 63) are present in human and rat ganglia during latent VZV infection (Cohrs et al., 1996; Lungu et al., 1998; Sadzot-Delvaux et al., 1990). Although their precise functions in PHN are unknown, the immediate early protein 62 (IE62) is essential for VZV gene expression in host cells (Sato et al., 2003).

A key factor in the neural plasticity underlying neuropathic pain is altered gene expression in sensory dorsal root ganglia (DRG) neurons (Cummins et al., 2000; Hökfelt et al., 1994; Woolf and Salter, 2000; Xiao et al., 2002). Injury to sensory nerves induces neurochemical, physiological and anatomical modifications to afferent and central neurons, such as afferent terminal sprouting and inhibitory interneuron loss (Moore et al., 2002; Woolf and Salter, 2000). Following nerve damage, Na^+ channel accumulation causes hyperexcitability (Matzner and Devor, 1994; Omana-Zapata et al., 1997), downregulation of the TTX-resistant $Na_v1.8$ (sensory neuron specific, SNS1) channel and upregulation of TTX-sensitive $Na_v1.3$ (brain type III) channels (Dib-Hajj et al., 1999; Kim et al., 2001). These changes contribute to increased NMDA glutamate receptor-dependent excitability of spinal dorsal horn neurons (Laird and Bennett, 1993; Mayer et al., 1999; Palecek et al., 1992) and are restricted to the ipsilateral (injured) side (Bennett and Xie, 1988; Kim et al., 1997). A combination of these factors could contribute to the neuropathic pain state of PHN.

Although the underlying pathophysiological mechanisms may be similar to other forms of neuropathic pain, it is unclear how latent VZV infection interacts with the nervous system to induce these changes. We therefore used markers to identify the subpopulation of sensory neurons that co-express the virus latency protein IE62 and to characterise sensory neuron phenotypic changes compared with other neuropathic pain models. Since the anticonvulsant gabapentin and sodium channel blockers are effective in the treatment of PHN pain (Pappagallo, 2003; Rowbotham et al., 1998), we investigated their effectiveness in this model.

2. Materials and methods

2.1. Cell infectivity and preparation prior to injection

VZV-infected cells (generated from a wild-type VZV isolate from an otherwise healthy child (designated strain KMcC; Neff et al., 1981) and passaged in MRC-5 human diploid fibroblast cells to passage 9) were stored in vapour phase liquid nitrogen. Prior to injection, 500 μl of infected cells were thawed and diluted in saline 1:10, centrifuged for 5 min at $1000 \times g$, supernatant was removed and the cells were resuspended in saline which displayed a titre of 3.2×10^7 plaque-forming cells/ml (64% infectious cells). Two serial 5-fold dilutions leading to titres of 6.4×10^5 (1:5) and 12.8×10^4 (1:25) plaque-forming cells/ml were also used.

All experiments were performed in accordance with the UK Animals (Scientific Procedures) Act, 1986. Adult male Wistar rats (200–300 g, Charles River, Kent, UK) were anaesthetised with halothane/O_2 (Zeneca, Cheshire, UK) and under aseptic conditions, VZV-infected cells were injected into the dorsum of the right hind paw at a volume of 65 μl per rat ($n=22$ for full dilution and $n=6$ for each of the five-fold dilutions) using a 25.1 g syringe. For sham infection, each rat ($n=8$) was briefly anaesthetised and cells (CCL-171, MRC-5 human fibroblast cells, LGC Promochem, Middlesex, UK) were injected at the same concentrations as above. Infectivity, not cell type, was the only defining factor, as VZV and sham-infected cells were both derived from human fibroblast cells.

2.2. Assessment of behavioral reflex responses in VZV and sham-infected animals

To establish a time course of VZV infection-induced behavioral sensitivity, baseline measurements for all animals were obtained immediately prior to injection, and behavioral testing recommenced on day 6/7, 1 week following infection and continued either every day or every week (depending on cell dilutions) until evidence of recovery was observed. Behavioral tests were carried out as previously described (Garry et al., 2003), using quantified, sensory stimuli delivered to the mid-plantar glabrous surface of the hind paw. Mechanical allodynia was assessed by measuring the paw withdrawal threshold (PWT) in response to graded mechanical stimuli with calibrated von Frey filaments (Stoelting, Wood Dale, IL, USA). Thermal hyperalgesia was monitored as paw withdrawal latency (PWL) from a quantified noxious radiant heat (48 °C; Hargreaves' thermal device, Linton Instruments, Diss, UK). The behavioral responses obtained at each time point were calculated as the mean ± SEM for each test and data were analysed by SigmaStat software (version 2.03). In tests of mechanical allodynia, the ipsilateral value was compared to the contralateral value at each time point using a Wilcoxon test and each compared to pre-injection or pre-drug baseline using a repeated measures ANOVA on ranks (Friedman test), with post hoc analysis using Dunn's test. In tests of thermal hyperalgesia, the ipsilateral value was compared to the contralateral value at each time point using a paired Student's *t*-test, then each was compared to pre-injection or pre-drug baseline using a one-way repeated measures ANOVA, with post hoc analysis using Dunnett's test.

2.3. Immunofluorescent/immunohistochemical localisation of VZV IE62 protein with NF-200 and peripherin and neuropeptide Y (NPY) with NF-200 in DRG

Fresh DRGs from lumbar segments L4–L6 were removed immediately following induction of anaesthesia with halothane/O_2 (Zeneca, Cheshire, UK) and the animals killed by decapitation. DRGs were either sham or ipsilateral or contralateral to VZV 28 days following administration, at maximal behavioral reflex sensory sensitivity ($n=4$ in each case). The tissue was snap frozen and embedded in OCT embedding matrix (Cell Path plc. Powys. Wales, UK) before being cryostat sectioned (10 μm)

and thaw-mounted on poly-L-lysine slides (Merck-BDH). VZV IE62-expressing fibroblast cells (PR Kinchington) were used as a positive control for VZV IE62 expression.

Sections were pre-incubated in buffer (0.1 M PBS, pH 7.4, 0.2% Triton X-100, 4% fish skin gelatin) containing 10% normal goat serum for 1 h at room temperature and then incubated with primary antibodies diluted in buffer (0.1 M PBS, pH 7.4, 0.2% Triton X-100, 2% gelatin) overnight at 4 °C. For VZV protein IE62, co-localisation with the A-afferent marker neurofilament-200 kDa (NF-200) or the C-afferent fiber marker, peripherin, or for NPY co-localisation with NF-200, antisera were used at the following concentrations: rabbit polyclonal anti-VZV IE62 (1:250, PR Kinchington), rabbit polyclonal anti-NPY (1:250, Peninsula Laboratories, Belmont, CA, USA), mouse monoclonal anti-NF-200 (1:1000, Sigma) and mouse monoclonal anti-peripherin (1:250, Chemicon). Sections were then washed in buffer and incubated with the appropriate secondary antibodies (goat anti-rabbit Alexa Flour 568, 1:1000 or goat anti-mouse Alexa Fluor 488, 1:500; Molecular Probes, OR, USA) for 2 h at room temperature. Following three washes with 0.1 M PBS, sections were incubated with the nuclear stain, To-Pro (1:1000, To-pro-3-iodide, Molecular Probes) and washed a further three times in 0.1 M PBS before coverslipping with Vecta Shield (Vector Laboratories, Burlingame, CA, USA). Control sections were processed as above omitting the primary antisera.

Analysis was carried out using a Leica TCSNT Confocal System (Leica Microsystems GMBH, Germany) on six randomly selected sections of DRG (separation of 100 μm) from each group of four animals. At least 500 neurons were counted per group and only neurons that were To-pro positive were used for analysis. Using Image Tool software (UTHSCSA Image Tool Version 3.0), the median point between the mean background intensity and the mean IE62- or NPY-immunopositive cell intensity was taken as the minimum intensity value required for a IE62- or NPY-immunopositive cell to be counted. All sections were counted for IE62 or NPY-immunopositive cells in this manner and for NF-200- or peripherin-positive cells that were To-pro positive. Results were expressed as the percentage of IE62/NF-200 or IE62/peripherin-positive or NPY/NF-200-positive cells from the total number of NF-200- or peripherin-positive cells, from all sections. Any statistically significant differences between groups were determined by a Mann–Whitney rank sum test.

2.4. Assessment of NPY, galanin, ATF-3, VZV IE62, $Na_v1.3$, $Na_v1.8$, and $\alpha2\delta1$ channel protein expression levels by Western immunoblotting

When animals were at the peak of behavioural sensitivity 28 days following VZV-infection, lumbar 4–6 DRG were pooled from five animals and Western blotting was carried out using methodology described previously (Garry et al., 2003). Blots were probed with rabbit polyclonal primary antibodies to VZV IE62 (1:100, Chemicon, International Ltd, Harrow, UK), NPY (1:100, Autogen Bioclear UK Ltd (Santa Cruz Biotechnology, Wiltshire), galanin (1:100, Autogen Bioclear UK Ltd) or ATF-3 (1:200, Autogen Bioclear UK Ltd), $\alpha2\delta1$ voltage-gated calcium channel (1:100, Chemicon), $Na_v1.3$ (1:200; Alomone Labs, Towcester, UK) or $Na_v1.8$ (Wallace et al., 2003) and detected by peroxidase-linked secondary antibody enhanced chemiluminescence. To assess any relationship between viral titre and the level of VZV IE62 expression in DRG, we also carried out western blotting on DRG from animals 2 weeks following infection with either 1:5 or the 1:25 cell titres and probed these samples for VZV IE62. The ubiquitous housekeeping enzyme glyceraldehyde-3-phosphate dehydrogenase (GAPDH, 1:750, Chemicon, International Ltd, Harrow, UK) was monitored as a control for protein level normalisation.

2.5. Gabapentin, sodium channel blocker and anti-inflammatory agent administration

We examined any effects of gabapentin, the sodium channel inhibitors, mexiletine and lamotrigine and the non-steroidal anti-inflammatory drug (NSAID), diclofenac. Drug doses were based on pharmacological characterisation of the Chung and spared nerve injury pain models (Merck in-house data; Erichsen and Blackburn-Munro, 2002). In experiments involving drug administration by oral gavage, only VZV-infected animals that showed clear signs of thermal hyperalgesia and mechanical allodynia were used. Due to solubility of drugs, gabapentin, mexiletine and diclofenac were both dissolved in sterile water, while lamotrigine was dissolved in a solution of 5% ethanol, 15% Tween80 and 8.5% sterile water and stirred overnight. Gabapentin (100 mg/kg), lamotrigine (100 mg/kg), mexiletine (100 mg/kg) and diclofenac (100 mg/kg) were administered once only by oral gavage, at a volume of 2 ml/kg. In all cases of oral gavage, animals ($n=8$ per group) fasted 10–12 h prior to gavage until the end of drug effect testing the following day. Behavioral testing commenced 1, 2, 4, 6 and 24 h post-gavage and at 48 h to ensure recovery of behavioral reflex sensitivity. Equivalent administration of vehicle was found to have no discernable effect on behavioral reflexes.

2.6. Intrathecal administration of NMDA receptor antagonist and μ opioid receptor agonist

Baseline measurements were carried out in VZV-infected animals at the peak of behavioural sensitivity for mechanical allodynia and thermal hyperalgesia prior to injection. Animals were briefly anaesthetised with halothane and O_2 and injected intrathecally at the level of the L5 spinal vertebra using a 25.1 g needle with either the NMDA receptor antagonist (R)-CPP ([3-((R)-2-carboxypiperazine-4-yl)-propyl-1-phosphonic acid] Tocris Cookson Ltd, Bristol, UK; 2.5 nmoles/50 μl saline) or the selective μ-opioid receptor agonist D-Ala_2, $MePhe_4$, Gly-ol enkephalin (DAMGO; Tocris Cookson; 1 μmol/50 μl saline). To determine the effects of the drugs on both mechanical allodynia and thermal hyperalgesia, behavioral reflex testing commenced 15 min following injection to allow recovery from anaesthesia and continued every 5 min thereafter until readings returned to baseline levels. Extensive control studies have shown that intrathecal injections of saline had no effect on these behavioral reflex measures.

3. Results

3.1. VZV infection induces behavioral mechanical allodynia and thermal hyperalgesia

Following preparation of the rat model of VZV infection by unilateral injection of virus into the hindpaw (Fleetwood-Walker et al., 1999; Sadzot-Delvaux et al., 1990),

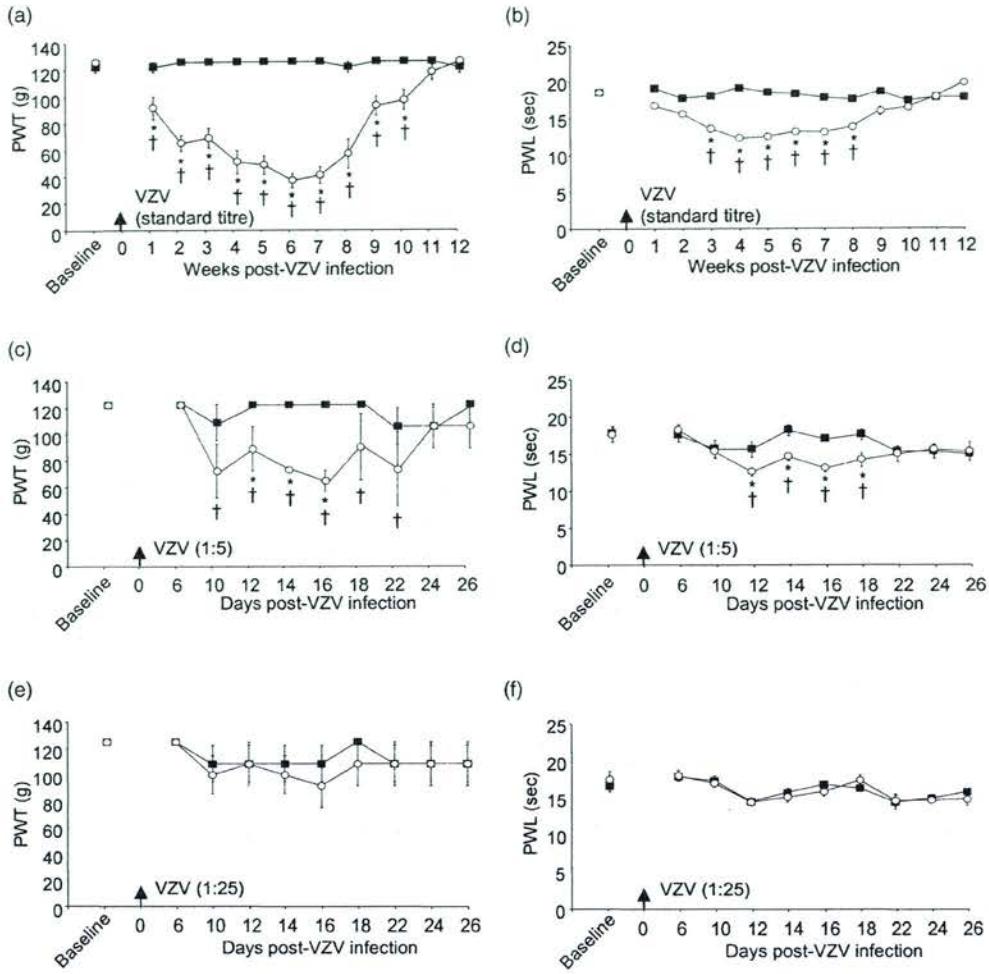

Fig. 1. Time course of VZV-induced neuropathic reflex behaviors. Mean ± SEM responses to sensory stimulation of the hindpaw for a week prior to (Baseline), and each week (a, b) or days (c–f) following VZV infection. (a) Paw withdrawal thresholds (PWT, g) from calibrated von Frey filaments ipsilateral to VZV-injection (○) showed significant differences between pre- and post-infection values ($^{\dagger}P<0.05$; Repeated measures ANOVA on ranks; Friedman's test with Dunn's post hoc analysis) and from post-operative, contralateral (■) values ($^{*}P<0.05$ by Wilcoxon test) from 1 to 10 weeks following VZV infection (standard titre). (b) Paw withdrawal latency (PWL, s) from a noxious thermal stimulus (Hargreaves' thermal stimulator) ipsilateral to VZV-injection (○) showed significant differences between post- and pre-infection values ($^{\dagger}P<0.05$; Repeated measures ANOVA with Dunnett's post-hoc analysis) and from post-operative, contralateral (■) values ($^{*}P<0.05$ by Student's paired *t*-test) from 3 to 8 weeks post infection (standard titre). (c and d) showed significant differences between post- and pre-infection values ($^{\dagger}P<0.05$; Repeated measures ANOVA on ranks; Friedman's test with Dunn's post hoc analysis) and from post-operative, contralateral (■) values ($^{*}P<0.05$ by Wilcoxon test) for PWT (c) and significant differences ($^{\dagger}P<0.05$; Repeated measures ANOVA with Dunnett's post hoc analysis) and from post-operative, contralateral (■) values ($^{*}P<0.05$ by Student's paired *t*-test) for PWL (d) following VZV infection (1:5). The second dilution (1:25) showed no significant differences between post- and pre-infection values or from post-operative, contralateral values for either PWT (e) or PWL (f).

VZV-infected rats ($n=22$) displayed a markedly lowered threshold in behavioral reflex tests of mechanical (Fig. 1a) and thermal (Fig. 1b) sensitisation ipsilateral, but not contralateral, to the site of injection. The heightened sensitivity to both tests was apparent from day 7 (week 1) after VZV infection, but reached peak values from day 28 (week 4) until day 56 (week 8) post-infection. Typically, at peak behavioral sensitivity following VZV infection, von Frey withdrawal thresholds were reduced from approximately 122 ± 3.5 to 36 ± 6.4 g on average (Fig. 1a) and thermal withdrawal latencies were reduced from approximately 18.5 ± 0.3 to 12 ± 0.6 s (Fig. 1b). All behavioral sensitivities recovered to baseline levels by 11 weeks for mechanical allodynia and by 9 weeks post-infection for thermal hyperalgesia. To establish whether there was a relationship between VZV-infected cell titre and the development of behavioural sensitisation, VZV-infected cells were diluted prior to injection. Behavioural sensitivity was dose-dependently diminished with each of two serial 5-fold dilutions of the original viral titre ($n=6$ in each case, Fig. 1, c–f). Approximately, half the level of sensitisation occurred at five times dilution (1:5; $n=6$) for both

mechanical withdrawal threshold (Fig. 1c) and thermal withdrawal latency (Fig. 1d). At peak behavioural sensitivity following infection with 1:5 of original cell concentration, von Frey withdrawal thresholds were reduced from 125.9±0.0g to 75.6±7.8 g (Fig. 1c) and thermal withdrawal latencies reduced from 15.1±0.7 to 12.0±0.5 s (Fig. 1d). Rats that received only 1:25 of the original viral cell titre ($n=6$) did not differ significantly post-infection with von Frey withdrawal thresholds maintained at 109.2±13.6 g (Fig. 1e) and thermal withdrawal thresholds of 14.9±0.7 s (Fig. 1f) on average throughout the time period tested. Furthermore, animals that had sham cell injections ($n=8$) showed no change from baseline, with von Frey threshold withdrawal values of between 117.5 and 125.9 g and thermal paw withdrawal latencies of approximately 17 s at all time points tested (data not shown). In both VZV- and sham-injected animals no consistent changes were detected contralateral to injection. There was no evidence of overt motor deficits or skin lesion development following either VZV or sham cell injection.

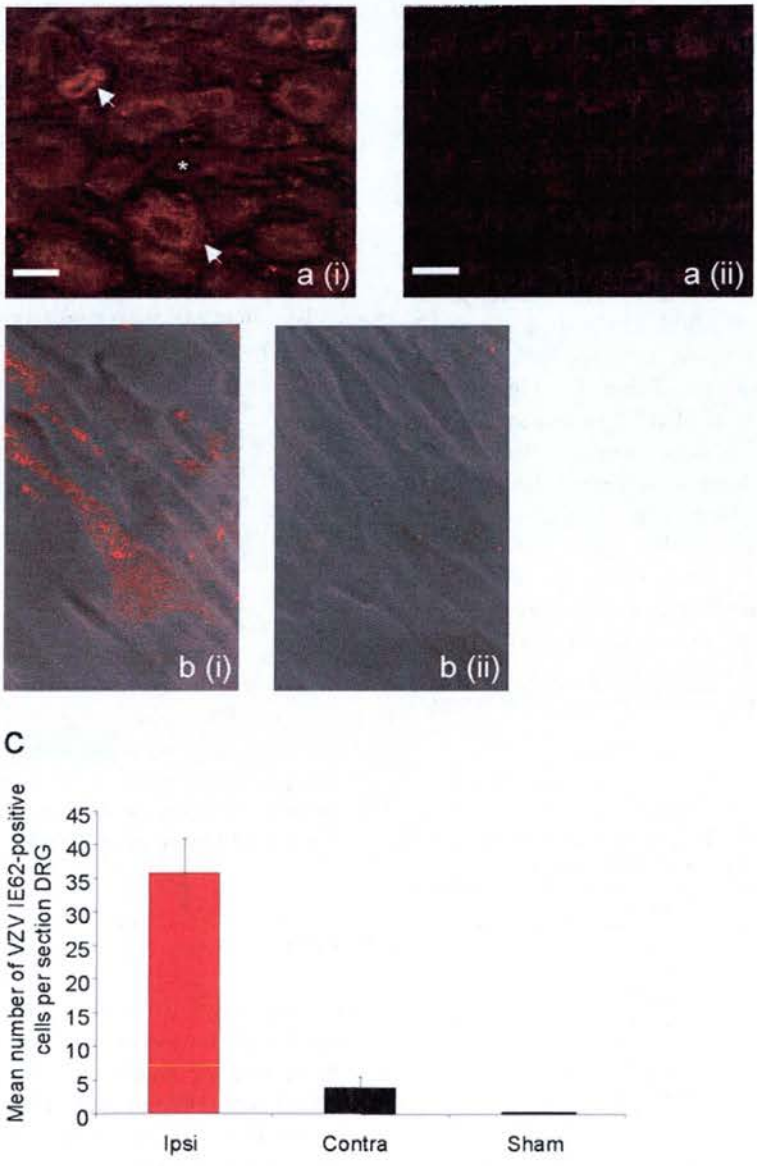

Fig. 2. VZV infection induces VZV IE62 protein expression in DRG. (a) Typical immunofluorescence images showing (i) the presence of VZV IE62 protein (red) in DRG neurons ipsilateral to VZV-infection 3 weeks following VZV infection. Positive- (arrow) and negative-labelled cells (asterisk) are indicated. (ii) Negligible expression of VZV IE62 is found in contralateral DRG neurons at the same time point (ii). Scale bar 25 μm. (b) Phase contrast images showing control VZV expressing fibroblast cells confirm VZV IE62 expression (i) while negatively expressing fibroblast cells show no expression (ii). (c) Mean (± SEM) number of neurons per DRG section that express VZV IE62 showing the marked induction of VZV IE62 in DRG neurons ipsilateral to VZV infection in comparison to contralateral and sham-infected DRG sections.

3.2. VZV protein IE62 is detected in DRG neurons of VZV-infected animals

The VZV immediate early protein IE62 is a major component of varicella zoster virus particles (Kinchington et al., 1992) and can act to alter neuropeptide expression (Meier and Straus, 1995). To confirm viral presence in sensory afferents, qualitative assessment of VZV IE62 protein in DRG from VZV-injected animals (at the peak of behavioral reflex sensitisation) and from sham-injected animals was carried out using immunofluorescence and Western blotting. VZV IE62 was present in VZV-infected tissue in a total of 609 small and large DRG cell bodies ipsilateral to injection (Fig. 2a(i), c), whilst expression in sham-treated tissue was negligible (Fig. 2c). While behavioral data indicated no significant contralateral effects of VZV injection, some contralateral staining (in a total of 77 cells) of VZV IE62 was found (Fig. 2a(ii), c). Control VZV IE62-expressing fibroblast cells confirmed positive protein expression (Fig. 2b(i)) compared with the negative fibroblast control cells, which did not express VZV IE62 (Fig. 2b(ii)). Positive VZV IE62 protein induction in VZV-infected DRG was also confirmed by Western blot, while expression in sham-infected DRGs was entirely absent (Fig. 5a, Table 1). Fig. 5c (and Table 1) shows that the level of IE62 expression in DRG, ipsilateral to infection, was proportional to the viral titre administered; matching behavioral reflex data (Fig. 1), indicating corresponding functional changes in nociceptive responsiveness. Naïve DRG cells also had no expression of VZV IE62 protein (data not shown). The housekeeping protein GAPDH was assessed as an internal control and showed similar expression in both VZV and sham-infected DRG samples, indicating no difference in overall levels of cellular proteins following VZV infection (Fig. 5b, Table 1).

Table 1
Immunoblot mean expression in VZV- or sham cell-infected DRG as percentage of GAPDH expression (arbitrary density units)

Protein	VZV-infected	Sham-infected	
VZV IE62	82.3±8.6*	0.0±0.0	
NPY	17.5±2.6*	5.4±1.9	
Galanin	23.8±4.6*	8.3±3.9	
ATF-3	16.5±2.7*	0.0±0.0	
α2δ1	46.0±5.3*	20.9±6.0	
$Na_v1.3$	29.7±5.0*	0.0±0.0	
$Na_v1.8$	53.8±4.7*	12.6±2.2	
VZV infectivity:	VZV (full titre)	VZV (1:5 dilution)	VZV (1:25 dilution)
VZV IE62	79.2±5.8	33.6±8.2	19.7±7.3

Values are mean %±SEM values ($n=5$) derived from quantitative densitometry of co-processed immunoblots for IE62 (shown in Fig. 5). Statistically significant differences in the levels of protein expression as percent GAPDH between VZV- and sham cell-infection controls are shown as *, $P<0.05$ by Wilcoxon test.

3.3. VZV protein IE62 is detected in both myelinated A- and unmyelinated C-afferent sensory neurons in VZV-infected animals, as revealed by co-expression with the cell markers peripherin and NF-200

To identify which sensory afferent neuronal subtypes express the viral latency protein, IE62, we analysed the expression of peripherin (Fig. 3a), a type III intermediate filament protein, which is normally expressed selectively by unmyelinated sensory neurons (Amaya et al., 2000) and NF-200 (Fig. 3b) which labels the larger diameter, myelinated DRG cell population (Lawson et al., 1993). No significant difference was observed in the number of either peripherin (ipsilateral 28.3±1.4; contralateral 22.9±1.6) or NF-200-positive (ipsilateral 13.7±1.2; contralateral 12.2±1.0) DRG neurons per section. This represents a mean proportion of NF-200-positive cells out of a total of NF-200- plus peripherin-positive cells of 33% (ipsilateral) and 35% (contralateral). We analysed the expression of IE62 in the DRG of VZV-infected rats, which were at the peak of neuropathic behavioral reflex sensitisation following infection. There we found expression of IE62 in 82.3±3.4% of DRG neurons also positive for peripherin (Fig. 3c) compared to 84.2±15.4% of DRG neurons also positive for NF-200 (Fig. 3d) ipsilateral to infection. This is compared with an IE62 expression of 12.0±9.0% for peripherin-positive and 21.3±9.1% for NF-200-positive neurons contralaterally. Under control sham-infected conditions we found no IE62-positive cells (Fig. 3c and d). There were no significant differences between the mean diameters of NF-200-positive cells that did or did not express IE62, ipsilateral to infection (33.3±0.9 and 30.0±0.8 μm, $n=85$, respectively) or for peripherin-positive cells, with corresponding values of 13.8±0.03 and 14.6±0.05 μm ($n=77$). Under the present experimental conditions, IE62 staining was only observed in the cytoplasm and not in the nucleus of VZV-infected NF-200 or peripherin-positive DRG neurons ($n=100$ randomly counted cells in each case), corresponding to the observations of Lungu et al. (1998).

3.4. VZV infection alters the expression of neuropeptide Y (NPY) in sensory DRG neurons co-expressing NF-200

Following traumatic injury to the peripheral nerve, a number of neurochemical and morphological changes take place both in peripheral nerve fibers and centrally in the spinal cord (Hökfelt et al., 1994). These changes contribute to the altered sensory transmission associated with chronic pain states. Phenotypic changes occur in many primary afferent DRG neurons, resulting in the altered expression of neuropeptides including downregulation of the afferent peptides SP and CGRP and upregulation of VIP, GAL and NPY (Hökfelt et al., 1994). We therefore investigated whether such changes occur in the VZV-induced

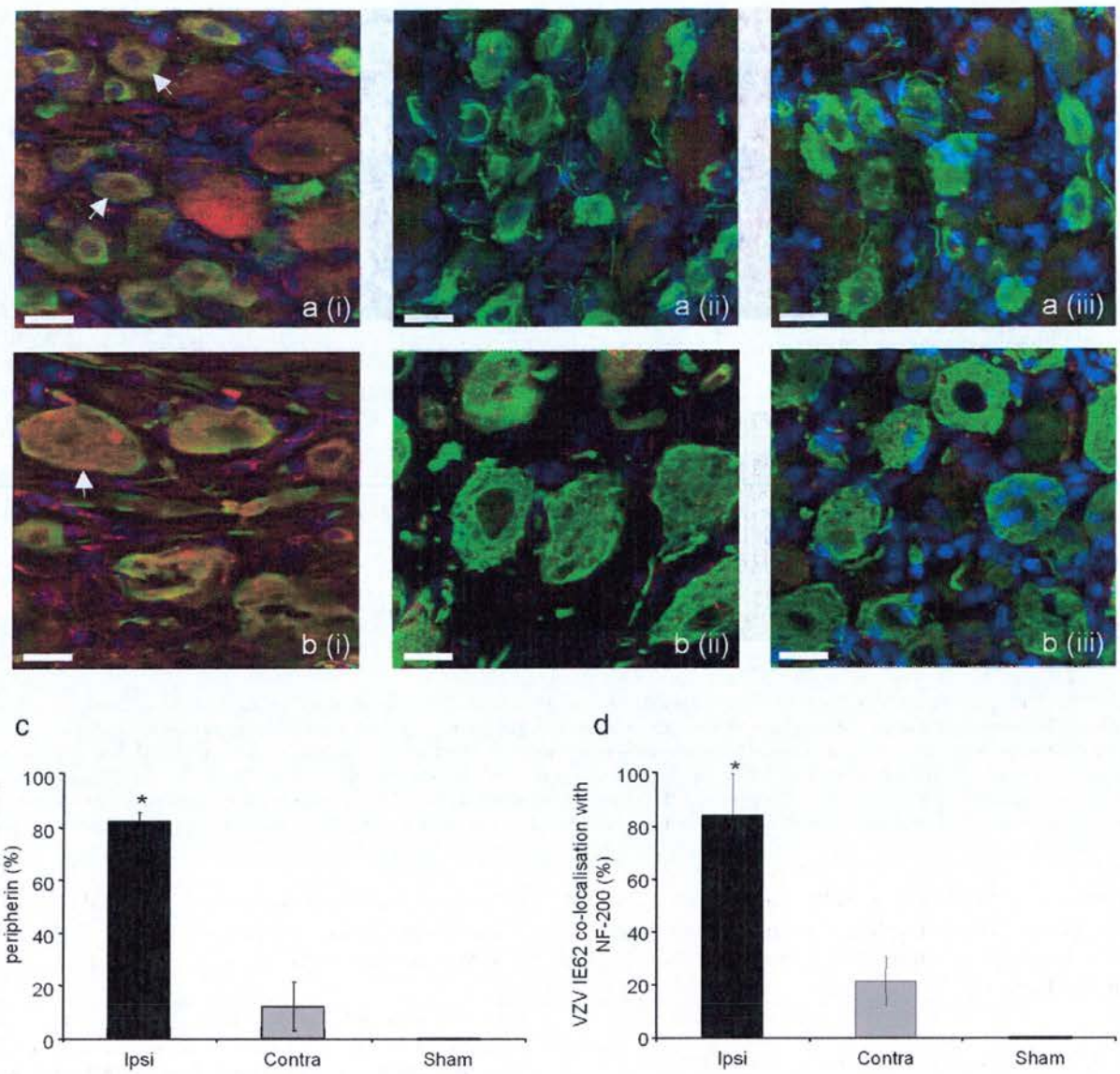

Fig. 3. Immunohistochemical co-localisation of unmyelinated C- and myelinated A-afferent markers, peripherin and NF-200 with VZV IE62 in DRG cells after VZV-infection. Immunohistochemical co-localisation of VZV IE62 with the C-fiber cell body marker peripherin (a) or the myelinated A fiber cell body marker NF-200 (b) in dorsal root ganglia sections taken three weeks following VZV infection (i) ipsilateral or (ii) contralateral to VZV-infection and (iii) following sham cell injection are shown. Images show VZV IE62 immunopositive cells (in a and b) labelled with Alexa Fluor 568 (red) and peripherin (in a) or NF-200 (in b) labelled with Alexa Fluor 488 (green). The nuclear stain To-Pro is shown (blue). Ipsilateral DRG neurons that were double labelled for VZV IE62 and either peripherin (a) or NF-200 (b) are indicated (arrow). Scale bar 25 μm. There was a significant increase in the expression of VZV IE62 co-localised with peripherin (c) or NF-200 (d) ipsilateral to VZV-infection when compared with contralateral or sham infection. Statistical significance ($*P<0.05$) was determined using a Mann–Whitney rank sum test.

hypersensitive state in order to compare the changes with those occurring in other models of neuropathic pain.

DRG cells express only low levels of NPY under normal conditions, but its expression is induced predominantly in the large neuron population following axotomy (Hökfelt et al., 1994), nerve injury (Ma and Bisby, 1998; Munglani et al., 1995) and demyelination (Wallace et al., 2003). Using NPY as a phenotypic marker, we therefore investigated whether any change in NPY expression occurs in sensory neurons of VZV-infected animals. Expression of NPY was co-localised with NF-200, which labels large diameter, myelinated DRG cells (Fig. 4a and c). We observed NPY immunoreactivity in approximately $90\pm1.0\%$ of NF-200 immunopositive cells after VZV infection (Fig. 4a and c) in comparison to approximately $12\pm0.7\%$ immunoreactivity in cells in naïve or sham-infected animals (Fig. 4b and c). Induction of NPY expression in VZV-infected DRG was confirmed by Western blot, while expression in sham-infected DRGs was entirely absent (Fig. 5a, Table 1). The housekeeping protein GAPDH was assessed as an internal

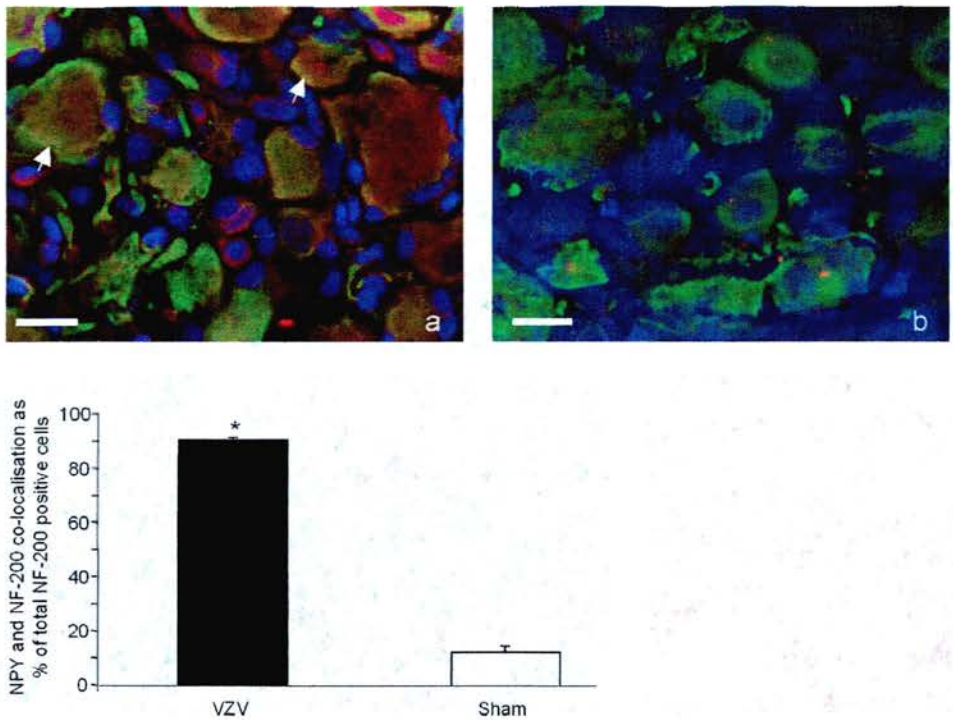

Fig. 4. VZV infection induces VZV IE62 and NPY expression in myelinated DRG cells. Immunohistochemical co-localisation of the larger-diameter, myelinated DRG cell population with neuropeptide NPY in VZV-infected (a) or sham infected (b) DRG sections three weeks following VZV infection. Images show NF-200 immunopositive cells labelled with Alexa Fluor 488 (green) and NF-200/NPY co-localised immunopositive cells labelled with Alexa Fluor 568 (red) in VZV treated DRG (a) with no NF-200/NPY co-localised immunopositive cells in sham DRG (b). Scale bar 25 μm. Double labelled cells are indicated by an arrow. (c) Number of NPY/NF-200 immunopositive cells expressed as a percent of total NF-200 immunopositive cells. Post-VZV treatment, there was a significant increase ($*P<0.05$; Mann–Whitney rank sum test) in the number of cells expressing NPY, which were all positive for NF-200, when compared to sham DRG.

control and showed similar expression in both VZV and sham-infected DRG samples, indicating no difference in overall levels of cellular proteins following VZV infection (Fig. 5a, Table 1).

3.5. Afferent expression of the neuropeptide galanin and nerve injury marker ATF-3, are induced following VZV infection

Galanin is expressed at very low levels under normal conditions and is upregulated mainly in unmyelinated small and medium DRG cells following peripheral nerve injury (Hökfelt et al., 1994). We observed a similar upregulation in galanin protein expression in DRG ipsilateral to VZV injection (Fig. 5a, Table 1). ATF-3 expression is induced in DRG neurons following nerve injury but not demyelination (Wallace et al., 2003) and is thus thought to be a marker of axonal damage (Tsujino et al., 2000). We also saw an increase in ATF-3 protein expression following VZV infection (Fig. 5a, Table 1), indicating axonal damage may occur in this model. The phenotypic changes reported here that mimic those seen following peripheral nerve injury may underlie the behavioral sensitisation resulting from VZV infection.

3.6. VZV infection induces upregulation of the α2δ1 voltage-gated calcium channel and $Na_v1.3$ and $Na_v1.8$ sodium channels in DRG

The anticonvulsant gabapentin can be an effective treatment in animal models of neuropathic pain (Chapman et al., 1998a; Christensen et al., 2001; Erichsen and Blackburn Munro, 2002; Kanai et al., 2004) and following PHN (Rowbotham et al., 1998). Gabapentin is thought to exert its actions via the α2δ1 subtype of voltage-gated calcium channel (Bayer et al., 2004). Fig. 5b shows that immunoreactivity for the α2δ1 calcium channel subunit was increased in extracts of DRG ipsilateral to VZV injection compared to sham controls.

The tetrodotoxin (TTX)-sensitive $Na_v1.3$ channel is normally only found in DRG during development and consistent with this we could not detect any expression of this channel in naive DRG (data not shown). However, expression of $Na_v1.3$ has been reported to increase in sensory neurons following axotomy (Cummins et al., 2000) and nerve ligation (Kim et al., 2001). As VZV infection shares the behavioral correlates of many nerve damage models, we investigated whether any changes in sodium channel expression occur in DRG of VZV-infected animals. We found that VZV infection can induce the expression of

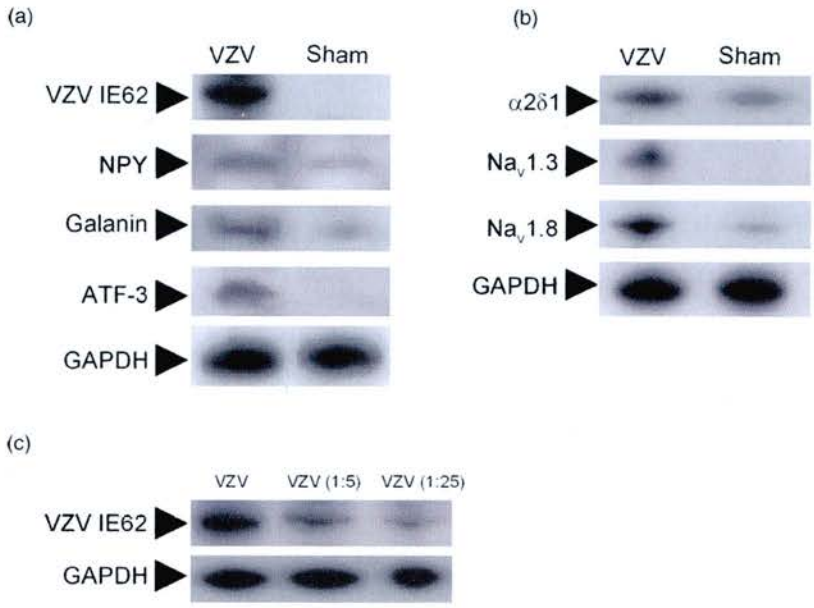

Fig. 5. VZV infection results in increased protein expression of $Na_v1.3$, $Na_v1.8$, galanin and ATF-3. (a) Immunoblots showing the presence of VZV IE62, NPY, galanin, ATF-3 and GAPDH in VZV- and sham cell-infected DRG. For full viral cell infection, samples were taken 3 weeks following VZV infection, the time of maximal behavioral sensitisation. There is positive expression of VZV IE62, NPY, galanin and ATF-3 protein in VZV-treated DRG, with minimal or no detectable expression in sham-treated DRG. (b) Immunoblots showing the expression of the $\alpha2\delta1$ subunit of Ca^{2+} channel and $Na_v1.3$ and $Na_v1.8$ sodium channel protein in VZV- and sham cell-infected DRG. All were upregulated ipsilateral to VZV infection with minimal or no detectable expression in sham-treated DRG. Normalised protein loading was determined by uniform expression of housekeeper gene GAPDH in both VZV- and sham cell-treated DRG ($n=5$ in each case). (c) There is reduced VZV IE62 expression with diluted viral infections in samples taken 2 weeks following infection, when maximal changes in behavioural sensitisation had been reached.

$Na_v1.3$ protein in ipsilateral DRG while no protein could be detected in sham cell-infected DRG (Fig. 5b, Table 1).

We also examined the TTX-resistant $Na_v1.8$ sodium channel, which has also been implicated in chronic pain (Gold et al., 2003; Novakovic et al., 1998; Porreca et al., 1999). We found that this channel was also upregulated in DRG following VZV infection (Fig. 5b, Table 1). Due to technical limitations of the available antibodies, we could not establish immunofluorescence of either $Na_v1.3$ or $Na_v1.8$. The presence of upregulated $Na_v1.3$ and $Na_v1.8$ sodium channels indicated that there are neuropathic type changes in VZV-infected rats.

3.7. Neuropathic pain behaviors are attenuated by gabapentin administration

Given the upregulation of the $\alpha2\delta1$ channel in VZV-infected tissue (Fig. 5b), we assessed the effect of orally administered gabapentin in VZV-infected rats. Rats at the peak of VZV-induced behavioral reflex sensitivity ($n=8$ at 4 weeks post-infection) received gabapentin (100 mg/kg) by oral gavage, and were tested 2, 4, 6, 24 and 48 h post-treatment. Gabapentin reversed the VZV-induced reduction in paw withdrawal threshold to mechanical stimulation using von Frey filaments (Fig. 6a) and the reduction in paw withdrawal latency to noxious heat (Fig. 6b). Effects were seen over a 24 h period for mechanical allodynia with recovery to VZV-induced sensitivity by 48 h. Results were similar for thermal hyperalgesia, although effects appeared to be shorter lasting, with recovery occurring between the 6 and 24 h periods of testing (Fig. 6a and b). Maximal effects of gabapentin were seen 2 h post-gavage with no significant difference between virus-treated and untreated sides for mean mechanical (contralateral and ipsilateral both 125.9 ± 0.0 g) or thermal (contralateral 19.4 ± 0.2 s; ipsilateral 18.7 ± 0.4 s) withdrawal responses. Thus, there appears to be a similar gabapentin sensitivity following VZV infection as seen in models of peripheral nerve injury.

3.8. Sodium channel blockers reduce VZV-induced neuropathic pain behaviors

Voltage-gated sodium channels initiate and propagate neuronal action potentials, thus regulating neuronal excitability. Post-injury changes in the distribution and activity of sodium channels within DRG neurons and at the site of injury can regulate a state of hyperexcitability (Baker and Wood, 2001; Cummins et al., 2000). The involvement of sodium channels in PHN has been suggested following effective use of peripheral analgesic lidocaine patches (Brau et al., 2001; Davies and Galer, 2004). Indeed, sodium channel blockers are also known to be effective in models of nerve damage (Cantrell and Catterall, 2001; Cummins et al., 2000). Since $Na_v1.3$ and $Na_v1.8$ sodium channel expression increased following VZV infection, we tested whether orally administered sodium channel blockers were effective

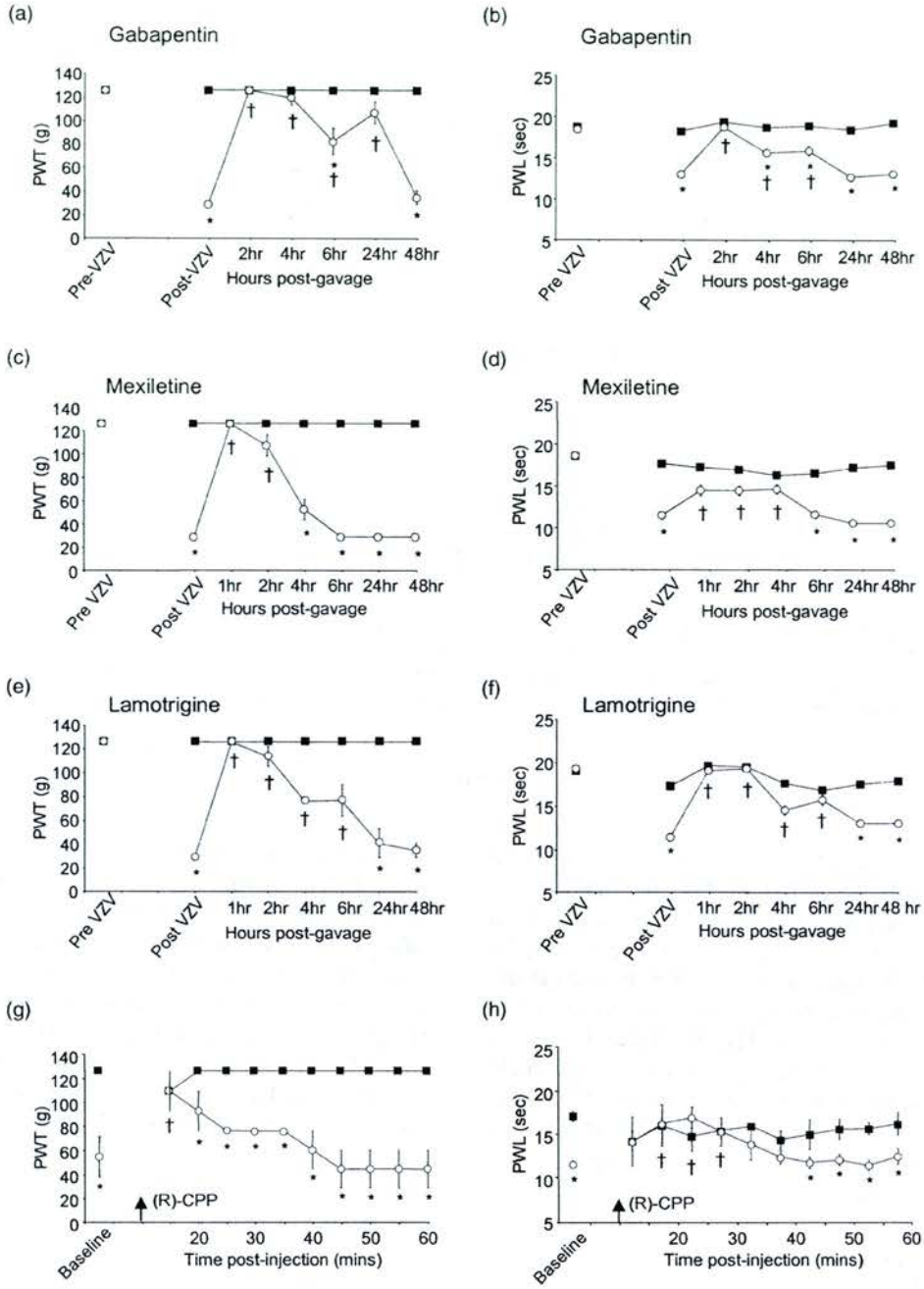

Fig. 6. Oral administration of the anticonvulsant, gabapentin and sodium channel blockers, mexiletine and lamotrigine attenuate sensitised behavioral reflex responses in VZV-infected animals. Mean ± SEM responses of the paw withdrawal threshold to an innocuous mechanical stimulus (a, c, e) and paw withdrawal latency to noxious thermal stimulation (b, d, f) following oral gavage of either gabapentin (a, b), lamotrigine (c, d) or mexiletine (e, f) ipsilateral (○) or contralateral (■) to VZV injection in animals at peak behavioral sensitivity following VZV infection. Mean ± SEM responses of withdrawal thresholds (g) and withdrawal latency (h) following the intrathecal injection of the NMDA receptor antagonist (R)-CPP. In (a, c, e, g), * represents a significant ipsilateral to contralateral difference at each time point, $P<0.05$ by Wilcoxon test, and † represents a significant difference at each time point when compared to pre-drug baseline, $P<0.05$ by repeated measures ANOVA on ranks (Friedman's test) followed by Dunn's post hoc test. In (b, d, f, h), * represents a significant ipsilateral to contralateral difference at each time point, $P<0.05$ by paired t-test and † represents a significant difference at each time point when compared to pre-drug baseline, $P<0.05$ by repeated measures ANOVA followed by Dunnett's post hoc test.

in reversing the sensitised pain behaviors observed. The effect of sodium channel blockers on VZV-induced neuropathic behaviors has not been previously investigated. We used two voltage-dependent sodium channel blockers, mexiletine and lamotrigine. Again, animals at the peak of VZV-induced behavioral reflex sensitivity ($n=8$ for each drug) received mexiletine and lamotrigine (both at 100 mg/kg) by oral gavage and were tested 1, 2, 4, 6, 24

and 48 h post-treatment. Mexiletine produced a reversal of behavioral sensitivity to mechanical (Fig. 6c) and thermal stimuli (Fig. 6d), whereby the inhibition of allodynia recovered to VZV-induced sensitivity after 2 h and for hyperalgesia after 4 h. Maximal effects of mexiletine were seen 2 h post-gavage with mean thermal withdrawals of 16.9 ± 0.3 s for contralateral and 14.5 ± 0.6 s for ipsilateral hindpaws. Mean mechanical responses for contralateral (125.9 ± 0.0 g) and ipsilateral (116.5 ± 9.4 g) paws were not significantly different. Lamotrigine also effectively reversed thermal hyperalgesia behaviors over a time course of 6 h (Fig. 6f), while similar effects were only seen for up to 2 h for mechanical allodynia (Fig. 6e). At peak reversal 1–2 h post-gavage, there was no significant difference in the mean mechanical responses (contralateral 125.9 ± 0.0 g; ipsilateral 119.6 ± 6.3 g) or in thermal responses (contralateral 19.6 ± 0.2 s; ipsilateral $19.1 + 0.3$ s). At the time of maximal analgesic effects of gabapentin, mexilitine and lamotrigine (2 h post-gavage), there was no significant effect seen with the NSAID diclofenac, which failed to reverse both the ipsilateral-specific mechanical allodynia (contralateral 125.9 ± 0.0 g; ipsilateral 17.2 ± 3.2 g) and thermal hyperalgesia (contralateral 17.0 ± 0.6 s; ipsilateral 10.3 ± 1.2 s), which was similar to that seen in untreated VZV-infected animals (Fig. 1).

3.9. VZV-induced neuropathic pain behaviors are dependent on spinal NMDA receptor-dependent changes

Sensitisation of cells in the dorsal horn of the spinal cord is a key change in other neuropathic pain states and is thought to crucially involve activation of the NMDA receptor (Coderre and Melzack, 1992). We found that spinal NMDA receptors also play a role in the mechanical allodynia seen in animals with VZV-infection, since behavioral sensitisation was reversed following spinal administration of the selective NMDA receptor antagonist (R)-CPP (Lehmann et al., 1987; Fig. 6g). Similarly, the reduction in thermal nociceptive response latency ipsilateral to VZV-infection was reversed by (R)-CPP (Fig. 6h). The mean percent reversal of sensitisation over the first 30 min of drug administration being 63.6 ± 4.2 and 90.4 ± 5.6 for mechanical allodynia (Fig. 6g) and thermal hyperalgesia (Fig. 6h), respectively (mean $\pm$ SEM; $n = 5$). There was no effect of (R)-CPP on thermal or mechanical responses contralateral to VZV-infection. Activation of spinal opioid receptors can produce analgesia in models of inflammation (Malmberg and Yaksh, 1993), but is largely ineffective in neuropathic pain conditions (Arner and Meyerson, 1988). To assess any potential opioid regulation of this model of VZV-induced sensitisation, we performed intrathecal injections with the highly selective μ-opioid receptor agonist, DAMGO. No discernable effect on thermal and mechanical nociceptive reflexes was seen following injection of DAMGO (at the highest dose possible before motor dysfunction was observed), indicating that opioids are not effective modulators of the behavioural sensitisation in this model (data not shown). Equivalent injections of the saline vehicle had no effect on mechanical or thermal reflex responses (data not shown). These findings suggest that the spinal NMDA receptor plays a key role in the development of VZV-induced neuropathic behavioral reflex sensitisation.

4. Discussion

Abnormal sensory phenomena including spontaneous pain, hyperalgesia and allodynia are associated with human primary VZV infection and its recurrence (Bowsher, 1995). Since the underlying mechanisms are poorly understood, it is important to characterise some of the functional and phenotypic changes occurring in a VZV-induced pain model.

4.1. VZV infection-induced allodynia and hyperalgesia

Sensory neuronal damage following VZV infection and PHN development often causes chronic pain and allodynia (Rowbotham and Fields, 1996). We show a unilateral mechanical allodynia and thermal hyperalgesia matched by increased DRG expression of the nerve injury marker, ATF-3. Evidence that central (spinal) changes in excitability are essential to this sensitised, VZV-induced pain state is provided by its marked attenuation by intrathecal injection of an antagonist of the NMDA receptor (a key mediator of synaptic sensitisation), but does not involve opioids. The time course of behavioral sensitisation is similar to that seen in other models of neuropathic pain and its persistence for up to 10 weeks is in agreement with another recent report of VZV-induced allodynia (Dalziel et al., 2004). Our finding that allodynia was longer lasting than thermal hyperalgesia mirrors the clinical finding of marked allodynia in PHN patients (Bowsher, 1995).

4.2. Presence of VZV viral protein in sensory neurons in the DRG

It is important to establish the presence of viral products, one of several viral genes, in subpopulations of sensory neurons in DRG. A number of viral genes are expressed in human DRG following latent infection with VZV, such as VZV IE62 (Cohrs et al., 1996; Kennedy et al., 2001). The function of these genes is unknown, but they may alter nociceptive processing. Extending previous findings in this model showing mRNA for genes 62, 63 and 4 (Sadzot- Delvaux et al., 1995) and IE63 protein (Fleetwood-Walker et al., 1999), we show that IE62 protein is co-localised in both A- (NF-200-) and C- (peripherin-) positive neurons in VZV-infected DRG and is largely localised to the sensitised side.

4.3. Phenotypic changes in neuropeptide and ion channel expression in sensory neurons in the DRG

Following peripheral nerve damage, phenotypic changes occur in peptide expression in DRG that may contribute to sensory sensitisation and chronic pain (Hökfelt et al., 1994). Neuropeptide changes in PHN have not previously been described. We observed an upregulation of NPY and galanin in the DRGs of VZV-infected rats, mimicking that seen in other nerve injury models (Hökfelt et al., 1994) with NPY being largely restricted to the NF-200-positive myelinated cells (Ma and Bisby, 1998; Munglani et al., 1995; Wallace et al., 2003).

Chronic nerve injury is also associated with subunit redistribution and altered subunit compositions of sodium and calcium channels that may predispose afferent neurons in sensory pathways to fire inappropriately (Cummins et al., 2000; Matzner and Devor, 1994; Rogawski and Löscher, 2004). After some peripheral nerve injuries, and here following VZV infection, the expression of the Ca^{2+} channel $\alpha 2\delta 1$ subunit in DRG neurons is upregulated (Luo et al., 2002; Newton et al., 2001). In such situations gabapentin does show antiallodynic effects, suggesting that gabapentin may block neuropathic pain by inhibiting the DRG hyperexcitability resulting from an upregulation of $\alpha 2\delta$ channels.

Changes accompanying both VZV infection and nerve injury include an increase in DRG $Na_v1.3$ (type III) Na^+ channels, leading to functional changes in afferent sodium currents (Cummins et al., 2000; Dib-Hajj et al., 1999; Kim et al., 2001). TTX-sensitive $Na_v1.3$ channels produce fast sodium currents that recover rapidly from inactivation, permitting high-frequency ectopic firing (Cummins et al., 2001).

Recent evidence indicates that increased expression of the $Na_v1.8$ channel (Akopian et al., 1996; Sangameswaran et al., 1996) in nociceptive sensory neurons near the site of injury results in spontaneous ectopic discharges and lowered mechanical activation thresholds leading to the consequences of neuropathic and inflammatory pain (Gold et al., 2003; Novakovic et al., 1998; Roza et al., 2003; Tanaka et al., 1998). Some reports suggest that nerve injury downregulates $Na_v1.8$ expression (Cummins et al., 2000; Decosterd et al., 2002), although antisense knockdown can alleviate sensitisation following nerve injury (Porreca et al., 1999). We saw increased expression of $Na_v1.8$ protein in DRG following VZV infection, which might explain why the agents used here, which block TTX-resistant sodium channels (Brau et al., 2001), were notably effective. Thus, specific sodium channel-blocking agents could be effective analgesics following VZV infection as in nerve injury-induced pain (Chabal et al., 1992; Devor et al., 1993; Omana-Zapata et al., 1997; Rizzo, 1997).

4.4. Gabapentin and sodium channel blockers alleviate VZV- induced sensitisation

Gabapentin inhibits both the allodynia following nerve injury and ectopic discharges of nociceptive afferents (Pan et al., 1999) as well as attenuating the increased responses of spinal cord dorsal horn neurons and afferents to noxious stimulation in the post-injury state (Chapman et al., 1998a; Kanai et al., 2004; Stanfa et al., 1997). Gabapentin binds with high affinity to the voltage-gated calcium channel $\alpha 2\delta 1$ and $\alpha 2\delta 2$ subunits and is thought to inhibit high voltage-activated Ca^{2+} currents through channels that contain these subunits (Rogawski and Löscher, 2004). Gabapentin is effective in the treatment of neuropathic pain, specifically post-herpetic neuralgia (Beydoun, 1999; Mao and Chen, 2000) and is antinociceptive following nerve injury (Erichsen and Blackburn Munro, 2002; Laughlin et al., 2002; Pan et al., 1999). We find gabapentin to be effective in reducing VZV-induced mechanical allodynia for up to 24 h and thermal hyperalgesia for up to 6 h following oral administration. This matches previous reports of effectiveness against PHN in humans (Rowbotham et al., 1998). Although the mechanism of analgesic action of gabapentin is unclear, recent findings suggest it reduces fast glutamatergic and glycinergic spinal synaptic transmission downstream of its inhibition of P/Q-type Ca^{2+} channels, the $\alpha 2\delta 1$ subunit of which it is thought to target and which is upregulated in the DRG and spinal cord following nerve injury (Bayer et al., 2004; Luo et al., 2002).

The sodium channel blockers, mexiletine and lamotrigine both block TTX-resistant sodium channel currents and are thought to act by direct channel binding, thus potentially preventing sodium influx and reducing action potential duration in nociceptive afferents (Brau et al., 2001; Clare et al., 2000; Ragsdale and Avoli, 1998). Mexiletine, currently in clinical use for neuropathic pain (Chabal et al., 1992), decreases spontaneous activity and mechanical sensitivity associated with neuroma formation, and the spontaneous activity of spinal neurons in nerve-ligated rats (Chabal et al., 1989; Chapman et al., 1998b). Mexiletine can alleviate hyperalgesia and allodynia in models of neuropathic pain (Erichsen and Blackburn Munro, 2002; Jett et al., 1997) and inhibits acute herpetic pain (Asano et al., 2003). Lamotrigine can also suppress repetitive firing of sodium-dependent, fast action potentials (Cheung et al., 1992) and attenuates both hyperalgesia (Erichsen et al., 2003) and allodynia (Laughlin et al., 2002) in models of neuropathic pain. It also reduces dorsal horn neuronal excitation elicited by the chemical algogen mustard oil (Blackburn-Munro and Fleetwood-Walker, 1997) and reverses prostaglandin E_2 and streptozotocin-induced mechanical hyperalgesia (Nakamura-Craig and Follenfant, 1995). Both lamotrigine and mexilitine were effective inhibitors of thermal hyperalgesia and allodynia in the present model.

In summary, we demonstrate a number of similarities between VZV infection and other neuropathic pain states in both functional changes and in the phenotypic changes that occur in the DRG. The presence of VZV in DRG neurons in this model was directly confirmed by both immunoblot and immunohistochemical evidence for the specific expression of VZV IE62. The induction of ATF-3 ipsilateral to VZV

infection indicates that sensory cells are stressed/injured following VZV infection. NPY is also upregulated in NF-200 positive DRG cells, whilst sodium channel involvement in the VZV-induced pain state is suggested by the observation that $Na_v1.3$ and $Na_v1.8$ channel subtypes as well as the neuropeptide, galanin are upregulated in the DRG.

The anticonvulsant, gabapentin and the sodium channel blockers lamotrigine and mexiletine were effective in reducing VZV-induced pain behaviors, while the anti-inflammatory agent diclofenac was not. Thus several aspects of the pharmacological sensitivity of VZV-induced pain behaviors and phenotypic changes are closely aligned with models of nerve injury-induced pain. Further work will reveal whether there are distinct biochemical and functional changes that are specific to this model.

Acknowledgements

We thank Gordon Goodall for expert histological skills, Linda Wilson for confocal assistance and staff at WARU and MFAA facilities for animal husbandry. Thanks to Paul J. Meechan for biosafety advice. PRK was supported by US PHS grants EY08098, EY07397, and funds from Research to Prevent Blindness, Inc. This work was supported by Merck & Co., Inc. and The Wellcome Trust.

References

Akopian AN, Sivilotti L, Wood JN. A tetrodotoxin-resistant voltage-gated sodium channel expressed by sensory neurons. Nature 1996;379(6562): 257–62.

Amaya F, Decosterd I, Samad TA, Plumpton C, Tate S, Mannion RJ, Costigan M, Woolf CJ. Diversity of expression of the sensory neuron-specific TTX-resistant voltage-gated sodium ion channels SNS and SNS2. Mol Cell Neurosci 2000;15(4):331–42.

Arner S, Meyerson MA. Lack of analgesic effect of opioids on neuropathic and idiopathic forms of pain. Pain 1988;33:11–23.

Arvin AM. Varicella zoster virus: overview and clinical manifestations. Semin Dermatol 1996;15(2 Suppl. 1):4–7.

Asano K, Sameshima T, Shirasawa H, Hisamitsu T. Attenuating effect of mexiletine hydrochloride on herpetic pain in mice infected with herpes simplex virus. J Pharm Pharmacol 2003;55:1365–70.

Baker D, Wood JN. Involvement of Na^+ channels in pain pathways. Trends Pharmacol Sci 2001;22:27–31.

Bayer K, Ahmadi S, Zeilhofer HU. Gabapentin may inhibit synaptic transmission in the mouse spinal cord dorsal horn through a preferential block of P/Q-type Ca^{2+} channels. Neuropharmacology 2004;46(5): 743–9.

Bennett GJ, Xie YK. A peripheral mononeuropathy in rat that produces disorders of pain sensation like those seen in man. Pain 1988;33: 87–107.

Beydoun A. Postherpetic neuralgia: role of gabapentin and other treatment modalities. Epilepsia 1999;40(Suppl 6):S51–S6.

Blackburn-Munro G, Fleetwood-Walker SM. The effects of Na^+ channel blockers on somatosensory processing by rat dorsal horn neurones. NeuroReport 1997;8:1549–54.

Bowsher D. Pathophysiology of postherpetic neuralgia: towards a rational treatment. Neurology 1995;45(Suppl. 8):S56–S7.

Brau ME, Dreimann M, Olschewski A, Vogel W, Hempelmann G. Effect of drugs used for neuropathic pain management on tetrodotoxin-resistant Na^+ currents in rat sensory neurones. Anesthesiology 2001;94:137–44.

Cantrell AR, Catterall WA. Neuromodulation of Na^+ channels: an unexpected form of cellular plasticity. Nat Rev Neurosci 2001;2: 397–407.

Chabal C, Russel LC, Burchiel KJ. The effect of intravenous lidocaine, tocainide, and mexiletine on spontaneously active fibers originating in rat sciatic neuromas. Pain 1989;38:333–8.

Chabal C, Jacobson L, Mariano A, Chaney E, Britell CW. The use of oral mexiletine for the treatment of pain after peripheral nerve injury. Anesthesiology 1992;76:513–7.

Chapman V, Suzuki R, Chamarette HL, Rygh LJ, Dickenson AH. Effects of systemic carbamazepine and gabapentin on spinal neuronal responses in spinal nerve ligated rats. Pain 1998a;75(2–3):261–72.

Chapman V, Ng J, Dickenson AH. A novel spinal action of mexiletine in spinal somatosensory transmission of nerve injured rats. Pain 1998b;77: 289–96.

Cheung H, Kamp D, Harris E. An in vitro investigation of the action of lamotrigine on neuronal voltage-activated sodium channels. Epilepsy Res 1992;13:107–12.

Christensen D, Gautron M, Guilbaud G, Kayser V. Effect of gabapentin and lamotrigine on mechanical allodynia-like behaviour in a rat model of trigeminal neuropathic pain. Pain 2001;93(2):147–53.

Clare JJ, Tate SN, Nobbs M, Romanos MA. Voltage-gated sodium channels as therapeutic targets. Drug Discov Today 2000;5:506–20.

Coderre TJ, Melzack R. The contribution of excitatory amino acids to central sensitization and persistent nociception after formalin-induced tissue injury. J Neurosci 1992;12:3665–70.

Cohrs RJ, Barbour M, Gilden DH. Varicella-zoster virus (VZV) transcription during latency in human ganglia: detection of transcripts mapping to genes 21, 29, 62, and 63 in a cDNA library enriched for VZV RNA. J Virol 1996;70(5):2789–96.

Cohrs RJ, Gilden DH, Mahalingam R. Varicella zoster virus latency, neurological disease and experimental models: an update. Front Biosci 2004;9:751–62.

Cummins TR, Dib-Hajj SD, Black JA, Waxman SG. Sodium channels and the molecular pathophysiology of pain. Prog Brain Res 2000;129:3–19.

Cummins TR, Aglieco F, Renganathan M, Herzog RI, Dib-Hajj SD, Waxman SG. $Na_V1.3$ sodium channels: rapid repriming and slow closed-state inactivation display quantitative differences after expression in a mammalian cell cine and in spinal sensory neurons. J Neurosci 2001;21:5952–61.

Dalziel RG, Bingham S, Sutton D, Grant D, Champion JM, Dennis SA, Quinn JP, Bountra C, Mark MA. Allodynia in rats infected with varicella zoster virus—a small animal model for post-herpetic neuralgia. Brain Res Rev 2004;46(2):234–42.

Davies PS, Galer BS. Review of lidocaine patch 5% studies in the treatment of postherpetic neuralgia. Drugs 2004;64(9):937–47.

Decosterd I, Ji RR, Abdi S, Tate S, Woolf CJ. The pattern of expression of the voltage-gated sodium channels $Na_V1.8$ and $Na_V1.9$ does not change in uninjured primary sensory neurons in experimental neuropathic pain models. Pain 2002;96:269–77.

Devor M, Govrin-Lippmann R, Angelides K. Na^+ channel immunolocalization in peripheral mammalian axons and changes following nerve injury and neuroma formation. J Neurosci 1993;13(5):1976–92.

Dib-Hajj SD, Fjell J, Cummins TR, Zheng Z, Fried K, LaMotte R, Black JA, Waxman EG. Plasticity of sodium channel expression in DRG neurons in the chronic constriction injury model of neuropathic pain. Pain 1999;83:591–600.

Erichsen HK, Blackburn-Munro G. Pharmacological characterisation of the spared nerve injury model of neuropathic pain. Pain 2002;98(1–2): 151–61.

Erichsen HK, Hao JX, Xu XJ, Blackburn-Munro G. A comparison of the antinociceptive effects of voltage-activated Na^+ channel blockers in

two rat models of neuropathic pain. Eur J Pharmacol 2003;458(3): 275–82.

Fleetwood-Walker SM, Quinn JP, Wallace C, Blackburn-Munro G, Kelly BG, Fiskerstrand CE, Nash AA, Dalziel RG. Behavioural changes in the rat following infection with varicella-zoster virus. J Gen Virol 1999;80(9):2433–6.

Garry EM, Moss A, Rosie R, Delaney A, Mitchell R, Fleetwood-Walker SM. Specific involvement in neuropathic pain of AMPA receptors and adapter proteins for the GluR2 subunit. Mol Cell Neurosci 2003;24(1):10–22.

Gold MS, Weinreich D, Kim CS, Wang R, Treanor J, Porreca F, Lai J. Redistribution of Na(V)1.8 in uninjured axons enables neuropathic pain. J Neurosci 2003;23(1):158–66.

Hökfelt T, Zhang X, Wiesenfeld-Hallin Z. Messenger plasticity in primary sensory neurons following axotomy and its functional implications. Trends Neurosci 1994;17:22–30.

Jett MF, McGuirk J, Waligora D, Hunter JC. The effects of mexiletine, desipramine and fluoxetine in rat models involving central sensitization. Pain 1997;69:161–9.

Kanai A, Sarantopoulos C, McCallum JB, Hogan Q. Painful neuropathy alters the effect of gabapentin on sensory neuron excitability in rats. Acta Anaesthesiol Scand 2004;48(4):507–12.

Kennedy PG, Grinfeld E, Bontems S, Sadzot-Delvaux C. Varicella-zoster virus gene expression in latently infected rat dorsal root ganglia. Virology 2001;289(2):218–23.

Kim KJ, Yoon YW, Chung JM. Comparison of three rodent neuropathic pain models. Exp Brain Res 1997;113(2):200–6.

Kim CH, Oh Y, Chung JM, Chung K. The changes in expression of three subtypes of TTX sensitive sodium channels in sensory neurons after spinal nerve ligation. Brain Res Mol Brain Res 2001;95:153–61.

Kinchington PR, Hougland JK, Arvin AM, Ruyechan WT, Hay J. The varicella-zoster virus immediate-early protein IE62 is a major component of virus particles. J Virol 1992;66:359–66.

Laird JM, Bennett GJ. An electrophysiological study of dorsal horn neurons in the spinal cord of rats with an experimental peripheral neuropathy. J Neurophysiol 1993;69(6):2072–85.

Laughlin TM, Tram KV, Wilcox GL, Birnbaum AK. Comparison of antiepileptic drugs tiagabine, lamotrigine, and gabapentin in mouse models of acute, prolonged, and chronic nociception. J Pharmacol Exp Ther 2002;302(3):1168–75.

Lawson SN, Perry MJ, Prabhakar E, McCarthy PW. Primary sensory neurones: neurofilament, neuropeptides, and conduction velocity. Brain Res Bull 1993;30:239–43.

Lehmann J, Schneider J, McPherson S, Murphy DE, Bernard P, Tsai C, Bennett DA, Pastor G, Steel DJ, Boehm C. CPP, a selective *N*-methyl-D-aspartate (NMDA)-type receptor antagonist: characterization in vitro and in vivo. J Pharmacol Exp Ther 1987;240:737–46.

Lungu O, Panagiotidis CA, Annunziato PW, Gershon AA, Silverstein SJ. Aberrant intracellular localization of Varicella–Zoster virus regulatory proteins during latency. Proc Natl Acad Sci USA 1998;95(12):7080–5.

Luo ZD, Calcutt NA, Higuera ES, Valder CR, Song YH, Svensson CI, Myers RR. Injury type-specific calcium channel alpha 2 delta-1 subunit up-regulation in rat neuropathic pain models correlates with anti-allodynic effects of gabapentin. J Pharmacol Exp Ther 2002;303(3): 1199–205.

Ma W, Bisby MA. Partial and complete sciatic nerve injuries induce similar increases of neuropeptide Y and vasoactive intestinal peptide immunoreactivities in primary sensory neurons and their central projections. Neuroscience 1998;86:1217–34.

Malmberg AB, Yaksh TL. Pharmacology of the spinal action of ketorolac, morphine, ST-91, U50488H, and L-PIA on the formalin test and an isobolographic analysis of the NSAID interaction. Anesthesia 1993;79: 270–81.

Mao J, Chen LL. Gabapentin in pain management. Anesth Analg 2000;91: 680–7.

Matzner O, Devor M. Hyperexcitability at sites of nerve injury depends on voltage-sensitive Na^+ channels. J Neurophysiol 1994;72(1):349–59.

Mayer DJ, Mao J, Holt J, Price DD. Cellular mechanisms of neuropathic pain, morphine tolerance, and their interactions. Proc Natl Acad Sci USA 1999;96:7731–6.

Meier JL, Straus SE. Interactions between varicella-zoster virus IE62 and cellular transcription factor USF in the coordinate activation of genes 28 and 29. Neurology 1995;45:S30–S2.

Moore KA, Kohno T, Karchewski LA, Scholz J, Baba H, Woolf CJ. Partial peripheral nerve injury promotes a selective loss of GABAergic inhibition in the superficial dorsal horn of the spinal cord. J Neurosci 2002;22:6724–31.

Munglani R, Bond A, Smith GD, Harrison SM, Elliot PJ, Birch PJ, Hunt SP. Changes in neuronal markers in a mononeuropathic rat model relationship between neuropeptide Y, pre-emptive drug treatment and long-term mechanical hyperalgesia. Pain 1995;63:21–31.

Nakamura-Craig M, Follenfant RL. Effect of lamotrigine in the acute and chronic hyperalgesia induced by PGE2 and in the chronic hyperalgesia in rats with streptozotocin-induced diabetes. Pain 1995; 63:33–7.

Neff BJ, Weibel RE, Villarejos VM, Buynak EB, McLean AA, Morton DM, Wolanski BS, Hilleman MR. Clinical and laboratory studies of KMcC strain live attenuated varicella virus. Proc Soc Exp Biol Med 1981;166: 339–47.

Newton RA, Bingham S, Case PC, Sanger GJ, Lawson SN. Dorsal root ganglion neurons show increased expression of the calcium channel $\alpha 2\delta$-1 subunit following partial sciatic nerve injury. Brain Res Mol Brain Res 2001;95:1–8.

Novakovic SD, Tzoumaka E, McGivern JG, Haraguchi M, Sangameswaran L, Gogas KR, Eglen RM, Hunter JC. Distribution of the tetrodotoxin-resistant sodium channel PN3 in rat sensory neurons in normal and neuropathic conditions. J Neurosci 1998;18: 2174–87.

Omana-Zapata I, Khabbaz MA, Hunter JC, Clarke DE, Bley KR. Tetrodotoxin inhibits neuropathic ectopic activity in neuromas, dorsal root ganglia and dorsal horn neurons. Pain 1997;72(1–2):41–9.

Palecek J, Paleckova V, Dougherty PM, Carlton SM, Willis WD. Responses of spinothalamic tract cells to mechanical and thermal stimulation of skin in rats with experimental peripheral neuropathy. J Neurophysiol 1992;67(6):1562–73.

Pan HJ, Eisenach JC, Chen SR. Gabapentin suppresses ectopic nerve discharges and reverses allodynia in neuropathic rats. J Pharamcol Exp Ther 1999;288:1026–30.

Pappagallo M. Newer antiepileptic drugs: possible uses in the treatment of neuropathic pain and migraine. Clin Ther 2003; 25(10):2506–38.

Porreca F, Lai J, Bian D, Wegert S, Ossipov MH, Eglen RM, Kassotakis L, Novakovic S, Rabert DK, Sangameswaran L, Hunter JC. A comparison of the potential role of the tetrodotoxin-insensitive sodium channels, PN3/SNS and NaN/SNS2, in rat models of chronic pain. Proc Natl Acad Sci USA 1999;96:7640–4.

Ragsdale DS, Avoli M. Sodium channels as molecular targets for antiepileptic drugs. Brain Res Rev 1998;26:16–28.

Rizzo MA. Successful treatment of painful traumatic mononeuropathy with carbamazepine: insights into a possible molecular pain mechanism. J Neurol Sci 1997;152(1):103–6.

Rogawski MA, Löscher W. The neurobiology of antiepileptic drugs for the treatment of nonepileptic conditions. Nat Med 2004;10:685–92.

Rowbotham MC, Fields HL. The relationship of pain, allodynia and thermal sensation in post-herpetic neuralgia. Brain 1996;119(2): 347–54.

Rowbotham M, Harden N, Stacey B. Gabapentin for the treatment of postherpetic neuralgia. J Am Med Assoc 1998;280:1837–42.

Roza C, Laird JM, Souslova V, Wood JN, Cervero F. The tetrodotoxin-resistant Na^+ channel $Na_v1.8$ is essential for the expression of spontaneous activity in damaged sensory axons of mice. J Physiol (London) 2003;550:921–6.

Sadzot-Delvaux C, Merville-Louis MP, Delree P, Marc P, Piette J, Moonen G, Rentier B. An in vivo model of varicella-zoster virus latent infection of dorsal root ganglia. J Neurosci Res 1990;26(1):83–9.

Sadzot-Delvaux C, Debrus S, Nikkels A, Piette J, Rentier B. Varicella-zoster virus latency in the adult rat is a useful model for human latent infection. Neurology 1995;45(12):S18–S20.

Sangameswaran L, Delgado SG, Fish LM, Koch BD, Jakeman LB, Stewart GR, Sze P, Hunter JC, Eglen RM, Herman RC. Structure and function of a novel voltage-gated, tetrodotoxin-resistant sodium channel specific to sensory neurons. J Biol Chem 1996;271:5953–6.

Sato B, Ito H, Hinchliffe S, Sommer MH, Zerboni L, Arvin AM. Mutational analysis of open reading frames 62 and 71, encoding the varicella-zoster virus immediate-early transactivating protein, IE62, and effects on replication in vitro and in skin xenografts in the SCID-hu mouse in vivo. J Virol 2003;77(10):5607–20.

Stanfa LC, Singh L, Williams RG, Dickenson AH. Gabapentin, ineffective in normal rats, markedly reduces C-fiber evoked responses after inflammation. NeuroReport 1997;8:587–90.

Tanaka M, Cummins TR, Ishikawa K, Dib-Hajj SD, Black JA, Waxman SG. SNS Na^+ channel expression increases in dorsal root ganglion neurons in the carrageenan inflammatory pain model. NeuroReport 1998;9:967–72.

Tenser RB. Herpes zoster infection and postherpetic neuralgia. Curr Neurol Neurosci Rep 2001;1(6):526–32.

Tsujino H, Kondo E, Fukuoka T, Dai Y, Tokunaga A, Miki K, Yonenobu K, Ochi T, Noguchi K. Activating transcription factor 3 (ATF3) induction by axotomy in sensory and motoneurons: a novel neuronal marker of nerve injury. Mol Cell Neurosci 2000;15(2): 170–82.

Wallace VC, Cottrell DF, Brophy PJ, Fleetwood-Walker SM. Focal lysolecithin-induced demyelination of peripheral afferents results in neuropathic pain behavior that is attenuated by cannabinoids. J Neurosci 2003;23(8):3221–33.

Woolf CJ, Salter MW. Neuronal plasticity: increasing the gain in pain. Science 2000;288(5472):1765–9.

Xiao HS, Huang QH, Zhang FX, Bao L, Lu YJ, Guo C, Yang L, Huang WJ, Fu G, Xu SH, Cheng XP, Yan Q, Zhu ZD, Zhang X, Chen Z, Han ZG, Zhang X. Identification of gene expression profile of dorsal root ganglion in the rat peripheral axotomy model of neuropathic pain. Proc Natl Acad Sci USA 2002;99(12):8360–5.

ACADEMIC PRESS

Available online at www.sciencedirect.com
SCIENCE DIRECT®

Molecular and Cellular Neuroscience 24 (2003) 10–22

MCN Molecular and Cellular Neuroscience

www.elsevier.com/locate/ymcne

Specific involvement in neuropathic pain of AMPA receptors and adapter proteins for the GluR2 subunit

Emer M. Garry,[a] Andrew Moss,[a,1] Roberta Rosie,[a] Ada Delaney,[a] Rory Mitchell,[b] and Susan M. Fleetwood-Walker[a,*]

[a] *Centre for Neuroscience Research, Division of Preclinical Veterinary Sciences, Royal (Dick) School of Veterinary Studies, University of Edinburgh, Summerhall, Edinburgh EH9 1QH, UK*

[b] *MRC Membrane and Adapter Proteins Co-operative Group and Membrane Biology Group, School of Biomedical and Clinical Laboratory Sciences, University of Edinburgh, Edinburgh EH8 9XD, UK*

Received 2 April 2003; revised 2 April 2003; accepted 8 April 2003

Abstract

Chronic pain states arise from peripheral nerve injury and are inadequately treated with current analgesics. Using intrathecal drug administration in a rat model of neuropathic pain, we demonstrate that AMPA receptors play a role in the central sensitisation that is thought to underpin chronic pain. The GluR2 subunit of the AMPA receptor binds to a number of intracellular adapter proteins including GRIP, PICK1 and NSF, which may link the receptor to proteins with signalling, scaffolding and other roles. We implicate for the first time a possible role for GRIP, PICK1 and NSF in neuropathic sensitisation from experiments with cell-permeable blocking peptides mimicking their GluR2 interaction motifs and also demonstrate differential changes in expression of these proteins following peripheral nerve injury. These studies suggest a critical involvement of protein:protein complexes associated with the AMPA receptor in neuropathic pain, and the possibility that they may have potential as novel therapeutic targets.

Introduction

Neuropathic pain is a hypersensitive chronic pain state, which is poorly treated with current analgesics. Glutamate is important in neurotransmission from primary afferent inputs and several studies suggest a role for the AMPA subtype of glutamate receptor in sensitisation. AMPA receptor agonists depolarise nociceptive spinal neurons and increase responses to noxious and innocuous stimulation as well as enhancing acute nociceptive behaviours (Aanonsen et al., 1990; Dougherty et al., 1992; Budai and Larson, 1994; Cumberbatch et al., 1994; Aanonsen and Wilcox, 1987), while AMPA receptor antagonists disrupt acute nociceptive behavioural responses and chronic pain, including neuropathic pain (Mao et al., 1992; Chaplan et al., 1997; Sorkin et al., 2001; Nishiyama et al., 1998). The molecular mechanisms underlying these actions of AMPA receptors are however unknown.

Of the four AMPA receptor subunits (GluR1-4; Hollmann and Heinemann, 1994), the GluR2/3 subunits have received particular attention since a number of proteins interact with a PDZ domain target motif at their C-terminus. GluR2, but not GluR3, is abundant in the dorsal spinal cord (Jakowec et al., 1995). The PDZ domain-containing proteins that can dock to GluR2 include the GRIP (Glutamate Receptor Interacting Protein) family (Dong et al., 1997, 1999; Srivastava et al., 1998; Brückner et al., 1999) and PICK1 (Protein Interacting with C Kinase 1) (Xia et al., 1999; Dev et al., 1999). GRIP is enriched in the postsynaptic density (PSD) but is also cytosolic (Wyszynski et al., 1998). PICK1 (originally identified by its interaction with PKCα; Xia et al., 1999; Dev et al., 1999) may act to bring

* Corresponding author. Fax: +44-131-650-6576.
E-mail address: s.m.fleetwood-walker@ed.ac.uk (S.M. Fleetwood-Walker).
[1] Current address: Department of Anatomy and Developmental Biology, Medawar Building, University College London, Gower St., London, WC1E 6BT, UK.

1044-7431/03/$ – see front matter © 2003 Elsevier Science (USA). All rights reserved.
doi:10.1016/S1044-7431(03)00134-9

the kinase close to plasma membrane substrates, including the AMPA receptor (Staudinger et al., 1997; Perez et al., 2001). Disruption of the GluR2 C-terminal SVKI motif interactions suggests that GRIP and PICK1 are important in the synaptic clustering of AMPA receptors (Dong et al., 1997; Osten et al., 2000) for unmasking silent glutamatergic synapses in somatosensory inputs (Li et al., 1999) and for the expression of long term changes in the excitability of hippocampal and cerebellar neurons (Xia et al., 2000; Kim et al., 2001). Both GRIP and PICK1 proteins have been implicated in the cell surface clustering of GluR2-containing AMPA receptors (Xia et al., 1999; Osten et al., 2000), while PICK1 appears to be involved in AMPA receptor endocytosis (Perez et al., 2001). NSF (N-ethylmaleimide-Sensitive Fusion protein), a non-PDZ domain protein involved in membrane fusion, is enriched in the PSD and has been shown to dock to the GluR2 subunit at a different site on its C-terminus (VAKNAQ, Osten et al., 1998; Song et al., 1998). This interaction may contribute to stabilising excitatory currents in hippocampal neurons (Nishimune et al., 1998; Song et al., 1998), to the movement of AMPA receptors to the cell surface (Noel et al., 1999; Lüthi et al., 1999; Luscher et al., 1999) and to Long Term Potentiation (LTD) (Lledo et al., 1998).

In the present study we asked whether AMPA receptors and GluR2 subunit adapter proteins might play a specific role in the sensitised responsiveness of spinal cord neurons that underlies neuropathic pain.

Results

AMPA receptor antagonists attenuate neuropathic reflex sensitisation following CCI

To examine the question of a role for the AMPA receptor in neuropathic pain conditions, we assessed the contribution of spinal AMPA receptors to CCI-induced changes in somatosensory behavioural reflexes by carrying out intrathecal administration of the AMPA receptor antagonists NBQX, NS-257 and SYM 2206 (Fig. 1a and b, Table 1). Intrathecal injection of the AMPA/kainate receptor antagonist NBQX and the highly selective AMPA receptor antagonists NS-257 and SYM 2206 in rats at the peak of behavioural reflex sensitisation attenuated the ipsilaterally sensitised behavioural measures of thermal hyperalgesia. NBQX, NS-257 and SYM 2206 had similar but somewhat less marked effects on mechanical allodynia following CCI. None of the antagonists caused any alteration in sensory responses elicited from the contralateral (uninjured) side of CCI animals or from sham/naïve animals at the concentrations that were found to clearly modify ipsilateral responses after CCI. Intrathecal injection of vehicle had no discemable effect on thermal hyperalgesia or mechanical allodynia following CCI (Table 1). These data indicate a pre-eminent role for AMPA receptors in the spinal cord in mediating the sensitised nociceptive transmission that occurs following peripheral nerve damage. This role of AMPA receptors in sensitisation is more readily disrupted by antagonists than the contribution of AMPA receptors to acute nociceptive or non-nociceptive inputs, since nociceptive reflexes from the contralateral (non-sensitised) side of CCI animals (Fig. 1) and in naïve animals (data not shown) were unaffected by the doses of AMPA receptor antagonists used here.

Effects of myristoylated GluR2 domain peptides on neuropathic sensitisation

Since there is little in vivo functional evidence on the spinal role of proteins that interact with the C-terminus of the GluR2 subunit, we assessed the effects of the local application of myristoylated peptides (designed to obscure the site of interaction of the GluR2 subunit with GRIP, PICK1 or NSF) on CCI-induced behavioural reflex changes. Intrathecal injection of the inhibitory peptide blocking the NSF binding site, myr-GluR2$_{846-856}$ significantly attenuated the thermal hyperalgesic state for up to 35 min (Fig. 1c) but had a much smaller and very short-lasting effect on mechanical allodynia (Fig. 1d). The inactive control peptide ([N854S]myr-GluR2$_{846-856}$; Noel et al., 1999) had no effect at any time tested (Fig. 2a, b). Similarly, administration of myr-GluR2$_{874-883}$ (to block the site of both GRIP and PICK1 binding on the extreme GluR2/3 C-terminus) markedly alleviated the CCI-induced ipsilateral thermal hyperalgesia for up to 50 min following injection (Table 1, Fig. 1e), but failed to significantly affect mechanical allodynia (Fig. 1f). Point mutation of S880 to E in this sequence produces a peptide that is no longer recognised by GRIP but still interacts with PICK1 (Li et al., 1999; Chung et al., 2000; Daw et al., 2000). [S880E]myr-GluR2$_{874-883}$ significantly attenuated thermal hyperalgesia (Fig. 2c), while effects on mechanical allodynia (Fig. 2d) were less pronounced. The inactive control peptide [1883E]myr-GluR2$_{874-883}$ (Li et al., 1999; Osten et al., 1999) had no effect on reflex behaviours at any time (Fig. 2ef), nor did a further control myristoylated peptide of unrelated sequence (Table 1).

These data indicate for the first time a functional role in vivo for AMPA receptor-interacting proteins in persistent neuropathic pain, suggesting that interactions of both GluR2:GRIP/PICK1 and GluR2:NSF docking domains may contribute to the maintenance of neuropathic thermal hyperalgesia with a lesser effect on mechanical allodynia. Since the effects of myr-GluR2$_{874-883}$ (which blocks both GRIP and PICK1 interactions) were essentially mimicked by [S880E]myr-GluR2$_{874-883}$, which still interacts with PICK1 but not GRIP, it appears that the PICK1 interaction in particular may be important in neuropathic sensitisation. None of the inhibitory peptides had any significant effect on contralateral responses or when tested in naïve rats (data not shown).

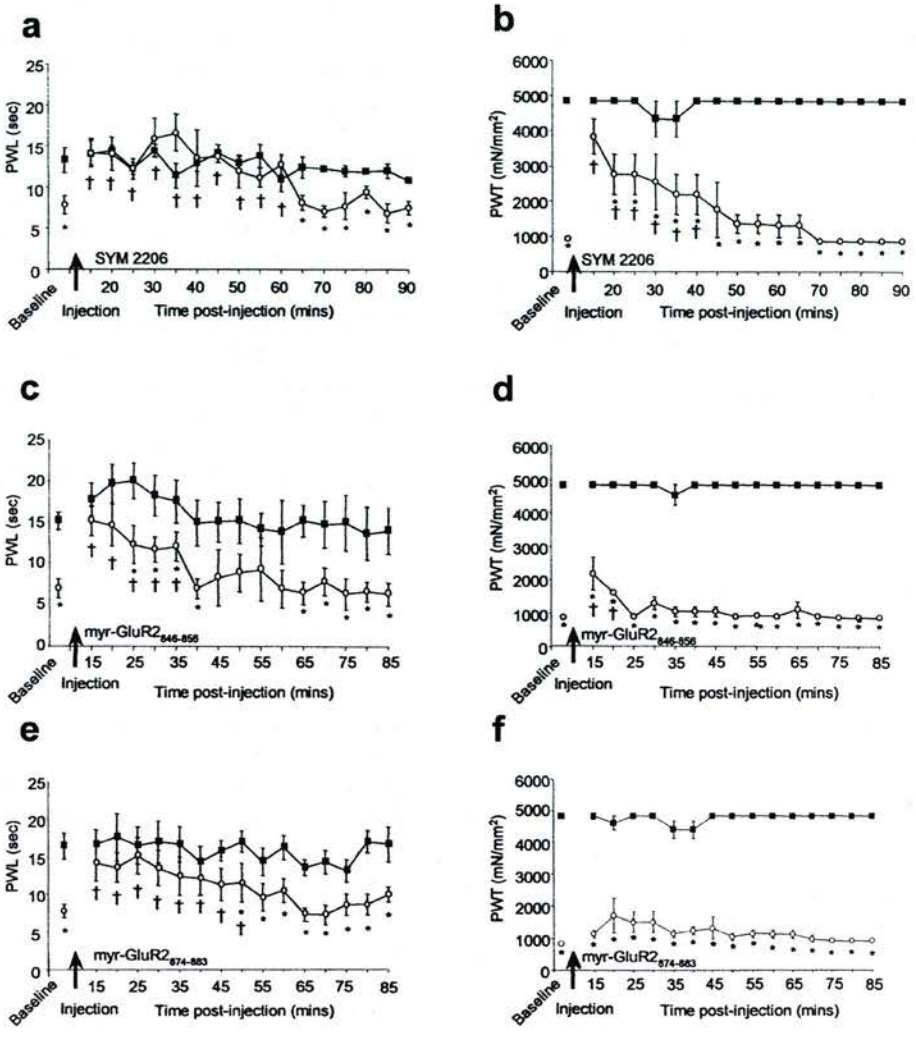

Fig. 1. Effects of intrathecal administration of the AMPA receptor antagonist SYM 2206, or the myristoylated peptides myr-GluR2$_{846-856}$ (NSF motif) and myr-GluR2$_{874-883}$ (PDZ target motif) on nerve injury-induced thermal hyperalgesia and mechanical allodynia. Data represent the average hindlimb withdrawal latency (sec) to noxious heat (a, c, e) and withdrawal threshold to mechanical stimuli (mN/mm^2; b, d, f) ± SEM before or following the intrathecal injection of either SYM 2206 (1.5 nmol/50 μl, a, b), myr-GluR2$_{846-856}$ (4.5 nmol/50 μl, c, d) or myr-GluR2$_{874-883}$ (4.5 nmol/50 μl, e, f). Rats at the peak of ipsilateral reflex sensitisation, as determined by a significant reduction in baseline ipsilateral paw withdrawal latency to thermal stimuli (PWL; *$P < 0.05$ Student's t-test, a, c, e) or paw withdrawal threshold to mechanical stimuli (PWT; *$P < 0.05$ Mann-Whitney Rank Sum test, b, d, f) compared to contralateral withdrawal responses, were intrathecally injected (at arrow). Following injection, SYM 2206 (a), myr-GluR2$_{846-856}$ (c) and myr-GluR2$_{874-883}$ (e) significantly attenuated the accentuated ipsilateral thermal responses (○) in comparison to pre-injection ipsilateral values (†$P < 0.05$, One-way ANOVA followed by a Dunnett's test) while there was no significant alteration in the contralateral (■) response. Paw withdrawal thresholds to mechanical stimulation ipsilateral to CCI (○) showed significant differences between pre- and post-injection values (†$P < 0.05$, Kruskal-Wallis ANOVA followed by a Dunn's test) for SYM 2206 (b) and a transient response only for myr-GluR2$_{846-856}$ (d), with no significant change due to myr-GluR2$_{874-883}$ (f). Contralateral responses (■) were not significantly altered by any of the reagents.

Immunoblotting for the GluR2 AMPA receptor subunit and associated proteins

In order to examine expression levels following CCI, semi-quantitative analysis of immunoblots following SDS-PAGE was carried out for GluR2, GRIP, NSF and PICK1 ipsilateral and contralateral to injury in CCI animals, compared to sham and naive spinal cord. An antibody that recognises both isoforms of GRIP was used. Expression levels were compared to those for GAPDH, a ubiquitous and constitutively expressed housekeeping enzyme, the expression of which does not change following peripheral nerve damage (Medhurst et al., 2000).

We found that levels of GluR2 (Fig. 3a, lane I, Table 2) and GRIP (Fig. 3b, lane I, Table 2) were selectively increased in the spinal cord ipsilateral to CCI with little variation in protein levels between contralateral (C), sham (S) and naïve (N) samples. Blots were stripped and reprobed for GAPDH (Fig. 3, lower panels) to ensure equivalent sample loading (as was also confirmed by Coomassie stain-

Table 1
Summary of the effects of AMPA receptor antagonists and GluR2 adapter protein-blocking peptides on pain-related behavioural reflex responses

Mean % reversal of ipsilateral sensitisation from 15–30 min following drug administration		
Blocker (dose)	Thermal hyperalgesia	Mechanical allodynia
a) General AMPA receptor antagonists		
NBQX (5 nmol)	88.9 ± 8.1*	55.1 ± 3.4†
NS-257 (83 nmol)	82.9 ± 8.2*	27.5 ± 2.9†
SYM 2206 (1.5 nmol)	87.4 ± 7.0*	48.5 ± 4.6†
Vehicle	9.0 ± 2.6	5.5 ± 3.0
b) Myristoylated domain-blocking peptides		
myr-GluR2$_{846-856}$ (4.5 nmol) (NSF target motif)	79.6 ± 10.5*	13.5 ± 2.6§
[N854S]myr-GluR2$_{846-856}$(4.5 nmol) (inactive on NSF motif)	−3.6 ± 4.2	9.9 ± 5.1
myr-GluR2$_{874-883}$ (4.5 nmol) (PDZ target motif)	74.2 ± 4.8*	12.4 ± 2.5
[S880E]myr-GluR2$_{874-883}$ (4.5 nmol) (inactive on GRIP but not PICK1 interaction)	91.9 ± 4.3*	44.8 ± 11.5§
[I883E]myr-GluR2$_{874-883}$ (4.5 nmol) (inactive on PDZ target motif)	11.3 ± 5.6*	11.2 ± 4.1
myr-GRRNAIHDE (4.5 nmol) (inactive unrelated control)	7.6 ± 3.4	3.7 ± 2.5

Note. Data represent mean percent reversal ± SEM from 15–30 min following intrathecal injection of each compound for measurements of thermal hyperalgesia and mechanical allodynia in rats at the peak of ipsilateral reflex sensitivity. * indicates a significantly attenuated ipsilateral thermal hyperalgesia in comparison to pre-injection ipsilateral values at each of the time points throughout this period ($P < 0.05$, One-way ANOVA followed by a Dunnett's test). †indicates a significant attenuation of ipsilateral mechanical allodynia in comparison to pre-injection ipsilateral values at each of the time points throughout this period ($P < 0.05$, Kruskal-Wallis ANOVA followed by a Dunn's test). §indicates results showing statistical significance only at some time points. There were no significant alterations in the pre-/post-injection contralateral responses.

ing of proteins). No significant increase was seen in the levels of PICK1 (Fig. 3c, Table 2) under the same conditions, but in contrast to this, levels of NSF protein (Fig. 3d, Table 2) were significantly decreased ipsilateral to injury (I).

ISHH examination of GluR2, GRIP and NSF mRNA levels following CCI

The distribution of AMPA receptors but not their docking proteins in the spinal cord has been previously documented under normal conditions. However, it is unknown whether the expression of GluR2-interacting proteins is altered in neuropathic pain states (Furuyama et al., 1993; Tölle et al., 1993; Harris et al., 1996). Indeed, there is little evidence for the specific localisation of AMPA receptor-associated proteins in the spinal cord and it was of interest to determine whether there were any localised alterations in their expression levels following the establishment of neuropathic sensitisation. Here we analysed expression of GluR2, GRIP, and NSF mRNA in the spinal cord following CCI. The GRIP2 isoform was examined in particular as it is reported to be the predominant form in the adult nervous system (Brückner et al., 1999). No probe for rat PICK1 was available. In naïve animals, GluR2, GRIP2, and NSF mRNA-labelled neurons were located throughout laminae I–V of the dorsal horn and to a lesser extent in ventral horn motoneurons (Fig. 4). Following CCI, there was a significant increase in the levels of both GluR2 (Fig. 4a) and GRIP2 mRNA (Fig. 4b) in superficial dorsal horn laminae I and II ipsilateral to injury (at the sites of primary afferent termination). While an increase in GluR2 expression was seen only in terms of silver grain density (Fig. 4a), the increase in GRIP2 mRNA was seen in terms of both the silver grain density of mRNA expression and in the number of cells expressing GRIP2 mRNA in LI and II (Fig. 4b). These increases in mRNA expression are in agreement with our assessment of protein levels of GluR2 and GRIP that were both significantly increased ipsilateral to CCI. Minimal alterations in GluR2 and GRIP expression levels were seen in the lower laminae (III–V), or indeed in the ventral horn motoneurons for GRIP, and levels did not significantly differ between contralateral, sham or naïve samples.

Following CCI, there was a small but significant decrease (in agreement with protein analysis for NSF) in the silver grain density of NSF mRNA ipsilateral to injury in LI of the superficial dorsal horn (Fig. 4c), while there was no detectable alteration in the number of cells expressing NSF mRNA. The level of NSF mRNA did not significantly differ between contralateral, sham or naïve samples.

Direct association of GluR2 with GRIP and PICK1

In order to investigate direct association between GluR2 and GRIP and PICK1 in the spinal cord we carried out GluR2-directed immunoprecipitations on spinal cord extracts solubilised under mild detergent conditions. Extracts were immunoprecipitated with a GluR2 antibody (directed against an N-terminal epitope) before probing Western blots of the immunoprecipitated complex for levels of the GluR2 C-terminus-interacting proteins GRIP and PICK1. Both GRIP and PICK1 were clearly co-immunoprecipitated with GluR2, but not in controls where non-immune IgG was used instead of the GluR2 immunoprecipitating antibody (Fig. 5a). As an example of the effectiveness of myr-peptides at interrupting GluR2 interactions, we showed that the co-immunoprecipitation of GRIP with GluR2 was reduced by topical treatment of the spinal cord with myr-GluR2$_{874-883}$ (but not myr-control peptide) prior to extraction (Fig. 5b). This confirms not only that motif selectivity is displayed by topically-applied myristoylated peptides, but also that they

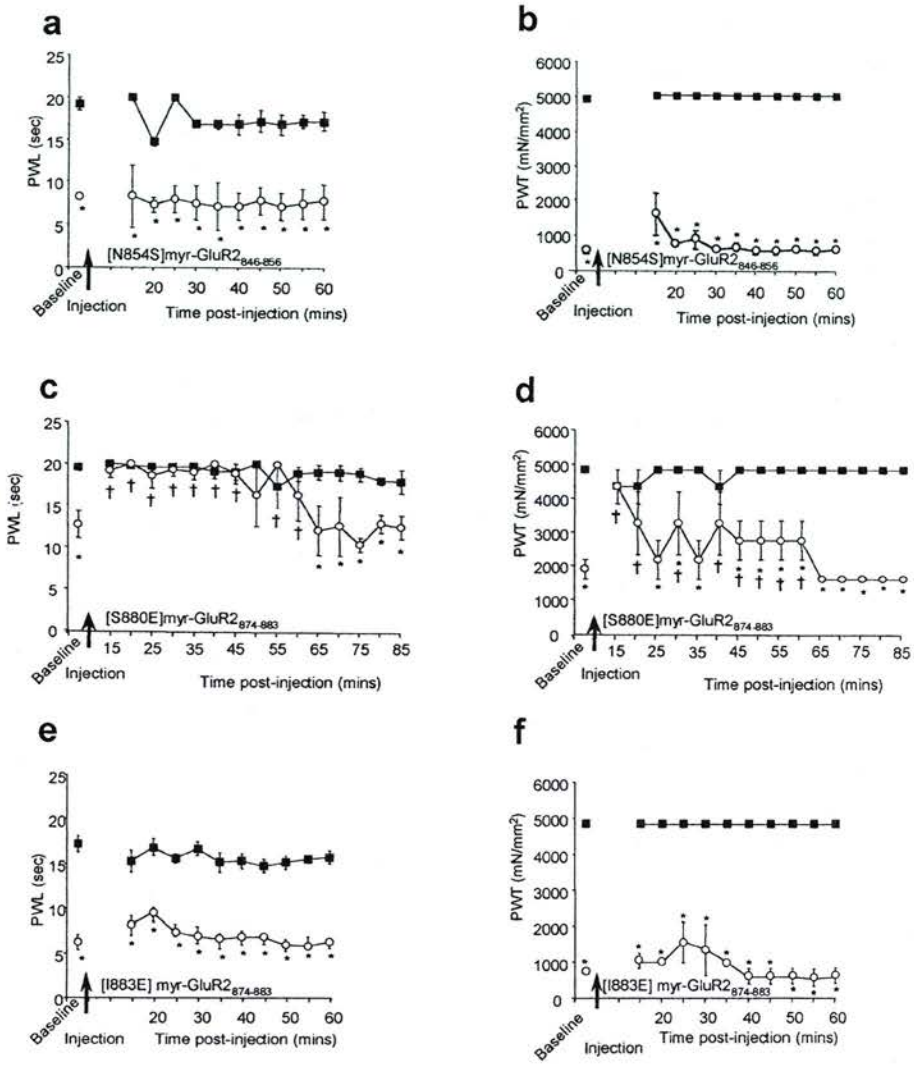

Fig. 2. Effects of myr-GluR2 domain peptides with point mutations on nerve injury-induced thermal hyperalgesia and mechanical allodynia. Data represent the average hindlimb withdrawal latency (sec) to noxious heat (a, c, e) and withdrawal threshold to mechanical stimuli (mN/mm^2; b, d, f) ± SEM before or following the intrathecal injection of [N854S]myr-GluR2$_{846-856}$ (an inactive NSF-binding motif peptide; 4.5 nmol/50 μl, a, b). [S880E]myr-GluR2$_{874-883}$ (a selective disruptor of PICK1, but not GRIP interaction; 4.5 nmol/50 μl, c, d) or [I883E]myr-GluR2$_{874-883}$ (an inactive analogue for the GRIP/PICK1 binding site; 4.5 nmol/50 μl, e, f). Rats at the peak of ipsilateral reflex sensitisation, as determined by a significant reduction in baseline ipsilateral paw withdrawal latency to thermal stimuli (PWL; *$P < 0.05$ Student's t-test, a, c, e) or paw withdrawal threshold to mechanical stimuli (PWT; *$P < 0.05$ Mann-Whitney Rank Sum test, b, d, f) compared to contralateral withdrawal responses, were intrathecally injected (at arrow). Following injection, [S880E]myr-GluR2$_{874-883}$ (c) significantly attenuated the accentuated ipsilateral thermal responses (○) in comparison to pre-injection ipsilateral values (†$P <$ 0.05, One-way ANOVA followed by a Dunnett's test) while there was no significant alteration in the contralateral (■) response. [N854S]myr-GluR2$_{846-856}$ (a) and [I883E]myr-GluR2$_{874-883}$ (e) had no discernable effect. Paw withdrawal thresholds to mechanical stimulation ipsilateral to CCI (○) showed significant differences between pre- and post-injection (†$P < 0.05$, Kruskal-Wallis ANOVA followed by a Dunn's test) for [S880E]myr-GluR2$_{874-883}$ only (d) and not for the other peptides (b) and (f). Contralateral responses (■) were not significantly altered by any of the reagents.

must penetrate to a significant degree into spinal cord tissue following this method of application.

Alterations in the subcellular distribution of GluR2, GRIP and PICK1 in spinal cord following topical AMPA treatment

These experiments involved the centrifugal fractionation of spinal cord homogenates into a dense membrane fraction and a light microsomal compartment in order to assess AMPA-induced translocation of GluR2, GRIP and PICK1 immunoreactivity. AMPA was topically administered to the dorsal surface of the spinal cord in naïve, anaesthetised rats. In whole spinal cord lysate, the overall levels of GluR2, GRIP and PICK1 were similar in either saline or AMPA-treated animals (Fig. 6a, b and c, respectively). Interestingly, there was a marked decrease in the amount of GluR2, GRIP or PICK1 associated with the dense membrane frac-

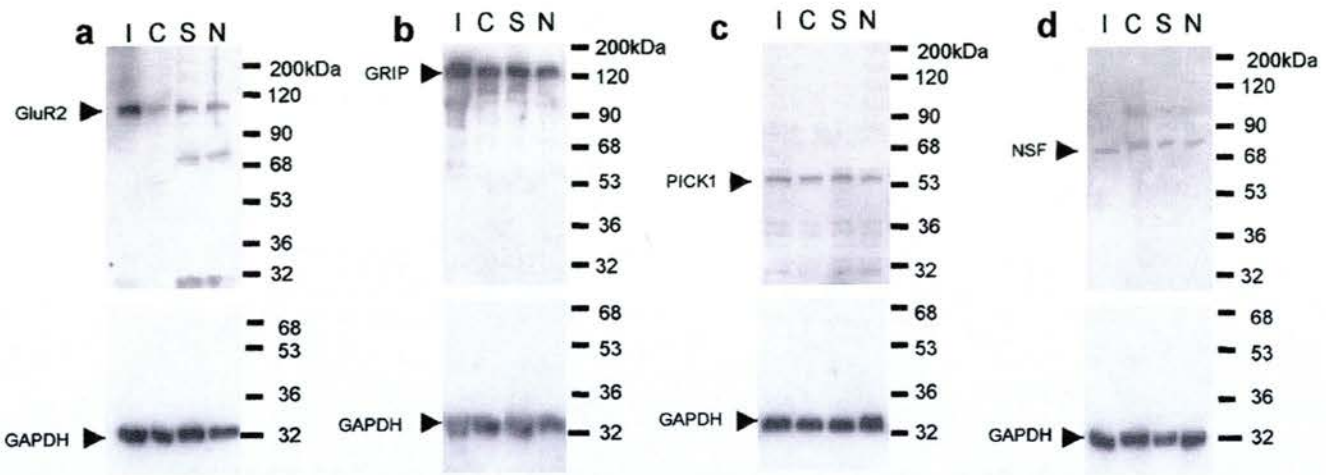

Fig. 3. Western blot analysis of GluR2, GRIP, PICK1 and NSF protein expression following CCI. Western blots of spinal cord samples from neuropathic, sham and naïve rats. (a) shows an increase in GluR2 protein levels ipsilateral (I) to CCI as compared to contralateral (C), sham (S) and naïve (N) controls. (b) shows an increase in GRIP protein levels ipsilateral to CCI as compared to contralateral, sham and naïve controls. (c) shows no apparent alteration in the levels of PICK1 protein in any of the conditions tested while (d) shows a small reduction in NSF protein levels ipsilateral to CCI as compared to contralateral, sham and naïve levels (see also Table 2). No significant difference was noted when contralateral protein levels were compared to sham or naïve samples. The lower panels in each case represent the levels of GAPDH, a ubiquitous housekeeping enzyme used to establish relative protein input levels between samples tested. See Table 2 for quantitative analysis. Molecular weights from standard marker proteins are shown on the right.

tion (M_1) after AMPA receptor stimulation when compared to saline treatment, while the levels of GRIP (b) and PICK1 (c) in the light microsomal fraction (S_1) were similar to control. Since the S_1 fraction reflects a much greater proportion of cell volume than M_1, it is only to be expected that translocation of proteins from M_1 to S_1 would not result in an obvious proportional increase in their S_1 content, despite an obvious loss from M_1. So, following AMPA receptor stimulation there was a significant movement of GluR2, GRIP and PICK1 from the membrane, presumably into the light microsomal fraction, since each protein was still detectable at its correct (not degraded) molecular weight. This indicates that a substantial proportion of GRIP and PICK1 in the spinal cord is associated with the GluR2 subunit of the AMPA receptor under normal conditions. This AMPA-induced translocation could be prevented by topical application of monodansylcadaverine and concanavalin A, inhibitors of endocytosis through the clathrin-coated vesicle pathway (Fig. 6d, Table 3). Therefore, AMPA-induced GluR2 translocation in the spinal cord appears to occur via clathrin-coated vesicle endocytosis and GRIP and PICK1 may share similar pathways of translocation, perhaps due to their (at least temporarily) continued association with GluR2.

Table 2
Densitometric analysis of Western blots for GluR2 and adapter proteins in spinal cord following CCI

Expression of protein in the spinal cord as % of GAPDH expression				
	Ipsilateral CCI	Contralateral CCI	Sham	Naïve
GluR2	55.8 ± 1.9*	41.6 ± 2.9	43.2 ± 2.9	43.5 ± 3.4
GRIP	126.6 ± 3.5*	98.9 ± 3.1	96.4 ± 2.5	97.8 ± 3.8
PICK1	17.5 ± 2.6	15.4 ± 2.4	14.1 ± 2.2	17.4 ± 2.8
NSF	8.5 ± 2.0*	11.2 ± 1.8	12.4 ± 6.5	14.3 ± 4.5

Note. Data represent GluR2, GRIP, PICK1 and NSF protein levels as a percentage of GAPDH expression in terms of relative arbitrary grey scale values following quantitative densitometry of ECL films. Data represent mean ± SEM (*$P < 0.05$ from corresponding contralateral CCI values, paired Student's t-test).

Discussion

Damage to peripheral nerves results in long-lasting physiological and phenotypic alterations in the peripheral and central nervous system and brings about a state of hypersensitivity within the dorsal horn of the spinal cord. This hypersensitivity contributes to the development of the hyperalgesia and allodynia that characterise the neuropathic pain condition. We provide evidence that proteins interacting with the C-terminal domain of the GluR2 subunit of AMPA receptor play an important role in the cellular mechanisms underlying neuropathic pain.

There is preliminary evidence that AMPA receptor antagonists can inhibit thermal hyperalgesia and mechanical allodynia following CCI (Mao et al., 1992; Chaplan et al., 1997). The characteristics of this effect and its cellular mechanism of action have been little investigated to date. Studies here utilising the intrathecal injection of several structurally distinct AMPA receptor antagonists confirmed this, whereby NBQX, NS-257, and SYM 2206 showed a reversible inhibition of neuropathic thermal hyperalgesia with less marked, but still clear effects on mechanical allo-

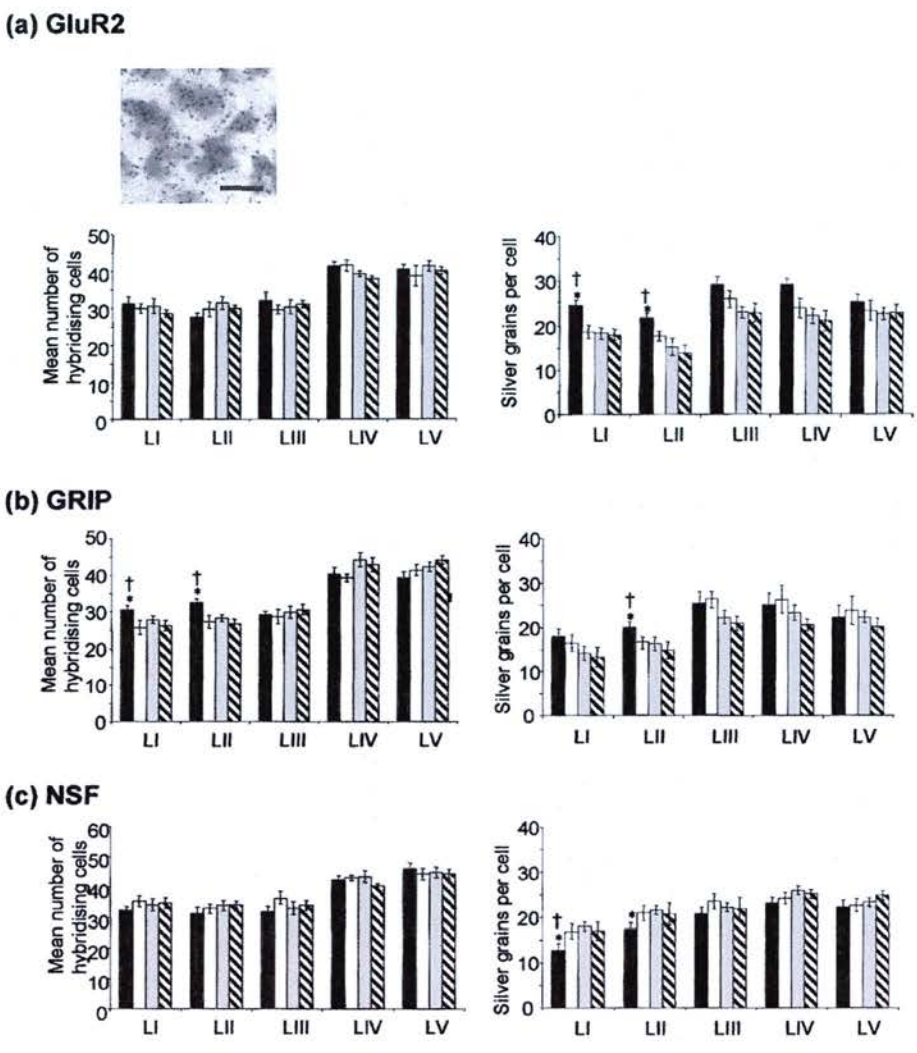

Fig. 4. In situ hybridisation analysis of the levels of GluR2, GRIP2 and NSF mRNA expression in the spinal cord following CCI. A photographic representation of the main region of GluR2 mRNA expression in lamina II of dorsal horn ipsilateral to CCI is shown as an example of silver grain expression levels (a) (Scale bar = 100 μm). In panels a, b and c, the histogram to the left shows the mean number of cells (± SEM) expressing GluR2, GRIP2 or NSF mRNA for the mediolateral dorsal horn laminae I–V (LI–V) ipsilateral and contralateral to CCI, compared to sham-operated and naïve animals (n = 4 rats, 5 sections per condition for each rat). Significant ipsilateral differences are indicated when compared to contralateral (*$P < 0.05$, Student's t-test) or to sham and naïve levels (†, $P < 0.05$, One-way ANOVA followed by a Dunnett's test). The histograms to the right represent the mean density (±SEM) of silver grains per cell expressing GluR2, GRIP2 or NSF mRNA for the mediolateral dorsal horn laminae I–V (LI–V). Significant ipsilateral differences are indicated when compared to contralateral (*$P < 0.05$, Student's t-test) or to sham and naïve levels (†$P < 0.05$, One-way ANOVA followed by a Dunnett's test). ■ = Ipsilateral; □ = contralateral; ▨ = sham; ▧ = naïve.

dynia (Table 1). There were no effects at these doses on the contralateral side or in sham or naïve animals. The limited effects of AMPA receptor agents alone on mechanical allodynia may be consistent with reports that co-activation of AMPA and metabotropic receptors is required for the development of mechanical allodynia (Meller et al., 1993).

GluR2 immunoreactivity is reported to increase in the ipsilateral dorsal horn following CCI (Harris et al., 1996). We confirmed this in the present study with immunoblotting (Fig. 3) and also at the level of ISHH, where quantitative analysis indicated a significant increase in the density of GluR2 mRNA expression in spinal cord LI and II cells from rats at the peak of behavioural reflex sensitisation, with no significant change in the number of cells expressing GluR2 mRNA in this region (Fig. 4a).

The functional impact of blocking the shared GRIP/PICK1 site within the GluR2 C-terminus was examined by the intrathecal injection of a myristoylated peptide corresponding to the interaction motif. This reagent was striking in its attenuation of thermal hyperalgesia following CCI (Fig. 1e). A similar reagent with a point mutation in this sequence [S880E], which markedly reduces its affinity for GRIP, but not for PICK1, also had a striking effect on thermal hyperalgesia (Fig 2c). Since the [S880E]myr-$GluR2_{874-883}$ peptide can still recognise PICK1, its effects here may be due to selective blockade of the GluR2:PICK1

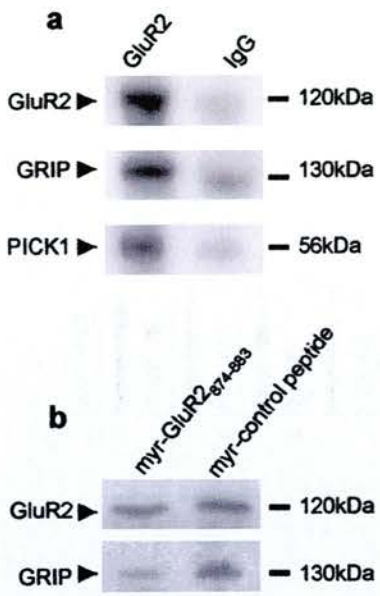

Fig. 5. Co-immunoprecipitation of GRIP and PICK1 with GluR2 from spinal cord and the effects of topical administration of the GRIP interaction-blocking peptide myr-GluR2$_{874-883}$. (a) shows GRIP and PICK1 immunoreactivity, recovered in association with GluR2-directed spinal cord immunoprecipitates from spinal cord (lower panels) together with confirmation that GluR2 was being specifically pulled down (upper panels). Non-immune IgG (IgG) was used as a negative control and produced negligible pull-down of GluR2, GRIP or PICK1 under these conditions. In b) the co-immunoprecipitation of GRIP with GluR2 was investigated in spinal cord from animals to which the GRIP:interaction site blocking peptide, myr-GluR2$_{874-883}$ had been topically applied for 30 min prior to extraction. An inactive myr-peptide was used as control. Mean relative densitometric values for GRIP:GluR2 ratios were 36.4 ± 2.3% for myr GluR2$_{874-883}$ and 78.1 ± 3.4 % for the control reagent.

interaction. The effects of these peptides on mechanical allodynia were however, much less (Figs. 1f and 2d), which may correspond to a differential involvement of AMPA receptors in the afferent pathways involved in the processing of thermal nociceptive and low intensity mechanical inputs. In addition, a significant increase in both the silver grain density and number of cells expressing GRIP2 mRNA was found in the superficial dorsal horn ipsilateral to CCI (Fig. 4b). Western blot analysis of spinal cord following CCI confirmed the increase in the overall levels of GRIP protein ipsilateral to injury (Fig. 3b). In contrast, PICK1 expression appeared to be unaltered ipsilateral to CCI (Fig. 3c). We showed that both GRIP and PICK1 proteins were specifically associated with GluR2 immunoprecipitates from spinal cord tissue and this interaction could be reduced by topical spinal application of a myristoylated peptide, designed to block the C-terminal PDZ target motif, prior to extraction (Fig. 5a, b). The turnover of GluR2:GRIP/PICK1 complexes may be increased by the additional glutamatergic input resulting from CCI. An increase in GluR2 and GRIP expression could contribute to replacing these components. The specific location of GluR2 in LII as well increases in GluR2 and GRIP mRNA (with corresponding increases in protein levels of GluR2 and GRIP) in areas innervated by specific subsets of fine afferents suggests that they may play a key role in mediating neuropathic pain. The role of GRIP in neuropathic sensitisation may relate to its involvement in synaptic accumulation of GluR2, which could depend on a reduction in rate of endocytosis (Osten et al., 2000), or to its additional PDZ domain interactions with other proteins.

Due to the lack of an available cDNA sequence for rat PICK1, in situ hybridisation analysis of PICK1 mRNA expression was not carried out, and the properties of the PICK1 antibody prevented immunohistochemical analysis of regional expression. Western blots indicated that there was no apparent alteration in the overall levels of PICK1 protein ipsilateral to CCI in the spinal cord (Fig. 3c). Nevertheless, our behavioural reflex results with the [S880E]myr-GluR2$_{874-883}$ peptide suggest that PICK1 is likely to play a role in neuropathic pain. Phosphorylation of the serine in the (−3) position in the carboxy terminal tail of GluR2 reduces the affinity of GluR2 for GRIP, but not PICK1 (Matsuda et al., 1999; Chung et al., 2000). Point mutation of this residue in GluR2 to the phosphoserine surrogate, glutamate or to alanine causes a similar effect (Matsuda et al., 1999; Chung et al., 2000; Osten et al., 2000). Peptides based on these modified sequences retain their selectivity, with the phosphoserine or glutamate-based sequences (that showed low affinity for GRIP) displaying minimal ability to disrupt GluR2:GRIP interactions (Matsuda et al., 1999; Li et al., 1999), while showing affinity for PICK1 (Li et al., 1999) and disrupting GluR2:PICK1 docking (Daw et al., 2000). Interestingly, a GluR2 tail peptide but not a mutant sequence (which should act as a selective disruptor of native GluR2:PICK1 interactions) prevents 5-HT-induced synaptic facilitation in dorsal horn neurons and LTD in hippocampal neurons (Li et al., 1999; Daw et al., 2000), whereas in our experiments on neuropathic sensitisation both peptides were effective. This suggests that whereas GRIP but not PICK1 may be involved in 5-HT-induced facilitation, or any LTD-like events in dorsal horn neurons, PICK1 is likely to play a role, probably in addition to GRIP, in neuropathic sensitisation. Disruption of PICK1 interactions with GluR2 may exert inhibitory effects here by inhibiting cell surface clustering of AMPA receptors or their organisation into complexes with signalling proteins, such as the PICK1-associating protein, PKCα (Xia et al., 1999; Perez et al., 2001). Any signalling events related to GluR2 endocytosis and perhaps receptor resensitisation might also be attenuated by disruption of GluR2:PICK1 interactions because PICK1 plays a key role in mediating GluR2 endocytosis (Perez et al., 2001).

The subcellular distributions of GluR2, GRIP and PICK1 were examined in response to topical application of either saline or AMPA to the dorsal spinal cord, in order to assess whether stimulation-induced intracellular translocation of these proteins might play a role in influencing their GluR2 association and overall function. In agreement with previous work (Wyszynski et al., 1998), we found that GRIP

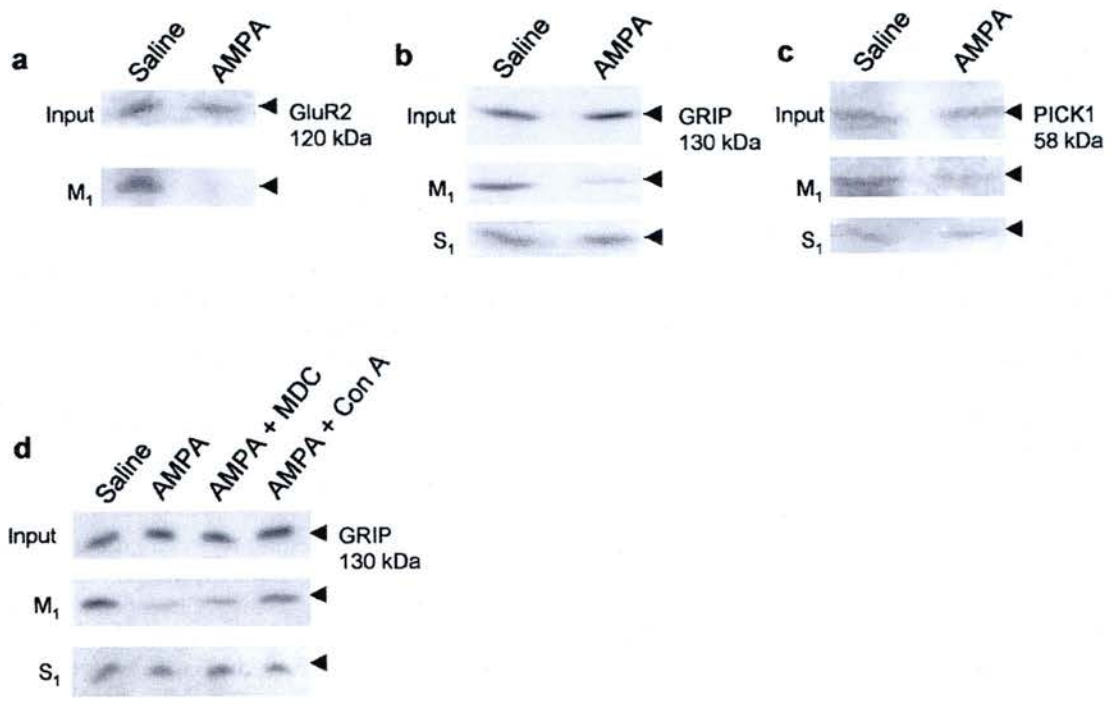

Fig. 6. Translocation of GluR2, GRIP and PICK1 from the membrane following AMPA stimulation is blocked by endocytosis inhibitors. Western blots for GluR2 (a) GRIP (b) and PICK1 (c) following topical application of either AMPA (500 μl of 50 μM AMPA in saline) or saline vehicle to the dorsal surface of the spinal cord. Whole spinal cord lysates showed no apparent difference in expression levels of GluR2, GRIP or PICK1 following either saline vehicle or AMPA topical administration. A corresponding mid-speed membrane fraction (M_1) and supernatant fraction containing light microsomal membrane fragments (S_1) originated from the same samples of spinal cord from which whole lysates were prepared. Membrane preparations (M_1) showed a marked reduction in the content of GluR2, GRIP and PICK1 following AMPA receptor stimulation in comparison to saline vehicle treatment. The light microsomal supernatant (S_1) preparations showed no difference in the content of both proteins following either saline or AMPA topical application. (d) Concurrent topical application of the endocytosis inhibitors, monodansylcadaverine and concanavalin A (20 μM and 0.25 mg/ml, respectively, 500 μl for 30 min), attenuated the AMPA-induced translocation of GRIP out of the dense membrane fraction without reducing the content in the light microsomal 'supernatant' fraction. See Table 3 for quantitative analysis.

appeared to be in both membrane and supernatant fractions and reveal that stimulation of AMPA receptors caused a relative translocation of GRIP out of the membrane-associated (M_1) fraction presumably towards a supernatant (microsomal, S_1) fraction (Fig. 6b). Even though disruption of GluR2 association with GRIP diminishes GluR2 synaptic surface accumulation, possibly by limiting its endocytosis (Xia et al., 1999), the present evidence suggests that not only GluR2 but also GRIP may be internalised following AMPA stimulation. A similar AMPA-induced translocation from the membrane was noted for PICK1 (Fig. 6c), which is consistent with the proposed role for PICK1 in endocytosis of GluR2 (Perez et al., 2001). PICK1 is diffusely distributed in transfected cells, although when co-transfected with GluR2 the proteins form clusters, some but not all of which may be at the cell surface (Xia et al., 1999; Dev et al., 1999). Activation-induced translocation of these docking proteins, as well as that of GluR2, is an important factor to consider in their possible roles during neuropathic pain states. NSF could not be examined under these conditions as there was

Table 3
Translocation of GRIP is prevented by endocytosis inhibitors

Relative densitometric values for GRIP immunoreactivity				
Treatment	Saline	AMPA	AMPA+monodansylcadaverine	AMPA+concanavalin A
Input (whole homogenates)	76.9 ± 3.2	72.4 ± 2.8	68.6 ± 3.2	69.3 ± 2.1
M_1	74.0 ± 4.1	48.5 ± 3.0*	54.9 ± 2.8*†	67.1 ± 3.3†
S_1	68.4 ± 2.9	65.3 ± 3.5	70.0 ± 4.1	62.9 ± 5.0

Note. Data represent means ± SEM for densitometric analysis of Western blots shown in Fig 6d. No values were significantly different for input levels. *$P < 0.05$ (Mann-Whitney Rank Sum test) represents a significant difference for AMPA and AMPA + monodansylcadaverine from saline in the M_1 fraction. †$P < 0.05$ (Mann-Whitney Rank Sum test) represents a significant reversal of the AMPA-induced loss of GluR2 from M_1 following topical AMPA + monodansylcadaverine and AMPA + concanavalin A treatment.

insufficient signal:noise ratio with the available reagents. The AMPA-induced translocation of GluR2, GRIP and PICK1 away from a dense membrane fraction, presumably to the light microsomal "supernatant" fraction, was attenuated by topical co-administration of inhibitors of endocytosis through the "clathrin-coated vesicle" pathway, monodansylcadaverine and concanavalin A (Fig. 6d). These observations on AMPA receptor internalisation in spinal cord are consistent with reports in hippocampal neurons (Carroll et al., 1999; Luscher et al., 1999; Lin et al., 1999) and additionally demonstrate AMPA-induced translocation of GRIP and PICK1.

Blocking the distinct NSF interaction site in the GluR2 C-terminal domain alleviated the thermal hyperalgesia characteristic of the CCI model with little effect on mechanical allodynia (Fig. 1c, d). Infusion of the same inhibitory peptide in hippocampal neurons reduces AMPA receptor current and synaptic abundance (Nishimune et al., 1998; Song et al., 1998; Noel et al., 1999). Given the role of NSF in vesicular trafficking, it would be predicted that blocking this site may affect AMPA receptor transport to the synapse and perhaps affect the receptor's ability to relay nociceptive information (Song et al., 1998; Lüthi et al., 1999). The levels of NSF mRNA decreased in silver grain density ipsilateral to injury specifically in LI, while there was no detectable alteration in the number of cells expressing NSF mRNA (Fig. 4c). NSF protein was also slightly decreased in the spinal cord ipsilateral to CCI (Fig 3d, Table 2). Since the GluR2:NSF interaction may play a role in moving GluR2 to the cell surface (Noel et al., 1999; Luthi, 1999; Luscher, 1999), a downregulation of NSF may imply a reduction in AMPA receptor recycling and such reduced trafficking of the AMPA receptor could limit the maintenance of the sensitised pain state.

In conclusion, we have shown that AMPA receptors play a greater role in the sensitised sensory responses that are brought about in a neuropathic pain model than in normal nociceptive or non-nociceptive reflex behavioural responses. Blocking interactions of GluR2/3 subunits with the intracellular proteins GRIP/PICK1 or NSF by means of intrathecally injected myristoylated peptides can selectively inhibit the neuropathic reflex sensitisation characteristic of peripheral nerve damage. It seems likely that there are distinct roles for GRIP, PICK1 and NSF in neuropathic sensitisation. Our observations on AMPA receptor-dependent sensitisation in neuropathic pain are consistent with observations from other parts of the CNS where the GRIP/PICK1 or NSF interactions of GluR2 play a role in AMPA receptor function or plasticity. Like GluR2, the expression of GRIP is increased in the spinal dorsal horn ipsilateral to injury, while the levels of NSF are decreased and the expression of PICK1 protein shows no apparent alteration. Furthermore, AMPA receptor activation causes relative translocation of GRIP and PICK1 (similar to GluR2) out of the membrane fraction, corresponding to a diminished presence of GRIP or PICK1 in association with GluR2 receptors on the cell surface. The interface between GluR2 and its adapter proteins, as well as cellular mechanisms that regulate these interactions may provide novel therapeutic targets for the alleviation of neuropathic pain.

Experimental methods

All experiments were performed in accordance with the UK Animals (Scientific Procedures) Act, 1986. Adult male Wistar rats (200–300 g, Charles River, Kent, UK) were anaesthetised under aseptic conditions. The Bennett and Xie (Bennett and Xie, 1988) chronic constriction injury model was performed as described previously (Moss et al., 2002).

Behavioural reflex testing

Sensory reflex testing was carried out to assess the development and progression of the neuropathic pain sensitisation characteristic to the CCI model, as indicated by the presence of hyperalgesia and allodynia. Thermal hyperalgesia was monitored using the Hargreaves' thermal stimulator (Linton Instrumentation, Diss, UK), as previously described (Moss et al., 2002). The latency of withdrawal was recorded for the ipsilateral (injured) and the contralateral (uninjured) hindpaws (PWL, paw withdrawal latency). Responses were recorded at 5 min intervals, which ensured no hypersensitivity to the test was established, and mean values taken. Mechanical allodynia was measured as the withdrawal threshold to calibrated Semmes-Weinstein von Frey filaments (Stoelting, Wood Dale; IL), as previously described (Moss et al, 2002). The mean threshold required to elicit a withdrawal response was recorded (PWT, paw withdrawal threshold). Data were expressed as the threshold indentation pressure (i.e. the bending force/per cross-sectional area at the tip of the filament, mN/mm^2).

Intrathecal injections

Drugs

All drugs were administered in a volume of 50 μl according to methods described previously (Moss et al. 2002). NBQX (2,3-dioxo-6-nitro-1,2,3,4-tetrahydrobenzo[f]quinoxaline-7-sulphonamide disodium; 1.5–15 nmol; Tocris-Cookson Ltd., Bristol, UK, Zeman and Lodge, 1992); NS-257 (1,2,3,6,7,8-hexahydro-3-(hydroxyimino)-N,N7-trimethyl-2-oxo-benzo[2,1-b 3,4-c']dipyrrole-5 sulfonamide) hydrochloride; 28–166 nmol; Sigma-RBI, Poole, Dorset or provided by NeuroSearch A/S, Wätjen et al., 1994); SYM 2206 ((±)-4-(4-aminophenyl)-1,2-dihydro-1-methyl-2-propylcarbamoyl-6,7-methylenedioxyphthalazine; 1.5 nmol; Tocris-Cookson Ltd., Bristol, UK, Pelletier et al., 1996). The myristoylated peptides, myr-GluR2$_{846-856}$ (myr-AKRMKVAKNAQ) and its inactive control, [N854S]myr-GluR2$_{846-856}$ (Nishimune et al., 1998; Song et al., 1998), myr-GluR2$_{874-883}$ (myr-NVYGIESVKI), its inactive control, [1883E]myr-GluR2$_{874-883}$ and the selec-

tive PICK1-targeting analogue, [S880E]myr-GluR2$_{874-883}$ (Matsuda et al., 1999; Li et al., 1999; Chung et al., 2000; Osten et al., 2000; Daw et al., 2000) were synthesised and purified by Pepsyn Ltd., University of Liverpool, UK. The inactive control myristoylated peptide of irrelevant sequence (myr-GRRNAIHDE) was a gift from Roger Clegg, Hannah Research Institute. All myristoylated peptides were administered intrathecally at a dose of 4.5 nmol and injections of vehicle (0.3% dimethylformamide in saline) or saline were shown to have no discernable effect on behavioural reflex responses.

The effects of each compound on behavioural reflex responses were examined. Baseline measurements were recorded for thermal hyperalgesia (Hargreaves' test) and mechanical allodynia (von Frey filament test) (n = 8 naïve; n = 10 neuropathic) in animals at the peak of neuropathic behavioural reflex sensitisation and intrathecal injections were carried out as described previously (Moss et al., 2002).

In situ hybridisation histochemistry (ISHH)

ISHH was carried out as described previously (Parker et al., 1993). Oligonucleotide probes (synthesised and HPLC purified by Oswel Chemicals, University of Southampton, UK) for GluR2, GRIP2, and NSF mRNA complementary to 2032–2076 for GluR2 (Keinänen et al., 1990), 2148–2186 for GRIP2 (Brückner et al., 1999), and 76–120 for NSF were used. Cell counts and silver grain analysis was carried out as described previously (Parker et al., 1993; Blackburn-Munro and Fleetwood-Walker, 1997) to assess any changes in the relative expression of mRNA following chronic constriction injury in comparison to sham and naïve expression (n = 5 sections, n = 4 animals per condition).

Western blotting

Western blotting was carried out using methodology described previously (Moss et al., 2002). Blots were probed with primary antibodies to GluR2 (1:1000, Chemicon International Ltd., Harrow, UK), GRIP (1:500, Becton Dickinson, London, UK), NSF (1:1,000, Chemicon), or PICK1 (1:200, Santa Cruz Biotechnology, Autogen Bioclear, Wiltshire, UK) and detected by peroxidase-linked secondary antibody enhanced chemiluminescence. The ubiquitous housekeeping enzyme glyceraldehyde-3-phosphate dehydrogenase (GAPDH, 1:750, Chemicon International Ltd., Harrow, UK) was used as a control, for protein level normalisation.

AMPA-induced translocation of GluR2, GRIP and PICK1

Prior to removal of L4–6 spinal cord segments, the cord was treated topically for 30 min with 500 μl saline or AMPA (50 μM) in saline. In some cases the treatment solution additionally contained 20 μM monodansylcadaverine or 0.25 mg/ml concanavalin A.

To examine the relative membrane and supernatant content of GluR2, GRIP and PICK1, samples of the spinal cord were homogenised to prepare whole lysates which were then centrifuged at 12,000 × g for 30 min at 4°C to prepare corresponding mid-speed membrane (M_1) and supernatant (S_1) fractions. The supernatant fraction was subsequently centrifuged at 82,000 × g for 30 min to obtain a microsomal pellet which constituted the vast majority of the relevant proteins recovered from the initial (S_1) supernatant fraction.

Co-immunoprecipitation of GluR2 with associated proteins

A laminectomy (L3–6) was performed on anaesthetised rats and the spinal cord was rapidly removed to cold buffer on ice. Following homogenisation (in IP buffer; PBS, pH 7.5 containing 1% CHAPS, 0.75% sodium deoxycholate, 2 μg/ml aprotinin, 4 μg/ml leupeptin, 1 mM AEBSF (4-(2-aminoethyl) benzene sulphonyl fluoride, Alexis Corporation, Nottingham, UK), 2 μg/ml pepstatin, 1 mM vanadate, 1 mM sodium fluoride, 5 mM sodium molybdate and soya bean trypsin inhibitor (50 μg/ml)), samples were incubated at 4°C for 1 h and centrifuged at 12,000 × g for 15 min at 4°C. Immunoprecipitation was carried out with an antibody directed against an N-terminal domain of the GluR2 receptor (Becton Dickinson) so as not to compromise C-terminal association of adapter proteins. The GluR2 immunoprecipitating antibody (10 μg/ml) was incubated with Protein G-Sepharose 4B fast flow (Sigma Aldrich Company Ltd., UK, 20 μl/ml) for ~1 h at 4°C before addition of supernatant and samples were then left rolling overnight at 4°C. The beads were precipitated by pulse centrifugation, washed in IP buffer and PBS before 40 μl of 2X Laemmli buffer was added for samples derived from 1 ml of original supernatant. Extracts were separated by electrophoresis on pre-cast polyacrylamide gels (BioRad, Hemel Hempstead, UK), transferred onto polyvinylidene difluoride membranes (ImmobilonP^{SQ}, Millipore UK Ltd.) and blocked overnight at 4°C in PBS with 5% Marvel and 0.1% Tween20. Blots were probed with primary antibodies to GluR2 (1:500, Chemicon), GRIP (1:500, Becton-Dickinson) or PICK1 (1:200, Santa Cruz Biotechnology) and detected by peroxidase-linked secondary antibody enhanced chemiluminescence.

Acknowledgments

This work was supported by The Wellcome Trust (S.F.-W.), the MRC (R.M.) and by the University of Edinburgh for the award of a studentship to E.G. and the M.R.C. for the award of Studentships to A.M. and A.D., respectively. We thank staff at the Wellcome Animal Research Unit (WARU) and the Medical Faculty Animal Area (MFAA) facilities for animal husbandry as well as R. Clegg and NeuroSearch A/S for gifts of the myr-GRRNAIDHE peptide and NS 257 respectively.

References

Aanonsen, L.M., Wilcox, G.L., 1987. Nociceptive action of excitatory amino acids in the mouse: effects of spinally administered opioids, phencyclidine and sigma agonists. J. Pharmacol. Exp. Ther. 243, 9–19.

Aanonsen, L.M., Lei, S., Wilcox, G.L., 1990. Excitatory amino acid receptors and nociceptive neurotransmission in rat spinal cord. Pain 41, 309–321.

Bennett, G.J., Xie, Y.K., 1988. A peripheral mononeuropathy in rat that produces disorders of pain sensation like those seen in man. Pain 33, 87–107.

Blackburn-Munro, G., Fleetwood-Walker, S.M., 1997. The effects of Na^+ channel blockers on somatosensory processing by rat dorsal horn neurons. Neuroreport 8, 1549–1554.

Brückner, K., Labrador, J.P., Scheiffele, P., Herb, A., Seeburg, P.H., Klein, R., 1999. EphrinB ligands recruit GRIP family PDZ adaptor proteins into raft membrane microdomains. Neuron 22, 511–524.

Budai, D., Larson, A.A., 1994. GYKI 52466 inhibits AMPA/kainate and peripheral mechanical sensory activity. Neuroreport 5, 881–884.

Carroll, R.C., Beattie, E.C., Xia, H., Luscher, C., Altschuler, Y., Nicoll, R.A., Malenka, R.C., von Zastrow, M., 1999. Dynamin-dependent endocytosis of ionotropic glutamate receptors. Proc. Natl. Acad. Sci. U.S.A. 96, 14112–7.

Chaplan, S.R., Malmberg, A.B., Yaksh, T.L., 1997. Efficacy of spinal NMDA receptor antagonism in formalin hyperalgesia and nerve injury evoked allodynia in the rat. J. Pharmacol. Exp. Ther. 280, 829–838.

Chung, H.J., Xia, J., Scannevin, R.H., Zhang, X., Huganir, R.L., 2000. Phosphorylation of the AMPA receptor subunit GluR2 differentially regulates its interaction with PDZ domain-containing proteins. J. Neurosci. 20, 7258–7267.

Cumberbatch, M.J., Chizh, B.A., Headley, P.M., 1994. AMPA receptors have an equal role in spinal nociceptive and non-nociceptive transmission. Neuroreport 5, 877–880.

Daw, M.I., Chittajallu, R., Bortolotto, Z.A., Dev, K.K., Duprat, F., Henley, J.M., Collingridge, G.L., Isaac, J.T.R., 2000. PDZ proteins interacting with C-terminal GluR2/3 are involved in a PKC-dependent regulation of AMPA receptors at hippocampal synapses. Neuron 28, 873–886.

Dev, K.K., Nishimune, A., Henley, J.M., Nakanishi, S., 1999. The protein kinase C alpha binding protein PICK1 interacts with short but not long form alternative splice variants of AMPA receptor subunits. Neuropharm. 38, 635–644.

Dong, H.L., Zhang, P.S., Song, I.S., Petralia, R.S., Liao, D.Z., Huganir, R.L., 1999b. Characterization of the glutamate receptor-interacting proteins GRIP1 and GRIP2. J. Neurosci. 19, 6930–6941.

Dong, H.L., O'Brien, R.J., Fung, E.T., Lanahan, A.A., Worley, P.F., Huganir, R.L., 1997. GRIP: A synaptic PDZ domain-containing protein that interacts with AMPA receptors. Nature 386, 279–284.

Dougherty, P.M., Palecek, J., Paleckova, V., Sorkin, L.S., Willis, W.D., 1992. The role of NMDA and non-NMDA excitatory amino acid receptors in the excitation of primate spinothalamic tract neurons by mechanical, chemical, thermal, and electrical stimuli. J. Neurosci. 12, 3025–3041.

Furuyama, T., Kiyama, H., Sato, K., Park, H.T., Maeno, H., Takagi, H., Tohyama, M., 1993. Region-specific expression of subunits of ionotropic glutamate receptors (AMPA-type, KA-type and NMDA receptors) in the rat spinal cord with special reference to nociception. Mol. Br. Res. 18, 141–151.

Harris, J.A., Corsi, M., Quartaroli, M., Arban, R., Bentivoglio, M., 1996. Upregulation of spinal glutamate receptors in chronic pain. Neurosci. 74, 7–12.

Hollmann, M., Heinemann, S., 1994. Cloned glutamate receptors. Ann. Rev. Neurosci. 17, 31–108.

Jakowec, M.W., Fox, A.J., Martin, L.J., Kalb, R.G., 1995. Quantitative and qualitative changes in AMPA receptor expression during spinal cord development. Neuroscience 67, 893–907.

Keinänen, K., Wisden, W., Sommer, B., Werner, P., Herb, A., Verdoorn, T.A., Sakmann, B., Seeburg, P.H., 1990. A family of AMPA-selective glutamate receptors. Science 249, 556–560.

Kim, C.H., Chung, H.J., Lee, H.K., Huganir, R.L., 2001. Interaction of the AMPA receptor subunit GluR2/3 with PDZ domains regulates hippocampal long-term depression. Proc. Natl. Acad. Sci. U.S.A. 98, 11725–30.

Li, P., Kerchner, G.A., Sala, C., Wei, F., Huettner, J.E., Sheng, M., Zhuo, M., 1999. AMPA receptor-PDZ interactions in facilitation of spinal sensory synapses. Nat. Neurosci. 2, 972–977.

Lin, J.W., Ju, W., Foster, K., Lee, S.H., Ahmadian, G., Wyszynski, M., Wang, Y.T., Sheng, M., 2002. Distinct molecular mechanisms and divergent endocytotic pathways of AMPA receptor internalization. Nat. Neurosci. 12, 1282–90.

Lledo, P.M., Zhang, X., Sudhof, T.C., Malenka, R.C., Nicoll, R.A., 1998. Postsynaptic membrane fusion and long-term potentiation. Science 279, 399–403.

Luscher, C., Xia, H., Beattie, E.C., Carroll, R.C., von Zastrow, M., Malenka, R.C., Nicoll, R.A., 1999. Role of AMPA receptor cycling in synaptic transmission and plasticity. Neuron 24, 649–58.

Lüthi, A., Chittajallu, R., Duprat, F., Palmer, M.J., Benke, T.A., Kidd, F.L., Henley, J.M., Isaac, J.T.R., Collingridge, G.L., 1999. Hippocampal LTD expression involves a pool of AMPARs regulated by the NSF-GluR2 interaction. Neuron 24, 389–399.

Mao, J., Price, D.D., Hayes, R.L., Lu, J., Mayer, D.J., 1992. Differential roles of NMDA and non-NMDA receptor activation in induction and maintenance of thermal hyperalgesia in rats with painful peripheral mononeuropathy. Brain Res. 598, 271–278.

Matsuda, S., Mikawa, S., Hirai, H., 1999. Phosphorylation of serine-880 in GluR2 by protein kinase C prevents its C terminus from binding with glutamate receptor-interacting protein. J. Neurochem. 73, 1765–1768.

Medhurst, A.D., Harrison, D.C., Read, S.J., Campbell, C.A., Robbins, M.J., Pangalos, M.N., 2000. The use of TaqMan RT-PCR assays for semiquantitative analysis of gene expression in CNS tissues and disease models. J. Neurosci. 98, 9–20.

Meller, S.T., Dykstra, C.L., Gebhart, G.F., 1993. Acute mechanical hyperalgesia is produced by coactivation of AMPA and metabotropic glutamate receptors. Neuroreport 4, 879–882.

Moss, A., Blackburn-Munro, G., Garry, E.M., Blakemore, J., Dickinson, T., Mitchell, R., Rosie, R., Fleetwood-Walker, S., 2002. A role of the ubiquitin-proteasome pathway in neuropathic pain. J. Neurosci. 22, 1363–1372.

Nishimune, A., Isaac, J.T.R., Molnar, E., Noel, J., Nash, S.R., Tagaya, M., Collingridge, G.L., Nakanishi, S., Henley, J.M., 1998. NSF binding to GluR2 regulates synaptic transmission. Neuron 21, 87–97.

Nishiyama, T., Yaksh, T.L., Weber, E., 1998. Effects of intrathecal NMDA and non-NMDA antagonists on acute thermal nociception and their interaction with morphine. Anesthesiology 89, 715–722.

Noel, J., Ralph, G.S., Pickard, L., Williams, J., Molnar, E., Uney, J.B., Collingridge, G.L., Henley, J.M., 1999. Surface expression of AMPA receptors in hippocampal neurons is regulated by an NSF-dependent mechanism. Neuron 23, 365–376.

Osten, P., Khatri, L., Perez, J.L., Kohr, G., Giese, G., Daly, C., Schulz, T.W., Wensky, A., Lee, L.M., Ziff, E.B., 2000. Mutagenesis reveals a role for ABP/GRIP binding to GluR2 in synaptic surface accumulation of the AMPA receptor. Neuron 27, 313–325.

Osten, P., Srivastava, S., Inman, G.J., Vilim, F.S., Khatri, L., Lee, L.M., States, B.A., Einheber, S., Milner, T.A., Hanson, P.I., Ziff, E.B., 1998. The AMPA receptor GluR2 C terminus can mediate a reversible, ATP-dependent interaction with NSF and alpha and beta-SNAPs. Neuron 21, 99–110.

Parker, R.M., Fleetwood-Walker, S.M., Rosie, R., Munro, F.E., Mitchell, R., 1993. Inhibition by NK2 but not NK1 antagonists of carrageenan-induced preprodynorphin mRNA expression in rat dorsal horn lamina 1 neurons. Neuropeptides 25, 213–22.

Pelletier, J.C., Hesson, D.P., Jones, K.A., Costa, A.M., 1996. Substituted 1,2-dihydrophthalazines: potent, selective, and noncompetitive inhibitors of the AMPA receptor. J. Med. Chem. 39, 343–346.

Perez, J.L., Khatri, L., Chang, C., Srivastava, S., Osten, P., Ziff, E.B., 2001. PICK1 targets activated protein kinase Cα to AMPA receptor clusters in spines of hippocampal neurons and reduces surface levels of the AMPA-type glutamate receptor subunit 2. J. Neurosci. 21, 5417–5428.

Song, I., Kamboj, S., Xia, J., Dong, H., Liao, D., Huganir, R.L., 1998. Interaction of the N-ethylmaleimide-sensitive factor with AMPA receptors. Neuron 21, 393–400.

Sorkin, L.S., Yaksh, T.L., Doom, C.M., 2001. Pain models display differential sensitivity to Ca^{2+}-permeable non-NMDA glutamate receptor antagonists. Anesthesiology 95, 965–973.

Srivastava, S., Osten, P., Vilim, F.S., Khatri, L., Inman, G., States, B., Daly, C., DeSouza, S., Abagyan, R., Valtschanoff, J.G., Weinberg, R.J., Ziff, E.B., 1998. Novel anchorage of GluR2/3 to the postsynaptic density by the AMPA receptor-binding protein ABP. Neuron 21, 581–591.

Staudinger, J., Lu, J.R., Olson, E.N., 1997. Specific interaction of the PDZ domain protein PICK1 with the COOH terminus of protein kinase c-α. J. Biol. Chem. 272, 32019–32024.

Tölle, T.R., Berthele, A., Zieglgänsberger, W., Seeburg, P.H., Wisden, W., 1993. The differential expression of 16 NMDA and non-NMDA receptor subunits in the rat spinal-cord and in periaqueductal gray. J. Neurosci. 13, 5009–5028.

Wätjen, F., Nielsen, E.Ø., Johansen, T.H., Drejer, J., 1994. NS 257 (1,2,3,6,7,8-hexahydro-3(hydroxyimino)-N,N,7-trimethyl-2-oxobenzol[2,1-b:3,4-c']dipyrrole-5-sulfonamide) is a potent systemically active AMPA receptor antagonist. Bioorg. Med. Chem. Lett. 4, 371–376.

Wyszynski, M., Kim, E., Yang, F.C., Sheng, M., 1998. Biochemical and immunocytochemical characterization of GRIP, a putative AMPA receptor anchoring protein, in rat brain. Neuropharm. 37, 1335–1344.

Xia, J., Chung, H.J., Wihler, C., Huganir, R.L., Linden, D.J., 2000. Cerebellar long-term depression requires PKC-regulated interactions between GluR2/3 and PDZ domain-containing proteins. Neuron 28, 499–510.

Xia, J., Zhang, X.Q., Staudinger, J., Huganir, R.L., 1999. Clustering of AMPA receptors by the synaptic PDZ domain-containing protein PICK1. Neuron 22, 179–187.

Zeman, S., Lodge, D., 1992. Pharmacological characterization of non-NMDA subtypes of glutamate receptor in the neonatal rat hemisected spinal cord in vitro. Br. J. Pharmacol. 106, 367–372.

Current Biology, Vol. 13, 321–328, February 18, 2003, ©2003 Elsevier Science Ltd. All rights reserved. PII S0960-9822(03)00084-8

Neuropathic Sensitization of Behavioral Reflexes and Spinal NMDA Receptor/CaM Kinase II Interactions Are Disrupted in PSD-95 Mutant Mice

Emer M. Garry,[1] Andrew Moss,[1,4] Ada Delaney,[1] Francis O'Neill,[1] James Blakemore,[1,5] Julian Bowen,[1] Holger Husi,[2] Rory Mitchell,[3] Seth G.N. Grant,[2] and Susan M. Fleetwood-Walker[1,*]

[1]Division of Preclinical Veterinary Sciences, R(D)SVS
University of Edinburgh
Summerhall, Edinburgh EH9 1QH
United Kingdom

[2]Division of Neuroscience
University of Edinburgh
1 George Square
Edinburgh EH8 9JZ
United Kingdom

[3]MRC Membrane and Adapter Proteins Co-operative Group and Membrane Biology Group
Division of Biomedical and Clinical Laboratory Sciences
University of Edinburgh
Edinburgh EH8 9XD
United Kingdom

Summary

Chronic pain due to nerve injury is resistant to current analgesics. Animal models of neuropathic pain show neuronal plasticity and behavioral reflex sensitization in the spinal cord that depend on the NMDA receptor [1, 2]. We reveal complexes of NMDA receptors with the multivalent adaptor protein PSD-95 [3, 4] in the dorsal horn of spinal cord and show that PSD-95 plays a key role in neuropathic reflex sensitization. Using mutant mice expressing a truncated form of the PSD-95 molecule [5], we show their failure to develop the NMDA receptor-dependent hyperalgesia and allodynia seen in the CCI model of neuropathic pain [6], but normal inflammatory nociceptive behavior following the injection of formalin. In wild-type mice following CCI, CaM kinase II inhibitors attenuate sensitization of behavioral reflexes, elevated constitutive (autophosphorylated) activity of CaM kinase II is detected in spinal cord, and increased amounts of phospho-Thr^{286} CaM kinase II coimmunoprecipitate with NMDA receptor NR2A/B subunits. Each of these changes is prevented in PSD-95 mutant mice although CaM kinase II is present and can be activated. Disruption of CaM kinase II docking to the NMDA receptor and activation may be responsible for the lack of neuropathic behavioral reflex sensitization in PSD-95 mutant mice.

*Correspondence: s.m.fleetwood-walker@ed.ac.uk

[4]Present address: Department of Anatomy and Developmental Biology, Medawar Building, University College London, Gower St., London WC1E 6BT, United Kingdom.

[5]Present address: Cell Factors plc, St. John's Innovation Centre, Cowley Road, Cambridge CB4 0WS, United Kingdom.

Results

PSD-95 Expression in Spinal Cord

Using histochemical staining for the β-galactosidase reporter gene, we showed that PSD-95 expression is specifically restricted to lamina II of the spinal dorsal horn, a prime location for the processing of nociceptive afferent inputs (Figure 1A), and is found throughout lumbar and thoracic spinal cord (Figure 1B). This distribution overlaps with those of NMDA receptor subunits (particularly NR2B) throughout lumbar and thoracic spinal cord [2]. PSD-95 expression was not detected in dorsal root entry zones (Figure 1B, arrow), dorsal root ganglion (DRG), dorsal roots, or sciatic nerve (data not shown). Using coimmunoprecipitation, we could isolate NMDA receptor complexes from spinal cord that contained NR1, NR2A, NR2B, and PSD-95, similar to those found in forebrain [3, 4] (Figure 1C).

PSD-95 Mutant Mice Lack Behavioral Reflex Sensitization Following CCI

We used the CCI model of neuropathic pain to examine the effects of sciatic nerve injury in homozygous PSD-95 mutant mice and their wild-type littermates. Over 7–10 days following CCI (under halothane anesthesia), wild-type mice progressively developed marked ipsilateral thermal hyperalgesia (reduced paw withdrawal latency, PWL; Figure 2A), mechanical allodynia (reduced paw withdrawal threshold, PWT; Figure 2C), and cold allodynia (increased suspended paw elevation time, SPET; Figure 2E). All responses from the contralateral hind limb remained unaltered. Thermal hyperalgesia and mechanical allodynia were absent in PSD-95 mutant mice (Figures 2B and 2D), while cold allodynia was severely attenuated, reaching statistical significance at only one time point (Figure 2F). No differences in motor function or coordination (as measured by the rotarod test) were observed in PSD-95 mutants compared to wild-type mice. In addition, there was no evidence for anatomical alterations in afferents of the mutant mice, with similar axon diameter and myelin thickness profiles for Aβ, Aδ, and C fibers between naive wild-type and homozygous PSD-95 mutant mice (in accordance with previous findings [7, 8]), and the extent of CCI-induced changes in afferent fibers was unaltered.

PSD-95 Mutant Mice Display Normal Responses to Inflammatory Nociceptive Stimuli

Sensitization of nociceptive reflexes can also be brought about by peripheral inflammatory stimuli [9], but inflammatory and neuropathic states display a number of distinct characteristics [1, 10]. We therefore tested whether PSD-95 mutant mice also display a deficit in behavioral responses to inflammation by intraplantar injection of formalin (10 μl of 1.5% solution in saline, during brief halothane anesthesia [11, 12]). PSD-95 mutant mice and wild-type littermates displayed the same responses of paw licking and flicking in the early acute phase of the

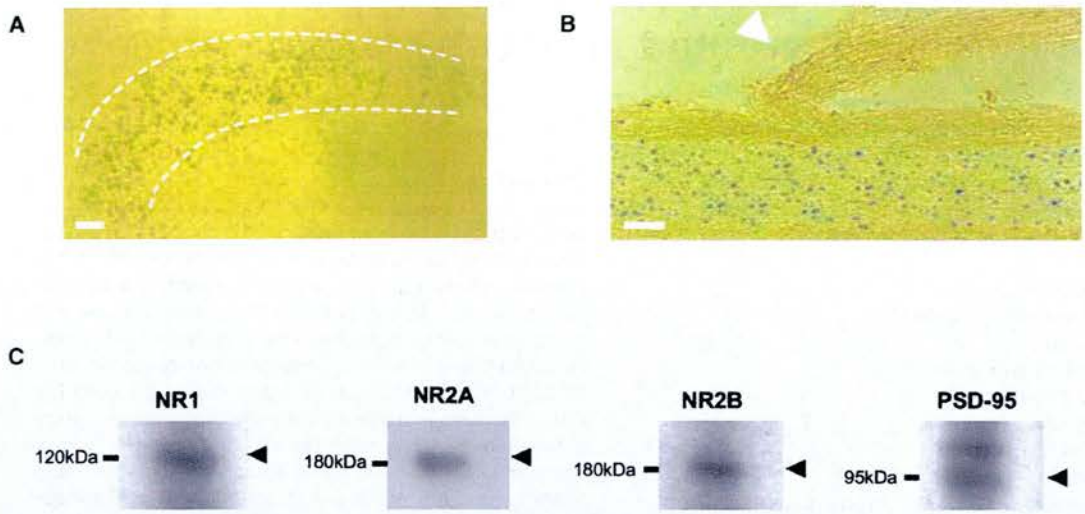

Figure 1. Expression of PSD-95 and Components of the NMDA Receptor Complex in Spinal Cord

Heterozygous PSD-95 (wt/mutant) animals (n = 5) were perfused with 4% paraformaldehyde in 0.1 M phosphate buffer. 10 μm sections were washed with ice-cold PBS/$MgCl_2$ and then 0.041% $MgCl_2$, 0.01% Na deoxycholate, 0.02% Nonidet-NP40, in 0.1 M PBS. Sections were stained at 22°C in 0.042% potassium ferrocyanide, 0.033% potassium ferricyanide in detergent buffer with 1 μg/ml 5-bromo-4-chloro-3-indolyl-β-D-galactoside, and incubated at 37°C in the dark for 4–6 hr.

(A) Transverse section, showing specific distribution of β-galactosidase-positive cells in lamina II (outlined with dashed line) of the superficial dorsal horn.

(B) Longitudinal section showing staining in dorsal horn, but not at the site of dorsal root entry (arrow). Scale bar equals 10 μm.

(C) Immunoblots for the presence of NMDA receptor complex proteins in NR2A/B-directed immunoprecipitates of L3-L6 spinal cord from wild-type mice.

formalin test (5–10 min following injection), and the late (inflammatory) phase of the response (25 min to 1 hr) was also indistinguishable between the mutant and wild-type mice (Figure 2G), in striking contrast to the lack of neuropathic behavioral reflex sensitization seen in the mutants. The degree of peripheral inflammation as assessed by paw volume was the same for PSD-95 mutant and wild-type mice.

NMDA Receptor-Dependent Hyperalgesia and Allodynia in Wild-Type, but not PSD-95 Mutant Mice

Intrathecal administration of the selective NMDA receptor antagonist (R)-CPP (under brief halothane anesthesia) completely reversed thermal hyperalgesia and mechanical allodynia that had developed ipsilateral to CCI in wild-type mice, with no detectable effect on contralateral responses or in naive animals. At 10–30 min following injection of (R)-CPP (100 pmole), the ipsilateral: contralateral differences in PWL and PWT (thermal hyperalgesia and mechanical allodynia) were reduced to 11.6% ± 5.9% and 8.3% ± 3.5% of predrug differences ($n = 6$, $p < 0.05$ by Wilcoxon test in each case). Recovery was complete by 60–80 min. The equivalent values for saline were 94.8% ± 3.9% and 90.0% ± 5.3%, respectively. The behavioral changes brought about following CCI were bilaterally mimicked in naive wild-type mice by intrathecal administration of NMDA (250 pmole), showing a 45.9% ± 5.1% reduction in mechanical paw withdrawal threshold (PWT) and a 36.2% ± 3.9% reduction in thermal paw withdrawal latency (PWL) over 10–30 min following injection ($p < 0.05$ in each case by Mann-Whitney U test). In contrast, behavioral responses of PSD-95 mutant mice following CCI were unaffected by intrathecal administration of (R)-CPP, with PWL and PWT values (which, as described, displayed no sensitization in these animals) remaining at 98.4% ± 7.2% and 94.5% ± 4.9% of predrug controls. Correspondingly, naive PSD-95 mutants showed no changes in PWL and PWT following intrathecal injection of NMDA, with values remaining at 96.4% ± 5.0% and 99.4% ± 6.3% of predrug controls. These findings suggest that NMDA receptor:PSD-95 interactions in spinal cord play a key role in the development of neuropathic behavioral reflex sensitization. In both wild-type mice and PSD-95 mutant mice, the second (inflammatory) phase of the nociceptive reflex response to formalin was completely inhibited by intrathecal injection of 100 pmol (R)-CPP. The mean number of paw flinches/flicks over the peak 15 min of the second phase formalin response was reduced by (R)-CPP to 11.5% ± 4.3% of control in wild-type and by 10.1% ± 5.2% in PSD-95 mutants ($n = 4$; $p < 0.05$ by Student's t test). Intrathecal injection of saline had no detectable effect on formalin responses with corresponding values remaining within 6% of those from uninjured controls. This indicates that while this inflammatory nociceptive behavioral response involves the NMDA receptor, it does not share the additional requirement for intact PSD-95 that is seen in the behavioral reflex sensitization induced by CCI.

CaM Kinase II Inhibitors Alleviate Neuropathic Sensitization

NMDA receptor:PSD-95 complexes in the forebrain incorporate the Ca^{2+}-dependent protein kinase, CaM kinase II, docked to NR2 subunits [3, 4, 13–15], where it

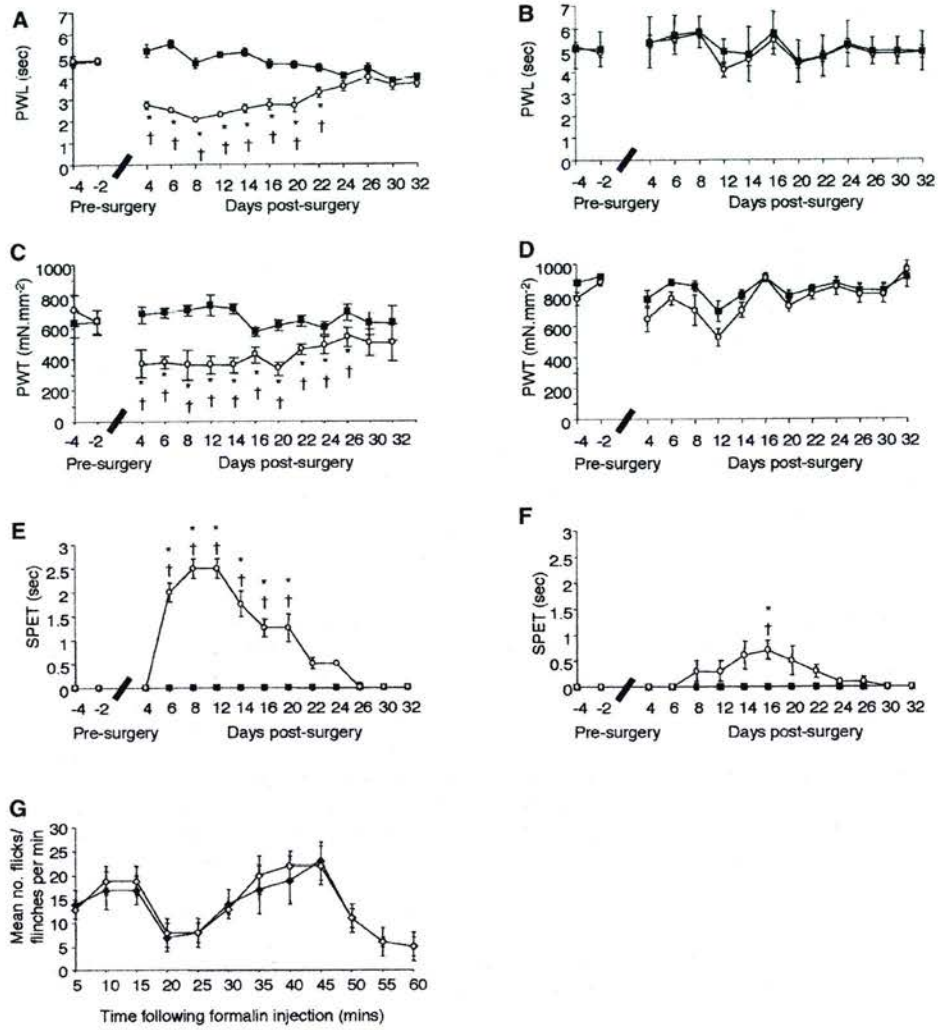

Figure 2. Behavioral Analysis of Wild-Type and PSD-95 Mutant Mice with Chronic Constriction Injury (CCI) to the Sciatic Nerve

Data show mean ± SEM responses for each day before and following the induction of CCI. A variation of the chronic constriction injury (CCI) model for rat [6] was used, whereby (under halothane anesthesia) three ligatures separated by 1 mm were tied loosely to constrict the tibial branch of the sciatic nerve.

(A and B) In wild-type mice (A), paw withdrawal latency (PWL) from a noxious thermal stimulus (Hargreaves' thermal stimulator) ipsilateral to CCI (open circle) showed significant differences between postoperative and preoperative values (dagger indicates $p < 0.05$; Kruskal-Wallis one-way ANOVA) and from postoperative, contralateral (closed square) values (asterisk indicates $p < 0.05$ by Student's t test). No thermal hyperalgesia was seen on the contralateral side (closed square) of wild-type mice (A) or in PSD-95 mutant mice (B) on either side.

(C and D) Paw withdrawal thresholds (PWT) from mechanical stimulation (von Frey filaments) for wild-type mice showed significant differences between postoperative and preoperative values on the side ipsilateral (open circle) to CCI (dagger indicates $p < 0.05$; Dunn's Method ANOVA on ranks) and between postoperative ipsilateral and contralateral values (asterisk indicates $p < 0.05$, Mann-Whitney U test). No significant differences were seen on the contralateral side (closed square) of wild-type mice (C) following nerve ligation or in PSD-95 mutants (D).

(E and F) The suspended paw elevation time (SPET) in response to a cold water (4°C) stimulus is shown for the ipsilateral paw (open circle) and contralateral paw (closed square) in wild-type mice (E) and in PSD-95 mutant mice (F). Following nerve ligation, SPET scores for the contralateral paw were always zero for both wild-type and mutant mice. Statistically significant differences between postsurgery and presurgery ipsilateral values are indicated by a dagger ($p < 0.05$, Dunn's Method ANOVA on ranks), and an asterisk ($p < 0.05$, Mann-Whitney U test) indicates statistically significant differences between postsurgery ipsilateral and contralateral responses.

(G) Data represent the number of paw flinch/flick responses per minute following the intraplantar injection of formalin. There was no significant difference between responses of wild-type (closed diamond) and PSD-95 mutant (open diamond) mice in either the initial stage or the second (inflammatory) stage of this test. $n = 5–9$ in each case.

is predicted to play a particular role in NMDA receptor-mediated synaptic plasticity [16]. Recent studies indicate that Ca^{2+}/calmodulin stimulation induces autophosphorylation at Thr^{286} CaM kinase II and docking of the active kinase to the C-terminal domain of NR2B [17]. We first investigated whether CaM kinase II is necessary for the NMDA receptor-dependent sensitization of spinal neurons in CCI. Intrathecal administration of the se-

Table 1. Effects of Acute Topical Drug Administration and of CCI on CaM Kinase II Activation in Spinal Cord of Wild-Type and PSD-95 Mutant Mice

Topical Application to Spinal Dorsal Horn	Constitutive CaM Kinase II Activity (% of Maximal Activity Evoked In Vitro by Ca^{2+}/Calmodulin)			
	Wild-Type		PSD-95 mutant	
In Naive Mice				
Saline	16.7 ± 3.1		13.9 ± 2.7	
NMDA/glycine (150 nmole/30 nmole)	39.4 ± 3.4*		37.0 ± 4.1*	
Ionomycin (5 nmole)	43.9 ± 2.7*		44.8 ± 5.2*	
In Mice with Established CCI	CCI Ipsi	CCI Contra	CCI Ipsi	CCI Contra
Saline	28.8 ± 3.1*	16.8 ± 2.0	16.1 ± 2.1	14.9 ± 1.7
(R)-CPP (5 nmole)	14.3 ± 1.5	17.5 ± 3.0	-	-

Agents were topically applied in a volume of 500 μl for 15 min to the dorsal surface of L3-L6 spinal cord before rapid removal of tissue and homogenization prior to CaM kinase II immunoprecipitation and kinase activity assay. The concentrations of NMDA/glycine and ionomycin used were selected to provide maximal intensity stimuli and ensure detectability of changes in enzyme activity within the heterogeneous tissue samples taken. The mean maximal CaM kinase II activity in immunoprecipitates from naive PSD-95 mutant mice spinal cord (stimulated by Ca^{2+}/calmodulin addition in vitro) was unaltered from that in wild-type mice (108.3 ± 13.7 and 97.8 ± 13.1 pmoles ^{33}P/min/μg original extract protein, respectively). Data are expressed as the percentage of maximal CaM kinase II activity (means ± SEM, n = 8–10). Statistically significant differences are indicated by asterisk ($p < 0.05$ by Mann Whitney U test, compared to corresponding saline values in naive mice and by Wilcoxon test compared to corresponding contralateral values in mice with established CCI).

lective CaM kinase II inhibitors, KN-93 (120 pmole [18]) and myristoyl-autocamtide 2-related inhibitory peptide (myr-AIP, myr-KKALRRQEAVDAL, 1 nmole [19]), clearly reversed the neuropathic thermal hyperalgesia and mechanical allodynia seen in wild-type mice following CCI, whereas a control myristoylated peptide (myr-GRRNAIHDE, 1 nmole) or saline vehicle were without effect. Cell permeability of myr-AIP has been documented [19], and we have shown that it can effectively attenuate CaM kinase II autophosphorylation in spinal cord following topical application (unpublished results). At 10–30 min following injection, the ipsilateral:contralateral difference in PWL (thermal hyperalgesia) was significantly reduced to 18.2% ± 3.6%* and 21.2 ± 2.3%* of predrug control values by KN-93 and myr-AIP, respectively (n = 6–9, *$p < 0.05$ by Wilcoxon test), but not by myr-control peptide (90.5% ± 8.6%) or saline (above). Corresponding values for the lateral difference in PWT (mechanical allodynia) were 3.3% ± 1.4%, 37.3% ± 5.9%*, and 96.3% ± 5.8%. Recovery from the effects of each reagent was largely complete by 60–80 min. Thus, the NMDA receptor-dependent sensitization of spinal neurons that is lacking in PSD-95 mutant mice crucially requires CaM kinase II to exert its functional influence.

CaM Kinase II Activation in Response to Spinal NMDA Receptor Stimulation or CCI

We directly monitored the activation state of spinal cord CaM kinase II, isolated by immunoprecipitation from tissue extracts. Following CCI, the proportion of CaM kinase II activity that was constitutive (a read-out of previous activation by Ca^{2+}/calmodulin) was significantly greater in spinal cord ipsilateral to nerve injury compared to contralateral in wild-type animals, but not in PSD-95 mutants (Table 1). This CCI-induced increment could be completely prevented by topical (R)-CPP, confirming the requirement for NMDA receptors in mediating the necessary Ca^{2+} entry. The maximal activity of CaM kinase II from spinal cord that could be evoked in vitro by Ca^{2+}/calmodulin addition was unchanged between wild-type and PSD-95 mutant mice. Furthermore, topical application of a maximally effective concentration of NMDA (with glycine) or of ionomycin elicited the same extent of CaM kinase II activation in naive PSD-95 mutant mice as seen in wild-type littermates (Table 1). Thus, the spinal complement of CaM kinase II is fully able to respond to Ca^{2+}-elevating stimuli in PSD-95 mutant mice. Nevertheless, the NMDA receptor-mediated Ca^{2+} entry that occurs physiologically during CCI appears to activate CaM kinase II more effectively in wild-type than in PSD-95 mutant mice. PSD-95 therefore seems to play an important role in facilitating the functional coupling between the NMDA receptor and CaM kinase II in CCI.

Molecular Mechanisms Disrupted in PSD-95 Mutant Mice

Changes either in protein phosphorylation or in protein:protein interactions might underlie the facilitated NMDA receptor:CaM kinase II coupling in CCI. The NMDA receptor is known to be phosphorylated by PKC and PKA at Ser^{896} and Ser^{897}, respectively, within the NR1 subunit [20], and PSD-95 is thought to bind the PKA/PKC-docking protein AKAP79/150 [21] through domains that are lacking in the mutant PSD-95 protein here, suggesting that regulatory phosphorylation of the NMDA receptor may be disturbed in the mutant mice. Figure 3A shows that NR1-directed immunoprecipitates demonstrated a small increase in phospho-Ser^{897}-NR1 immunoreactivity ipsilateral to CCI, which tended to be less in PSD-95 mutant mice. No clear signal was obtained for phospho-Ser^{896} immunoreactivity. Pan-NR1 control blots were also carried out to confirm that the proportion of NR1 phosphorylated at Ser^{897} was increased (Figure 3A). Small reductions in the levels of pan-NR1 immunoreactivity were seen ipsilateral to CCI (in accordance with a previous report [22] and our unpublished data from the rat CCI model), and these reductions were similar in PSD-95 mutant mice to those in

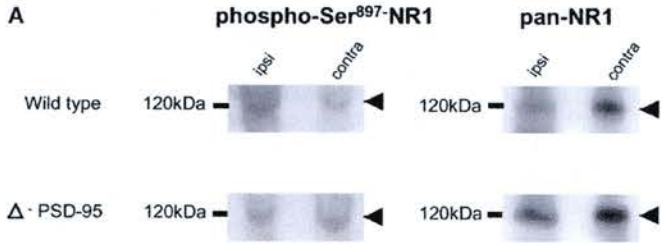

Mean relative phospho-Ser 897 NR1: pan NR1 immunoreactivity (grey scale ratios relative to wt contra)	
Wild type ipsi	4.67 ± .63
Wild type contra	1.0 (as defined)
Δ- ipsi	1.35 ± 0.22
Δ- contra	1.02 ± 0.17

Figure 3. Immunoblots for Phospho-Ser[897]-NR1 and PKA-Related Proteins in NR1 and NR2 Immunoprecipitates from Wild-Type and PSD-95 Mutant Mice Either Following CCI Surgery or in Naive Samples

(A) Western blot analysis of NR1 immunoprecipitates from spinal cord following sciatic CCI carried out 12 days previously. Immunoprecipitates from wild-type (wt) or PSD-95 mutant (open triangle) mice, ipsilateral or contralateral to the injury, were probed for phospho-Ser[897]-NR1 or pan-NR1 (n = 5). The mean ratio of phospho-Ser[897]-NR1:pan-NR1 immunoreactivity appeared to be increased in wild-type ipsilateral samples, but not those from the mutant mice. Approximate molecular weights are shown on the left.

(B) Western blot analysis of spinal cord proteins captured by "pep6" NR2B C-terminal (SIESDV) peptide-affinity resin [4]. Samples derived from wild-type (wt) or PSD-95 mutant (open triangle) mice were probed with antibodies for NR1, PKA-RIIα, PKA-RIIβ, and AKAP150 (n = 8). There was no detectable difference in the levels of any of these captured proteins when wild-type extracts were compared to PSD-95 mutant extracts.

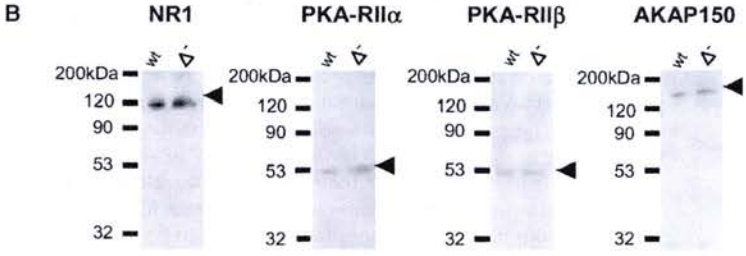

wild-type littermates. However, affinity capture of NMDA receptor complexes and associated proteins using an NR2B tail peptide affinity resin [3, 4] showed consistently no changes in NR1, PKA-RIIα, PKA-RIIβ, or AKAP150 immunoreactivity between complexes from wild-type or PSD-95 mutant spinal cord (Figure 3B). This suggests that altered AKAP-mediated kinase targeting to the NMDA receptor complex in the PSD-95 mutant mice does not underlie their neuropathic sensitization-resistant phenotype.

To examine the coexistence of CaM kinase II and NMDA receptors in molecular complexes in the spinal cord following CCI and to assess any difference caused by the mutant PSD-95 protein, we immunoprecipitated NR2A/B subunits from spinal cord following CCI and probed for the levels of total and autophosphorylated (activated) CaM kinase IIα immunoreactivity bound to the receptor. In wild-type spinal cord, we found high levels of CaM kinase IIα associated with the receptor, with an increase in CaM kinase IIα levels ipsilateral to CCI compared to contralateral (Figure 4A). Similarly, there was a marked increase in the levels of NR2A/B bound phospho-Thr[286] CaM kinase IIα ipsilateral to injury in wild-type mice (Figure 4B) where under the same conditions in PSD-95 mutant mice, minimal levels of CaM kinase IIα (Figure 4A) or phospho-Thr[286] CaM kinase IIα (Figure 4B) were bound to NR2A/B subunits. When blots were probed for control pull-down of NR2A and NR2B subunits, uniform immunoreactivity was seen in wild-type and PSD-95 mutant tissue (Figure 4C). Similarly, the tissue levels of CaM kinase II expression were unaltered between wild-type and PSD-95 mutant mice (Figure 4D). These data reveal a profound loss of NMDA receptor-associated CaM kinase IIα and phospho-Thr[286] CaM kinase IIα (an autonomously active form of the enzyme) in the PSD-95 mutant mice. Disruption of this interaction could provide a unified explanation of the linked dependence of sensitization on NMDA receptors and CaM kinase II, together with the lack of CCI-induced behavioral reflex sensitization and CCI-induced CaM kinase II activation seen in the PSD-95 mutants.

Discussion

Using transgenic mice and a behavioral reflex model of central sensitization following nerve injury [5, 6], we have

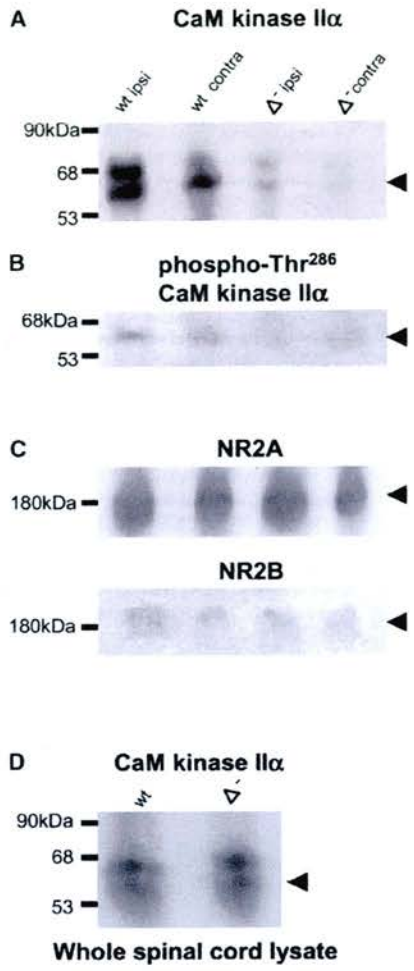

Figure 4. Immunoblots for CaM Kinase IIα Association with Spinal NR2A/B Immunoprecipitates

(A) Western blot of NR2A/B immunoprecipitates from wild-type (wt) and PSD-95 mutant (open triangle) spinal cord at the peak of behavioral sensitization following CCI (n = 8). Ipsilateral to injury (ipsi) wild-type mice show increased levels of receptor bound CaM kinase II when compared to the contralateral (contra) spinal cord. In comparison, the levels of receptor bound CaM kinase II in PSD-95 mutant spinal cord were greatly reduced both ipsilateral and contralateral to injury. Approximate molecular weights are shown on the left.

(B) Western blots probed for phospho-Thr^{286} CaM kinase II show increased levels of NR-associated immunoreactivity ipsilateral to nerve injury in wild-type mice, but not PSD-95 (open triangle) mutants.

(C) Recovery of NR2A and NR2B from the immunoprecipitates showed no detectable differences between wild-type and PSD-95 mutant samples.

(D) Western blot of whole spinal cord lysate from naive wild-type (wt) mice and PSD-95 mutant mice (open triangle) probed for CaM kinase II shows that the total content of CaM kinase II was similar in wild-type and PSD-95 mutant mice.

addressed the role of the NMDA receptor-adaptor protein PSD-95 in neuropathic pain. Histochemical staining for the β-galactosidase reporter incorporated into the mutant construct showed specific expression in many cells within lamina II of the superficial dorsal horn. This corresponds to regions of high NMDA receptor expression, to the termination of fine sensory afferents, and matches a recent report of native PSD-95 immunoreactivity in spinal cord [23]. In spinal cord of wild-type mice, NR2 subunit immunoprecipitates additionally pulled down both NR1 and PSD-95, confirming the presence of spinal complexes of NMDA receptor subunits with PSD-95.

The functional impact of the mutant PSD-95 construct on neuropathic behavioral reflex sensitization was striking. Thermal hyperalgesia, mechanical allodynia, and cold allodynia brought about by peripheral nerve injury were all virtually absent in homozygous PSD-95 mutant mice, despite the entirely undiminished nociceptive reflex behavior that they displayed following intraplantar formalin. The enduring lack of neuropathic sensitization seen in this phenotype is consistent with a brief report of transient delays in the development of such sensitization following a PSD-95 antisense reagent [23]. The current report reveals for the first time that the requirement for PSD-95 is both selective for neuropathic rather than inflammatory sensitization and is absolute. Intrathecal injection of NMDA receptor antagonist confirmed that the neuropathic hyperalgesia and allodynia are dependent on spinal NMDA receptors, matching other results in neuropathic pain models [1]. Similar sensitivity to NMDA receptor antagonist was seen for the late phase inflammatory formalin response, as in other reports [11, 12]. Intrathecal injection of NMDA did not produce hyperalgesia and allodynia in PSD-95 mutant mice, at a dose that was effective in naive wild-type mice. This is consistent with a recent report of attenuated NMDA-induced thermal hyperalgesia in the tail flick test when animals were treated with a PSD-95 antisense reagent [24]. The present data demonstrate that failure of a key signal from spinal NMDA receptors in the PSD-95 mutant mice is likely to underlie their inability to develop neuropathic sensitization. Inflammatory sensitization, although also requiring NMDA receptors, appears to be independent of such PSD-95-mediated coupling of the NMDA receptor to other proteins.

The sensitivity of NMDA receptor/PSD-95-dependent neuropathic sensitization to CaM kinase II inhibitors suggests that this enzyme may play a key role downstream of the complex in producing the sensitized state. This idea is consistent with evidence that NMDA receptor-mediated CaM kinase II translocation to synapses and activation is important in long-term potentiation in hippocampus [13, 25, 26], and spinal cord data showing that CaM kinase II can elicit and mediate sensitization caused by the activator of nociceptive afferent fibers, capsaicin [27, 28]. Accordingly, we found that CCI caused a partial activation of CaM kinase II in spinal cord. This was monitored by ex vivo enzyme assays, as a constitutively active (autophosphorylated, previously activated) form of the enzyme. PSD-95 mutant mice failed to show CCI-induced activation of CaM kinase II, however, suggesting that PSD-95 is essential in assembling an in vivo connection between the NMDA receptor and CaM kinase II under these conditions. Total CaM kinase II activity and immunoreactivity were unaltered by CCI or by the PSD-95 mutation. The fact that a high concentration of NMDA (plus glycine) could readily evoke CaM kinase II activation in PSD-95 mutant ani-

mals while CCI-induced enzyme activation was prevented could suggest that the CCI response involves a particular subpopulation of the enzyme, perhaps assembled in a specific functional arrangement.

An alternative hypothesis could be that the CCI-induced CaM kinase II response, but not that induced by NMDA (plus glycine) alone, might rely on auxiliary regulatory events, for which phosphorylation of the NMDA receptor would be a strong candidate. Although we detected some increase in phosphorylation of NR1-Ser^{897} (a PKA target) in CCI, we could find no evidence for altered association of PKA or AKAP79/150 with spinal NMDA receptor complexes in PSD-95 mutant mice. This argues against a failure of AKAP-mediated localization of kinases in the proximity of the NMDA receptor being the functionally critical deficit in the PSD-95 mutant mice.

In contrast, we found that the levels of overall CaM kinase IIα and phospho-Thr^{286} CaM kinase IIα that could be immunoprecipitated with NR2A/B subunits were clearly increased ipsilateral to CCI in wild-type, but not PSD-95 mutant mice. CaM kinase II is a major component of NMDA receptor complexes [3, 4] and can translocate to synapses upon further NMDA receptor activation [25]. It is known that CaM kinase II can associate directly with NR2A/B subunits, and this interaction may be reduced when PSD-95 is docked to receptor carboxy-tail sequences [29]. Nevertheless, here in a physiological model of neuropathic pain, the injury-induced association of CaM kinase II with the NMDA receptor is shown to be PSD-95 dependent, suggesting that its assembly into multiprotein complexes may be a key factor for in vivo function. Such functional microdomains organized in the vicinity of NMDA receptor complexes [30] may well be critical for neuropathic sensitization. While altered interactions of PSD-95 with other potential partners in the mutant mice may make a contribution to their lack of neuropathic reflex sensitization, the present evidence indicates that disruption of NMDA receptor:PSD-95:CaM kinase II functional microdomains plays a key role.

Supplementary Material

Supplementary material including detailed Experimental Procedures and data on morphological analysis of sciatic nerve fibers is available at http://images.cellpress.com/supmat/supmatin.htm.

Acknowledgments

This work was supported by the Wellcome Trust (S.M.F.-W., H.H., and S.G.N.G.) and the Medical Research Council (R.M.). Thanks to Louise Anderson and Jane Robinson for technical support and to the Faculty of Veterinary Medicine, University of Edinburgh for the award of a postgraduate studentship to E.M.G. and a summer vacation studentship to J. Bowen.

Received: September 30, 2002
Revised: November 22, 2002
Accepted: December 9, 2002
Published: February 18, 2003

References

1. Mayer, D.J., Mao, J., Holt, J., and Price, D.D. (1999). Cellular mechanisms of neuropathic pain, morphine tolerance, and their interactions. Proc. Natl. Acad. Sci. USA *96*, 7731–7736.
2. Boyce, S., Wyatt, A., Webb, J.K., O'Donnell, R., Mason, G., Rigby, M., Sirinathsinghji, D., Hill, R.G., and Rupniak, N.M.J. (1999). Selective NMDA NR2B antagonists induce antinociception without motor dysfunction: correlation with restricted localisation of NR2B subunit in dorsal horn. Neuropharmacology *38*, 611–623.
3. Husi, H., and Grant, S.G. (2001). Isolation of 2000-kDa complexes of N-methyl-D-aspartate receptor and postsynaptic density 95 from mouse brain. J. Neurochem. *77*, 281–291.
4. Husi, H., Ward, M.A., Choudhary, J.S., Blackstock, W.P., and Grant, S.G. (2000). Proteomic analysis of NMDA receptor-adhesion protein signaling complexes. Nat. Neurosci. *3*, 661–669.
5. Migaud, M., Charlesworth, P., Dempster, M., Webster, L.C., Watabe, A.M., Makhinson, M., He, Y., Ramsay, M.F., Morris, R.G.M., Morrison, J.H., et al. (1998). Enhanced long-term potentiation and impaired learning in mice with mutant postsynaptic density-95 protein. Nature *396*, 433–439.
6. Bennett, G.J., and Xie, Y.K. (1988). A peripheral mononeuropathy in rat that produces disorders of pain sensation like those seen in man. Pain *33*, 87–107.
7. Guilbaud, G., Gautron, M., Jazat, F., Ratinahirana, H., Hassig, R., and Hauw, J.J. (1993). Time-course of degeneration and regeneration of myelinated nerve fibers following chronic loose ligatures of the rat sciatic nerve—can nerve lesions be linked to the abnormal pain-related behaviors. Pain *53*, 147–158.
8. Sommer, C., Laonde, A., Heckman, H.M., Rodriguez, M., and Myers, R.R. (1995). Quantitative neuropathology of a focal nerve injury causing hyperalgesia. J. Neuropathol. Exp. Neurol. *54*, 635–643.
9. Woolf, C.J., and Costigan, M. (1999). Transcriptional and posttranslational plasticity and the generation of inflammatory pain. Proc. Natl. Acad. Sci. USA *96*, 7723–7730.
10. Arner, S., and Meyerson, B.A. (1988). Lack of analgesic effect of opioids on neuropathic and idiopathic forms of pain. Pain *33*, 11–23.
11. Coderre, T.J., and Melzack, R. (1992). The contribution of excitatory amino-acids to central sensitization and persistent nociception after formalin-induced tissue-injury. J. Neurosci. *12*, 3665–3670.
12. Chaplan, S.R., Malmberg, A.B., and Yaksh, T.L. (1997). Efficacy of spinal NMDA receptor antagonism in formalin hyperalgesia and nerve injury evoked allodynia in the rat. J. Pharmacol. Exp. Ther. *280*, 829–838.
13. Gardoni, F., Caputi, A., Cimino, M., Pastorino, L., Cattabeni, F., and Di Luca, M. (1998). Calcium/calmodulin-dependent protein kinase II is associated with NR2A/B subunits of NMDA receptor in postsynaptic densities. J. Neurochem. *71*, 1733–1741.
14. Strack, S., McNeill, R.B., and Colbran, R.J. (2000). Mechanism and regulation of calcium/calmodulin-dependent protein kinase II targeting to the NR2B subunit of the N-methyl-D-aspartate receptor. J. Biol. Chem. *275*, 23798–23806.
15. Gardoni, F., Schrama, L.H., van Dalen, J.J., Gispen, W.H., Cattabeni, F., and Di Luca, M. (1999). αCaMKII binding to the C-terminal tail of NMDA receptor subunit NR2A and its modulation by autophosphorylation. FEBS Lett. *456*, 394–398.
16. Lisman, J., Malenka, R.C., Nicoll, R.A., and Malinow, R. (1997). Learning mechanisms: the case for CaM-KII. Science *276*, 2001–2002.
17. Bayer, K.U., De Koninck, P., Leonard, A.S., Hell, J.W., and Schulman, H. (2001). Interaction with the NMDA receptor locks CaMKII in an active conformation. Nature *411*, 801–805.
18. Sumi, M., Kiuchi, K., Ishikawa, T., Ishii, A., Hagiwara, M., Nagatsu, T., and Hidaka, H. (1991). The newly synthesized selective Ca^{2+}/calmodulin dependent protein kinase II inhibitor KN-93 reduces dopamine contents in PC12h cells. Biochem. Biophys. Res. Commun. *181*, 968–975.
19. Gailly, P. (1998). Ca^{2+} entry in CHO cells, after Ca^{2+} stores depletion, is mediated by arachidonic acid. Cell Calcium *24*, 293–304.
20. Tingley, W.G., Ehlers, M.D., Kameyama, K., Doherty, C., Ptak, J.B., Riley, C.T., and Huganir, R.L. (1997). Characterization of protein kinase A and protein kinase C phosphorylation of the N-methyl-D-aspartate receptor NR1 subunit using phosphorylation site-specific antibodies. J. Biol. Chem. *272*, 5157–5166.
21. Colledge, M., Dean, R.A., Scott, G.K., Langeberg, L.K., Huganir,

R.L., and Scott, J.D. (2000). Targeting of PKA to glutamate receptors through a MAGUK-AKAP complex. Neuron *27*, 107–119.

22. Siegan, J.B., and Sagen, J. (1995). Attenuation of NMDA-induced spinal hypersensitivity by adrenal medullary transplants. Brain Res. *680*, 88–98.
23. Tao, F., Tao, Y.X., Gonzales, J.A., Fanf, M., Mao, P., and Johns, R.A. (2001). Knockdown of PSD-95/SAP90 delays the development of neuropathic pain in rats. Neuroreport *12*, 3251–3255.
24. Tao, Y., Huang, Y., Mei, L., and Johns, R.A. (2000). Expression of PSD-95/SAP90 is critical for N-methyl-D-aspartate receptor-mediated thermal hyperalgesia in the spinal cord. Neuroscience *98*, 201–206.
25. Shen, K., and Meyer, T. (1999). Dynamic control of CaMKII translocation and localization in hippocampal neurons by NMDA receptor stimulation. Science *284*, 162–166.
26. Fukunaga, K., Rich, D.P., and Soderling, T.R. (1989). Generation of the $Ca^{2(+)}$-independent form of Ca^{2+}/calmodulin-dependent protein kinase II in cerebellar granule cells. J. Biol. Chem. *264*, 21830–21836.
27. Fang, L., Wu, J., Lin, Q., and Willis, W.D. (2002). Calcium-calmodulin-dependent protein kinase II contributes to spinal cord central sensitization. J. Neurosci. *22*, 4196–4204.
28. Kolaj, M., Cerne, R., Cheng, G., Brickey, D.A., and Randic, M. (1994). Alpha subunit of calcium/calmodulin-dependent protein kinase enhances excitatory amino acid and synaptic responses of rat spinal dorsal horn neurons. J. Neurophysiol. *72*, 2525–2531.
29. Gardoni, F., Schrama, L.H., Kamel, A., Gespen, W.H., Cattabeni, F., and Di Luca, M. (2001). Hippocampal synaptic plasticity involves competition between Ca^{2+}/calmodulin-dependent protein kinase II and postsynaptic density 95 for binding to the NR2A subunit of the NMDA receptor. J. Neurosci. *21*, 1501–1509.
30. Zhabotinsky, A.M. (2000). Bistability in the $Ca^{(2+)}$/calmodulin-dependent protein kinase-phosphatase system. Biophys. J. *79*, 2211–2221.